Linking fungal secondary metabolites and pathways to their genes in Aspergillus

Petersen, Lene Maj

Publication date:
2014

Document Version
Publisher's PDF, also known as Version of record

Linking fungal secondary metabolites and pathways to their genes in *Aspergillus*

Lene Maj Petersen

PhD thesis

DTU Systems Biology

September 15th 2014

DTU Systems Biology
Department of Systems Biology

Preface

This thesis is submitted to the Technical University of Denmark as part of the requirements for the Degree of Doctor of Philosophy in Chemistry. The work was carried out from September 15th 2011 to September 15th 2014 at the Department of Systems Biology under the main supervision of associate professor Thomas Ostenfeld Larsen (DTU Systems Biology) and co-supervision by associate professor Charlotte Held Gotfredsen (Department of Chemistry, DTU) and assistant professor Jakob Blæsbjerg Nielsen (DTU Systems Biology).

Many people have contributed to making my PhD project not only a highly educational experience but also very pleasant and exciting. First and foremost I want to thank my supervisors. Thomas; for giving me the opportunity to work on this project and for all the guidance throughout the years. You are a great mentor and source of inspiration for me, and I will always admire your enthusiasm and ability to see the big picture. Charlotte and Jakob for all of their guidance and help on their areas of expertise. I could not have asked for better supervisors!

Secondly, I want to thank all of my amazing colleagues. Especially I want to thank Dorte Holm for our close and fruitful collaborations, Kristian Fog, Jens Frisvad and Carsten Christophersen for guidance and invaluable discussions, the technical staff Hanne Jacobsen, Lisette Knoth-Nielsen, Kir Lyhne and Anne Hector, who's help has been vital, Louise Kjærulff for good NMR support, Silas, Kasper and Aaron for being the best officemates, and rest of the lot: Ana, Marie-Louise, Tanja, Sara, Maria, Livia, Anita, Olivera, Ina, Andreas, Alexander, Paiman, and Mikael for being the best colleagues imaginable. I would also like to thank a number of productive students, especially Casper Hoeck.

During my PhD project I had the privilege to spend six months in Professor Yi Tang's group at the University of California Los Angeles (UCLA), USA. I would like to thank Professor Tang for letting me join his lab and enjoy the Californian sun. Also I would like to thank the entire group for welcoming me and providing guidance in the lab. Especially Wenbing Yin for guidance, Angelica, Nidhi, Anthony, and Sameh for new friendships, and Jackie for showing me the world of American football and how to spend American Christmas.

As part of a PhD course I also got to spend two weeks at the University of Aberdeen in Scotland, and here I want to thank professor Marcel Jaspars. Not only for organizing a great course, but also for valuable NMR guidance for structure elucidation of *A. indologenus* compounds.

I also had the pleasure to participate in a number of conferences, which has been a great source of inspiration, as well as a great opportunity to present my own work. Funding from Knud Højgaards Fond, Augustinus Fonden, Oticon Fonden, Otto Mønsteds Fond and G.A. Hagemann's Mindefond, making the conferences and especially my external stay at UCLA possible, is greatly acknowledged.

Also thanks to Solveig Kallesøe (University of Copenhagen) for helping obtaining CD data and to the Danish Instrument Center for NMR Spectroscopy of Biological Macromolecules at Carlsberg laboratory for NMR time.

My biggest appreciation goes to everybody at the former CMB, for creating an amazing working environment. You have made this whole project a true pleasure and I feel privileged to have worked with such talented people and now be able to call so many of you my friends.

Lastly, thanks to my friends and family, who maybe not always understood my weird fungus-language, but none the less listened and provided the support needed. You are the best!

Kgs. Lyngby, September 15, 2014

Lene Maj Petersen

Summary

Filamentous fungi are producers of small bioactive molecules termed secondary metabolites (SMs), which display a wide range of functional and structural diversity. The compounds have several important activities including antifungal, antibacterial, anticancer, antiparasitic, antiinsectan and immunosuppressive activities. The rapid increase in genomes sequences of filamentous fungi has revealed that the biosynthetic potential is enormous, due to the presence of huge numbers of biosynthetic gene clusters. Thus, there is an enormous potential of previously undiscovered SMs waiting to be exploited, which can potentially be used as pharmaceuticals.

The work has focused on filamentous fungi from the important genus *Aspergillus*. It contains species that are both food and feed contaminants, some that are used for industrial applications for production of small compounds and enzymes, as well as model organisms for genetic studies and human opportunistic pathogens.

The aim of this PhD study has been divided into two major topics:

1) Discovery and characterization of novel SMs from filamentous fungi
2) Linking of fungal SMs to genes and elucidation of biosynthetic pathways

The first part of this study, the discovery of novel SMs, has resulted in characterization of 22 novel SMs from selected Aspergilli. Two different approaches were undertaken: Dereplication based discovery and discovery by induction of sclerotium formation. The outcome included characterization of the following novel compounds: aculenes A-D, acucalbistrins A-B, acu-dioxomorpholine, okaramine S, and epi-10,23-dihydro-24,25-dehydroaflavinin from *A. aculeatus*, aspiperidine oxide from *A. indologenus*, homomorphosins A-F from *A. homomorphus*, sclerotionigrins A-B from *A. sclerotioniger*, as well as emindole SC, sclerolizine and carbonarins I-J from *A. sclerotiicarbonarius*. In addition, several known compounds could be reported from the different species for the first time. Furthermore it was discovered how sclerotia formation could be induced in black Aspergilli, using a combination of natural substrates and by introduction of a pre-freezing step prior to inoculation. This is of general interest for the discovery of novel bioactive SMs, since sclerotia formation trigger otherwise silent biosynthetic pathways, resulting in greatly altered metabolic profiles.

The second part of the study, linking genes to SMs and elucidating biosynthetic pathways, led to insights into the biosynthetic potential of a number of Aspergilli. This included comparative metabolic profiling of *A. oryzae* and *A. flavus*, two species with an overall high homology of 99.5 % on genome level, but surprisingly high degree of chemical differences. Elucidation of structures from novel *A. oryzae* metabolites, however, revealed the chemical link between the two species.

In two parallel projects, involving *A. niger* and *A. aculeatus* respectively, the polyketide 6-methyl salicylic acid (6-MSA), and corresponding biosynthetic pathways, were investigated. In *A. niger*, 6-MSA was converted into meroterpenoid yanuthone D. The biosynthetic pathway was investigated by a multidisciplinary approach. As a result the cluster responsible for production of yanuthone D was identified and a biosynthetic pathway presented, where 6-MSA is converted into yanuthone D in eight steps. Furthermore a total of ten novel yanuthones were characterized, whereof two did not originate from 6-MSA, but did utilize several of the enzymes encoded by the cluster, defining a new class of yanuthones. In *A. aculeatus* the 6-MSA pathway was found to differ, with conversion of 6-MSA into the terpenoid/non-ribosomal peptide/polyketide hybrids aculins A-B, for which a biosynthetic pathway has been proposed. By overexpression of a TF located immediately downstream of the 6-MSA synthase gene, two non-6-MSA derived compounds were additionally discovered.

In *A. nidulans* a supercluster consisting of a non-ribosomal peptide synthase and a prenyltransferase was predicted, by full genome gene expression comparison, which ultimately linked to the tetracyclopeptide nidulanin A, illustrating the strength of bioinformatic tools to predict superclusters and structures of NRPs. Finally, it was investigated how entire gene clusters from filamentous fungi could be reconstituted in the model organism *A. nidulans*. This project would improve discovery, and ease characterization, of genes. As proof of concept, the cytochalasin gene cluster from *A. clavatus* was successfully reconstituted in *A. nidulans*, allowing further biochemical characterization.

The work of this thesis represents a major step forward in extending the chemical knowledge on the complex secondary metabolism of important filamentous fungi and at the same time illustrates the enormous potential for still discovering novel SMs. A focused collaboration between bioinformatics, molecular biology, analytical and natural products chemistry is critical for advances in both the linking of fungal SMs to genes and unraveling the biosynthetic pathways, as well as for the discovery of novel SMs hidden in a treasury of biosynthetic potential of filamentous fungi.

Sammenfatning

Filamentiøse svampe producerer små bioaktive molekyler, betegnet sekundære metabolitter, som spænder bredt i både funktionel og strukturel diversitet. De sekundære metabolitter kan være biologisk aktive mod f.eks. bakterier, insekter, humane celler eller andre svampe. Genomerne for adskillige filamentiøse svampe er på det seneste blevet sekventeret, hvilket har afsløret et stort antal genklustre, der koder for biosynteser, og dermed blotlagt et enormt potentiale af hidtil uopdagede sekundære metabolitter, der potentielt kan udnyttes til medicinske formål.

Arbejdet, der præsenteres i denne afhandling, har fokuseret på filamentiøse svampe indenfor den vigtige og spændende slægt *Aspergillus*. Den indeholder arter der; kontaminerer fødevarer og foder, bruges som modelsystemer til genetiske undersøgelser, er patogene overfor mennesker, og bruges til industrielle applikationer, f.eks. til produktion af både små molekyler og enzymer.

Formålet for dette PhD studie har været opdelt i to hovedtemaer:

1) Opdagelse og karakterisering af nye metabolitter fra filamentiøse svampe
2) Kobling af svampe sekundære metabolitter til gener, samt udredning af biosynteseveje

Den første del af dette studie, opdagelsen af nye sekundære metabolitter, har resulteret i karakterisering af 22 nye sekundære metabolitter fra udvalgte Aspergiller. To forskellige tilgange blev udforsket: Dereplikerings baseret opdagelse samt opdagelse ved induktion af sclerotium dannelse. Resultatet omfatter karakterisering af følgende nye metabolitter: aculene A-D, acucalbistrin A-B, acu-dioxomorpholine, okaramine S, samt epi-10,23-dihydro-24,25-dehydroaflavinin fra *A. aculeatus*, aspiperidine oxide fra *A. indologenus*, homomorphosin A-F fra *A. homomorphus*, sclerotionigrin A-B fra *A. sclerotioniger*, emindole SC, sclerolizine samt carbonarin I-J fra *A. sclerotiicarbonarius*. Desuden blev flere kendte metabolitter, rapporteret i de forskellige arter for første gang. Et vigtigt resultat af dette studie, er opdagelsen af, hvordan svampe relaterede strukturer kaldet sclerotier, kan induceres i sorte Aspergiller, ved at kombinere brugen af naturlige substrater og indførelse af et frysningstrin forud for podning. Dette er af generel interesse for opdagelsen af nye bioaktive metabolitter, da sclerotiedannelse, aktiver biosynteseveje, der ellers ikke er udtrykte, og som en direkte konsekvens, ses en stor ændring i metabolitprofilen.

Den anden del af PhD studiet, hvor gener kobles til sekundære metabolitter og biosynteseveje udledes, førte til indsigt i det biosyntetiske potentiale i en række

Aspergiller. Dette omfattede en sammenligning af den kemiske profil af *A. oryzae* og *A. flavus*, der er to nærtbeslægtede arter (99,5% homologi på genomniveau), men som viser en overraskende høj grad af forskelle i deres kemiske profiler. Opklaring af kemiske strukturer for nye stoffer fra *A. oryzae*, afslørede dog hidtil usete kemiske link mellem de to arter.

I to parallelle projekter, i henholdsvist *A. niger* og *A. aculeatus*, blev polyketidet 6-methyl-salicylsyre (6-MSA) og de respektive biosynteseveje med udgangspunkt i 6-MSA undersøgt. I *A. niger* blev 6-MSA omdannet til meroterpenoidet yanuthone D. Via en multidisciplinær tilgang kunne generne, i et genkluster, ansvarligt for produktionen af yanuthone D identificeres, og biosyntesevejen over 8 trin udledes. Desuden blev ti nye yanuthoner karakteriseret, hvoraf to viste sig ikke at være afledt af 6-MSA. Dog var produktionen af disse to yanuthoner afhængig af flere af enzymerne kodet af det pågældende genkluster ansvarlig for yanuthone D, hvilket, definererede en ny klasse af yanuthoner. *A. aculeatus* 6-MSA biosyntesevejen varierede. Her blev 6-MSA omdannet til aculiner, hybrider af terpener/ikke-ribosomale peptider/polyketider, for hvilke der blev foreslået en biosyntesevej, baseret på bioinformatiske og strukturkemiske betragtninger. En transskriptionsfaktor tæt på 6-MSA synthasen, blev overudtrykt, hvilket resulterede i karakterisering af yderligere to stoffer, der dog ikke var afledte fra 6-MSA.

I *A. nidulans* blev to fysisk adskilte gener, bestående af en non-ribosomal peptidsynthetase og en prenyltransferase forudset til at være koblet til den samme biosyntesevej. Dette blev eftervist og forbundet med biosyntesen af tetra-cyclopeptidet nidulanin A, hvilket illustrerede styrken af bioinformatiske værktøjer til at forudsige sammenhænge mellem fysisk adskilte gener, samt strukturer af non-ribosomale peptider. Endelig blev det undersøgt, hvordan hele genklustre fra svampe kunne udtrykkes heterologt i modelorganismen *A. nidulans*. Dette projekt vil forbedre opdagelse samt karakterisering af gener involveret i biosynteser. Cytochalasin biosyntesevejen fra *A. clavatus* blev undersøgt og med succes rekonstrueret i *A. nidulans*.

Resultaterne af dette PhD studie bringer ny kemisk viden om den komplekse sekundære metabolisme af vigtige filamentiøse svampe og illustrerer samtidig det enorme potentiale for at opdage nye sekundære metabolitter. Et målrettet samarbejde mellem bioinformatik, molekylærbiologi, analytisk kemi og naturstof kemi er afgørende for fremskridt i både koblingen af svampe metabolitter til gener og udledning af biosynteseveje, samt til opdagelsen af de mange nye metabolitter, der stadig ligger skjult i de filamentiøse svampe.

List of papers

Paper 1: **Petersen, L.M.**; Hoeck, C.; Frisvad, J.C.; Gotfredsen, C.H.; Larsen, T.O. "Dereplication guided discovery of secondary metabolites of mixed biosynthetic origin from *Aspergillus aculeatus" Molecules*, **2014**, *19*, 10898-10921.

Paper 2: **Petersen L.M.**; Kildgaard, S.; Jaspars, M.; Larsen, T.O. "Aspiperidine oxide, a new rare piperidine *N*-oxide, from the filamentous fungus *Aspergillus indologenus*" Intended for publication in Phytochemistry Letters.

Paper 3: Hoeck, C.; **Petersen, L.M.**; Frisvad, J.C.; Gotfredsen, C.H.; Larsen, T.O. "Novel metabolites from *Aspergillus homomorphus"* Intended for publication in Magnetic Resonance in Chemistry.

Paper 4: Frisvad, J.C.; **Petersen, L.M.**; Lyhne, K.E.; Larsen, T.O. "Formation of sclerotia and production of indoloterpenes by *Aspergillus niger* and other species in section *Nigri*" *PLoS One*, **2014**, *9* (4), e94857

Paper 5: **Petersen L.M.**; Bladt, T.T.; Dürr, C.; Seiffert, M.; Frisvad, J.C.; Gotfredsen, C.H.; Larsen, T.O. "Isolation, structural analyses and biological activity assays against chronic lymphocytic leukemia of two novel cytochalasins, sclerotionigrin A and B" *Molecules*, **2014**, *19*, 9786-9797

Paper 6: **Petersen, L.M.**; Frisvad, J.C.; Knudsen, P.B.; Rohlfs, M. Gotfredsen, C.H.; Larsen, T.O. "Induced sclerotium formation exposes new bioactive metabolites from *Aspergillus sclerotiicarbonarius*" Intended for publication in Journal of Antibiotics.

Paper 7: Rank, C.; Klejnstrup, M. L.; **Petersen, L. M.**; Kildgaard, S.; Frisvad, J. C.; Gotfredsen, C. H.; & Larsen, T. O. "Comparative chemistry of *Aspergillus oryzae* (RIB40) and *A. flavus* (NRRL 3357)" *Metabolites*, **2012**, *2* (1), 39–56. doi:10.3390/metabo2010039

Paper 8: Andersen, M.R.; Nielsen, J.B.; Klitgaard, A.; **Petersen, L.M.**; Zachariasen, M.; Hansen, T.J.; Blicher, L.H.; Gotfredsen, C.H.; Larsen, T.O.; Nielsen, K.F.; Mortensen, U.H. "Accurate prediction of secondary metabolite gene clusters in filamentous fungi" *Proceedings of the National Academy of Sciences of the United States of America*, **2013**, *110* (1), E99–107. doi:10.1073/pnas.1205532110

Paper 9: Holm, D.K.; **Petersen, L.M. (Joint 1st author)**; Klitgaard, A.; Knudsen, P.B.; Jarczynska, Z.D.; Nielsen, K.F.; Gotfredsen, C.H.; Larsen, T.O.; Mortensen, U.H. "Molecular and chemical characterization of the biosynthesis of the 6-MSA derived meroterpenoid yanuthone D in *Aspergillus niger" Chemistry & Biology*, **2014**, *21*, 519-529.

Paper 10: **Petersen, L.M.**; Holm, D.K.; Klitgaard, A.; Knudsen, P.B.; Nielsen, K.F.; Gotfredsen, C.H.; Mortensen, U.H.; Larsen, T.O. "Characterization of four new antifungal yanuthones from *Aspergillus niger" Journal of Antibiotics*, **2014**, In Press.

Paper 11: **Petersen, L.M.**; Holm, D.K.; Gotfredsen, C.H.; Mortensen, U.H.; Larsen, T.O. "Investigation of a 6-MSA synthase gene cluster in *Aspergillus aculeatus* reveals 6-MSA derived aculins A-B and non-6-MSA derived pyrrolidinones" Intended for publication in Chemistry & Biology.

Paper 12: **Petersen, L.M.**; Tang, Y. "Reconstitution of the cytochalasin gene cluster from *Aspergillus clavatus* in *Aspergillus nidulans*" Draft.

Conference contributions

Petersen L.M. "Unraveling cryptic chemistry in black Aspergilli" Oral presentation at the Annual Meeting of the American Society of Pharmacognosy (ASP), Oxford, MS, USA, **2014**.
Abstract published in Planta Medica 2014, Volume 80, P760.

Petersen, L.M.; Holm, D.K.; Gotfredsen, C.H.; Mortensen, U.H.; Larsen, T.O. "Discovery of novel secondary metabolites in *Aspergillus aculeatus"* Poster presentation at Directing Biosynthesis III, Nottingham, UK, **2012**.

Petersen, L.M.; Holm, D.K.; Gotfredsen, C.H.; Mortensen, U.H.; Larsen, T.O. "Discovery of novel secondary metabolites in *Aspergillus aculeatus*". Poster presentation at the International Congress on Natural Products Research (ICNPR), New York, NY, USA, **2012**.
Abstract published in Planta Medica 2012, Volume 78, P1159-1160.

Petersen, L.M.; Holm, D.K.; Gotfredsen, C.H.; Mortensen, U.H.; Larsen, T.O. "Activation of a silent meroterpenoid pathway in *Aspergillus aculeatus*". Poster presentation at the 7th Danish Conference on Biotechnology and Molecular Biology, Vejle, Denmark, **2012**.

Petersen, L.M.; Rank, C.; Klejnstrup, M.L.; Kildgaard, S.; Frisvad, J.C.; Gotfredsen, C.H.; Larsen, T.O. "Comparative Chemistry of *Aspergillus oryzae* and *A. flavus*". Poster at the 33rd Danish NMR Meeting, Århus, Denmark, **2012**.

Petersen, L.M.; Gotfredsen, C.H.; Hjorth, C.; Larsen, T.O. "Linking of fungal secondary metabolites and pathways to their synthase genes" Poster at Novo Scholarship Symposium, Bagsværd, Denmark, **2012**.

Abbreviations

A	Adenylation
AA	Amino Acid
Aad	2-aminoadipicacid
ACN	Acetonitrile
ACP	Acyl Carrier Protein
AMA1	Autonomous Maintenance in *Aspergillus*
AT	Acyltransferase
BLAST	Basic Local Alignment Tool
Bp	Base Pairs
BPC	Base Peak Chromatogram
C	Condensation
CD	Circular Dichroism
CLL	Chronic Lymphocytic Leukemia
CoA	Coenzyme A
COSY	Correlation Spectroscopy
CLC	Claisen Cyclase
CMB	Center For Microbial Biotechnology
CYA	Czapek Yeast Agar
CYAR	Czapek Yeast Agar Raisin
CYC	Cyclase
1D	1 Dimensional
2D	2 Dimensional
DAD	Diode Array Detector
DCM	Dichloromethane
DH	Dehydratase
DMAPP	Dimethylallyl Diphosphate
DMSO	Dimethyl Sulfoxide
DNA	Deoxyribonucleic Acid
DQF-COSY	Double Quantum Filtered COrrelated SpectroscopY
DTU	Technical University of Denmark
EIC	Extracted Ion Chromatogram
ESI	Electrospray Ionization
E-SPE	Explorative Solid Phase Extraction
EtOAc	Ethyl Acetate
ER	Enoyl Reductase
FA	Formic Acid
FAS	Fatty-acid Synthases
FDAA	1-fluoro-2,4-dinitrophenyl-5-L-alanineamide
GMM	Glucose Minimal Medium
H2BC	Heteronuclear two Bond Correlation
HMBC	Heteronuclear Multiple Bond Correlation
HPLC	High Performance Liquid Chromatography
HR	Highly Reduced
HR	Homologous Recombination
HRMS	High-Resolution Mass Spectrometry
HSQC	Heteronuclear Single Quantum Coherence
IBT	Institute for Biotechnology
IC_{50}	Median Inhibitory Concentration
IPP	Isopentenyl Diphosphate
kb	Kilobasepair
KR	Ketoreductase

KS	β-ketoacyl Synthase
Kyn	Kynurenine
LB	Luria-Bertani
LC_{50}	Median Lethal Concentration
MAT	Malonyl Acyl Transferase
MAX	Mixed mode anion-exchanger
MeOH	Methanol
MM	Minimal medium
MS	Mass Spectrometry
MS/MS	Tandem Mass Spectrometry
6-MSA	6-methylsalicylic Acid
MT	Methyl Transferase
MQ	MilliQ-water
m/z	Mass-to-charge ratio
NHEJ	Non-Homologous End-Joining
NMR	Nuclear Magnetic Resonance
NOESY	Nuclear Overhauser Effect Spectroscopy
NP	Natural Product
NR	Non Reduced
NRP	Non Ribosomal Peptide
NRPS	Non Ribosomal Peptide Synthetase
OAT	Oat meal agar
OSMAC	One Strain Many Compounds
PCP	Peptidyl Carrier Protein
PCR	Polymerase Chain Reaction
Phe	Phenylalanine
PK	Polyketide
PKS	Polyketide Synthase
Ppm	Parts Per Million
PR	Partially Reduced
PT	Product Template
qRT PCR	quantitative Reverse Transcription Polymerase Chain Reaction
RNA	Ribonucleic Acid
RP	Reverse Phase
RT	Rentention Time
SAM	S-adenosylmethionine
SAT	Starter unit ACP Transacylase
SAX	Strong Anion-Exchanger
SCX	Strong Cation-Exchanger
SM	Secondary Metabolite
Sp.	Species
T	Thiolation
TAR	Transformation-Associated Recombination
TE	Thioesterase
TF	Transcription Factor
TOCSY	Total Correlation Spectroscopy
TOF	Time Of Flight
UHPLC	Ultra High Performance Liquid Chromatography
UV	Ultraviolet
UV/VIS	Ultraviolet/Visual
Val	Valine
WATM	Wickerhams Antibiotic Test Medium
YES	Yeast Extract Sucrose

Table of Contents

1 Introduction

Natural products (NPs) have played a major role in the history of drug discovery, and they continue to be important as drugs and targets of study for synthetical and analytical chemists. NPs display a wide range of functional and structural diversity and the compounds have several important activities including antifungal, antibacterial, anticancer, antiparasitic, antiinsectan and immunosuppressive activities. Originating with the discovery of penicillin in 1929 [1], NPs have been used as a source of inspiration for drug discovery. Of all new approved drugs in a 30 years period from 1981 to the end of 2010, 65% was either NPs or directly derived thereof [2][3]. Today the discovery of novel NPs is still important. First and foremost, since novel drugs are still needed. A growing problem is that bacteria become resistant to existing antibiotics, and at the same time fewer novel antibiotics are being approved [4].

The major sources of NPs are bacteria, plants, and filamentous fungi; marine as well as terrestrial. The focus of this study has been on secondary metabolites (SMs) from filamentous fungi. The genus *Aspergillus* has been investigated due to the high importance of numerous species from this family. Several species produce relevant pharmaceutical compounds (e.g. cholesterol-lowering lovastatin from *A. terreus* [5]), others are used in the industry for production of small compounds or enzymes (e.g. citric acid and various enzymes from *A. niger* [6]) and finally another species is important for use as model organism for genetic studies (*A. nidulans* [7][8][9]). Yet others are pathogenic (*A. flavus* [10]) and some are food and feed contaminants (*A. niger* [11], *A. aculeatus* [11][12]).

Genome sequencing projects have exposed a high amount of biosynthetic gene clusters in filamentous fungi and revealed an enormous potential of previously undiscovered SMs: The number of SM gene clusters by far exceeds the number of known metabolites, which can be linked to these clusters. Consequently, there is an unexplored potential of SM diversity in filamentous fungi.

In this work, the aim has been two-sided: Partly to explore the SM potential of a number of black Aspergilli by discovery and characterization of novel SMs (chapter 3). Partly to link these compounds to their biosynthetic genes and pathways in the organism (chapter 4). This first chapter gives a general introduction to SMs from filamentous fungi with emphasis on the biosynthesis of SMs (section 1.2), the genetics of SMs (section 1.3) and the metabolite analysis (section 1.4).

1.1 Filamentous fungi

Filamentous fungi, or moulds, belongs to the kingdom of fungi, and constitute a large and diverse group of multicellular eukaryotes [13][14]. Fungi are widespread in nature and many species have more than one preferred habitat and can survive in very diverse environments; fungi are very tolerant to a range of pH and temperatures, and can degrade and consume a wide range of substrates. Filamentous fungi are essential to the ecosystem for degradation of organic matter.

It has been estimated that as much as 1.5 million different fungal species exist [15], and of these only 75.000 have so far been collected and described [16], and hereof only a minority have been investigated for their chemical potential.

The genus *Aspergillus* is one of the most significant due to both their role as food and feed contaminants (*A. niger*, *A. aculeatus*), for uses as industrial workhorses (*A. niger*, *A. aculeatus*, *A. oryzae*) and for use as model organisms for genetic studies (*A. nidulans*), see Figure 1.1.

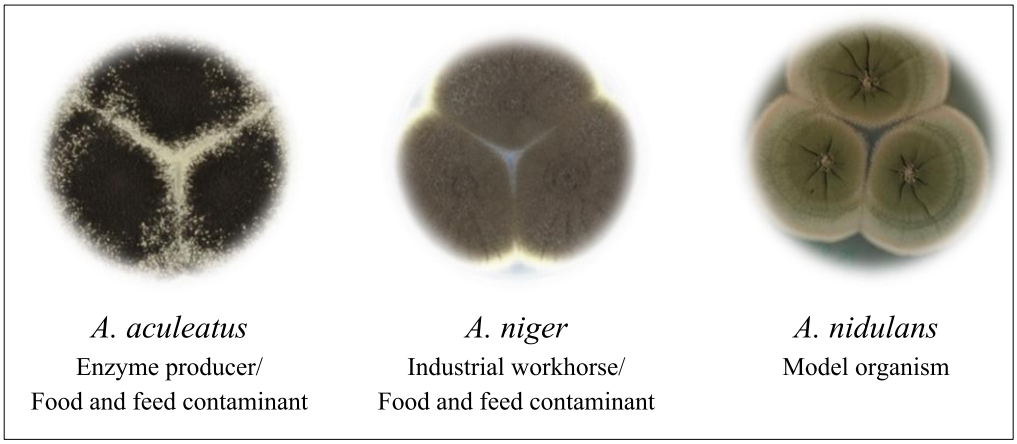

Figure 1.1 Physical appearance on solid growth media of selected filamentous fungi used in this study. Heavy black sporulation is observed for the black Aspergilli *A. aculeatus* and *A. niger*.

While some species, such as *A. nidulans*, has been widely studied, many of the black Aspergilli are unexplored. This group has been the focus in this thesis, and is described in the following section.

1.1.1 Black Aspergilli

Within the genus *Aspergillus* are the black Aspergilli (*Aspergillus* section *Nigri*), which constitute an important group, with both species utilized for industrial purposes and species being food and feed contaminants [17]. Members of the group are further divided into clades; an overview is given in Table 1.1.

Amongst the black Aspergilli, an important and widely studied species is *A. niger*. This species is industrially important and several processes using this fungus have been granted the "generally regarded as safe" (GRAS) certified status by the U.S. Food and Drug Administration (FDA) [6]. *A. niger* is utilized in several industrial processes and is used for production of organic acids such as citric acid and gluconic acid as well as enzymes such as amylases and lipases [6]. In addition to its wide use in the fermentation industry, *A. niger* is also a contaminant of food and feed [11]. Some strains are able to produce mycotoxins, such as fumonisins [18][19][20] and ochratoxin A [21].

Table 1.1 The black Aspergilli divided into clades [17][22]. Species in bold have been investigated in this thesis.

Clade	Species
A. niger	*A. neoniger, A. costaricaencis, A. vadensis, A. eucalypticola, A. piperis, A. acidus, A. coreannus, A. tubingensis, A. awamori,* ***A. niger****, A. lacticoffeatus, A. foetidus, A. brasiliensis*
A. carbonarius	*A. ibericus,* ***A. sclerotiicarbonarius****, A. carbonarius,* ***A. sclerotioniger***
A. heteromorphus	*A. ellipticus, A. heteromorphus*
A. homomorphus	*A. saccharolyticus,* ***A. homomorphus***
A. aculeatus	*A. fijiensis,* ***A. indologenus****,* ***A. flavus****, A. violaceofuscus,* ***A. aculeatus****, A. aculeatinus, A. uvarum, A. japonicus*

Another black *Aspergillus* is *A. aculeatus*; which is also used by the industry for enzyme production. *A. aculeatus* has been used to produce enzymes such as cellulases [23], xylanases [24][25] and proteases [26], which are used commercially in food and feed industries. *A. aculeatus* is among the most common fungi in postharvest decay of fruit, beans and nuts [11][12]. Only a few SMs have been reported for this fungus, however, genome sequencing has revealed its large genetic potential for production of SMs (section 3.1.1).

In Table 1.2 an overview of metabolites for some of the black Aspergilli investigated in this study is given.

Table 1.2 Metabolites reported from selected black Aspergilli prior to and after this study.

Species	Metabolites	This study
A. aculeatus	Aculeacins A–G [27][28] CJ-15,183 [29] Secalonic acids D and F [30] Okaramines H and I [31] Asperaculin A [32] Aspergillusol A [33] Aculeatusquinones A–D [34]	Okaramine J and S (Paper 1) Aculene A-D (Paper 1) Acu-calbistrins A-B (Paper 1) Acu-dioxomorpholine (Paper 1) Epi-10,23-dihydro-24,25-dehydroaflavinine (Paper 1) Calbistrin A and C (Paper 1) Aculins A and B (Paper 11) Aculinic acid (Paper 11) RKB-3384B (Paper 11)
A. niger	Yanuthone A-E [35] 1-hydroxy yanuthone A [35] 1-hydroxyyanuthone C [35] 22-deacetylyanuthone A [35] Azanigerones A–F [36] Fumonisins [18][19][20] Ochratoxin A [21] Aurasperone B [37] And several more, see [38]	Yanuthone F-J (Paper 9) Yanuthone X_1 (Paper 9) Yanuthone K-L (Paper 10) Yanuthone X_2 (Paper 10 Anominine (formerly known as nominine [39]) (Paper 4) 10,23-dihydro-24,25-dehydroaflavinine (Paper 4) Aflavinine analogs (Paper 4)
A. indologenus	Okaramines A,B and H [22]	Aspiperidine oxide (Paper 2) JBIR-74 (Paper 2) Fellutanine C (Paper 2) Aspergillicin A (Paper 2)
A. homomorphus	Dehydrocarolic acid [40] Secalonic acid D and F [40][41]	Homomorphins A-F (Paper 3) Q-20547-E (Paper 3) L-valyl-L-tryptophan anhydride (Paper 3) α-pyrone A and B (Paper 3)
A. sclerotioniger	Ochratoxins A and B [38][41]	Sclerotionigrin A (Paper 5) Sclerotionigrin B (Paper 5) Proxiphomin (Paper 5)
A. sclerotieecarbonarius	Naphtho-γ-pyrones [17] Pyranonigrin A [17]	Sclerolizine (Paper 6) Emindole SC (Paper 6) Carbonarin I (Paper 6) Carbonarin J (Paper 6)

1.1.2 Secondary metabolites from filamentous fungi

Metabolites from filamentous fungi are divided into two types: Primary metabolites and secondary metabolites. In general primary metabolites are essential for growth and reproduction, whereas secondary metabolites, are not. Secondary metabolites are, however, produced by the organisms for specific purposes and often play essential roles in chemical communication, signaling or as defense compounds (antibiotics, insecticides, antifungals). Secondary metabolites are of great interest as pharmaceuticals, as they are often pharmacological active. The borders between primary and secondary metabolism are often hard to define. One reason is that most secondary metabolites are built up from primary metabolite precursors. The correlation between primary and secondary metabolites is presented in Figure 1.2.

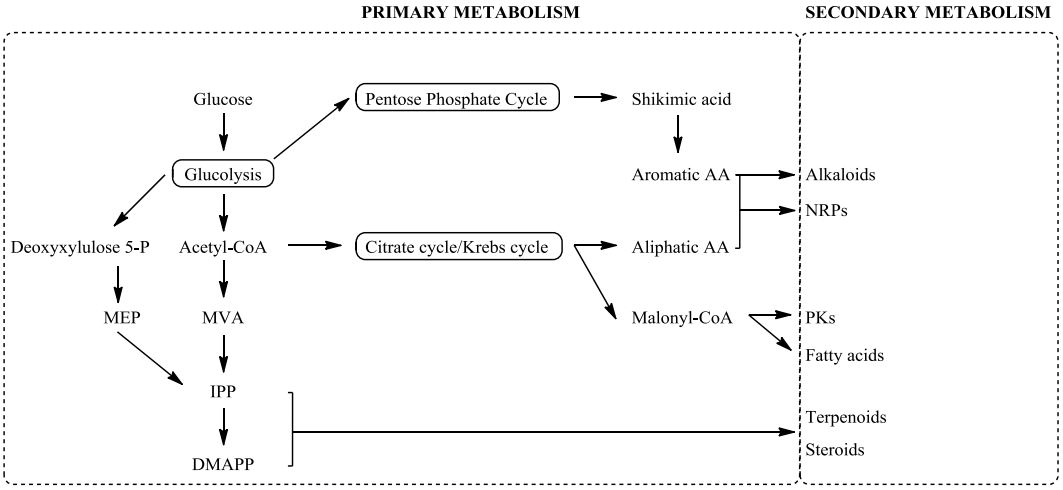

Figure 1.2 Simplified correlations between primary and secondary metabolism. MEP = methylerythritol phosphate. MVA = mevalonic acid. IPP = isopentenyl diphosphate. DMAPP = dimethylallyl diphosphate. CoA = coenzyme A. AA = amino acid. NRPs = nonribosomal peptides. PKs = polyketides.

Filamentous fungi often live in competitive environments, and it is believed that their SM repertoire reflects selection pressures from other organisms and environment. It is therefore likely to find interesting biological activities amongst the fungal SMs, such as antifungal, antibacterial, insecticides and so forth. Furthermore the fungal SMs can be utilized as pigments and colorants [42], which is another reason for investigation these compounds.

Main classes of secondary metabolites with interesting biological activities are polyketides (PKs), nonribosomal peptides (NRPs), terpenoids or hybrids thereof. Figure 1.3 displays examples of all three classes as well as combinations of the three types (hybrids). The SMs shown are all compounds discovered or investigated in this work, and will be further described in chapter 3 and 4.

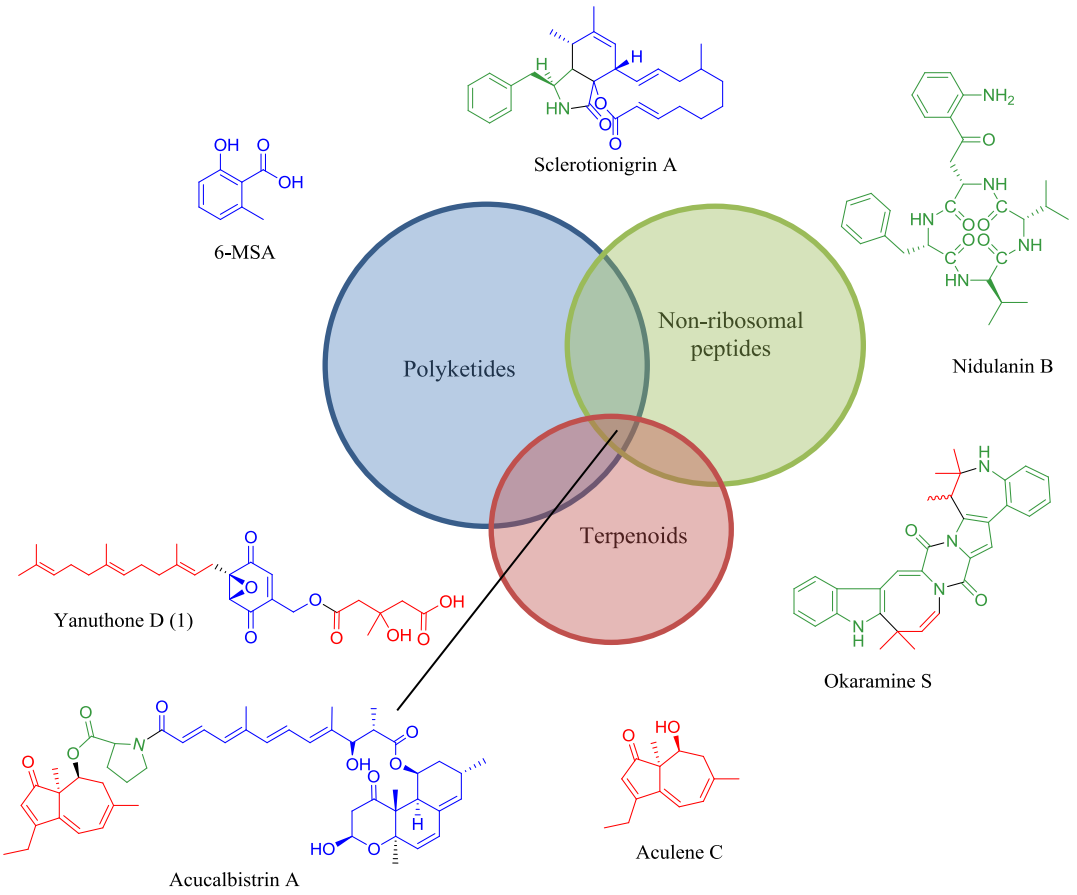

Figure 1.3 Illustration of three major classes of fungal SMs: PKs, NRPs and terpenoids; compound types found during this study. Compounds may also be hybrids. Here exemplified by SMs discovered or investigated in this thesis: The PK 6-MSA (section 4.3 and 4.4), NRP nidulanin A (section 4.1), terpenoid aculene C (section 3.1.1), PK-NRP sclerotionigrin A (section 3.2.2), NRP-terpenoid okaramine S (section 3.1.1), PK-terpenoid (meroterpenoid) yanuthone D (section 4.3) as well as acucalbistrin A, a putative hybrid of all three classes (section 3.1.1).

1.2 Biosynthesis of secondary metabolites

The SMs produced by filamentous fungi are, based on their mode of biosynthesis, divided into different groups. The general biosynthetic pathway for four main groups, polyketides (PKs), non-ribosomal peptides (NRPs)/alkaloids, terpenoids, and the shikimate derived SMs, are depicted in Figure 1.4.

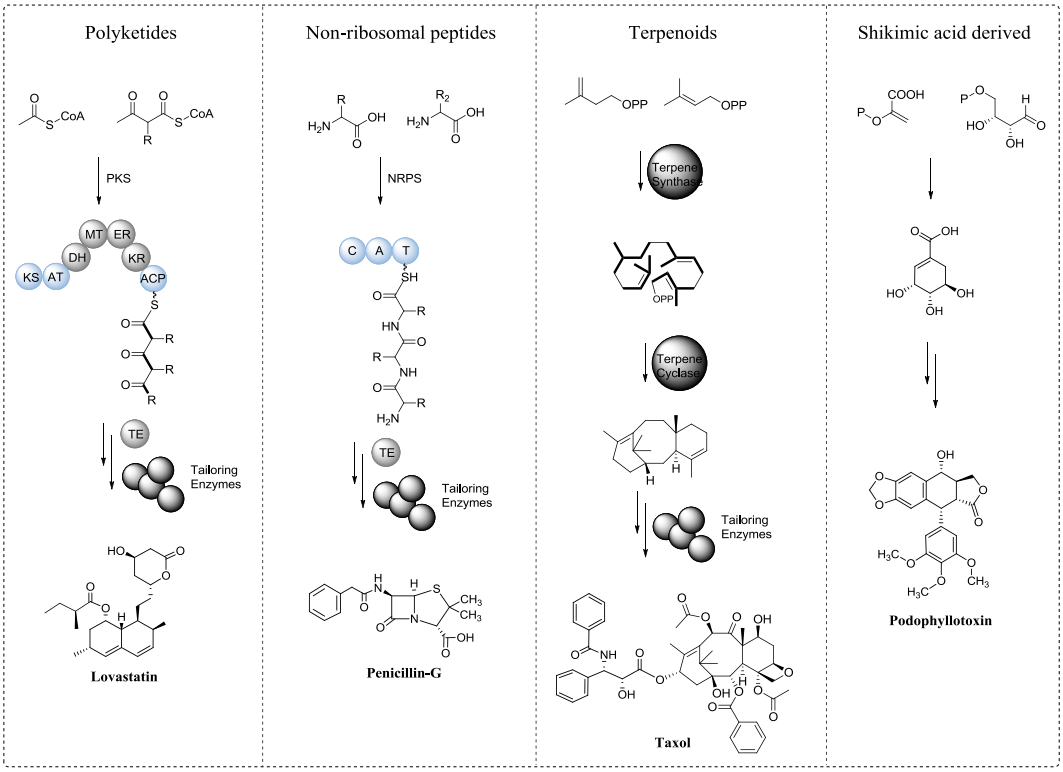

Figure 1.4 General biosynthetic pathways for polyketides, non-ribosomal peptides, terpenoids and shikimic acid derived compounds. Exemplified by the NPs lovastatin (cholesterol-lowering drug), penicillin-G (antibiotic), taxol (anti-cancer) and podophyllotoxin (anti-cancer) respectively.

The biosynthesis of the four types is in brief as follows: PKs are synthesized by large multifunctional enzymes with individual functional domains, polyketide synthases (PKSs), by assembly of ketide units. NRPs are peptides not synthesized by a ribosome, but by NRP synthetases (NRPSs) which are multimodular enzymes, which select specific amino acids and forms peptide bonds. Terpenoids are hydrocarbons which are built up by C_5 isoprene units. Shikimic acid is a C_7 unit, which can be incorporated into other SMs. The focus of this thesis, and therefore the SMs that will be discussed in this chapter, are PKs, NRPs and terpenoids. The following sections will give a description of the three types of SMs and how they are biosynthesized in the organism (section 1.2.1, 1.2.2, 1.2.3).

1.2.1 Polyketides

PKs constitute one of the major classes of SMs and are known from fungi, but also bacteria, plants and animals [43][44]. It is an enormously diverse group spanning compounds with a wide range of functional and structural diversity. The many important biological activities covers antibacterial, anticancer, antifungal, antiparasitic, cholesterol lowering, and immunosuppressive properties. Examples of important fungal PKs are lovastatin (cholesterol lowering) [5], mycophenolic acid (antimicrobial and immunosuppressive) [45] and griseofulvin (antibiotic) [46].

The structures of PKs vary greatly and they are solely grouped based on the way they are biosynthesized. This is by enzymes called polyketide synthases (PKSs) [44], which resemble eukaryotic fatty-acid synthases (FASs) in domain architecture. The PKSs can be classified into three different types based on their different architectural organization; type I, II and III, see Table 1.3.

Table 1.3 Division of PKSs. Adapted from [44]**.**

PKS type	Description	Mechanism	Organisms
I (modular)	Large multifunctional proteins with individual functional domains. Multiple modules.	Linear assembly line. Active site only used once.	Bacteria
I (Iterative) Subtypes: NR-, PR- and HR-PKS	Large multifunctional proteins with individual functional domains. One module.	Iterative, active sites may be reused.	Fungi Some bacteria
II	Complex of individual monofunctional proteins. Single active site for each.	Iterative, active sites may be reused.	Exclusively bacteria
III	Single protein with multiple modules.	Iterative, active sites may be reused.	Mainly plants Some bacteria and fungi

PKs are assembled by repetitive decarboxylative Claisen condensations usually of an activated acyl starter unit with malonyl-CoA derived extender units. Most fungal PKs are synthesized by iterative type I PKSs. These are large multifunctional proteins containing a single module, which is used iteratively. The PKS module consists of different domains, where each domain has a specific catalytically function, see Table 1.4 and Figure 1.5 A.

Table 1.4 Overview of catalytic domains found in PKSs.

Domain	Function
Necessary domains	
Acyl carrier protein (ACP)	Holds the growing polyketide chain
β-ketoacyl synthase (KS)	Catalyzes the Claisen condensation
(malonyl)acyl transferase (MAT)/(AT)	Transfers acyl/malonyl units
Reductive domains	
Ketoreductase (KR)	Reduction of β-ketone to hydroxyl
Dehydratase (DH)	Reduction of hydroxyl yielding an enoyl group
Enoyl reductase (ER)	Reduction of enoyl group to saturated alkyl
Other	
Product template (PT)	Control folding pattern of non-reduced PKs
Thioesterase (TE)	Hydrolysis of the thiolester, releases PK
Methyl transferase (MT)	Methylation using S-adenosylmethionine (SAM)
Cyclisation (CYC)	Cyclisation of reduced polyketide
Starter unit AT transacylase (SAT)	Loading of the starter unit

Three domains are essential for biosynthesis of PKs: the acyl carrier protein (ACP), the β-ketoacyl synthase (KS), and the acyltransferase (AT). The ACP domain is responsible for holding the growing PK chain, hereby allowing loading of the extender units. The KS domain catalyzes C-C bond formation through decarboxylative Claisen condensations (Figure 1.5 B). The MAT or AT domain recognizes the specific extender unit that is going to be incorporated into the growing PK chain.

PKSs can furthermore have reductive domains also known as β-keto processing domains, which can reduce the β-keto group, see Table 1.4 and Figure 1.5 C. The three domains are ketoreductase (KR), dehydratase (DH) and enoyl reductase (ER), that reduces the keto group to a hydroxyl group, dehydrates the hydroxyl group to an enoyl group, and reduces the enoyl group to the saturated alkyl, respectively. PKSs are divided into three groups accordingly to the presence or absence of β-keto processing domains: nonreducing (NR), partly reducing (PR), and highly reducing (HR) PKSs [47]. The NR PKSs do not contain any of the reducing domains, whereas the reducing PKSs contain either KR or KR/DH (partly reducing), or all three domains (highly reducing).

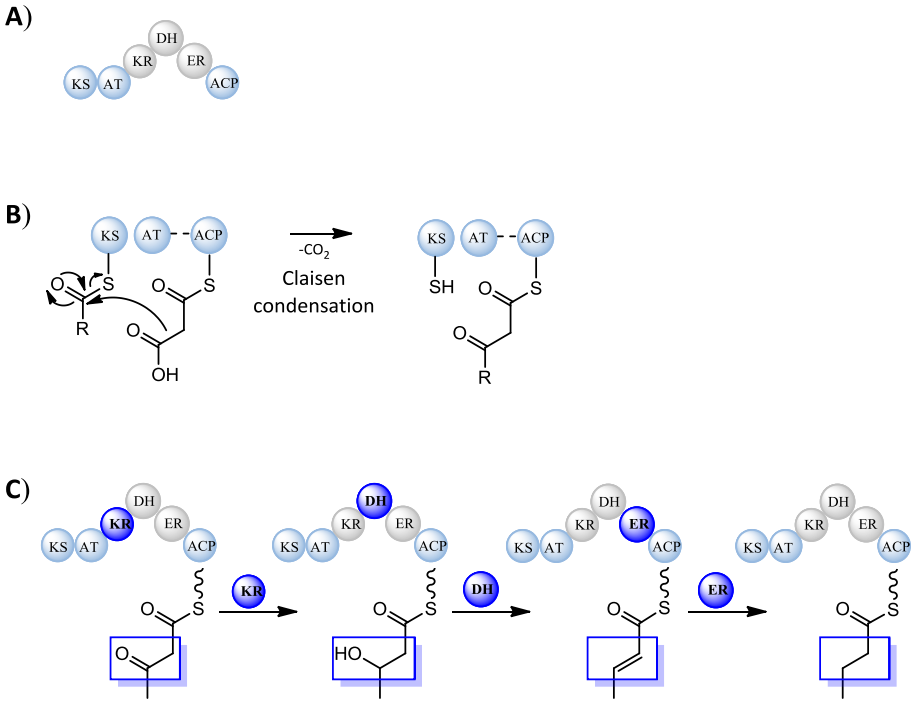

Figure 1.5 A) Example of the domain organization of a HR-PKS. The blue domains are necessary for functionality of the PKS. B) Chain extension of the PK chain through Claisen condensations of the extender unit (here malonyl-CoA) and starter unit (here acetyl-CoA). C) β-keto processing. The KR reduces the keto group to a hydroxyl group, the DH dehydrates the hydroxyl group to an enoyl group, and the ER reduces the enoyl group to the saturated alkyl. KS = β-ketoacyl synthase, AT = acyl transferase, ACP = acyl carrier protein, KR = ketoreductase, DH = dehydratase, ER = enoyl reductase.

Even with the presence of the reductive domains, the reductive steps can be partly of fully omitted in each round of elongation, see Figure 1.6. This will give rise to more diverse and complex functionalities in the final PK. The PK backbone can be further modified e.g. be methylation by a methyltransferase domain (MT), which catalyzes methylation of the growing PK chain using S-adenosylmethionine (SAM) as a carbon-donor [48]. Elongation and reduction cycles will be repeated until a defined chain length is obtained. The thioester bound substrates are then released from the enzyme complex, catalyzed by a thioesterase (TE), cyclase (CYC) or other enzymes [49][50].

After release the PK product often undergoes additional modifications by tailoring enzymes. This post-PKS processing is another source of diversity in PKs. The modifications can range from small changes such as methylations, reductions and oxidations, to larger modifications including ring formation or linking to other metabolites such as sugar moieties or terpenoids.

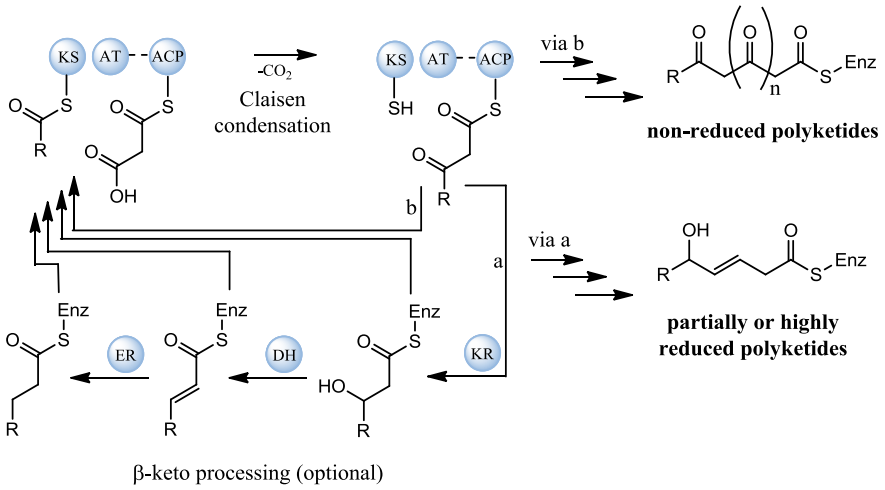

Figure 1.6 Mechanisms involved in PK biosynthesis. In each chain elongation the PK chain is extended with one ketide unit as a result of the Claisen condensation. The reductive steps can be partly of fully omitted in each round of elongation. Enz = Enzyme, KS = Ketoacylsynthase, AT = Acyl Transferase, ACP = Acyl carrier protein, ER = Enoyl reductase, DH = Dehydratase, KR = Ketoreductase. Adapted from [44].

The iterative nature of the PKSs makes it difficult to predict the structure of the final PK product [51] both with respect to the degree of saturation, methylation pattern and size. It has been demonstrated, that there is a correlation between the volume of the active site pocket of the KS domain and the size of the final PK product [52], however, the number of the iterations in the PKS still cannot be predicted.

1.2.2 Non-ribosomal peptides

In contrast to the ribosomal biosynthesis of peptides and proteins, many smaller natural peptides are non-ribosomally synthesized [53]. The biosynthesis happens in a sequence of enzyme-controlled processes, where each amino acid is added due to the specificity of the enzyme involved. The non-ribosomal peptides are assembled on multimodular enzymes called non-ribosomal peptide synthetases (NRPSs) [53][54].

The NRPSs have a modular arrangement, where each module is responsible for incorporation and modification of one defined amino acid. The number of modules corresponds to the number of amino acids in the final NRP product and their order follows the order of the adenylation domains. Each module consists of several catalytic domains, see Table 1.5. Three domains are necessary for biosynthesis, which is a condensation (C) domain, an adenylation (A) domain and a thiolation (T) domain (also referred to as peptidyl carrier protein (PCP) domain) [54]. The A domain is catalyzing selection for each amino acid, which is adenylated and loaded onto the T domain, where the C domain catalyzes formation of the peptide bond between two amino acids, see Figure 1.7.

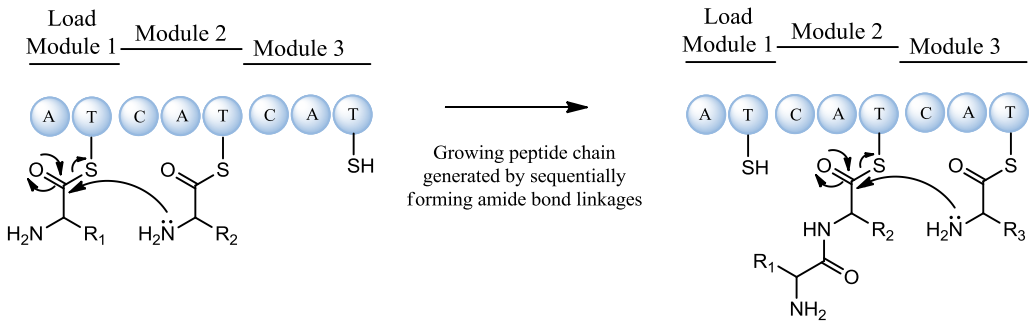

Figure 1.7 Peptide bond formation catalyzed by the C domain is resulting in a growing peptide chain. Adapted from [54].

The residues are lined up to allow a sequential series of peptide bond formations until the peptide are released from the enzyme. The release can result in either a linear or a cyclic peptide depending on whether it is released by hydrolysis or lactamization. Release to give a linear peptide is often achieved by a thioesterase (TE) domain in the final module whereas cyclization occurs by terminal C-like domains [49][55][56][57]. Structural variance in NRPs occurs by tailoring domains, a brief description of some are given in Table 1.5.

Table 1.5 Overview of domains in NRPSs.

Domain	Description
Necessary domains	
Adenylation (A)	Selection and activation of specific amino acids
Condensation (C)	Catalyzes formation of peptide bond
Thiolation (T)	Holds the growing chain. Also referred to as peptidyl carrier protein (PCP) domain
Tailoring domains	
Epimerization (E)	Located downstream of T and catalyzes the generation of D-configured amino acids from the corresponding L-isomers
N-methyltransferase (Mt)	Responsible for the *N*-methylation of the peptide products. Usually integrated at the C-terminal region of the A-domains
C-methyltransferase (C-Mt)	Responsible for the C-methylation of C_α atoms of cysteine residues. Located downstream of T domains
Cyclization (Cy)	In addition to peptide bond formation it catalyzes a heterocyclic ring formation to the corresponding thiazoline or oxazoline rings
Oxidation (Ox)	Catalyze the formation of thiazoles and oxazoles. Integrated within the C-terminal region of A-domains
Reduction (R)	Catalyze the NADPH-dependent formation of thiazolidine andoxazolidine rings

The structures of NRPs vary as a result of the tailoring domains, but also from incorporation of AAs (not necessarily proteogenic AAs) as well as variations in release from the enzymes.

Prediction of the products of NRPSs is more straightforward than that of fungal PKSs, because of their modular nature, as also demonstrated in this thesis. For the peptide nidulanin A, discovered in *A. nidulans*, bioinformatic analysis could, based on the domain structure, predict a tetracyclic structure including suggestions for incorporated AAs, which was verified by isolation and structure elucidation of the compound (see section 4.2 and Paper 8).

1.2.3 Terpenoids

The terpenoids or isoprenoids, is a group of NPs build by activated C_5 units [58][59]. What is now known as "the isoprene rule" was observed as far back as 1887, where Wallack noted that many NPs apparently were comprised of isoprene units (C_5H_8) [60], see Figure 1.8. The rule states that terpenoids are formed by linking isoprene units in a head-to-tail fashion. The typical terpenoid structure therefore contain a carbon skeleton built up of isoprene units (C_5H_8) represented by $(C_5)_n$, see Table 1.6.

Most terpenoids are further modified by cyclisation reactions, and can also be oxidized, reduced or fused to other metabolites. However, in the final product it is most often possible to identify the original arrangement of the head-to-tail isoprene units.

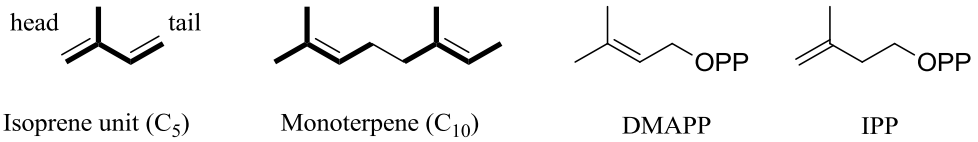

Figure 1.8 Structure of the isoprene unit, showing the head and tail, and a monoterpene consisting of two individual isoprene units marked in bold. DMAPP = dimethylallyl diphosphate. IPP = isopentenyl diphosphate.

The isoprene units may be derived from two different pathways: either from intermediates of mevalonic acid or methylerythritol phosphate [61]. In both pathways the activated C_5 isoprene units dimethylallyl diphosphate (DMAPP) and isopentenyl diphosphate (IPP) are utilized (Figure 1.8), which are condensed in a head to tail fashion.

Table 1.6 Nomenclature of terpenoids [61].

Isoprenoid units	Name
1	Hemiterpenes (C_5)
2	Monoterpenes (C_{10})
3	Sesquiterpenes (C_{15})
4	Diterpenes (C_{20})
5	Sesterterpenes (C_{25})
6	Triterpenes (C_{30})
8	Tetraterpenes (C_{40})
≥ 9	Polyterpenes ($\geq C_{45}$)

Terpenoid elements are often incorporated into other types of NPs. This is true for PKs (section 1.2.1) and NRPs (section 1.2.2). In fungi this process is catalyzed by a class of enzymes called prenyltransferases that transfer allylic prenyl groups to acceptor molecules, as seen in e.g. nidulanin A and meroterpenoid yanuthone D in this thesis (section 4.2, Paper 8 and section 4.3, Paper 9, respectively).

1.3 Genetics of secondary metabolites biosynthesis

The work of this thesis has been carried out in what is referred to as the post-genomic era. Before the genomic era, the study of biosynthesis of SMs were time consuming, difficult and limited to random mutations or purification of pathway enzymes followed by reconstruction of the biosynthetic steps in the lab [62]. The modern high-throughput DNA sequencing has exposed a high amount of biosynthetic gene clusters and revealed an enormous biosynthetic potential of previously undiscovered SMs in filamentous fungi, and opened for more genome driven research [63][64][65]. This section covers the genetics of SMs biosynthesis and different approaches to express/activate silent genes.

1.3.1 Secondary metabolite gene clusters

In contrast to primary metabolites, whose biosynthetic genes are distributed across the genome, the genes involved in biosynthesis of SMs in filamentous fungi are often clustered [66]. The compilation of genes, that together is responsible for production of a final SM, is referred to as a gene cluster. A typical gene cluster will usually consist of a synthase/synthetase gene such as a PKS or NRPS (see section 1.2.1 and 1.2.2), genes encoding enzymes for post modifications often referred to as tailoring enzymes, genes to regulate the expression of the gene cluster, and potentially genes necessary for exporting the final SM out of the cell.

From the Aspergilli sequenced so far, those with a genome size of 28-40 Mb, typically contain around 50 gene clusters [67], where one cluster can span more than 10,000 bases. There are, however, exceptions from the physically clustered genes, such as the biosynthetic pathway for meroterpenoids austinol and dehydroaustinol in *A. nidulans* which requires two separate gene clusters located on separate chromosomes [68] or the biosynthetic pathway of nidulanin A, where the NRPS and a prenyltransferase are physically separated in the genome (section 4.2 and Paper 8).

As briefly described in section 1.1.2, SMs are not necessary for cell growth, but exhibit other specific functions such as defense or signaling. Therefore a strict regulation of production is necessary to ensure that the SMs are only being produced when needed. This regulation can occur by regulatory genes, embedded in the SMs gene clusters, encoding transcription factors (TFs), that transcriptionally control the structural genes involved in biosynthesis. From fungi, a total of twelve TF superfamilies have been identified, and of these, three are exclusively present in fungi [69]. The TF can work in one of two ways: either by facilitating transcription (activators) or by blocking

transcription (repressors) [70]. In either way, experiments with expression of the TF may provide useful information about the pathway.

1.3.2 Activation of silent genes

Most of the gene clusters in filamentous fungi are silenced or expressed in minute amounts under standard laboratory conditions [71]. To this end, genomic sequencing has revealed, that there are many more genes for biosynthesis of SMs than metabolites already identified [19][72][73]. As a direct consequence the number of gene clusters by far exceeds the number of known metabolites, which can be linked to these clusters. Gene clusters encoding biosynthetic systems not associated with production of a known SM are often referred to as "cryptic." There is a further difference between uncharacterized genes and genes that are not expressed. Orphan biosynthetic pathways are defined gene clusters for which the corresponding metabolite is unknown, while silent genes refers to genes which are not expressed under given growth conditions [74].

The growing evidence, that fungal genomes contain a substantial number of SM genes that remains silent under standard laboratories conditions is especially true for PKS and NRPS genes [75][76]. Consequently there are therefore a large number of undiscovered NPs, representing a big pool of novel and possibly bioactive compounds just awaiting discovery.

Some of the strategies used to trigger activation of silent genes are:

- OSMAC [77][78]
- Co-cultivation [79]
- Epigenetic modifiers [80][81]
- Transcription factors [82]
- Heterologous expression [83]

The classical way of triggering silent pathways in filamentous fungi is by the "one-strain – many compounds" (OSMAC) approach [77][78]. This is achieved by altering the cultivating conditions such as temperature, pH, cultivation time, light, aeration and/or media composition, since a change in these conditions can influence the production of SMs. One example of use of the OSMAC approach is by Nielsen and co-workers, who investigated the metabolic profile of *A. nidulans* on seven complex media resulting in a large difference in production of metabolites [84]. Although powerful, the OSMAC approach can be exhaustive, and it can be tedious to find the specific growth conditions

under a variety of parameters and organisms, and the exact mechanisms and understanding of the linkage between culturing conditions and metabolic profile are not fully understood and moreover difficult to predict.

In this study it has been demonstrated that silent gene clusters can be activated by induction of sclerotia formation. It was here demonstrated that under sclerotium producing conditions, the metabolic profile was highly altered in a number of black Aspergilli. This is further described in section 3.2, Paper 4 and Paper 6.

Another way to activate silent gene clusters is by genome mining. The more classical way to use genome mining for investigation of SMs is to delete or inactivate a biosynthetic gene followed by comparative metabolic profile analysis by HPLC-UV or –MS (see section 2.1.2). This is, however, restricted to the smaller number of SMs that are produced under laboratories conditions. Instead, two other ways of investigating the silent clusters are often utilized: The use of TFs and by heterologous expression. Employing TFs, these are (if activators) typically overexpressed in the native organism to ensure activation of the cluster. Using heterologous expression, one synthase/synthetase gene or an entire gene cluster is expressed heterologous in a host organism.

For the filamentous fungus *A. niger* investigated in this study, sequencing and gene annotation suggests that there are 944 regulatory genes [19]. In the biosynthetic gene cluster for yanuthone D, one TF was embedded in the cluster, which was shown to work as a repressor, giving insights into the span of the cluster. For this, see section 4.3 and Paper 9. In *A. aculeatus* the overexpression of a TF activated a biosynthetic pathway leading to the discovery of diastereomers of RKB-3384B, see section 4.4 and Paper 11. This study exemplifies the use of TFs for discovery of novel SMs. Heterologous expression was also used in both of these projects for investigation of the pathways. Furthermore a way to quickly expressing genes or whole gene clusters from filamentous fungi has been investigated in this thesis (section 4.5).

The use of genome mining for investigation of gene clusters [85] will be further discussed in the following section.

1.3.3 Genome mining

Gene prediction

To elucidate the biosynthetic pathway of fungal SMs in a genome sequenced organism, the first step is to predict the genes belonging to the gene cluster. Through computational analysis it is possible to identify putative SM genes within genomes. This is achieved by use of one or several gene prediction algorithms creating automated annotations based on domain predictions and homology search, followed by manual inspection. These predictions grow more powerful, but as it is merely predictions, these should always be followed up by experiments. In Table 1.7 the genome sequenced strains used in this study are displayed.

Table 1.7. Overview of the fully genome sequenced strains used in this studies including the predicted number of synthase/synthetase genes and examples of metabolites that have been linked to genes.

Species	Strain	Sequencing	Predictions	Linking of metabolites to genes	
A. niger	ATCC 1015	DOE Joint Genome Institute [73]	32 PKSs 15 NRPSs 9 hybrids [81]	**PKs** Azaphilones [36] TAN-1612 [86] Dihydroxynaphthalene (DHN) Melanin [87] Naphtho-γ-pyrone [87] Fumonisin [18][19][20]	**PK-NRPs** Pyranonigrin E [88] Ochratoxin A [19] **Meroterpenoids** Yanuthone D [89] (see section 4.3)
A. nidulans	FGSC A4	Broad institute[75]	32 PKSs 27 NRPSs 1 hybrid [55][84]	**PKs** Sterigmatocystin [90] Naphthopyrone [91] Asperthecin [92] Monodictyphenone/ emodin [93][94] austinol/dehydroaustinol[84], arugosins [84], Orsellinic acid/ Lecanoric acid/F9775A/F9775B [93] [79][95] Asperfuranone [96] Alternariol/cichorine [97]	**PK-NRPs** Aspyridone A-B [82] Emericellamide [98] **Meroterpenoids** Aspernidine A-B [99] **NRPs** Nidulanin A [100] (See section 4.2)
A. aculeatus	ATCC 16872	DOE Joint Genome Institute [101]	24 PKSs 19 NRPSs 9 terpenoid synthases 5 hybrids [102]	**PK-NRP-terpenoid** Aculins A-B, epi-aculin A and PK aculinic acid (Section 4.4, Paper 11)	

Many strategies exist for the investigation of biosynthetic pathways [74][103][104]. In the following only the approaches used in this study will be described: gene inactivation and heterologous expressions.

Genetic manipulations in fungal native host

A widely used technique for discovery of novel metabolites is to delete or inactivate a biosynthetic gene, followed by comparative metabolic profile analysis by HPLC-UV or -MS. This procedure can identify the compounds affected by the gene deletion and thereby link genes to compounds.

To execute this experiment a knockout cassette containing a resistance marker or prototrophic gene is specifically integrated into the specified locus. The deletions of genes can, besides abolishment of production of the final SM also, lead to accumulation of intermediates, which can provide further insights into the biosynthetic pathway. Thereby a series of individual deletions of all genes in a cluster can lead to understanding of every step in a biosynthetic pathway from production of the first precursor through all modifications and intermediates into the final SM.

There are limitations to these experiments, as they will depend on the ease of genetic manipulations of the fungal host. To improve efficiency of homologous recombination (HR) to ensure specific integration, strains can be engineered to favor HR over non-homologues end-joining (NHEJ). In *A. nidulans* the deletion of the Ku70-Ku80 heterodimer resulted in > 90 % gene targeting efficiencies [9][105], while the elimination of the homologue *kusA* in *A. niger* enhanced the efficiency in this species to > 80 % [106]. The efficiency can further be enhanced in combination with bipartite transformation substrates [8].

In this study the biosynthetic pathway of yanuthone D was investigated in the native host by gene deletions of all genes in the cluster. This is described in section 4.3 and Paper 9.

Heterologous expression of individual genes or clusters in model organisms

There can be many reasons why manipulations in the native host, is not the most optimal approach. The organism of interest can be difficult or hazardous to work with, expensive or impossible to cultivate in the laboratory, or insusceptible to genetic manipulations. In these cases it can be advantageous to move the gene or gene cluster of interest to a host organism. Some of the advantages of using a host organism include that it will be amenable to genetic modifications, the optimal conditions for growth will already be known and its genome sequence and metabolite profile are already known [107]. Furthermore, competing gene clusters can be deleted. Bacteria and yeast have been used as host organisms, but for production of fungal SMs, filamentous fungi are preferred as hosts. Both since they themselves are producers of SMs, why they have the required accessory enzymes to facilitate the products, and secondly since they are capable of

splicing introns, which is not the case for bacteria and yeast. Among filamentous fungi *A. nidulans* has been well-studied and is often used as host organism.

Heterologous expression can be achieved by different methods. One way is by heterologous integration in a well-defined locus in the host organism, for example *A. nidulans*. For heterologous gene expression a genomic insertion site is needed. The foreign gene should be expressed from a specific well-characterized locus and preferably the new gene should be inserted with no interference with the strain and allowing high and stable expression. Investigations of such a site in *A. nidulans* have led to the insertion site IS1 [83], but several other sites have also been used [108][109]. An example of the strength of heterologous expression by integration is the reconstitution of the entire geodin cluster from *A. terreus* [109]. Heterologous expression was also used in this PhD study, where the cytochalasin gene cluster from *A. clavatus* was reconstituted in *A. nidulans*, (section 4.5, Paper 12), as well as for investigation of 6-MSA PKS gene from both *A. niger* (section 4.3, Paper 9) and *A. aculeatus* (section 4.4, Paper 11).

Heterologous expression can also be achieved by use of non-integrative vectors; autonomously replicating plasmids. In this study AMA1 (Autonomous Maintenance in *Aspergillus*) plasmids [110] have been used. These are designed with the AMA1 sequence with the purpose of doing extrachromosomal replication [102][110]. The autonomously replicating plasmids have the advantage over the integrative systems, in that transformation rates are high [111]. Drawbacks are that the plasmids are unstable and easily lost if selection is not maintained. The AMA1 based plasmids are hence good for rapid screenings. The AMA1 based self-replicating plasmids are not limited to *A. nidulans* but have become available for use in a number *Aspergillus* species such as *A. niger* [112][113], *A. fumigatus* [114], *A. oryzae* [110] and in this study also been used in *A. aculeatus* for the first time (section 4.4 and Paper 11).

1.4 Metabolite profile analysis

Metabolite profile analysis refers to the qualitative analysis or identification of metabolites produced of an organism (the metabolome). In this thesis this is achieved by use of UHPLC-DAD-HRMS, utilizing the exact mass of the metabolite and hence the molecular formula as well as the UV spectrum, which serves as a fingerprint of the specific SM. This is exemplified under experimental work in section 2.1.2. In this section a description of the MS-based dereplication is described (section 1.4.1) as well as explorative solid phase extractions (E-SPE), (section 1.4.2), which can serve as an aid in dereplication.

1.4.1 MS-based dereplication

Filamentous fungi produce a wide variety of SMs, wherefore a fungal extract will be a complex mixture. A major goal in the discovery of novel NPs, is early in the process, to implement a strategy for detection of already known compounds, so time and resources are not wasted in purification hereof. The process of tentatively identifying the already known compounds is termed dereplication [115]. Different techniques can be used, for instance LC-NMR [116], but the core technology used for dereplication is LC-UV-MS in combination with subsequent database search [115].

The process can roughly be divided into three steps:

1. Identifying the pseudo molecular ion (MS data)
2. Search based on the elemental composition in database of choice (Database)
3. Evaluation of hits and final determination (UV data, RT, E-SPE)

The dereplication approach is based on the MS data, first finding the monoisotopic mass and hence the elemental composition of the compound of interest. Caution must be taking in this part to identify the correct pseudo molecular ion. Some compounds can have strong sodiated or ammoniated adducts, others can predominantly form di- and trimeric ions, yet others will fragment easily or will simply ionize poorly. In all cases identification is prone to errors, since the mass spectrum is easily misinterpreted. The pseudo molecular ion should be assigned with care; the more adducts to confirm the mass, the better, and confirmation in positive as well as negative mode is preferable. Once the pseudo molecular ion is determined the monoisotopic mass and isotopic pattern should be used to generate the elemental composition [115][117], which is then used for a query in an appropriate database.

SciFinder and MarinLit are examples of databases used for NP dereplication; in this work the commercial database Antibase 2012 (40065 compounds) [118] has been used as well as an in-house library of microbial metabolites (7237 compounds) [115]. A high mass accuracy will ensure the database search to result in fewest possible candidates. The number of hits in the databases can, however, vary, and elimination of candidates may be necessary. This can be achieved by UV-data and the by using the RT. Many NPs have unique UV-spectra wherefore comparison of measured data with spectra from databases or the literature, can result in elimination of candidates [115][119]. On the same note, the RT may reduce the number of candidates. This can be by simple considerations of the polarity of the compound in question, or preferably if the RT is known for a given compound. The latter requires detection on the same instruments, since RT vary from different setups; a standard is optimal for reliable identification.

As an aid in dereplication E-SPE can be used [120]. In the E-SPE approach, described in section 1.4.2, important information about the physical chemical properties of the compound such as acid and basic properties are attained; which can help to accelerate dereplication by reducing the number of potential candidates.

Recent advances within dereplication speeds up the process by "aggressive dereplication" [121], which has also been used in this study. In this approach, TargetAnalysis (Bruker Daltonics), is used to screen extracts for several thousands of compounds, by use of the internal compound database, based on an in-house-built Excel application. This is achieved by comparison with the accurate mass, as well as isotope pattern and RT consistency. EICs are automatically generated for all compounds in the database and overlaid with the BPC. Compounds available as reference standards, previously identified compounds, known contaminants (from solvents, media, filters etc.) are labeled and potentially novel compounds are easily visualized. Manual inspection is still necessary as adduct formation and simple fragmentations may result in false-negative results. A way of optimizing the aggressive dereplication process, is by use of MS-MS libraries, as these will eliminate false-negative results [122]. This is a robust and reliable way of tentatively identifying known compounds, but is highly depended on MS-MS libraries of standards of NPs.

1.4.2 Explorative solid phase extractions

Explorative solid phase extractions (E-SPE) is an approach of targeted exploration of chemical functionalities [120]. It uses small pre-packed columns with orthogonal stationary phases for a quick screening. The E-SPE strategy used in this project was developed by Månsson and co-workers [120] and uses ion-exchangers, size exclusion and normal phase columns. Three ion exchangers are tested: One strong anion-exchanger (SAX), a strong cation-exchanger (SCX) and a mixed mode anion-exchanger (MAX). The size exclusion chromatography is performed using self-packed columns of LH-20, and finally, two normal phase columns are used, a diol and one amino column. As illustrated in Figure 1.9, a test of all six columns, results in 27 fractions, which are subsequently analyzed by UHPLC-DAD-HRMS. Analysis of the fractions will reveal if a compound of interest carry any basic or acidic functionalities, a valuable information that can be exploited in the dereplication process. Furthermore, the use of orthogonal stationary phases enable separation of compounds with different functionalities, even though they would co-elute on traditionally RP chromatography, which can be used to easily establish a purification strategy.

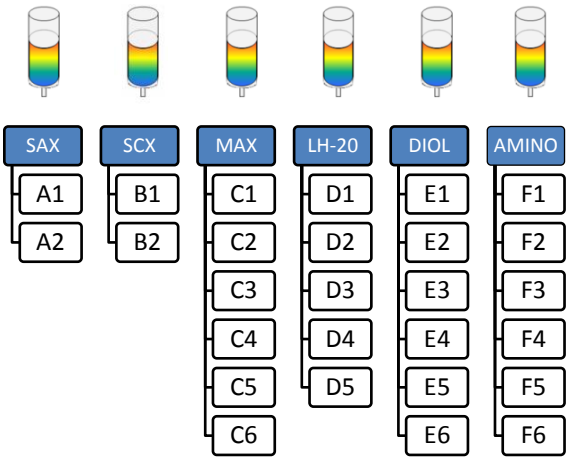

Figure 1.9 Overview of the columns used in the E-SPE setup. Three ion-exchangers are used (SAX, SCX, MAX), one size exclusion (LH-20), and two normal phases (diol and amino).

The optimal outcome of a dereplication for the NP chemist is *not* to find hits matching a given compound, since this indicates a novel structure. There are, however, no guaranties. There are no databases with all compounds described in literature, and new structures are continuously being submitted both from natural sources and from synthetic approaches. Furthermore the compounds of interest may be novel but only contain smaller modifications compared to a known compound. For instance an additional methyl group

would result in no hits in the databases due to the change in mass, though the structure would merely be an analogue.

2 Overview of experimental work

An overview of the experimental work performed and the resulting papers is given in Figure 2.1. The results are presented in chapter 3-4.

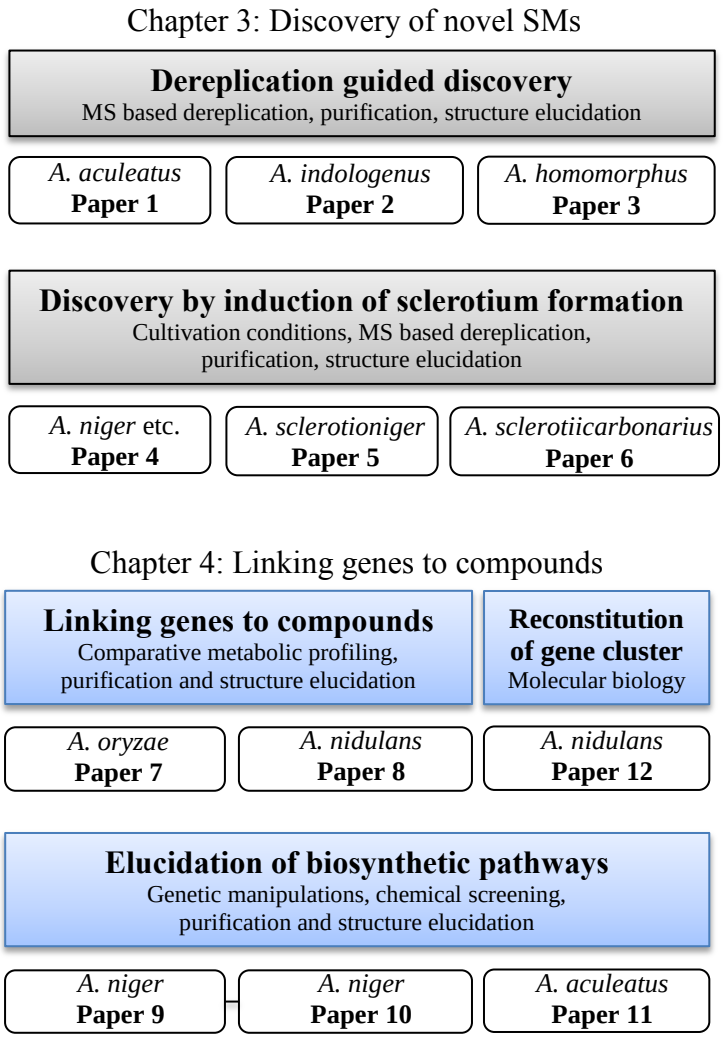

Figure 2.1 Overview of the experimental work performed in this thesis.

The following sections outline the workflow, strategies and instruments applied in this study. Detailed experimental descriptions are presented in Paper 1-12.

2.1 Workflow

The workflow used throughout this study is summarized in Figure 2.2. Depending on the type of project, the first step was to genetically modify the strain. The strain of interest was then cultivated, typically on a set of different media, to get insight into the full metabolic repertoire. SMs were then extracted and often the next step was often E-SPE using a series of different columns. This step was introduced with two purposes: Firstly as an aid in dereplication as information of functional groups provide valuable information. Secondly, to provide a strategy for purification. Extensive dereplication was then performed mapping all SMs produced and identifying already known compounds. When the chemical analyses revealed new compounds or intermediates of interest, the cultivation was scaled up to allow for isolation and structure elucidation. After extraction of the metabolites a process of purification followed, using several consecutive purification steps and going back and forth between chemical analysis and purification. When pure compounds were obtained, their structures were elucidated by use of 1D and 2D NMR experiments.

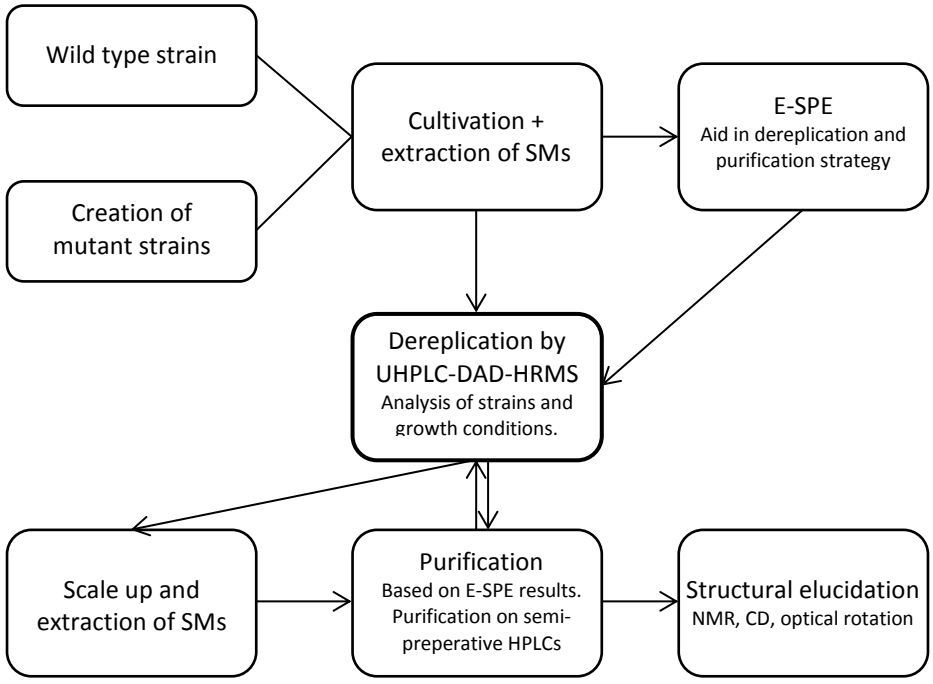

Figure 2.2 The workflow and purification strategy used throughout this study. See text for details.

2.1.1 Purification strategy

For isolations of all SMs in this work, solid cultures were used. Strains were inoculated as three point inoculations on 50-200 plates of selected media and incubated at 25-37 °C for 5-7 days in the dark. The plates were harvested and extracted twice overnight with ethyl acetate (EtOAc) with or without 1 % formic acid. After extraction of the SMs, a step of removing both very polar (e.g. sugars from the media) as well as very apolar (e.g. fatty acids) compounds was accomplished through liquid-liquid extractions.

A crude fractionation using an Isolera flash purification system (Biotage) followed. In this particular step, the data from the preliminary E-SPE experiments was used. This was crucial in order to find orthogonal purification methods to obtain a good separation of compounds. This is exemplified by the purification of two yanuthones (section 4.3). Chromatograms from the E-SPE are depicted in Figure 2.3. The BPC of the *A. niger* crude extract showed that two of the targets, 7-deacetoxyyanuthone A and yanuthone D, eluded close together on a traditional C_{18} column. Two of the fractions from the E-SPE experiment with a diol column, however, showed complete separation of the two compounds in two consecutive fractions; fraction four (DCM) and fraction five (DCM/EtOAC 1:1). A diol column was therefore used at the Isolera, providing optimal separation of the two compounds.

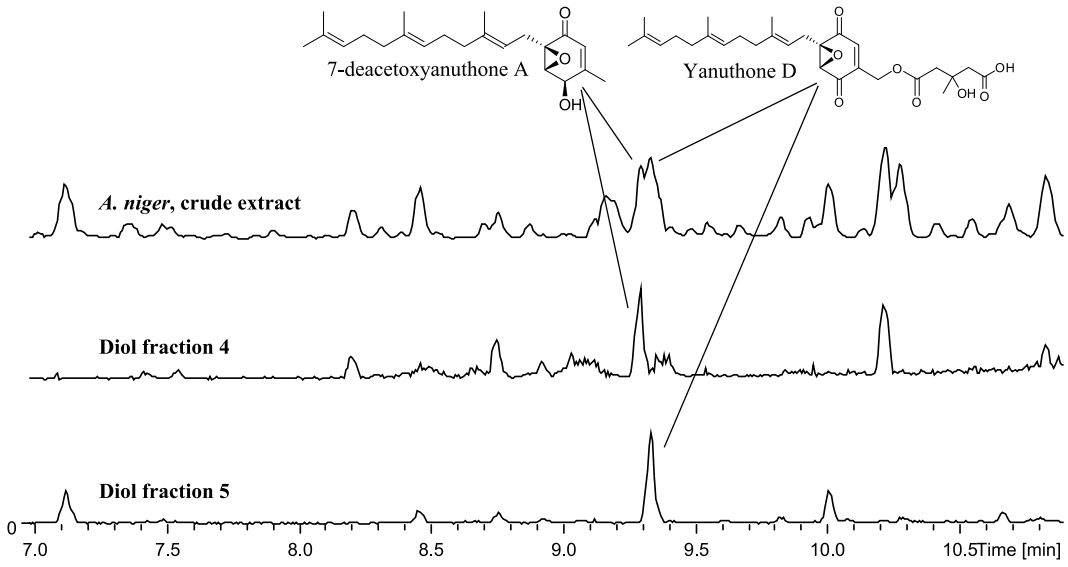

Figure 2.3 ESI+ BPC chromatograms of *A. niger* extract showing the metabolic profile of the crude extract and two fractions from E-SPE using a diol column.

The Isolera fractions were subjected to further purification on a semi-preparative HPLCs which was either a Waters 600 Controller with a 996 photodiode array detector (Waters, Milford, MA, USA) or a Gilson 322 Controller connected to a 215 Liquid Handler, 819 Injection Module and a 172 DAD (Gilson, Middleton, WI, USA). This was typically achieved using a Luna II C_{18} column (250 x 10 mm, 5 µm, Phenomenex) or a Gemini C6-Phenyl 110A column (250 x 10.00 mm, 5 µm, Phenomenex). The choice of system, solvents, flow rate, column and gradients depended on the given sample mixture for the project.

2.1.2 Metabolic analysis

The chemical analysis performed during this study was primarily performed on a maXis 3G QTOF (Bruker Daltonics). This was equipped with an electrospray ionization (ESI) source and connected to an Ultimate 3000 UHPLC system (Dionex). The column used was a reverse-phase Kinetex 2.6 µm C_{18}, 100 mm x 2.1 mm (Phenomenex), and the column temperature was maintained at 40 ˚C. A linear water-acetonitrile (LC-MS grade) gradient was used (both solvents were buffered with 20 mM formic acid) starting from 10% (v/v) ACN and increased to 100% in 10 min, maintaining this rate for 3 min before returning to the starting conditions in 0.1 min and staying there for 2.4 min before the following run. A flow rate of 0.4 ml/min was used. TOFMS was performed in ESI+ with a data acquisition range of 10 scans per second at *m/z* 100–1,000. The TOFMS was calibrated using Bruker Daltonics high precision calibration algorithm by means of the use of the internal standard sodium formate, which was automatically infused before each run. This provided a mass accuracy of better than 1.5 ppm in MS mode. UV-visible spectra were collected at wavelengths from 200 to 700 nm. Data processing was performed using Data Analysis 4.0 and Target Analysis 1.2 software (Bruker Daltonics).

Comparative metabolic profiling was used for analysis of strains. This is illustrated for a PKS deletion strain and reference strain of *A. niger* (section 4.3, Paper 9), see Figure 2.4. It is here illustrated how a SM (RT = 9.4 min) is disappearing in the deletion strain. This was always verified by extracted ion chromatograms (EICs) of the *m/z* of the compound in question (not shown in Figure 2.4). The peak would then be analyzed by MS and UV data, and a search in the two databases Antibase 2012 (commercial database, 40065 compounds) [118] and the in-house library of microbial metabolites (7349 compounds)[115] conducted, in order to tentatively identify already known compounds, as described in section 1.4.1.

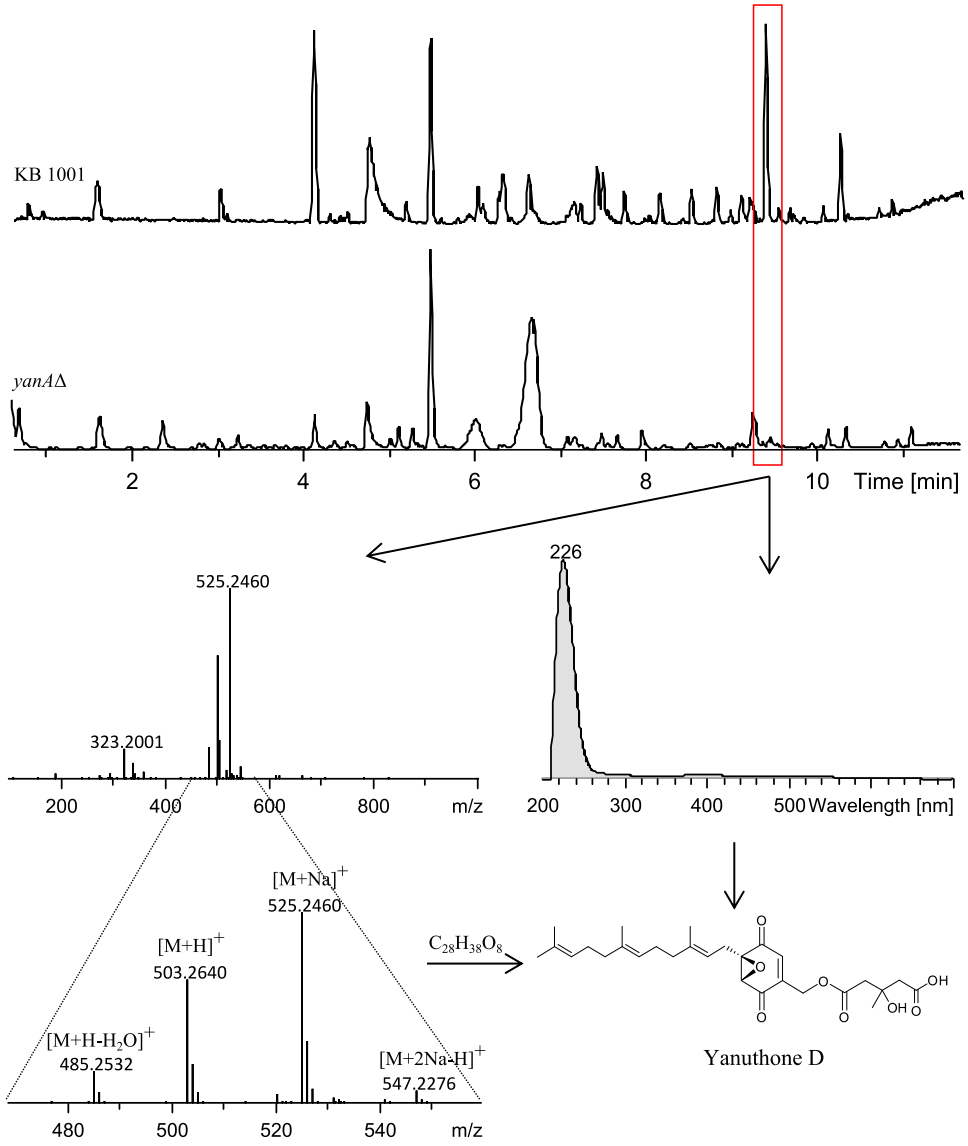

Figure 2.4 Example of comparative metabolic profiling, identifying abolishment of a SM in the deletion strain (RT = 9.4 min). Analysis by HRMS and UV and subsequent database search allowed for determination of the compound as the meroterpenoid yanuthone D.

2.1.3 Structural analysis

The structure elucidation of isolated metabolites was performed in combination of UHPLC-DAD-HRMS data and 1D- and 2D NMR experiments. The latter were achieved on a Varian Unity Inova-500 MHz spectrometer or a Bruker 400 MHz spectrometer, both located at DTU Chemistry. When minute amounts of compounds were obtained, NMR data was recorded on a 800 MHz Bruker Daltonics Avance spectrometer located at the Danish Instrument Centre for NMR Spectroscopy of Biological Macromolecules at Carlsberg Laboratory. Generally ^{1}H, DQF-COSY, NOESY, HSQC and HMBC spectra

were recorded for all compounds. The general workflow is presented in Figure 2.5. It is noted that a ^{13}C spectrum was generally not obtained; the $^{13}CNMR$ chemical shifts were determined from HSQC and HMBC experiments. With some structures, for instance carbonarin I and J with molecular formulas of $C_{34}H_{31}NO_{10}$ and $C_{34}H_{29}NO_9$ respectively (section 3.2.5, and Paper 6), the few proton resonances made it impossible to assign all carbon resonances from the heteronuclear experiments, why 1D ^{13}C spectra were recorded. Other experiments, which were utilized to confirm or aid an assignment, were H2BC, edited-HSQC and HSQC-TOCSY.

To obtain the absolute configuration different techniques were used, depending on the compounds. These included optical rotation, CD, NOESY experiments and Marfey's method.

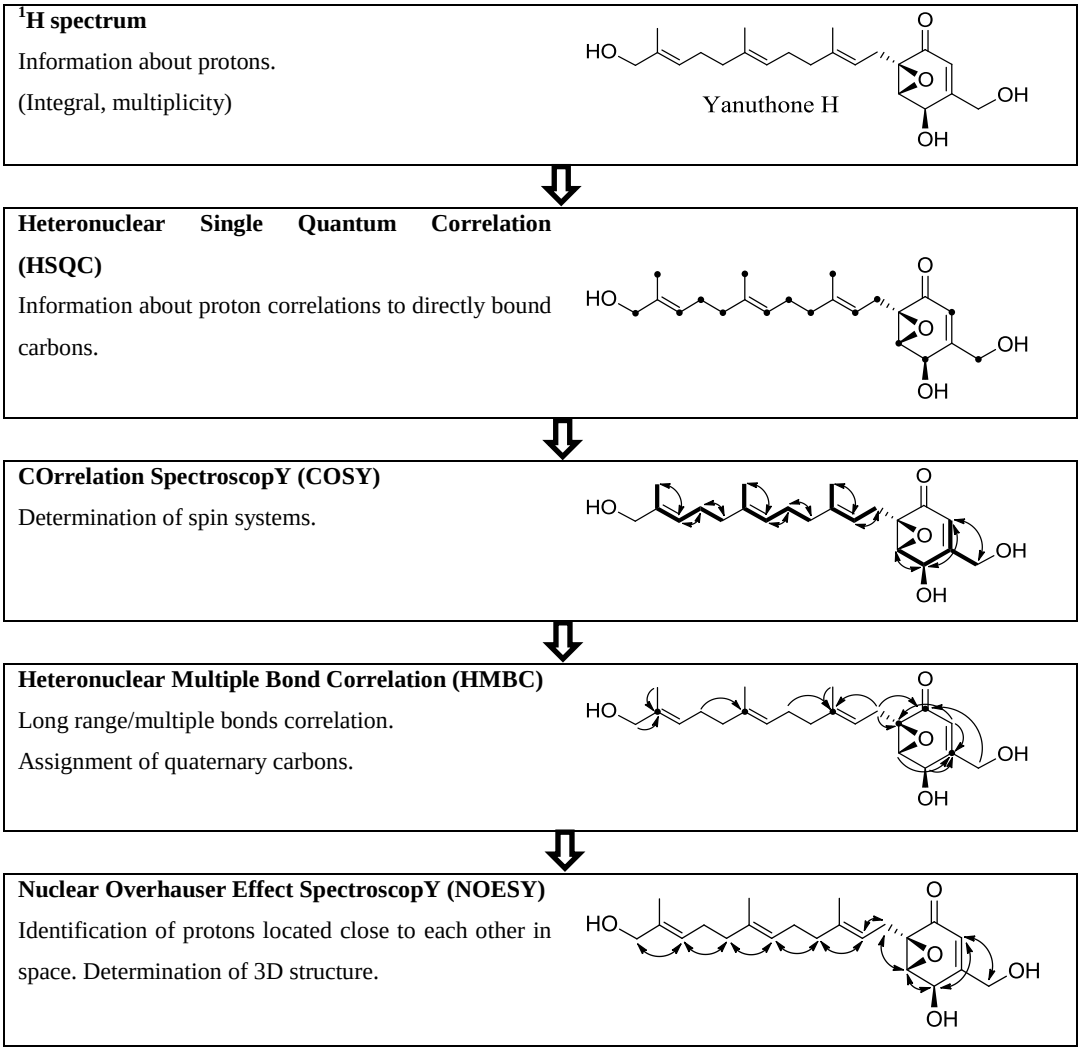

Figure 2.5 Workflow for structure elucidation by 1D and 2D NMR exemplified with yanuthone H.

3 Discovery of novel secondary metabolites

A significant part of the experimental work performed during this thesis has focused on the discovery of novel SMs, and is the theme of this chapter. Two different approaches have been undertaken wherefore the chapter is parted in two. The discovery has been achieved by dereplication (section 3.1) as well as sclerotium formation (section 3.2). Several species of the black Aspergilli have been studied; however, the main efforts have been on *A. aculeatus* and *A. niger*.

3.1 Dereplication based discovery

The dereplication based discovery is driven by the premise that biodiversity leads to chemodiversity: by studying the more exotic or unstudied species belonging to the black Aspergilli, we hypothesized that novel chemistry would likely be discovered. Using dereplication for fast tentative identification of already known compounds (section 1.4.1), targets for unknown and uncharacterized compounds can be identified. These can subsequently be explicitly targeted for purification. This section describes three black Aspergilli, *A. aculeatus*, *A. indologenus* and *A. homomorphus*, for which the metabolic profile was analyzed and possible unknown metabolites, were isolated and characterized.

3.1.1 *Aspergillus aculeatus*

This section presents the manuscript "Dereplication guided discovery of secondary metabolites of mixed biosynthetic origin from *Aspergillus* aculeatus" (Paper 1), published in Molecules in 2014.

The study presents a thorough investigation of the industrially important black filamentous fungi *A. aculeatus* by UHPLC-DAD-HRMS.

From fungal species identified as *A. aculeatus* metabolites such as aculeacins A–G [27][28], CJ-15,183 [29], secalonic acids D and F [30] and okaramines H and I [31] have been reported. Furthermore asperaculin A [32], aspergillusol A [33] and aculeatusquinones A–D [34] have been reported from marine strains of *A. aculeatus*. From these, different biological activities are reported, such as antifungal (aculeacins A-G and CJ-15,183), enzymatic inhibitory (CJ-15,183 and aspergillusol A), antimicrobial activities (secalonic D and F) and cytotoxicity (aculeatusquinone B and D).

The metabolic profile of *A. aculeatus* (IBT = 21030) is depicted in Figure 3.1, which also illustrates the results of the study: Complete assignment of all major metabolites. This entailed identification of four compounds already known to be produced by *A. aculeatus*,

identification of three compounds reported from *A. aculeatus* for the first time and last but not least, the discovery of nine novel compounds reported for the very first time.

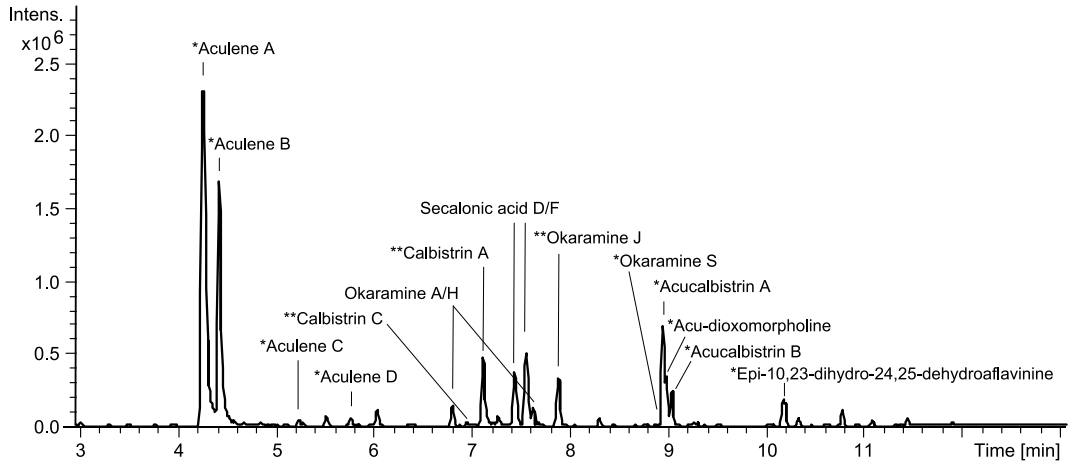

Figure 3.1 ESI+ base peak chromatogram illustrating the dereplication of some of the major compounds in the extract from *A. aculeatus* IBT 21030 as well as the results of purification and structure elucidation of novel compounds. Based on cultivation on YES media for 7 days at 25 °C in the dark. *Novel compounds reported for the first time. **Known compounds reported from *A. aculeatus* for the first time.

The use of dereplication for discovery of novel SMs proved strong in this project, as known compounds could easily be identified by use of the HRMS and subsequent database search as described in section 1.4.1. Purification followed by structure elucidation may still be necessary for complete assignment. For instance, it was clear from both UV and HRMS data that *A. aculeatus* produced calbistrins, which have not been reported from this organism before. It was, however, unclear which two calbistrins were produced, as calbistrin A and B have the same molecular formula and likewise for calbistrins C and D. If standards of the compounds are available the identity can be decided by comparison of RT, adducts, fragmentation and if necessary MS/MS, but no standards were available for the calbistrins. Depending on the project this information may be enough. If the purpose is solely to discover novel structures, it does not matter exactly which calbistrin it is; it is enough to know that the compounds are calbistrins and therefore of no interest. In this project, we did, however, have an interest in knowing the identity; since the calbistrins were incorporated into the novel structures, the acucalbistrins. The two compounds were therefore isolated and their structures elucidated by 1D and 2D NMR, whereby it was shown that the two compounds produced by *A. aculeatus* were calbistrins A and C. The same situation was true for okaramine J, which could not be unambiguously dereplicated, since the HRMS and UV data pointed towards either okaramine C, J *or* L. The novel compounds discovered in *A. aculeatus* are depicted

in Figure 3.2. A detailed description of the structure elucidation of these compounds is given in Paper 1.

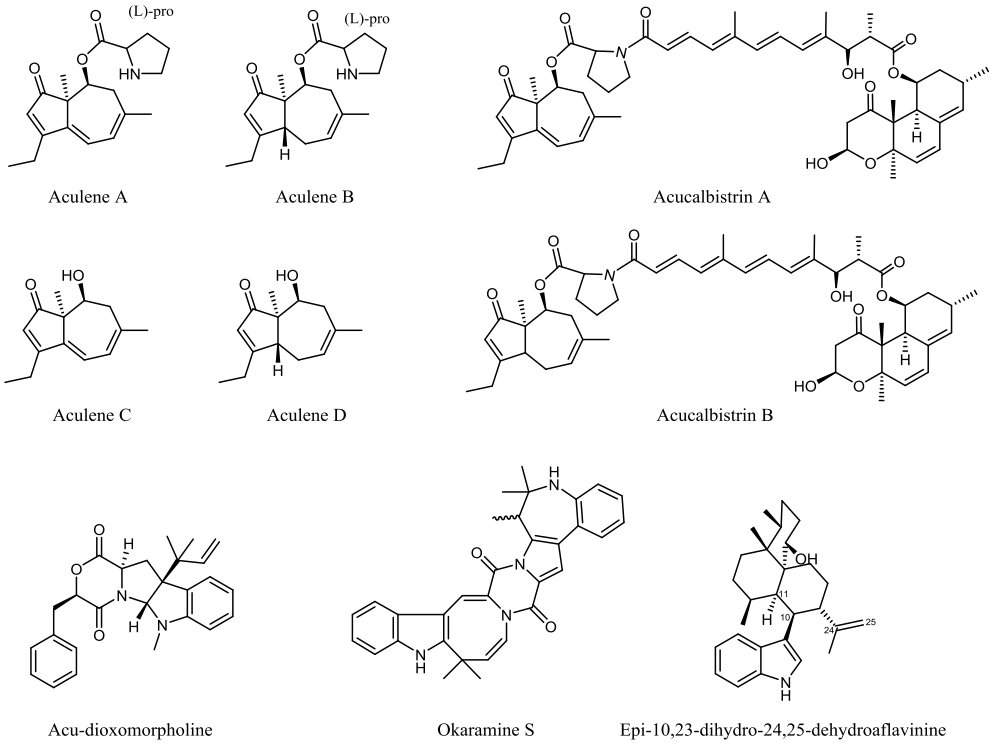

Figure 3.2 Structures of the novel compounds isolated from *A. aculeatus*. The structures of aculenes A-C, acu-dioxomorpholine, okaramine S and epi-10,23-dihydro-24,25-dehydroaflavinine has been verified by 1D and 2D NMR spectroscopy, while they remaining have been suggested based on UHPLC-DAD-HRMS data.

As depicted, the novel *A. aculeatus* structures are of different biosynthetic origin. We propose that aculenes A-B are assembled from three isoprene units and the AA proline (further elaborated in section 4.4). The calbistrin part of the acucalbistrins has been hypothesized to be of PK origin [123], while acu-dioxomorpholine, okaramine S and epi-10,23-dihydro-24,25-dehydroaflavinine are of NRP/indole terpenoid origin.

Working on this project it was by serendipity discovered that *A. aculeatus* was capable of producing sclerotia, when spores were maintained at -18˚C prior to inoculation. This discovery was of great interest, as the metabolic profile was greatly altered under sclerotia producing conditions. This led to further investigations including other *Aspergillus* species, which are described in section 3.2.

3.1.2 *Aspergillus indologenus*

This section presents the manuscript "Aspiperidine oxide, a new rare piperidine *N*-oxide, from the filamentous fungus *Aspergillus* indologenus" (Paper 2), intended for submission to Phytochemistry Letters. The structure elucidation of the novel compound aspiperidine oxide, was performed under supervision of professor Marcel Jaspars as part of a PhD course at the University of Aberdeen.

In the same clade as *A. aculeatus* is another black *Aspergillus*: *A. indologenus* (IBT 3679 = CBS 114.80) (see Table 1.1). This species was isolated from Indian soil in 2011 and was subsequently described by Varga and co-workers [22]. This work showed that *A. indologenus* is a producer of the insecticidal compounds okaramines A, B, and H, which is also the case for the closely related *A. aculeatus* (section 3.1.1). A further analysis of the metabolic profile showed that it produced indol-alkaloids related to aflavinines [22]. Being a relatively unstudied species, the hypothesis was that *A. indologenus* would likely produce new chemical entities, other than the SMs already reported from this clade. Initial dereplication revealed compounds, which were already known. This included the three compounds JBIR-74 [124], aspergillicin A [125] and fellutanine C [126], see Figure 3.3.

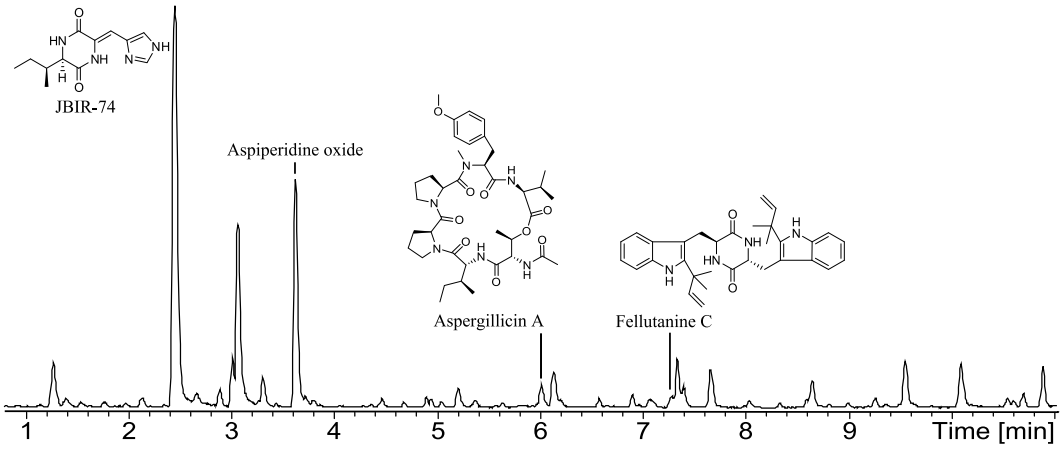

Figure 3.3 ESI+ Base peak chromatogram illustrating some of the major compounds in the extract from *A. indologenus*. Based on microscale extraction after cultivation on CYA media for 7 days at 25 °C in the dark.

These compounds have, however, not been described from *A. indologenus* before. JBIR-74 was originally isolated from a sponge-derived *Aspergillus* species, aspergillicin A from a marine-derived *A. carneus* and fellutanine C from *Penicillium fellutanum*. Aspiperidine oxide, (RT = 3.65 min, Figure 3.3) was identified as a possible novel compound and isolated and structure elucidated from *A. indologenus*. The structure is

depicted in Figure 3.4, a thorough description of the structure elucidation is found in Paper 2.

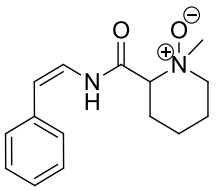

Figure 3.4 The chemical structure of aspiperidine oxide.

Aspiperidine oxide was tested towards GRAM negative bacteria *P. aeruginosa*, *A. baumannii* and *E. coli*, GRAM positive *MSSA* and *MRSA*, the yeast *C. albicans* and for fungal activity against *A. fumigatus*, but did not display any biological activity.
The structure of aspiperidine oxide was found to contain the *N*-oxide displayed in Figure 3.4. This type of structure has, to the best of our knowledge, never been seen in any fungal SM. The piperidine *N*-oxide has recently been observed in two alkaloids isolated from the plant *Microcos paniculata* [127]. The chemical shifts were comparable to our observations.

We hypothesized aspiperidine oxide to originate from amino acids, as the other metabolites JBIR-74, aspergillicin A and fellutanine C also produced by *A. indologenus* (Figure 3.3). We suggest aspiperidine oxide to originate from phenylalanine and the non-proteinogenic amino acid pipecolic acid. The proposed biosynthetic pathway is depicted in Figure 3.5. The putative decarboxylation step of the carboxylic acid group of phenylalanine moiety, have been observed for the oryzamide $A_{1\text{-}2}$ from *A. flavus*, described in section 4.1.

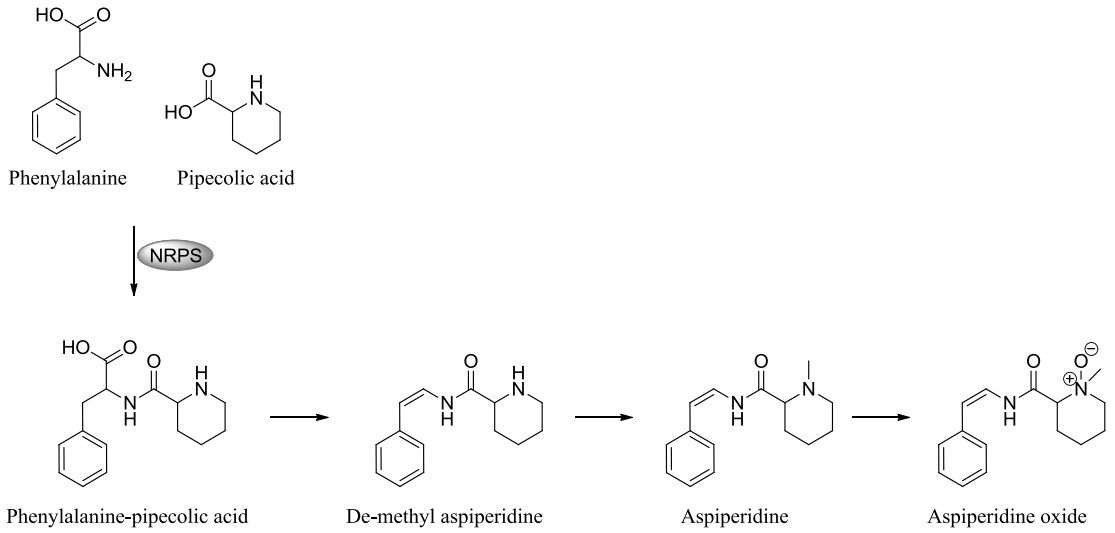

Figure 3.5 Proposed steps towards the biosynthesis of aspiperidine oxide.

The *A. indologenus* extract was scrutinized for possible intermediates, see Paper 2. This resulted in tentative identification of both the dipeptide phenylalanine-pipecolic acid (trace amounts), de-methyl aspiperidine and aspiperidine. Phenylalanine was also observed, though no traces were found of the non-proteinogenic amino acids pipecolic acid. The tentative identification of the suggested intermediates supports the suggested biosynthesis of aspiperidine oxide. Further verification of the suggested biosynthetic pathway could be achieved by feeding experiments with labelled amino acids, testing if these were incorporated into aspiperidine oxide and the suggested metabolites.

The finding of aspiperidine oxide in *A. indologenus* is an example of the potential of discovering novel SMs in the more unstudied species.

3.1.3 *Aspergillus homomorphus*

This section presents the manuscript "Novel metabolites from *Aspergillus homomorphus*" (Paper 3), intended for submission to Magnetic Resonance in Chemistry.

A. aculeatus and *A. indologenus* described in the previous sections belong to the same clade, the *A. aculeatus* clade. Another clade within the black Aspergilli, is the *A. homomorphus* clade, see Table 1.1. From this, the species *Aspergillus homomorphus* (IBT 21893) was investigated. *A. homomorphus* was originally identified from soil near the Dead Sea in Israel [128]. The SMs dehydrocarolic acid and secalonic acids D and F have earlier been reported to be produced from this species [40][41].

The metabolic profile of *A. homomorphus* is depicted in Figure 3.6. We were able to identify secalonic acids D and F, as well as other known compounds, not reported from *A. homomorphus* previously: Q-20547-E, L-valyl-L-tryptophan anhydride, originally isolated from the fungus *Phoma lingam* [129] and α-pyrone A and B, which has previously only been described from a synthetic study [130][131]. Dehydrocarolic acid was not identified from incubation on any medium.

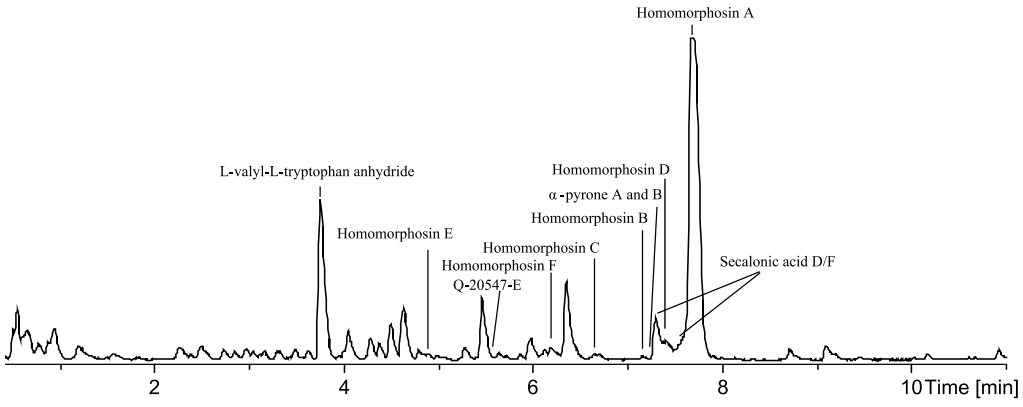

Figure 3.6 ESI+ base peak chromatogram illustrating compounds in the extract from *A. homomorphus* IBT 21893. Based on microscale extraction after cultivation on YES media for 7 days at 25 °C in the dark.

Furthermore we isolated and characterized six novel, related compounds, which we named by their fungal origin: homomorphosins A-F. A thorough description of the structure elucidations is given in Paper 3; their structures are depicted in Figure 3.7.

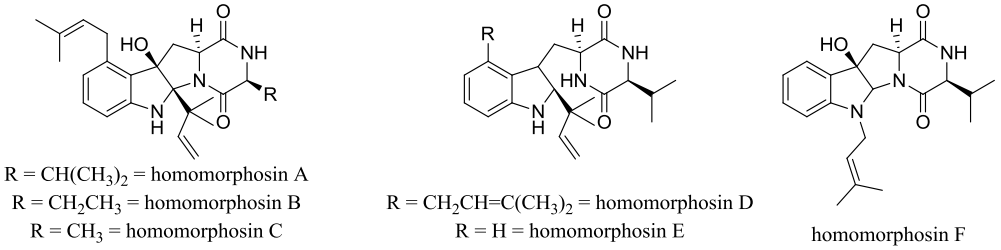

Figure 3.7 The chemical structures of homomorphosin A-F

Homomorphosin A was unquestionable the major compound being product by *A. homomorphus*. It was isolated in a crude Isolera fraction during pre-fractionation in staggering 180.7 mg. The isolation of homomorphosin A led to a hypothetical biosynthesis proposed in Figure 3.8, which in turn led to the discovery of the other homomorphosins. The biosynthesis was proposed utilizing known reactions from organic and biochemical synthesis, starting from L-valine and L-tryptophan. The mechanisms needed to obtain the compounds are two *C*-prenylations and an epoxidation and subsequent intramolecular ring-closure. Both mechanisms have been previously described or suggested in the biosynthesis of other natural products [54][129][132][133][134][135][136].

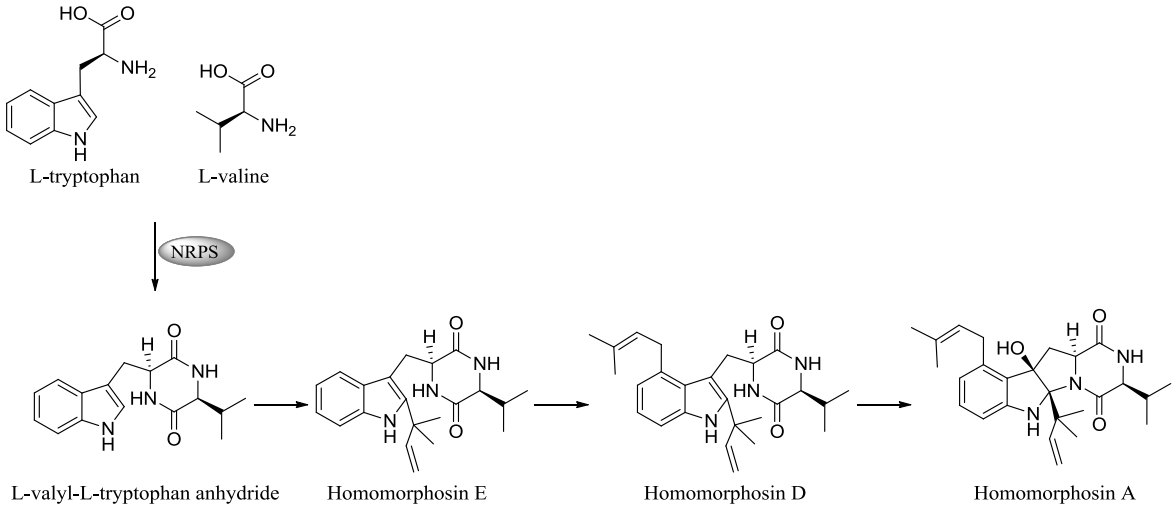

Figure 3.8 The suggested biosynthesis of homomorphosin A.

Homomorphosins B and C (Figure 3.7) are believed to follow the same pathway, but with the exchange of L-valine for L-alanine as precursor for homomorphosin C, while homomorphosin B may originate from a non-proteinogenic AA, or from L-valine or L-alanine which subsequently were demethylated or methylated respectively.

Homomorphosin F is most likely also derived from L-tryptophan and L-valine, but differs in the prenylation pattern, as it is *N*-prenylated, rather than *C*-prenylated.

The bioactivity of compounds similar to the homomorphosins against bacteria, fungi and protozoa has been tested and bioactivities have been reported against e.g. *S. aureus* [137][138]. Homomorphosin A was tested against *C. albicans* and chronic lymphatic leukemia, but no activity was observed.

3.2 Production of sclerotium for discovery

This section presents results from three different papers. Firstly, the manuscript "Formation of sclerotia and production of indoloterpenes by *Aspergillus niger* and other species in section *Nigri*" (Paper 4), published in Plos One in 2014, secondly, "Isolation, structural analyses and biological activity assays against chronic lymphocytic leukemia of two novel cytochalasins, sclerotionigrin A and B" (Paper 5), published in Molecules in 2014, and finally, "Induced sclerotium formation exposes new bioactive metabolites from *Aspergillus* sclerotiicarbonarius" (Paper 6), intended for publication in Journal of Antibiotics. The section also presents additional previously unpublished data.

3.2.1 Induction of sclerotium formation

Paper 4 presents results from our study involving a range of natural substrates, as well as pre-freezing of spores prior to inoculation, in order to induce the formation of sclerotia in various members of the black Aspergilli as well as characterization of the metabolic profile during sclerotia formation.

Sclerotial development in filamentous fungi is considered to be an important prerequisite for sexual development, wherefore the ability to induce sclerotium production could be a step forward towards finding a perfect state in a given *Aspergillus* species. Several species of the black Aspergilli have been reported as being able to produce sclerotia such as *A. aculeatus*, *A. sclerotioniger*, *A. carbonarius*, and *A. sclerotiicarbonarius* [41], whereas no sclerotia has been reported from the industrially important *A. niger*, and this organism is thought to be a purely asexual organism. Sclerotium production by *A. niger* and other black Aspergilli would have many biological, biotechnological and food safety consequences, due to possible production of mycotoxins such as aflatoxins and ochratoxin A [17][22][41][139][140][141][142].

Besides the interesting biological aspects of this study another reason to pursue this project has been for the discovery of novel SMs from previously silent gene clusters. In section 1.3 it is described that genome sequencing projects have revealed that many organisms have a great genetic potential to produce a large range of SMs, many of which are currently unknown. Our hypothesis was, that the induction of sclerotium formation would alter the metabolic profile and lead to production of sclerotial related SMs, wherefore induction of sclerotium formation could be a way of inducing the production of new SMs, especially indoloterpenes, from previously silent gene clusters in black Aspergilli.

The attempt to induce sclerotium formation involved various members of the black Aspergilli. We presented data showing the metabolic profile of *A. niger* (IBT 29019) and *A. tubingensis* (IBT 16833 = CBS 161.79 = NRRL 4700) under growth conditions with and without sclerotium formation. Comparative metabolic studies were, besides for these two species, also performed for several other members of the black Aspergilli. Appendix A, Figure A1, shows some of the common SMs found in the black Aspergilli during this study, while Figure A2 shows the comparative metabolic profiles of several black Aspergilli.

A common trend is production of more apolar compounds in the sclerotial extractions. These are apolar indoloterpenes; several tentatively identified as aflavinine analogous. Another common trend is production or upregulation of the naphtho-γ-pyrone aurasperone B. This was observed for *A. carbonarius* (IBT 21089), *A. acidus* (IBT 24821), *A. tubingensis* (IBT 16833), *A. tubingensis* (IBT 23488), *A. niger* (IBT 28999), *A. niger* (IBT 24631), *A. sclerotiicarbonarius* (IBT 28362) and *A. sclerotioniger* (IBT 22905). Aurasperone B thus seems to be an important sclerotial metabolite. It has earlier been demonstrated that aurasperone B is depending of the *fwnA* gene responsible for encoding the major PKS involved in formation of conidial melanin [143]. The work demonstrated a partial redundancy to synthesize aurasperone B. This also illustrates the importance of aurasperone B for the organism and could perhaps be connected to the upregulation observed during sclerotia formation.

In the following sections a more detailed description of the changes in metabolic profile for four of the black Aspergilli is given: *A. aculeatus*, *A. niger*, *A. sclerotioniger* and *A. sclerotiicarbonarius*.

3.2.2 *Aspergillus niger*

Sclerotia formation had prior to our study only been reported from a few strains of *A. niger* [144][145][146][147], however, these have later been assigned as other species [22][40][41]. The strains of *A. niger* that we tested in our study had not previously been shown to produce sclerotia. We first learned that several fruits stimulated sclerotium production. This included raisins, mulberry, blueberry, cranberry, apricot, prune, and mango peel. Inducing the sclerotial formation by raisins, was achieved by adding three, whole sterilized pieces of raisin on top of the CYA media (CYAR) and subsequently doing three-point inoculations close to each of the raisins, see Figure 3.9. If macerated raisins were added, no sclerotia were observed.

Figure 3.9 Left: Numerous white to cream-colored sclerotia produced on CYAR agar can be seen surrounding the raisins (highlighted in yellow ellipses) and the usual heavy sporulation caused by *A. niger* IBT 29019 heads. Right: Close-up showing white to cream-colored sclerotia. The clear or brown exudate droplets associated with sclerotia are also visible.

Sclerotium production was not fully consistent only by use of the CYAR medium. We learned that pre-freezing of spores used for inoculation in a freezer at -18 ˚C for minimum two weeks highly affected the production, which was originally discovered in the *A. aculeatus* work described in section 3.1.1. With the pre-freezing step, sclerotium production was entirely consistent in *A. niger* IBT 29190 and IBT 24631. From this first part of the study we therefore learned that sclerotium can be induced by a combination of using CYAR media and pre-freezing step. We were hereby able to induce sclerotium formation for the first time in the following other species of the black Aspergilli: *A. brasiliensis*, *A. floridensis*, *A. ibericus*, *A. luchuensis*, *A. neoniger*, *A. trinidadensis*, and *A. saccharolyticus*.

A. niger is known to produce a wide range of SMs, but have never been reported to produce aflavinine related indoloterpenes [38]. However, with the induction of sclerotium

formation the metabolic profile changed noticeably. Figure 3.10 displays the metabolic profile of three different extractions of *A. niger* IBT 29019; A: Plug extraction from growing and sporulating culture with no sclerotium production (CYA agar with biotin); B: Plug extraction from growth with sclerotium production (CYAR with biotin); C: Sclerotium extraction (from CYAR with biotin). From the standard plug extraction with no sclerotium formation, several known metabolites could be tentatively identified using the UHPLC-DAD-HRMS data by comparison of retention time, monoisotopic mass for the pseudomolecular ion, adducts and UV spectrum to a standard.

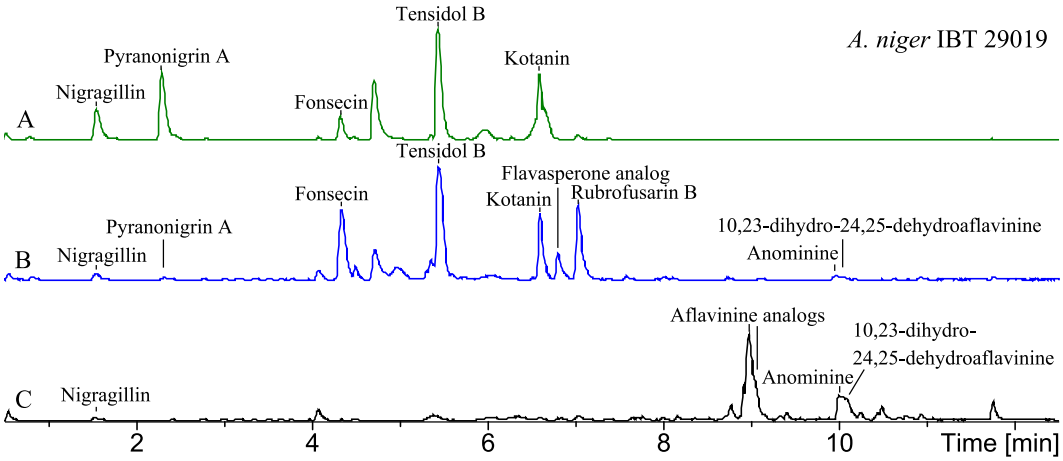

Figure 3.10 BPC chromatograms of *A. niger* (IBT 29019**)** A: Plug extraction from growing and sporulating culture with no sclerotium production (CYA agar with biotin). B: Plug extraction from growth with sclerotium production (CYAR with biotin). C: Sclerotium extraction (from CYAR with biotin). For structures of these compounds, see Appendix A.

From both the plug extraction with sclerotia present and the true sclerotial extraction, several indoloterpenes were detected. This included anominine (formerly known as nominine [39]) and 10,23-dihydro-24,25-dehydroaflavinine, but also several other compounds which based on UV chromophore and elemental composition were identified as aflavinine analogs. It is interesting that these indoloterpenes are exclusively found in the sclerotia. Many indoloterpenes have been reported to be antiinsectan [148][149][150][151][152][153][154]; and sclerotia related indoloterpenes have been suggested to be produced to protect against insects.

3.2.3 *Aspergillus aculeatus*

During the dereplication guided discovery of novel compounds from *A. aculeatus*, described in section 3.1.1 it was found that the strain was capable of producing sclerotia in vast amount, Figure 3.11.

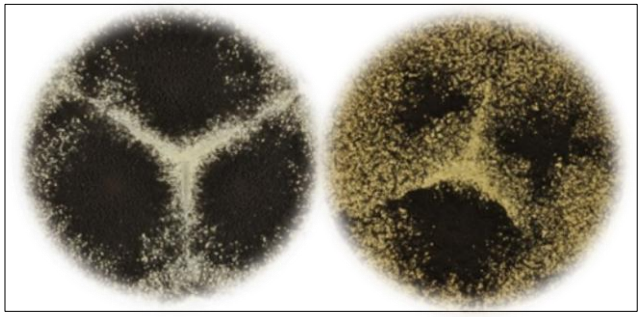

Figure 3.11 The figure shows production of sclerotia on YES (left) and CYA (right) media after growth for 7 days at 25 °C in the dark. The sclerotia are the white to cream-colored structures seen among the black conidial *Aspergillus* heads.

Comparative metabolic profiling showed that some metabolites were highly upregulated inside the sclerotia, compared to the metabolites in the mycelium. Analyses of extracts of sclerotia from MM, CYA and YES showed large upregulations of okaramines, see Figure 3.12. Aculenes A-C were still produced, though in smaller amounts. Furthermore the analysis showed that production of secalonic acids abolished on MM and CYA. The calbistrins were still produced and the same were acucalbistrins A-B, though in trace amounts. Some okaramine analogues have shown activity against silkworms [155][156][157] and the substantial upregulation of okaramines can be connected to sclerotium production as a defense mechanism to protect against insects.

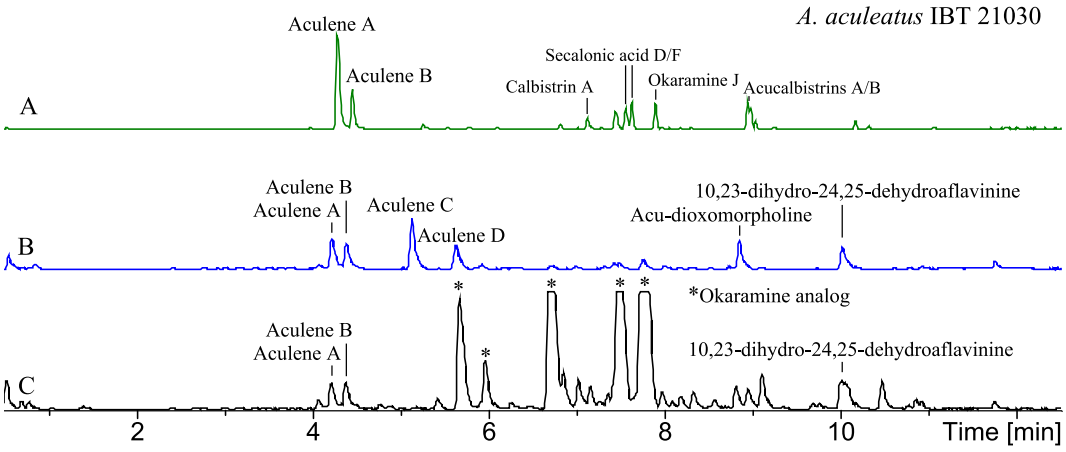

Figure 3.12 BPC chromatograms of *A. aculeatus* (IBT 21030**)** A: Plug extraction from growing and sporulating culture with no sclerotium production (CYA agar with biotin). B: Plug extraction from growth with sclerotium production (CYAR with biotin). C: Sclerotium extraction (from CYAR with biotin). For full description of metabolites produced by *A. aculeatus*, see section 3.1.1.

3.2.4 *Aspergillus sclerotioniger*

From the study involving several black Aspergilli, described in section 3.2.1, the metabolic profile of *A. sclerotioniger* caught our attention, since several compounds were produced, tentatively identified as novel cytochalasans.

The possible production of cytochalasins caught our attention as it is a diverse group of compounds with a wide range of biological functions [158], including inhibitory activities towards lung, ovarian, and human colon cancer as well as human leukemia [159,160]. Another reason to pursue this compound class is that our lab recently demonstrated that chaetoglobosin A, produced by *Penicillium aquamarinum*, selectively induce apoptosis in CLL cells with a median lethal concentration (LC_{50}) value of 2.8 µM [161]. A more thorough description of cytochalasins can be found in section 4.5.1.

It was furthermore interesting, since the only indication of production of any cytochalasans in *Aspergillus* subgenus *Circumdati* section *Nigri* is aspergillin PZ, for which the precursor aspochalasin C or D has been suggested [162][163]. However, in the sister clade *Aspergillus* subgenus *Circumdati* section *Flavipedes*, many cytochalasans have been reported, including aspochalasin A-D [164], E [165], F & G [166], D & H [167], I-K [168][169], L [170], U [171] and TMC-169 [172] in addition to aspochalamin A-D, aspochalasin D & Z [173], rosellichalasin [174], and cytochalasin E, 5,6-dehydro-7-hydroxy cytochalasin E, and a $\Delta^{6,12}$-5,6-dehydro-7-hydroxy cytochalasin E, 10-phenyl-[12]-cytochalasin Z16, 10-phenyl-[12]-cytochalasin Z17, cytochalasin Z11, cytochalasin Z13, Z16-Z20, and rosellichalasin [175][176][177][178][179]. In another species of *Aspergillus* subgenus *Circumdati* section *Circumdati*, *Aspergillus elegans* aspochalasin A1, B, D, H, I, J, cytochalasin Z24, zygosporin D, rosellichalasin and aspergillin PZ were found [180] supporting the view that aspochalasin D is a precursor of aspergillin PZ. Finally in the less closely related *Aspergillus clavatus* in *Aspergillus* subgenus *Fumigati* section *Clavati*, cytochalasin E and K have been isolated [181][182].

The chemical profiles of *A. sclerotioniger* did not display a great alteration in the different extractions (Figure 3.13), in contrary to many of the other black Aspergilli. This was a result of sclerotium being produced even without induction. The sclerotium extraction (trace C), did however show aurasperone B in higher amounts, also observed for many other black Aspergilli in this PhD study. Upregulation of the mycotoxin ochratoxin A has earlier been associated with sclerotium production in *A. carbonarius*

[139], and also in *A. sclerotioniger* [17][22][41]. Our observations were, however, quite opposite, as seen in Figure 3.13.

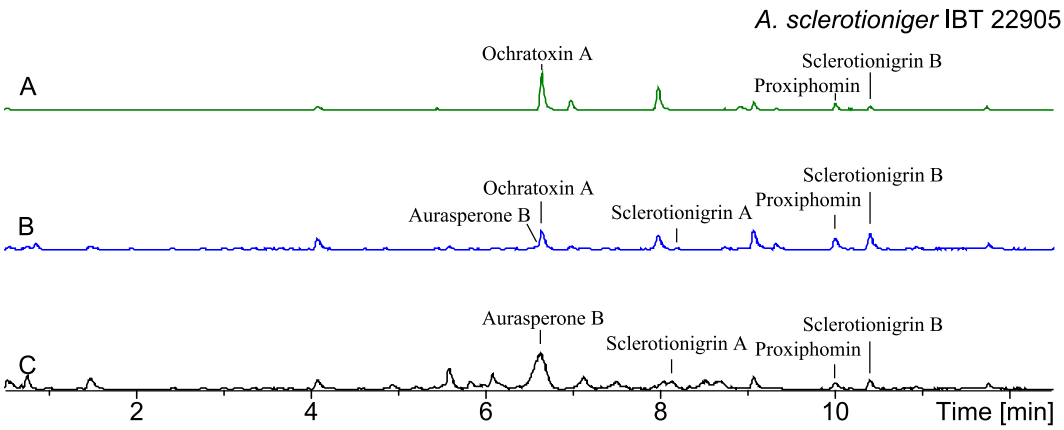

Figure 3.13 BPC chromatograms of *A. sclerotioniger* (IBT 22905**)** A: Plug extraction from growing and sporulating culture with no sclerotium production (CYA agar with biotin). B: Plug extraction from growth with sclerotium production (CYAR with biotin). C: Sclerotium extraction (from CYAR with biotin).

By cultivation of *A. sclerotioniger* in a larger scale, three cytochalasins were purified and their structures elucidated, see Figure 3.14. One of the cytochalasins, proxiphomin, was previously isolated from cultures of *Phoma* species [183]. The other two were novel cytochalasins, which we named by their fungal origin: sclerotionigrin A and B. A thorough description of the structure elucidation is given in Paper 5, but one interesting structural feature, was the stereochemistry at the central carbon of the tricyclic core, which we found to differ compared to other cytochalasans.

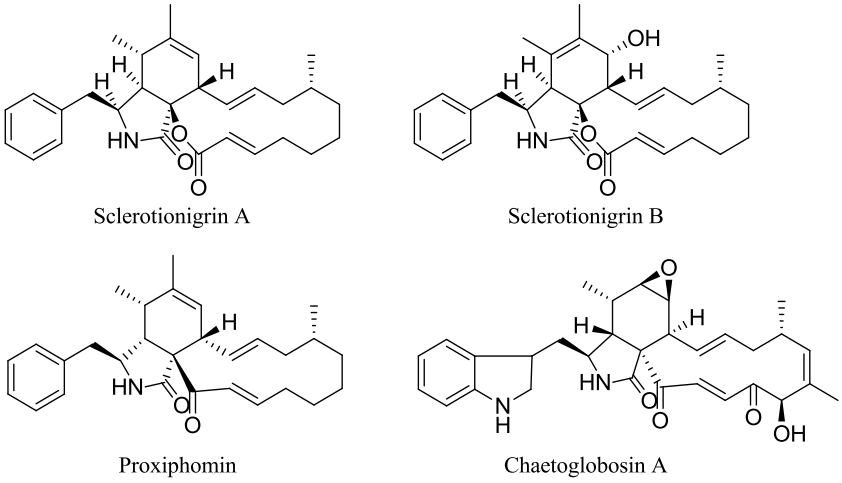

Figure 3.14 Structures of sclerotionigrin A, sclerotionigrin B, proxiphomin and chaetoglobosin A.

Based on the findings that chaetoglobosin A selectively induce apoptosis in CLL cells with a median lethal concentration (LC_{50}) value of 2.8 µM, we wanted to test the effect of CLL cells of both sclerotionigrin A and B as well as proxiphomin. Sclerotionigrin B was found to have no effect, while sclerotionigrin A had a LC_{50} of 72 µM, and proximorphin 48 µM. The decrease in activity observed for the sclerotionigrins, as compared to chaetoglobosin A, could be due to a number of things, since there are several structural differences. One suggestion could be the absence of the epoxide, the exchange of tryptophan to phenylalanine or perhaps the change of stereochemistry at the central carbon of the tricyclic core.

3.2.5 *Aspergillus sclerotiicarbonarius*

During the sclerotial study another species that caught our attention was *A. sclerotiicarbonarius*, a black Aspergilli, originally isolated from Thai coffee beans [184] belonging to the *A. carbonarius* clade [22]. *A. sclerotiicarbonarius* has, as the name implies, been known as a producer of sclerotia. Nonetheless sclerotium formation was not observed for *A. sclerotiicarbonarius* (IBT 28362) on standard media, why the CYAR media as described in section 3.2.1 was utilized. Comparative metabolic profiling showed a great alteration in SMs, see Figure 3.15.

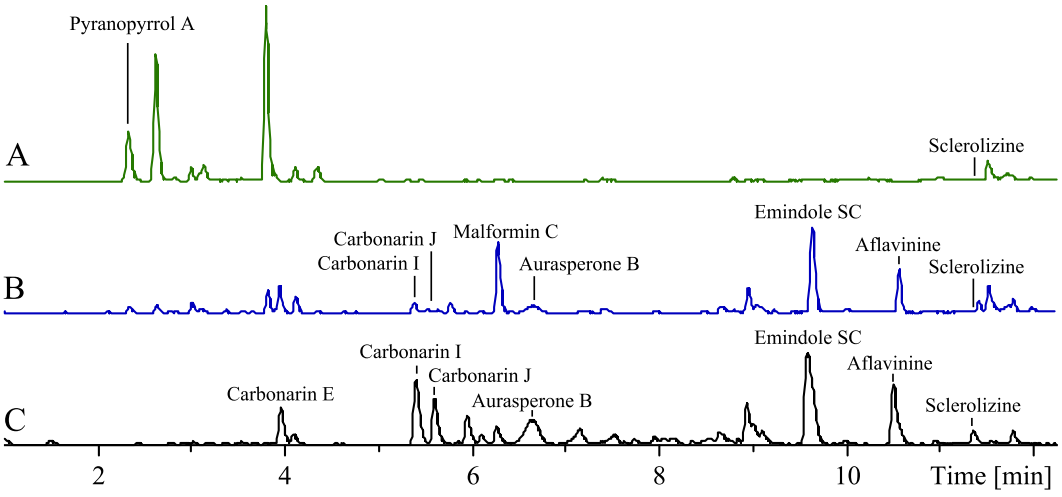

Figure 3.15 UHPLC-TOF-HRMS ESI+ BPC chromatogram of *Aspergillus sclerotiicarbonarius* (IBT = 28362) extractions. Scaled to RT between 1-12 minutes, intensities are to scale. A: Plug extraction from growth with no sclerotium production. B: Plug extraction from growth with sclerotium production. C: Sclerotial extraction. The extractions under sclerotium production (B + C) show the presence of the four novel compounds sclerolizine, emindole SC, carbonarin I and J.

Two general observations were made: firstly, the SMs produced under sclerotium producing conditions were more apolar, and secondly, the naphtho-γ-pyrone aurasperone B was produced, as also seen for other black Aspergilli (section 3.2.1). Several compounds could not be unambiguously dereplicated, thus a large scale extraction was prepared followed by purification and structure elucidation. This led to the four novel compounds depicted in Figure 3.16. A detailed description of the structure elucidations is given in Paper 6.

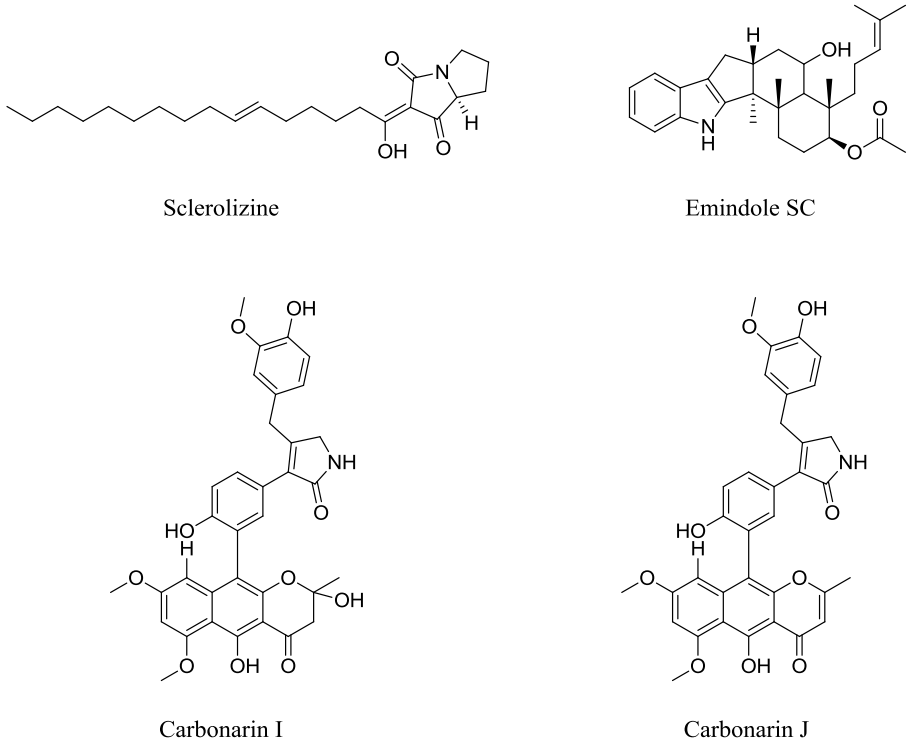

Figure 3.16 Structures of the novel compounds isolated from *A. sclerotiicarbonarius*.

For verification of whether the compounds were true sclerotial metabolites, or if they were produced in trace amounts in the non-sclerotium extract, extracted ion chromatograms (EICs) were created in the UHPLC-HRMS data from the plug extractions with and without sclerotium formation as well as the sclerotial extraction, see Table 3.1. It was here found that all metabolites were present in both the sclerotial extracts and the plug extracts under sclerotium formation. In the plug extraction, where no sclerotium was formed, all compounds but sclerolizine were absent, strongly indicating that emindole SC, carbonarin I, and carbonarin J are true sclerotial metabolites.

Table 3.1 Presence of compound **1-4** with and without sclerotium production. Detected by Extracted Ion Chromatograms (EICs) with a mass tolerance of *m/z* +/- 0.005.

	Plug extraction CYA (No sclerotia formation)	**Plug extraction CYA (Sclerotia formation)**	**Sclerotia extraction**
Sclerolizine	x	x	x
Emindole SC	-	x	x
Carbonarin I	-	x	x
Carbonarin J	-	x	x

To further investigate this, a search for carbonarin A-H in the UHPLC-UV-HRMS data from the sclerotial extract was conducted. This showed trace amounts of carbonarin A-D, high production of carbonarin E and F, while no carbonarin G nor H could be detected (Tentatively identified by HRMS with a mass tolerance of *m/z* +/- 0.005). An equivalent search for carbonarins in the *A. sclerotiicarbonarius* extract with no sclerotium production showed no traces of any of the carbonarins, suggestion this group of compounds to be related to sclerotium production.

As sclerotial compounds have often been found to possess insecticidal properties, all compounds were tested for larvicial activity towards *Drosophila melanogaster* larvae. The results showed that with increasing concentrations all compounds were affecting the survival of the insect larvae ($p < 0.001$), yet there was no compound-specific variation in this effect. Overall, at a concentration of only 1.83 ±0.08 µmol, 50 % of the larvae were found dead. The compounds were also tested for antifungal activity. Sclerolizine and carbonarin I displayed moderate antifungal activity, with sclerolizine as the most active (IC_{50} 8.5 ± 2.0 µM).

3.3 Chapter 3 Summary and part conclusion

The discovery of novel SMs from black Aspergilli has been addressed by two different approached: Traditional dereplication based discovery and by induction of sclerotium formation.

The first mentioned approach, dereplication based discovery, utilizes dereplication by HRMS to get an overview of the metabolic profile of a species and identify putative novel SMs, so these can efficiently be targeted. Three fungi were investigated by this approach. For *A. aculeatus* this led to discovery of a number of new compounds: A dioxomorpholine, a unique okaramine, an aflavinine and related, novel structures of mixed biosynthetic origin, which were named aculenes A–D and acucalbistrins A-B. From *A. indologenus*, aspiperidine oxide was discovered, which entails a piperidine *N*-oxide, a structural feature not seen in fungal SMs. From *A. homomorphus* five related compounds, homomorphosins A-F were characterized.

The work with *A. aculeatus* led to the discovery, that when spores were maintained at -18 ˚C for a period of time prior to inoculation this resulted in production of sclerotium. This discovery was of great interest, as the metabolic profile was greatly altered under sclerotium formation conditions, and led directly to the second theme for this chapter: Induction of sclerotium formation for discovery. The pre-freezing step was combined with use of natural substrates and especially the addition of raisins to the solid media would lead to induction of sclerotium. By use of this combined approach, sclerotium formation, was observed for the first time for *A. niger, A. brasiliensis, A. floridensis, A. ibericus, A. luchuensis, A. neoniger, A. trinidadensis* and *A. saccharolyticus*. Two species were further investigated: *A. sclerotioniger* and *A. sclerotiicarbonarius*. From the first mentioned it was found that cytochalasins were produced when sclerotia was formed, which led to discovery of two novel cytochalasins: Sclerotionigrin A and B in addition to the known cytochalasin proxiphomin. For *A. sclerotiicarbonarius* the metabolic profile was also highly altered, and four novel SMs were discovered, whereof three were identified as true sclerotial metabolites. The finding that induction of sclerotium formation can trigger otherwise silent biosynthetic pathways in filamentous fungi, is of general interest for the discovery of novel bioactive SMs.

Overall, the findings presented in this section confirm, that there are still many novel SMs to be discovered from filamentous fungi.

4 Linking genes to compounds

The second big theme for this study has been to link fungal SMs to their synthase/synthetase genes and to elucidate biosynthetic pathways. The results are given in this chapter in separate sections for each of the studied fungi: *A. oryzae* (4.1), *A. nidulans* (4.2), *A. niger* (4.3), *A. aculeatus* (4.4), and *A. nidulans*/*A. clavatus* (4.5).

4.1 *Aspergillus oryzae*

This section presents some of the results from the manuscript "Comparative Chemistry of *Aspergillus oryzae* (RIB40) and *A.* flavus (NRRL 3357)" (Paper 7), published in Metabolites in 2012.

4.1.1 Comparative metabolic profiling

A. oryzae has been used for centuries in Asian food fermentation of e.g. soy sauce, sake and vinegar [185]. It has been assumed to be a domesticated form of the related species *A. flavus*, which contrary is a pathogenic species, capable of producing the carcinogenic aflatoxins. Due to their high importance, the two species were some of the first Aspergilli having their genome sequenced, and bioinformatic analysis revealed a high homology between the two species: 99.5 % genome homology and 98 % at the protein level for RIB40/ATCC 42149 and NRRL 3357 [186].

Despite their high similarity only few metabolites had been reported from both species. The aim for this project has been to perform a comparative investigation of the metabolic profile of two genome sequenced strains of *A. oryzae* (RIB40) and *A. flavus* (NRRL 3357), in order to get insights into possible similarities and differences in SM production for these two important species.

The comparative metabolic profiling of the two strains and initial dereplication revealed a surprisingly high degree of chemical differences, as depicted in Figure 4.1. Besides kojic acid (shown in box) and analogues in the beginning of chromatogram and ergosterol in the end (not shown), there were very few identical compounds between the strains. This was in sharp contrast to the high gene homology.

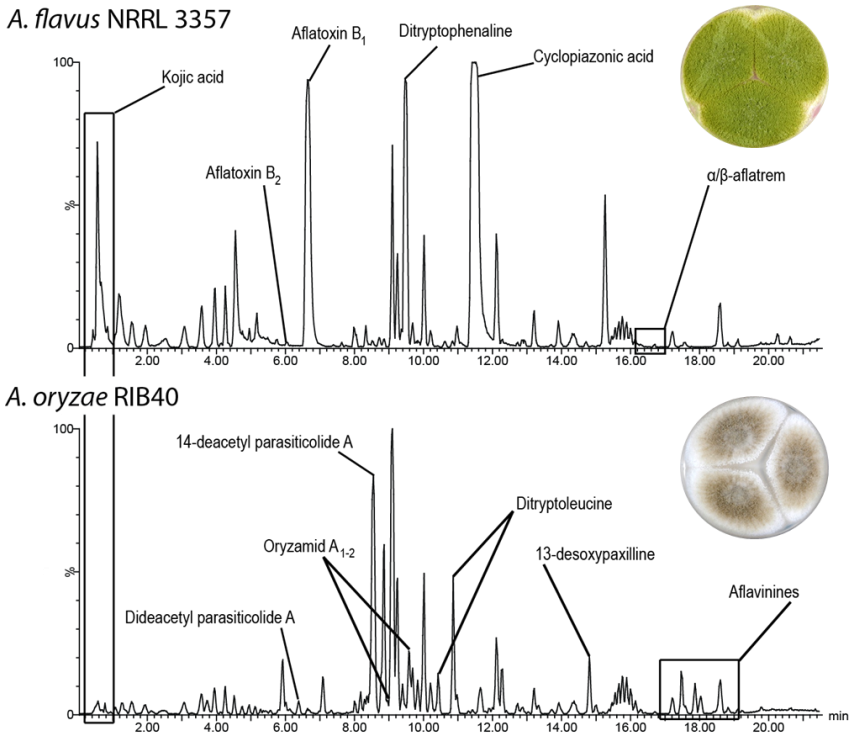

Figure 4.1 ESI+ BPI chromatogram of 7 day micro scale extract from WATM. Top: *A. flavus* NRRL 3357. Bottom: *A. oryzae* RIB40.

Besides previously reported *A. oryzae* metabolites, aflavinine analogues were detected for the first time, and several metabolites were purified and characterized including parasiticolides and 13-desoxypaxilline for the first time from *A. oryzae* and the novel compounds oryzamide $A_{1\text{-}2,}$ and ditryptoleucine.

4.1.2 Metabolites in *Aspergillus oryzae* and the link to *A. flavus*

During this project several *A. oryzae* metabolites were characterized, giving insights into the similarities as well as differences to *A. flavus*. Some of the findings are here briefly described.

A shared pathway with different end products

A known metabolite of *A. flavus* is the toxin aflatrem [187][188]; the last steps of the biosynthesis [189] are depicted in Figure 4.2. In *A. oryzae* no traces of aflatrem were detected, but one of the compounds we characterized in *A. oryzae*, was the aflatrem precursor 13-desoxypaxilline (13-dehydroxypaxilline). This was present in several media micro-scale extracts including YES, CYA, OAT and WATM. Furthermore no other intermediates in the biosynthetic pathway towards aflatrem were detected with the exception of one sample (WATM, 7d) showing traces of paspaline, a precursor for 13-desoxypaxilline.

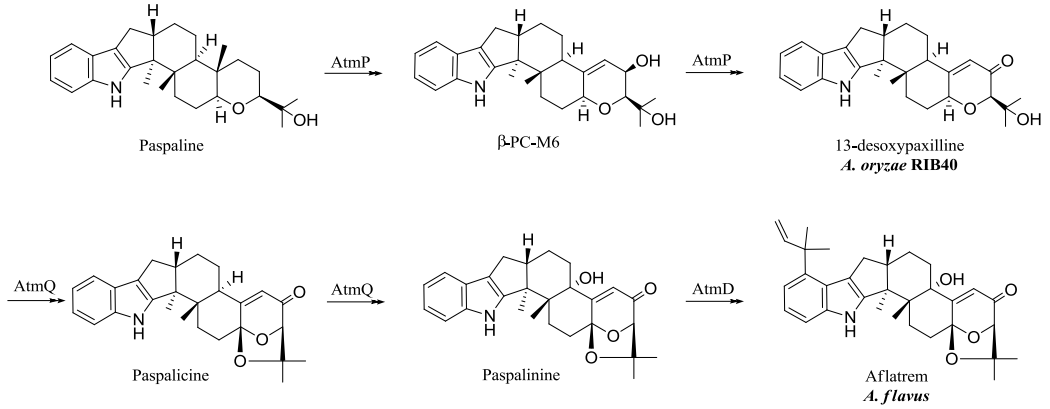

Figure 4.2 The final steps in the proposed biosynthesis of aflatrem (in *A. flavus*). *A. oryzae* RIB40 biosynthesis stops at 13-desoxypaxilline.

The identification of 13-desoxypaxilline as the end-product in the pathway from *A. oryzae* was in agreement with the analysis of Nicholson and co-workers, who showed that a frame shift mutation in the *atmQ* gene presumably accounts for the 13-desoxypaxilline not being converted into paspalicine and paspalinine [189]. In the work by Nicholson and co-workers, it was demonstrated that AtmQ is a multifunctional cytochrome P450 monooxygenase likely to catalyze several oxidative steps needed for biosynthesis of the acetal ring present in the structures of paspalicine, paspalinine and aflatrem, altogether pointing towards a more complex biosynthesis than shown in Figure 4.2.

Variation in incorporation of amino acids between the two species

Depicted in Figure 4.3 are the novel *A. oryzae* metabolites compared to known *A. flavus* metabolites, miyakamides B_{1-2} [190] and ditryptophenaline [191]. Apparently, the *A. oryzae* metabolites have exchanged phenylalanine with leucine compared to the corresponding *A. flavus* metabolites. This could indicate a common trait in the domestication process.

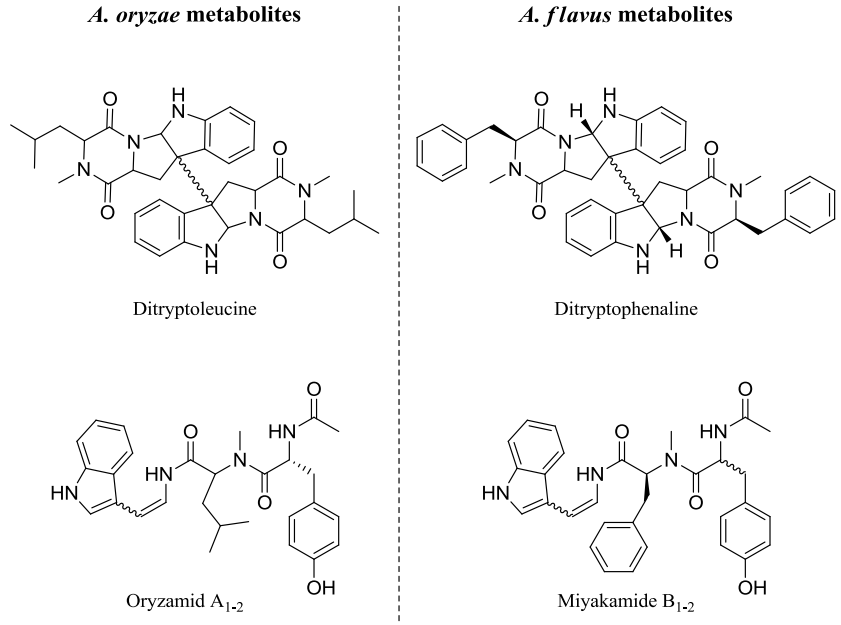

Figure 4.3 Novel metabolites from *A. oryzae* isolated and characterized in this study compared to known *A. flavus* metabolites. The *A. oryzae* metabolites have apparently exchanged phenylalanine with leucine compared to the similar *A. flavus* metabolites ditryptophenaline and miyakamides.

Although *A. oryzae* and *A. flavus* are very closely related with highly similar genomes, their ESI+ profiles appeared very different. Novel compounds characterized from *A. oryzae*, however, revealed to be either closely related or precursors for metabolites in *A. flavus*. This connection between the metabolites emphasizes the genetic coherence, but also indicates a path for the domestication process.

Altogether the findings show, how a combination of genome comparisons and comparative metabolic profiling, can exploit the chemical potential of different strains and give insights into differences at the genomic level, even without use of any genetic manipulations.

4.2 *Aspergillus nidulans*

This section presents the manuscript "Accurate prediction of secondary metabolite gene clusters in filamentous fungi" (Paper 8), published in Proceedings of the National Academy of Sciences of the United States of America in 2013.

The study presents a new method to predict fungal secondary metabolite clusters using DNA expression arrays in combination with legacy data, where expression profiles for neighboring genes are compared. As part of this study a "supercluster" (physically separated genes) consisting of a NRPS (AN1242) and a prenyltransferase (AN11080) was investigated in *A. nidulans*, which ultimately could be linked to the tetracyclopeptide nidulanin A.

4.2.1 Investigation of a supercluster in *A. nidulans*

A. nidulans is an important model organism for both biological model systems and genetic engineering. It was genetically characterized by Pontecorvo and co-workers in 1953 [7] and has ever since been widely studied, wherefore there today is several efficient, genetic tools developed [8][9]. Genome sequencing in 2005 [75] has further facilitated the possibilities of genome mining within this organism. As a result several biosynthetic pathways have been investigated, such as sterigmacotycin [90], naphthopyrone [91], aspyridone A-B [82], asperthecin [92], emericellamide [98], monodictyphenone/emodin [93][94], austinol/dehydroaustinol [84], arugosins [84], orsellinic acid/lecanoric acid/F9775A/F9775B [93][79][95], asperfuranone [96], and alternariol/cichorine [97].

In filamentous fungi biosynthetic genes tend to be clustered as described in section 1.3.1. The genes can, however, also be located various places in the genome, in which case they are referred to as a supercluster. Our investigation of *A. nidulans* led to a discovery of such a supercluster, consisting of a NRPS (AN1242) located on chromosome VIII and a putative prenyltransferase (AN11080) located on chromosome V. The data indicated crosschemistry between the two, which could be verified by deletion experiments of the synthetase and the prenyltransferase. In Figure 4.4, UHPLC-DAD-HRMS data from the *A. nidulans* reference strain and ΔAN1242 and ΔAN11080 strains are shown. The first conclusion to be drawn, is the linking of both genes (AN1242 and AN11080) to the compound at RT = 8.74 min, as this compound was absent in both deletion strains. This confirmed the cross-chemistry between the two genes. The *m/z* for $[M+H]^+$ of the affected compound (nidulanin A) was found to be 604.3493, corresponding to a molecular

formula of $C_{34}H_{45}N_5O_5$. The EICs in Figure 4.4 is for this *m/z*, but also for a related compound (nidulanin B), differing by the loss of a prenyl group. This compound is suggested to be the unprenylated precursor to nidulanin A. As seen in Figure 4.4 both nidulanin A and the precursor is present in the *A. nidulans* reference strain but neither in the NRPS deletion strain (ΔAN1242). In the prenyltransferase deletion strain (ΔAN11080) nidulanin A is not present, linking the gene to nidulanin A. However, the tentatively identified unprenylated precursor, nidulanin B, is still being produced; highly supporting the hypothesis, that AN11080 is responsible for prenylation of the NRPS product.

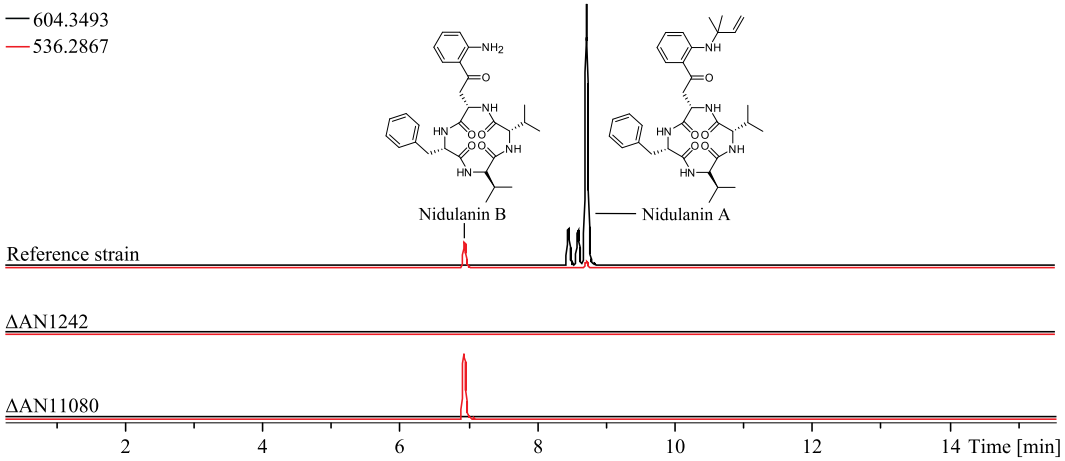

Figure 4.4 Extracted ion chromatograms for nidulanin A ($C_{34}H_{45}N_5O_5$, $[M+H]^+$ = 604.3493, black) and nidulanin B (nidulanin A – C_5H_8) ($[M+H]^+$ = 536.2867, red) with a mass tolerance +/- 0.005 Da. Data from UHPLC-DAD-HRMS of chemical extractions from the *A. nidulans* reference strain and ΔAN1242 and ΔAN11080 strains.

Due to the modular nature of the biosynthesis of NRPs (section 1.2.2) the product (nidulanin A) could be predicted as a tetracyclopeptide. The NRPS was predicted to contain four modules and here both adenylation domains and epimerase domains were identified. The adenylation domain specificities were predicted using NRPS predictor [192], whereby the sequence -Phe-Aad-Val-Val- was predicted as likely. Aad is the non-proteogenic amino acid 2-aminoadipicacid, and the prediction was "Aad-like". The UHPLC-DAD-HRMS data deduced the molecular formula to be $C_{34}H_{45}N_5O_5$, which was in some agreement with this prediction, though with some doubt about the Aad-like moiety. Even though the assembly of nidulanin A, could be predicted, structure elucidation was still necessary to complete the structure and to investigate the location of the isoprene unit.

4.2.2 Structure elucidation of nidulanin A

Purification and structure elucidation of the compound indeed confirmed this to be a tetracyclopeptide. It was found to have the sequence -L-Phe-L-Kyn-L-Val-D-Val- with an isoprene unit *N*-linked to the amino group of L-kynurenine unit. The absolute structure of nidulans A is depicted in Figure 4.5.

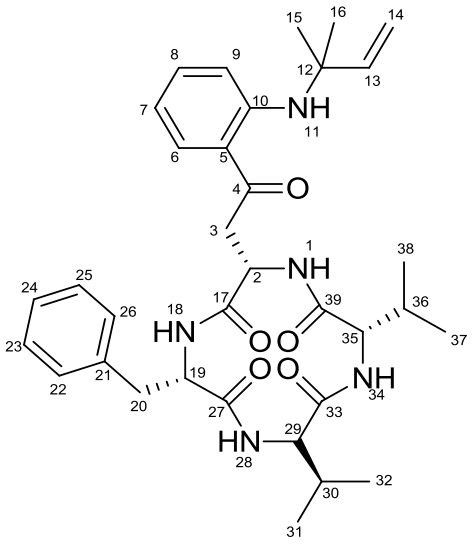

Figure 4.5 The structure of nidulanin A isolated from *A. nidulans*.

The classical approach for structure elucidation of peptides is to use COSY connectivities to link NH and Hα in the same residue and use NOESY connectivities to link NH from one residue to Hα in the neighboring residue. In this way the peptide backbone can be assembled. This approach was also used for nidulanin A. The ^{1}H NMR spectrum displayed four resonances at δ_H 8.16, 7.91, 7.64, and 7.51 ppm, which were identified as amide protons. For each resonance, a COSY correlation to a proton further up-field in the α-proton area could be observed. This coupled each of the amide protons to Hα protons at resonances of δ_H 4.82, 3.92, 4.56, and 3.85 ppm, respectively. Investigation of the NOESY connectivities allowed for assembling of the peptide backbone, which revealed a cyclical tetrapeptide as illustrated in Figure 4.6. The amino acids Phe and the two Val residues were elucidated by use of the COSY, HSQC and HMBC experimental data. The prenylated Kyn residue consisted of three different spin system as well as two isolated methyl groups. These were linked together by the NOESY and HMBC connectivities as depicted in Figure 4.6. The first spin system consisted of the amide proton at δ_H 8.16 ppm, the Hα proton at 4.82 ppm, and a diastereotopic pair of protons at δ_H 3.63 (1H, dd, 17.7, 9.7) and 3.09 (1H, dd, 17.6, 4.9) ppm. The second spin system consisted of four

aromatic protons at δ_H 7.79 (1H, dd, 8.2, 1.5), 7.28 (1H, ddd, 8.6, 7.0, 1.5), 6.81 (1H, dd, 8.7, 0.7), and 6.57 (1H, ddd, 8.6, 7.0, 1.1) ppm, whereas the third and final spin system contained three protons located in the double-bond area at δ_H 5.95 (1H, dd, 17.6, 10.7), 5.13 (1H, dd, 10.7, 1.0), and 5.15 (1H, dd, 17.6, 1.0) ppm. The latter was shown to be connected to the two methyl groups at δ_H 1.39 (3H, s) and 1.38 (3H, s) ppm, and the presence of a quaternary carbon at δ_C 53.7 ppm linked this part as an isoprene unit.

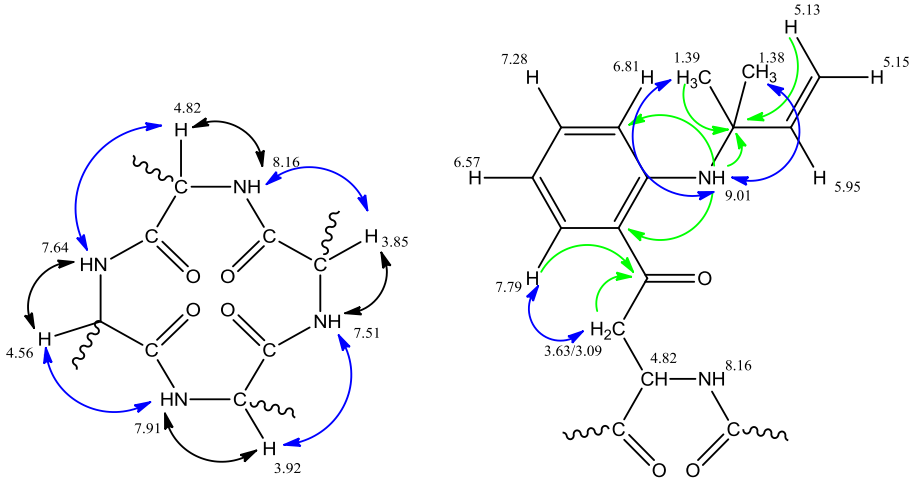

Figure 4.6 COSY (black) and NOESY (blue) connectivities that lead to the cyclic tetrapeptide, as well as the key HMBC (green) and NOESY connectivities used to link the different spin system.

To obtain the absolute stereochemistry of nidulanin A, Marfey's analysis was conducted. This is widely used for NRPs since this approach can differentiate between L- and D-amino acids (AAs). The derivation agent is 1-fluoro-2,4-dinitrophenyl-5-L-alanineamide (FDAA), also called Marfey's reagent and can react with AAs to give a diastereomer. L- and D AAs are enantiomers and can consequently not be distinguished on a HPLC setup; Marfey's derived diastereomer can. NRPs can therefore be hydrolyzed, reacted with FDAA and a comparison to Marfey's derived enantiomeric pure D- and L-AAs will thereby reveal the stereochemistry [193][194].

For the case of nidulanin A, Marfey's analysis was able to confirm the Phe residue present as L-Phe, whereas the analysis for Val showed equal amounts of L- and D-Val. As no standards for L- and D-Kyn was available, this was not investigated. These results did, however, not clarify which of the Val residues was L-form and which was in the D-form. The final proposal for the stereochemistry of nidulanin A was therefore given as a combination of the experimental data from Marfey's analysis and the bioinformatic studies. The latter predicted the Phe, Kyn and first Val module not to contain an

epimerase domain, while the last Val module did contain an epimerase domain. This resulted in the sequence -L-Phe-L-Kyn-L-Val-D-Val- which is also depicted in Figure 4.5.

The result found in this work illustrates how close collaboration of two fields: bioinformatics and structural chemistry, can lead to discoveries that neither could have achieved separately. The stereochemistry of nidulanin A was in the end suggested based on the results from both bioinformatic analysis and results of Marfey's analysis. Furthermore the study illustrates how fungal NRPs can be predicted, due to their modular nature. Fungal PK pathways are more complicated, since the PKSs are functioning in an iterative way, and other experiments are needed, which will be demonstrated in the following two sections in elucidation of the PK 6-MSA related pathways in *A. niger* and *A. aculeatus*, respectively.

4.3 *Aspergillus niger*

This section presents the manuscript "Molecular and chemical characterization of the biosynthesis of the 6-MSA derived meroterpenoid yanuthone D in *Aspergillus niger*" (Paper 9), published in Chemistry & Biology in 2013.

The study was carried out in close collaboration with PhD Dorte Koefoed Holm and investigated the biosynthetic pathway of the meroterpenoid yanuthone D in *A. niger*. A multidisciplinary approach for solving the biosynthetic pathway was employed, applying gene deletions, heterologous gene expression, analytical chemistry covering UHPLC-DAD-MS and MS/MS, structure elucidation by NMR spectroscopy and CD, as well as feeding experiments with labeled and unlabeled metabolites. As a result the cluster responsible for production of yanuthone D was identified, 6-MSA was determined as the precursor, the biosynthetic pathway for yanuthone D, where 6-MSA is converted into yanuthone D in eight steps, was presented, a novel enzymatic activity, an O-mevalon transferase, was found, six novel structures were characterized and finally a novel class of yanuthones (class II yanuthones) was defined, which utilizes some of the enzymes from the cluster, but does not origin from 6-MSA. Altogether the paper represents a major step forward in understanding the complex secondary metabolism in the industrially important filamentous fungus *A. niger*.

Following this work we investigated the possible production of other analogues of class II yanuthones in *A. niger*. We scrutinized the *A. niger* KB1001 strain for other yanuthones and were able to isolate four further yanuthones, whereof one was a class II yanuthone. This resulted in the manuscript "Characterization of four novel antifungal yanuthones from *Aspergillus* niger" (Paper 10), published in Journal of Antibiotics in 2014.

4.3.1 The biosynthesis of yanuthone D

Our investigations of the biosynthesis of yanuthone D in *A. niger* originated with the gene PKS48/ASPNIDRAFT_44965 which had been predicted to encode a 6-MSA synthase [81]. The gene was transferred to our model organism *A. nidulans* into the integration site IS1 [83], which verified that the gene was indeed encoding a 6-MSA synthase as 6-MSA was produced. Next the gene was deleted in *A. niger*. This step was eased by the use of the ATCC1015-derived strain KB1001 (pyrGΔ kusA::AFpyrG). This resulted in abolishment of not just one, but two major *A. niger* metabolites: Yanuthone D and E were both depending on the 6-MSA synthase. In order to elucidate the entire biosynthetic pathway we predicted and deleted the genes surrounding the 6-MSA synthase gene. From

UHPLC-DAD-HRMS analysis of the resulting deletion strains we were able to deduce the boundaries of the gene cluster. Additionally eight genes were needed for yanuthone D production and a TF gene was also linked to the cluster resulting in a total of 10 genes in what was named the *yan* gene cluster. In the elucidation of the biosynthesis of yanuthone D, three deletion strains were essential: Δ*yanH*, Δ*yanI*, and Δ*yanF*. Large scale extracts were prepared of the three strains for purification and structure elucidation of intermediates, see Figure 4.7.

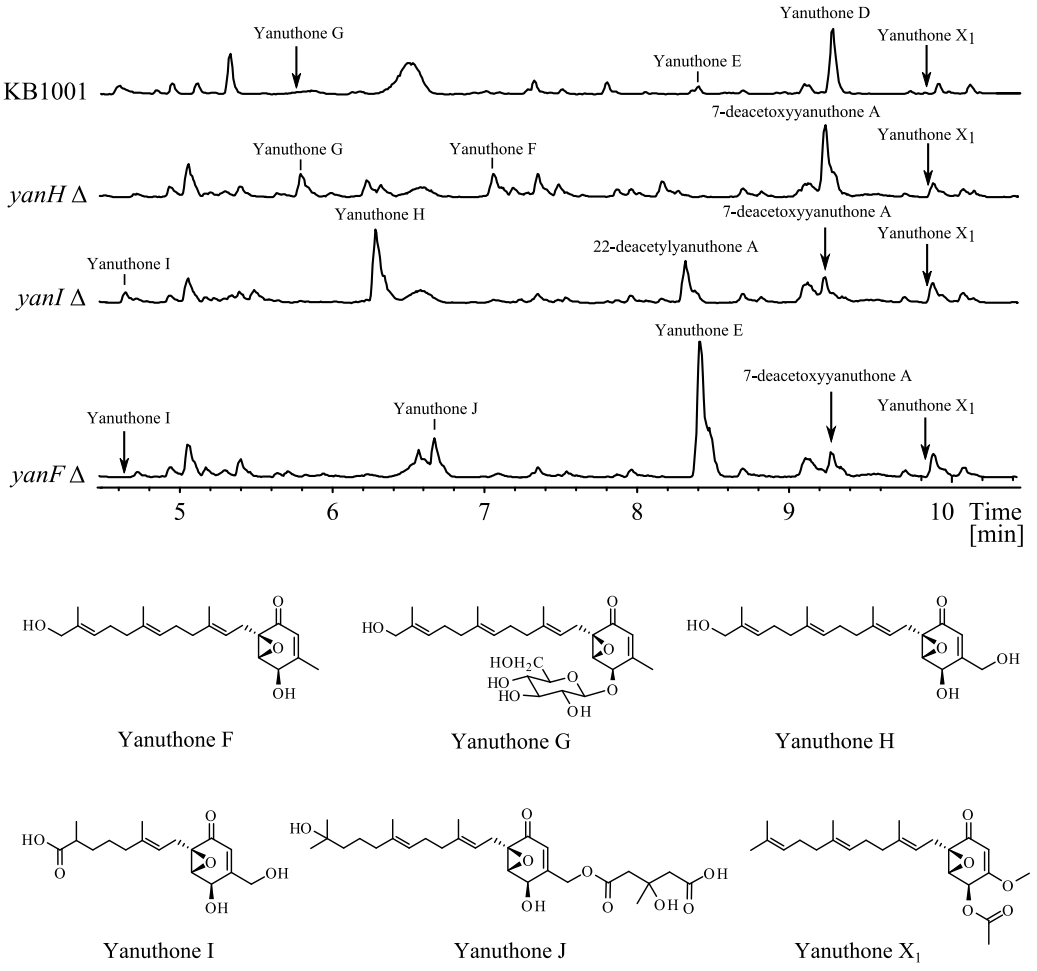

Figure 4.7 BPC *m/z* 100-1000 of reference strain (KB1001), *yanH*Δ, *yanI*Δ, and *yanF*Δ. All NMR-elucidated compounds are shown for comparison of intensity and relative retention times. Below are structures of the novel yanuthones identified in this study. The structures of the remaining yanuthones are seen in Figure 4.8.

From the Δ*yanF* strain we learned that YanF converts yanuthone E into yanuthone D, which we could conclude was the true end product of the pathway. From the Δ*yanH* and Δ*yanI* strains, we purified the intermediates 7-deacetoxyyanuthone A and 22-deacetylyanuhone A respectively. These were key intermediates, and led to understanding

of the oxidating specificity of the cytochrome P450 YanH and the O-mevalon transferase YanI. Thereby the biosynthesis from 6-MSA to yanuthone D was deduced (Figure 4.8).

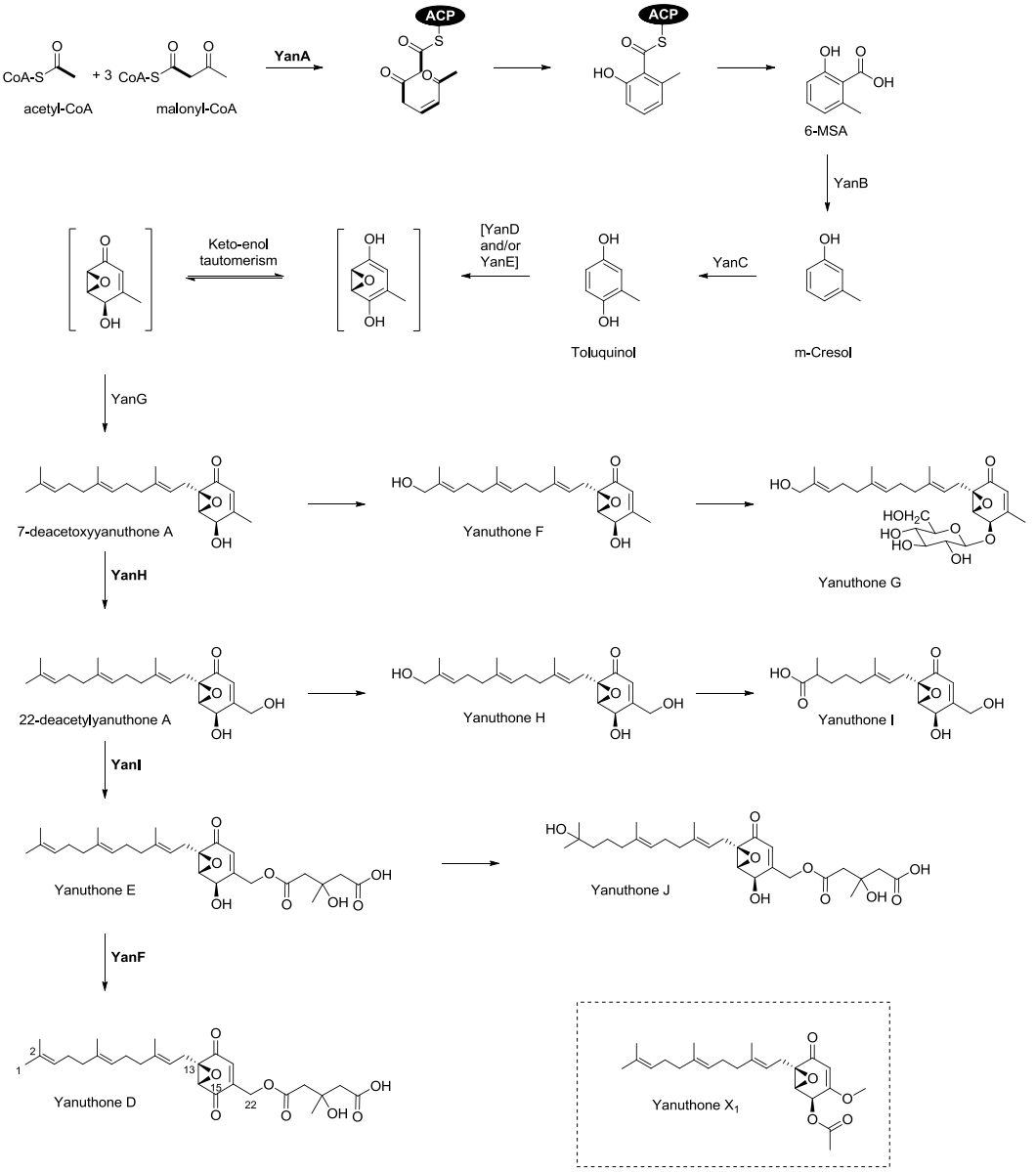

Figure 4.8 Proposed biosynthesis of yanuthone D. Structures and enzymatic activities in brackets are hypothesized, activities in plain text have been proposed from bioinformatics, and activities in bold have been experimentally verified. The structure of yanuthone X_1, utilizing YanC, YanD, YanE and YanG, is showed for reference.

An important part of the investigation of the biosynthesis of yanuthone D was the feeding experiments using fully labeled $^{13}C_8$-6-MSA. First and foremost the experiment was necessary to establish 6-MSA as a precursor for yanuthone D and later to establish exactly which yanuthones utilized 6-MSA. The execution of this experiment

demonstrated the interdisciplinary approach we utilized, and the strengths of several specialists working together. When we learned we needed fully labeled $^{13}C_8$-6-MSA, we found that this was not commercially available. Instead we had to produce it ourselves, starting with the molecular biology work of creating a 6-MSA producing *A. nidulans* strain, followed by fermentation using fully labeled glucose, purification of the product and finally the feeding experiments and HRMS analysis.

4.3.2 Verification of intermediates

A major challenge in the investigation of the biosynthesis of yanuthone D, was the lack of detecting any of the smaller intermediates preceding 7-deacetoxyyanuthone A, Figure 4.8. No intermediates were detected in either of the yanB, yanC, yanD, yanE and yan G deletion strains. To address this problem we tried optimizing our detection of small compounds (< 200 Da) on the UHPLC-DAD-HRMS setup, but as these efforts did not provide new information and since we could easily detect 6-MSA in the *A. nidulans* strain where we integrated the 6-MSA synthase gene, it became evident that it was not a problem of detecting these compounds, rather they were simply not present. We did not at any time detect 6-MSA or any of the other small aromatic compounds (e.g. *m*-cresol or toluqinol) in any *A. niger* deletion strain, and we suggest that they are toxic to the cell, why they are rapidly degraded, converted into other compounds, or they may be incorporated into insoluble material such as the cell wall.

To gain information about this part of the biosynthesis, we instead used bioinformatics and feeding experiments. In the biosynthesis of patulin in *A. floccosus* (previously identified as *A. terreus*; Jens C. Frisvad, personal communication) and in *A. clavatus*, 6-MSA is decarboxylated into *m*-cresol by the decarboxylase PatG and then further modified into toluquinol by the cytochrome P450 PatI [195][196]. Inspection of the *yan* gene cluster for similar activities resulted in the putative 6-MSA decarboxylase (YanB) and a cytochrome P450 (YanC). This suggested that *m*-cresol and toluquinol could be likely intermediates. To verify this we fed the two compounds to the *yanA* deletion strain and a subsequent analysis of the metabolic profile revealed that addition of either of the two compounds, restored production of yanuthone D, see Figure 4.9.

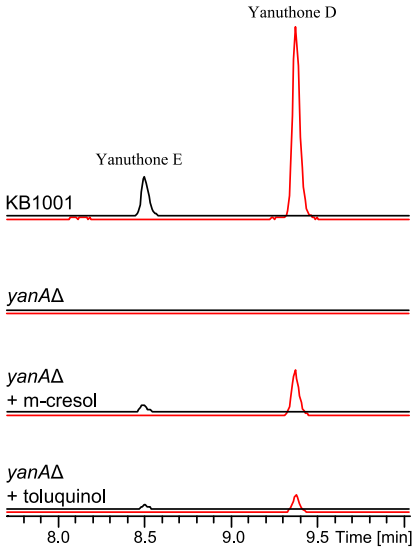

Figure 4.9 Feeding with unlabeled *m*-cresol and toluquinol. EICs of yanuthone D (1) 503.2640±0.005 (red) and yanuthone E (2) 505.2791±0.005 (black) for KB1001 and the *yanA*Δ strain with and without feeding. Chromatograms are to scale.

Besides this evidence for *m*-cresol and toluquinol as intermediates, we observed that the 6-MSA production in the heterologous expression of YanA in *A. nidulans* would disappear if the strain also expresses YanB. This also indicated that 6-MSA was the substrate for the putative 6-MSA decarboxylase YanB.

The intermediates and exact mechanisms from toluquinol to 7-deacetoxyyanuthone A including formation of the epoxide remain unclear, but could be investigated by purification of YanD and YanC followed by in vitro experiments with toluquinol.

4.3.3 Branching points reveals novel yanuthones

In the elucidation of the biosynthesis of yanuthone D, three deletion strains were central: Δ*yanH*, Δ*yanI*, and Δ*yanF*. Large scale extracts of the three strains were prepared for purification and structure elucidation of intermediates. The intermediates 7-deacetoxyyanuthone A, 22-deacetylyanuhone A and yanuthone E were discovered from the three strains respectively, and were key intermediates in the elucidation of the pathway, as well as revealing the enzyme functions of YanH, YanI and YanF.

A common trend for all three strains was that not only one new intermediate would be produced; rather 2-3 different intermediates were observed in each extract. This led to several branching points in the biosynthesis, as displayed in Figure 4.8. All three intermediates in the three different strains were oxidized: 7-deacetoxyyanuthone A and

22-deacetylyanuhone A at C1 resulting in yanuthone F and yanuthone H respectively, while yanuthone E was oxidized at C2 leading to yanuthone J.

It is interesting to note that a disruption of the biosynthetic pathway toward yanuthone D results in formation of branch points, and in all cases, the first step is an oxidation of the sesquiterpene ether on C1 or C2. Since hydroxylation is a known detoxification mode [197], we speculate, if the abnormally high amount of potentially toxic intermediates, triggers the cell to initiate phase I type of detoxification processes, in which the toxic intermediates are hydroxylated. This hypothesis is supported by the fact that we could not link any enzyme to the hydroxylation processes.

Besides the hydroxylated intermediates one further compound was found in each of the *yanH* and *yanI* deletion strains. A variant of yanuthone F was identified in the *yanH* deletion strain, in which yanuthone F is glycosylated at the hydroxyl group at C15 to form yanuthone G. The glucose moiety of yanuthone G is intriguing because sugar moieties are rare in fungal SMs. Besides detecting the compound in the deletion strain we also detected it in the KB1001 strain, which shows that it is a naturally occurring compound. Because yanuthone G production is upregulated in *yanH* deletion strain, we suggest that glycosylation poses a second (phase II conjugation) type of mechanism for further detoxification of possible toxic intermediates.

Another variant of 22-deacetylyanuthone A, besides the oxidized yanuthone H, was detected in the *yanI* deletion strain. Yanuthone I, is identical to 22-deacetylyanuthone A and yanuthone H but with a shorter and oxidized sesquiterpene chain. A similar modification has been observed in the biosynthetic pathway for production of mycophenolic acid [198]. In the mycophenolic acid pathway it was proposed to occur by oxidative cleavage between C4 and C5 of the sesquiterpene chain, which could also be the case here, but alternatively, it could occur by terminal oxidation of a geranyl side chain.

4.3.4 The diversity of yanuthones in *Aspergillus niger*

It has earlier been reported how heterologous expression of a whole pathway revealed eight compounds in addition to the one already known from the pathway [199] (One pathway, many compounds). The biosynthetic potential of a single pathway was also demonstrated in this work in the native organism: In the elucidation process of the biosynthesis of yanuthone D, a total of nine yanuthones were purified from four different strains, Figure 4.8. We showed that all of these were derived from the small aromatic PK

6-MSA both by feeding fully labeled $^{13}C_8$-6-MSA into the yanuthones in vivo, but also by investigation of the 6-MSA synthase gene deletion strain, where production of the compounds were shown to be abolished. One further compound, yanuthone X_1, was also purified, and the structure elucidation revealed a structure very similar to the known yanuthones, see Figure 4.8. This compound was still present in the 6-MSA synthase gene deletion strain and the feeding studies showed that 6-MSA was not incorporated. This revealed, that not all yanuthones depend on 6-MSA and we therefore defined two classes of yanuthones: those based on 6-MSA (class I) and those who are not (class II).

It was very interesting for us to learn that the two classes share several enzymatic steps: Yanuthone X_1 was depending on YanC, YanD, YanE and YanG. Together this suggests that the precursor is a small aromatic compound similar to 6-MSA, but lacking the carboxylic acid, since it did not depend on the enzymatic activity of YanB, the decarboxylase. For instance it could be anisole, known to be produced by several *Aspergillus* species, or 3-methoxy phenol.

Importantly, the main difference between yanuthone X_1 and the other yanuthones are the group attached to C16. In the case of yanuthone X_1, this position is oxidized, whereas in other yanuthones there is a carbon-carbon bond that originates from the methyl group of 6-MSA. Consequently, yanuthone X_1 cannot be mevalonated by YanI wherefore there is no class II analog with the mevalon side chain.

In continuation of the study of yanuthone D biosynthesis, further four yanuthones were purified from the *A. niger* KB1001 strain: Yanuthone K-M, all class I yanuthones and yanuthone X_2, which we showed was a class II yanuthone.

Some of the yanuthones described in this study were only discovered as a consequence of the deletion strains: accumulation of intermediates and the branching points, as described in section 4.3.3. A great number was, however, found in the reference strain of *A. niger*. This included yanuthone D and E, yanuthone G and I in trace amounts, yanuthone K-M and both of the class II yanuthones, yanuthone X_1 and X_2. On top of, this *A. niger* has previously been reported to produce yanuthones A, B, and C, 1-hydroxyyanuthone A, 1-hydroxyyanuthone C, and 22-deacetylyanuthone A [35]. The great variety of the yanuthones from a single species, plus the fact that yanuthone D is one of the main metabolites being produced of all compounds from *A. niger*, point towards that these compounds have a great significance for the organism.

We tested all 14 yanuthones towards the pathogenic yeast *Candida albicans*, which accounts for the highest source of fungal infections worldwide [200], wherefore it is of great interest to find new drug candidates. The result of the assay is displayed in Figure 4.10.

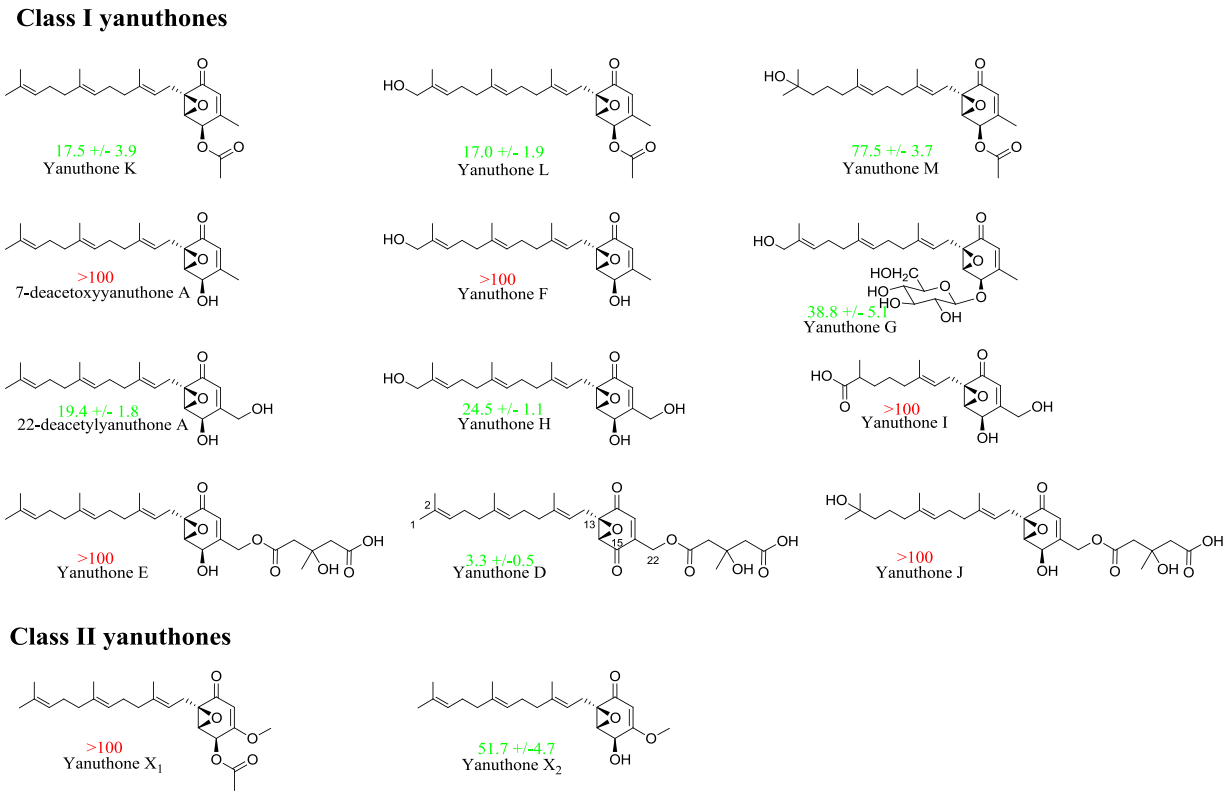

Figure 4.10 Overview of class I and II yanuthones as well as their IC_{50} towards *Candida albicans*.

Our analysis identified yanuthone D as the most active compound, justifying it as the end product of the pathway. Otherwise several of the yanuthones displayed antifungal activities and due to the vast number tested, we gained valuable insights to structural features important for the potency towards *C. albicans*. A discussion on this topic can be found in Paper 9, but in summary we learned that the ketone at C15 for yanuthone D was of high importance for the activity. Hydroxylation of C22 and acetylation at C15 would increase the antifungal activity, while chain shortening of hydroxylation of C2 would decrease activity. This work demonstrates the strengths of having several natural analogs, to accommodate structure-activity relationship to identify key structural features for potency.

4.4 *Aspergillus aculeatus*

This section presents the manuscript "Investigation of a 6-MSA synthase gene cluster in *Aspergillus aculeatus* reveals 6-MSA derived aculins A-B and non-6-MSA derived pyrrolidinones" (Paper 11), intended for publication in Chemistry & Biology.

In parallel to the elucidation of the biosynthetic pathway from 6-MSA to yanuthone D in *A. niger* (section 4.3), a putative 6-MSA synthase was identified in *A. aculeatus*. We investigated the 6-MSA pathway in *A. aculeatus*, which turned out to be quite different from the yanuthone pathway. The results are described in this section.

4.4.1 Investigation of 6-MSA synthase gene

To verify that the putative 6-MSAS gene encoded a 6-MSA synthase, the gene was integrated into the IS1 locus of *A. nidulans.* Comparative metabolic profiling (see Figure 4.11) of the resulting strain to a reference strain by UHPLC-DAD-HRMS indeed confirmed the 6-MSAS gene, as production of 6-MSA could be verified by comparison to an authentic standard.

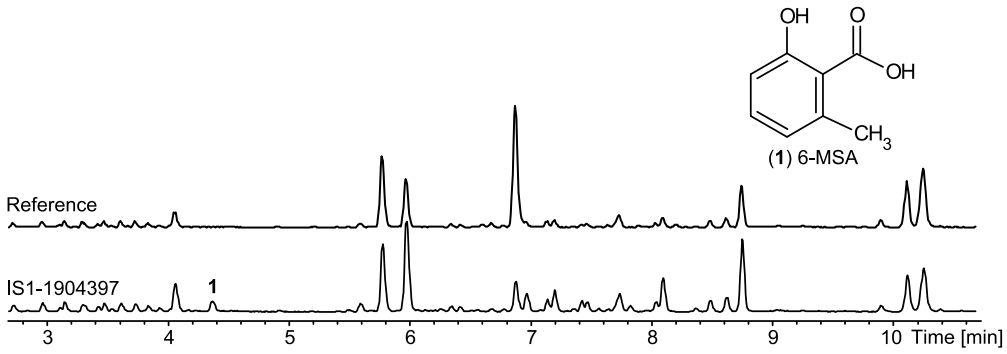

Figure 4.11 BPC of the *A. nidulans* strain expressing the putative 6-MSA synthase 1904397 compared to an *A. nidulans* reference.

We further investigated the 6-MSA synthase gene. We hypothesized that over-expression of the 6-MSAS would result in an up regulation of the end product of the pathway, either revealing a new compound or higher amounts of a known compound. The gene was expressed in *A. aculeatus* from an AMA1-based plasmid. The metabolic profile analysis verified that the strain produced 6-MSA (not normally produced by *A. aculeatus*), but otherwise there were no significant changes observed in the rest of the metabolite profile.

4.4.2 Over-expression of transcription factor

Examination of the predicted gene cluster revealed that a putative TF was located immediately downstream of the 6-MSA synthase gene, why this could possibly be a regulator of the 6-MSA gene cluster. When the TF was overexpressed by AMA-1 based plasmids, two compounds were affected on MM, see Figure 4.12.

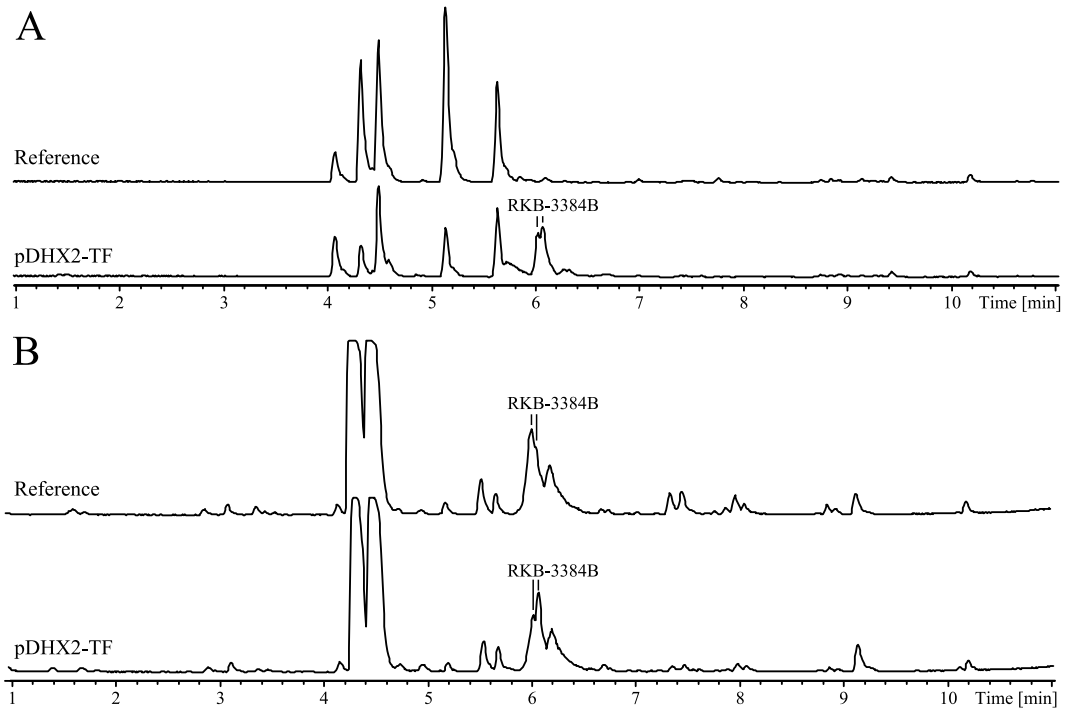

Figure 4.12 BPC of *A. aculeatus* expressing putative transcription factor from plasmid (pDHX2-TF) compared to a reference, cultivated on minimal medium (A) and YES (B).

The two compounds were structure elucidated to be diastereomers of RKB-3384B [201]. They were produced by both the reference strain and the TF overexpression strain, when cultivated on YES, indicating that the biosynthesis of these compounds is normally active when cultivated on YES medium, but not on minimal medium. The two compounds only differ by the stereochemistry at one or both of the stereocenters, see Figure 4.13.

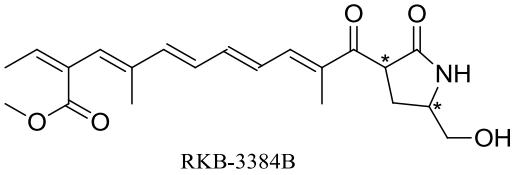

RKB-3384B

Figure 4.13 The isolated compounds are diastereomers of RKB-3384B. Stereocenters are marked with *.

The backbone of the compounds have previously been observed e.g. in lucilactaene produced by a *Fusarium sp*. [202], epolactaene from a marine *Penicilium sp*. [203] and fusarin C from *Fusarium moniliforme* [204]. All of these compounds contain the long chain observed in RKB-3384B, but differs in the attached moiety. Lucilactaene contains two fused five-membered rings, epolactaene a single five-membered lactam entailing an epoxide, and the fusarins display different structures. The biosynthesis of the backbone chain has been investigated by labeling studies for the fusarins, which verified that it was of PK origin [205]. Furthermore, labeling and genetic studies [206] showed that the final part originates from a C_4-unit. Assuming that RKB-3384B has the same PK chain, the final part must consist of a nitrogen-containing C_3 unit e.g. serine.

4.4.3 Identification of 6-MSA related compounds

Based on the structure of RKB-3384B, a connection to 6-MSA was not immediately obvious. For the 6-MSA derived pathway in *A. niger* the end product of the pathway was established by gene deletion of the 6-MSA PKS gene. Gene deletions were not easily obtained in *A. aculeatus*, wherefore the biosynthetic pathway could not be investigated with the same approach. Instead, we fed fully labeled 6-MSA ($^{13}C_8$-6-MSA) to the strain to test whether 6-MSA was incorporated into the RKB-3384B diastereomers, see Figure 4.14.

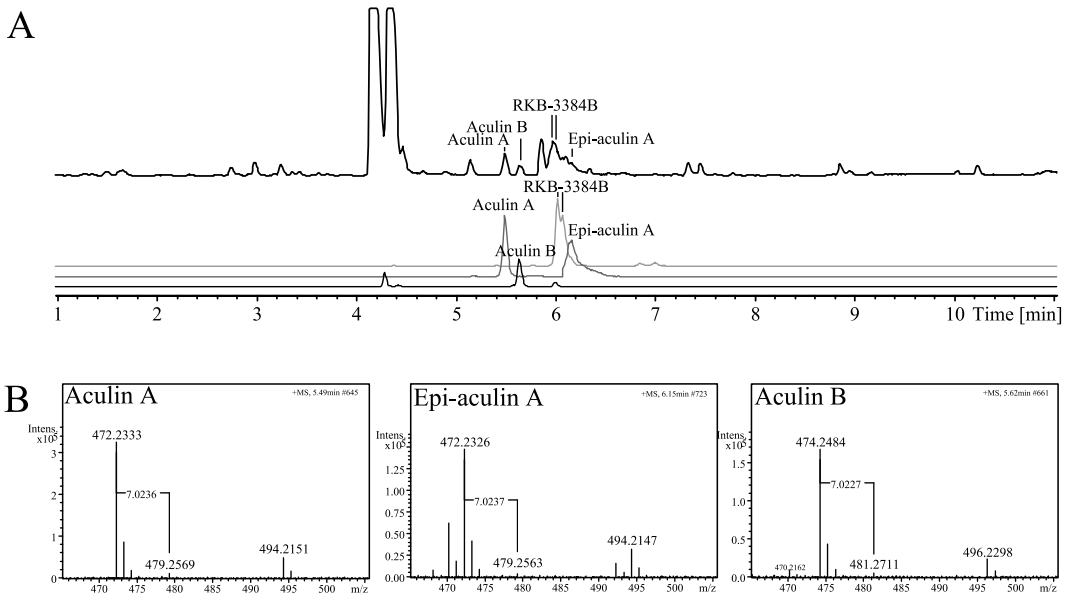

Figure 4.14 A. BPC (black) of pDHX2-TF on YES+$^{13}C_8$-6-MSA, EIC 374.1963±0.005 (light grey), EIC 472.2333 ± 0.005 (dark grey), EIC 474.2484 ± 0.005 (black). **B.** Mass spectra of the 6-MSA incorporating aculins.

Careful inspection of the metabolite profile revealed a mass shift of 7.023 Da for three related compounds, which we named aculins. Interestingly, but not surprisingly, 6-MSA was not incorporated into the diastereomers of RKB-3384B. Thus these compounds do not origin from 6-MSA although production of the two compounds appeared to be activated by expression of the TF located immediately downstream of the 6-MSA synthase gene. We therefore hypothesized the TF to be unrelated to the 6-MSAS and pathway.

We now turned our attention to the 6-MSA incorporating compounds. The fact that a mass shift equivalent of seven ^{13}C atoms, and not the eight ^{13}C atoms that are present in $^{13}C_8$-6-MSA, suggests that one carbon atom is eliminated from 6-MSA during modification into the end products. A mass shift of 7.023 Da was also observed in feeding studies of the yanuthone D biosynthesis, where one carbon atom is eliminated from 6-MSA by decarboxylation (section 4.3, Paper 9).

Isolation of the 6-MSA related compounds was challenging as the compounds degraded even at the mildest conditions during purification. It is noted that a similar trend was observed for the acu-calbistrins (section 3.1.1 and Paper 1), also produced by *A. aculeatus*. In the case of the aculins, aculin A these were degrading to a small acid (present as two diastereomers) and aculene A, a compound characterized from *A. aculeatus* (section 3.1.1 and Paper 1), see Figure 4.15. Likewise aculin B was degrading to aculene B and the same small acid. Although impossible to isolate the aculins, we solved the structure of the degradation products, see Figure 4.15.

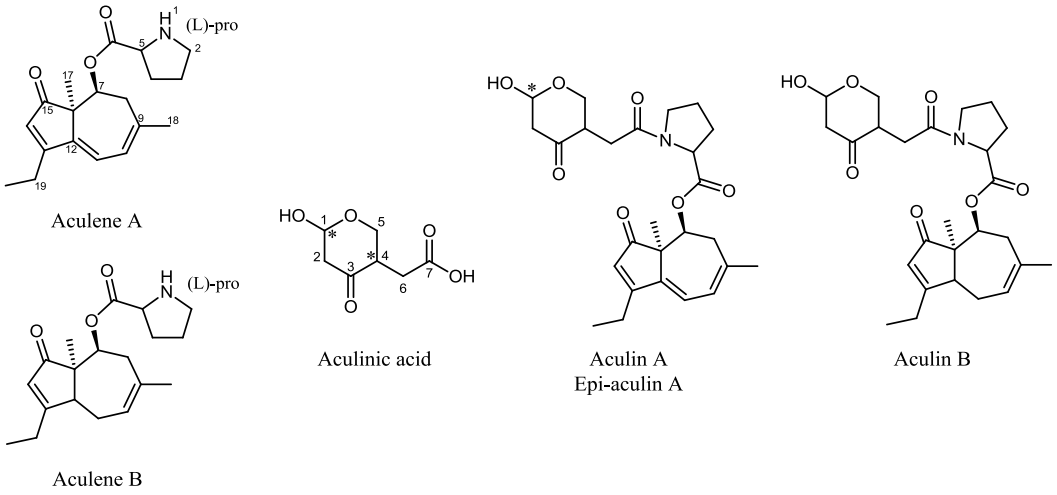

Figure 4.15 Structures of the degradation products of the aculins: Aculenes A-B and aculinic acid, and the suggested structure of the aculins.

The fragments were structure elucidated by 1D and 2D NMR from a mixture of aculin A and the degradation products, whereby a suggestion for their structures could be given. Resonances, identical to those we observed for aculene A, were identified as well as two set of signals for a smaller compound, we identified as aculinic acid. We suggest the two structures to be alike, and only differing at the stereocenter at C1. The degradation products of aculin B have not been confirmed by NMR experiments, but have been verified by UHPLC-DAD-HRMS data.

4.4.4 Biosynthetic pathway from 6-MSA

The 6-MSA synthase gene and surrounding genes are depicted in Figure 4.16. We define the *acu* gene cluster as the genes *acuA-acuI* spanning 23.6 kb with no disruption from unrelated genes.

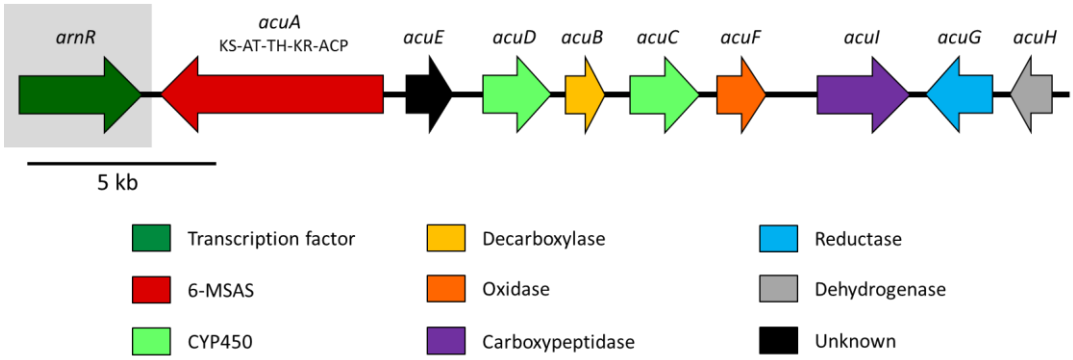

Figure 4.16 The *acuA* 6-MSA synthase encoding gene is flanked by eight genes, which we define as the *acu* gene cluster. The *arnR* TF is not part of the *acu* cluster, but is located immediately upstream of *acuA*.

Utilizing knowledge of the two other 6-MSA derived pathways towards yanuthone D [207] and patulin [196], as well as the predicted activities encoded by the *acu* cluster, we proposed the biosynthetic pathway from 6-MSA towards aculin A, see Figure 8.

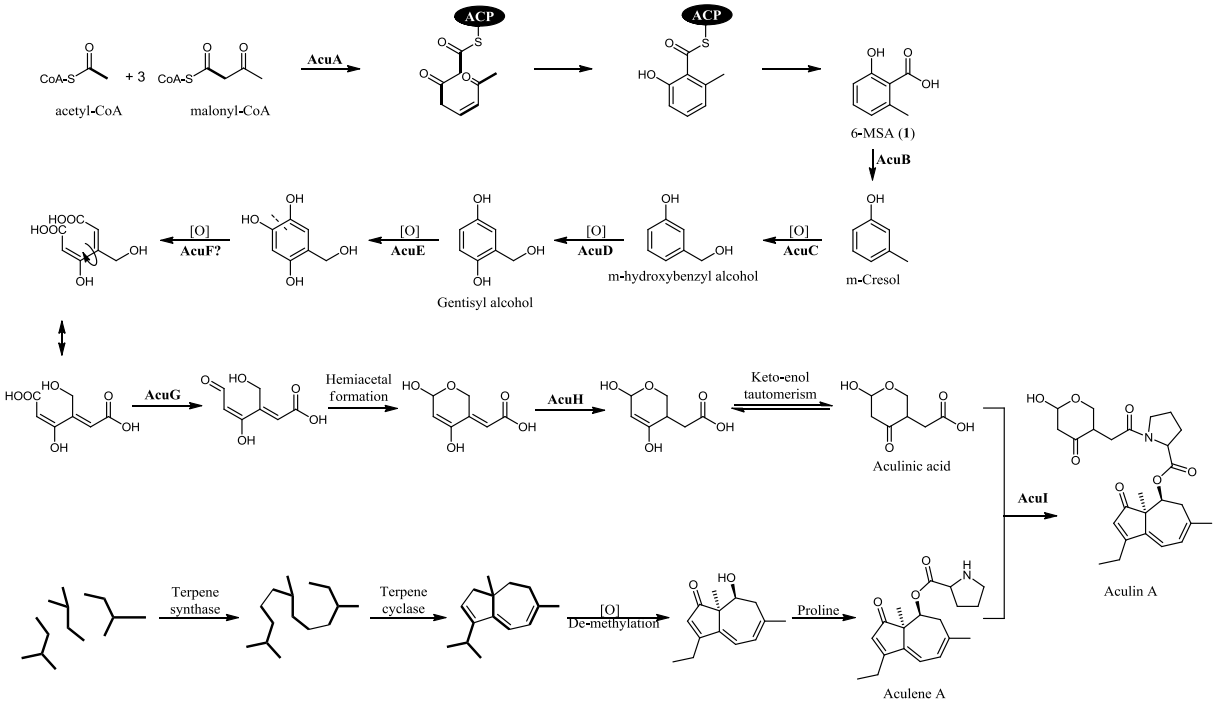

Figure 4.17 Proposed biosynthetic pathway of aculin A.

Many of the enzymatic steps could be justified by high homologies to enzymes from the yanuthone D and patulin pathways. It is also noted that aculinic acid has a high resembles to neo-patulin, which only differs by having an additional double bond and a lactone formed from the oxygen at C3 to the carboxylic acid.

The elucidation of the *A. aculeatus* 6-MSA derived pathway proved more challenging than the 6-MSA pathway in *A. niger*. This was a consequence of both molecular biology challenges (deletions not easily obtained) and chemical challenges (degradation of the end products). Nonetheless we were capable of proposing a biosynthetic pathway from 6-MSA to aculin A, based on structures of the precursor and proposed end product as well as the predicted enzymatic activities of the cluster. Two diastereomers of RKB-3384B were found to be unrelated to the *acu* gene cluster, but none the less overexpression of the TF led to upregulation of the compounds on MM, whereby they caught our attention, and they were discovered as a direct consequence.

4.5 Reconstitution of gene clusters

This section presents previously unpublished work, performed in Professor Yi Tang's research group at UCLA, Los Angeles, USA.

The aim of this work has been to reconstitute entire gene clusters from filamentous fungi in the model organism *A. nidulans*. Many microbes including filamentous fungi have not yet been cultured for investigation of the chemical profile, and of the microbes that have been cultured many are difficult to work with. They can either be difficult to propagate, hazardous to work with or expensive to cultivate. Cloning of genes or even whole gene clusters from these organisms would improve discovery and characterization. The reconstitution of gene clusters has the potential to provide access to the chemical diversity encoded in the genomes of otherwise uncultured filamentous fungi. In this section unpublished results are described, where reconstitution of entire gene clusters from filamentous fungi is investigated by the cytochalasin gene cluster from *A. clavatus*, which has been reconstituted in *A. nidulans.* Further details are presented in Paper 12.

4.5.1 Biosynthesis of cytochalasins

Cytochalasans constitute a class of PK-NRP hybrids containing a highly reduced PK backbone and an amino acid. In a parallel study of this thesis, three cytochalasans were characterized from *A. sclerotioniger*: Sclerotionigrin A, sclerotionigrin B and proxiphomin (Section 3.2.4, Paper 5 and Figure 4.18). Characteristic for the cytochalasans is their tricyclic core consisting of a macrocycle fused to a bicyclic lactam (isoindolone) system. The macrocycle origins from the reduced PK part and can be fused to the isoindolone system by a cyclic ketone, a lactone or a cyclic carbonate. The cytochalasans are classified based on the amino acid incorporated into the PK backbone.

The name origins from Greek and refers to the best known property of the cytochalasans: Kytos (cell) and chalasis (relaxation) refers to the capping of actin filaments [208][209]. The group displays a wide range of biological functions. This is exemplified by the earliest reported cytochalasin A and B [210][211] which can repress glucose transport in human erythrocyte membrane [212] and cytochalasin E, which have been reported to show inhibitory activities towards ovarian, and human colon cancer [159] and possess strong anti-angiogenic activities [213].

A subclass of the cytochalasans is cytochalasins, distinguishing by having the amino acid phenylalanine. The structures of selected cytochalasins are depicted in Figure 4.18.

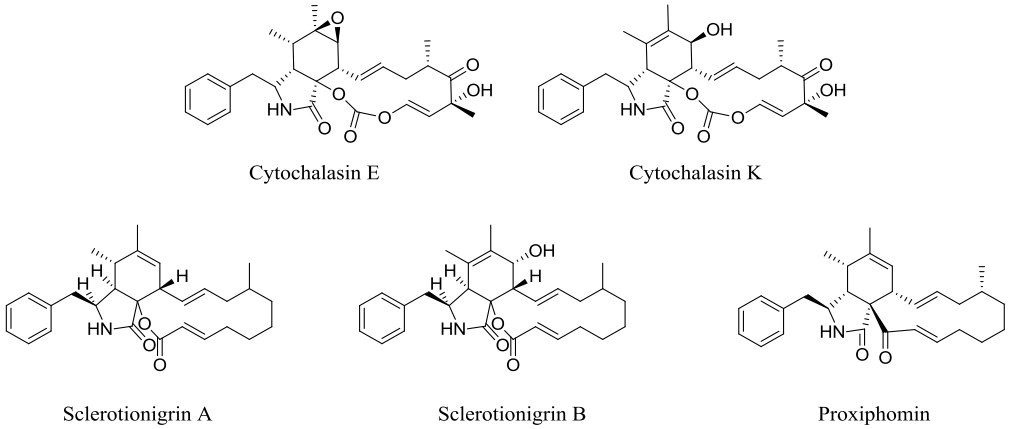

Figure 4.18 Structures of selected cytochalasins. Cytochalasin E and K are known from *A. clavatus* [214], while proxiphomin and sclerotionigrin A and B are known from *A. sclerotioniger*, see section 3.2.4 and Paper 5.

Isotope labeling studies have revealed that the cytochalasans origin from malonyl building blocks as well as amino acid [215][216], suggesting the mixed biosynthetic pathway. The genetic and molecular basis of cytochalasin biosynthesis have been studied by Hertweck and co-workers for chaetoglobosin A, from *Penicillium expansum* [158] and by Tang and co-workers for cytochalasin E and K from *A. clavatus* [214][217]. The biosynthetic genes responsible for cytochalasin production in *A. clavatus* are depicted in Figure 4.19. The genes *ccsA-ccsG* and the TF *ccsR* comprises the *ccs* biosynthetic gene cluster spanning 29,819 kb of DNA.

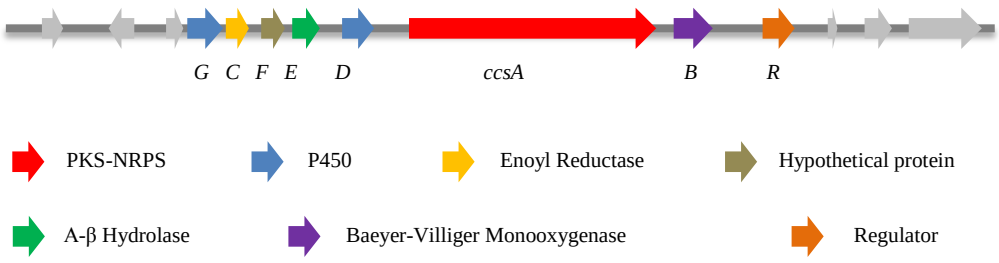

Figure 4.19 Organization of the *ccs* gene cluster in the genome of *A. clavatus* NRRL 1. Adapted from [214].

The proposed biosynthetic pathway towards cytochalasin K is depicted in Figure 4.20. The first step in the biosynthetic pathway is formation of the backbone by the PKS-NRPS (CcsA). A more thorough description of the biosynthesis is given in Paper 12.

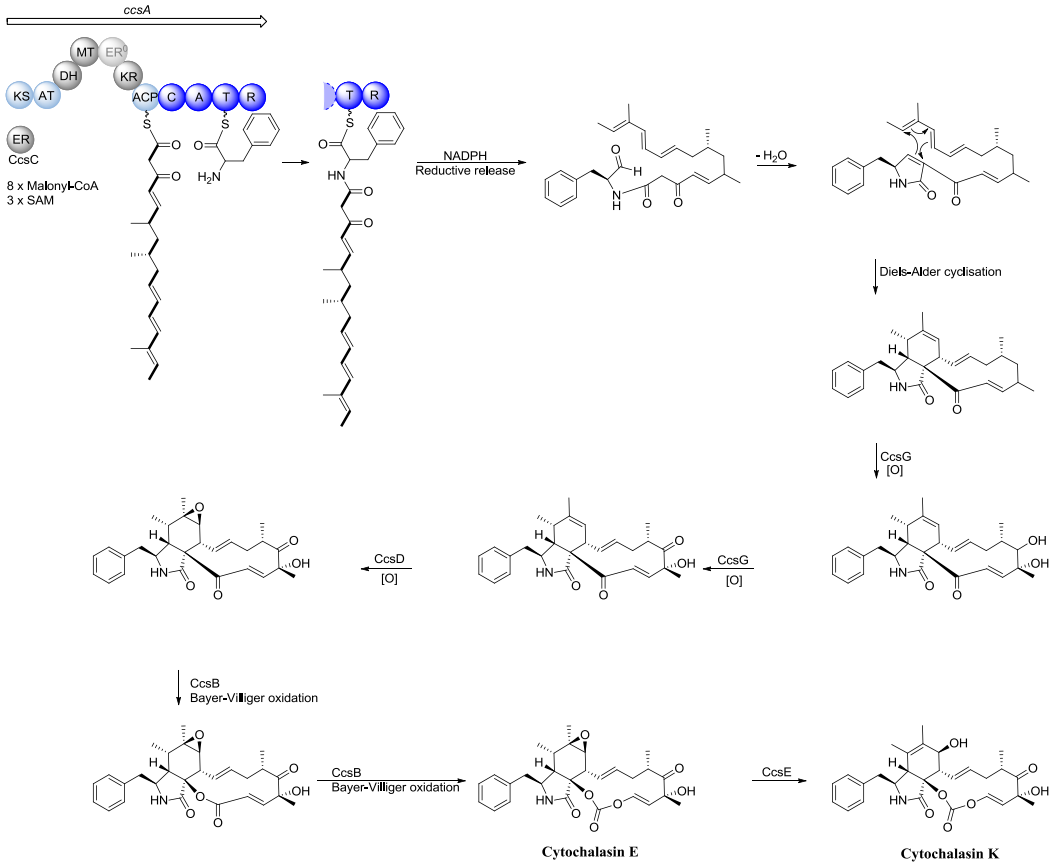

Figure 4.20 Proposed biosynthesis of cytochalasin E. The PKS-NRPS **CcsA** is responsible for formation of the octaketide with incorporation of phenylalanine in combination with **CcsC** a functional enoyl reductase. After release an intramolecular condensation followed by a Diels-Alder cyclisation is forming the tricycle core. The P450s **CcsG** and **CcsD** introduce a hydroxyl group, a keto group and the epoxide. Finally **CcsB**, a Bayer-Villiger oxidase, introduces two oxygens to form the carbonate moiety. **CcsE** converts cytochalasin E to cytochalasin K, while **CcsF** may be involved in a post-PKS-NRPS tailoring, resistance or transport. Adapted from [214].

4.5.2 Transformation-Associated Recombination (TAR)

Transformation-Associated Recombination (TAR) [218][219] is becoming a generically useful tool for reconstructing large biosynthetic gene clusters from gDNA and eDNA [220]. With TAR it is possible to explore large gene clusters (~40 kb) by reassembling them from sets of smaller overlapping fragments in *Saccharomyces cerevisiae*. This yeast is used since it has an extremely efficient DNA recombination system [218]. TAR was developed as a recombinational cloning strategy, to isolate large genomic fragments from human DNA [219][221].

TAR has been used to reassemble eDNA derived type II PKS gene cluster from *Streptomyces albus* for production of fluostatins [222]. General descriptions of how to

recover large NP biosynthetic gene clusters from eDNA using TAR have been described [220] and the TAR approach has been applied to several organisms including human [219][221], mouse [223], fish [224], parasites [225] and bacteria [222].

In this study TAR was used to reconstitute the cytochalasin gene cluster from *A. clavatus* and express it in the model organism *A. nidulans*.

4.5.3 Reconstitution of the cytochalasin gene cluster from *A. clavatus*

A CEN-based vector was designed for transformation in three different organisms: Transformation in *S. cerevisiae*, replication in *E. coli* and transformation in *A. nidulans*. It therefore contained elements for all three organisms. DNA fragments of 5 kb, spanning the entire *ccs* gene cluster, were first amplified by PCR. The primers were designed to create overlapping regions of 150-200 bp between each PCR fragment. This is illustrated in Figure 4.21. The resulting sets of overlapping PCR fragments and the linearized vector, engineered to carry small homolog regions corresponding to regions of the exterior primers, were introduced in *S. cerevisiae* by co-transformation. The fragments and vector undergo recombination to yield a stable plasmid containing the targeted genomic region.

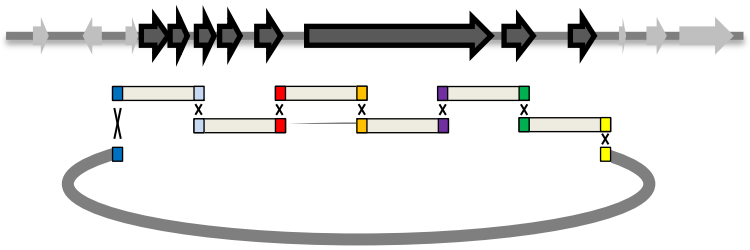

Figure 4.21 General illustration of the cluster reconstitution by PCR amplification and TAR in yeast. Primers are designed to create 150-200 bp overlapping regions between each PCR fragment, and with a 30-50 bp overlapping region to the linearized vector.

The regulator gene *ccsR* was amplified separately and the plasmid was constructed with the strong constitutive promoter *gpdA* followed by the TF encoding gene *ccsR* and then the remaining cluster. The resulting plasmid, pLP1, is depicted in Figure 4.22. The plasmid was verified by four enzymatic digestions, PCR of pieces spanning the cluster and into the plasmid as well as sequencing.

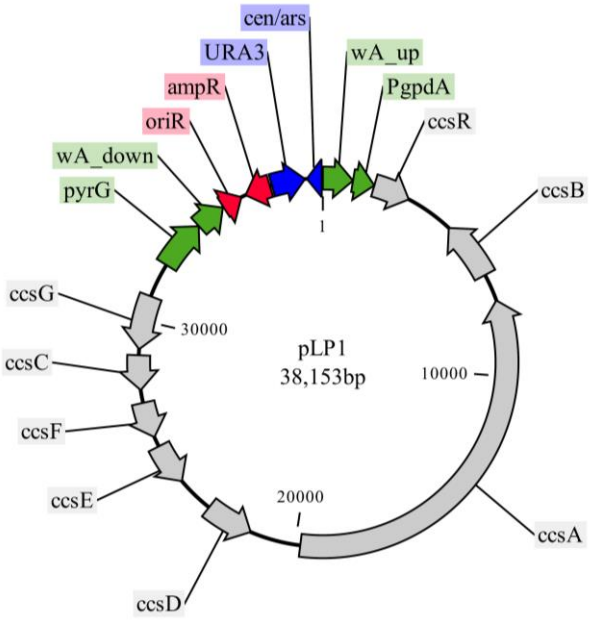

Figure 4.22 The plasmid, pLP1, designed for rapid assembly and transformation in yeast (CEN/ARS, URA3), transformation in *E. coli* (ORI, *ampR*) and for integrative transformation in *A. nidulans* (*pyrG*, *wA* PKS gene targeting sequences). It contains the gpdA promoter directly followed by the TF encoding gene *ccsR* and the remaining *ccs* cluster.

The plasmid was cleaved creating a linearized plasmid for transformation in *A. nidulans*. Transformation in *A. nidulans* was achieved as earlier described [226][8][227], disrupting the WA PKS gene *wA*, responsible for the green melanin production in *A. nidulans*, wherefore transformants appear white.

To determine if the *ccs* cluster was transcribed; RT-PCR analysis was performed. In addition to the PKS-NRPS *ccsA*, all other genes believed to belong to the cluster were transcribed (*ccsB*-*ccsG*). The transformants were incubated on solid and liquid MM and extracted, and the metabolic profile examined by HPLC-MS. EICs of *m/z* corresponding to the sodiated adduct of cytochalasin E and K are depicted in Figure 4.23, from a liquid extraction after three days.

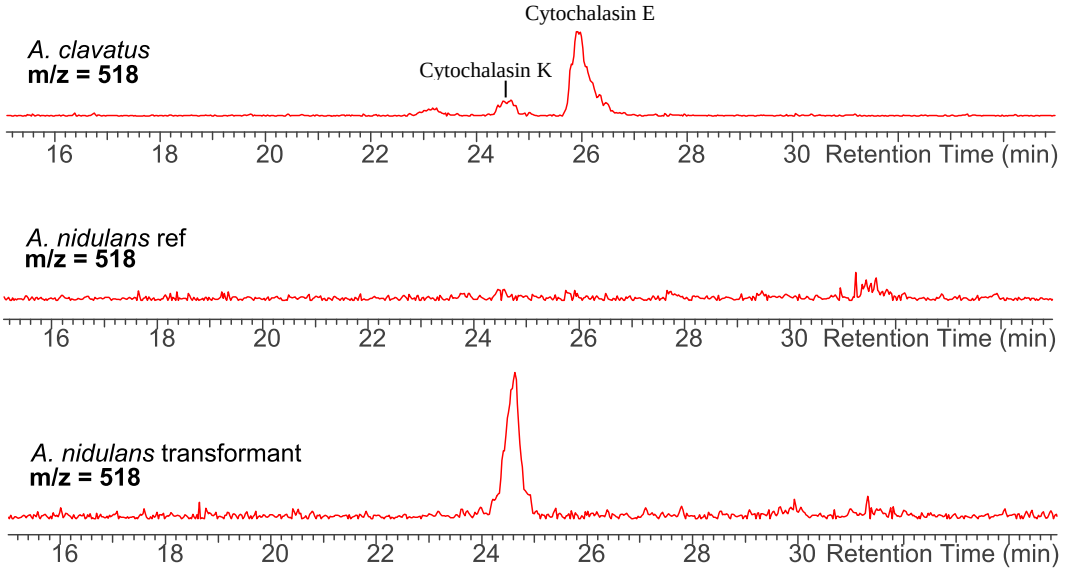

Figure 4.23 EIC of *m/z* = 518 (the most abundant adduct for both cytochalasin E and K, $[M+Na]^+$) in *A. clavatus*, the *A. nidulans* reference and the *A. nidulans* mutant containing the *ccs* cluster.

Cytochalasin E and K have the same molecular formula (see Figure 4.18) and hence the same *m/z* of 518 for the most abundant adduct $[M+Na]^+$. EICs of extracts from the host organism *A. clavatus*, show this was producing small amounts of cytochalasin K and vast amounts of cytochalasin E. In the *A. nidulans* transformants no cytochalasin E was observed, however, cytochalasin K was detected. It is interestingly why cytochalasin E is favored in *A. clavatus*, while it is not produced even in trace amounts in *A. nidulans*. Cytochalasin E could be toxic to *A. nidulans* wherefore the biosynthesis is driven to the end product cytochalasin K. Nonetheless, the *ccs* gene cluster was successfully reconstituted and the end product cytochalasin K produced in *A. nidulans*.

This work demonstrates how TAR can be used to fast and efficiently reconstitute gene clusters from filamentous fungi in the model organism *A. nidulans*. The major remaining challenge is how to express the product in significant amounts.

4.6 Chapter 4 Summary and part conclusion

The theme for this chapter has been to link fungal SMs to their biosynthetic pathways and synthase/synthetase genes; the filamentous fungi studied were *A. oryzae*, *A. nidulans*, *A. niger* and *A. aculeatus*.

Bioinformatic analysis revealed a high homology between *A. oryzae* and *A. flavus* (99.5 % genome homology), but despite of this, comparative metabolic profiling revealed a surprisingly high degree of chemical differences. Investigation of metabolites in *A. oryzae,* however, revealed clear links to *A. flavus* metabolites. Both species for instance share genes for the aflatrem biosynthetic pathway, but in *A. oryzae* the pathway stops at 13-desoxypailline. The novel compounds ditryptoleucine and the oryzamides $A_{1\text{-}2}$ discovered and characterized from *A. oryzae*, had high similarities to the *A. flavus* metabolites, ditryptophenaline and miyakamides. The latter incorporated phenylalanine while *A. oryzae* incorporated leucine.

In *A. nidulans* a supercluster consisting of a NRPS (AN1242) and a prenyltransferase (AN11080) was investigated, which eventually was linked to the tetracyclopeptide nidulanin A. Due to the modular nature of the biosynthesis of NRPs the product of the NRPS could be predicted as a tetracyclopeptide, and this was confirmed by purification and structure elucidation, indeed revealing a tetracyclopeptide with an isoprene unit incorporated.

In *A. niger* the entire biosynthetic pathway of the meroterpenoid yanuthone D was elucidated, starting with the 6-MSA PKS, and going from 6-MSA to yanuthone D in eight steps. Besides showing that 6-MSA is the precursor of yanuthone D, a novel enzymatic activity, an O-mevalon transferase, was discovered as well as six novel yanuthones. One of these were not derived from 6-MSA, why a novel class of yanuthones was defined. The new class of yanuthones was, however, utilizing several of the enzymes from the *yan* cluster. Another 6-MSA pathway was investigated in the related *Aspergillus* species *A. aculeatus*. This was found to differ significantly from the yanuthone pathway in *A. niger*. Here 6-MSA was modified into the terpenoid-NRP-PK hybrids, the aculins, and a biosynthetic pathway for this was suggested. Altogether these works represent a major step forward in understanding the complex secondary metabolism in the industrially important filamentous fungi *A. niger* and *A. aculeatus*.

Linking of genes to compounds by genetic modifications is difficult for several organisms. In this study it was investigated how to reconstitute entire gene clusters of

filamentous fungi in the model organism *A. nidulans*. This project would improve discovery, and ease characterization of genes. As a proof of concept, the cytochalasin gene cluster from *A. clavatus* was investigated. This was successfully reconstituted in *A. nidulans*. The reconstitution has the potential to provide access to the chemical diversity encoded in the genomes of otherwise uncultured filamentous fungi.

Overall the results of this chapter demonstrates important key points: The power of bioinformatic tools for prediction of superclusters (exemplified by nidulanin A), how to elucidate entire biosynthetic pathway and the small mysteries from nature that are unraveled along the way (exemplified by the 6-MSA pathways), and a method to explore the biosynthetic potential of uncultivable filamentous fungi (exemplified by the reconstitution of the cytochalasin pathway).

5 Overall discussion and conclusion

The work of this thesis has been divided into two major topics: Discovery of novel secondary metabolites from filamentous fungi and linking of fungal compounds to genes and biosynthetic pathways.

The discovery part (chapter 3) has led to extended chemical knowledge of important filamentous fungi and several novel SMs have been characterized. To achieve this, different approaches were undertaken: Dereplication based discovery and discovery by induction of sclerotium formation. The outcome included characterization of 22 novel compounds. From *A. aculeatus* this entailed aculenes A-D, acucalbistrins A-B, acu-dioxomorpholine, okaramine S and epi-10,23-dihydro-24,25-dehydroaflavinin (Paper 1). The biological function of the *A. aculeatus* metabolites remain unclear, but nonetheless a great diversity of SMs from the species have been established, as compounds are both of PK, NRP and terpenoid origin including hybrids of all three classes. From *A. indologenus* aspiperidine oxide was discovered (Paper 2). This entailed a piperidine *N*-oxide, a structural feature not seen previously in fungal SMs. From *A. homomorphus* six related structures, the homomorphosins A-F were discovered (Paper 3). By scrutinizing of the fungal extracts for possible intermediates, a biosynthetic pathway was proposed for both aspiperidine oxide and homomorphosin A. In the latter case, the intermediates were verified by isolation and structure elucidation. In addition several known compounds could be reported from the three species for the first time. The use of dereplication for discovery of novel SMs proved strong in these projects, as known compounds could easily be identified, so laborative isolation efforts could be focused on the putative novel SMs

The progress on how to induce sclerotium formation in black Aspergilli (Paper 4) is of general interest for the discovery of novel bioactive SMs, since formation of sclerotia trigger otherwise silent biosynthetic pathways, resulting in a great alteration in the metabolic profile. As a result of sclerotium formation, sclerotionigrins A-B from *A. sclerotioniger* (Paper 5), as well as emindole SC, sclerolizine and carbonarins I-J from *A. sclerotiicarbonarius* (Paper 6) were discovered. It would be interesting to investigate, which genes are responsible for the sclerotial formation and related metabolites. The novel compounds characterized from *A. sclerotioniger* and *A. sclerotiicarbonarius*, illustrate how novel slerotial compounds can be discovered utilizing inducion of sclerotial formation.

The *A. carbonarius* compounds, were found to possess both antifungal and larvicial activity. In addition, a general trend in other black Aspergilli was production of insectan aflavinines under sclerotium production. For *A. aculeatus* okaramines were upregulated, compounds that are active against silkworms. Altogether the sclerotial metabolites seem to posses insecticidal properties, in accordance with earlier reports [148][149][150][151][152][153][154].

Overall the combined findings of chapter 3 demonstrate, that there are still a vast biosynthetic potential in filamentous fungi and many novel SMs to be discovered. Both as a consequence of unexplored species, but also by utilizing different approaches such as the sclerotium formation.

The second part, linking genes to SMs and elucidating biosynthetic pathways (chapter 4), led to several insights into the biosynthetic potential of industrially very important Aspergilli. The first study described was the comparative metabolic profiling of *A. oryzae* and *A. flavus* (Paper 7). Bioinformatic analysis revealed a high homology between the two species (99.5 % genome homology), but despite of this, initial dereplication revealed a surprisingly high degree of chemical differences. Characterization of metabolites in *A. oryzae*, however, revealed the link to *A. flavus* metabolites. For some, the end products in biosynthetic pathways of *A. flavus*, were not reached in *A. oryzae*. This was the case in the aflatrem pathway, that stops at 13-desoxypaxilline in *A. oryzae*, which could also be justified by bioinformatics: A mutation in the *atmQ* was observed in *A. oryzae*, the gene responsible for the final steps of the biosynthesis of aflatrem in *A. flavus*. Other *A. oryzae* metabolites were found to be very similar to *A. flavus* metabolites, only differing in the AAs incorporated. Ditryptoleucine and the oryzamides discovered and characterized from *A. oryzae* incorporated leucine while the corresponding *A. flavus* metabolite, ditryptophenaline and miyakamides, incorporated phenylalanine. This study is an example of how a combination of genome comparisons and comparative metabolic profiling can exploit the chemical potential of different strains and give insights at the genome level even without use of genetic modifications in the organisms.

In another project a “supercluster” (physically separated genes) consisting of a NRPS (AN1242) and a prenyltransferase (AN11080) was investigated in *A. nidulans*, which ultimately could be linked to the tetracyclopeptide nidulanin A (Paper 8). The results of this work illustrated the strengths of collaboration between bioinformatics and structural chemistry; the stereochemistry of nidulanin A was suggested based on combined efforts

of the two fields. Furthermore the study illustrates how fungal superclusters can be predicted, and also NRP structures. Improvements of bioinformatic tools have made it easier to predict the structure of SMs. This is especially true for NRPs, due to the modular nature of the NRPSs. In the case of PKs it remains difficult to predict the end product since neither the size, degree of saturation or methylation pattern can be predicted as a consequence of the iterative mode of action of the fungal PKSs. Presence of tailoring enzymes further complicates the prediction.

A key result of this thesis has been the characterization of the biosynthesis of the meroterpenoid yanuthone D, which was investigated by a multidisciplinary approach (Paper 9). We were able to identify the cluster responsible for production of yanuthone D, and to show that 6-MSA is the precursor. We presented a biosynthetic pathway, where 6-MSA is converted into yanuthone D in eight steps and present a novel enzymatic activity, an O-mevalon transferase. In this work and a follow up study we characterized ten novel yanuthones (Paper 9 and Paper 10) and defined a novel class of yanuthones utilizing several of the tailoring enzymes from the cluster, but not originating from 6-MSA. Altogether the work represents a major step forward in understanding the complex secondary metabolism in the industrially important filamentous fungus *A. niger* and furthermore the results of this particular work are an example of the fruitful outcome of close collaborations between different fields, especially of natural product chemistry and molecular biology.

In parallel to this project, a 6-MSA pathway in the related black *Aspergillus A. aculeatus* was also explored (Paper 11). Several obstacles were faced in this project. Firstly, gene deletions were not easily obtained in this species, wherefore the biosynthetic pathway could not be investigated with the same approach as the *A. niger* pathway. By heterologous gene expression of the PKS gene, this was, however, established as a 6-MSA synthase gene. The end product of the pathway could not be established by gene knock-out and comparative metabolic profiling, but instead feeding experiments with fully labeled 6-MSA established incorporation into three related compounds, identifying these as pathways related products. The second complication was in the isolation of the 6-MSA related compounds: These were degrading, wherefore the structures of these could not be established by traditional methods. Instead the fragments were structure elucidated by 1D and 2D NMR from a mixture of compounds, whereby a suggestion for their structures could be given. By combination of the structures and the information from the bioinformatic analysis of the surrounding genes, the biosynthetic pathway from 6-MSA to

the end products, (novel compounds aculin A-B and epi-aculin A), was proposed, in spite of the obstacles in this project. The first steps of the pathway is proposed to be similar to the yanuthone D biosynthesis: decarboxylation of 6-MSA to *m*-cresol and oxidation by CYP450 enzymes with high homologies. Aside from this the pathways are divergent. In *A. aculeatus* it results in the aculins, which are PK-NRP-terpene hybrids. By overexpression of a TF located immediately downstream of the 6-MSA synthase gene, two non-6-MSA derived compounds, were additionally discovered.

It was furthermore investigated how to reconstitute entire gene clusters from filamentous fungi in the model organism *A. nidulans* (Paper 12). This project would improve discovery, and ease characterization of genes. As a proof of concept, the cytochalasin gene cluster from *A. clavatus* was investigated and it was successfully reconstituted in *A. nidulans*. The reconstitution approach has the potential to provide access to the chemical diversity encoded in the genomes of otherwise uncultivable filamentous fungi and also allow for further biochemical characterization, but optimization of the titer of the target product is still necessary.

Novel metabolites from *A. aculeatus*

During the mapping of metabolites from *A. aculeatus*, the major metabolites were determined as aculene A and B, discovered during this work. The metabolites are possibly of terpenoid origin with incorporation of the amino acid proline. Two other metabolites from *A. aculeatus* (IBT 21030) were acu-calbistrins A and B. The structure elucidations of these two compounds were complicated by the fact that they were degrading even at mild conditions. Structures were, however, proposed based on the degradation products: aculenes A or B as well as calbistrin A. In an unrelated project, with another *A. aculeatus* strain, 6-MSA derived metabolites were explored. Purifying these other compounds it came as quite a surprise, that not only did these apparently unrelated compounds also degrade: furthermore they degraded also to aculene A or B and another part we identified as the small acid aculinic acid. In close proximity to the 6-MSA cluster responsible for production of aculinic acid, we did not identify any terpenoid related genes we could connect to the biosynthesis of the aculenes. This could indicate a super cluster. Since the aculenes are produced in a higher amount than any of the remaining metabolites in both strains, these are hypothesized to be important metabolites for the organism. It is, however, interesting, why they are linked to two so different moieties as calbistrin A and aculinic acid respectively in two different strains, and why both hybrids are so chemically unstable, that purification has not been possible.

An explanation could also be that the hybrids are artefacts. Only few chimeric compounds are reported from filamentous fungi. Cryptoechinulin B and D [228] isolated from *A. amstelodami* have earlier been suggested to be artefacts formed by Diels-Alder addition.

Improvements of techniques aiding NP drug discovery

Analytical techniques for rapid dereplication of known compounds and their analogues are imperative to not waste time on already known metabolites. Dereplication is getting automated by "aggressive dereplication" [121], also used throughout this thesis, which can be further optimized by use of MS-MS libraries as these will eliminate false-negative results [122]. Furthermore multivariate data analysis is a great aid, since this method can identify small variations in large amounts of data.

On the NMR side, several programs are now available for automated or computer assisted structure elucidation such as CMC-se structure elucidator from Bruker [229] or Structure Elucidator Suite from ACD/Labs [230]. The outcome of any of these is ideally to generate all possible structures that are consistent with a given set of spectroscopic data. An advantage of using this is that the bias of human interpretation is avoided, as one may have an idea of the structure e.g. based on a biosynthetic pathway.

Discovering novel SMs

When discovering novel SMs from filamentous fungi two things should be taking into consideration in order to ensure maximization of chemodiversity. One is the OSMAC approach [77][78], since variations in growth conditions (media, temperature, incubation time, pH, etc.) will lead to variations in the compounds produced. This is also exemplified during this work, as formation of sclerotia led to discovery of novel SMs (Paper 4, Paper 5 and Paper 6). The other aspect is "one pathway – many compounds" [199]. In filamentous fungi one biosynthetic pathway will seldom lead to just a single end product. Rather a series of compounds will be connected to the pathway. This was evident in the biosynthetic pathway of yanuthone D (Paper 9), where not only a number of intermediates were identified, but also several novel yanuthones as a result of branching in the pathway, only discovered due to the individual deletion strains.

Even having the above in mind, not all metabolites are necessarily easily discovered. Some may not be extracted by the standard methods utilized in several labs. Others may not contain a chromophore, wherefore they would be missed in UV-guided purification. Yet others may be present in too low amounts for detection, and there can be challenges in the reproducibility as even small variations in media composition, temperature

fluctuations or similar, may alter the SMs being produced. Finally and maybe most importantly: not all SMs will be produced on any set of lab conditions, wherefore other ways of investigation will be necessary.

The importance of NP chemistry and elucidation of pathways

There can be no question that NPs have played a major role in the history of drug discovery. A more relevant question is: Will they keep their status and inspire new pharmaceuticals? And in that case – where will the new NPs come from? As illustrated in this thesis the answer to this question is not unambiguous. Novel NPs can come from more rare and unexploited species (as illustrated for *A. aculeatus*, *A. homomorphus*, *A. indologenus*), they can arise from triggering well-studied species into activating otherwise silenced gene clusters (as illustrated by induction of sclerotium formation in several black Aspergilli and overexpression of a TF in *A. aculeatus*), or it could be by investigation of pathways, both with known end products (as illustrated by the 6-MSA pathway in *A. niger* leading to characterization of 10 novel yanuthone analogs) or with unknown end products (as illustrated by the 6-MSA pathway in *A. aculeatus*). Altogether there are many different approaches; no matter what: There is still a vast potential for finding novel SMs in filamentous fungi.

The second theme of this thesis, where entire biosynthetic pathways were elucidated, is important for several reasons. Firstly, novel SMs may be discovered in the process, as illustrated in both of the 6-MSA derived pathways (Paper 9 and Paper 11). Discovery of new SMs and structures enhances the possibility of discovering novel drugs. Secondly, on the basis of the growing knowledge, PK and NRP pathways may be manipulated or redesigned for the production of novel drug candidates. A growing research area is synthetic biology, where pathways are engineered by swapping of genes or domains, resulting in new, designed metabolites [231][232][233][234]. This field of research utilized enzymes that can carry out complicated chemical reactions and thereby create unnatural metabolites containing enhanced structural features otherwise inaccessible.
Also, for the filamentous fungi used in industrial processes, it would be beneficial knowing the genetic potential, to avoid unwanted by-products, e.g. mycotoxins, and to easily identify new metabolites.

NP chemistry – next steps

PKs and NRPs are two groups of fungal SMs, which have attracted massive attention and have been widely studied. A more overlooked group is the terpenoids. A major reason for this can be limitations in detection of this type of compounds. Terpenoids are

hydrocarbons and though some undergo enzymatic modifications, e.g. oxidations, not all will contain heteroatoms, and consequently they will be difficult to detect by MS, the method of choice in many labs. Furthermore many are not giving rise to a chromophore detectable or standing out in a UV analysis, wherefore they might also be missed by this analytical method. To this end, it is noted that the structure of terpenoids are difficult to predict by bioinformatics. Altogether this leads to fewer discoveries of the terpenoids. None the less, their structures are highly diverse, and they do possess pharmaceutical relevant bioactivities, such as anticancer properties [235], why this group could very likely be the follower of the intensive studies currently directed towards PKs and NRPs.

NP research was earlier more limited to chemists, purifying and elucidation structures; today and in the future NP research is highly linked with other areas, especially the disciplines of bioinformatics and synthetic biology. The still growing availability of entire genomes has changed the focus and it has become easier to predict biosynthetic products, especially with the bioinformatical accessibility of both PKs and NRPs. Manipulation with SMs in synthetic biology have further opened for both getting a better knowledge of existing biosynthetic pathways, but also to design new ones.

Concluding remarks

The work of this thesis represents a major step forward in extending the chemical knowledge on the complex secondary metabolism of industrially important filamentous fungi and at the same time illustrates the enormous potential for still discovering novel SMs. Through discovery 22 novel compounds were characterized, and in the elucidation of biosynthetic pathways, numerous other SMs have been characterized. On top of this, biosynthetic pathways for nidulanin A in *A. nidulans*, yanuthone D in *A. niger* and aculin A in *A. aculeatus* have been described, and the metabolites linked to genes. These findings, also illustrate the strengths, of close collaborations between fields. Interactions between bioinformatics, molecular biology, analytical and NP chemistry are crucial for advances in linking fungal SMs to genes and unraveling the biosynthetic pathways. A continued, focused collaboration is needed both for understanding the important known metabolites of a given species as well as for the discovery of novel SMs hidden in the still large biosynthetic potential of filamentous fungi.

6 References

1. Fleming, A. On the antibacterial action of cultures of a *Penicillium*, with special reference to their use in the isolation of *B. indluenzæ*. *Br. J. Exp. Pathol.* **1929**, *10*, 226–236.

2. Newman, D. J.; Cragg, G. M. Natural products as sources of new drugs over the 30 years from 1981 to 2010. *J. Nat. Prod.* **2012**, *75*, 311–335.

3. Cragg, G. M.; Newman, D. J. Natural products: a continuing source of novel drug leads. *Biochim. Biophys. Acta* **2013**, *1830*, 3670–3695.

4. Cooper, M. A.; Shlaes, D. Fix the antibiotics pipeline. *Nature* **2011**, *472*, 32.

5. Lopezt, M.; Joshuat, H.; Harrist, E.; Patchettt, A.; Monaghan, R.; Currie, S.; Stapleyt, E.; Hirshfieldt, J.; Hoogsteent, K.; Liescht, J.; Springeri, J. Mevinolin: a highly potent competitive inhibitor of hydroxymethylglutaryl-coenzyme A reductase and a cholesterol-lowering agent. *Proc. Natl. Acad. Sci. U. S. A.* **1980**, *77*, 3957–3961.

6. Schuster, E.; Dunn-Coleman, N. S.; Frisvad, J. C.; Van Dijck, P. W. M. On the safety of *Aspergillus niger* - a review. *Appl. Microbiol. Biotechnol.* **2002**, *59*, 426–435.

7. Pontecorvo, G.; Roper, J. A.; Hemmons, L. M.; Bufton, A. W. The genetics of *Aspergillus nidulans*. *Adv. Genet.* **1953**, *5*, 141–238.

8. Nielsen, M. L.; Albertsen, L.; Lettier, G.; Nielsen, J. B.; Mortensen, U. H. Efficient PCR-based gene targeting with a recyclable marker for *Aspergillus nidulans*. *Fungal Genet. Biol.* **2006**, *43*, 54–64.

9. Nielsen, J. B.; Nielsen, M. L.; Mortensen, U. H. Transient disruption of non-homologous end-joining facilitates targeted genome manipulations in the filamentous fungus *Aspergillus nidulans*. *Fungal Genet. Biol.* **2008**, *45*, 165–170.

10. Cotty, P. J. Influence of field application of an atoxigenic strain of *Aspergillus flavus* on the populations of *A. flavus* infecting cotton bolls and on the aflatoxin content of cottonseed. *Phytopathology* **1994**, *84*, 1270–1277.

11. Perrone, G.; Susca, A.; Cozzi, G.; Ehrlich, K. C.; Varga, J.; Frisvad, J. C.; Meijer, M.; Noonim, P.; Mahakarnchanakul, W.; Samson, R. A. Biodiversity of *Aspergillus* species in some important agricultural products. *Stud. Mycol.* **2007**, *59*, 53–66.

12. Adisa, V. A. Pectic enzymes of *Aspergillus aculeatus* associated with post-harvest deterioration of citrus sinensis fruit. *J. Food Biochem.* **1989**, *13*, 243–252.

13. Madigan, M.T.; Martinko, J.M.; Dunlap, P.V.; Clark, D. P. *Biology of microorganisms*; 12th ed.; Pearson Benjamin Cummings: San Francisco, 2009; pp. 535–545.

14. Solomon, E. P.; Berg, L. R.; Martin, D. W.; Villee, C. *Biology*; 4th ed.; Saunders College Publishing: Fort Worth, 1996; pp. 551–565.

15. Hawksworth, D. L. The fungal dimension of biodiversity: magnitude, significance, and conservation. *Mycol. Res.* **1991**, *95*, 641–655.

16. Cox, R. J. Polyketides, proteins and genes in fungi: programmed nano-machines begin to reveal their secrets. *Org. Biomol. Chem.* **2007**, *5*, 2010–2026.

17. Samson, R. A.; Noonim, P.; Meijer, M.; Houbraken, J.; Frisvad, J. C.; Varga, J. Diagnostic tools to identify black Aspergilli. *Stud. Mycol.* **2007**, *59*, 129–145.

18. Baker, S. E. *Aspergillus niger* genomics: past, present and into the future. *Med. Mycol.* **2006**, *44*, 17–21.

19. Pel, H. J.; de Winde, J. H.; Archer, D. B.; Dyer, P. S.; Hofmann, G.; Schaap, P. J.; Turner, G.; de Vries, R. P.; Albang, R.; Albermann, K.; Andersen, M. R.; Bendtsen, J. D.; Benen, J. A. E.; van Den Berg, M.; Breestraat, S.; Caddick, M. X.; Contreras, R.; Cornell, M.; Coutinho, P. M.; Danchin, E. G. J.; Debets, A. J. M.; Dekker, P.; van Dijck, P. W. M.; van Dijk, A.; Dijkhuizen, L.; Driessen, A. J. M.; D'Enfert, C.; Geysens, S.; Goosen, C.; Groot, G. S. P.; de Groot, P. W. J.; Guillemette, T.; Henrissat, B.; Herweijer, M.; van den Hombergh, J. P. T. W.; van den Hondel, C. A. M. J. J.; van der Heijden, R. T. J. M.; van der Kaaij, R. M.; Klis, F. M.; Kools, H. J.; Kubicek, C. P.; van Kuyk, P. A.; Lauber, J.; Lu, X.; van der Maarel, M. J. E. C.; Meulenberg, R.; Menke, H.; Mortimer, M. A.; Nielsen, J.; Oliver, S. G.; Olsthoorn, M.; Pal, K.; van Peij, N. N. M. E.; Ram, A. F. J.; Rinas, U.; Roubos, J. A.; Sagt, C. M. J.; Schmoll, M.; Sun, J. B.; Ussery, D. W.; Varga, J.; Vervecken, W.; de Vondervoort, P. J. J.; Wedler, H.; Wosten, H. A. B.; Zeng, A. P.; van Ooyen, A. J. J.; Visser, J.; Stam, H. Genome sequencing and analysis of the versatile cell factory *Aspergillus niger* CBS 513.88. *Nat. Biotechnol.* **2007**, *25*, 221–231.

20. Frisvad, J. C.; Smedsgaard, J.; Samson, R. A.; Larsen, T. O.; Thrane, U. Fumonisin B2 production by *Aspergillus niger*. *J. Agric. Food Chem.* **2007**, *55*, 9727–9732.

21. Lucchetta, G.; Bazzo, I.; Cortivo, G. D.; Stringher, L.; Bellotto, D.; Borgo, M.; Angelini, E. Occurrence of black Aspergilli and ochratoxin A on grapes in Italy. *Toxins (Basel).* **2010**, *2*, 840–855.

22. Varga, J.; Frisvad, J. C.; Kocsubé, S.; Brankovics, B.; Tóth, B.; Szigeti, G.; Samson, R. A. New and revisited species in *Aspergillus* section *Nigri*. *Stud. Mycol.* **2011**, *69*, 1–17.

23. Bhat, M. K. Cellulases and related enzymes in biotechnology. *Biotechnol. Adv.* **2000**, *18*, 355–383.

24. Fujimoto, H.; Ooi, T.; Wang, S.; Takizawa, T. Purification and properties of three xylanases from *Aspergillus aculeatus*. *Biosci. Biotechnol. Biochem.* **1995**, *59*, 538–540.

25. Polizeli, M. L. T. M.; Rizzatti, a C. S.; Monti, R.; Terenzi, H. F.; Jorge, J. a; Amorim, D. S. Xylanases from fungi: properties and industrial applications. *Appl. Microbiol. Biotechnol.* **2005**, *67*, 577–591.

26. Olutiola, P. O.; Nwaogwugwu, R. I. Growth, sporulation and production of maltase and proteolytic enzymes in *Aspergillus aculeatus*. *Trans. Br. Mycol. Soc.* **1982**, *78*, 105–113.

27. Mizuno, K.; Yagi, A.; Satoi, S.; Takada, M.; Hayashi, M.; Asano, K.; Matsuda, T. Studies on aculeacin. I. Isolation and characterization of aculeacin A. *J. Antibiot.* **1977**, *4*, 297–302.

28. Satoi, S.; Yagi, A.; Asano, K.; Misuno, K.; Watanabe, T. Studies on aculeacin. II. Isolation and characterization of aculeacins B, C, D, E, F and G. *J. Antibiot.* **1977**, *30*, 303–307.

29. Watanabe, S.; Hirai, H.; Ishiguro, M.; Kambara, T.; Kojima, Y.; Matsunaga, T.; Nishida, H.; Suzuki, Y.; Harwood, H. J.; Huang, L. H.; Kojima, N. CJ-15,183, a new inhibitor of squalene synthase produced by a fungus, *Aspergillus aculeatus*. *J. Antibiot. (Tokyo).* **2001**, *54*, 904–910.

30. Andersen, R.; Buechi, G.; Kobbe, B.; Demain, A. L. Secalonic acids D and F are toxic metabolites of *Aspergillus aculeatus*. *J. Org. Chem.* **1977**, *42*, 352–353.

31. Hayashi, H.; Furutsuka, K.; Shiono, Y. Okaramines H and I, new okaramine congeners, from *Aspergillus aculeatus* . *J. Nat. Prod.* **1999**, *62*, 315–317.

32. Ingavat, N.; Mahidol, C.; Ruchirawat, S.; Kittakoop, P. Asperaculin A, a sesquiterpenoid from a marine-derived fungus, *Aspergillus aculeatus*. *J. Nat. Prod.* **2011**, *74*, 1650–1652.

33. Ingavat, N.; Dobereiner, J.; Wiyakrutta, S.; Mahidol, C.; Ruchirawat, S.; Kittakoop, P. Aspergillusol A, an alpha-glucosidase inhibitor from the marine-derived fungus *Aspergillus aculeatus*. *J. Nat. Prod.* **2009**, *72*, 2049–2052.

34. Chen, L.; Zhang, Q.-Q.; Zhang, W.-W.; Liu, Q.-Y.; Zheng, Q.-H.; Zhong, P.; Hu, X.; Fang, Z.-X. Aculeatusquinones A-D, novel metabolites from the marine-derived fungus *Aspergillus aculeatus*. *Heterocycles* **2013**, *87*, 861–868.

35. Bugni, T. S.; Abbanat, D.; Bernan, V. S.; Maiese, W. M.; Greenstein, M.; Wagoner, R. M. Van; Ireland, C. M. Yanuthones: novel metabolites from a marine isolate of *Aspergillus niger*. *J. Org. Chem.* **2000**, *65*, 7195–7200.

36. Zabala, A. O.; Xu, W.; Chooi, Y.-H.; Tang, Y. Characterization of a silent azaphilone gene cluster from *Aspergillus niger* ATCC 1015 reveals a hydroxylation-mediated pyran-ring formation. *Chem. Biol.* **2012**, *19*, 1049–1059.

37. Wang, P.-L.; Tanaka, H. Yellow Pigments of *Aspergillus niger* and *Asp. awamori* Part II. *Agric. Biol. Chem.* **1966**, *30*, 683–687.

38. Nielsen, K. F.; Mogensen, J. M.; Johansen, M.; Larsen, T. O.; Frisvad, J. C. Review of secondary metabolites and mycotoxins from the *Aspergillus niger* group. *Anal. Bioanal. Chem.* **2009**, *395*, 1225–1242.

39. Bradshaw, B.; Etxebarria-Jardí, G.; Bonjoch, J. Polycyclic framework synthesis of anominine and tubingensin A indole diterpenoids. *Org. Biomol. Chem.* **2008**, *6*, 772–778.

40. Samson, R. A.; Noonim, P.; Meijer, M.; Houbraken, J.; Frisvad, J. C.; Varga, J. Diagnostic tools to identify black Aspergilli. *Stud. Mycol.* **2007**, *59*, 129–145.

41. Samson, R.; Houbraken, J.; Kuijpers, A. New ochratoxin A or sclerotium producing species in *Aspergillus* section *Nigri*. *Stud Mycol* **2004**, *2*, 45–61.

42. Dufossé, L.; Fouillaud, M.; Caro, Y.; Mapari, S. A.; Sutthiwong, N. Filamentous fungi are large-scale producers of pigments and colorants for the food industry. *Curr. Opin. Biotechnol.* **2014**, *26*, 56–61.

43. Cox, R. J.; Simpson, T. J. Fungal type I polyketide synthases. *Methods Enzymol.* **2009**, *459*, 49–78.

44. Hertweck, C. The biosynthetic logic of polyketide diversity. *Angew. Chem. Int. Ed. Engl.* **2009**, *48*, 4688–4716.

45. Bentley, R. Mycophenolic Acid: a one hundred year odyssey from antibiotic to immunosuppressant. *Chem. Rev.* **2000**, *100*, 3801–3826.

46. Chooi, Y.-H.; Cacho, R.; Tang, Y. Identification of the viridicatumtoxin and griseofulvin gene clusters from *Penicillium aethiopicum*. *Chem. Biol.* **2010**, *17*, 483–494.

47. Schümann, J.; Hertweck, C. Advances in cloning, functional analysis and heterologous expression of fungal polyketide synthase genes. *J. Biotechnol.* **2006**, *124*, 690–703.

48. Fischbach, M. A.; Walsh, C. T. Assembly-line enzymology for polyketide and nonribosomal Peptide antibiotics: logic, machinery, and mechanisms. *Chem. Rev.* **2006**, *106*, 3468–3496.

49. Du, L.; Lou, L. PKS and NRPS release mechanisms. *Nat. Prod. Rep.* **2010**, *27*, 255–278.

50. Weissman, K. J. Biochemistry. Anatomy of a fungal polyketide synthase. *Science* **2008**, *320*, 186–187.

51. Keller, N. P.; Turner, G.; Bennett, J. W. Fungal secondary metabolism - From biochemistry to genomics. *Nat. Rev. Microbiol.* **2005**, *3*, 937–947.

52. Yadav, G.; Gokhale, R. S.; Mohanty, D. Towards prediction of metabolic products of polyketide synthases: An in silico analysis. *Plos Comput. Biol.* **2009**, *5*, e1000351.

53. Marahiel, M. A. Working outside the protein-synthesis rules: insights into non-ribosomal peptide synthesis. *J. Pept. Sci.* **2009**, *15*, 799–807.

54. Dewick, P. M. *Medicinal Natural Products. A Biosynthetic Approach*; 3rd ed.; John Wiley & Sons Ltd: Chichester, West Sussex, United Kingdom, 2009.

55. Von Döhren, H. A survey of nonribosomal peptide synthetase (NRPS) genes in *Aspergillus nidulans*. *Fungal Genet. Biol.* **2009**, *46*, 45–52.

56. Kopp, F.; Marahiel, M. a Macrocyclization strategies in polyketide and nonribosomal peptide biosynthesis. *Nat. Prod. Rep.* **2007**, *24*, 735–749.

57. Gao, X.; Haynes, S. W.; Ames, B. D.; Wang, P.; Vien, L. P.; Walsh, C. T.; Tang, Y. Cyclization of fungal nonribosomal peptides by a terminal condensation-like domain. *Nat. Chem. Biol.* **2012**, *8*, 823–830.

58. Dewick, P. M. The biosynthesis of C5-C25 terpenoid compounds. *Nat. Prod. Rep.* **2002**, *19*, 181–222.

59. Oldfield, E.; Lin, F.-Y. Terpene biosynthesis: modularity rules. *Angew. Chem. Int. Ed. Engl.* **2012**, *51*, 1124–1137.

60. Bentley, R. Secondary metabolite biosynthesis: the first century. *Crit. Rev. Biotechnol.* **1999**, *19*, 1–40.

61. Dewick, P. M. *Medicinal Natural Products. A Biosynthetic Approach.*; 3rd ed.; John Wiley & Sons Ltd: Chichester, West Sussex, United Kingdom, 2009.

62. Davies, J. Specialized microbial metabolites: functions and origins. *J. Antibiot. (Tokyo).* **2013**, *66*, 361–364.

63. Winter, J. M.; Behnken, S.; Hertweck, C. Genomics-inspired discovery of natural products. *Curr. Opin. Chem. Biol.* **2011**, *15*, 22–31.

64. Heine, D.; Martin, K.; Hertweck, C. Genomics-guided discovery of endophenazines from Kitasatospora sp. HKI 714. *J. Nat. Prod.* **2014**, *77*, 1083–1087.

65. Walsh, C. T.; Fischbach, M. Natural products version 2.0: connecting genes to molecules. *J. Am. Chem. Soc.* **2010**, *132*, 2469–2493.

66. Keller, N.; Hohn, T. Metabolic pathway gene clusters in filamentous fungi. *Fungal Genet. Biol.* **1997**, *21*, 17–29.

67. Brakhage, A. A. Regulation of fungal secondary metabolism. *Nat. Rev. Microbiol.* **2013**, *11*, 21–32.

68. Lo, H.-C.; Entwistle, R.; Guo, C.-J.; Ahuja, M.; Szewczyk, E.; Hung, J.-H.; Chiang, Y.-M.; Oakley, B. R.; Wang, C. C. C. Two separate gene clusters encode the biosynthetic pathway for the meroterpenoids austinol and dehydroaustinol in *Aspergillus nidulans*. *J. Am. Chem. Soc.* **2012**, *134*, 4709–4720.

69. Shelest, E. Transcription factors in fungi. *FEMS Microbiol. Lett.* **2008**, *286*, 145–151.

70. Latchman, D. S. Transcription factors: an overview. *Int. J. Biochem. Cell Biol.* **1997**, *29*, 1305–1312.

71. Hertweck, C. Hidden biosynthetic treasures brought to light. *Nat. Chem. Biol.* **2009**, *5*, 450–452.

72. Andersen, M. R.; Salazar, M. P.; Schaap, P. J.; van de Vondervoort, P. J. I.; Culley, D.; Thykaer, J.; Frisvad, J. C.; Nielsen, K. F.; Albang, R.; Albermann, K.; Berka, R. M.; Braus, G. H.; Braus-Stromeyer, S. a; Corrochano, L. M.; Dai, Z.; van Dijck, P. W. M.; Hofmann, G.; Lasure, L. L.; Magnuson, J. K.; Menke, H.; Meijer, M.; Meijer, S. L.; Nielsen, J. B.; Nielsen, M. L.; van Ooyen, A. J. J.; Pel, H. J.; Poulsen, L.; Samson, R. a; Stam, H.; Tsang, A.; van den Brink, J. M.; Atkins, A.; Aerts, A.; Shapiro, H.; Pangilinan, J.; Salamov, A.; Lou, Y.; Lindquist, E.; Lucas, S.; Grimwood, J.; Grigoriev, I. V; Kubicek, C. P.; Martinez, D.; van Peij, N. N. M. E.; Roubos, J. a; Nielsen, J.; Baker, S. E. Comparative genomics of citric-acid-producing *Aspergillus niger* ATCC 1015 versus enzyme-producing CBS 513.88. *Genome Res.* **2011**, *21*, 885–897.

73. Baker, S. E. *Aspergillus niger* genomics: past, present and into the future. *Med. Mycol.* **2006**, *44*, 17–21.

74. Gross, H. Strategies to unravel the function of orphan biosynthesis pathways: recent examples and future prospects. *Appl. Microbiol. Biotechnol.* **2007**, *75*, 267–277.

75. Galagan, J. E.; Calvo, S. E.; Cuomo, C.; Ma, L. J.; Wortman, J. R.; Batzoglou, S.; Lee, S. I.; Basturkmen, M.; Spevak, C. C.; Clutterbuck, J.; Kapitonov, V.; Jurka, J.; Scazzocchio, C.; Farman, M.; Butler, J.; Purcell, S.; Harris, S.; Braus, G. H.; Draht, O.; Busch, S.; D'Enfert, C.; Bouchier, C.; Goldman, G. H.; Bell-Pedersen, D.; Griffiths-Jones, S.; Doonan, J. H.; Yu, J.; Vienken, K.; Pain, A.; Freitag, M.; Selker, E. U.; Archer, D. B.; Penalva, M. A.; Oakley, B. R.; Momany, M.; Tanaka, T.; Kumagai, T.; Asai, K.; Machida, M.; Nierman, W. C.; Denning, D. W.; Caddick, M. X.; Hynes, M.; Paoletti, M.; Fischer, R.; Miller, B. L.; Dyer, P. S.; Sachs, M. S.; Osmani, S. A.; Birren, B. W. Sequencing of *Aspergillus nidulans* and comparative analysis with *A. fumigatus* and *A. oryzae*. *Nature* **2005**, *438*, 1105–1115.

76. Machida, M.; Asai, K.; Sano, M.; Tanaka, T.; Kumagai, T.; Terai, G.; Kusumoto, K. I.; Arima, T.; Akita, O.; Kashiwagi, Y.; Abe, K.; Gomi, K.; Horiuchi, H.; Kitamoto, K.; Kobayashi, T.; Takeuchi, M.; Denning, D. W.; Galagan, J. E.; Nierman, W. C.; Yu, J. J.; Archer, D. B.; Bennett, J. W.; Bhatnagar, D.; Cleveland, T. E.; Fedorova, N. D.; Gotoh, O.; Horikawa, H.; Hosoyama, A.; Ichinomiya, M.; Igarashi, R.; Iwashita, K.; Juvvadi, P. R.; Kato, M.; Kato, Y.; Kin, T.; Kokubun, A.; Maeda, H.; Maeyama, N.; Maruyama, J.; Nagasaki, H.; Nakajima, T.; Oda, K.; Okada, K.; Paulsen, I.; Sakamoto, K.; Sawano, T.; Takahashi, M.; Takase, K.; Terabayashi, Y.; Wortman, J. R.; Yamada, O.; Yamagata, Y.; Anazawa, H.; Hata, Y.; Koide, Y.; Komori, T.; Koyama, Y.; Minetoki, T.; Suharnan, S.; Tanaka, A.; Isono, K.; Kuhara, S.; Ogasawara, N.; Kikuchi, H. Genome sequencing and analysis of *Aspergillus oryzae*. *Nature* **2005**, *438*, 1157–1161.

77. Bode, H.; Bethe, B.; Höfs, R.; Zeeck, A. Big effects from small changes: possible ways to explore nature's chemical diversity. *ChemBioChem* **2002**, *3*, 619–627.

78. Sinica, A. M. OSMAC (One Strain Many Compounds) approach in the research of microbial metabolites-A review. *Acta Microbiol. Sin.* **2010**, *50*, 701–709.

79. Schroeckh, V.; Scherlach, K.; Nützmann, H. W.; Shelest, E.; Schmidt-Heck, W.; Schuemann, J.; Martin, K.; Hertweck, C.; Brakhage, A. A. Intimate bacterial-fungal

interaction triggers biosynthesis of archetypal polyketides in *Aspergillus nidulans*. *Proc. Natl. Acad. Sci. U. S. A.* **2009**, *106*, 14558–14563.

80. Williams, R. B.; Henrikson, J. C.; Hoover, A. R.; Lee, A. E.; Cichewicz, R. H. Epigenetic remodeling of the fungal secondary metabolome. *Org. Biomol. Chem.* **2008**, *6*, 1895–1897.

81. Fisch, K. M.; Gillaspy, A. F.; Gipson, M.; Henrikson, J. C.; Hoover, A. R.; Jackson, L.; Najar, F. Z.; Wagele, H.; Cichewicz, R. H. Chemical induction of silent biosynthetic pathway transcription in *Aspergillus niger*. *J. Ind. Microbiol. Biotechnol.* **2009**, *36*, 1199–1213.

82. Bergmann, S.; Schümann, J.; Scherlach, K.; Lange, C.; Brakhage, A. a; Hertweck, C. Genomics-driven discovery of PKS-NRPS hybrid metabolites from *Aspergillus nidulans*. *Nat. Chem. Biol.* **2007**, *3*, 213–217.

83. Hansen, B. G.; Salomonsen, B.; Nielsen, M. T.; Nielsen, J. B.; Hansen, N. B.; Nielsen, K. F.; Regueira, T. B.; Nielsen, J.; Patil, K. R.; Mortensen, U. H. Versatile enzyme expression and characterization system for *Aspergillus nidulans*, with the *Penicillium brevicompactum* polyketide synthase gene from the mycophenolic acid gene cluster as a test case. *Appl. Environ. Microbiol.* **2011**, *77*, 3044–3051.

84. Nielsen, M. L.; Nielsen, J. B.; Rank, C.; Klejnstrup, M. L.; Holm, D. K.; Brogaard, K. H.; Hansen, B. G.; Frisvad, J. C.; Larsen, T. O.; Mortensen, U. H. A genome-wide polyketide synthase deletion library uncovers novel genetic links to polyketides and meroterpenoids in *Aspergillus nidulans*. *FEMS Microbiol. Lett.* **2011**, *321*, 157–166.

85. Bok, J. W.; Hoffmeister, D.; Maggio-Hall, L. A.; Murillo, R.; Glasner, J. D.; Keller, N. P. Genomic mining for *Aspergillus* natural products. *Chem. Biol.* **2006**, *13*, 31–37.

86. Li, Y.; Chooi, Y.-H.; Sheng, Y.; Valentine, J. S.; Tang, Y. Comparative characterization of fungal anthracenone and naphthacenedione biosynthetic pathways reveals an α-hydroxylation-dependent Claisen-like cyclization catalyzed by a dimanganese thioesterase. *J. Am. Chem. Soc.* **2011**, *133*, 15773–85.

87. Chiang, Y.-M.; Meyer, K. M.; Praseuth, M.; Baker, S. E.; Bruno, K. S.; Wang, C. C. C. Characterization of a polyketide synthase in *Aspergillus niger* whose product is a precursor for both dihydroxynaphthalene (DHN) melanin and naphtho-γ-pyrone. *Fungal Genet. Biol.* **2011**, *48*, 430–437.

88. Awakawa, T.; Yang, X.-L.; Wakimoto, T.; Abe, I. Pyranonigrin E: A PKS-NRPS Hybrid Metabolite from *Aspergillus niger* Identified by Genome Mining. *Chembiochem* **2013**, 2095–2099.

89. Holm, D. K.; Petersen, L. M.; Klitgaard, A.; Knudsen, P. B.; Jarczynska, Z. D.; Nielsen, K. F.; Gotfredsen, C. H.; Larsen, T. O.; Mortensen, U. H. Molecular and chemical characterization of the biosynthesis of the 6-MSA-derived meroterpenoid yanuthone D in *Aspergillus niger*. *Chem. Biol.* **2014**, *21*, 519–529.

90. Brown, D. W.; Yu, J. H.; Kelkar, H. S.; Fernandes, M.; Nesbitt, T. C.; Keller, N. P.; Adams, T. H.; Leonard, T. J. Twenty-five coregulated transcripts define a

sterigmatocystin gene cluster in *Aspergillus nidulans*. *Proc. Natl. Acad. Sci. U. S. A.* **1996**, *93*, 1418–1422.

91. Watanabe, A.; Fujii, I.; Sankawa, U.; Mayorga, M. E.; Timberlake, W. E.; Ebizuka, Y. Re-identification of *Aspergillus nidulans* wA gene to code for a polyketide synthase of naphthopyrone. *Tetrahedron Lett.* **1999**, *40*, 91–94.

92. Szewczyk, E.; Chiang, Y.-M.; Oakley, C. E.; Davidson, A. D.; Wang, C. C. C.; Oakley, B. R. Identification and characterization of the asperthecin gene cluster of *Aspergillus nidulans*. *Appl. Environ. Microbiol.* **2008**, *74*, 7607–7612.

93. Bok, J. W.; Chiang, Y. M.; Szewczyk, E.; Reyes-Dominguez, Y.; Davidson, A. D.; Sanchez, J. F.; Lo, H. C.; Watanabe, K.; Strauss, J.; Oakley, B. R.; Wang, C. C.; Keller, N. P. Chromatin-level regulation of biosynthetic gene clusters. *Nat. Chem. Biol.* **2009**, *5*, 462–464.

94. Chiang, Y.-M.; Szewczyk, E.; Davidson, A. D.; Entwistle, R.; Keller, N. P.; Wang, C. C. C.; Oakley, B. R. Characterization of the *Aspergillus nidulans* monodictyphenone gene cluster. *Appl. Environ. Microbiol.* **2010**, *76*, 2067–2074.

95. Sanchez, J. F.; Chiang, Y.-M.; Szewczyk, E.; Davidson, A. D.; Ahuja, M.; Elizabeth Oakley, C.; Woo Bok, J.; Keller, N.; Oakley, B. R.; Wang, C. C. C. Molecular genetic analysis of the orsellinic acid/F9775 gene cluster of *Aspergillus nidulans*. *Mol. Biosyst.* **2010**, *6*, 587–593.

96. Chiang, Y.-M.; Szewczyk, E.; Davidson, A. D.; Keller, N.; Oakley, B. R.; Wang, C. C. C. A gene cluster containing two fungal polyketide synthases encodes the biosynthetic pathway for a polyketide, asperfuranone, in *Aspergillus nidulans*. *J. Am. Chem. Soc.* **2009**, *131*, 2965–2970.

97. Ahuja, M.; Chiang, Y.-M.; Chang, S.-L.; Praseuth, M. B.; Entwistle, R.; Sanchez, J. F.; Lo, H.-C.; Yeh, H.-H.; Oakley, B. R.; Wang, C. C. C. Illuminating the diversity of aromatic polyketide synthases in *Aspergillus nidulans*. *J. Am. Chem. Soc.* **2012**, *134*, 8212–8221.

98. Chiang, Y. M.; Szewczyk, E.; Nayak, T.; Davidson, A. D.; Sanchez, J. F.; Lo, H. C.; Ho, W. Y.; Simityan, H.; Kuo, E.; Praseuth, A.; Watanabe, K.; Oakley, B. R.; Wang, C. C. C. Molecular genetic mining of the *Aspergillus* secondary metabolome: Discovery of the emericellamide biosynthetic pathway. *Chem. Biol.* **2008**, *15*, 527–532.

99. Yaegashi, J.; Praseuth, M. B.; Tyan, S. W.; Sanchez, J. F.; Entwistly, R.; Chiang, Y.; Oakley, B. R.; Wang, C. C. C. Molecular genetic characterization of the biosynthesis cluster of a prenylated isoindolinone alkaloid aspernidine A in *Aspergillus nidulans*. *Org. Lett.* **2013**, *15*, 2862–2865.

100. Andersen, M. R.; Nielsen, J. B.; Klitgaard, A.; Petersen, L. M.; Zachariasen, M.; Hansen, T. J.; Blicher, L. H.; Gotfredsen, C. H.; Larsen, T. O.; Nielsen, K. F.; Mortensen, U. H. Accurate prediction of secondary metabolite gene clusters in filamentous fungi. *Proc. Natl. Acad. Sci. U. S. A.* **2013**, *110*, E99–107.

101. http://genome.jgi-psf.org/Aspac1/Aspac1.home.html. *DOE Jt. Genome Inst. Aspergillus aculeatus ATCC16872 Genome portal v.1.1*.

102. Holm, D. M. K. Development and implementation of novel genetic tools for investigation of fungal secondary metabolism. *PhD thesis* **2013**, Technical University of Denmark.

103. Zerikly, M.; Challis, G. L. Strategies for the discovery of new natural products by genome mining. *Chembiochem* **2009**, *10*, 625–633.

104. Corre, C.; Challis, G. L. New natural product biosynthetic chemistry discovered by genome mining. *Nat. Prod. Rep.* **2009**, *26*, 977–86.

105. Nayak, T.; Szewczyk, E.; Oakley, C. E.; Osmani, A.; Ukil, L.; Murray, S. L.; Hynes, M. J.; Osmani, S. a; Oakley, B. R. A versatile and efficient gene-targeting system for *Aspergillus nidulans*. *Genetics* **2006**, *172*, 1557–1566.

106. Meyer, V.; Arentshorst, M.; El-Ghezal, A.; Drews, A.-C.; Kooistra, R.; van den Hondel, C. a M. J. J.; Ram, A. F. J. Highly efficient gene targeting in the *Aspergillus niger kusA* mutant. *J. Biotechnol.* **2007**, *128*, 770–775.

107. Ongley, S. E.; Bian, X.; Neilan, B. a; Müller, R. Recent advances in the heterologous expression of microbial natural product biosynthetic pathways. *Nat. Prod. Rep.* **2013**, *30*, 1121–1138.

108. Hansen, B. G.; Mnich, E.; Nielsen, K. F.; Nielsen, J. B.; Nielsen, M. T.; Mortensen, U. H.; Larsen, T. O.; Patil, K. R. Involvement of a natural fusion of a cytochrome P450 and a hydrolase in mycophenolic acid biosynthesis. *Appl. Environ. Microbiol.* **2012**, *78*, 4908–4913.

109. Nielsen, M. T.; Nielsen, J. B.; Anyaogu, D. C.; Anyaogu, D. C.; Holm, D. K.; Nielsen, K. F.; Larsen, T. O.; Mortensen, U. H. Heterologous reconstitution of the intact geodin gene cluster in *Aspergillus nidulans* through a simple and versatile PCR based approach. *PLoS One* **2013**, *8*, e72871.

110. Gems, D.; Johnstone, I. L.; Clutterbuck, A. J. An autonomously replicating plasmid transforms *Aspergillus nidulans* at high frequency. *Gene* **1991**, *98*, 61–67.

111. Aleksenko, A.; Nikolaev, I.; Vinetski, Y.; Clutterbuck, A. Gene expression from replicating plasmids in *Aspergillus nidulans*. *Mol. Gen. Genet. MGG* **1996**, *253*, 242–246.

112. Verdoes, J. C.; Punt, P. J.; van der Berg, P.; Debets, F.; Stouthamer, A. H.; van den Hondel, C. A. Characterization of an efficient gene cloning strategy for *Aspergillus niger* based on an autonomously replicating plasmid: cloning of the *nicB* gene of *A. niger*. *Gene* **1994**, *146*, 159–165.

113. Storms, R.; Zheng, Y.; Li, H.; Sillaots, S.; Martinez-Perez, A.; Tsang, A. Plasmid vectors for protein production, gene expression and molecular manipulations in *Aspergillus niger*. *Plasmid* **2005**, *53*, 191–204.

114. Liu, W.; May, G. S.; Lionakis, M. S.; Lewis, R. E.; Kontoyiannis, D. P. Extra copies of the *Aspergillus fumigatus* squalene epoxidase gene confer resistance to terbinafine: genetic approach to studying gene dose-dependent resistance to antifungals in *A. fumigatus*. *Antimicrob. Agents Chemother.* **2004**, *48*, 2490–2496.

115. Nielsen, K. F.; Ma, M.; Rank, C.; Frisvad, J. C.; Larsen, T. O. Dereplication of Microbial Natural Products by LC-DAD-TOFMS. *J. Nat. Prod.* **2011**, *74*, 2338–2348.

116. Bobzin, S. C.; Yang, S.; Kasten, T. P. LC-NMR: a new tool to expedite the dereplication and identification of natural products. *J. Ind. Microbiol. Biotechnol.* **2000**, *25*, 342–345.

117. Sleno, L. The use of mass defect in modern mass spectrometry. *J. mass Spectrom.* **2012**, *47*, 226–236.

118. Laatsch, H. Antibase 2012. http://www.wiley-vch.de/stmdata/antibase.php (accessed on 1 February 2014).

119. Hansen, M. E.; Smedsgaard, J.; Larsen, T. O. X-hitting: An algorithm for novelty detection and dereplication by UV spectra of complex mixtures of natural products. *Anal. Chem.* **2005**, *77*, 6805–6817.

120. Månsson, M.; Phipps, R. K.; Gram, L.; Munro, M. H. G.; Larsen, T. O.; Nielsen, K. F. Explorative solid-phase extraction (E-SPE) for accelerated microbial natural product discovery, dereplication, and purification. *J. Nat. Prod.* **2010**, *73*, 1126–1132.

121. Klitgaard, A.; Iversen, A.; Andersen, M. R.; Larsen, T. O.; Frisvad, J. C.; Nielsen, K. F. Aggressive dereplication using UHPLC-DAD-QTOF: screening extracts for up to 3000 fungal secondary metabolites. *Anal. Bioanal. Chem.* **2014**, *406*, 1933–1943.

122. Kildgaard, S.; Mansson, M.; Dosen, I.; Klitgaard, A.; Frisvad, J. C.; Larsen, T. O.; Nielsen, K. F. Accurate dereplication of bioactive secondary metabolites from marine-derived fungi by UHPLC-DAD-QTOFMS and a MS/HRMS library. *Mar. Drugs* **2014**, *12*, 3681–3705.

123. Brill, G.; Chen, R.; Rasmussen, R. Calbistrins, novel antifungal agents produced by *Penicillium restrictum*. II: Isolation and elucidation of structure. *J. Antibiot. (Tokyo).* **1993**, *46*, 39–47.

124. Takagi, M.; Motohashi, K.; Motohashi, K.; Shin-ya, K. Isolation of 2 new metabolites, JBIR-74 and JBIR-75, from the sponge-derived *Aspergillus* sp. fS14. *J. Antibiot. (Tokyo).* **2010**, *63*, 393–395.

125. Capon, R. J.; Skene, C.; Stewart, M.; Ford, J.; O'Hair, R. a J.; Williams, L.; Lacey, E.; Gill, J. H.; Heiland, K.; Friedel, T. Aspergillicins A-E: five novel depsipeptides from the marine-derived fungus *Aspergillus carneus*. *Org. Biomol. Chem.* **2003**, *1*, 1856–1862.

126. Kozlovsky, A. G.; Vinokurova, N. G.; Adanin, V. M.; Burkhardt, G.; Dahse, H. M.; Gräfe, U. New diketopiperazine alkaloids from *Penicillium fellutanum*. *J. Nat. Prod.* **2000**, *63*, 698–700.

127. Still, P. C.; Yi, B.; González-Cestari, T. F.; Pan, L.; Pavlovicz, R. E.; Chai, H.-B.; Ninh, T. N.; Li, C.; Soejarto, D. D.; McKay, D. B.; Kinghorn, D. A. Alkaloids from Micrococ paniculata with cytotoxic and nicotinic receptor antagonistic activities. *J. Nat. Prod.* **2013**, *76*, 243–249.

128. Steiman, R.; Guiraud, P.; Sage, L.; Seigle-Murandi, F. New Strains from Israel in the *Aspergillus niger* Group. *Syst. Appl. Microbiol.* **1995**, *17*, 620–624.

129. Pedras, M. S. C.; Smith, K. C.; Taylor, J. L. Production of 2,5-dioxopiperazine by a new isolate type of the blackleg fungus *Phoma lingam*. *Phytochemistry* **1998**, *49*, 1575–1577.

130. Kayser, O.; Waters, W. R.; Woods, K. M.; Upton, S. J.; Keithly, J. S.; Kiderlen, A. F. Evalutaion of in vitro activity of aurones and related compounds against *Cryptosporidium parvum*. *Planta Med.* **2001**, *67*, 722–725.

131. McCracken, S. T.; Kaiser, M.; Boshoff, H. I.; Boyd, P. D. W.; Copp, B. R. Synthesis and antimalarial and antituberculosis activities of a series of natural and unnatural 4-methoxy-6-styryl-pyran-2-ones, dihydro analogues and photo-dimers. *Bioorg. Med. Chem.* **2012**, *20*, 1482–1493.

132. Metzger, U.; Schall, C.; Zocher, G.; Unsöld, I.; Stec, E.; Li, S.-M.; Heide, L.; Stehle, T. The structure of dimethylallyl tryptophan synthase reveals a common architecture of aromatic prenyltransferases in fungi and bacteria. *Proc. Natl. Acad. Sci. U. S. A.* **2009**, *106*, 14309–14314.

133. Guo, J.-P.; Tan, J.-L.; Wang, Y.-L.; Wu, H.-Y.; Zhang, C.-P.; Niu, X.-M.; Pan, W.-Z.; Huang, X.-W.; Zhang, K.-Q. Isolation of talathermophilins from the thermophilic fungus *Talaromyces thermophilus* YM3-4. *J. Nat. Prod.* **2011**, *74*, 2278–2281.

134. Zhou, L.; Zhu, T.; Cai, S. Three new indole-containing diketopiperazine alkaloids from a deep-ocean sediment derived fungus *Penicillium griseofulvum*. *Helv. Chim. Acta* **2010**, *93*, 1758–1763.

135. Hollenhorst, M. a; Bumpus, S. B.; Matthews, M. L.; Bollinger, J. M.; Kelleher, N. L.; Walsh, C. T. The nonribosomal peptide synthetase enzyme DdaD tethers N(β)-fumaramoyl-l-2,3-diaminopropionate for Fe(II)/α-ketoglutarate-dependent epoxidation by DdaC during dapdiamide antibiotic biosynthesis. *J. Am. Chem. Soc.* **2010**, *132*, 15773–15781.

136. Lorenz, N.; Olsovská, J.; Sulc, M.; Tudzynski, P. Alkaloid cluster gene ccsA of the ergot fungus Claviceps purpurea encodes chanoclavine I synthase, a flavin adenine dinucleotide-containing oxidoreductase mediating the transformation of N-methyl-dimethylallyltryptophan to chanoclavine I. *Appl. Environ. Microbiol.* **2010**, *76*, 1822–1830.

137. Gao, J.; Radwan, M. M.; León, F.; Wang, X.; Jacob, M. R.; Tekwani, B. L.; Khan, S. I.; Lupien, S.; Hill, R. a; Dugan, F. M.; Cutler, H. G.; Cutler, S. J. Antimicrobial and antiprotozoal activities of secondary metabolites from the fungus Eurotium repens. *Med. Chem. Res.* **2012**, *21*, 3080–3086.

138. Du, F.-Y.; Li, X.-M.; Li, C.-S.; Shang, Z.; Wang, B.-G. Cristatumins A-D, new indole alkaloids from the marine-derived endophytic fungus *Eurotium cristatum* EN-220. *Bioorg. Med. Chem. Lett.* **2012**, *22*, 4650–4653.

139. Wicklow, D. T.; Dowd, P. F.; Alfatafta, a a; Gloer, J. B. Ochratoxin A: an antiinsectan metabolite from the sclerotia of *Aspergillus carbonarius* NRRL 369. *Can. J. Microbiol.* **1996**, *42*, 1100–1103.

140. Mogensen, J. M.; Nielsen, K. F.; Samson, R. a; Frisvad, J. C.; Thrane, U. Effect of temperature and water activity on the production of fumonisins by *Aspergillus niger* and different *Fusarium* species. *BMC Microbiol.* **2009**, *9*, 281.

141. Noonim, P.; Mahakarnchanakul, W.; Nielsen, K. F.; Frisvad, J. C.; Samson, R. a Isolation, identification and toxigenic potential of ochratoxin A-producing *Aspergillus* species from coffee beans grown in two regions of Thailand. *Int. J. Food Microbiol.* **2008**, *128*, 197–202.

142. Moore, G. G.; Elliott, J. L.; Singh, R.; Horn, B. W.; Dorner, J. W.; Stone, E. a; Chulze, S. N.; Barros, G. G.; Naik, M. K.; Wright, G. C.; Hell, K.; Carbone, I. Sexuality generates diversity in the aflatoxin gene cluster: evidence on a global scale. *PLoS Pathog.* **2013**, *9*, e1003574.

143. Jørgensen, T. R.; Nielsen, K. F.; Arentshorst, M.; Park, J.; van den Hondel, C. a; Frisvad, J. C.; Ram, A. F. Submerged conidiation and product formation by *Aspergillus niger* at low specific growth rates are affected in aerial developmental mutants. *Appl. Environ. Microbiol.* **2011**, *77*, 5270–5277.

144. Raper, K. B.; Fennell, D. I. *The genus Aspergillus*; Williams and Wilkins: Baltimore, MD, USA, 1965; p. 686.

145. Al-Musallam, A. *Revision of the black Aspergillus species*; Centraalbureau voor Schimmelcultures: Baarn, 1980; p. 92.

146. Agnihotri, V. P. Effects of nitrogenous compounds on sclerotium formation in *Aspergillus niger*. *Can. J. Microbiol.* **1968**, *14*, 1253–1258.

147. Agnihotri, V. P. Some nutritional and environmental factors affecting growth and production of sclerotia by a strain of *Aspergillus niger*. *Can. J. Microbiol.* **1969**, *15*, 835–840.

148. Wicklow, D. T. Metabolites in the coevolution of fungal chemical defence systems. In *Coevolution of fungi with plant and animals*; Pirozynski, K.; Hawksworth, D., Eds.; Academic Press: London, 1988; pp. 173–201.

149. Tepaske, M. R.; Gloer, J. B.; Wicklow, D. T.; Dowd, P. F. 3 new aflavinines from the sclerotia of *Aspergillus tubingensis*. *Tetrahedron* **1989**, *45*, 4961–4968.

150. Tepaske, M. R.; Gloer, J. B.; Wicklow, D. T.; Dowd, P. F. Tubingensin A: An antiviral carbazole alkaloid from the sclerotia of *Aspergillus tubingensis*. *J. Org. Chem.* **1989**, *54*, 4743–4746.

151. Swenson, D. C.; TePaske, M. R.; Baenziger, N. C.; Gloer, J. B. Tubingensin B, a cytotoxic carbazole alkaloid from the sclerotia of *Aspergillus tubingensis*. *Acta Crystallogr. Sect. C Cryst. Struct. Commun.* **1997**, *53*, 1447–1449.

152. Sings, H. L.; Harris, G. H.; Dombrowski, a W. Dihydrocarbazole alkaloids from *Aspergillus tubingensis* . *J. Nat. Prod.* **2001**, *64*, 836–838.

153. Staub, G. M.; Gloer, J. B.; Wicklow, D. T.; Dowd, P. F. Aspernomine: A cytotoxic antiinsectan metabolite with a novel ring-system from the sclerotia of *Aspergillus nomius*. *J. Am. Chem. Soc.* **1992**, *114*, 1015–1017.

154. Gloer, J. B. Antiinsectan natural products from fungal sclerotia. *Acc. Chem. Res.* **1995**, *28*, 343–350.

155. Murao, S.; Hayashi, H.; Takiuchi, K.; Arai, M. Okaramine A, a novel indole alkaloid with insecticidal activity, from *Penicillium simplicissimum* AK-40. *Agric. Biol. Chem.* **1988**, *52*, 885–886.

156. Hayashi, H.; Takiuchi, K.; Murao, S.; Arai, M. Okaramine B, an insecticidal indole alkaloid, produced by *Penicillium simplicissimum* AK-40. *Agric. Biol. Chem.* **1988**, *52*, 2131–2133.

157. Hayashi, H.; Asabu, Y.; Murao, S.; Arai, M. New Okaramine Congeners, Okaramins D, E, and F, from *Penicillium simplicissimum* ATCC 90288. *Japan Soc. Biosci. Biotechnol. Agrochem.* **1995**, *59*, 246–250.

158. Schümann, J.; Hertweck, C. Molecular basis of cytochalasan biosynthesis in fungi: gene cluster analysis and evidence for the involvement of a PKS-NRPS hybrid synthase by RNA silencing. *J. Am. Chem. Soc.* **2007**, *129*, 9564–9565.

159. Wagenaar, M. M.; Corwin, J.; Strobel, G.; Clardy, J. Three new cytochalasins produced by an endophytic fungus in the genus *Rhinocladiella*. *J. Nat. Prod.* **2000**, *63*, 1692–1695.

160. Liu, R.; Gu, Q.; Zhu, W.; Cui, C.; Fan, G.; Fang, Y.; Zhu, T.; Liu, H. 10-Phenyl-[12]-cytochalasins Z7, Z8, and Z9 from the marine-derived fungus *Spicaria elegans*. *J. Nat. Prod.* **2006**, *69*, 871–875.

161. Knudsen, P. B.; Hanna, B.; Ohl, S.; Sellner, L.; Zenz, T.; Döhner, H.; Stilgenbauer, S.; Larsen, T. O.; Lichter, P.; Seiffert, M. Chaetoglobosin A preferentially induces apoptosis in chronic lymphocytic leukemia cells by targeting the cytoskeleton. *Leukemia* **2014**, 1–10.

162. Zhang, Y.; Wang, T.; Pei, Y.; Hua, H.; Feng, B. Aspergillin PZ, a novel isoindole-alkaloid from *Aspergillus awamori*. *J. Antibiot. (Tokyo).* **2002**, *55*, 693–695.

163. Canham, S. M.; Overman, L. E.; Tanis, P. S. Identification of an unexpected 2-oxonia[3,3]sigmatropic rearrangement/aldol pathway in the formation of oxacyclic rings. Total synthesis of (+)-aspergillin PZ. *Tetrahedron* **2011**, *67*, 9837–9843.

164. Keller-Schierlein, W.; Kupfer, E. Metabolites of microorganisms. 186. The aspochalasins A, B, C, and D. *Helv. Chim. Acta* **1979**, *62*, 1501–1524.

165. Naruse, N.; Yamamoto, S.; Yamamoto, H. β-cyanoglutamic acid, a new antifungal amino acid from a streptomycete. *J. Antibiot. (Tokyo).* **1993**, *46*, 685–686.

166. Fang, F.; Ui, H.; Shiomi, K.; Masuma, R.; Yamaguchi, Y.; Zhang, C. G.; Zhang, X. W.; Tanaka, Y.; Omura, S. Two new components of the aspochalasins produced by *Aspergillus* sp. *J. Antibiot. (Tokyo).* **1997**, *50*, 919–925.

167. Tomikawa, T.; Kazuo, S.; Seto, H.; Okusa, N.; Kajiura, T.; Hayakawa, Y. Structure of aspochalasin H, a new member of the aspochalasin family. *J. Antibiot. (Tokyo).* **2002**, *55*, 666–668.

168. Choo, S.-J.; Yun, B.-S.; Ryoo, I.-J.; Kim, Y.-H.; Bae, K.-H.; Yoo, I.-D. Aspochalasin I, a Melanogenesis Inhibitor from *Aspergillus* sp. *J. Microbiol. Biotechnol.* **2009**, *19*, 368–371.

169. Zhou, G.-X.; Wijeratne, K. E. M.; Bigelow, D.; Pierson, L. S.; VanEtten, H. D.; Gunatilaka, L. A. A. Aspochalasins I, J, and K: three new cytotoxic cytochalasans of *Aspergillus flavipes* from the rhizosphere of *Ericameria laricifolia* of the Sonoran Desert. *J. Nat. Prod.* **2004**, *67*, 328–332.

170. Rochfort, S.; Ford, J.; Ovenden, S.; George, S.; Wildman, H.; Tait, R. M.; Meurer-Grimes, B.; Coxd, S.; Coatesd, J.; Rhodes, D. A novel aspochalasin with HIV-1 integrase inhibitory activity from *Aspergillus flavipes*. *J. Antibiot. (Tokyo).* **2005**, *58*, 279–283.

171. Liu, J.; Hu, Z.; Huang, H.; Zheng, Z.; Xu, Q. Aspochalasin U, a moderate TNF-α inhibitor from *Aspergillus* sp. *J. Antibiot. (Tokyo).* **2012**, *65*, 49–52.

172. Kohno, J.; Nonaka, N.; Nishio, M.; Ohnuki, T.; Kawano, K.; Okuda, T.; Komatsubara, S. TMC-169, a new antibiotic of the aspochalasin group produced by *Aspergillus flavipes*. *J. Antibiot. (Tokyo).* **1999**, *52*, 575–577.

173. Gebhardt, K.; Schimana, J.; Holitzel, A.; Dettner, K.; Draeger, S.; Beil, W.; Rheinheimer, J.; Fiedler, H.-P. Aspochalamins A-D and aspochalasin Z produced by the endosymbiotic fungus *Aspergillus niveus* LU 9574. *J. Antibiot. (Tokyo).* **2004**, *57*, 707–714.

174. Barrow, C.; Sedlock, D.; Sun, H.; Cooper, R.; Gillum, A. M. WIN 66306, a new neurokinin antagonist produced by an *Aspergillus* species: fermentation, isolation and physico-chemical properties. *J. Antibiot. (Tokyo).* **1994**, *47*, 1182–1187.

175. Fujishima, T.; Ichikawa, M.; Ishige, H.; Yoshino, H.; Ohishi, J.; Ikegami, S. Production of cytochalasin E by *Aspergillus terreus*. *Hakkokogaku Kaishi – J. Soc. Ferment. Technol.* **1979**, *57*, 15–19.

176. Lin, Z.; Zhang, G.; Zhu, T.; Liu, R.; Wei, H.-J.; Gu, Q.-Q. Bioactive cytochalasins from *Aspergillus flavipes*, an endophytic fungus associated with the mangrove plant *Acanthus ilicifolius*. *Helv. Chim. Acta* **2009**, *92*, 1538–1544.

177. Ge, H. M.; Peng, H.; Guo, Z. K.; Cui, J. T.; Song, Y. C.; Tan, R. X. Bioactive alkaloids from the plant endophytic fungus *Aspergillus terreus*. *Planta Med.* **2010**, *76*, 822–824.

178. Zhang, H.-W.; Zhang, J.; Hu, S.; Zhang, Z.-J.; Zhu, C.-J.; Ng, S. W.; Tan, R.-X. Ardeemins and cytochalasins from *Aspergillus terreus* residing in *Artemisia annua*. *Planta Med.* **2010**, *76*, 1616–1621.

179. Xiao, L.; Liu, H.; Wu, N.; Liu, M.; Wei, J.; Zhang, Y.; Lin, X. Characterization of the high cytochalasin E and rosellichalasin producing-*Aspergillus* sp. nov. F1 isolated from marine solar saltern in China. *World J. Microbiol. Biotechnol.* **2013**, *29*, 11–17.

180. Zheng, C.-J.; Shao, C.-L.; Wu, L.-Y.; Chen, M.; Wang, K.-L.; Zhao, D.-L.; Sun, X.-P.; Chen, G.-Y.; Wang, C.-Y. Bioactive phenylalanine derivatives and cytochalasins from the soft coral-derived fungus, *Aspergillus elegans*. *Mar. Drugs* **2013**, *11*, 2054–2068.

181. Büchi, G.; Kitaura, Y.; Yuan, S. Structure of cytochalasin E, a toxic metabolite of *Aspergillus clavatus*. *J. Am. Chem. Soc.* **1973**, *95*, 5423–5425.

182. Steyn, P. S.; van Heerden, F. R.; Rabie, C. J. Cytochalasin-E and cytochalasin-K, toxic metabolites from *Aspergillus clavatus*. *J. Am. Chem. Soc. Perkin I* **1982**, 541–544.

183. Binder, M.; Tamm, C. Proxiphomin and Protophomin, 2 new cytochalasanes. *Helv. Chim. Acta* **1973**, *7*, 2387–2396.

184. Noonim, P.; Mahakarnchanakul, W.; Varga, J.; Frisvad, J. C.; Samson, R. a Two novel species of *Aspergillus* section *Nigri* from Thai coffee beans. *Int. J. Syst. Evol. Microbiol.* **2008**, *58*, 1727–1734.

185. Machida, M.; Yamada, O.; Gomi, K. Genomics of *Aspergillus oryzae*: learning from the history of Koji mold and exploration of its future. *DNA Res.* **2008**, *15*, 173–183.

186. Rokas, A.; Payne, G. A.; Fedorova, N.; Baker, S. E.; Machida, M.; Yu, J.; Georgianna, D. R.; Dean, R. A.; Bhatnagar, D.; Cleveland, T. E.; Wortman, J. R.; Maiti, R.; Joardar, V.; Amedeo, P.; Denning, D. W.; Nierman, W. C. What can comparative genomics tell us about species concepts in the genus *Aspergillus*? *Stud. Mycol.* **2007**, *59*, 11–17.

187. Wilson, B. J.; Wilson, C. H. Toxin from *Aspergillus Flavus*: Production on food materials of a substance causing tremors in mice. *Science.* **1964**, *144*, 177–178.

188. Gallagher, R.; Wilson, B. Aflatrem, the tremorgenic mycotoxin from *Aspergillus flavus*. *Mycopathologia* **1978**, *66*, 183–185.

189. Nicholson, M. J.; Koulman, A.; Monahan, B. J.; Pritchard, B. L.; Payne, G. a; Scott, B. Identification of two aflatrem biosynthesis gene loci in *Aspergillus flavus* and metabolic engineering of *Penicillium paxilli* to elucidate their function. *Appl. Environ. Microbiol.* **2009**, *75*, 7469–7481.

190. Shiomi, K.; Hatae, K.; Yamaguchi, Y.; Masuma, R.; Tomoda, H.; Kobayashi, S.; Omura, S. New antibiotics miyakamides produced by a fungus. *J. Antibiot. (Tokyo).* **2002**, *55*, 952–961.

191. Springer, J. P.; Bűchi, G.; Kobbe, B.; Demain, A. L.; J, C. The structure of ditryptophenaline-a new metabolite of *Aspergillus flavus*. *Tetrahedron Lett.* **1977**, *28*, 2403–2406.

192. Rausch, C.; Weber, T.; Kohlbacher, O.; Wohlleben, W.; Huson, D. H. Specificity prediction of adenylation domains in nonribosomal peptide synthetases (NRPS) using transductive support vector machines (TSVMs). *Nucleic Acids Res.* **2005**, *33*, 5799–5808.

193. Marfey, P. Determination of D-amino acids. II. Use of a bifunctional reagent, 1,5-difluoro-2,4-dinitrobenzen. *Carlsb. Res. Commun.* **1984**, *49*, 591–596.

194. Bhushan, R.; Brückner, H. Marfey's reagent for chiral amino acid analysis: a review. *Amino Acids* **2004**, *27*, 231–47.

195. Artigot, M. P.; Loiseau, N.; Laffitte, J.; Mas-Reguieg, L.; Tadrist, S.; Oswald, I. P.; Puel, O. Molecular cloning and functional characterization of two CYP619 cytochrome P450s involved in biosynthesis of patulin in *Aspergillus clavatus*. *Microbiology* **2009**, *155*, 1738–1747.

196. Puel, O.; Galtier, P.; Oswald, I. P. Biosynthesis and toxicological effects of patulin. *Toxins (Basel).* **2010**, *2*, 613–631.

197. Dewick, P. M. *Medicinal Natural Prdoducts. A Biosynthetic Approach*; 3rd ed.; John Wiley & Sons Ltd: Chichester, West Sussex, United Kingdom, 2009; pp. 39–132.

198. Regueira, T. B.; Kildegaard, K. R.; Hansen, B. G.; Mortensen, U. H.; Hertweck, C.; Nielsen, J. Molecular basis for mycophenolic acid biosynthesis in *Penicillium brevicompactum*. *Appl. Environ. Microbiol.* **2011**, *77*, 3035–3043.

199. Wasil, Z.; Pahirulzaman, K. A. K.; Butts, C.; Simpson, T. J.; Lazarus, C. M.; Cox, R. J. One pathway, many compounds: heterologous expression of a fungal biosynthetic pathway reveals its intrinsic potential for diversity. *Chem. Sci.* **2013**, *4*, 3845–3856.

200. Richards, M.; Edwards, J. Nosocomial infections in combined medical-surgical intensive care units in the United States. *Infect. Control Hosp. Epidemiol.* **2000**, *21*, 510–515.

201. Nagata, H.; Kakeya, H.; Konno, H.; Kanazawa, S. JP2002322149-A ; JP4870276-B2: RKB-3384 analogs from *Aspergillus* species, and pharmaceuticals containing them.

202. Kakeya, H.; Kageyama, S.; Nie, L.; Onose, R.; Okada, G.; Beppu, T.; Norbury, C. J.; Osada, H. Lucilactaene, a new cell cycle inhibitor in p53-transfected cancer cells, produced by a *Fusarium* sp. *J. Antibiot. (Tokyo).* **2001**, *54*, 850–854.

203. Kakeya, H.; Takahashi, I.; Okada, G.; Isono, K.; Osada, H. Epolactaene, a novel neuritogenic compound in human neuroblastoma cells, produced by a marine fungus. *J. Antibiot. (Tokyo).* **1995**, *48*, 733–735.

204. Gelderblom, W.; Marasas, W.; Steyn, P.; PG, T.; Van der Merwe, K. J.; Rooyen, P.; Vleggaar, R.; Wessels, P. L. Structure elucidation of fusarin C, a mutagen produced by *Fusarium moniliforme*. *J. Chem. Soc., Chem.Commun.* **1984**, 122–124.

205. Steyn, P.; Vleggaar, R. Biosynthetic studies on the fusarins, metabolites of *Fusarium moniliforme*. *J. Chem. Soc. Chem. Commun.* **1985**, 1189–1191.

206. Song, Z.; Cox, R. J.; Lazarus, C. M.; Simpson, T. J. Fusarin C biosynthesis in *Fusarium moniliforme* and *Fusarium venenatum*. *ChemBioChem* **2004**, *5*, 1196–1203.

207. Holm, D. K.; Petersen, L. M.; Klitgaard, A.; Knudsen, P. B.; Jarczynska, Z. D.; Nielsen, K. F.; Gotfredsen, C. H.; Larsen, T. O.; Mortensen, U. H. Molecular and chemical characterization of the biosynthesis of the 6-MSA derived meroterpenoid yanuthone D in *Aspergillus niger*. *Chem. Biol.* **2014**, *21*, 519–529.

208. Flanagan, M. D.; Lin, S. Cytochalasins block actin filament elongation by binding to high affinity sites associated with F-actin. *J. Biol. Chem.* **1980**, *255*, 835–838.

209. Brown, S. S.; Spudich, J. A. Mechanism of action of cytochalasin: evidence that it binds to actin filament ends. *J. Cell Biol.* **1981**, *88*, 487–491.

210. Aldridge, D. C.; Armstron, J. J.; Speake, R. N.; Turner, W. B. Cytochalasins, a new class of biologically active mould metabolites. *Chem. Commun.* **1967**, 26–27.

211. Aldridge, D. C.; Armstrong, J. J.; Speake, R. N.; Turner, W. B. The structures of cytochalasins A and B. *J. Chem. Soc.* **1967**, 1667–1676.

212. Rampal, A.; Pinkofsky, H.; Jung, C. Structure of cytochalasins and cytochalasin B binding sites in human erythrocyte membranes. *Biochemistry* **1980**, 679–683.

213. Udagawa, T.; Yuan, J.; Panigrahy, D.; Chang, Y. H.; Shah, J.; D'Amato, R. J. Cytochalasin E, an epoxide containing *Aspergillus*-derived fungal metabolite, inhibits angiogenesis and tumor growth. *J. Pharmacol. Exp. Ther.* **2000**, *294*, 421–427.

214. Qiao, K.; Chooi, Y.-H.; Tang, Y. Identification and engineering of the cytochalasin gene cluster from *Aspergillus clavatus* NRRL 1. *Metab. Eng.* **2011**, *13*, 723–732.

215. Binder, V. M.; Kiechel, J.-R.; Tamm, C. Zur Biogenese des Antibioticums Phomin. *Helv. Chim. Acta* **1970**, *53*, 1797–1812.

216. Probst, A.; Tamm, C. Biosynthetic Studies on Chaetoglobosin A and 19-O-Acetylchaetoglobosin A. *Helv. Chim. Acta* **1981**, *64*, 2065–2077.

217. Hu, Y.; Dietrich, D.; Xu, W.; Patel, A.; Thuss, J. a J.; Wang, J.; Yin, W.-B.; Qiao, K.; Houk, K. N.; Vederas, J. C.; Tang, Y. A carbonate-forming Baeyer-Villiger monooxygenase. *Nat. Chem. Biol.* **2014**, *10*, 552–554.

218. Larionov, V.; Kouprina, N.; Eldarov, M.; Perkins, E.; Porter, G.; Resnick, M. A. Transformation-associated recombination between diverged and homologous DNA repeats is induced by strand breaks. *Yeast* **1994**, *10*, 93–104.

219. Larionov, V.; Kouprina, N.; Graves, J.; Resnick, M. A. Highly selective isolation of human DNAs from rodent-human hybrid cells as circular yeast artificial chromosomes by transformation-associated recombination cloning. *Proc. Natl. Acad. Sci. U. S. A.* **1996**, *93*, 13925–13930.

220. Kim, J. H.; Feng, Z.; Bauer, J. D.; Kallifidas, D.; Calle, P. Y.; Brady, S. F. Cloning large natural product gene clusters from the environment: piecing environmental DNA gene clusters back together with TAR. *Biopolymers* **2010**, *93*, 833–844.

221. Larionov, V.; Kouprina, N. Specific cloning of human DNA as yeast artificial chromosomes by transformation-associated recombination. *Proc. Natl. Acad. Sci. U. S. A.* **1996**, *93*, 491–496.

222. Feng, Z.; Kim, J.; Brady, S. Fluostatins produced by the heterologous expression of a TAR reassembled environmental DNA derived type II PKS gene cluster. *J. Am. Chem. Soc.* **2010**, *132*, 11902–11903.

223. Candlla, M.; Graves, J.; Matesic, L.; Reeves, R.; Tainton, K.; Choo, K.; Resnick, M.; Larionov, V.; Kouprina, N. Rapid cloning of mouse DNA as yeast artificial chromosomes by transformation-associated recombination (TAR). *Mamm. Genome* **1998**, *9*, 157–159.

224. Kirchner, J. M.; Ivanova, V.; Samson, A.; Noskov, V. N.; Volff, J. N.; Resnick, M. a; Walter, R. B. Transformation-associated recombination (TAR) cloning of tumor-inducing Xmrk2 gene from *Xiphophorus maculatus*. *Mar. Biotechnol.* **2001**, *3*, 168–176.

225. Gaida, A.; Becker, M. M.; Schmid, C. D.; Bühlmann, T.; Louis, E. J.; Beck, H.-P. Cloning of the repertoire of individual *Plasmodium falciparum* var genes using transformation associated recombination (TAR). *PLoS One* **2011**, *6*, e17782.

226. Johnstone, I. L.; Hughes, S. G.; Clutterbuck, A. J. Cloning an *Aspergillus nidulans* developmental gene by transformation. *EMBO J.* **1985**, *4*, 1307–1311.

227. Yin, W.-B.; Chooi, Y. H.; Smith, A. R.; Cacho, R. A.; Hu, Y.; White, T. C.; Tang, Y. Discovery of cryptic polyketide metabolites from dermatophytes using heterologous expression in *Aspergillus nidulans*. *ACS Synth. Biol.* **2013**, *2*, 629–634.

228. Gatti, G.; Cardillo, R.; Fuganti, C.; Gheringhelli, D. Structure determination of two extractives from *Aspergillus amstelodami* by nuclear magnetic resonance spectroscopy. *Chem. Commun.* **1976**, 435–436.

229. CMC-se structure elucidator http://www.bruker.com/products/mr/nmr/nmr-software/software/complete-molecular-confidence/cmc-se/overview.html (Accessed on 1 September 2014).

230. ACD/Structure elucidator http://www.acdlabs.com/products/com_iden/elucidation/struc_eluc/(Accessed on 1 September 2014).

231. Church, G. M.; Elowitz, M. B.; Smolke, C. D.; Voigt, C. a; Weiss, R. Realizing the potential of synthetic biology. *Nat. Rev. Mol. Cell Biol.* **2014**, *15*, 289–294.

232. Khalil, A. S.; Collins, J. J. Synthetic biology: applications come of age. *Nat. Rev. Genet.* **2010**, *11*, 367–379.

233. Winter, J. M.; Tang, Y. Synthetic biological approaches to natural product biosynthesis. *Curr. Opin. Biotechnol.* **2012**, *23*, 736–43.

234. Cameron, D. E.; Bashor, C. J.; Collins, J. J. A brief history of synthetic biology. *Nat. Rev. Microbiol.* **2014**, *12*, 381–390.

235. Huang, M.; Lu, J.-J.; Huang, M.-Q.; Bao, J.-L.; Chen, X.-P.; Wang, Y.-T. Terpenoids: natural products for cancer therapy. *Expert Opin. Investig. Drugs* **2012**, *21*, 1801–1818.

7 Appendix A

Sclerotium formation in black Aspergilli

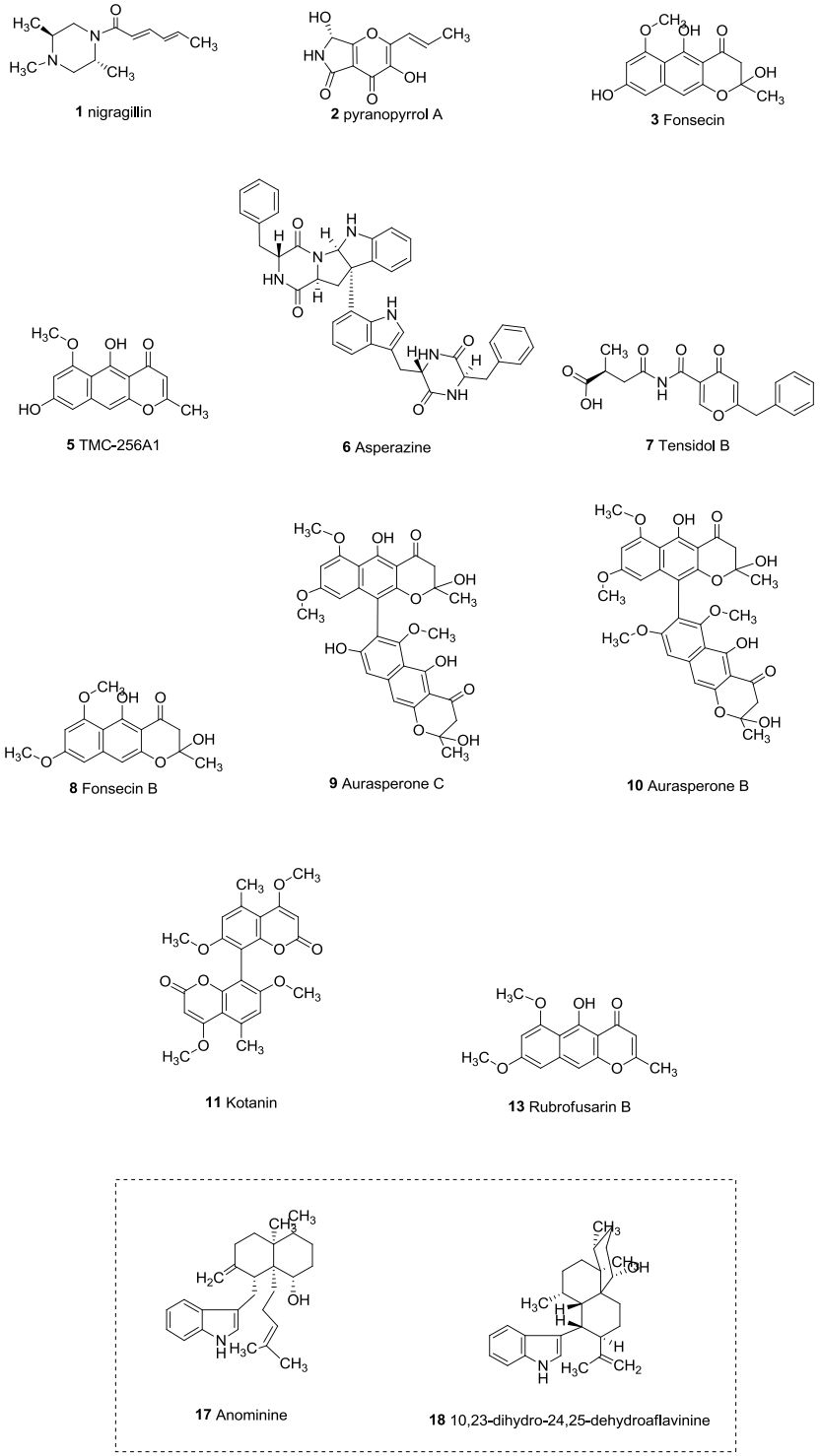

Figure A1 Chemical structures of selected SMs from the black Aspergilli and the sclerotium related indoloterpenes anominine (**17**) and 10,23-dihydro-24,25-dehydroaflavinine (**18**). For distribution, see Figure A2.

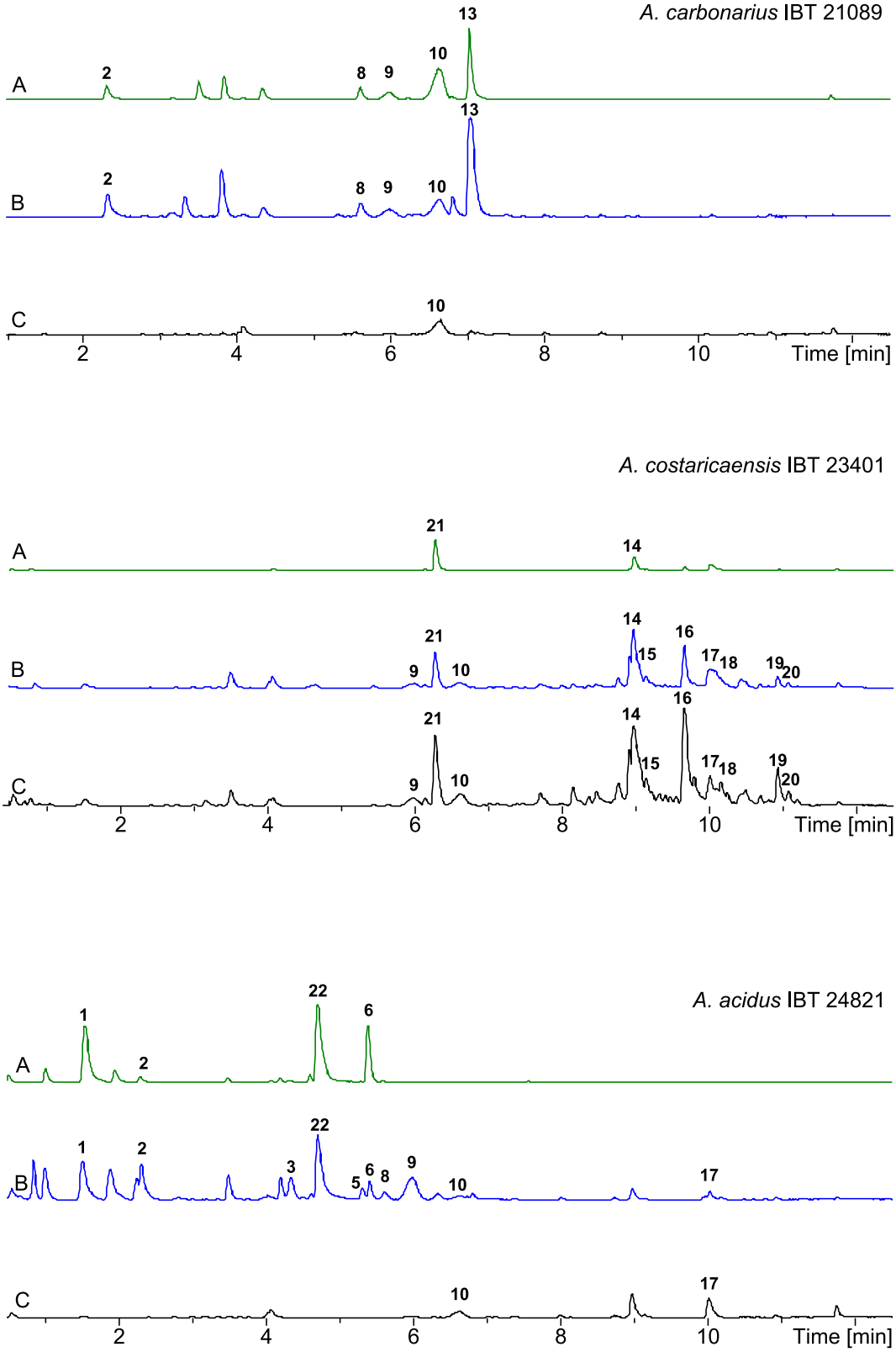

(*Figure A2 continued*)

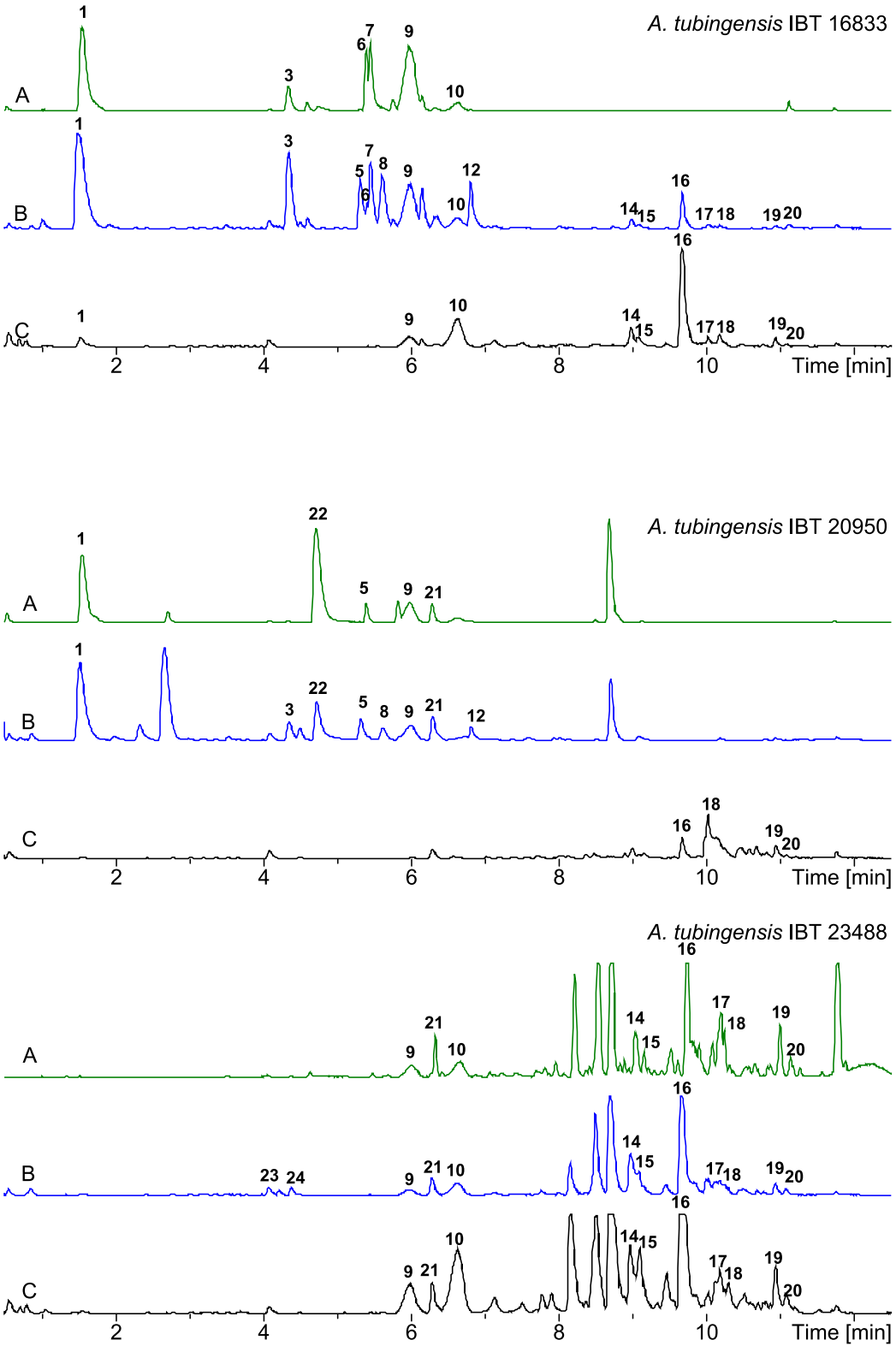

(*Figure A2 continued*)

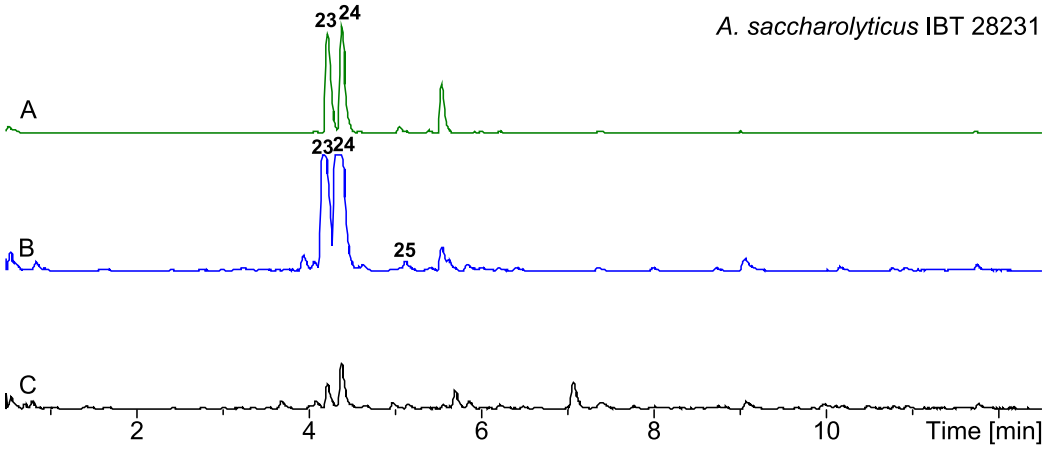

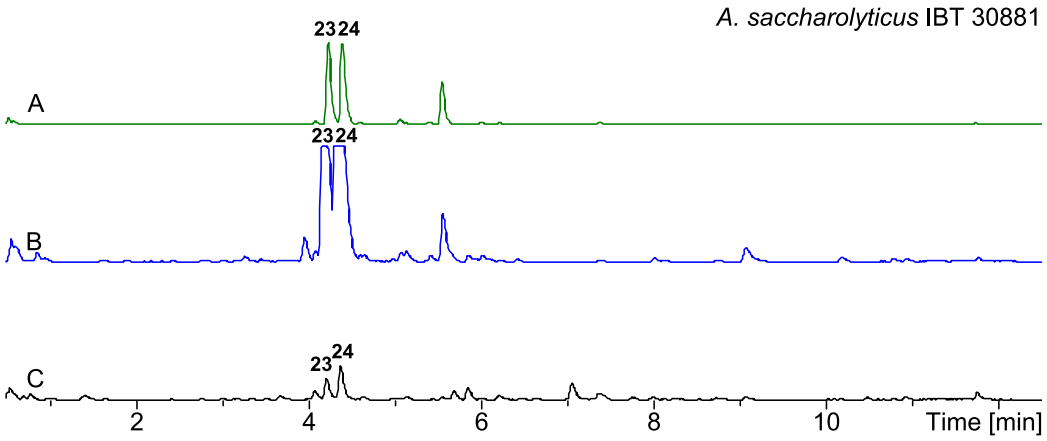

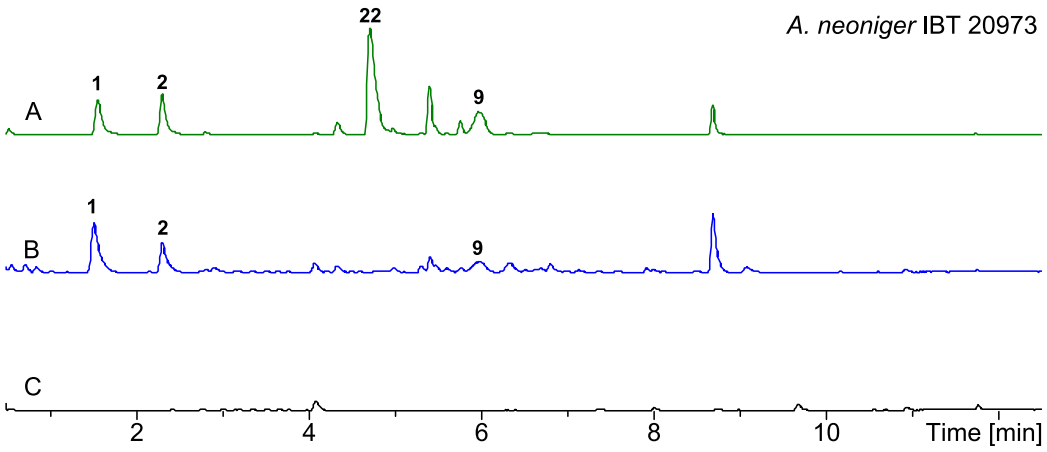

(*Figure A2 continued*)

A. niger IBT 24631

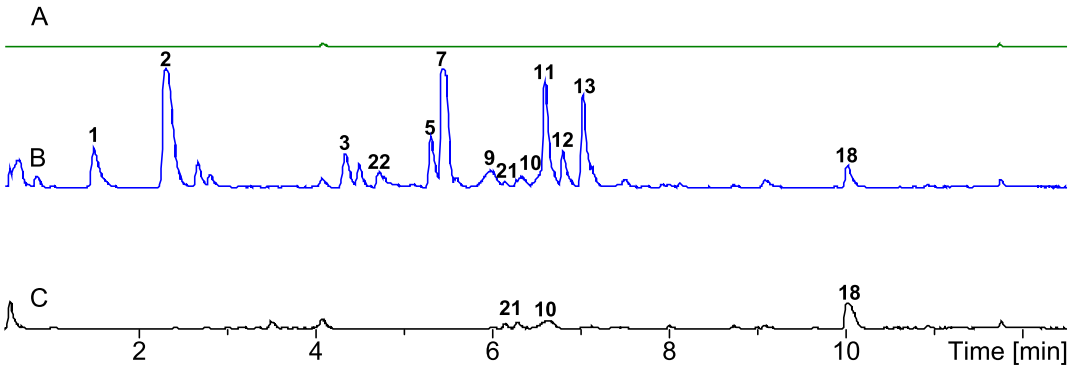

A. niger IBT 28999

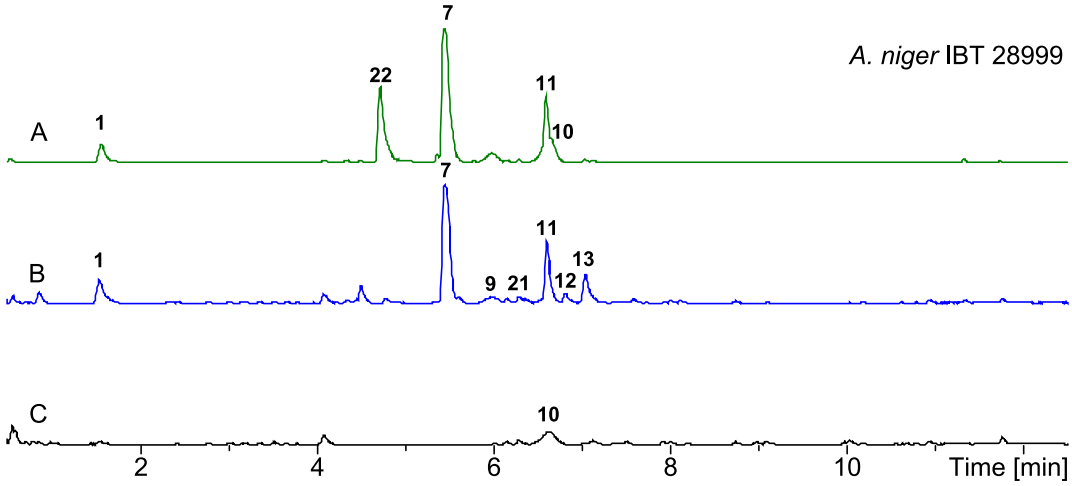

A. niger IBT 29019

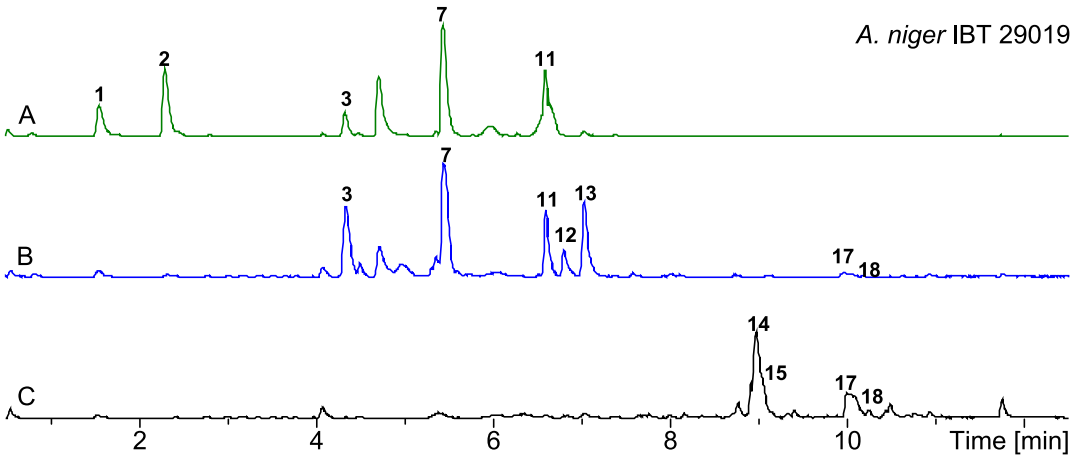

(Figure A2 continued)

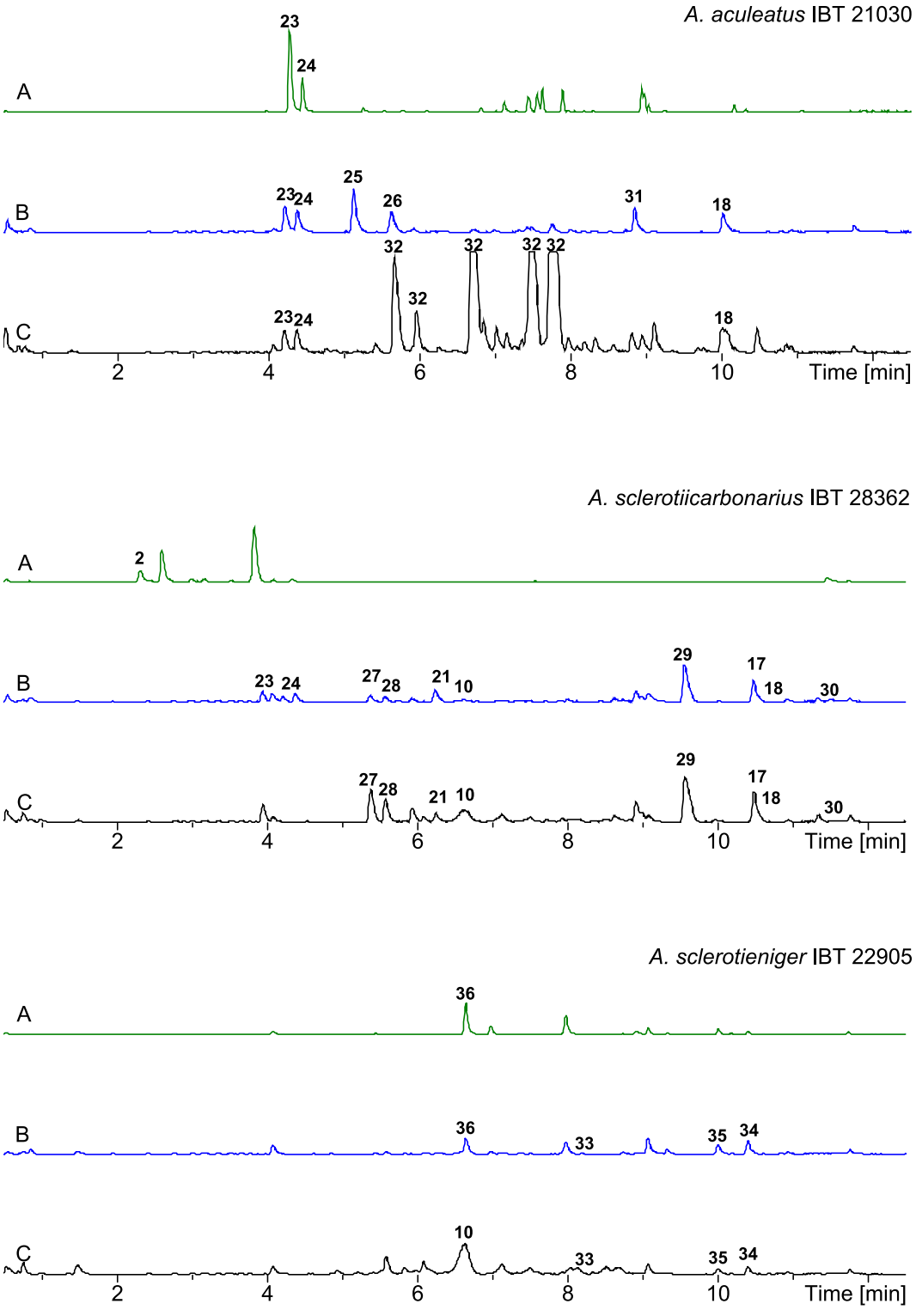

(*Figure A2 continued*)

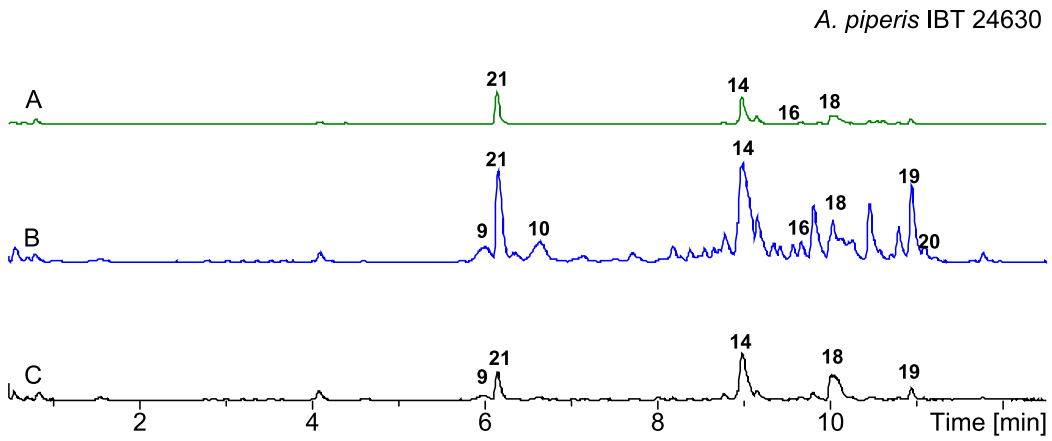

Figure A2 A: Plug extraction from growing and sporulating culture with no sclerotium production (CYA agar with biotin). B: Plug extraction from growth with sclerotium production (CYAR with biotin). C: Sclerotium extraction (from CYAR with biotin). 1) Nigragillin, 2) Pyranonigrin A, 3) Fonsecin, 4) Aurasperone/nigerasperone analog, 5) TMC-256A1, 6) Asperazine, 7) Tensidol B, 8) Fonsecin B, 9) AurasperoneC, 10) Aurasperone B, 11) Kotanin, 12) Flavasperone analog, 13) Rubrofusarin B, 14) Aflavinine analog, 15) Aflavinine analog, 16) Aflavinine analog, 17) Anominine, 18) 10,23-dihydro- 24,25-dehydroaflavinine, 19) Aflavinine analog, 20) Aflavinine analog, 21) malformin C, 22) Funalenone, 23) Aculene A, 24) Aculene B, 25) Aculene C, 26) Aculene D, 27) Carbonarin I, 28) Carbonarin J, 29) Emindole SC, 30) Sclerolizine, 31) Acudioxomorpholine, 32) Okaramine analog, 33) Sclerotionigrin A, 34) Sclerotionigrin B, 35) Proxiphomin, 36) Ochratoxin A. For structures of a selection of these compounds, see Figure A1.

Paper 1

"Dereplication guided discovery of secondary metabolites of mixed biosynthetic origin from *Aspergillus aculeatus*"

Petersen, L.M.; Hoeck, C.; Frisvad, J.C.; Gotfredsen, C.H.; Larsen, T.O.

Molecules, **2014**, *19*, 10898-10921

Molecules **2014**, *19*, 10898-10921; doi:10.3390/molecules190810898

OPEN ACCESS

molecules

ISSN 1420-3049
www.mdpi.com/journal/molecules

Article

Dereplication Guided Discovery of Secondary Metabolites of Mixed Biosynthetic Origin from *Aspergillus aculeatus*

Lene M. Petersen [1], Casper Hoeck [2], Jens C. Frisvad [1], Charlotte H. Gotfredsen [2] and Thomas O. Larsen [1,*]

[1] Chemodiversity Group, Department of Systems Biology, Søltofts Plads B221, Technical University of Denmark, Kgs. Lyngby DK-2800, Denmark; E-Mails: lmape@bio.dtu.dk (L.M.P.); jcf@bio.dtu.dk (J.C.F.)

[2] Department of Chemistry, Kemitorvet B201, Technical University of Denmark, Kgs. Lyngby DK-2800, Denmark; E-Mails: casho@kemi.dtu.dk (C.H.); chg@kemi.dtu.dk (C.H.G.)

* Author to whom correspondence should be addressed; E-Mail: tol@bio.dtu.dk; Tel.: +45-2425-2632; Fax: +45-4588-4922.

Received: 16 June 2014; in revised form: 15 July 2014 / Accepted: 16 July 2014 / Published: 25 July 2014

Abstract: Investigation of the chemical profile of the industrially important black filamentous fungus *Aspergillus aculeatus* by UHPLC-DAD-HRMS and subsequent dereplication has led to the discovery of several novel compounds. Isolation and extensive 1D and 2D NMR spectroscopic analyses allowed for structural elucidation of a dioxomorpholine, a unique okaramine, an aflavinine and three novel structures of mixed biosynthetic origin, which we have named aculenes A–C. Moreover, known analogues of calbistrins, okaramines and secalonic acids were detected. All novel compounds were tested for antifungal activity against *Candida albicans*, however all showed only weak or no activity. *Aspergillus aculeatus* IBT 21030 was additionally shown to be capable of producing sclerotia. Examination of the sclerotia revealed a highly regulated production of metabolites in these morphological structures.

Keywords: *Aspergillus aculeatus*; Aspergilli; natural products; secondary metabolism; dereplication; sclerotia

---

1. Introduction

Aspergillus aculeatus is a filamentous fungus belonging to *Aspergillus* section *Nigri*—the black aspergilli. At least 145 metabolites have been characterized from the black aspergilli [1], many of which are biologically active. Naphtho-γ-pyrones (NGPs) such as aurasperone A and rubrofusarin B from *A. niger* are known to be antifungal [2], while other NGPs are reported to have antitumor activities [3]. Mycotoxins produced by *A. niger*, such as ochratoxin A [4] or the fumonisins [5] are also known.

The black aspergilli can be divided into different clades. *A. aculeatus* belongs to the uniseriate black aspergilli and is closely related to *A. aculeatinus*, *A. uvarum*, *A. japonicus*, *A. fijiensis*, *A. trinidadensis*, *A. floridensis*, *A. brunneoviolaceus* and *A. violaceofuscus* [6,7]. These fungi differ from the other black aspergilli in their morphology, physiological behavior and in the production of secondary metabolites. The fungi belonging to this group can produce secondary metabolites, which can be both polyketide (PK) and nonribosomal peptide (NRP) derived or of mixed biosynthetic origin [1]. Several metabolites, including aculeacins A–G [8,9], CJ-15,183 [10], secalonic acids D and F [11] and okaramines H and I [12], have been reported in fungi identified as *A. aculeatus*. Furthermore, asperaculin A [13], aspergillusol A [14] and aculeatusquinones A–D [15] have been reported in marine strains of *A. aculeatus*. Different biological activities are reported for these metabolites, including antifungal (aculeacins A-G and CJ-15,183), enzyme inhibitory (CJ-15,183 and aspergilluson A), antimicrobial activities (secalonic D and F) and cytotoxicity (aculeatusquinone B and D).

While some black aspergilli are important in the biotechnological industry for production of enzymes and organic acids [16,17], some species can also be food and feed contaminants [18]. In fact, the black aspergilli are among the most common fungi connected to postharvest decay of fruit, beans and nuts, and *A. aculeatus* is no exception [18,19].

A. aculeatus is used to produce important industrial enzymes such as cellulases [20], xylanases [21,22] and proteases [23], which are used commercially in the food and feed industries. Moreover a marine strain of *A. aculeatus* has tested active against *Staphylococcus aureus* [24]. Based on both the industrial applications of *A. aculeatus* as well as food and feed contamination hazards it is of great importance to know what metabolites are being produced by this fungus. The aim of the current work has been to investigate the chemical profile of *A. aculeatus* seeking to discover novel compounds and to test for the antifungal activity of its metabolites.

2. Results and Discussion

Initial analysis of the chemistry of *A. aculeatus* involved two strains (IBT 21030 and IBT 3244) which were investigated on a series of solid media (YES, CYA, MEA, OAT and CREA) [25]. The strains were cultivated at 25 and 30 °C in the dark for 7 days and were investigated with micro-scale extractions [26]. The secondary metabolite profiles were analyzed with UHPLC-DAD-HRMS, which demonstrated that the strains showed highly similar chemical profiles. However, more metabolites were produced by the *A. aculeatus* IBT 21030 strain, hence this strain was chosen for further work. The medium used in the cultivations had varying effect on metabolite production. While cultivation on MEA, OAT and CREA did not lead to diverse production, cultivation on both CYA and YES lead to production of several different metabolites. The YES medium was selected for further work, and it was

found that the optimal cultivation temperature was 25 °C. The *A. aculeatus* strain was inoculated on YES media and incubated at 25 °C and analyzed after 2, 4, 7, and 10 days to test the effect of incubation time on the metabolite production. These experiments showed that 7 days of incubation gave the optimum production of secondary metabolites. Based on these initial experiments, *A. aculeatus* was inoculated on 200 plates of YES and incubated at 25 °C for seven days in the dark. The results of the dereplication as well as isolation and elucidation of novel compounds are depicted in Figure 1.

Figure 1. Base peak chromatogram illustrating the dereplication of some of the major compounds in the extract from *A. aculeatus* IBT 21030 as well as the results of purification and structural elucidation of novel compounds. Based on cultivation on YES media for 7 days at 25 °C in the dark. * Novel compounds reported here for the first time. ** Compounds reported from *A. aculeatus* for the first time.

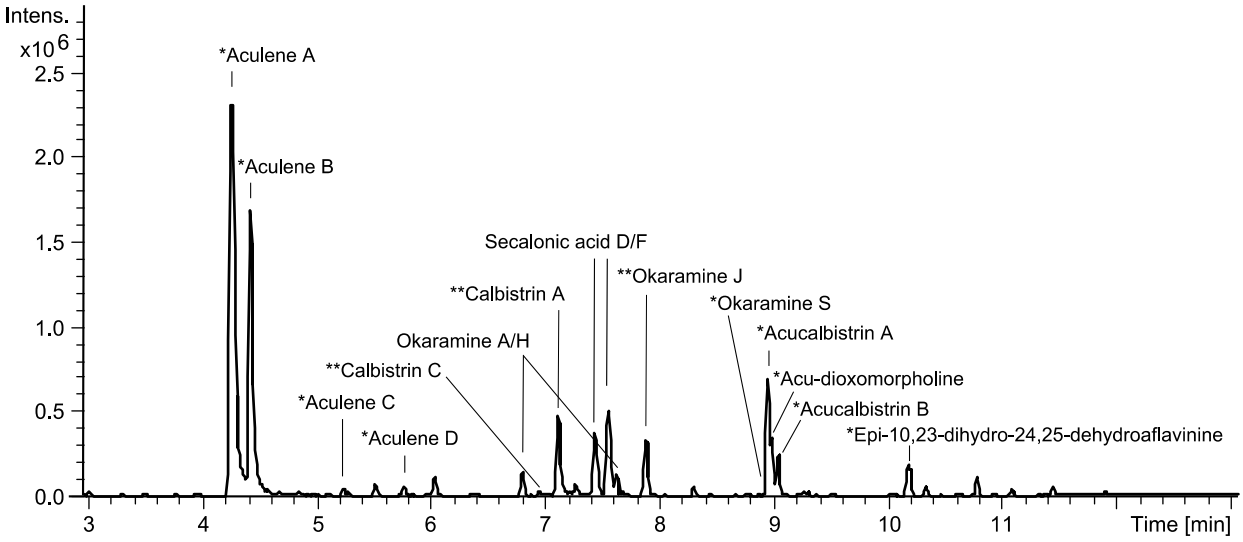

Dereplication was performed by UV- and HRMS-data to identify known compounds. An in-house library of microbial metabolites [27] as well as the AntiBase 2012 natural products database [28] were used for identification. Many of the major peaks could be dereplicated as compounds already known to be produced by *A. aculeatus* (Figures 1 and 2). This included secalonic acids D and F [11], as well as okaramines A and H [12]. One further okaramine was produced, which could not be unambiguously dereplicated, since the HRMS and UV data pointed towards either okaramine C, J *or* L. The compound was isolated and the structure was elucidated by 1D and 2D NMR and the structure was established to correspond to okaramine J, which has previously been described from *Penicillium ochrochloron* (formerly identified as *Penicillium simplicissimum*) [29,30].

Two calbistrin analogues could also be dereplicated from *A. aculeatus*. Calbistrins A–D, have been described from *Penicillium restrictum* by Jackson *et al.* [31] and the structures of the four compounds were later elucidated by the same group [32]. Calbistrin A is biologically active as an antifungal agent, a promoter of nerve growth factor production and a cholesterol lowering agent. Identification of the two calbistrins was not possible solely based on HRMS and DAD data, as calbistrins pairwise have the same molecular formula (A and B have the same molecular formula and likewise for calbistrins C and D). The

two compounds were therefore isolated and their structures elucidated by 1D and 2D NMR, and it was shown that the two compounds produced by *A. aculeatus* were calbistrin A and C, Figure 2.

Figure 2. Known compounds dereplicated from *A. aculeatus*. Okaramines A and H as well as secalonic acids have previously been reported from the organism, whereas the calbistrins and okaramine J are reported from *A. aculeatus* for the first time.

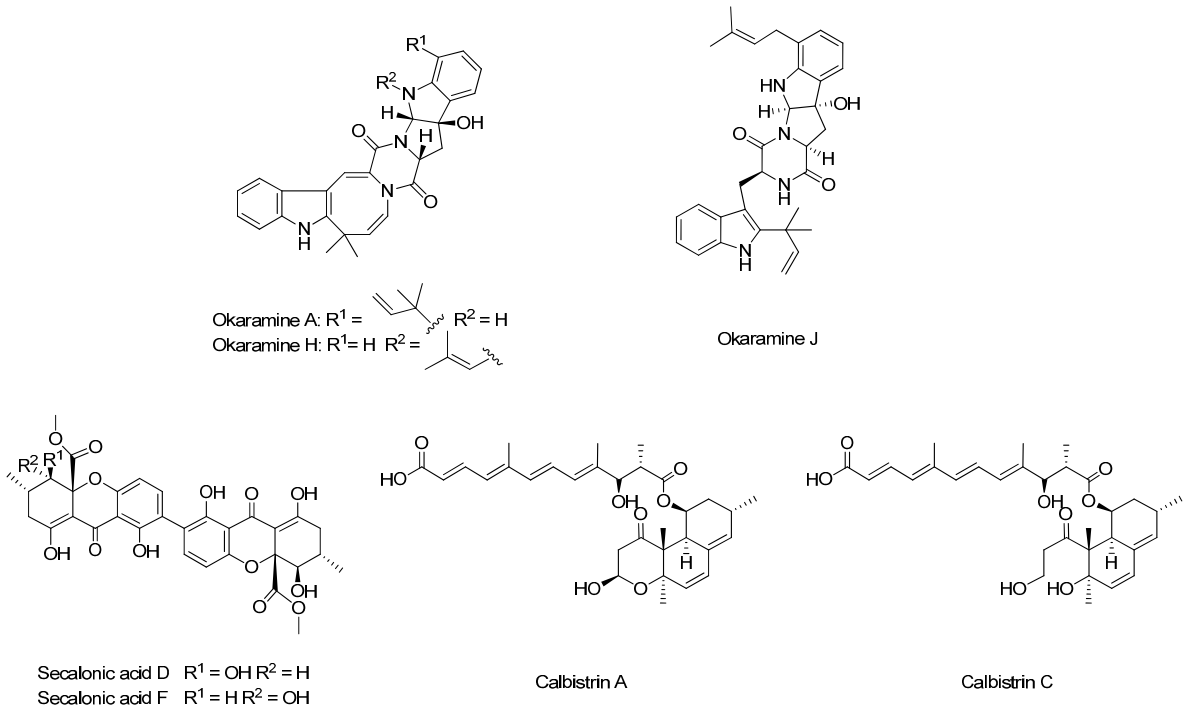

2.1. A Novel Class of Compounds, Named the aculenes, Has a Mixed Biosynthetic Origin

The two major metabolites produced by *A. aculeatus*, aculenes A and B (Figure 1) have previously been detected by UHPLC-DAD-HRMS in the related black aspergillus *A. saccharolyticus* [33], but the structures have not been elucidated. The molecular formulae of the two compounds were determined by HRMS to be $C_{19}H_{25}NO_3$ and $C_{19}H_{27}NO_3$, respectively. The mass difference of 2 Da and the fact that the two compounds eluted very close to each other suggested that the compounds were related and only differed by a double bond. The UV-spectra differed greatly as depicted in Figure 3, indeed indicating aculene A to contain a more conjugated chromophore.

The structures of the two compounds were elucidated by 1D- and 2D NMR spectroscopy and the structures of aculenes A and B are depicted in Figure 4. The conjugation in aculene A was in agreement with the recorded UV spectrum. The only difference with aculene B is the absent double bond between C-11 and C-12 and as seen, this structure was also in accordance with the obtained UV spectrum. The ^{1}H-NMR spectra of both aculenes A and B revealed the presence of one H_α proton (H-5), which was found to be in a COSY spin system with three methylene groups (H-2, H-3 and H-4), which where elucidated as a proline ring. The remaining resonances in the ^{1}H-NMR spectra belonged to a fused five and seven membered ring system. The linking between the COSY spin systems for this part and assignments of the quaternary carbons were accomplished through detailed analysis of the

HMBC experimental data. Some of the important HMBC correlations for the elucidation of aculene B are depicted in Figure 5.

Figure 3. UV-spectra of selected *A. aculeatus* metabolites. The remaining UV spectra can be found in the Supporting Information.

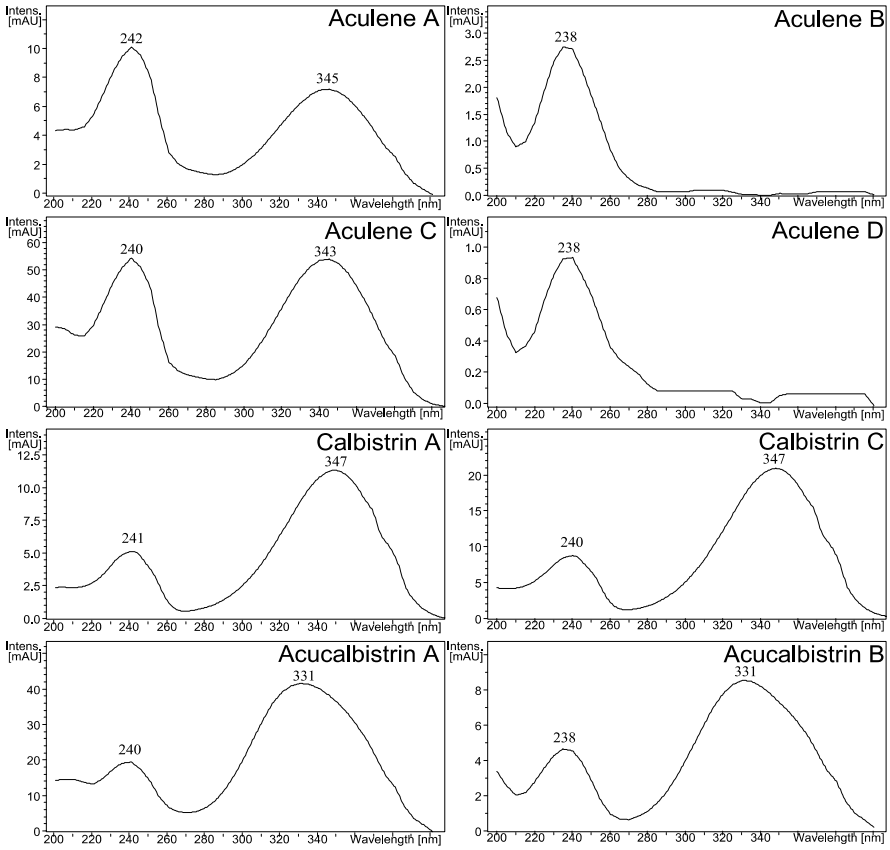

Figure 4. The structure of aculenes A–D. The structures of aculenes A–C have been verified by 1D and 2D NMR spectroscopy, whereas the structure of aculene D has been suggested based on UHPLC-DAD-HRMS data. The stereochemistry shown is relative.

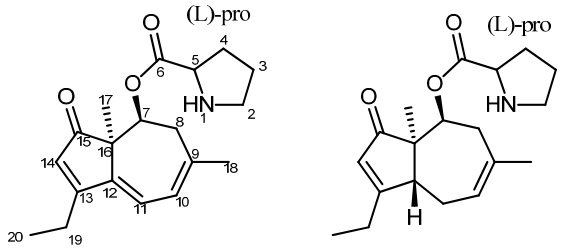

Aculene A Aculene B

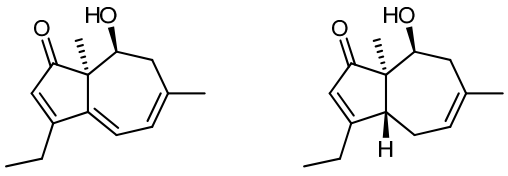

Aculene C Aculene D

Figure 5. A. Important HMBC correlations in the elucidation of aculene B. **B**. The NOEs used to solve the stereochemistry. Similar HMBCs and NOEs were observed for aculenes A and C, see Table 1 and Supplementary Table S2.

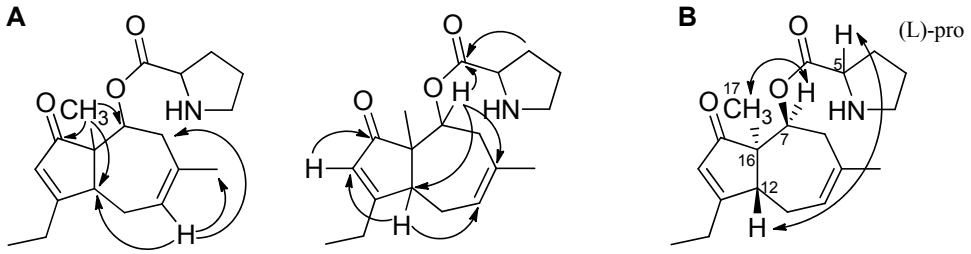

Table 1. ^{1}H-NMR spectroscopic data (500 and 800 MHz, DMSO-d_6) and HMBCs for aculenes A–C.

	Aculene A		Aculene B		Aculene C	
Position	**δ_H (*J* in Hz)**	**HMBC**	**δ_H (*J* in Hz)**	**HMBC**	**δ_H (*J* in Hz)**	**HMBC**
1	-	-	-	-		
2	3.15 (m)	-	3.21 (m)	3,4,5		
2'	3.09 (m)	-	3.14 (m)	3,4,5		
3	1.83 (m)	-	1.84 (m)	2,4,5		
3'	1.67 (m)	-	1.76 (m)	2,4,5		
4	1.94 (m)	2,6	2.05 (m)	2,3,5,6		
4'	1.46 (m)	2,6	1.55 (m)	2,6		
5	4.23 (t 7.7)	6	4.31 (t 7.8)	2,3,4,6		
6	-	-	-	-		
7	5.33 (dd 4.4, 2.4)	-	5.28 (dd 5.3, 2.3)	6,9,12,16	3.95 (t 3.5)	9,13,15
8	2.82(br.d 20.8)	-	2.67 (br. d 19.1)	16	2.52 (br. d 20.1)	
8'	2.55 (m)	9,10,16	2.37 (m)	7,9,10,16	2.31 (m)	7,9,10,16
9	-	-	-	-	-	-
10	5.98 (d 7.4)	8,12,18	5.56 (m)	8,11,12,18	5.87 (d 7.3)	8,12,18
11	6.24 (d 7.4)	9,13,16	2.12 (m)	-	6.08 (d 7.4)	9,13,16
11'	-	-	2.52 (m)	18	-	-
12	-	-	3.31 (m)	10,11,14	-	-
13	-	-	-	-	-	-
14	6.03 (s)	12,13,15,16,19	5.81 (q 1.8)	12,13,15,16,19	5.93 (s)	12,13,15,16, 19
15	-	-	-	-	-	-
16	-	-	-	-	-	-
17	0.96 (s)	7,12,15,16	0.96 (s)	7,12,15,16	0.79 (s)	7,12,15,16
18	1.85 (s)	8,9,10	1.68 (s)	8,9,10	1.82 (s)	8, 9,10
19	2.55 (m)	13,20	2.39 (m)	13,14,20	2.48 (m)	12,13,14,20
20	1.16 (t 7.4)	13,19	1.11 (t 7.3)	13,19	1.14 (t 7.4)	13,19
-OH	-	-	-	-	4.43 (s)	-

The NMR data for aculene A were very comparable to those of aculene B (Tables 1 and 2), yet differences were observed corresponding to the additional double bond in aculene A. The chemical shift of H-10 and H-14 is seen to differ slightly and furthermore an additional resonance was present in the ^{1}H-NMR spectrum in the aromatic/alkene area for compound A. This was located at a chemical

shift of δ_H = 6.24 ppm and assigned H-11. The only other location where the spectrum differed significantly was due to the extra diastereotopic CH_2 groups in the 7-membered ring of aculene B. For this, and the diastereotopic CH_2 group H8/H8' present in both compounds, rather large coupling constants were observed due to the geminal coupling. In compound A the H-8 doublet had a coupling constant of 20.8 Hz. Another notable chemical shift is the carbon chemical shift of C-13. This was at δ_C = 175.3 and 183.8 ppm, respectively for the two compounds, which is rather far downfield.

Table 2. ^{13}C-NMR spectroscopic data (125 and 200 MHz, DMSO-d_6) for aculenes A–C.

Position	Aculene A	Aculene B	Aculene C
	δ_C	δ_C	δ_C
1	-	-	-
2	45.1	44.7	-
3	22.3	22.3	-
4	27.6	27.6	-
5	58.4	58.3	-
6	168.0	167.8	-
7	72.9	73.5	67.6
8	36.5	35.5	40.2
9	141.7	130.7	142.5
10	120.0	122.7	119.7
11	118.5	24.9	117.8
12	142.5	44.6	144.3
13	175.3	183.8	174.3
14	125.3	122.8	125.6
15	205.8	208.2	208.2
16	51.7	54.4	53.6
17	17.9	17.1	18.3
18	26.9	28.3	27.1
19	20.1	23.1	19.8
20	12.0	10.8	11.8

A third and related compound (aculene C) was also characterized. The UV spectrum was similar to the UV spectrum observed for aculene A (Figure 3) and the molecular formula was determined by HRMS to be $C_{14}H_{18}O_2$. The NMR data was comparable to that of aculene A (Tables 1 and 2), though with an absence of resonances originating from the proline part. Elucidation of the structure revealed that the compound was related to the aculenes, therefore it was named aculene C (Figure 4). Aculene C is a likely precursor to aculene A, having the same carbon skeleton, but missing the proline moiety. Analysis of the UHPLC-DAD-HRMS data showed a fourth compound, eluting close by aculene C, present in minute amounts, with a mass difference of 2 Da compared to aculene C, and with a UV spectrum very similar to aculene B (Figure 3). The HRMS data displayed the same adducts and fragmentation pattern as observed for aculene C. This compound, aculene D, is believed to have a similar structure as aculene C, but with the absence of the double bond between C-11 and C-12, as seen with the relation between aculenes A and B. This structure has not been verified by NMR experiments.

The stereochemistry of aculenes A-C was elucidated by NOEs, *J*-couplings and Marfey's reaction [34], from which it was determined that aculenes A and B contained L-proline. The stereocenters (C-5, C-7 and C-16) of aculenes A and B could not be connected, due to lack of NOEs from the proline to the bicyclic system and the free rotation of proline. The relative stereochemistry of stereocenters C-7 and C-16, as well as C-12 for aculene B, is depicted in Figure 4, suggested by NOEs and backcalculated ^{3}J-couplings of H-7 (see Supplementary Figure S37 and Supplementary Tables S1 and S2). Relevant NOEs are depicted for aculene B in Figure 5.

We hypothesize the biosynthesis of the aculenes to originate from a terpene pathway. Aculene C and D consist of fourteen carbons, which could originate from a sesquiterpene with the loss of one carbon atom, possibly at C9. Aculene A and B furthermore contain the amino acid proline.

The two compounds marked as acucalbistrin A and B in Figure 1 were also targeted. These compounds were intriguing because they could not be dereplicated, and because the HRMS data suggested that the size were somewhat larger than typical secondary metabolites. The molecular formulas for the two compounds were determined to be $C_{50}H_{63}NO_{10}$ and $C_{50}H_{65}NO_{10}$, the mass spectra are depicted in Figure 6.

Figure 6. Mass spectra of acucalbistrin A (top) and acucalbistrin B (bottom). A fragment corresponding to *m/z* of the molecular ion $[M+H]^+$ of aculene A (*) and aculene B (**) are observed for acucalbistrin A and B respectively.

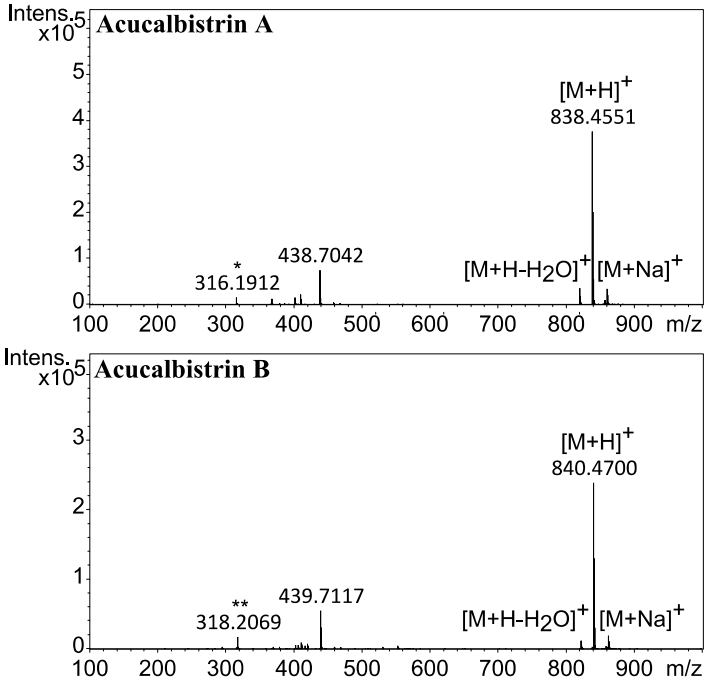

A feature noted in both mass spectra was a fragment corresponding to the mass of aculenes A and aculene B, respectively. Different chromatographic approaches were taken to purify both compounds, which however proved challenging as the compounds were unstable even under mild conditions. Apparently acucalbistrin A was degrading to aculene A and another compound X, while acucalbistrin B was degrading to aculene B and the same compound X. Analysis by UHPLC-DAD-HRMS of a small semipreparative proportion of this degradation product revealed to our surprise this compound to

be calbistrin A. This was verified by the UHPLC-DAD-HRMS data by comparison to the known compounds, see Supplementary Figure S39.

The combined mass of aculene A and calbistrin A is higher than that of acucalbistrin A (and the same for the case of acucalbistrin B), where the difference corresponds to a single water molecule. We therefore hypothesize that the acucalbistrins undergo hydrolysis and with knowledge on the structures of aculenes A–B and calbistrin A, a possible structure could therefore be an amide bond between the nitrogen in the proline moiety in aculene to the carbonyl in the carboxylic acid part of calbistrin A (see Supplementary Figure S38). This would account for the observed masses. These acucalbistrin structures have not been verified by NMR spectroscopy. We note that the UV spectra of acucalbistrin A and B have UV_{max} values comparable to those observed for calbistrin A (Figure 3). The slight shift observed may be due to the aculene moiety being attached directly to the carboxylic acid, which is part of the conjugated system in calbistrin A. The proposed structures are given in Supplementary Figure S38.

2.2. Discovery of Novel Indole Terpenoids

Three other compounds were isolated and structure elucidated resulting in the novel compounds acu-dioxomorpholine, okaramine S and epi-10,23-dihydro-24,25-dehydroaflavinine with the structures shown in Figure 7.

Figure 7. The structure of acu-dioxomorpholine, okaramine S and epi-10,23-dihydro-24,25-dehydroaflavinine.

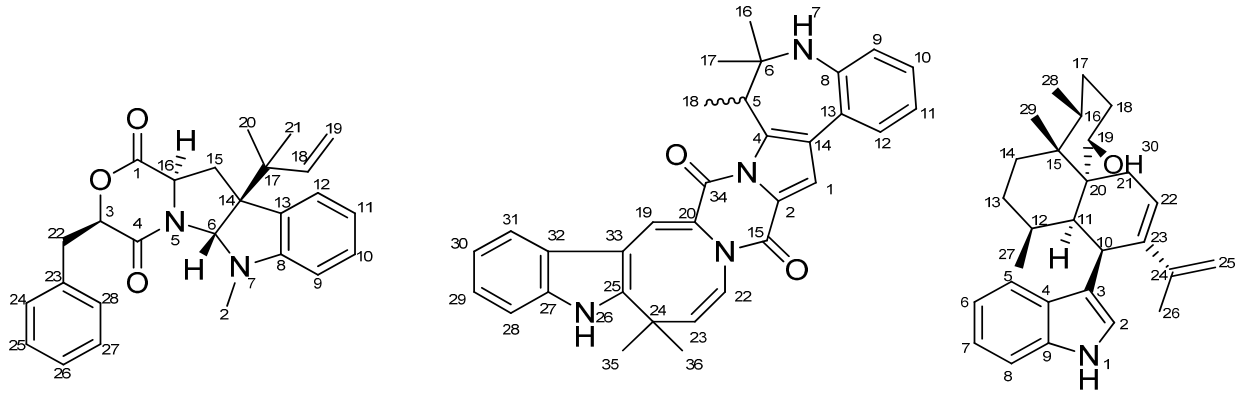

NMR data for the compounds are presented in Table 3, Table 4, and Table 5, respectively. The structure of acu-dioxomorpholine reminds one of a diketopiperazine, but this structure differs in that it contains a lactone. The chemical shift of the proton adjacent to the lactone oxygen (H-3) clearly differs compared to the chemical shift of a proton in ordinary diketopiperazines, which is typically reported to be around δ_H = 3.50–4.50 ppm [35,36]. For acu-dioxomorpholine the proton chemical shift is δ_H = 5.32 ppm. The carbon chemical shift of C-3 is also shifted significantly downfield, with δ_C = 78.1 ppm for the acu-dioxomorpholine, compared to around 60 ppm for diketopiperazines. Two compounds have been reported by Wang *et al.* with the same lactone feature [37], but differ by having leucine

incorporated instead of phenylalanine and by lacking the *N*-methylation. Otherwise the NMR data are comparable.

NOESY experiments enabled determination of the relative stereochemistry of acu-dioxomorpholine. NOE connectivities were found between H-3 and H-16 placing these protons on the same side of the ring system. These had no NOE connectivities to H-6, which however displayed NOE connectivities to H-22 as well as several of the protons in the prenyl moiety (H-18, H-19, H-19' and H-20), strongly indicating the positioning of the prenyl group and H-6 on the other side of the ring system as compared to H-3 and H-16.

Table 3. NMR spectroscopic data (500 and 800 MHz, DMSO-d_6) for acu-dioxomorpholine.

Position	δ_H (*J* in Hz)	δ_C	HMBC	Noesy
1	-	168.0	-	-
2	2.96 (3H, s)	32.7	6, 8	6,9
3	5.32 (1H, dd, 8.8, 3.4)	78.1	4, 22, 23	16, 22, 22', 24/28
4	-	163.5	-	-
5	-	-	-	-
6	5.43 (1H, s)	81.9	2, 4, 8, 13, 14, 15, 16, 17	12, 18, 19, 19', 20, 22
7	-	-	-	-
8	-	150.8	-	-
9	6.44 (1H, d, 7.6)	105.6	11, 13	2, 10
10	7.09 (1H, td, 7.6, 0.8)	128.5	8, 12	9, 11
11	6.64 (1H, t, 7.3)	116.9	9, 12, 13	10, 12
12	7.17 (1H, d, 7.3)	124.1	8, 10, 14	11, 15, 18, 20, 21
13	-	128.8	-	-
14	-	59.6	-	-
15	2.43 (1H, dd, 12.7, 6.6)	36.6	1, 6, 13, 14, 16	12, 15', 16
15'	2.21 (1H, dd, 12.7, 11.1)	36.6	1, 13, 14, 16	15, 16, 18, 20, 21
16	4.17 (1H, dd, 11.1, 6.6)	56.7	1, 15	3, 15, 15'
17	-	40.1	-	-
18	5.87 (1H, dd, 17.4, 11.0)	143.3	14, 17, 21	6, 12, 15', 19, 19', 20, 21
19	5.02 (1H, dd, 17.4, 1.1)	113.7	14, 17, 18	6, 18, 19', 20, 21
19'	5.06 (1H, dd, 11.0, 1.1)	113.6	14, 17, 18	6, 18, 19, 20, 21
20	0.82 (3H, s)	22.4	14, 17, 18, 21	6, 12, 15', 18, 19, 19', 21
21	0.97 (3H, s)	21.7	14, 17, 18, 20	12, 15', 18, 19, 19', 20
22	2.98 (1H, dd, 14.8, 8.8)	34.9	3, 4, 23, 28	3, 6, 22', 24/28
22'	3.33 (1H, m)	34.9	3, 4, 23, 28	3, 22, 24/28
23	-	136.3	-	-
24	7.26 (1H, m)	129.2	22, 26, 28	3, 22, 22'
25	7.28 (1H, m)	127.7	-	26
26	7.22 (1H, tt, 7.2, 1.6)	126.2	28	25
27	7.28 (1H, m)	127.7	23, 25	-
28	7.26 (1H, m)	129.2	-	3, 22, 22'

Table 4. NMR spectroscopic data (500 and 800 MHz, DMSO-d_6) for okaramine S.

Position	δ_H (*J* in Hz)	δ_C	Hmbc	Noesy
1	7.64 (1H, s)	114.7	2, 4, 14, 15	-
2	-	123.8	-	-
4	-	137.6	-	-
5	4.26 (1H, q, 6.5)	43.2	4, 14, 18	18
6	-	51.2	-	-
7	5.87 (1H, s)	-	5, 9, 13, 17	9
8	-	144.5	-	-
9	6.90 (1H, d, 7.6)	118.8	11, 13	10
10	6.99 (1H, t, 7.6)	127.4	8, 12	9
11	6.65 (1H, t, 7.6)	116.8	9, 13	12
12	7.74 (1H, d, 7.6)	128.3	8, 10, 14	1,11
13	-	115.3	-	-
14	-	124.9	-	-
15	-	153.4	-	-
16	0.95 (3H, s)	27.1	5, 6, 17	17
17	1.39 (3H, s)	29.3	5, 6, 16	16
18	1.18 (3H, d, 7.2)	18.1	4, 5, 6	-
19	7.76 (1H, s)	117.5	20, 25, 32, 33, 34	-
20	-	125.2	-	-
22	5.90 (1H, d, 8.3)	123.6	23, 24	23
23	6.15 (1H, d, 8.3)	140.2	22, 24, 35/36	22
24	-	35.8	-	-
25	-	149.8	-	-
26	11.70 (1H, s)	-	25, 32, 33	-
27	-	134.2	-	-
28	7.44 (1H, m)	112.3	-	29/30
29	7.17 (1H, m)	121.7	31	28, 31
30	7.17 (1H, m)	121.7	31	28, 31
31	7.63 (1H, m)	116.1	27, 29/30	12, 29/30
32	-	105.3	-	-
33	-	129.5	-	-
34	-	157.6	-	-
35	1.69 (3H, s)	26.7	23, 24, 25, 35/36	-
36	1.69 (3H, s)	26.7	23, 24, 25, 35/36	-

For okaramine S the molecular formula was by HRMS predicted to be $C_{32}H_{30}N_4O_2$. The azocinoindole part of the novel okaramine (Figure 7) is identical to that observed in okaramines A and H (Scheme 1), also produced by *A. aculeatus* [12]. The remaining part is highly similar, also originating from tryptophan and an isoprene unit, but in okaramine S, the terpene is fused with the ring system of the tryptophan moiety resulting in an intriguing, additional seven-membered ring, not previously reported in any okaramine. Key HMBCs from this part of okaramine S are depicted in Figure 8.

Table 5. NMR spectroscopic data (500 MHz, DMSO-d_6) for epi-10,23-dihydro-24,25-dehydroaflavinine.

Position	δ_H (*J* in Hz)	δ_C	HMBC	H2BC	NOESY
1	10.66 (s)	-	2, 3, 4, 9	2	2,8
2	7.07 (d 2.0)	122.7	3, 4, 9	-	1, 23, 25, 27
3	-	114.4	-	-	
4	-	126.7	-	-	
5	7.38 (d 7.8)	116.8	7, 9	6	10, 11, 18
6	6.96 (t 7.2)	117.7	4, 8	5, 7	
7	7.02 (t 7.3)	120.0	5, 9	6, 8	
8	7.29 (d 8.0)	110.9	4, 6	7	1
9	-	135.5	-	-	
10	3.59 (dd 13.3, 5.0)	33.4	2, 3, 11, 12, 23, 24	11, 23	5, 11, 19, 25, 26
11	2.47 (m)	37.6	10, 12, 23	10, 12	5, 10, 12, 13, 16, 19
12	1.27 (m)	28.9	-	17	11
13	1.53 (m)	28.1	29	-	11, 13', 16
13'	0.81 (d 12.9)	28.1	-	-	13
14	1.46 (m)	27.4	-	-	
14'	1.08 (d 13.7)	27.4	27	-	28
15	-	38.2	-	-	
16	2.04 (m)	30.4	-	17, 28	11, 13, 17', 28
17	1.71 (m)	24.8	-	18	
17'	1.22 (m)	24.8	-	-	
18	1.99 (d 11.3)	29.6	-	-	5, 19
18'	1.74 (m)	29.6	-	-	19, 30
19	4.64 (s)	65.6	-	-	10, 11, 18, 18', 22, 26
20	-	42.9	-	-	
21	2.07 (m)	23.5	-	-	29, 30
21'	1.65 (m)	23.5	19, 23	-	27
22	1.85 (m)	26.6	20, 24	21, 23	19, 30
22'	1.54 (m)	26.6	-	-	
23	3.13 (m)	42.3	24, 25, 26	10, 22	2, 25, 27
24	-	149.8	-	-	
25	4.81 (d 1.8)	110.4	23, 26	26	2, 10, 23, 25'
25'	4.58 (d 1.8)	110.4	23, 26	26	25, 26
26	1.45 (s)	17.7	23, 24, 25	-	10, 19, 25'
27	1.21 (s)	21.1	11, 12	12	2, 21', 23
28	0.71 (d 6.7)	15.4	15, 16, 17	16	14', 16, 17'
29	0.92 (s)	17.7	13, 15, 16, 20	-	17, 21, 30
30	4.28 (d 4.3)	-	19, 20	19	18', 21, 22, 29

The molecular formula of the aflavinine analogue was predicted by HRMS to be $C_{28}H_{39}NO$ and dereplication indicated it could be aflavinine or an analogue. Since no aflavinine or analogue was previously described in *A. aculeatus*, this compound was also a target for isolation and structural elucidation. The NMR data, see Table 5, suggested the structure of 10,23-dihydro-24,25-dehydroaflavinine.

Figure 8. Key HMBCs substantiating the seven-membered ring in okaramine S.

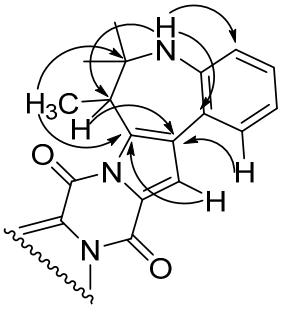

10,23-Dihydro-24,25-dehydroaflavinine has earlier been reported from sclerotia from *A. flavus*, *A. parasiticus* and *A. tubingensis* [38]. The compound has not been reported from *A. aculeatus*, but it is known to be produced by the related black *Aspergillus A. costaricaensis* [39]. The stereochemistry of epi-10,23-dihydro-24,25-dehydroaflavinine was solved by the use of NOEs and *J*-couplings. The relative stereochemistry was found to be equal to that of 10,23-dihydro-24,25-dehydroaflavinine [38]. For investigation of the absolute configuration of the purified compound, optical rotation was measured. Two different values were obtained, [α] = 63.58° and [α] = 9.08° in MeOH and $CHCl_3$ respectively. These values were compared to the value of $[\alpha]_D = -1.20°$, which has earlier been reported for 10,23-dihydro-24,25-dehydroaflavinine in $CHCl_3$ [38]. Due to those opposite signs, our result suggests that the compound from *A. aculeatus* is the enantiomer of 10,23-dihydro-24,25-dehydroaflavinine, wherefore we have named it epi-10,23-dihydro-24,25-dehydroaflavinine. The 3D structure (see Supplementary Figure S40) was suggested by the isolated spin pair approximation [40].

2.3. Biological Testing of the Novel A. aculeatus Metabolites

Aculenes A–C, acu-dioxomorpholine, okaramine S and epi-10,23-dihydro-24,25-dehydroaflavinine were tested for antifungal activity against *Candida albicans*. Endpoint optical density from compound screens were normalized with the negative controls and susceptibility evaluated as percentage reduction in optical density. None of the compounds showed significant antifungal activity.

2.4. Production of Sclerotia Reveals a Highly Regulated Metabolic Profile

It has recently been demonstrated that sclerotium production can be prompted under specific conditions for a number of the black aspergilla [41]. This study showed that some metabolites are highly upregulated inside the sclerotia, compared to the metabolites in the mycelium. *A. aculeatus* is capable of producing sclerotia in vast amounts. Production was demonstrated on CYA and YES media, see Figure 9.

Analysis of extracts of sclerotia from MM, CYA and YES showed large upregulations of okaramines, see Figure 10. Aculenes A–C were still produced, though in smaller amounts. Furthermore the analysis showed that production of secalonic acids abolished on MM and CYA. The calbistrins were still produced and the same were acucalbistrins A–B, though in trace amounts. Some okaramine analogues have shown activity against silkworms [42–44] and the substantial upregulation of okaramines can be connected to sclerotium production as a defense mechanism to protect

against insects. Sclerotia are survival structures and the production is often provoked by extreme conditions [41,45].

Figure 9. The figure shows production of sclerotia on YES (left) and CYA media (right) after growth for 7 days at 25 °C in the dark. The sclerotia are the white to cream-colored structures seen among the black conidial *Aspergillus* heads.

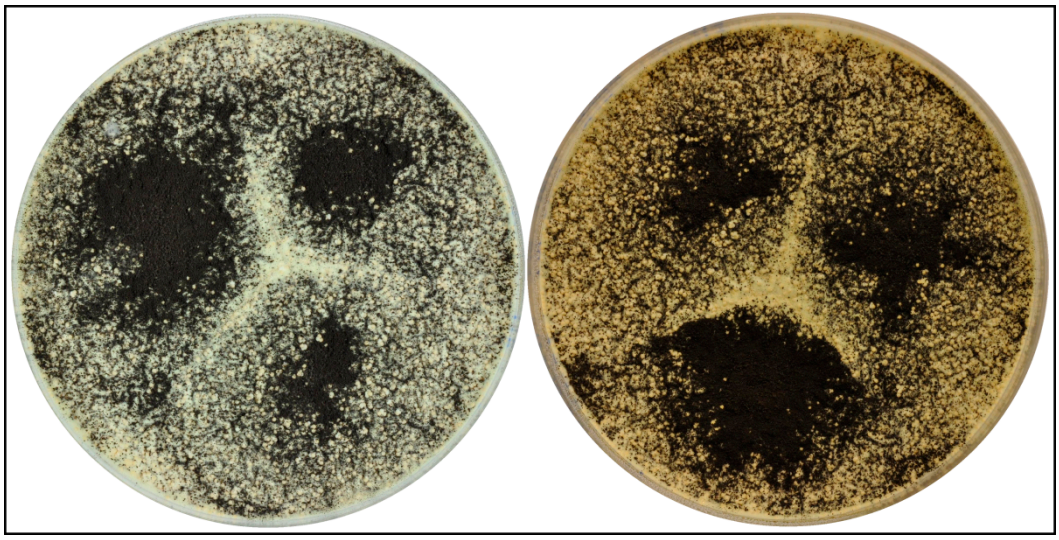

Figure 10. Base peak chromatograms of extraction from sclerotia (top) and plug extractions of *A. aculeatus* IBT 21030 after cultivation on YES agar for 7 days at 25 °C in the dark (bottom) for reference. The chromatograms are to scale. Stars indicate okaramines produced in the sclerotium extract.

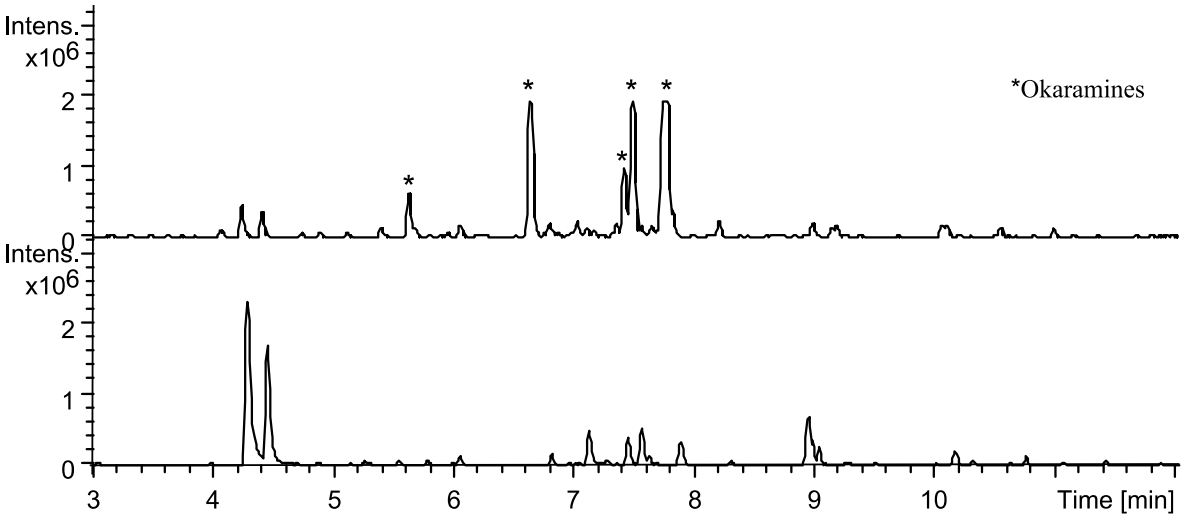

3. Experimental Section

3.1. Fungal Growth, Strains and Media

For standard screening the fungal strain was inoculated as three point stabs on solid media and incubated for seven days at 25 °C. Media was prepared as described by Samson *et al.* [25] The strain

IBT 21030 was compared to the culture ex type IBT 3244 = CBS 172.66 = ATCC 16872 = IMI 211388 = WB 5094, in order to authenticate the identity of the isolate.

3.2. Large Scale Extraction

For the large scale preparation, *A. aculeatus* (IBT 21030) was inoculated as three point stabs on 200 plates of solid YES medium, and incubated in the dark for 7 days at 25 °C. The fungi were harvested and extracted. Ten Petri plates of fungi were transferred to separate stomacher bags. To each bag 100 mL of ethyl acetate (EtOAc) containing 1% formic acid (FA) were added and the bags were subsequently crushed using a stomacher for 30–60 s. After one hour the liquid phase was filtered and concentrated *in vacuo*. The stomacher bags still containing the fungi were again filled with EtOAc containing 1% FA, and then left overnight. The following day the solution was filtered and then concentrated *in vacuo*. The combined extract was dissolved in 800 mL methanol (MeOH) and H_2O purified and deionized by a Millipore system through a 0.22 μm membrane filter (MQ H_2O) (9:1) and 800 mL of heptane added, whereafter the phases were separated. To the MeOH/MQ H_2O phase 800 mL MQ H_2O was added, and metabolites were then extracted with 4 × 400 mL dichloromethane (DCM). The phases were then concentrated separately *in vacuo.*

3.3. Plug Extraction

For standard screening three plugs were taken from one colony by use of a 6 mm plug drill; one from the center of the colony, one from the edge near the other colonies and one from the edge as far away from the other colonies. The plugs were transferred to 2 mL vials and 500 μL extraction solvent were added. A mixture of MeOH/DCM/EtOAc (1:2:3 v/v/v) containing 1% FA was used. To each sample 40 μL chloramphenicol in ethanol (500 μg/mL) was added as an internal standard. The vials were placed in an ultrasonic bath (Branson 2510 or 3520) for 60 min. The extract was then transferred to a clean vial and evaporated to dryness. This was either achieved by leaving the vials in a fume hood over night or by applying nitrogen airflow at 25–32 °C. After evaporation 500 μL MeOH was added and the sample was then ultrasonicated for 20 minutes. The extract was then filtered using a 0.45 μm PTFE filter.

3.4. Sclerotium Extraction

A. aculeatus IBT 21030 was three-point inoculated on YES, CYA and MM plates and incubated at 30 °C for ten days and then at room temperature for eight days. Sclerotia were harvested by applying MQ H_2O to the plate and carefully harvest with Drigalski spatula. The liquid including the sclerotia and spores was filtred through sterilised Miracloth and washed with MQ H_2O, allowing for the spores to pass through, while sclerotia were staying in the filter. Sclerotia were transferred to true Eppendorf tubes and washed with water to remove remaining spores. After evaporation of excess MQ H_2O, two big and two small steel balls was added to each tube and the tubes were shaken at 2000 rpm for 2 × 60 s. To each tube 40 μL chloramphenicol (internal standard) and 1 mL MeOH/DCM/EtOAc (1:2:3 v/v/v) containing 1% FA was added and the extract was transferred to clean 2 mL vials. The samples were ultrasonicated for 1 h and the extract was transferred to clean vials and solvent was evaporated by applying airflow at

25–32 °C. The samples were redissolved in 500 µL MeOH, ultrasonicated for 20 min and filtrated to fresh vials using 0.45 µm PTFE filters.

3.5. UHPLC-DAD-HRMS Analysis

Analysis was performed using ultra-high-performance liquid chromatography (UPHLC) UV/Vis diode array detector (DAD) high-resolution MS (TOFMS) on a maXis 3G orthogonal acceleration quadrupole time of flight mass spectrometer (Bruker Daltonics, Bremen, Germany) equipped with an electrospray ionization (ESI) source and connected to an Ultimate 3000 UHPLC system (Dionex, Sunnyvale, CA, USA). The column used was a reverse-phase Kinetex 2.6-µm C_{18}, 100 × 2.1 mm (Phenomenex, Torrance, CA, USA), and the column temperature was maintained at 40 °C. A linear water-acetonitrile (ACN) (LCMS-grade) gradient was used (both solvents were buffered with 20 mM FA) starting from 10% (vol/vol) ACN and increased to 100% in 10 min, maintaining this rate for 3 min before returning to the starting conditions in 0.1 min and staying there for 2.4 min before the following run. A flow rate of 0.4 $mL \cdot min^{-1}$ was used. TOFMS was performed in ESI+ with a data acquisition range of 10 scans per second at *m/z* 100–1000. The TOFMS was calibrated using Bruker Daltonics high precision calibration algorithm (HPC) by means of the use of the internal standard sodium formate, which was automatically infused before each run. UV/VIS spectra were collected at wavelengths from 200 to 700 nm. Data processing was performed using DataAnalysis 4.0 software (Bruker Daltonics).

3.6. NMR

The 1D and 2D spectra were recorded on a Varian Unity Inova-500 MHz spectrometer located at DTU, or on a Bruker Avance 800 MHz spectrometer located at the Danish Instrument Centre for NMR Spectroscopy of Biological Macromolecules at Carlsberg Laboratory. Spectra were acquired using standard pulse sequences. The deuterated solvent was DMSO-d_6 and signals were referenced by solvent signals for DMSO-d_6 at δ_H = 2.49 ppm and δ_C = 39.5 ppm. The NMR data was processed in MestReNova V.6.0.1–5391 or Bruker Topspin. Chemical shifts are in ppm (δ) and scalar couplings are reported in hertz (Hz). The sizes of the *J* coupling constants reported in the tables are the experimentally measured values from the 1D ^{1}H and DQF-COSY spectra. There are minor variations in the measurements which may be explained by the uncertainty of *J* and the spectral digital resolution.

Distances for the epi-10,23-dihydro-24,25-dehydroaflavinine were obtained from 2D NOESY experiments using the isolated spin pair approximation (ISPA) [40]. The linear range was increased by the method suggested by Macura *et al.* [46,47]. The used mixing time was 150 ms. Different mixing times were used to construct a buildup curve to ensure that only crosspeaks which fitted the ISPA were used.

The ^3J-couplings from angles in the 3D structures of epi-10,23-dihydro-24,25-dehydroaflavinine and the aculenes were calculated by the Haasnoot-DeLeeuw-Altona (HLA) equation and by DFT computations of the final structure [48,49].

The simulations were conducted using the program Maestro (Version 9.3.515, MMshare Version 2.1.515) from the Schrödinger suite. Conformational searches in implicit solvents (DMSO) were run by MacroModel (version 9.9, Schrödinger, LLC, New York, NY, USA, 2012) using the force

fields OPLS2005 and MMFFs. Monte Carlo torsional sampling was used to generate the structures and the minimization method was PRCG. The number of steps were 20,000, and only conformations within 30 kJ/mol of the found minimum were considered. The solvent DMSO was treated as a constant dielectric constant of 47.0. Both force fields gave similar results.

Selected structures were further optimized by HF/3-21G using Jaguar (Jaguar, version 7.9, 2012, Schrödinger, LLC, New York, NY, USA,) followed by DFT (for epi-10,23-dihydro-24,25-dehydroaflavinine) [50]. DFT calculations were carried out by Gaussian09 [51] using cam-B3LYP/6-311++G(d,p) for optimization and B3LYP/6-31G(d,p) u+1s for calculating *J*-coupling constants (only Fermi Contact contribution considered, see reference [49]).

3.7. Marfey's Reaction

Aculenes A and B (100 µg) were hydrolyzed with 6 M HCl (200 µL) in 2 mL analytical vials with lids, and were left at 110 °C for 22 h. The solvent was removed at a speedvac. For reference, 50 µL (2.5 µmol) standard L- and D-proline were prepared. To all vials 50 µL H_2O, 20 µL 1 M $NaHCO_3$ and 100 µL 1% 1-fluoro-2,4-dinitrophenyl-5-L-alanineamide (FDAA) in acetone were added. The vials were left for 40 °C for 1 h. 10 µL 2 M HCl was added followed by 820 µL MeOH and HPLC-DAD-MS data were acquired.

3.8. Purification of Metabolites

The DCM phase from the large scale extraction consisting of 2.375 g was absorbed onto Sepra ZT C18 (Phenomenex) and dried before packing into a 50 g (~66 mL) SNAP column (Biotage, Uppsala, Sweden) with Septra ZT C18 material. The extract was then fractionated using an Isolera flash purification system (Biotage). The gradient started with 15:100 MeOH/H_2O in the first three column volumes (CV), then went to 100% MeOH over 18 CVs and stayed here for 3 CVs using a flow rate of 40 mL/min. MeOH was of HPLC grade and H_2O was purified and deionized by Millipore system through 0.22 µm membrane filter (MQ H_2O) and both were added 50 ppm trifluoroacetic acid (TFA). Fractions were automatically collected 1 CV at a time. The fractions were subjected to further purification on a semi-preparative HPLC, which was either a Waters 600 Controller with a 996 photodiode array detector (Waters, Milford, MA, USA) or a Gilson 322 Controller connected to a 215 Liquid Handler, 819 Injection Module and a 172 DAD (Gilson, Middleton, WI, USA). This was achieved using a Luna II C18 column (250 × 10 mm, 5 µm, Phenomenex). 50 ppm TFA was added to ACN of HPLC grade and MQ H_2O. For choice of system, flow rate, gradients and yields see descriptions for the specific compound.

Aculenes A and B. The three first Isolera flash chromatography fractions, eluding with 10%–25% MeOH, were subjected to further purification on the waters semi-preparative HPLC. A linear water-ACN gradient was used starting with 15% ACN and increasing to 100% over twenty minutes using a flow rate of 4 mL/min. Two compounds eluting with 54% and 56% ACN respectively, were collected. This yielded two pure compounds, 3.0 mg of aculene A and 3.7 mg of aculene B.

Aculene A: HRMS: *m/z* = 316.1910. $[M+H]^+$, calculated for $[C_{19}H_{25}NO_3+H]^+$: *m/z* = 316.1907. $[\alpha]_D^{20}$ = +0.63° (MeOH). ^{1}H- and ^{13}C-NMR (see Tables 1 and 2).

Aculene B: HRMS: *m/z* = 318.2068. $[M+H]^+$, calculated for $[C_{19}H_{27}NO_3+H]^+$: *m/z* = 318.2064. $[\alpha]_D^{20}$ = +6.96° (MeOH). ^{1}H- and ^{13}C-NMR (see Tables 1 and 2).

Aculene C. One of the Isolera flash chromatography fractions, eluding with 50% MeOH, was subjected to further purification on the waters semi-preparative HPLC. An isocratic water-ACN gradient was used starting with 40% ACN over twenty minutes using a flow rate of 4 mL/min. A compound eluding with 40% ACN was collected. This yielded 2.0 mg of aculene C.

HRMS: *m/z* = 319.1382 $[M+H]^+$, calculated for $[C_{14}H_{18}O_2+H]^+$: *m/z* = 319.1379. $[\alpha]_D^{20}$ = 0.00° (MeOH). ^{1}H- and ^{13}C-NMR (see Tables 1 and 2).

Calbistrin A and C. One of the Isolera flash chromatography fractions, eluding with 100% MeOH, was subjected to further purification on the waters semi-preparative HPLC. An isocratic water-ACN method was used with 52% ACN over eighteen minutes using a flow rate of 4 mL/min. Two compounds eluding at 52% ACN were collected. This yielded 5.2 mg of calbistrin A and 4.6 mg of calbistrin C.

Calbistrin A: HRMS: *m/z* = 563.2622 $[M+Na]^+$, calculated for $[C_{31}H_{40}O_8+Na]^+$: *m/z* = 563.2615. $[\alpha]_D^{20}$ = +46.1° (MeOH). ^{1}H-NMR (499.87 MHz, DMSO-*d*$_6$, 25 °C, 2.49 ppm): 0.77 (3H, d, *J* = 7.1 Hz), 0.97 (3H, d, *J* = 7.1 Hz), 1.13 (3H, s), 1.22 (3H, s), 1.32 (1H, m), 1.69 (3H, s), 1.98 (3H, s), 2.02 (1H, m), 2.30 (1H, dd, *J* = 13.8, 3.8 Hz), 2.37 (1H, m), 2.41 (1H, m), 2.69 (1H, dd, *J* = 13.8, 8.2 Hz), 2.80 (1H, m), 3.94 (1H, d, *J* = 9.4 Hz), 5.06 (1H, m, -OH), 5.10 (1H, m), 5.59 (1H, d, *J* = 9.6 Hz), 5.70 (1H, s), 5.86 (1H, m), 5.88 (1H, d, *J* = 14.9 Hz), 5.97 (1H, d, *J* = 9.8 Hz), 6.05 (1H, d, *J* = 11.2 Hz), 6.30 (1H, d, *J* = 12.0 Hz), 6.38 (1H, d, *J* = 15.1 Hz), 6.68 (1H, dd, *J* = 15.1, 11.2 Hz), 7.51 (1H, dd, *J* = 14.9, 12.0 Hz; ^{13}C-NMR (125.70 MHz, DMSO-*d*$_6$, 25 °C, 39.5 ppm): 10.9, 12.3, 13.0, 13.7, 20.6, 25.4, 26.0, 34.7, 39.8, 43.6, 43.7, 56.2, 56.3, 68.3, 78.3, 121.2, 126.4, 127.0, 127.2, 130.8, 132.7, 133.8, 135.7, 139.4, 140.9, 143.4, 173.9, 212.8.

Calbistrin C: HRMS: *m/z* = 565.2776 $[M+Na]^+$, calculated for $[C_{31}H_{42}O_8+Na]^+$: *m/z* = 565.2772. $[\alpha]_D^{20}$ = +8.67° (MeOH); ^{1}H-NMR (499.87 MHz, DMSO-*d*$_6$, 25 °C, 2.49 ppm): 0.77 (3H, d, *J* = 7.1 Hz), 0.95 (3H, d, *J* = 7.1 Hz), 1.01 (3H, s), 1.21 (1H, m), 1.27 (3H, s), 1.71 (3H, s), 1.93 (1H, m), 1.98 (3H, s), 2.35 (1H, m), 2.38 (1H, qin, *J* = 8.4), 2.56 (1H, m), 2.92 (1H, dt, *J* = 17.5, 7.5 Hz), 2.99 (1H, m), 3.56 (2H, m), 3.95 (1H, dd, *J* = 9.4, 3.1 Hz), 5.09 (1H, br.d, *J* = 3.5 Hz, -OH), 5.05 (1H, s, -OH), 5.20 (1H, m), 5.37 (1H, d, *J* = 9.9 Hz), 5.59 (1H, m), 5.88 (1H, d, *J* = 14.9 Hz), 5.90 (1H, d, *J* = 9.9 Hz), 6.07 (1H, d, *J* = 11.1 Hz), 6.31 (1H, d, *J* = 12.0 Hz), 6.39 (1H, d, *J* = 15.1 Hz), 6.69 (1H, dd, *J* = 15.1, 11.1 Hz), 7.51 (1H, dd, *J* = 14.9, 12.0); ^{13}C-NMR (125.70 MHz, DMSO-*d*$_6$, 25 °C, 39.5 ppm): 10.9, 12.3, 13.0, 13.7, 20.6, 25.4, 26.0, 34.7, 39.8, 43.6, 43.7, 56.2, 56.3, 68.3, 78.3, 121.2, 126.4, 127.0, 127.2, 130.8, 132.7, 133.8, 135.7, 139.4, 140.9, 143.4, 173.9, 212.8.

Acu-dioxomorpholine. One of the Isolera flash chromatography fractions, eluding with 95% ACN, was subjected to further purification on the waters semi-preparative HPLC). A linear water-ACN gradient was used starting with 60% ACN increasing to 100% over twenty minutes using a flow rate of 4 mL/min. A compound eluding with 85% ACN was collected. This yielded 2.1 mg of acu-dioxomorpholine. HRMS: *m/z* = 417.2176 $[M+H]^+$, calculated for $[C_{26}H_{29}N_2O_3+H]^+$: *m/z* = 417.2173. $[\alpha]_D^{20}$ = −49.23° (MeOH). ^{1}H- and ^{13}C-NMR (see Table 3).

Epi-10,23-dihydro-24,25-dehydroaflavinine. One Isolera flash chromatography fraction eluding with 100% MeOH, was subjected to purification on the waters semi-preparative HPLC. A gradient of 15%–100% ACN over twenty minutes was used and the flow rate was 4 mL/min. A compound eluding with 100% ACN was collected. This yielded 8.7 mg of epi-10,23-dihydro-24,25-dehydroaflavinine. HRMS: *m/z* = 406.3113 $[M+H]^+$, calculated for $[C_{28}H_{39}NO+H]^+$: *m/z* = 406.3104. $[\alpha]_D^{20}$ = +63.58° (MeOH); ^{1}H- and ^{13}C-NMR (see Table 5).

Okaramine S. One Isolera flash chromatography fraction, eluding with 100% MeOH, was subjected to purification on the Gilson semi-preparative HPLC. This was done using a gradient of 70%–100% ACN over fifteen minutes using a flow rate was 5 mL/min. A compound eluding with 80% ACN was collected. This yielded 1.7 mg of the pure compound. HRMS: *m/z* = 503.2447 $[M+H]^+$, calculated for $[C_{32}H_{30}N_4O_2+H]^+$: *m/z* = 503.2441. $[\alpha]_D^{20}$ = −15.29° (MeOH); ^{1}H- and ^{13}C-NMR (see Table 4).

Okaramine J. One Isolera flash chromatography fraction, eluding with 74% MeOH, was subjected to purification on the waters semi-preparative HPLC. This was done using a gradient of 50%–100% ACN over twenty minutes using a flow rate of 4 mL/min. A compound eluding with 82% ACN was collected. This yielded 2.5 mg of the pure compound. HRESIMS: *m/z* = 525.2865 $[M+H]^+$, calculated for $[C_{32}H_{36}N_4O_3+H]^+$: *m/z* = 525.2860. $[\alpha]_D^{20}$ = +15.38° (MeOH); ^{1}H-NMR (499.87 MHz, DMSO-d_6, 25 °C, 2.49 ppm): 1.52 (6H, s, H-17, H-18), 1.68 (3H, s, H-34), 1.73 (3H, s, H-35), 1.86 (1H, m, H-20), 2.42 (1H, dd, 13.2, 6.8, H-20'), 2.99 (1H, dd, 15.2, 9.4, H-1), 3.14 (1H, dd, 16.3, 7.1, H-31), 3.23 (1H, dd, 16.8, 7.5, H-31'), 3.59 (1H, dd, 15.2, 4.2, H-1'), 4.46 (1H, dd, 9.1, 4.4, H-2), 4.67 (1H, dd, 11.3, 6.4, H-19), 5.05 (1H, dd, 10.5, 1.1, H-4), 5.08 (1H, dd, 17.4, 1.1, H-4'), 5.26 (1H, t, 7.4, H-32), 5.33 (1H, d, 4.5, H-29), 6.01 (1H, s , H-36), 6.12 (1H, d, 4.4, H-28), 6.22 (1H, dd, 17.4, 10.5, H-5), 6.32 (1H, s, H-3), 6.67 (1H, t, 7.5, H-24), 6.88 (1H, d, 7.5, H-25), 6.96 (1H, t, 7.5, H-12), 6.96 (H-26), 7.05 (2H, H-11, H-23), 7.35 (1H, s, H-10), 7.53 (1H, s, H-13), 10.67 (1H, s, H-8); ^{13}C-NMR (125.70 MHz, DMSO-d_6, 25 °C, 39.5 ppm): 17.5 (C-34), 24.7 (C-1), 25.2 (C-35), 27.6 (C-17,C-18), 28.2 (C-31), 39.0 (C-6), 40.8 (C-20), 55.1 (C-2), 58.2 (C-19), 83.5 (C-29), 85.5 (C-21), 104.3 (C-15), 110.7 (C-10), 110.9 (C-4), 117.6 (C-13), 118.4 (C-12, C-24), 118.9 (C-23), 120.0 (C-11), 121.5 (C-32), 122.7 (C-22), 128.3 (C-14), 131.0 (C-26), 132.0 (C-33), 134.5 (C-9), 141.1 (C-7), 145.8 (C-27), 146.0 (C-5), 167.5 (C-16), 169.7 (C-30).

3.9. Antifungal Susceptibility Testing

All compounds were screened for antifungal activity towards *Candida albicans* in accordance with the CLSI standards using RPMI-1640 medium adjusted to pH 7 with 0.165 M MOPS buffer [52]. The screening was performed as described by Holm *et al.* [53].

4. Conclusions

Investigation of the chemical profile of *Aspergillus aculeatus* by UHPLC-DAD-HRMS has identified several novel compounds some of which have been selected, purified and their structure elucidated by 1D and 2D NMR spectroscopy. A novel class of related compounds – the aculenes – has been discovered. Aculenes A and B are hybrids containing the amino acid proline but also a fourteen carbon moeity we hypothesize to originate from a sesquiterpene with the loss of one carbon atom. Aculene C is believed to be a precursor to aculene A, missing the proline part of the molecule.

Moreover there is UHPLC-DAD-HRMS evidence suggesting a fourth structure, aculene D, a possible precursor to aculene B. Two other larger, however chemically unstable metabolites have been discovered. As they apparently were degrading to two known parts, aculene A and B respectively and calbistrin A, a tentative suggestion for their structures have been given. Two further novel compounds, acu-dioxomorpholine and okaramine S has also been discovered to be produced by *A. aculeatus*. Acu-dioxomorpholine has a remarkable structure, reminding of diketopiperazine, but with a lactone instead of the one lactame part and okaramine S displays a seven-membered ring, not previously seen in any reported okaramine. Furthermore the aflavinine analogue epi-10,23-dihydro-25,25-dehydroaflavinine was detected. Production of sclerotia was observed under specific conditions, and here an upregulation of okaramines was observed. Altogether the chemical profile of *Aspergillus aculeatus* has been examined and several novel compounds have been characterized.

Supplementary Materials

^{1}H, DQF-COSY, HSQC, HMBC, NOESY and UV spectra for the novel compounds as well as suggestion for the structures of acucalbistrin A and B and elucidation of the stereochemistry of aculenes A–D and epi-10,23-dihydro-24,25-dehydroaflavinine are available in the supplementary. Supplementary materials can be accessed at: http://www.mdpi.com/1420-3049/19/8/10898/s1.

Acknowledgments

We thank the Danish Instrument Center for NMR Spectroscopy of Biological Macromolecules for 800 MHz NMR time. This work was supported by grant 09-064967 from the Danish Council for Independent Research, Technology, and Production Sciences. We thank James B. Gloer for supplying us with an authentic standard of 10,23-dihydro-24,25-dehydroaflavinine. We thank Peter B. Knudsen for running the antifungal assay.

Author Contributions

LMP executed the experiments, isolated and elucidated the structures of the compounds and wrote the paper. CH assisted in purification and structural elucidation and performed the investigation of the stereochemistry. JCF assisted in the sclerotial study. CHG assisted with structural elucidations. TOL planned the study and guided preparation of the manuscript.

Conflicts of Interest

The authors declare no conflict of interest.

References

1. Nielsen, K.F.; Mogensen, J.M.; Johansen, M.; Larsen, T.O.; Frisvad, J.C. Review of secondary metabolites and mycotoxins from the *Aspergillus niger* group. *Anal. Bioanal. Chem.* **2009**, *395*, 1225–1242.

2. Song, Y.C.; Li, H.; Ye, Y.H.; Shan, C.Y.; Yang, Y.M.; Tan, R.X. Endophytic naphthopyrone metabolites are co-inhibitors of xanthine oxidase, SW1116 cell and some microbial growths. *FEMS Microbiol. Lett.* **2004**, *241*, 67–72.
3. Koyama, K.; Ominato, K.; Natori, S.; Tashiro, T.; Tsuruo, T. Cytotoxicity and antitumor activities of fungal bis(naphtho-gamma-pyrone) derivatives. *J. Pharmacobio-Dyn.* **1988**, *11*, 630–635.
4. Abarca, M.; Bragulat, M. Ochratoxin A production by strains of Aspergillus niger var. niger. *Appl. Environ. Microbiol.* **1994**, *60*, 2650–2652.
5. Frisvad, J.C.; Smedsgaard, J.; Samson, R.A.; Larsen, T.O.; Thrane, U. Fumonisin B2 Production by *Aspergillus niger*. *J. Agric. Food Chem.* **2007**, *55*, 9727–9732.
6. Varga, J.; Frisvad, J.C.; Kocsubé, S.; Brankovics, B.; Tóth, B.; Szigeti, G.; Samson, R.A. New and revisited species in *Aspergillus* section *Nigri*. *Stud. Mycol.* **2011**, *69*, 1–17.
7. Jurjević, Z.; Peterson, S.W.; Stea, G.; Solfrizzo, M.; Varga, J.; Hubka, V.; Perrone, G. Two novel species of *Aspergillus* section *Nigri* from indoor air. *IMA Fungus* **2012**, *3*, 159–173.
8. Mizuno, K.; Yagi, A.; Satoi, S.; Takada, M.; Hayashi, M.; Asano, K.; Matsuda, T. Studies on aculeacin. I. Isolation and characterization of aculeacin A. *J. Antibiot.* **1977**, *4*, 297–302.
9. Satoi, S.; Yagi, A.; Asano, K.; Misuno, K.; Watanabe, T. Studies on aculeacin. II. Isolation and characterization of aculeacins B, C, D, E, F and G. *J. Antibiot.* **1977**, *30*, 303–307.
10. Watanabe, S.; Hirai, H.; Ishiguro, M.; Kambara, T.; Kojima, Y.; Matsunaga, T.; Nishida, H.; Suzuki, Y.; Harwood, H.J.; Huang, L.H.; *et al.* CJ-15,183, a new inhibitor of squalene synthase produced by a fungus, *Aspergillus aculeatus*. *J. Antibiot.* **2001**, *54*, 904–910.
11. Andersen, R.; Buechi, G.; Kobbe, B.; Demain, A.L. Secalonic acids D and F are toxic metabolites of *Aspergillus aculeatus* . *J. Org. Chem.* **1977**, *42*, 352–353.
12. Hayashi, H.; Furutsuka, K.; Shiono, Y. Okaramines H and I, new Okaramine Congeners, from *Aspergillus aculeatus* . *J. Nat. Prod.* **1999**, *62*, 315–317.
13. Ingavat, N.; Mahidol, C.; Ruchirawat, S.; Kittakoop, P. Asperaculin A, a sesquiterpenoid from a marine-derived fungus, Aspergillus aculeatus. *J. Nat. Prod.* **2011**, *74*, 1650–1652.
14. Ingavat, N.; Dobereiner, J.; Wiyakrutta, S.; Mahidol, C.; Ruchirawat, S.; Kittakoop, P. Aspergillusol A, an alpha-glucosidase inhibitor from the marine-derived fungus Aspergillus aculeatus. *J. Nat. Prod.* **2009**, *72*, 2049–2052.
15. Chen, L.; Zhang, Q.-Q.; Zhang, W.-W.; Liu, Q.-Y.; Zheng, Q.-H.; Zhong, P.; Hu, X.; Fang, Z.-X. Aculeatusquinones A-D, novel metabolites from the marine-derived fungus Aspergillus aculeatus. *Heterocycles* **2013**, *87*, 861–868.
16. Goldberg, I.; Rokem, J.; Pines, O. Organic acids: Old metabolites, new themes. *J. Chem. Technol. Biotechnol.* **2006**, *81*, 1601–1611.
17. Pel, H.J.; de Winde, J.H.; Archer, D.B.; Dyer, P.S.; Hofmann, G.; Schaap, P.J.; Turner, G.; de Vries, R.P.; Albang, R.; Albermann, K.; *et al.* Genome sequencing and analysis of the versatile cell factory *Aspergillus niger* CBS 513.88. *Nat. Biotechnol.* **2007**, *25*, 221–231.
18. Perrone, G.; Susca, A.; Cozzi, G.; Ehrlich, K.C.; Varga, J.; Frisvad, J.C.; Meijer, M.; Noonim, P.; Mahakarnchanakul, W.; Samson, R.A. Biodiversity of Aspergillus species in some important agricultural products. *Stud. Mycol.* **2007**, *59*, 53–66.

19. Adisa, V.A. Pectic enzymes of Aspergillus aculeatus associated with post-harvest deterioration of citrus sinensis fruit. *J. Food Biochem.* **1989**, *13*, 243–252.
20. Bhat, M.K. Cellulases and related enzymes in biotechnology. *Biotechnol. Adv.* **2000**, *18*, 355–383.
21. Fujimoto, H.; Ooi, T.; Wang, S.; Takizawa, T. Purification and properties of three xylanases from Aspergillus aculeatus. *Biosci. Biotechnol. Biochem.* **1995**, *59*, 538–540.
22. Polizeli, M.L.T.M.; Rizzatti, A.C.S.; Monti, R.; Terenzi, H.F.; Jorge, J.A.; Amorim, D.S. Xylanases from fungi: Properties and industrial applications. *Appl. Microbiol. Biotechnol.* **2005**, *67*, 577–591.
23. Olutiola, P.O.; Nwaogwugwu, R.I. Growth, sporulation and production of maltase and proteolytic enzymes in Aspergillus aculeatus. *Trans. Br. Mycol. Soc.* **1982**, *78*, 105–113.
24. Christophersen, C.; Crescente, O.; Frisvad, J.C.; Gram, L.; Nielsen, J.; Nielsen, P.H.; Rahbaek, L. Antibacterial activity of marine-derived fungi. *Mycopathologia* **1999**, *143*, 135–138.
25. Samson, R.A.; Houbraken, J.; Thrane, U.; Frisvad, J.C.; Andersen, B. *Food and Indoor Fungi*; CBS-KNAW Fungal Biodiversity Centre: Utrecht, The Netherlands, 2010.
26. Smedsgaard, J. Micro-scale extraction procedure for standardized screening of fungal metabolite production in cultures. *J. Chromatogr. A* **1997**, *760*, 264–270.
27. Nielsen, K.F.; Ma, M.; Rank, C.; Frisvad, J.C.; Larsen, T.O. Dereplication of microbial natural products by LC-DAD-TOFMS. *J. Nat. Prod.* **2011**, *74*, 2338–2348.
28. Laatsch, H. Antibase 2012. Available online: http://www.wiley-vch.de/stmdata/antibase.php (accessed on 1 February 2014).
29. Shiono, Y.; Akiyama, K.; Hayashi, H. New okaramine congeners, okaramines J, K, L, M and related compounds, from *Penicillium Simplicissimum* ATCC90288. *Biosci. Biotechnol. Biochem.* **1999**, *63*, 1910–1920.
30. Nielsen, K.F.; Smedsgaard, J. Fungal metabolite screening: Database of 474 mycotoxins and fungal metabolites for dereplication by standardised liquid chromatography-UV-mass spectrometry methodology. *J. Chromatogr. A* **2003**, *1002*, 111–136.
31. Jackson, M.; Karwowski, J.; Humphrey, P. Calbistrins, novel antifungal agents produced by Penicillium restrictum. I: Production, taxonomy of the producing organism and biological activity. *J. Antibiot.* **1993**, *46*, 34–38.
32. Brill, G.; Chen, R.; Rasmussen, R. Calbistrins, novel antifungal agents produced by Penicillium restrictum. II: Isolation and elucidation of structure. *J. Antibiot.* **1993**, *46*, 39–47.
33. Sørensen, A.; Lübeck, P.S.; Lübeck, M.; Nielsen, K.F.; Ahring, B.K.; Teller, P.J.; Frisvad, J.C. Aspergillus saccharolyticus sp. nov., a black Aspergillus species isolated in Denmark. *Int. J. Syst. Evol. Microbiol.* **2011**, *61*, 3077–3083.
34. Marfey, P. Determination of D-amino acids. II. Use of a bifunctional reagent, 1,5-di-fluoro-2,4-dinitrobenzen. *Carlsb. Res. Commun.* **1984**, *49*, 591–596.
35. Rank, C.; Klejnstrup, M.L.; Petersen, L.M.; Kildgaard, S.; Frisvad, J.C.; Gotfredsen, C.H.; Larsen, T.O. Comparative chemistry of Aspergillus oryzae (RIB40) and A. flavus (NRRL 3357). *Metabolites* **2012**, *2*, 39–56.

36. Boyes-Korkis, J.; Gurney, K.; Penn, J. Anacine, a new benzodiazepine metabolite of Penicillium aurantiogriseum produced with other alkaloids in submerged fermentation. *J. Nat. Prod.* **1993**, *56*, 1707–1717.
37. Wang, H.J.; Gloer, J.B.; Wicklow, D.T.; Dowd, P.F. Mollenines A and B: new dioxomorpholines from the ascostromata of Eupenicillium molle. *J. Nat. Prod.* **1998**, *61*, 804–807.
38. TePaske, M.R.; Gloer, J.B.; Wicklow, D.T.; Dowd, P.F. Three new aflavinines from the sclerotia of *Aspergillus tubingensis*. *Tetrahedron* **1989**, *45*, 4961–4968.
39. Samson, R.A.; Noonim, P.; Meijer, M.; Houbraken, J.; Frisvad, J.C.; Varga, J. Diagnostic tools to identify black aspergilli. *Stud. Mycol.* **2007**, *59*, 129–145.
40. Butts, C.P.; Jones, C.R.; Towers, E.C.; Flynn, J.L.; Appleby, L.; Barron, N.J. Interproton distance determinations by NOE--surprising accuracy and precision in a rigid organic molecule. *Org. Biomol. Chem.* **2011**, *9*, 177–184.
41. Frisvad, J.C.; Petersen, L.M.; Lyhne, E.K.; Larsen, T.O. Formation of sclerotia and production of indoloterpenes by *Aspergillus niger* and other species in section *Nigri*. *PLoS One* **2014**, *9*, e94857.
42. Murao, S.; Hayashi, H.; Takiuchi, K.; Arai, M. Okaramine A, a novel indole alkaloid with insecticidal activity, from Penicillium simplicissimum AK-40. *Agric. Biol. Chem.* **1988**, *52*, 885–886.
43. Hayashi, H.; Takiuchi, K.; Murao, S.; Arai, M. Okaramine B, an insecticidal indole alkaloid, produced by Penicillium simplicissimum AK-40. *Agric. Biol. Chem.* **1988**, *52*, 2131–2133.
44. Hayashi, H.; Asabu, Y.; Murao, S.; Arai, M. New Okaramine Congeners, Okaramins D, E, and F, from Penicillium simplicissimum ATCC 90288. *Jpn. Soc. Biosci. Biotechnol. Agrochem.* **1995**, *59*, 246–250.
45. Wicklow, D.T. Metabolites in the coevolution of fungal chemical defence systems. In *Coevolution of Fungi with Plant and Animals*; Pirozynski, K., Hawksworth, D., Eds.; Academic Press: London, UK, 1988; pp. 173–201.
46. Macura, S.; Farmer, B., II; Brown, L. An improved method for the determination of cross-relaxation rates from NOE data. *J. Magn. Reson.* **1986**, *70*, 493–499.
47. Hu, H.; Krishnamurthy, K. Revisiting the initial rate approximation in kinetic NOE measurements. *J. Magn. Reson.* **2006**, *182*, 173–177.
48. Haasnoot, C.A.G.; de Leeuw, F.A.A.M.; Altona, C. The relationship between proton-proton NMR coupling constants and substituents electronegativitis-I. *Tetrahedron* **1979**, *36*, 2783–2792.
49. Bally, T.; Rablen, P.R. Quantum-chemical simulation of 1H-NMR spectra. 2. Comparison of DFT-based procedures for computing proton-proton coupling constants in organic molecules. *J. Org. Chem.* **2011**, *76*, 4818–4830.
50. Bochevarov, A.; Harder, E.; Hughes, T.; Greenwood, J.; Braden, D.A.; Philipp, D.; Rinaldo, D.; Halls, M.; Zhang, J.; Friesner, R. Jaguar: A high-performance quantum chemistry software program with strengths in life and materials sciences. *Int. J. Quantum Chem.* **2013**, *113*, 2110–2142.
51. Frisch, M.J.; Trucks, G.W.; Schlegel, H.B.; Scuseria, G.E.; Robb, M.A.; Cheeseman, J.R.; Scalmani, G.; Barone, V.; Menucci, B.; Petersson, G.A. *Gaussian 09,* Revision B.01; Available online: http://www.gaussian.com/ (accessed on 1 February 2014).

52. Reference methods for broth dilution antifungal susceptibility testing of yeasts; *Fourth International Supplement*; CLSI Document M27-S4; Clinical and Laboratory Standards Institute: Wayne, PA, USA, 2012.
53. Holm, D.K.; Petersen, L.M.; Klitgaard, A.; Knudsen, P.B.; Jarczynska, Z.D.; Nielsen, K.F.; Gotfredsen, C.H.; Larsen, T.O.; Mortensen, U.H. Molecular and chemical characterization of the biosynthesis of the 6-MSA derived meroterpenoid yanuthone D in *Aspergillus niger*. *Chem. Biol.* **2014**, *21*, 519–529.

Sample Availability: Not available.

Supplementary Materials

Figure S1. ^{1}H-NMR (500 MHz, DMSO-d_6 spectrum) of the new compound aculene A.

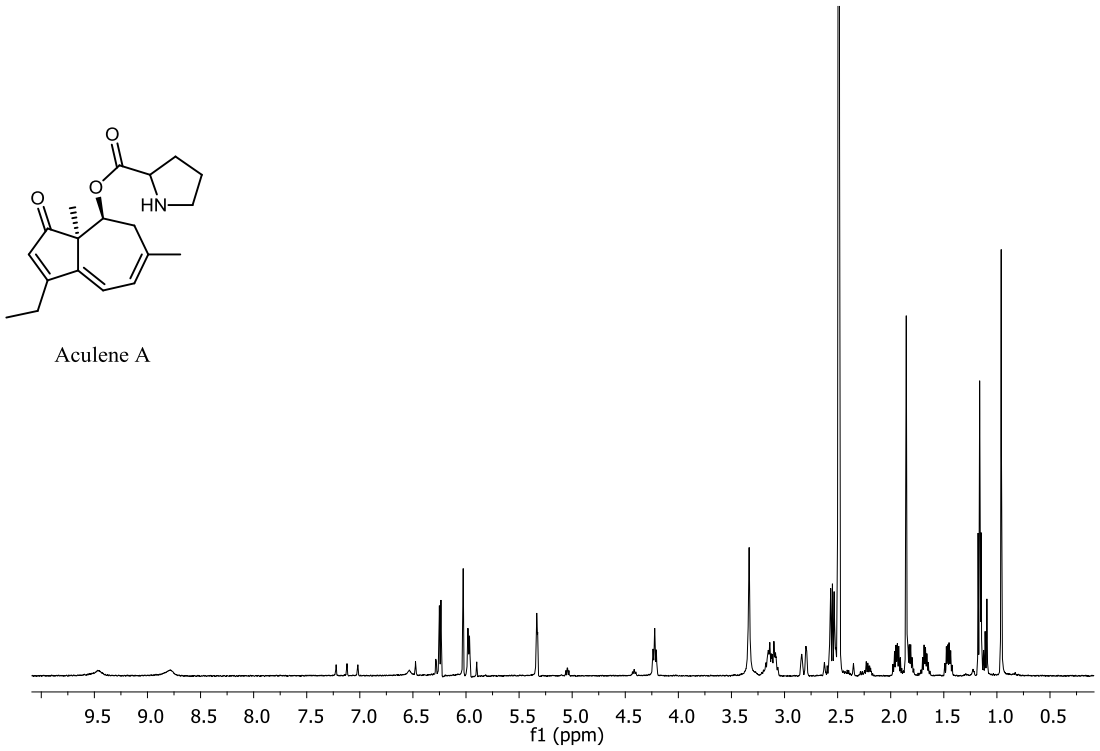

Figure S2. DQF-COSY spectrum of the new compound aculene A.

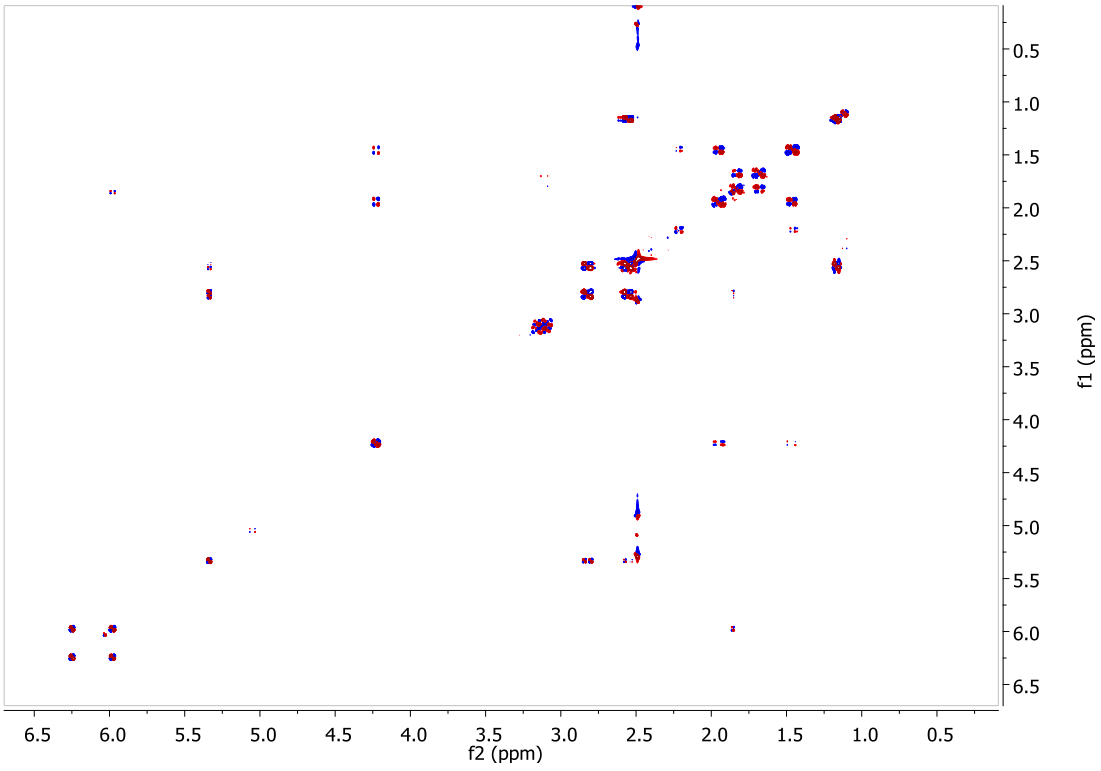

Figure S3. NOESY spectrum of the new compound aculene A.

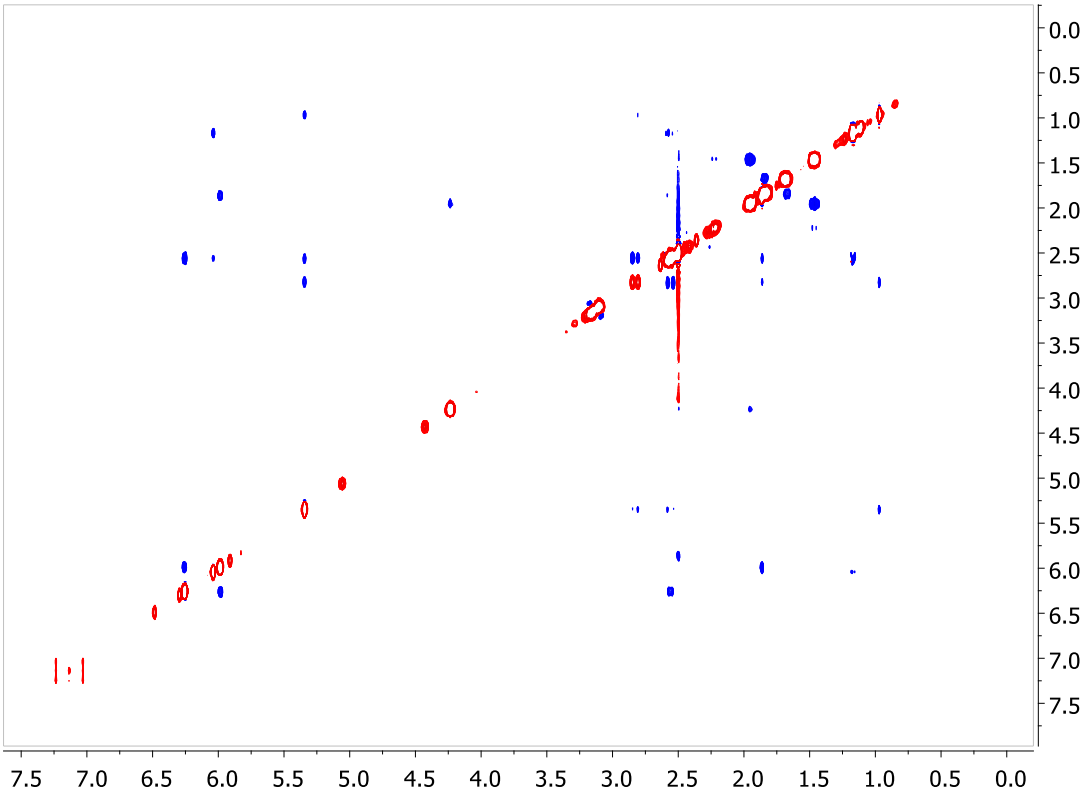

Figure S4. HSQC spectrum of the new compound aculene A.

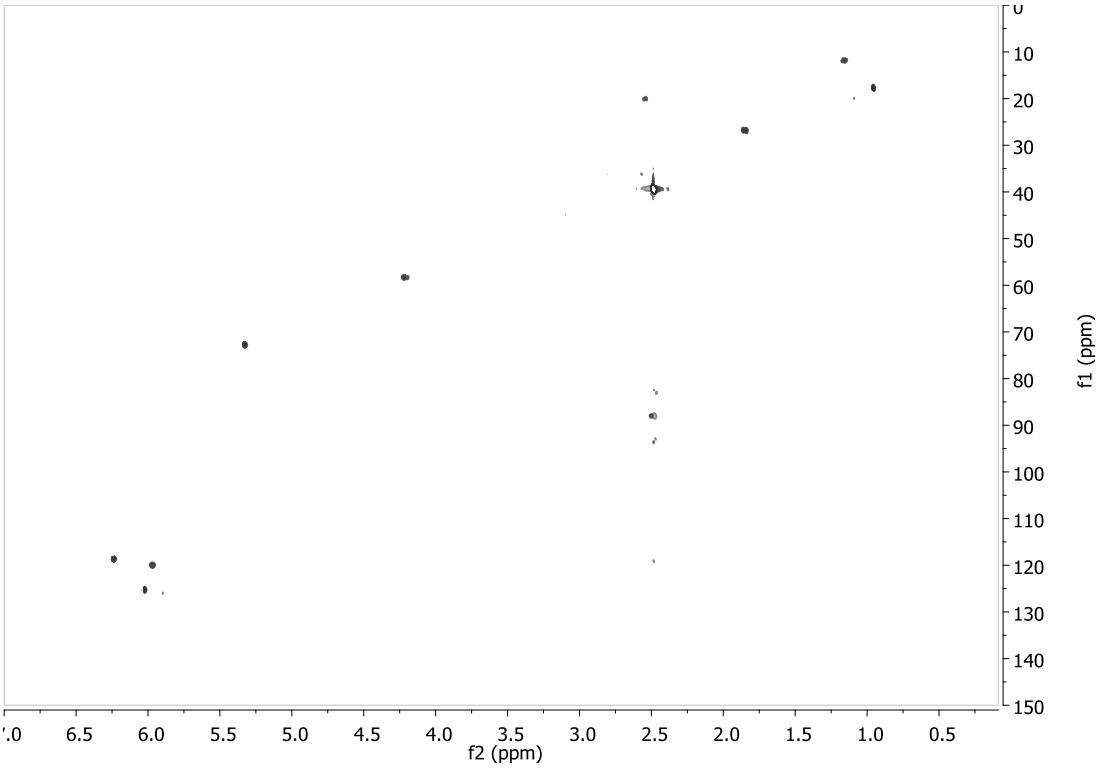

Figure S5. HMBC spectrum of the new compound aculene A.

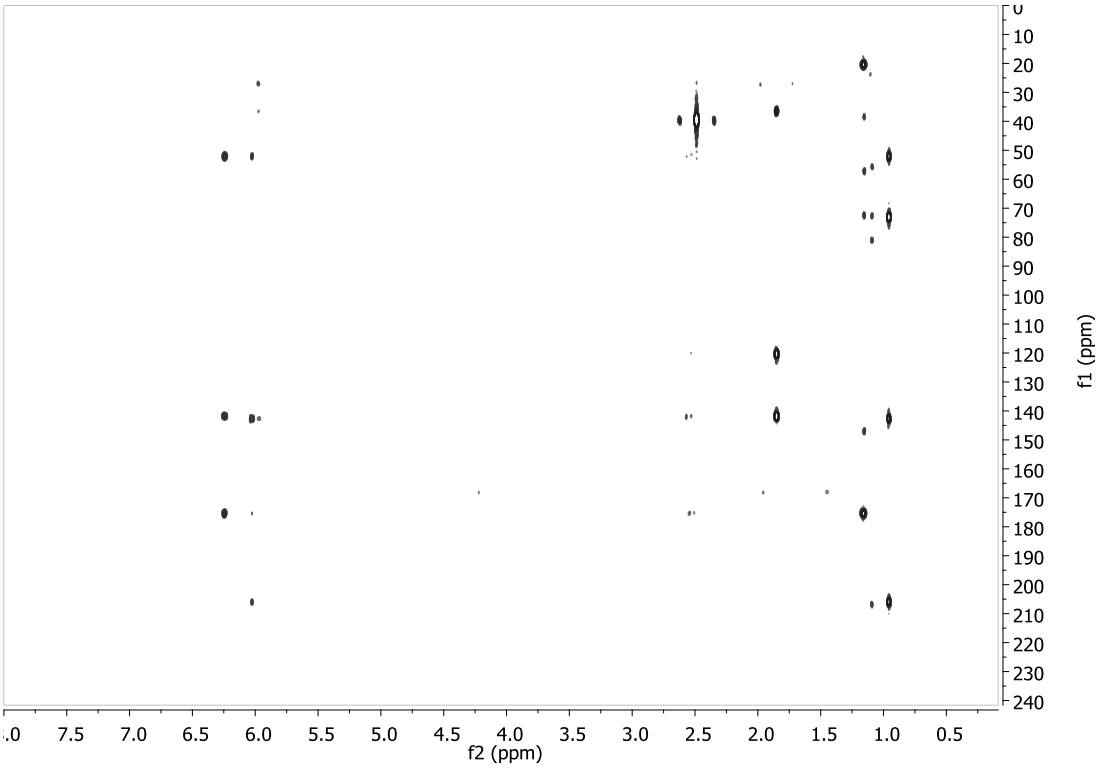

Figure S6. UV spectrum of the new compound aculene A.

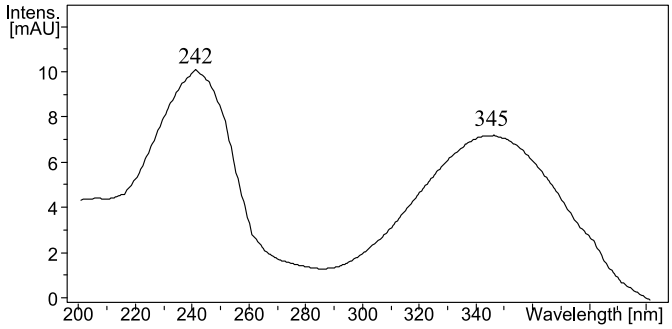

Figure S7. [1]H-NMR (500 MHz, DMSO-d_6 spectrum) of the new compound aculene B.

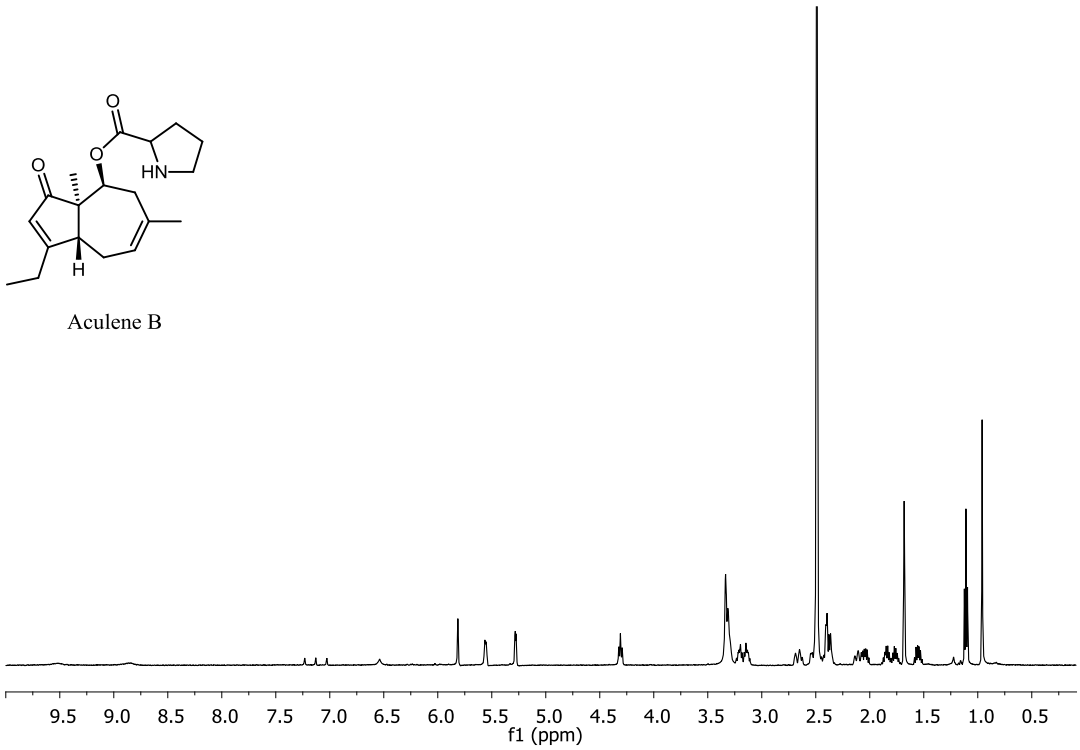

Figure S8. DQF-COSY spectrum of the new compound aculene B.

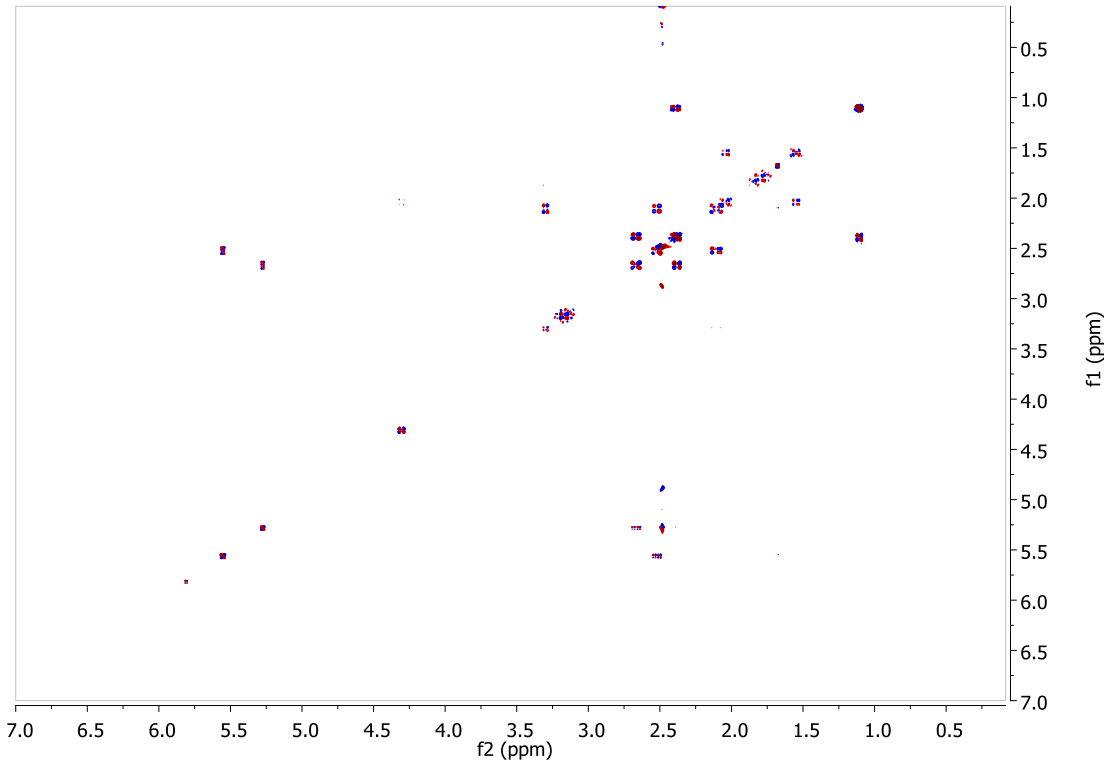

Figure S9. NOESY spectrum of the new compound aculene B.

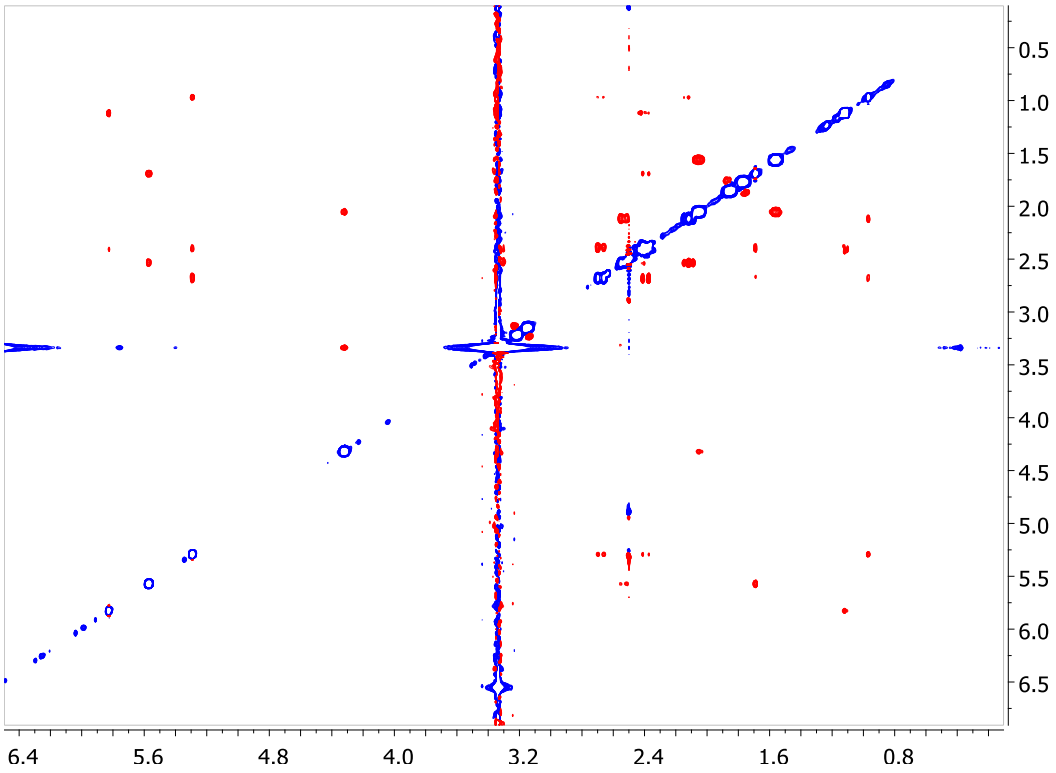

Figure S10. HSQC spectrum of the new compound aculene B

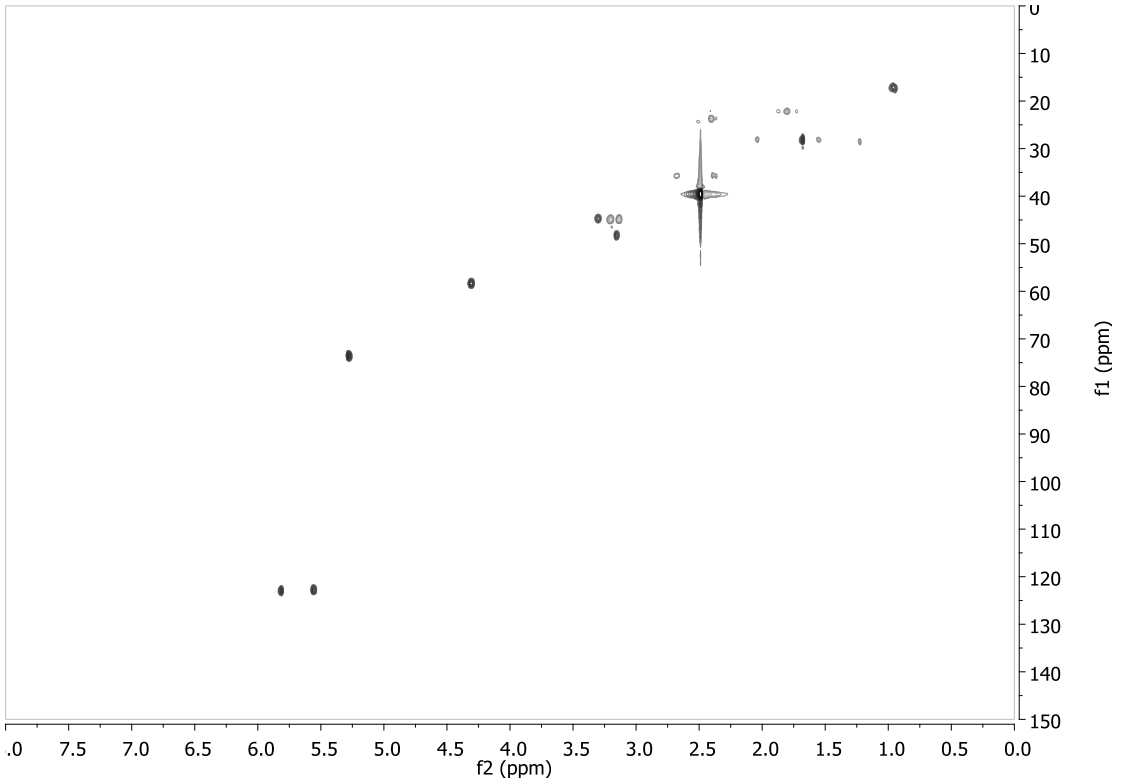

Figure S11. HMBC spectrum of the new compound aculene B.

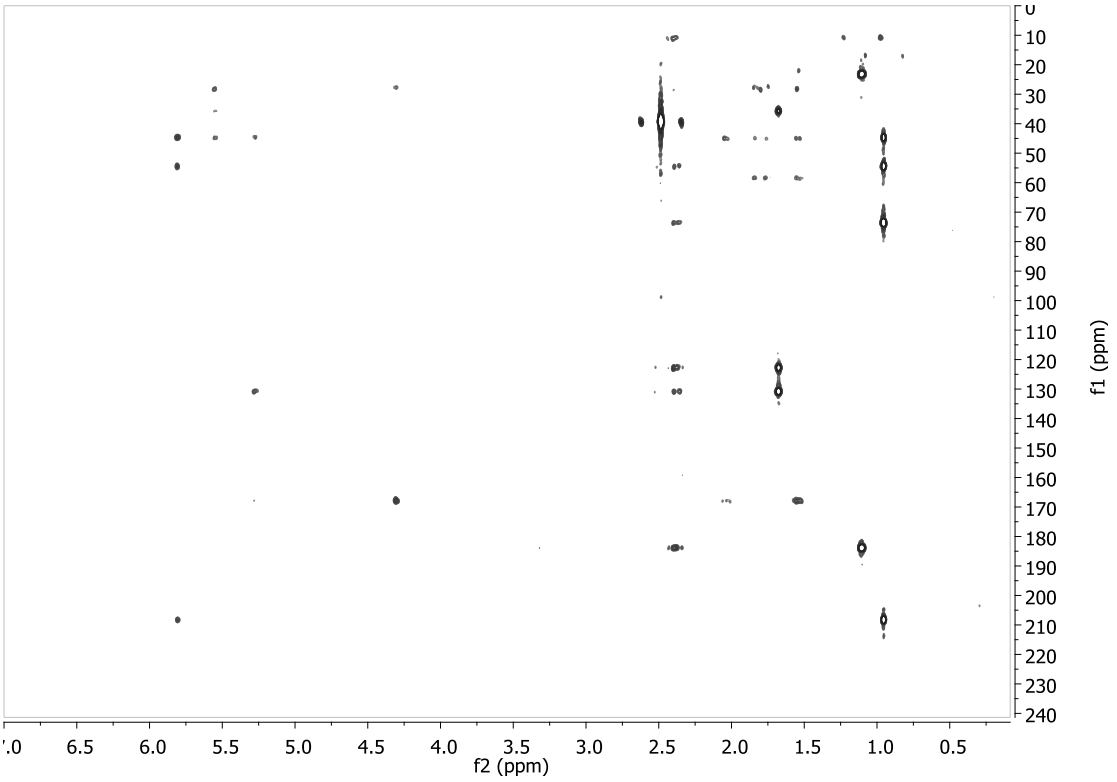

Figure S12. UV spectrum of the new compound aculene B.

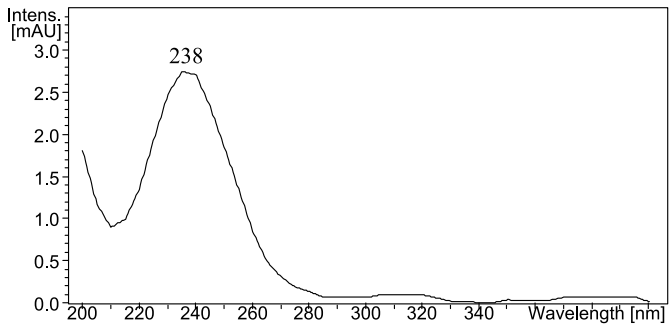

Figure S13. ^{1}H-NMR (800 MHz, DMSO-d_6 spectrum) of the new compound aculene C.

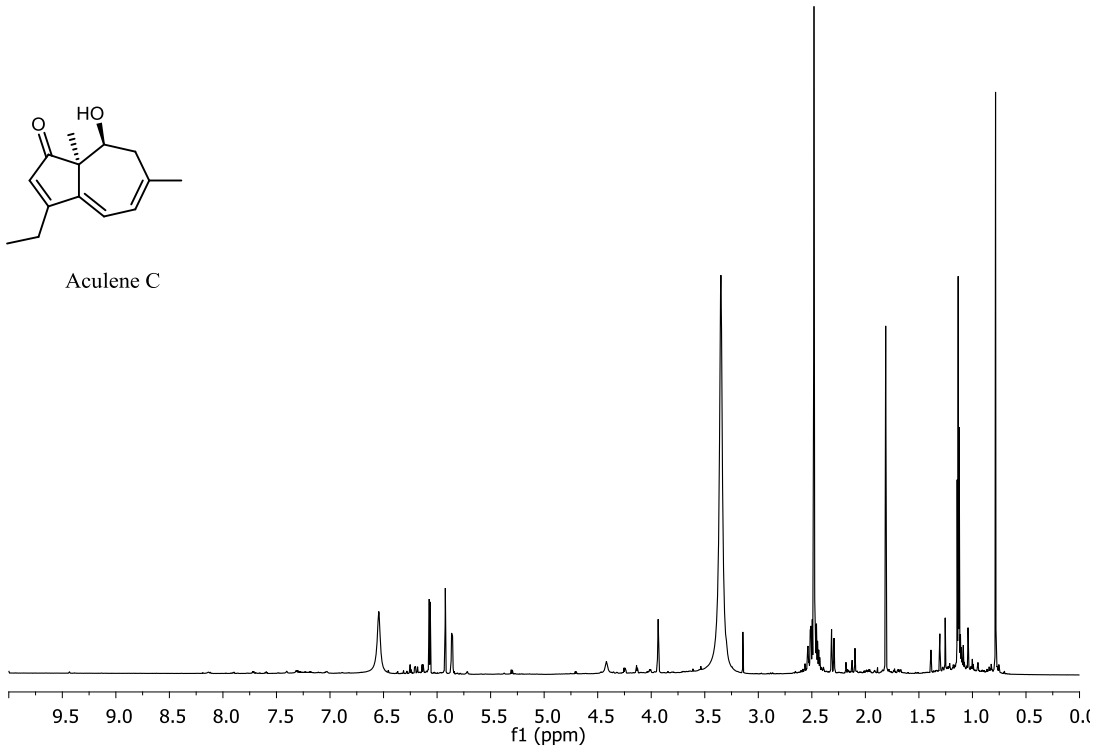

Figure S14. DQF-COSY spectrum of the new compound aculene C.

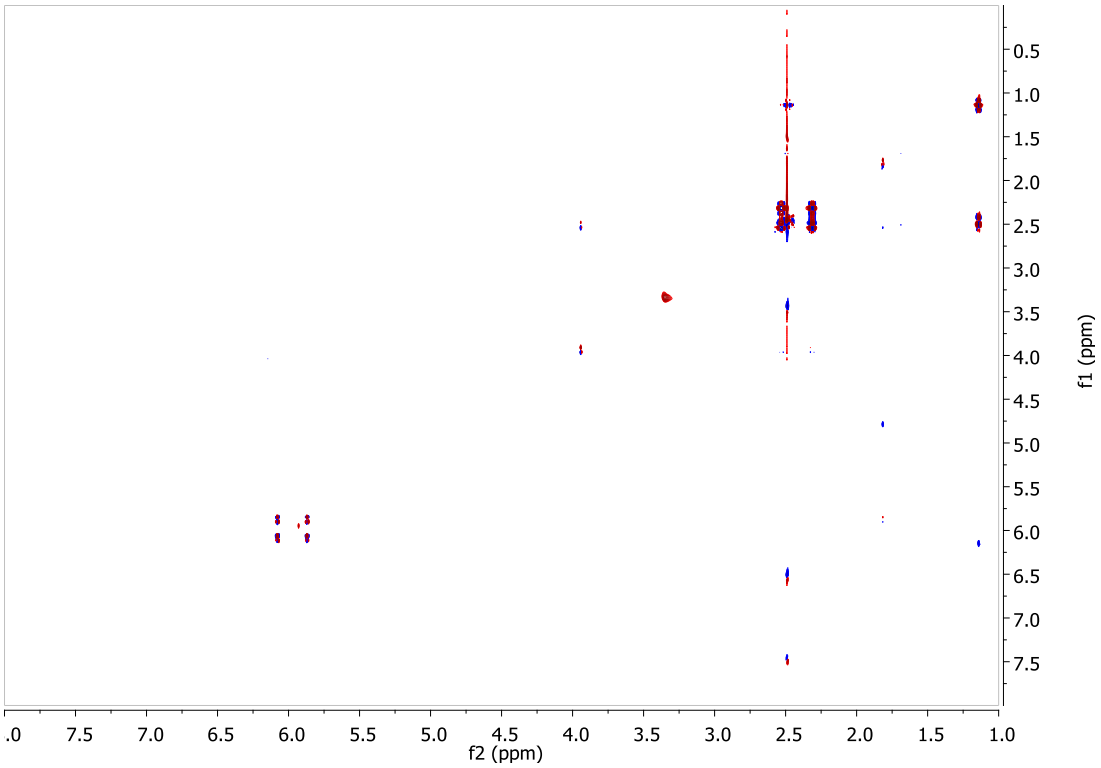

Figure S15. NOESY spectrum of the new compound aculene C.

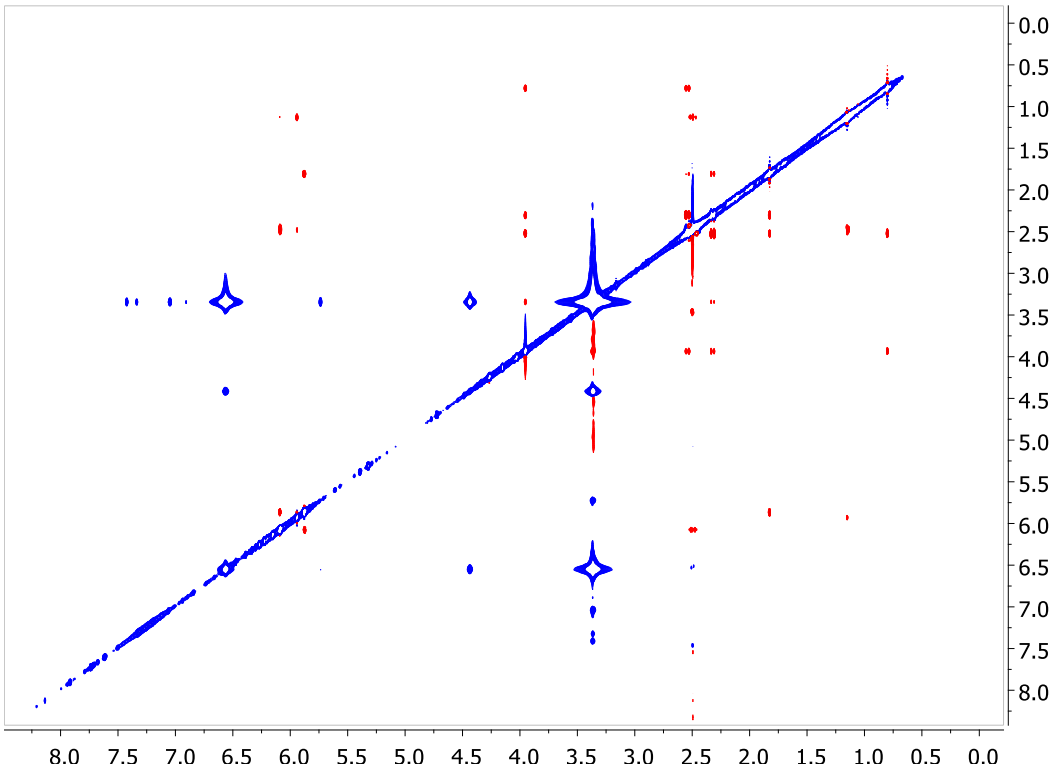

Figure S16. HSQC spectrum of the new compound aculene C.

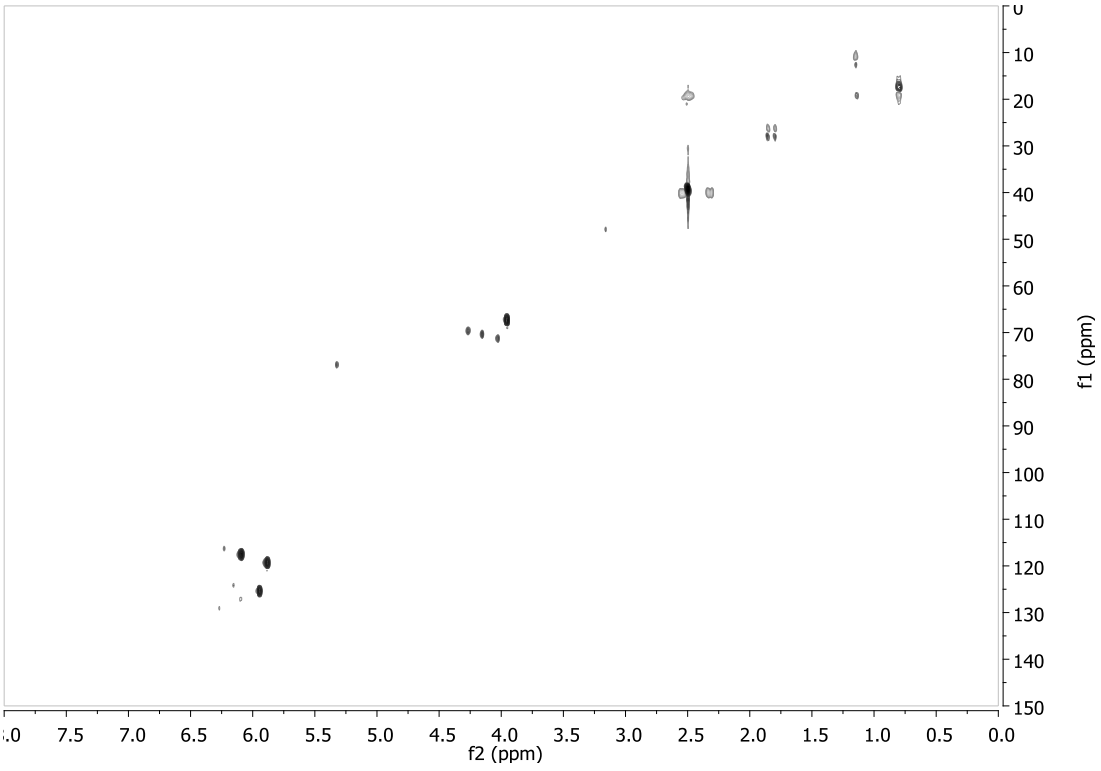

Figure S17. HMBC spectrum of the new compound aculene C.

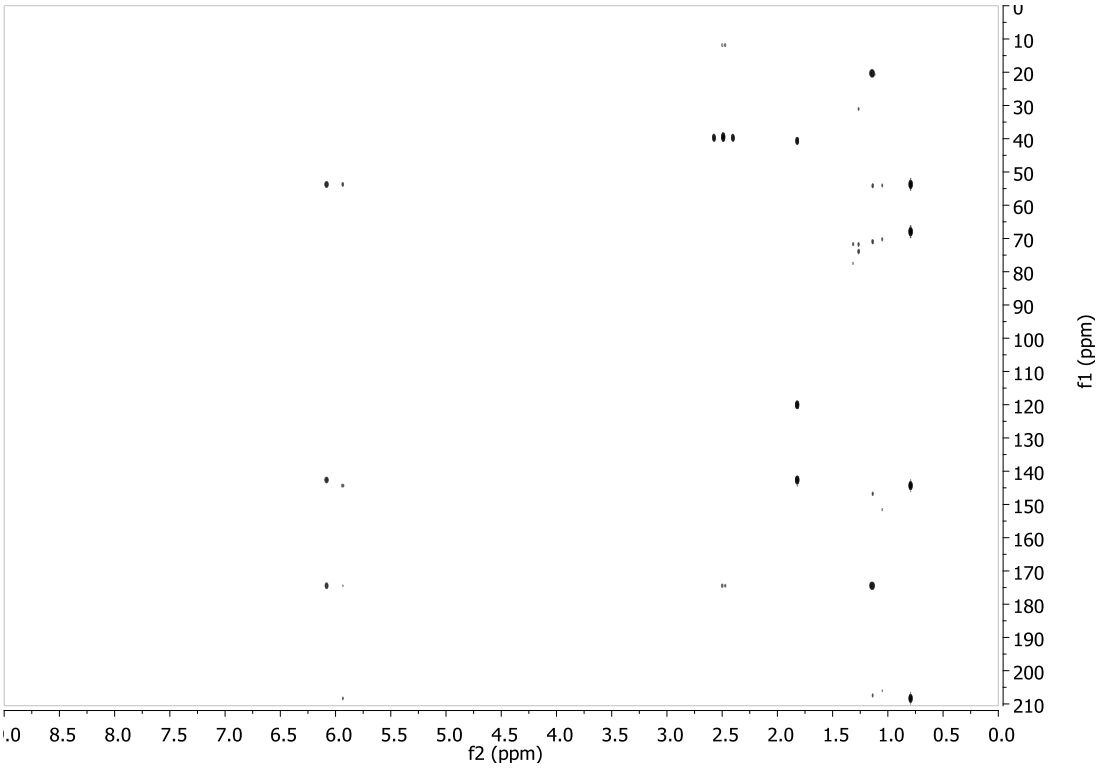

Figure S18.UV spectrum of the new compound aculene C.

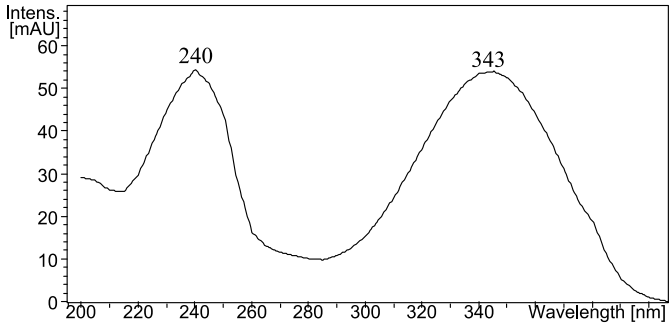

Figure S19. ^{1}H-NMR (500 MHz, DMSO-d_6 spectrum) of the new compound acu-dioxomorhpoline.

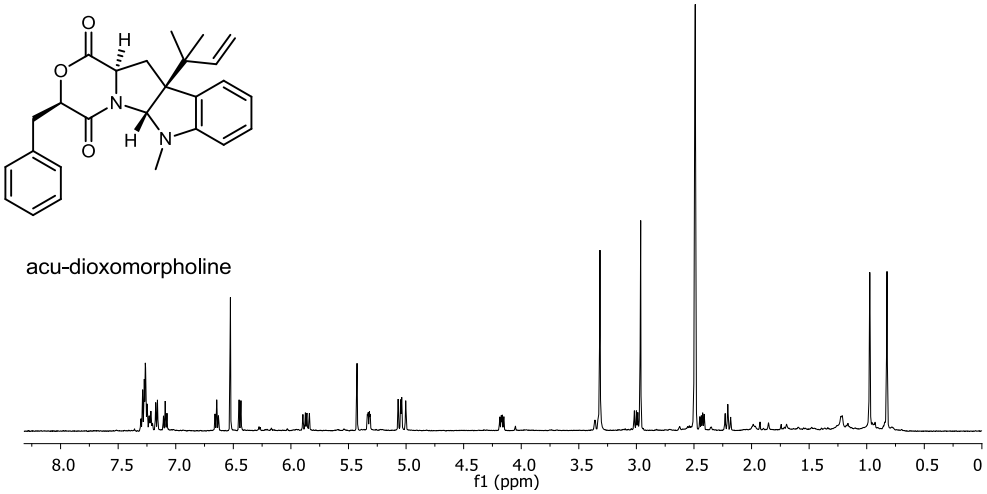

Figure S20. DQF-COSY spectrum of the new compound acu-dioxomorhpoline.

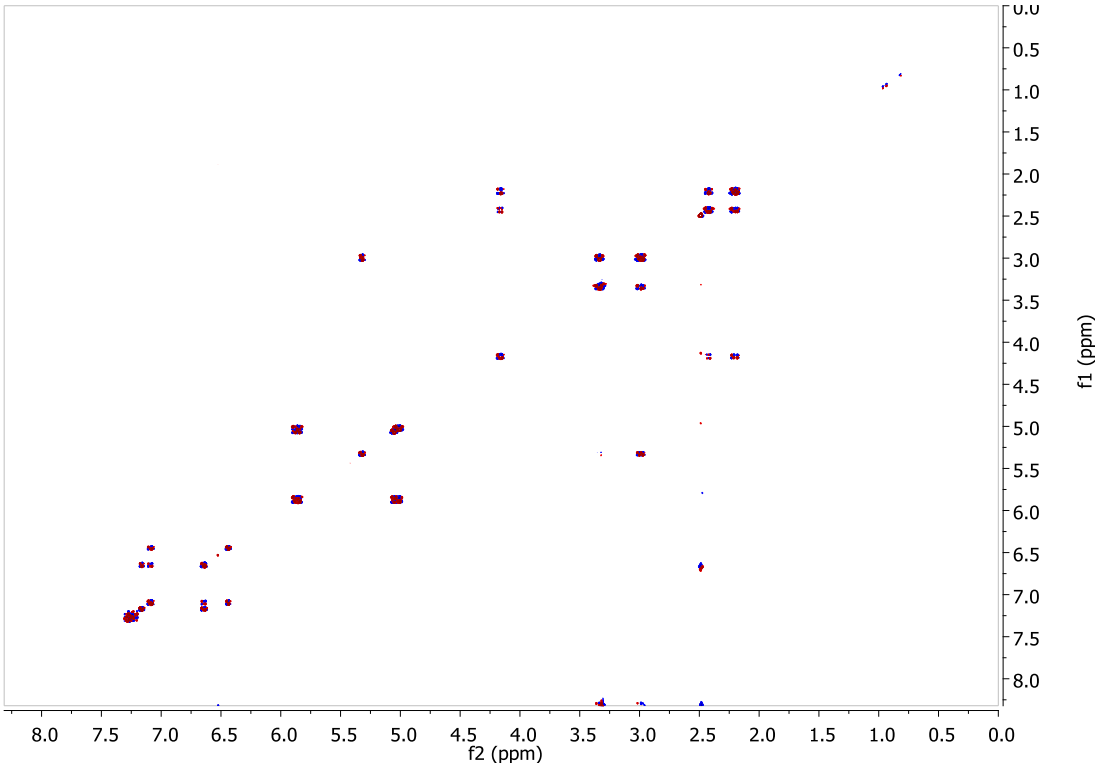

Figure S21. NOESY spectrum of the new compound acu-dioxomorhpoline.

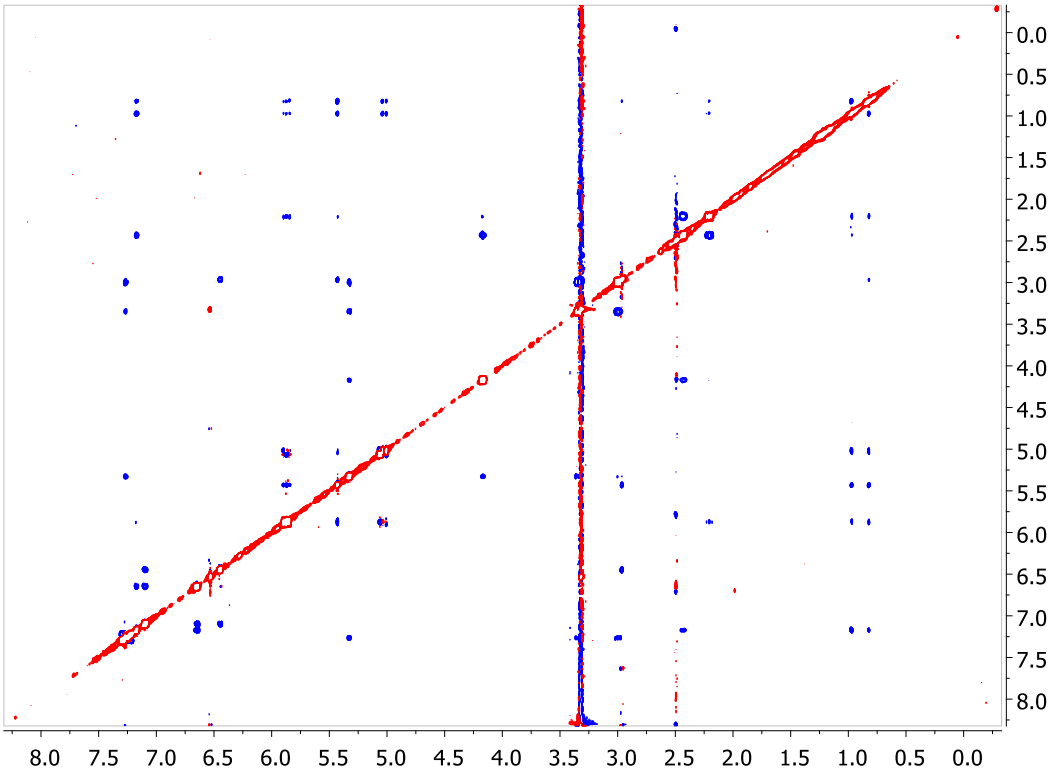

Figure S22. HSQC spectrum of the new compound acu-dioxomorhpoline.

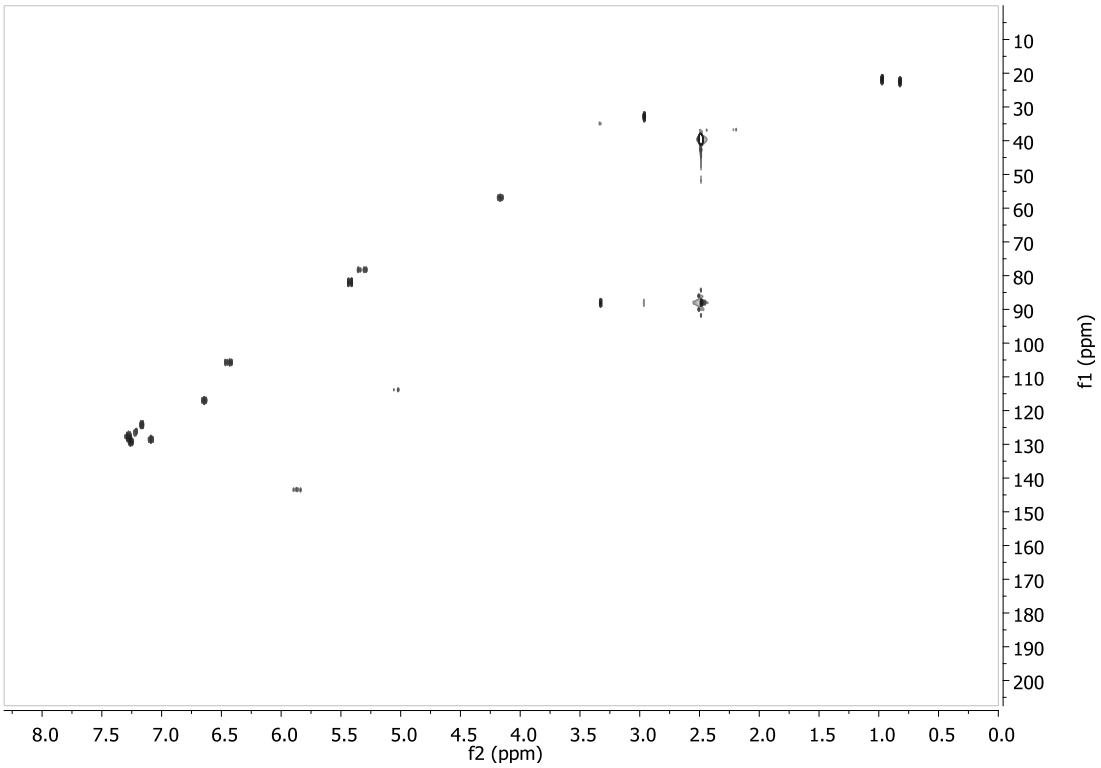

Figure S23. MBC spectrum of the new compound acu-dioxomorhpoline.

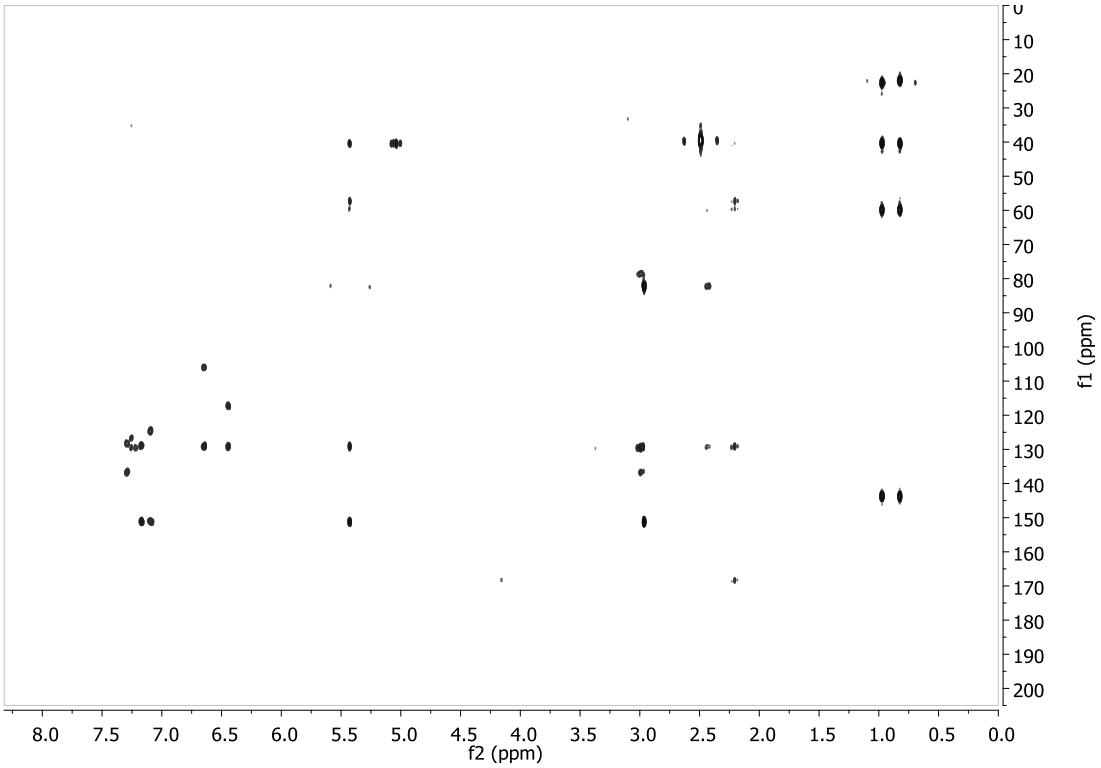

Figure S24. UV spectrum of the new compound acu-dioxomorhpoline.

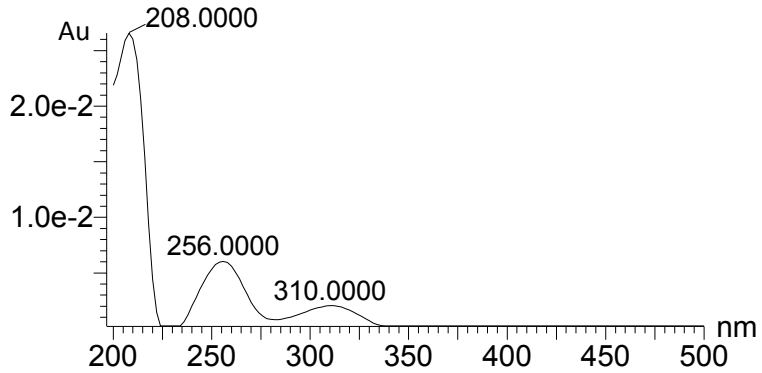

Figure S25. ^{1}H-NMR (500 MHz, DMSO-d_6 spectrum) of the new compound okaramine S.

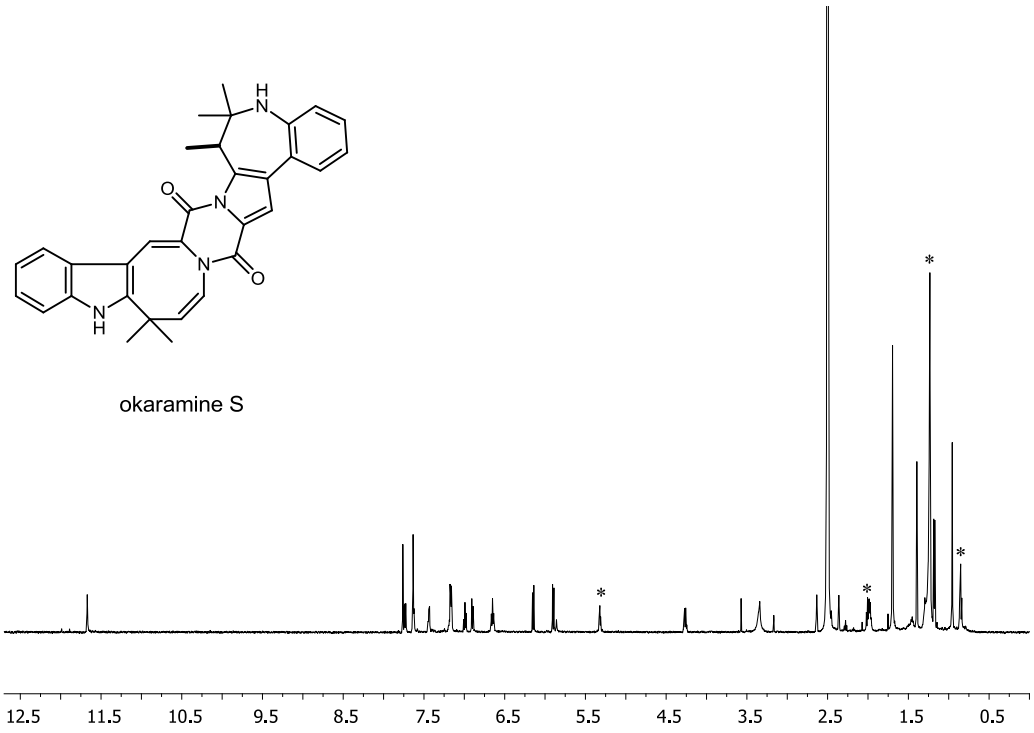

* Impurity (Isolated spinsystem, not part of the compound).

Figure S26. DQF-COSY spectrum of the new compound okaramine S.

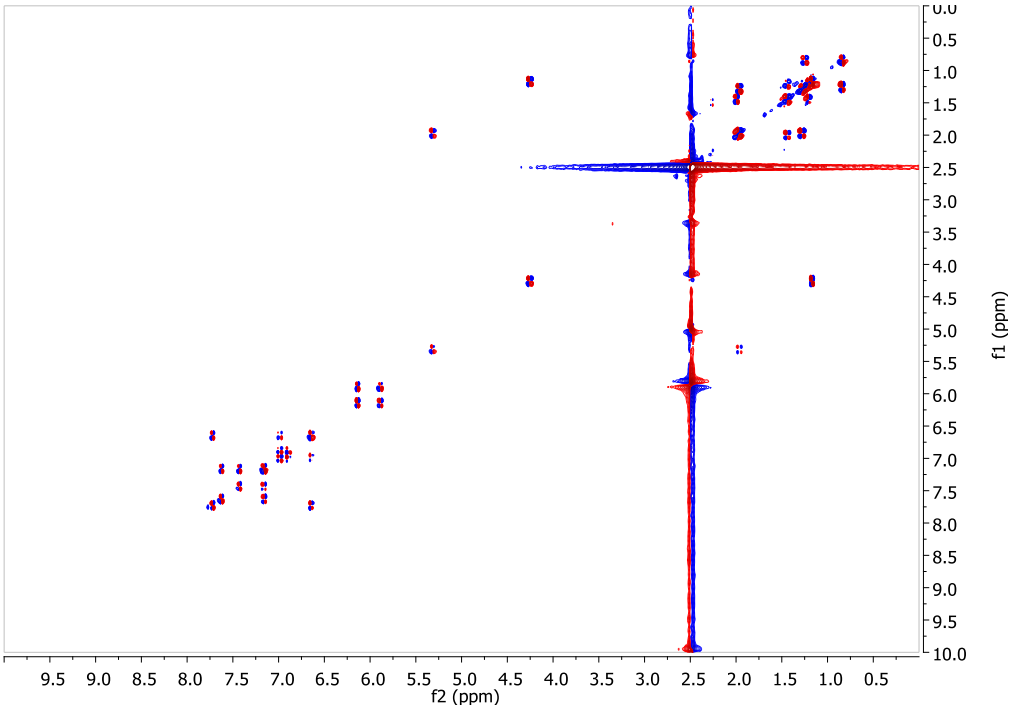

Figure S27. NOESY spectrum of the new compound okaramine S.

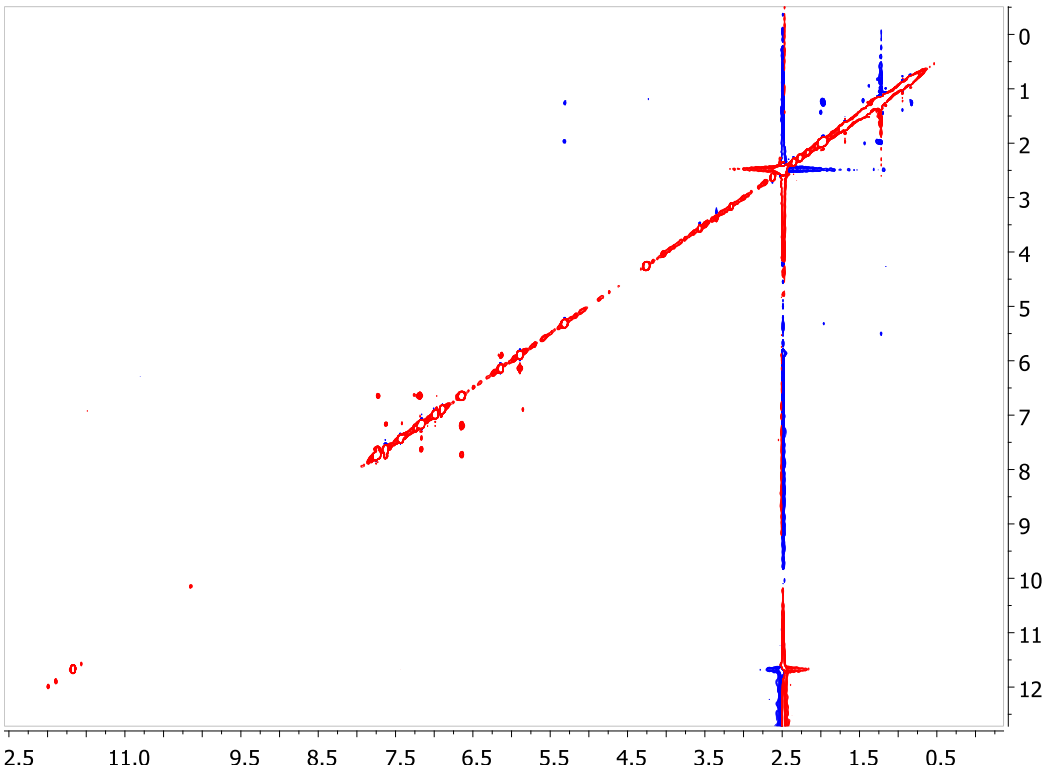

Figure S28. HSQC spectrum of the new compound okaramine S.

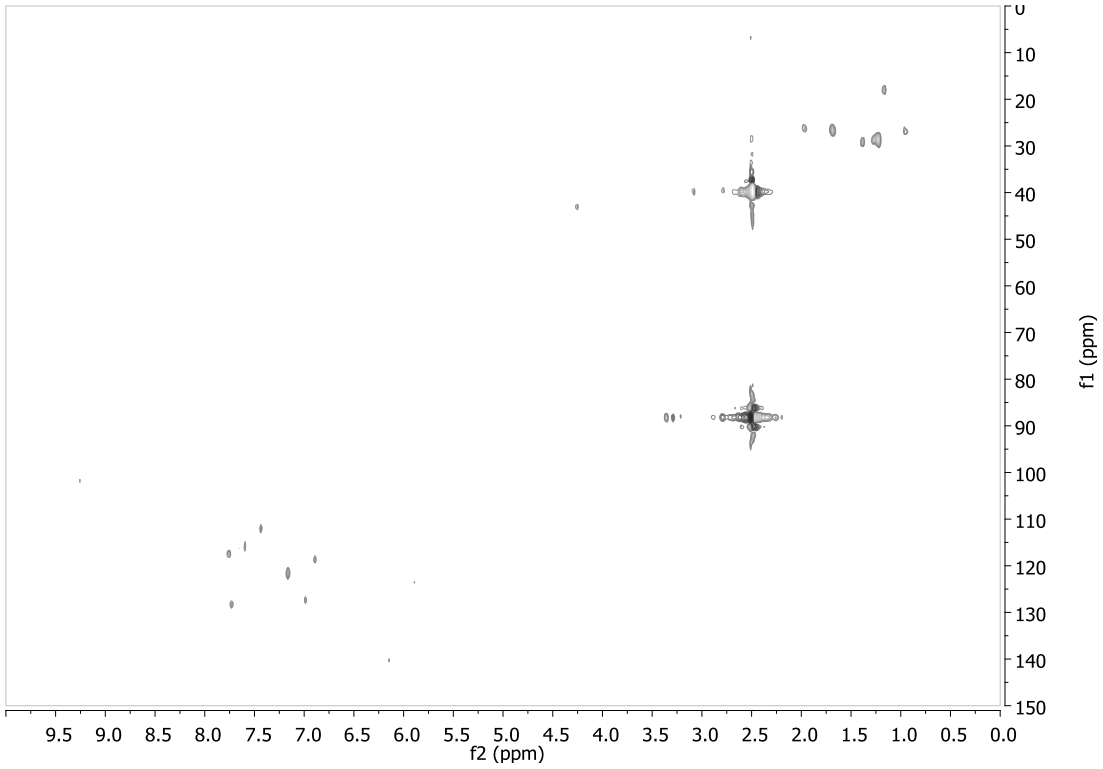

Figure S29. HMBC spectrum of the new compound okaramine S.

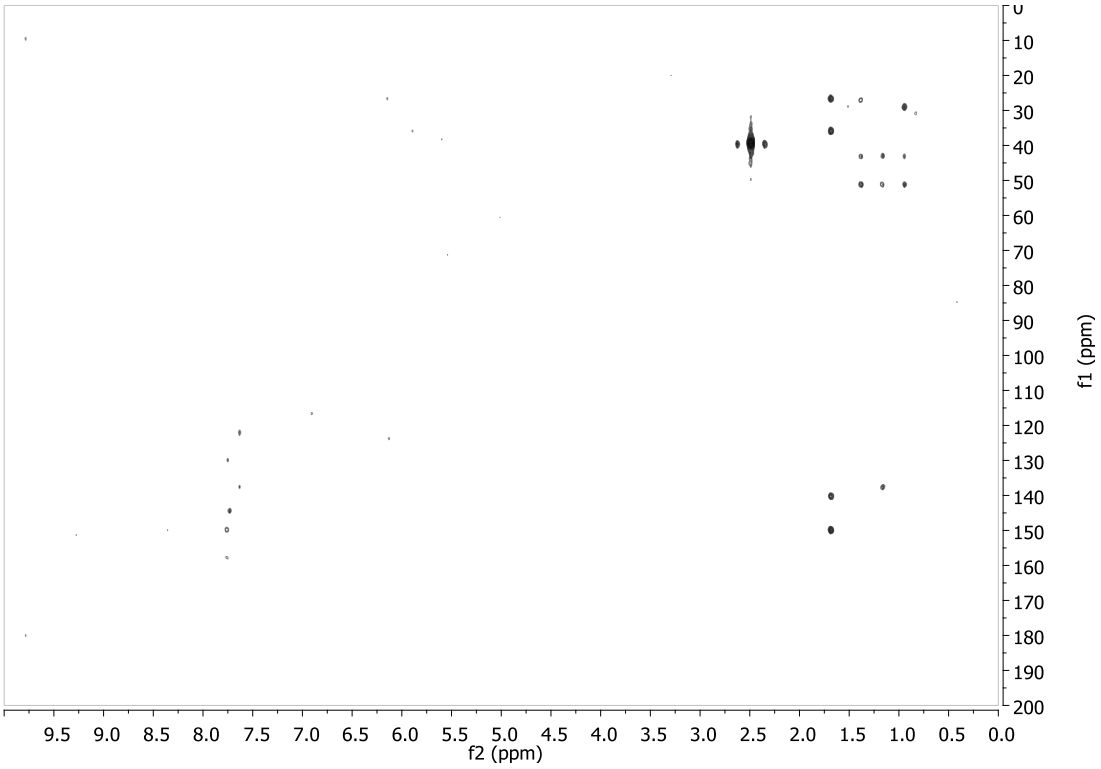

Figure S30. UV spectrum of the new compound okaramine S.

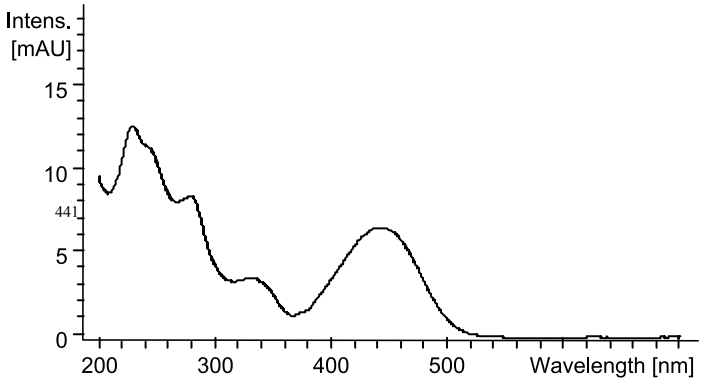

Figure S31. ^{1}H-NMR (500 MHz, DMSO-d_6 spectrum) of epi-10,23-dihydro-24,25-dehydroaflavinine.

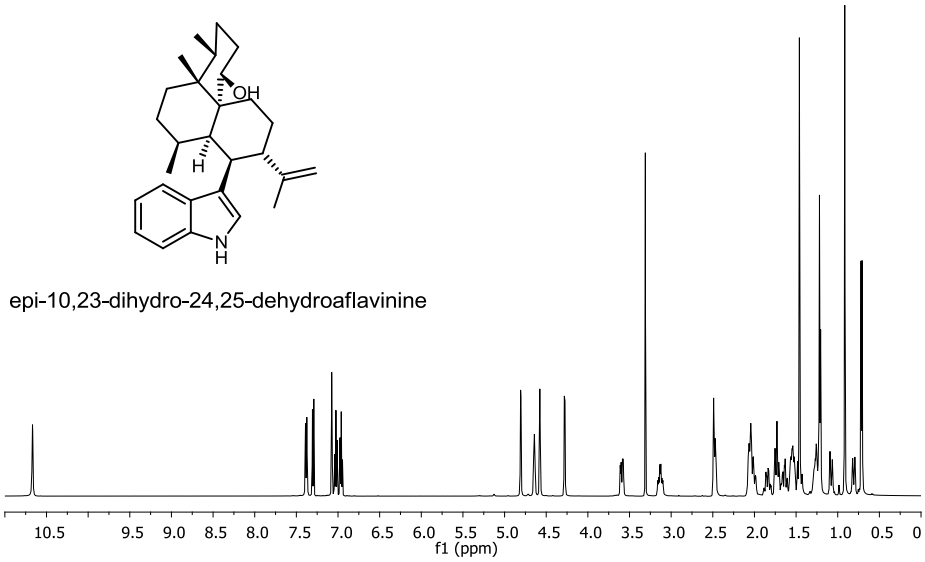

Figure S32. DQF-COSY spectrum of the new compound epi-10,23-dihydro-24,25-dehydroaflavinine.

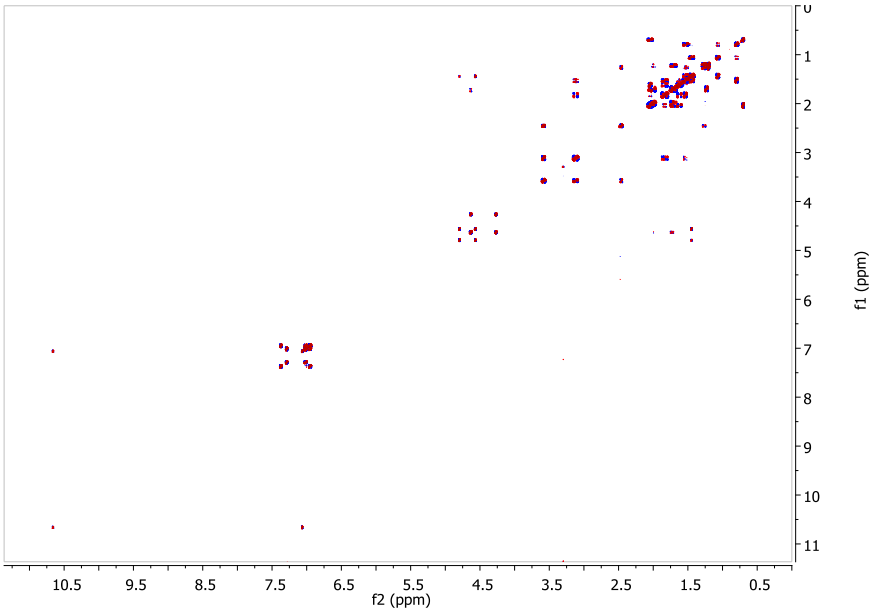

Figure S33. NOESY spectrum of the new compound epi-10,23-dihydro-24,25-dehydroaflavinine.

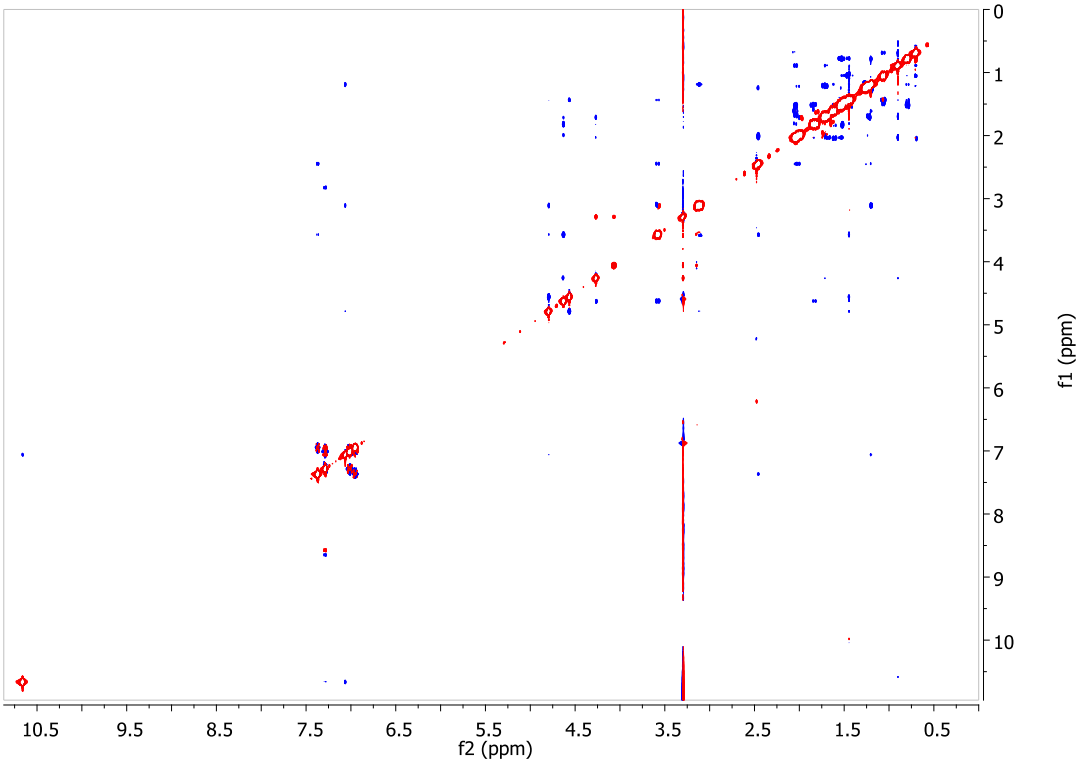

Figure S34. HSQC spectrum of the new compound epi-10,23-dihydro-24,25-dehydroaflavinine.

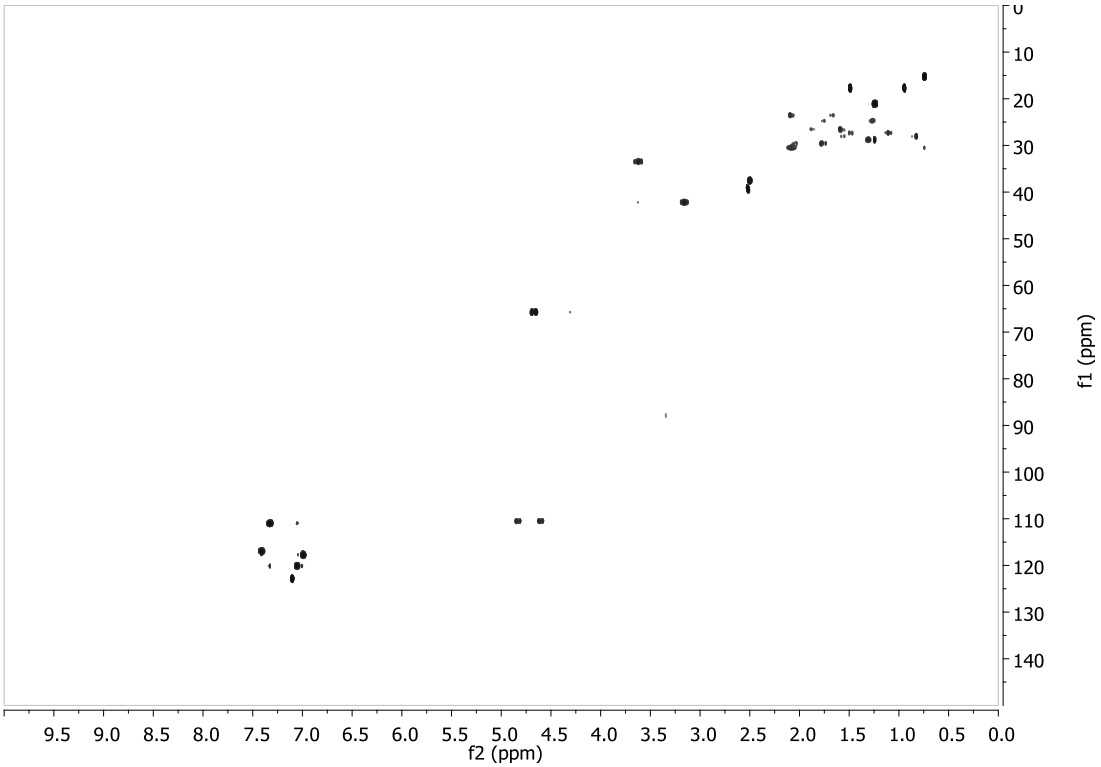

Figure S35. HMBC spectrum of the new compound epi-10,23-dihydro-24,25-dehydroaflavinine.

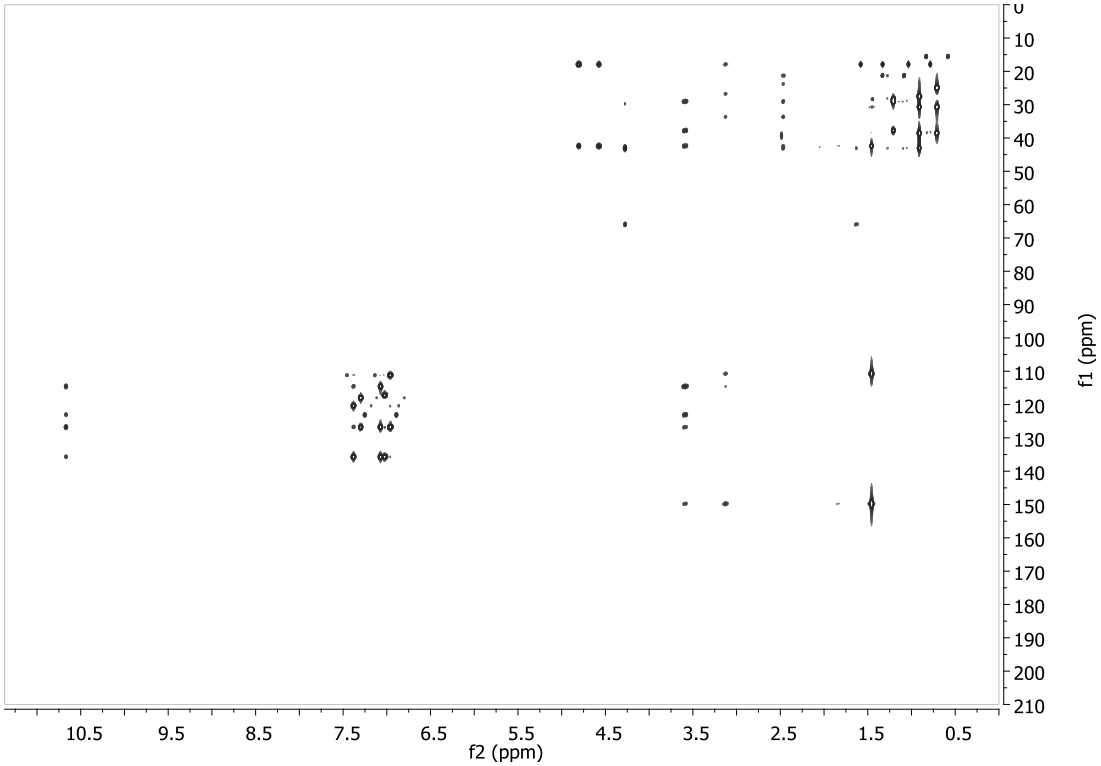

Figure S36. UV spectrum of the new compound epi-10,23-dihydro-24,25-dehydroaflavinine.

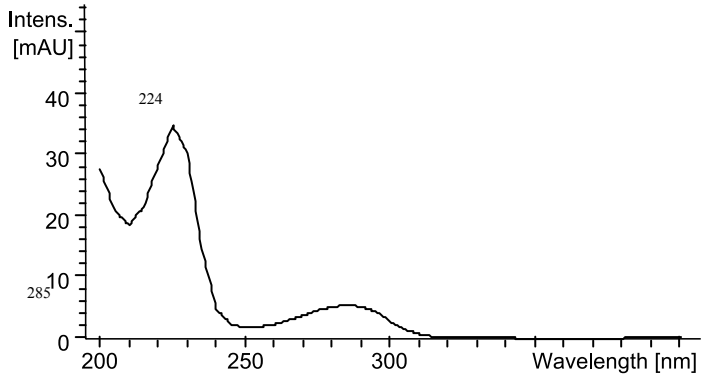

Figure S37. Selected NOEs for aculenes A and B.

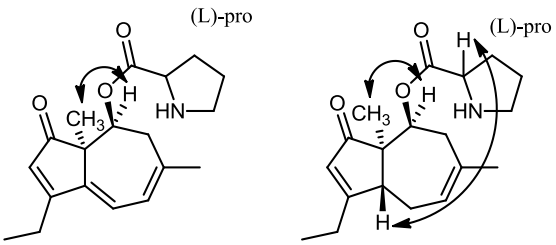

Aculene A Aculene B

Stereochemistry of aculenes A–D: The relative stereochemistry of the stereocenters C-7 and C-16 was investigated by performing conformational searches on the two diastereomers of aculenes A-C.

The strain of the ring resulted in mainly two possible configurations per structure. Only the configuration which is seen in Figure S37 will result in the observed ^{3}J-coupling constants of H-7 as seen in Table S1.

Table S1 for aculene A. A similar trend was observed for aculenes B and C. The observed NOESY peaks (Table S2) fit the suggested structures the best. The final stereocenter (C-12) of aculene B is suggested from NOEs and from the rather large *J*-coupling from H-12 to H-11, which displays an NOE to H-17.

Table S1. Observed ^{3}J-couplings in Hz of H-7 of aculene A compared to values calculated by DFT.

Nucleus1	Nucleus2	Meas	(RS) or (SR) conf. 1	(RS) or (SR) conf. 2	(RR) or (SS) conf. 1	(RR) or (SS) conf. 2
7	8	4.4	4.5	11.0	9.3	11.3
7	8'	2.8	2.6	5.2	0.6	5.9

Table S2. NOESY correlations for aculenes A–C.

Position	Aculene A	Aculene B	Aculene C
1			
2		2'	
2'		2	
3	3'	3'	
3'	3	3,4'	
4	4',5	4',5	
4'	4	3',4	
5	4	4,12	
6			
7	8,8',17	8,8',17	8,8',17
8	7,8',17	7,8',17,18	7,8',17,18
8'	7,8	7,8	7,8,18
9			
10	11,18	11,11',18	11,18
11	10,19	10,11',17	10,19,20
11'		10,11	
12		5	
13			
14	19,20	17,19,20	17,19,20
15			
16			
17	7,8	7,8,11,14	7,8,14
18	10	8,10,19	8,8',10
19	11,14,20	14,18,20	11,14,20
20	14,19	14,19	11,14,19
-OH			

Figure S38. Proposed structures of acucalbistrin A and B.

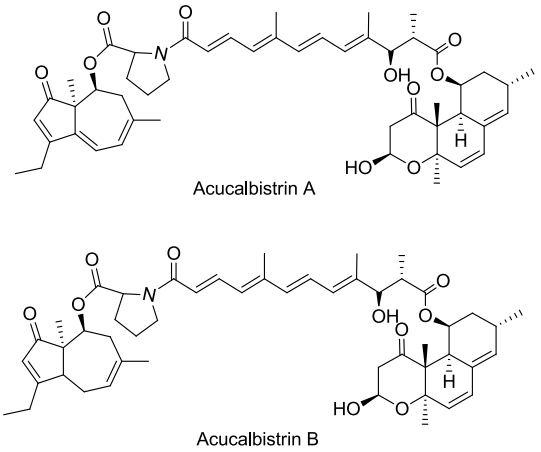

A. BPC and EICs of a fraction from attempted purification of acucalbistrin A. Fraction contains aculene A ($[M+H]^+$ = 316.1907), calbistrin A ($[M+Na]^+$ = 563.2615, ionizing poorly in positive ion mode) and acucalbistrin A ($[M+H]^+$ = 838.4524). Both acucalbistrin A and calbistrin A epimerize during purification. **B.** BPC and EICs of a fraction from attempted purification of acucalbistrin B. Fraction contains aculene B ($[M+H]^+$ = 318.2064), calbistrin A ($[M+Na]^+$ = 563.2615, ionizing poorly in positive ion mode) and acucalbistrin B ($[M+H]^+$ = 840.4681). Both acucalbistrin B and calbistrin A epimerize during purification.

Figure S39. Degradation of the acucalbistrins.

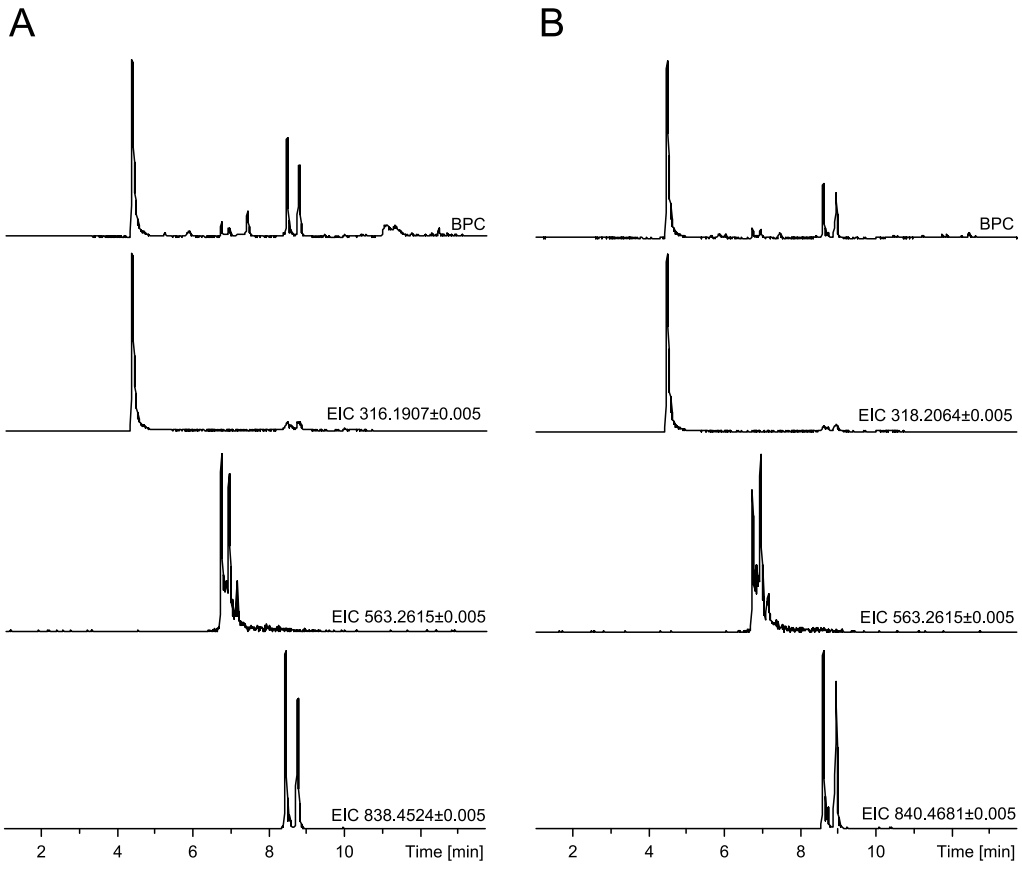

Figure S40. 3D-structure of 10,23-dihydro-24,25-dehydroaflavinine. Epi-10,23-dihydro-24,25-dehydroaflavinine is suggested to be the enantiomer

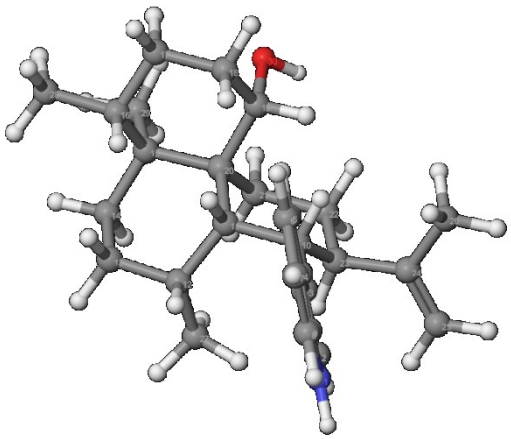

The relative stereochemistry of epi-10,23-dihydro-24,25-dehydroaflavinine was established by performing conformational searches on different diastereomers and comparing observed distances to the back-calculated distances from ISPA, as well as comparing ^{3}J-couplings. The structure which fitted the data the best was further optimized by HF and DFT to give the reported structure.

Table S3. ISPA derived distances in Å of epi-10,23-dihydro-24,25-dehydroaflavinine, a: reference, b: error due to freely rotating bond.

Nucleus1	Nucleus2	Meas	Calc	Diff	Lower bound	Violation	Upper bound	Violation
1	2	2.50	2.64	0.14	2.38		2.90	
1	5	2.83	3.03	0.20	2.72		3.33	
5	18	2.40	2.72	0.32	2.45	0.05	2.99	
5	11	2.37	2.41	0.04	2.17		2.65	
5	10	2.67	2.54	0.13	2.29		2.79	
2	27	2.54	2.48	0.06	2.23		2.73	
2	23	2.46	2.58	0.12	2.32		2.83	
2	25	2.96	3.01	0.05	2.71		3.32	
25	23	2.31	2.39	0.07	2.15		2.62	
25	10	4.58	2.78	1.80[b]	2.51		3.06	1.52
25	25'	1.85	1.85	0.00[a]	1.66		2.03	
19	26	2.95	2.98	0.04	2.68		3.28	
19	18'	2.43	2.51	0.08	2.25		2.76	
19	22	2.14	2.02	0.12	1.82		2.22	
19	18	2.41	2.32	0.08	2.09		2.56	
19	11	2.83	3.37	0.53	3.03	0.20	3.70	
19	10	1.88	1.95	0.07	1.75		2.14	
30	29	2.83	2.88	0.05	2.59		3.17	
30	18'	3.32	2.48	0.84[b]	2.23		2.73	0.59
30	22	2.25	2.68	0.44[b]	2.41	0.16	2.94	
30	21	2.06	2.65	0.59[b]	2.39	0.33	2.92	

Table S3. *Cont.*

Nucleus1	Nucleus2	Meas	Calc	Diff	Lower bound	Violation	Upper bound	Violation
10	26	2.33	2.28	0.05	2.05		2.50	
10	11	2.32	2.24	0.08	2.02		2.47	
23	27	2.05	2.06	0.02	1.86		2.27	
11	12	2.24	2.12	0.12	1.90		2.33	
11	13	2.61	2.70	0.09	2.43		2.97	
11	16	2.21	1.86	0.35	1.68		2.05	0.16
16	28	2.37	2.23	0.14	2.01		2.46	
21	29	2.18	2.05	0.12	1.85		2.26	
16	17'	2.44	2.10	0.34	1.89		2.31	0.13
16	13	2.02	1.93	0.09	1.73		2.12	
22	22'	1.74	1.75	0.01	1.58		1.93	
17	29	2.33	2.31	0.02	2.08		2.54	
17	17'	1.75	1.93	0.18	1.74		2.13	
21'	27	2.07	2.12	0.04	1.91		2.33	
13	13'	1.75	1.75	0.00	1.57		1.92	
17'	28	2.46	2.35	0.11	2.12		2.59	
14'	28	2.16	2.11	0.04	1.90		2.33	
25’	26	2.44	2.38	0.06	2.14		2.62	

Table S4. HLA and DFT ^{3}J-coupling constants in Hz of epi-10,23-dihydro-24,25-dehydroaflavinine.

Nucleus1	Nucleus2	Meas	Calc (HLA)	Diff	Calc (DFT)	Diff
10	23	13.3	11.1	2.2	12.4	0.9
10	11	5.0	5.4	0.4	5.1	0.1
21'	22	13.5	11.8	1.7	11.9	1.6
22	23	13.5	10.6	2.8	13.7	0.2
16	17	11.3	11.4	0.1	13.7	0.2
17	18	11.3	12.1	0.8	14.1	2.8
21'	22'	3.4	4.9	1.5	4.4	1
21	22	4.3	4.6	0.3	4.4	0.1
22'	23	5.6	5.4	0.2	5.3	0.3

Paper 2

"Aspiperidine oxide, a new rare piperidine *N*-oxide, from the filamentous fungus *Aspergillus indologenus*"

Petersen L.M.; Kildgaard, S.; Jaspars, M.; Larsen, T.O.

Intended for publication in Phytochemistry Letters

Aspiperidine oxide, a new rare piperidine *N*-oxide, from the filamentous fungus *Aspergillus indologenus*

Lene M. Petersen[1], Sara Kildgaard[1], Marcel Jaspars[2], Thomas O. Larsen[1*]

[1]Technical University of Denmark, Department of Systems Biology, Chemodiversity Group, Søltofts Plads B221, DK-2800 Kgs. Lyngby, Denmark

[2]Marine Biodiscovery Centre, Department of Chemistry, University of Aberdeen, Old Aberdeen AB24 3UE, Scotland, UK.

ABSTRACT: A novel secondary metabolite, aspiperidine oxide, was isolated from the filamentous fungus *Aspergillus indologenus*. The structure of aspiperidine oxide was determined from extensive 1D and 2D NMR spectroscopic analysis supported by high resolution mass spectrometry. The structure revealed a rare piperidine *N*-oxide, not observed in filamentous fungi before. A biosynthetic pathway of aspiperidine oxide is proposed, based on tentative identification of intermediates from UHPLC-DAD-HRMS data.

1. Introduction

Black Aspergilli constitute an important group of fungi within the genus *Aspergillus*. The group both entails species used for industrial production as well as common food and feed contaminants. A famous member of the group is *A. niger*, which is utilized in several industrial processes for production of organic acids such as citric acid and gluconic acid as well as enzymes such as amylases and lipases[1]. In addition, *A. niger* is also one of the most widespread food and feed contaminants[2]. This comprises a health hazard, since some strains are able to produce mycotoxins, such as fumonisins[3][4][5] and ochratoxin A[6]. Another member of the black Aspergilli is *A. aculeatus*, which similarly is both a contaminant and an industrial workhorse a[2][7].

In the same clade as *A. aculeatus* is another black *Aspergillus*: *A. indologenus* (IBT 3679 = CBS 114.80). This species was isolated from Indian soil in 2011 and was subsequently described by Varga and co-workers[8]. This work showed that *A. indologenus* is a producer of the insecticidal compounds okaramins A, B, and H, which is also the case for the closely related *A. aculeatus*[9]. A further analysis of the metabolic profile indicated that the species can produce indol-alkaloids related to aflavinines[8]. Being a relatively unstudied species and the only isolate of this species ever reported, our hypothesis was that *A. indologenus*

(IBT 3679 = CBS 114.80) would likely produce new chemical entities, other than the SMs already reported from this clade.

2. Results and discussion

Initial dereplication of a CYA derived extract, revealed production of the previously described metabolites JBIR-74, aspergillicin A and fellutanine C, see Figure 1.

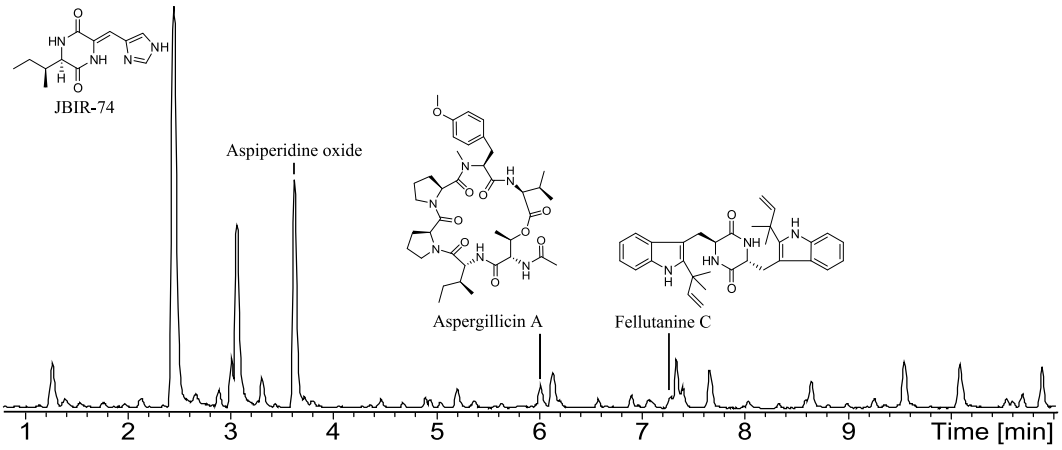

Figure 1 ESI+ Base peak chromatogram illustrating some of the major compounds in the extract from *A. indologenus*. Based on microscale extraction after cultivation on CYA media for 7 days at 25 °C in the dark.

These compounds have not been described from *A. indologenus* before. JBIR-74 was originally isolated from a sponge-derived *Aspergillus* species[10] and displayed no cytotoxic activity against several cancer cell lines and no antimicrobial acitivity against *Candida albicans*, *Micrococcus luteus* or *Escherichia coli*. Aspergillicin A was isolated from a marine-derived *Aspergillus carneus* and showed modest cytotoxic activity (LD_{99} 25–50 µg/mL) [11]. Fellutanine C was isolated from *Penicillium fellutanum* and showed no cytotoxic activity [12]. Dereplication of one of the major peaks eluting at 3.65 min gave no hits in Antibase[13], why a large extract was prepared for isolation and structural elucidation of what indeed turned out to be a novel compound, which we have named aspiperidine oxide. The resulting structure is depicted in Figure 2.

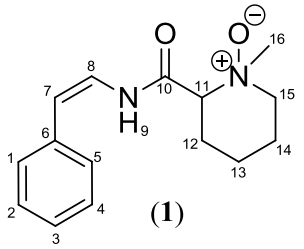

Figure 2 The chemical structure of aspiperidine oxide.

2.1 Structural elucidation of aspiperidine oxide

The ESI^+ spectrum of aspiperidine oxide showed an adduct pattern consisting of $[M+H]^+$ and $[2M+H]^+$. The molecular formula $C_{15}H_{20}N_2O_2$ was obtained from HRMS of $[M+H]^+$ of *m/z* 261.1588 (261.1597 calculated for $[C_{15}H_{20}N_2O_2 + H]^+$). The UV spectrum displayed absorption maxima at 273 nm indicating a conjugated chromophore. For MS and UV spectra see Supporting Information.

The ^1H NMR spectrum revealed the presence of one amide proton, eight methines (one aliphatic, two vinylic and five aromatic), four methylenes, and one methyl group (Figure 3). The DQF-COSY spectrum of **1** defined three spin systems besides the single methyl group; one spin system for the aromatic protons, one connecting the two vinylic protons with the amide proton, and the final spinsystem constituting the four methylene groups (three of these diastereotopic) and the aliphatic methine proton. The linking between these COSY spin systems and assignments of the remaining signals and quaternary carbons were accomplished through thorough analysis of HMBC experimental data (Figure 3).

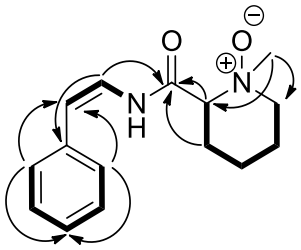

Figure 3 Important HMBC correlations connecting the three COSY spin systems (marked in bold) for aspiperidine oxide. The remaining HMBC correlations are found in Table 1.

The aromatic protons H1, H2, H4, and H5 had overlapping resonances at δ_H 7.38 ppm and δ_C 128.9 ppm. From these both COSY and HMBC correlations were observed to the final aromatic proton H3 (δ_H 7.26 ppm, δ_C 127.5 ppm). Furthermore HMBC correlations were observed to the quaternary carbon at δ_C 135.2 ppm identified as H6. A further correlation was observed to this carbon from H8 (δ_H 6.73 ppm) connecting the aromatic part to the vinyllic part of the molecule. HMBC correlations were also observed from the aromatic system to C7 verifying this relation. The size of the vicinal coupling constants ($^3J_{HH}$) for H7/H8 was measured to 9.9 Hz, suggesting *trans* stereochemistry. A strong COSY correlation was observed between the two and one further COSY correlation was observed from H8 to what was identified as the amide proton at δ_H 10.23 ppm. Correlations to the C10 carbonyl (δ_C 164.9 ppm) was observed from H8, but also from protons at δ_H 4.64 ppm (H11), δ_H 2.04 ppm and 2.12 ppm (H12 and H12'). H11 and H12 could by COSY and HMBC correlations be connected to the three remaining methylene groups C13, C14 and C15. The chemical shift of H11 (δ_H 4.64 ppm) and H15/15' (δ_H 3.58/4.07 ppm) indicated C11 and C15 to be directly connected to the remaining nitrogen, leading to the 6-membered aliphatic ring of aspiperidine oxide. Finally the methyl group appearing as a singlet at δ_H 3.56 ppm (H16) could be linked to this 6-membered ring through HMBC correlations to C11 and C15. The chemical shifts suggested it to be directly attached to the

nitrogen resulting in the *N*-oxide shown in Figure 3. This type of structure, has to the best of our knowledge, never been seen in any fungal SM. The piperidine *N*-oxide has recently been observed in two alkaloids isolated from the shrub *Microcos paniculata*[14]. The chemical shifts were comparable to our observations.

Table 1. NMR data for aspiperidine oxide. ^{1}H NMR data were obtained at 600 MHz in DMSO-d_6 and ^{13}C data were obtained at 150 MHz in DMSO-d_6. ^{13}C-NMR chemical shifts determined from HSQC and HMBC experiments. It was not possible to distinguish between no. 1, 2, 4 and 5.

Atom #	^{1}H-chemical shift [ppm]/ (Intg., mult., *J* [Hz])	^{13}C-chemical shift [ppm]	COSY correlations	HMBC connectivities
1	7.38 (1H, m)	128.9	2/4, 3/5	2/4/5, 3, 6, 7
2	7.38 (1H, m)	128.9	1/3/5, 2/4	1/4/5, 3, 6, 7
3	7.26 (1H, m)	127.5	1/5, 2/4	1/2/4/5
4	7.38 (1H, m)	128.9	1/3/5, 2	1/2/5, 3, 6, 7
5	7.38 (1H, m)	128.9	1/3, 2/4	1/2/4, 3, 6, 7
6	-	135.2	-	-
7	5.86 (1H, d, 9.9)	113.6	8	1/5, 8
8	6.73 (1H, t, 9.9)	121.5	7, 9	6, 7, 10
9	10.23 (1H, d, 9.9)	-	8	10
10	-	164.9		-
11	4.64 (1H, m)	74.2	12, 12’	10, 12/12’, 13/13’,
12	2.04 (1H, m)	25.5	11, 12’, 13, 13’	10, 11, 13/13’, 14
12’	2.12 (1H, m)	25.5	11, 12, 13, 13’	10, 11, 13/13’, 14
13	1.52 (1H, m)	19.3	12, 12’, 13’, 14	11, 12/12’, 14
13’	1.68 (1H, m)	19.3	12, 12’, 13, 14	11, 14
14	1.91 (2H, m)	21.4	13, 13’ 15, 15’	12/12’, 13/13’, 15/15’
15	3.58 (1H, m)	67.4	14, 15’	11, 13/13’, 14, 16
15’	4.07 (1H, m)	67.4	14, 15	11, 13/13’, 14
16	3.56 (3H, s)	51.4	-	11, 15/15’

2.2 Biological activity

Aspiperidine oxide was tested towards GRAM-negative bacteria *P. aeruginosa*, *A. baumannii* and *E. coli*, GRAM positive *MSSA* and *MRSA*, the yeast *C. albicans* and for fungal activity against *A. fumigatus*, but did not display any biological activity. Plant related metabolites partly containing an piperidine *N*-oxide moiety, have been shown to display cytotoxic as well as nicotinic receptor antagonistic activities[14], why we speculate that aspiperidine oxide may play a role in fungal plant interactions.

2.3 Biosynthetic origin

Aspiperidine oxide is likely to originate from amino acids, as are the metabolites JBIR-74, aspergillicin A and fellutanine C also produced by *A. indologenus* (Figure 1). We suggest aspiperidine oxide to originate from phenylalanine and the non-proteinogenic amino acid pipecolic acid. The proposed biosynthetic pathway is depicted in Figure 4. The putative decarboxylation step of (**4**) to (**5**) have been observed for other fungal metabolites, e.g. in the oryzamide A_{1-2} from *A. flavus*[15]. The next step is the *N*-methylation to (**6**) and finally the *N*-oxide is formed, resulting in the final structure of aspiperidine oxide (**1**). We hypothesize that L- pipecolinic acid is incorporated into the compound; feeding studies is ongoing in our laboratory to reveal whether L- or D- pipecolinic acid is one of the amino acid precursors.

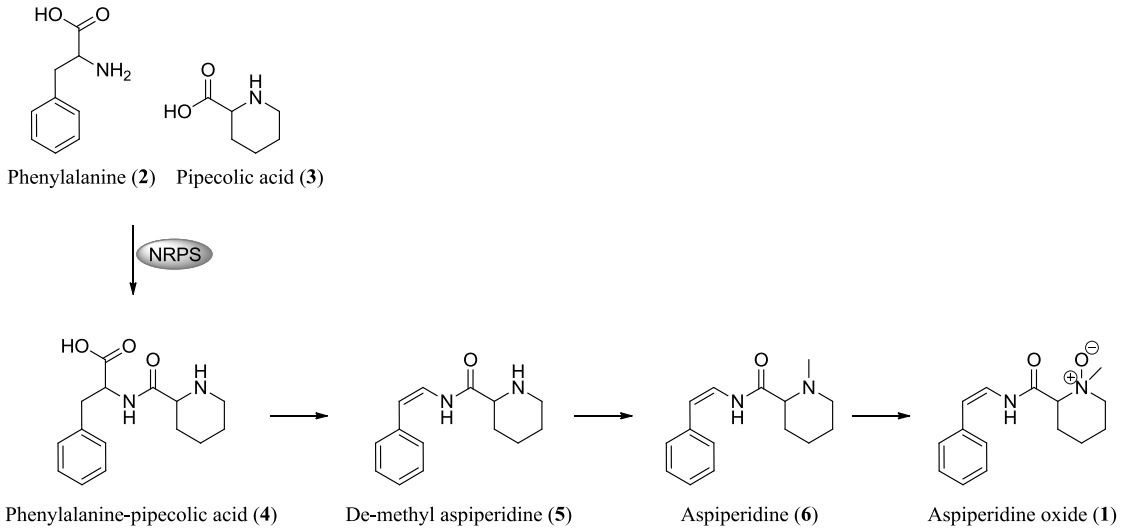

Figure 4 Proposed steps towards the biosynthesis of aspiperidine oxide. NRPS = non-ribosomal peptide synthetase.

The *A. indologenus* extract was scrutinized for the putative intermediates, see Figure 5. This resulted in tentatively identification of both the dipeptide phenylalanine-pipecolic acid (**4**) (trace amounts), de-methyl aspiperidine (**5**) and aspiperidine (**6**). Phenylalanine (**2**) was also observed, though no traces were found of the non-proteinogenic amino acid pipecolic acid (**3**).

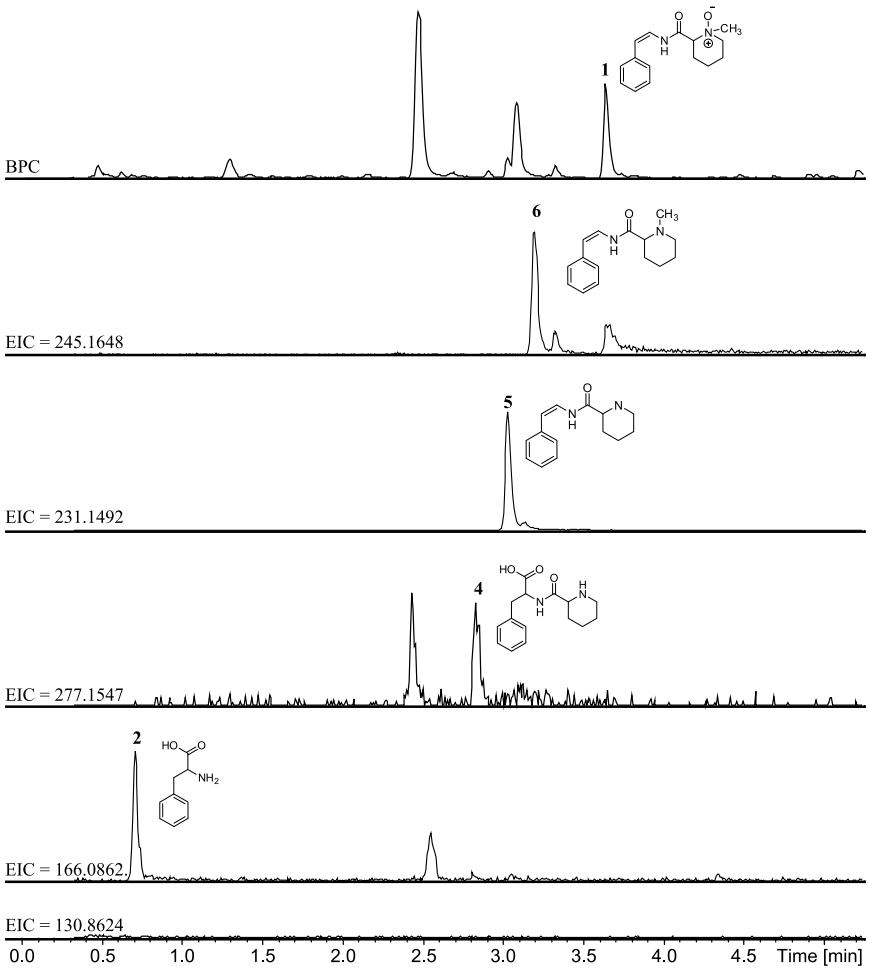

Figure 5. Extracted ion chromatograms (EICs) for compounds **1**–**6** with a mass tolerance ± 0.005 Da. From UHPLC-DAD-HRMS data of microscale extraction after cultivation of *A. indologenus* on CYA media for 7 days at 25 °C in the dark. The EICs are not to scale.

The decreasing polarity of the intermediates is in accordance with the observed retention times. The tentative identification of the suggested intermediates supports the suggested biosynthesis of aspiperidine oxide.

3. Materials and methods

3.1 Chemical analysis of strains.

Strains were cultivated on solid CYA media at 25 °C for 7 days in the dark. Extraction of metabolites was performed as described by Smedsgaard[16]. Analysis was performed using reversed phase ultra-high-performance liquid chromatography (UPHLC) UV/Vis diode array detector (DAD) high-resolution time-op-flight mass spectrometer (TOFMS) on a maXis G3 orthogonal acceleration quadrupole time of flight (Q-TOF) mass spectrometer (Bruker Daltonics, Bremen) as described by Holm *et al.*[17].

3.2 Strains, media and purification of metabolites.

Solid plates with CYA media were prepared as described by Frisvad and Samson[18]. *A. indologenus* (IBT 3679) was cultivated on 200 plates of CYA medium at 30 °C for 5 days in the dark. Extraction and workup was performed as described by Holm *et al.*[17]. Pre-fractionation of the extract was achieved by using an Isolera flash purification system (Biotage) using a 25g C18 Septra ZT column and a gradient of ACN and water going from 30 % to 100% ACN. ACN was of HPLC grade, and water was purified and deionized by a Millipore system through a 0.22 mmmembrane filter (Milli-Q water). The Isolera fractions were subjected to further purification on a semipreparative high-performance liquid chromatography (HPLC), which was a Gilson 322 controller connected to a 215 Liquid Handler, 819 Injection Module, and a 172 DAD (Gilson). This was achieved using a Luna II C18 column (250 310 mm, 5 mm; Phenomenex) and a gradient from 15 to 20 % ACN over 20 minutes. 50 ppm TFA was added to ACN of HPLC grade and Milli-Q water. This yielded 2.3 mg of aspiperidine oxide.

3.3 NMR and structural elucidation.

The 1D and 2D spectra were recorded on a Varian VNMRS 600 MHz spectrometer. Spectra were acquired using standard pulse sequences and ^{1}H spectra as well as DQF-COSY, ed-HSQC and HMBC spectra were acquired. The deuterated solvent was DMSO-d_6 and signals were referenced by solvent signals for DMSO-d_6 at δ_H = 2.49 ppm and δ_C = 39.5 ppm. Chemical shifts are reported in ppm (δ) and scalar couplings in hertz (Hz).

References

1. Schuster, E.; Dunn-Coleman, N. S.; Frisvad, J. C.; Van Dijck, P. W. M. On the safety of *Aspergillus niger* - a review. *Appl. Microbiol. Biotechnol.* **2002**, *59*, 426–435.

2. Perrone, G.; Susca, A.; Cozzi, G.; Ehrlich, K. C.; Varga, J.; Frisvad, J. C.; Meijer, M.; Noonim, P.; Mahakarnchanakul, W.; Samson, R. A. Biodiversity of *Aspergillus* species in some important agricultural products. *Stud. Mycol.* **2007**, *59*, 53–66.

3. Baker, S. E. *Aspergillus niger* genomics: past, present and into the future. *Med. Mycol.* **2006**, *44*, 17–21.

4. Pel, H. J.; de Winde, J. H.; Archer, D. B.; Dyer, P. S.; Hofmann, G.; Schaap, P. J.; Turner, G.; de Vries, R. P.; Albang, R.; Albermann, K.; Andersen, M. R.; Bendtsen, J. D.; Benen, J. A. E.; van Den Berg, M.; Breestraat, S.; Caddick, M. X.; Contreras, R.; Cornell, M.; Coutinho, P. M.; Danchin, E. G. J.; Debets, A. J. M.; Dekker, P.; van Dijck, P. W. M.; van Dijk, A.; Dijkhuizen, L.; Driessen, A. J. M.; D'Enfert, C.; Geysens, S.; Goosen, C.; Groot, G. S. P.; de Groot, P. W. J.; Guillemette, T.; Henrissat, B.; Herweijer, M.; van den Hombergh, J. P. T. W.; van den Hondel, C. A. M. J. J.; van der Heijden, R. T. J. M.; van der Kaaij, R. M.; Klis, F. M.; Kools, H. J.; Kubicek, C. P.; van Kuyk, P. A.; Lauber, J.; Lu, X.; van der Maarel, M. J. E. C.; Meulenberg, R.; Menke, H.; Mortimer, M. A.; Nielsen, J.; Oliver, S. G.; Olsthoorn, M.; Pal, K.; van Peij, N. N. M. E.; Ram, A. F. J.; Rinas, U.; Roubos, J. A.; Sagt, C. M. J.; Schmoll, M.; Sun, J. B.; Ussery, D. W.; Varga, J.; Vervecken, W.; de Vondervoort, P. J. J.; Wedler, H.; Wosten, H. A. B.; Zeng, A. P.; van Ooyen, A. J. J.; Visser, J.; Stam, H. Genome sequencing and analysis of the versatile cell factory *Aspergillus niger* CBS 513.88. *Nat. Biotechnol.* **2007**, *25*, 221–231.

5. Frisvad, J. C.; Smedsgaard, J.; Samson, R. A.; Larsen, T. O.; Thrane, U. Fumonisin B2 production by *Aspergillus niger*. *J. Agric. Food Chem.* **2007**, *55*, 9727–9732.

6. Lucchetta, G.; Bazzo, I.; Cortivo, G. D.; Stringher, L.; Bellotto, D.; Borgo, M.; Angelini, E. Occurrence of black Aspergilli and ochratoxin A on grapes in Italy. *Toxins (Basel).* **2010**, *2*, 840–855.

7. Adisa, V. A. Pectic enzymes of *Aspergillus aculeatus* associated with post-harvest deterioration of citrus sinensis fruit. *J. Food Biochem.* **1989**, *13*, 243–252.

8. Varga, J.; Frisvad, J. C.; Kocsubé, S.; Brankovics, B.; Tóth, B.; Szigeti, G.; Samson, R. A. New and revisited species in *Aspergillus* section *Nigri*. *Stud. Mycol.* **2011**, *69*, 1–17.

9. Petersen, L. M.; Hoeck, C.; Frisvad, J. C.; Gotfredsen, C. H.; Larsen, T. O. Dereplication guided discovery of secondary metabolites of mixed biosynthetic origin from *Aspergillus aculeatus*. *Molecules* **2014**, *19*, 10898–10921.

10. Takagi, M.; Motohashi, K.; Motohashi, K.; Shin-ya, K. Isolation of 2 new metabolites, JBIR-74 and JBIR-75, from the sponge-derived *Aspergillus* sp. fS14. *J. Antibiot. (Tokyo).* **2010**, *63*, 393–395.

11. Capon, R. J.; Skene, C.; Stewart, M.; Ford, J.; O'Hair, R. a J.; Williams, L.; Lacey, E.; Gill, J. H.; Heiland, K.; Friedel, T. Aspergillicins A-E: five novel depsipeptides from the marine-derived fungus *Aspergillus carneus*. *Org. Biomol. Chem.* **2003**, *1*, 1856–1862.

12. Kozlovsky, A. G.; Vinokurova, N. G.; Adanin, V. M.; Burkhardt, G.; Dahse, H. M.; Gräfe, U. New diketopiperazine alkaloids from *Penicillium fellutanum*. *J. Nat. Prod.* **2000**, *63*, 698–700.

13. Laatsch, H. Antibase 2012. http://www.wiley-vch.de/stmdata/antibase.php (accessed on 1 February 2014).

14. Still, P. C.; Yi, B.; González-Cestari, T. F.; Pan, L.; Pavlovicz, R. E.; Chai, H.-B.; Ninh, T. N.; Li, C.; Soejarto, D. D.; McKay, D. B.; Kinghorn, D. A. Alkaloids from Microcos paniculata with cytotoxic and nicotinic receptor antagonistic activities. *J. Nat. Prod.* **2013**, *76*, 243–249.

15. Rank, C.; Klejnstrup, M. L.; Petersen, L. M.; Kildgaard, S.; Frisvad, J. C.; Gotfredsen, C. H.; Larsen, T. O. Comparative chemistry of *Aspergillus oryzae* (RIB40) and *A. flavus* (NRRL 3357). *Metabolites* **2012**, *2*, 39–56.

16. Smedsgaard, J. Micro-scale extraction procedure for standardized screening of fungal metabolite production in cultures. *J. Chromatogr. A* **1997**, *760*, 264–270.

17. Holm, D. K.; Petersen, L. M.; Klitgaard, A.; Knudsen, P. B.; Jarczynska, Z. D.; Nielsen, K. F.; Gotfredsen, C. H.; Larsen, T. O.; Mortensen, U. H. Molecular and chemical characterization of the biosynthesis of the 6-MSA derived meroterpenoid yanuthone D in *Aspergillus niger*. *Chem. Biol.* **2014**, *21*, 519–529.

18. Samson, R. A.; Houbraken, J.; Thrane, U.; Frisvad, J. C.; Andersen, B. *Food and Indoor Fungi*; CBS-KNAW Fungal Biodiversity Centre: Utrecht (NL), 2010.

^{1}H NMR (600 MHz, DMSO-d_6 spectrum) of the new compound aspiperidine oxid

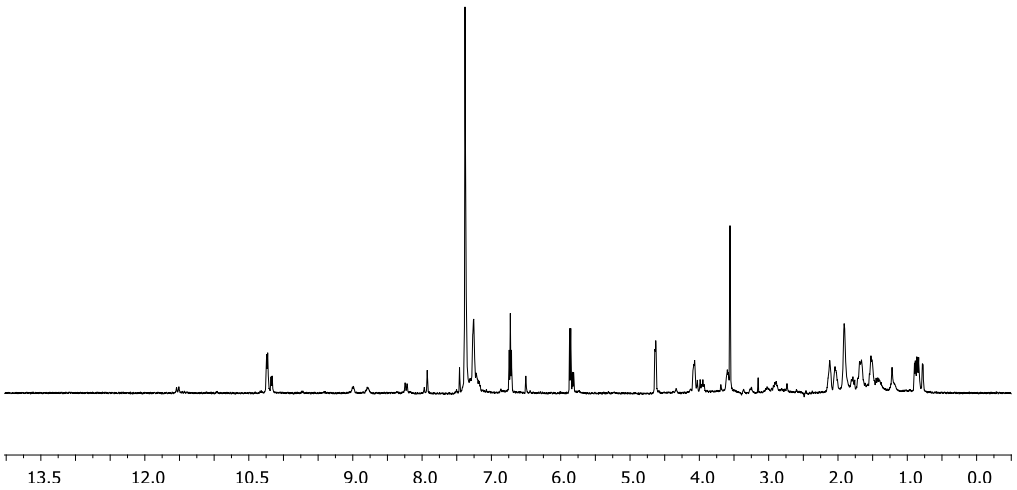

DQF-COSY spectrum of the new compound aspiperidine oxid

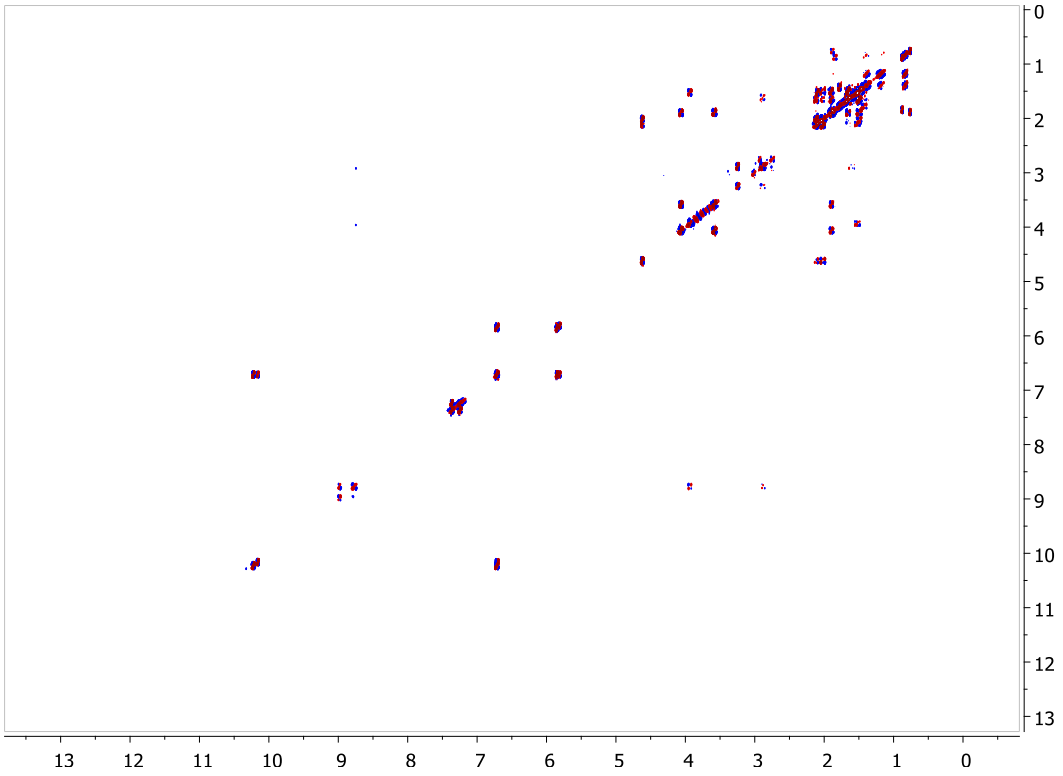

Edited HSQC spectrum of the new compound aspiperidine oxid

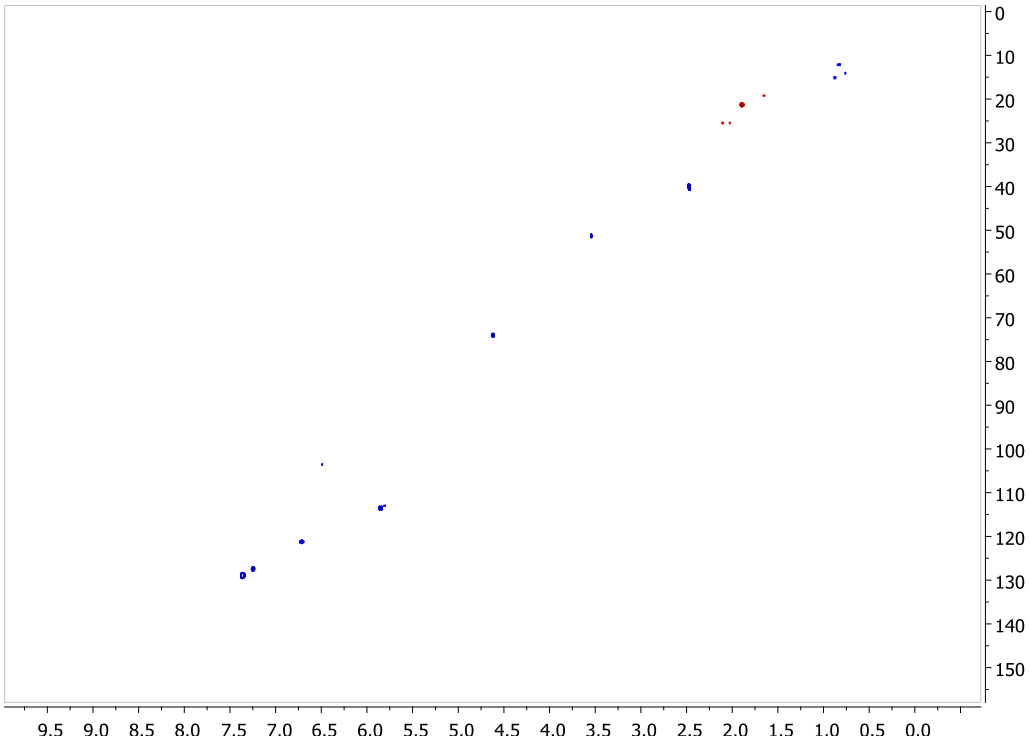

HMBC spectrum of the new compound aspiperidine oxid

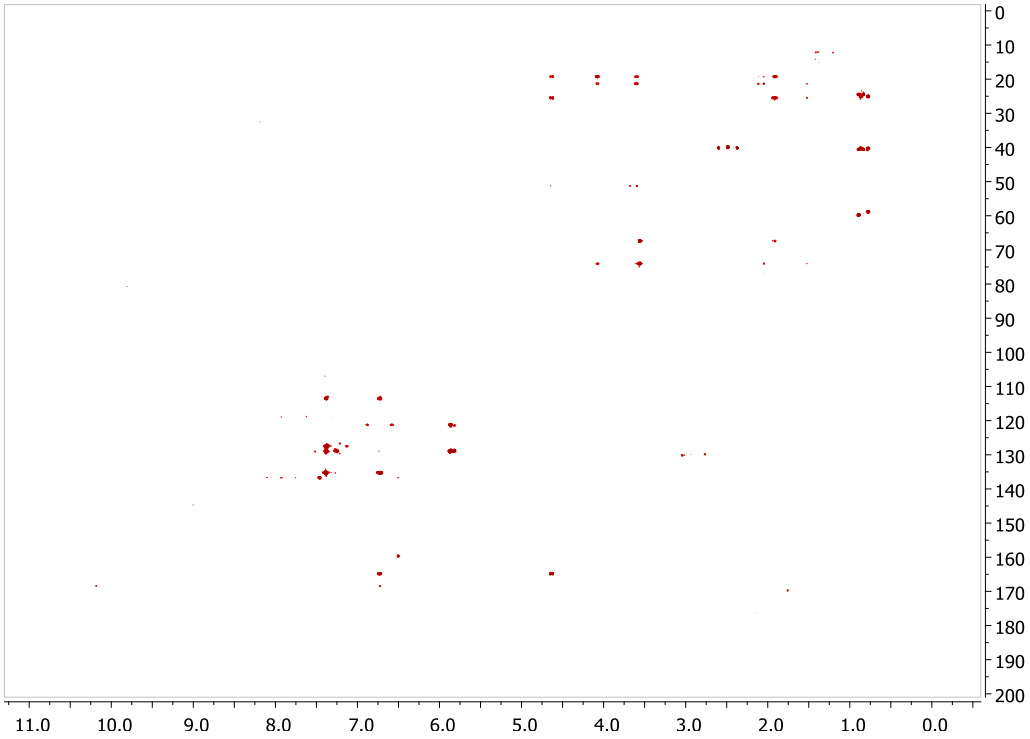

MS and UV spectra of the new compound aspiperidine oxid

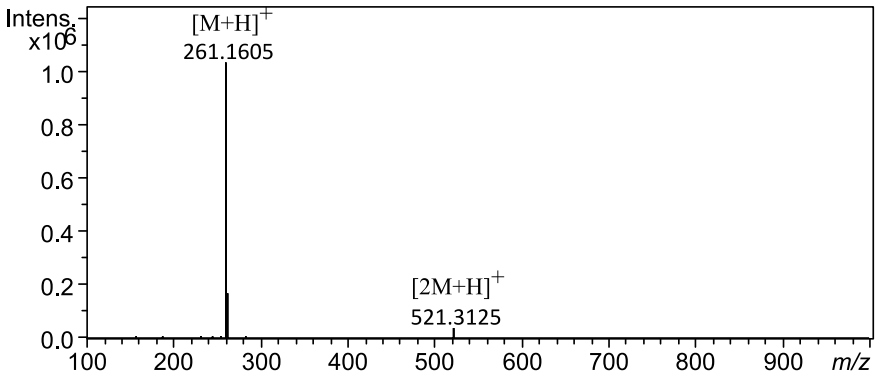
Intens.
x10^6
1.0
0.8
0.6
0.4
0.2
0.0
[M+H]+
261.1605
[2M+H]+
521.3125
100
200
300
400
500
600
700
800
900
m/z

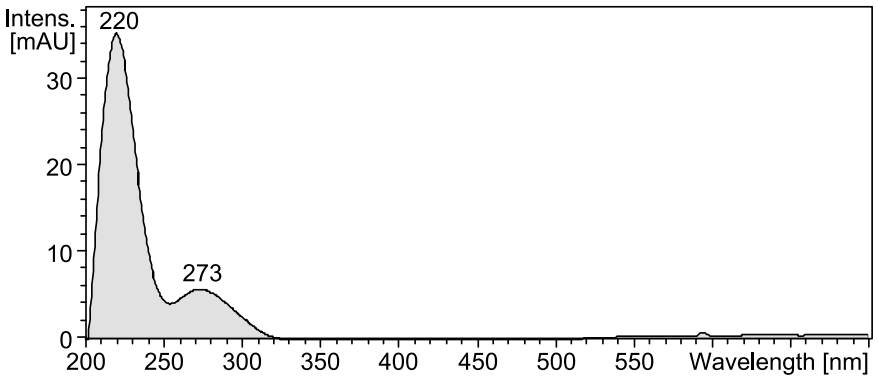
Intens.
[mAU]
30
20
10
0
220
273
200
250
300
350
400
450
500
550
Wavelength [nm]

Paper 3

"Novel metabolites from *Aspergillus homomorphus*"

Hoeck, C.; **Petersen, L.M.**; Frisvad, J.C.; Gotfredsen, C.H.; Larsen, T.O.

Intended for publication in Magnetic Resonance in Chemistry

Novel metabolites from *Aspergillus homomorphus*

Casper Hoeck[1], Lene M. Petersen[2], Thomas O. Larsen[2] and Charlotte H. Gotfredsen[1,*]

[1] Department of Chemistry, Kemitorvet B201, Technical University of Denmark, Kgs. Lyngby DK-2800, Denmark; E-Mails: casho@kemi.dtu.dk (C.H.)

[2] Chemodiversity Group, Department of Systems Biology, Søltofts Plads B221, Technical University of Denmark, Kgs. Lyngby DK-2800, Denmark; E-Mails: lmape@bio.dtu.dk (L.M.P.); : tol@bio.dtu.dk (T.O.L.)

* Author to whom correspondence should be addressed; E-Mail: chg@kemi.dtu.dk.

Keywords: NMR, ^{1}H, ^{13}C, *Aspergillus homomorphus*, Aspergilli, natural products, secondary metabolism

Introduction

Aspergilus homomorphus (*A. homomorphus*) is a lesser known fungus of the *Aspergillus* genus residing in section *Nigri* (or the black Aspergilli), which includes fungi such *A. niger* and *A. carbonarius*.[1] *A. homomorphus* was first identified by R. Steiman *et al.* from soil near the Dead Sea in Israel.[2] Black aspergilli are commonly known to cause food spoilage and are also of industrial use.[3] An example of the latter is *A. niger* which is used in large scale production of citric acid but may also produce ochratoxin A and fumonisin B_2.[4,5] *A. homomorphus* belong in a clade which, among other species, includes the industrially important *A. aculeatus*.[1]

Through the years a wide variety of secondary metabolites (SMs) have been reported from black Aspergilli.[6] The continued search for new chemical entities (NCEs) in the section is thus spurred by the ability of related species to produce quite different SMs.[7,8] *A. homomorphus* have previously been reported to produce the SMs secalonic acid D and F as well as dehydrocarolic acid.[1] Here the SM chemistry of *A. homomorphus* is explored using UHPLC-DAD-MS and NMR spectroscopy in the continued search for both NCEs and the elucidation of their biosynthetic origin.

Most of these structures share features and were identified through a proposed shared biosynthetic relationship, which was used to guide the identification and isolation of novel precursor compounds. This is proposed without any knowledge from genetics, as the genome of *A. homomorphus* has not yet been sequenced.

Results and discussions

The structures of metabolites isolated and characterized from *A. homomorphus* are shown in Figure 1. Most of these are non-ribosomal peptides (NRPs) with attached isoprene units. They are thereby related to other natural compounds such as okaramines, which are produced by other black aspergilli, e.g. *A. aculeatus* and *A. indologenus*, as well as *Penicillium simplicissimum.*[9–14] All relevant MS, UV and NMR data are found in the Supporting Information.

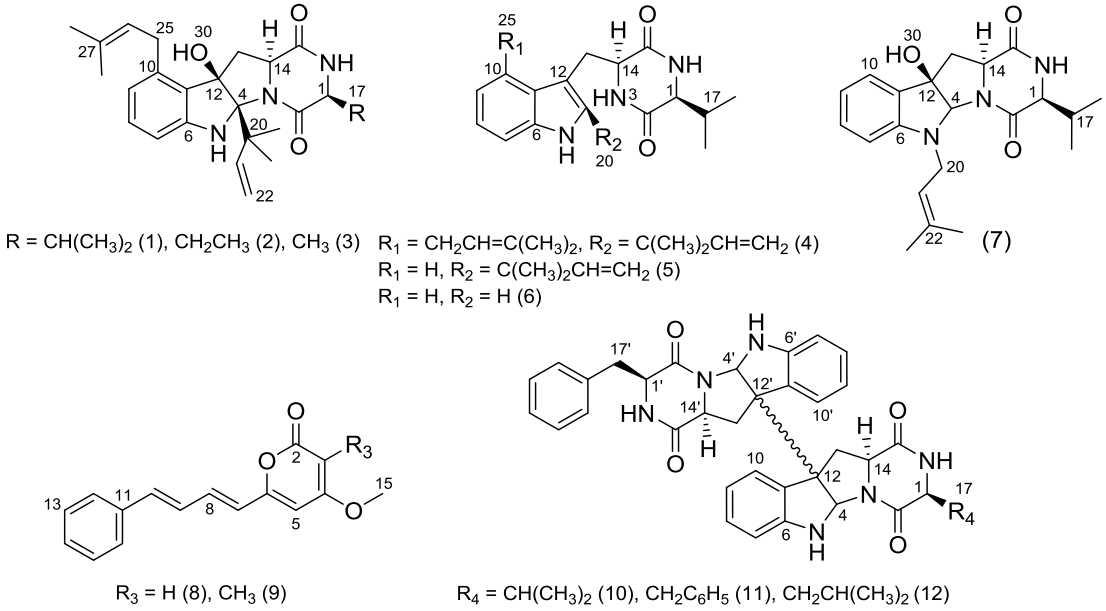

Figure 1 Novel compounds from A. homomorphus (1-6), compounds previously reported as "unnatural" (8,9) and rediscovered compounds (7,[15] 10-12). 7 is included due to biosynthetic relationship with 1, 4, 5 and 6. Data of 8-10 may be found in the Structural data section. Also secalonic acid D and F were reconfirmed to be produced via UHPLC-DAD-MS in accordance with previous publications.[1] Dehydrocarolic acid was not identified from incubation on any medium.

Novel metabolites

The common name of the novel compounds, homomorphosin, was chosen due to their fungal origin. The NMR data for the related compounds **1**-**6** is found in Table 1 and Table 2.

Table 1. ^{1}H-NMR data for the homomorphosins A-F acquired in DMSO-d_6 at 500 or 800 MHz. Chemical shifts in ppm and *J*-coupling constants in Hz.

	A (1)	**B (2)**	**C (3)**	**D (4)**	**E (5)**	**F (6)**
#	δ_H (*I*, mult, *J*)	δ_H (*I*, mult, *J*)	δ_H (*I*, mult, *J*)	δ_H (*I*, mult, *J*)	δ_H (*I*, mult, *J*)	δ_H (*I*, mult, *J*)
1	3.77 (1H,d,1.9)	3.84 (1H,t,4.5)	3.89 (1H,q,6.8)	3.57b (1H,m)	3.48 (1H,m)	4.02 (1H, m)
2						
3				6.84 (1H,s)	7.49 (1,d,3.0)	
4						5.31 (1H,s)
5	6.72 (1H,s)	6.69 (1H,1,s)	6.66 (1H,s)	10.59 (1H,s)	10.51 (1H,s)	
6						
7	6.56 (1H,d,7.8)	6.57 (1H,d,7.6)	6.57 (1H,d,7.4)	7.21 (1H,d,7.9)	7.30 (1H,d,8.0)	6.45 (1H, d, 7.9)
8	6.99 (1H,t,7.7)	6.99 (1H,t,7.7)	6.99 (1H,t,7.7)	6.92 (1H,t,7.6)	7.00 (1H,t,7.1)	7.11 (1H, t, 7.5)
9	6.47 (1H,d,7.6)	6.47 (1H,d,7.4)	6.47 (1H,d,7.4)	6.69 (1H,d,7.1)	6.92 (1H,t,7.1)	6.72 (1H, t, 7.4)
10					7.42 (1H,d,7.8)	7.17 (1H,d, 7.2)
11						
12						
13a	2.54 (1H,m)	2.53 (1H,m)	2.53 (1H,m)	3.13 (1H,dd,14.8,10.7)	2.99 (1H,dd,14.5,9.2)	1.78 (1H, m)
13b	2.62 (1H,dd,13.0,7.4)	2.62 (1H,m)	2.63 (1H,dd,11.5,7.4)	3.57a (1H,m)	3.41 (1H,dd,14.5,4.3)	2.40b (1H, m)
14	3.66 (1H,dd,11.5,7.3)	3.68 (1H,dd,11.5,7.3)	3.72 (1H,dd,11.5,7.5)	4.03 (1H,d,10.4,)	3.99 (1H,m)	4.57 (1H, dd, 11.6, 6.3)
15						
16	7.95 (1H,s)	8.05 (1H,s)	8.10 (1H,s)	8.12 (1H,s)	8.18 (1H,d,2.7)	7.98 (1H, s)
17a	2.32 (1H,septd,7.1,2.0)	1.68 (1H,m)	1.16 (3H,m)	2.13 (1H,m)	1.98 (1H,dd,12.4,6.8)	2.40a (1H, m)
17b		1.71 (1H,m)				
18	0.86 (3H,d,6.8)	0.85 (3H,t,7.3)		0.91 (3H,d,6.7)	0.89 (3H,d,6.8)	0.87 (3H, d, 6.8)
19	0.98 (3H,d,7.2)			0.99 (3H,d,7.0)	0.96 (3H,d,6.9)	1.02 (3H, d, 7.2)
20a						3.93 (1H, m)
20b						4.00 (1H, m)
21	6.27 (1H,dd,17.6,10.8)	6.27 (1H,dd,17.6,10.9)	6.26 (1H,dd,17.6,10.8)	6.16 (1H,dd,17.5,10.5)	6.15 (1H,dd,17.5,10.5)	5.08 (1H, t, 5.8)
22a	4.85 (1H,m)	4.84 (1H,d,11.1)	4.85 (1H,dd,12.8,1.7)	5.03 (1H,d,14.2)	5.00 (1H,m)	
22b	4.85 (1H,m)	4.87 (1H,d,17.6)	4.88 (1H,dd,17.9,1.7)	5.04 (1H,d,17.2)	5.03 (1H,m)	
23	1.17 (3H,s)	1.17 (3H,s)	1.17 (3H,s)	1.49 (3H,s)	1.47 (3H,s)	1.60 (3H, s)
24	1.20 (3H,s)	1.20 (3H,s)	1.19 (3H,s)	1.52 (3H,s)	1.48 (3H,s)	1.67 (3H, s)
25a	3.33 (1H,m)	3.34 (1H,m)	3.34 (1H,m)	3.67 (1H,m)		
25b	3.47 (1H,dd,15.6,7.3)	3.46 (1H,dd,15.7,6.9)	3.47 (1H,dd,15.7,7.5)	3.75 (1H,m)		

26	5.22 (1H,t,6.9)	5.23 (1,td,6.7,1.4)	5.23 (1H,t,6.9)	5.21 (1H,t,6.7)
27				
28	1.70 (3H,s)	1.70 (3H,s)	1.71 (3H,s)	1.68a (3H,s)
29	1.70 (3H,s)	1.69 (3H,s)	1.70 (3H,s)	1.68b (3H,s)
30	5.70 (1H,s)	5.69 (1H,s)	5.69 (1H,s)	

Table 2. ^{13}C-NMR data for the homomorphosins A-F acquired in DMSO-d_6 at 500 or 800 MHz. Chemical shifts in ppm.

	A (1)	**B (2)**	**C (3)**	**D (4)**	**E (5)**	**F (6)**
#	δ_C	δ_C	δ_C	δ_C	δ_C	δ_C
1	60.4	56.1	51.3	59.2	59.6	60.4
2	171.8	172.1	172.8	168.3	166.1	170.1
3						
4	90.8	90.7	90.3	141.2	140.9	88.0
5						
6	149.6	149.5	149.4	135.7	134.6	148.8
7	107.8	108.1	108.2	108.9	110.6	108.7
8	129.4	129.3	129.5	120.4	120.3	129.7
9	119.3	119.5	119.6	119.2	118.2	118.5
10	139.3	139.3	139.3	132.7	117.8	122.3
11	127.3	127.1	127.2	125.7	128.9	131.8
12	89.1	89.2	89.0	105.6	104.8	85.5
13	34.6	34.9	34.6	30.2	31.2	40.6
14	57.0	57.3	57.4	55.9	55.4	59.2
15	170.4	170.2	169.7	166.2	167.6	171.8
16						
17	26.7	21.2	14.9	31.3	31.87	27.9
18	15.8	8.7		17.4	17.4	16.5
19	18.1			18.5	18.4	18.5
20	44.6	44.4	44.5	38.9	39.4	46.0
21	145.2	145.4	145.6	146.7	146.3	119.9
22	110.6	110.6	110.7	110.7	110.8	134.8
23	24.2	24.2	24.2	27.3	27.5	26.0
24	24.5	24.6	24.6	27.8	27.5	18.4
25a	28.6	28.5	28.8	31.0		
25b	28.6	28.5	28.8	31.0		
26	123.0	123.1	123.2	123.9		
27	131.5	131.5	131.4	131.1		
28	17.7	25.2	25.3	17.7		
29	25.2	17.6	17.6	25.5		

Homomorphosin A (**1**) was isolated as a white solid. The $[M+H]^+$ of **1**, *m/z* 438.2754, corresponds to a constituent formula of $C_{26}H_{35}N_3O_3$ (theoretical *m/z* 438.2751). The 35 protons found in the 1D ^{1}H spectrum were divided among six methyl groups at δ_H 0.86 (3H, d,), 0.98 (3H, d, *J*=7.2, H_3-19), 1.17 (3H, s, H_3-19), 1.20 (3H, s, H_3-19) and 1.70 (6H, s, H_3-19/20), three aromatic protons at δ_H

6.47 (1H, d, *J*=7.6, H-9), 6.56 (1H, d, *J*=7.8, H-7) and 6.99 (1H, t, *J*=7.7, H-8), four olefinic protons at δ_H 4.85 (2H, m, H_2-22), 5.22 (1H, t, *J*=6.9, H-26) and 6.27 (1H, dd, *J*=17.6, 10.8, H-21), two methines with neighboring heteroatoms at δ_H 3.66 (1H, dd, *J*=11.5, 7.3, H-14) and 3.77 (1H, d, *J*=1.9, H-1), two diastereotopic methylenes at δ_H 2.54 (1H, m, H-13a), 2.62 (1H, dd, *J*=13.0, 7.4, H-13b), 3.33 (1H, m, H-25a) and 3.47 (1H, dd, *J*=15.6,7.3, H-25b), a methine at δ_H 2.32 (1H, septd, *J*=7.1, 2.0, H-17) along with exchangeable protons at δ_H 5.70 (1H, s, H-30), 6.72 (1H, s, H-5) and 7.95 (1H, s, H-16). All protons could be coupled to their respective carbons (as in Table 1) through gHSQC correlations with the exception of the exchangeable protons. The diastereotopic protons and the resonance at 1.70 ppm could thus be elucidated. Five spin systems were established from the DQF-COSY experiment; an aromatic, an olefinic and three aliphatic, and the spin systems and quaternary carbons were joined through gHMBC correlations as illustrated in Figure 2a.

The relative stereochemistry of **1** is suggested from a network of NOEs obtained from NOESY and ROESY experiments with the key NOEs being H-1/H-14. This NOE established that the amino acids share handedness. NOEs H-13b/H-14, H-13a/H-30, H-13a/H_3-23/24 and H-21/H-30 were used to solve the remaining relative stereochemistry. The couplings constants of H-13a/b and H-14 fit to the proposed diastereotopicity of the methylene group with a smaller *J*-coupling originating from H-13b/H-14 in comparison to H-13a/H-14 which shows a large J-coupling constant. Figure 2b includes the important NOEs, while c shows the 3D structure with the best fit to the correlating distances obtained by the isolated spin pair approximations (ISPA). The absolute configuration was solved by hydrolyses and reaction with Marfey's reagent which suggested an L-configuration of valine.[16] The ^3J-coupling of H-1 and H-13 is 2.0 Hz which suggests a restriction in the rotation of the isopropane group attached to C-1.

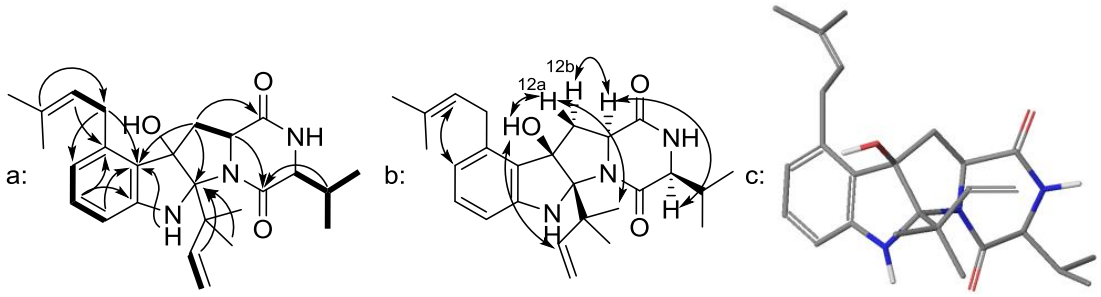

Figure 2 a: COSY spin systems (-) and chosen HMBC correlations (→) of 1. **b:** Chosen NOEs (→) of 1**. c:** The 3D structure of 1 which fit the NOESY data the best.

Biosynthesis of the homomorphosins

The isolation of **1** led to a hypothetical biosynthesis proposed in Figure 3, which in turn led to the discovery of more NRPs. This methodology of discovering new metabolites was used, as **1** was by far the main metabolite produced on the used media. The biosynthesis was proposed utilizing known reactions from organic and biochemical synthesis, starting from L-valine and L-tryptophan (not shown in figure). The mechanisms needed to obtain the compounds are two *C*-prenylations and an epoxidation and subsequent intramolecular ring-closure. Both mechanisms have been previously described or suggested in the biosynthesis of natural products. [17–26]

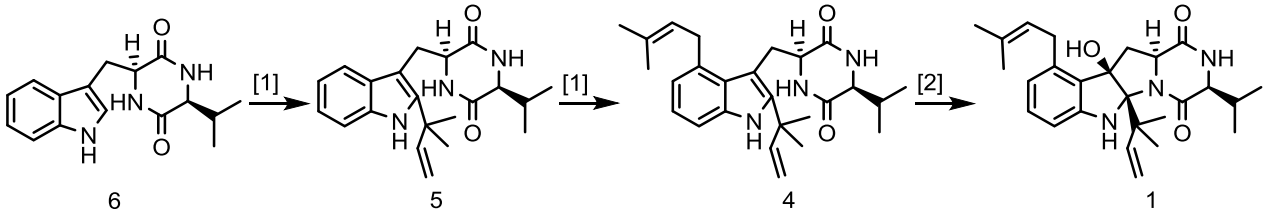

Figure 3 The suggested biosynthesis of (1). Compound 6 is proposed to be made by the cyclization of L-valine and L-tryptophan (not shown). [1] *C*-prenylation, [2] epoxidation/ring closure.

A dereplication, utilizing UHPLC-DAD-MS (chromatograms in Figure 4), was then conducted for proposed stable intermediates, which were all isolated and structure elucidated.

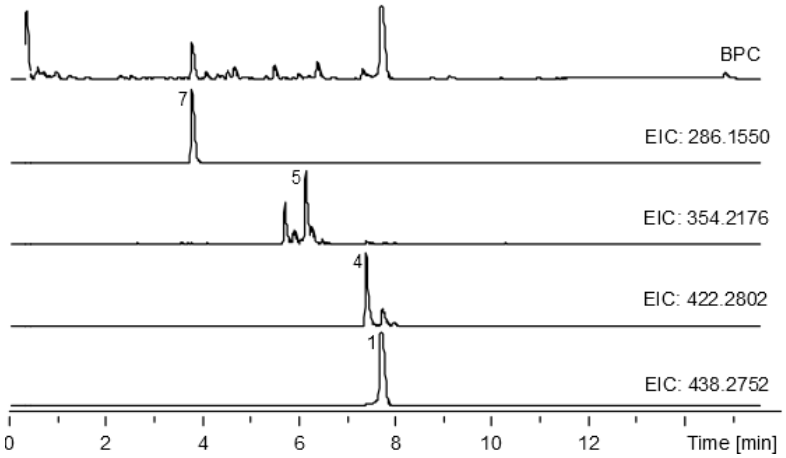

Figure 4 Chromatogram of extract of *A. homomorphus* (top) and extracted ion chromatograms (EICs) of the *m/z* values for suggested compounds in the biosynthesis of (1). Chromatograms are scaled.

Homomorphosins D (**4**), E (**5**) and L-valyl-L-tryptophan anhydride (**7**) were isolated as white solids. The NMR data resembles that of **1** where structural features are shared. The homomorphosins are novel diketopiperazines. The data of the rediscovered **7** corresponds to that found in the literature.[15] The NMR data and UV^{max} suggested that these compounds contain an

indole ring which differentiates them from **1**.[27] The compounds **4**, **5** and **7** are suggested to share biosynthetic pathway though the genome have yet to be sequenced.

Due to the successful identification of precursors for **1**, a new dereplication to identify structural analogues of **1** was conducted, with tryptophan coupled to other amino acids, which revealed compounds **2** and **3**.

Homomorphosins B (**2**) and C (**3**) were both white solids. The NMR data corresponds to that of **1**, except that valine is exchanged with alanine (**3**) or the "unnatural" amino acid 2-aminobutyrate (**2**). The latter amino acid is not commonly found in natural diketopiperazines of amino acids, and though some have been published, these were functionalized at the α-position.[28–30] The ^{3}J-coupling of H-1 and H-16 increases as the size of the substituent attached to C-1 decreases which may support the suggested rotational restriction for **1**.

Homomorphosin F (**6**) was isolated as a white solid (data found in supporting info). The compound differs from the other homomophosins, and compound isolated from *A. homomorphus* in general, as it is *N*-prenylated. As for **1**, **2** and **3** the UV^{max} of **6** showed a reduction of the indole ring. The resonance from the alcohol proton did not appear in the NMR spectra, probably due to a high water content of the sample. The structure was thus suggested due to the constituent formula obtained from HRMS, the chemical shift of C-11 and the UV spectrum. The respective UV-spectra are compared in Supporting Information.

The absolute stereochemistry of **2-6** is believed to be the same as that of **1** due to a similar relative stereochemistry in between the compounds, and the possible involvement of **4** and **5** in the biosynthesis of **1**. The absolute stereochemistry of **7** was established by Marfey's to be that of **1**. No NOE between H-1 and H-13 was found in the NOESY spectra of **3**, which might suggest another relative configuration. The reason for this could also be due to the sparse amount of compound, as the sign of the optical rotation is equal to **1** and **2**.

Bioactivity

The bioactivity of compounds similar to the homomorphosins against bacteria, fungi and protozoa has been tested and bioactivity have been reported against e.g. *S. aureus*.[31,32] Homomorphosin A was tested against *C. albicans* and chronic lymphatic leukaemia but no activity was observed.

Conclusion

A large scale cultivation of *A. homomorphus* led to the discovery of six novel NRPs based metabolites with a diketopiperazines skeleton. They were all characterized using UHPLC-DAD-MS and NMR spectroscopy. Based on NOESY and ROESY NMR data, *J*-coupling constants and structural simulations the relative stereochemistry and a possible 3D structure for the compounds are proposed. For compound 1 the absolute stereochemistry relations were obtained using Marfey's analysis. It is speculated that all the new compounds have a shared biosynthetic origin. The proposed biosynthesis were used to identify new metabolites and gained credibility by the isolated structures.

Experimental

Fungal growth, extraction and the isolation of compounds.

A. homomorphus (IBT 21893) was inoculated on different media to determine the preferred growth media and time in order to get as diverse a chemical profile as possible. The used media were Yeast Sucrose Agar (YES), Czapek yeast extract agar (CYA), Malt Extract Agar (MEA), Oatmeal agar (OAT) and Creatine sucrose agar (CREA) for 2, 5, 7 and 9 days.[33] The major metabolites from most growth media were homomorphosin A (**1**) and a 4-methoxy-α-pyrone (**9**) which could originate from polyketide and Shikimi pathways.[34] The chosen media and time were YES for 7 days.

A. homomorphus was inoculated as three-point stabs on agar plates and incubated in the dark at 30 °C for 7 days. The used media were YES for the NRPs (200 plates) and MEA for the other isolated metabolites (50 plates). The fungi were harvested and extracted twice with EtOAc (1 % FA) (once overnight), m(YES) = 7.8 g, m(MEA) = 217.1 mg. The combined extract was dissolved in 9:1 MeOH:H_2O and washed with heptane. Water was added to give 1:1 MeOH/H_2O and compounds were extracted with DCM followed by concentration *in vacuo*, m(YES) = 4.90 g, m(MEA) = 36.3 mg. The DCM phase (YES) was absorbed onto reverse phase column material and fractioned by an Isolera One flash chromatography system by Biotage with auto-fractionation and a 120 g Biotage Snap KP-C18-HS column. The column volume used 132 mL and fractions of 115 mL (max) were collected. The gradient ranged from 30 to 100 % MeCN/H_2O with a flow rate of 40 mL/min over 65 min.

The fractions (see table below) which showed possible targets after UHPLC-DAD-MS analysis were further purified on a semi-preparative HPLC; the Waters 600 Controller coupled to a Waters

996 Photodiode Array Detector with a flow rate of 5 mL/min. The columns used were Luna II C18, 5 µm, 250 × 10 mm by Phenomenex and Gemini C6-Phenyl, 5 µm, 250 × 10 mm by Phenomenex.

	Isolera fraction %MeCN/H_2O	m [mg]	Waters run %MeCN/H_2O Time [min]	Waters elution time [min] %MeCN/H_2O	Yield [mg]
1	15/70-74	180.7	-	-	180.7
2	13/64-68	72.0	Iso/65/15	7.3/65	2.7
3	11/56-60	14.6	Grad/40-70/20	14.5/63	0.9
4	13/64-68	72.0	Iso/65/15	7.7/65	3.6
5	8/45-49	36.9	Iso/45/15	7.5/45	1.7
6	4/30-34	72.6	Grad/30-40/15	5.3/34	8.1
7	10/52-56	27.0	Iso/40/20	15.5/40	1.9
8	-	36.3	Iso/55/20	13.4/55	1.7
9	-	36.3	Iso/55/20	15.8/55	2.5
10	8/45-49	36.9	Iso/45/15	6.35/45	3.5

NMR

All NMR spectra were acquired using standard pulse sequences on a Unity Inova 500 by Varian or on a Bruker Avance 800 spectrometer of the Danish Instrument Center for NMR Spectroscopy of Biological Macromolecules at 298 °C. The deuterated solvent used for all compounds was DMSO-d_6 which was used as internal standard (δ_H = 2.49 ppm, δ_C = 39.5 ppm). Typical acquisition conditions were as follows (conditions for homomorphosin A). 1D ^{1}H: Spectrometer frequency (sf) = 499.87 MHz, Spectral width (sw) = 5000.0 Hz, Fourier transform size (si) = 20480, acquisition time (aq) = 2.05 s, 90 ° pulse width (pw) = 7.0 µs, line broadening (lb) = 0.3, relaxation delay (rd) = 2 s, number of scans (ns) = 32, number of dummy scans (ds) = 8. gHSQC: sf = 499.87 MHz, sw(^{1}H) = 5000.0 Hz, sw(^{13}C) = 30007.7 Hz, si = 2048, ni = 512, aq = 0.20 s, pw = 6.9 µs, rd = 1.5 s, ns = 8, ds = 64. DQF-COSY: sf = 499.87 MHz, sw = 5000.0 Hz, si = 2048, ni = 1024, aq = 0.20 s, pw = 6.9 µs, rd = 1.5 s, ns = 8, ds = 16. gHMBC: sf = 499.87 MHz, sw(^{1}H) = 5000.0 Hz, sw(^{13}C) = 34999.7 Hz, si = 2048, ni = 512, aq = 0.20 s, pw = 6.9 µs, rd = 1.5 s, ns = 8, ds = 64. NOESY/ROESY: sf = 499.87 MHz, sw = 5000.0 Hz, si = 2048, ni = 512, aq = 0.20 s, pw = 7 µs, rd = 2 s, ns = 8, ds = 16.

Structural parameters from NMR

To check the stereochemical assignment of homomorphosin A the isolated spin-pair approximation (ISPA) method, with increased linear range as suggested by Macura *et al.*, was applied.[35] The mixing time was 150 ms which was found to be within the linear range (50, 100, 150, 200 ms was used). The volumes from the peaks in the ROESY spectra were extracted by integration in Topspin3.1. For the calculation of *J*-couplings from dihedral angles the Karplus equation for amino acids was used.[36,37] Experimental couplings constants were measured in 1D ^{1}H or DQF-COSY spectra. Structures were generated using Macromodel in the Maestro (Schrödinger Release 2013-2: Maestro, version 9.5, Schrödinger, LLC, New York, NY, 2013). A conformational search was conducted in implicit DMSO, treated as a constant dielectric constant of 46. The mixed mode option was used with 10,000 steps and PRCG as minimization method using the force field MMFFs. Structures within 25 kJ of the found minimum was considered. From the conformational search 364 conformations was found. The structure which fitted the data the best was found by comparing back-calculated distances and *J*-couplings with the found values. Averaging of NMR parameters was done iteratively over 10,000 steps were each step included the structure which would give the best average fit to the data. NOE to *J*-couplings were weighted 10:1. Distances was averaged according to $r_{ave} = \langle r_i^{-6} \rangle^{1/6}$. The script was written in-house in Matlab (R2013b, 8.2.0.701, The MathWorks, Inc., Natick, MA).

UHPLC-DAD-MS

UHPLC-DAD-MS data was acquired by the Maxis 3G UHR-QTOF-MS by Bruker Daltonics (Bremen, Germany) with an electrospray ionization (ESI) source combined with an UltiMate 3000 Rapid Separation LC by system Thermo Scientific Dionex (Sunnyvale, CA, USA). The column used was a Kinetex C18, 100x2.1 mm, 2.6 μm, by Phenomenex (Torrance, CA, USA) maintained at 40 °C. Solvents were acetonitrile (ACN) and H_2O (buffered with 20 mM FA) and a linear gradient from 10 to 100 % (v/v) ACN over 10 min with a flow rate was 0.4 mL/min was used. MS was run in positive mode (ESI+) with a mass range of m/z 100–1000. Sodium formate was used as internal standard for mass calibration. UV/VIS spectra from the DAD were collected at wavelengths from 200-700 nm.

Marfey's reagent

Stereoisometry of the amino acid valine was elucidated using Marfey's method.[16] 100 μg of **1** and **7** was hydrolyzed with 200 μL of 6 M HCl at 110 °C for 20 h. To the hydrolysis product and vials

with 2.5 μmol of standard D- and L-amino acids were added 50 μL of water, 20 μL of 1 M $NaHCO_3$ solution, and 100 μL of 1 % 1-fluoro-2-4-dinitrophenyl-5-L-alanine amide (FDAA) in acetone and left at 40 °C for 1 h to react. The reaction mixture was removed from the heat and neutralized with 10 μL of 2 M HCl, and the solution was diluted with 820 μL of MeOH. See supporting information.

Structural data

Homomorphosin A (1): HRMS: *m/z* = 438.2754. $[M+H]^+$, calculated for $[C_{26}H_{35}N_3O_3+H]^+$: *m/z* = 438.2751. Adducts: 460 $[M+Na]^+$. $[\alpha]_{589.3}^{20\,C}$ = -1.37°.

Homomorphosin B (2): HRMS: *m/z* = 422.2803. $[M+H]^+$, calculated for $[C_{26}H_{35}N_3O_2+H]^+$: *m/z* = 422.2802. Adducts: 444 $[M+Na]^+$. $[\alpha]_{589.3}^{20\,C}$ = -0.14°.

Homomorphosin C (3): HRMS: *m/z* = 354.2181. $[M+H]^+$, calculated for $[C_{21}H_{27}N_3O_2+H]^+$: *m/z* = 354.2176. Adducts: 376 $[M+Na]^+$, 707 $[2M+H]^+$, 729 $[2M+Na]^+$. $[\alpha]_{589.3}^{20\,C}$ = -0.15°.

Homomorphosin D (4): HRMS: *m/z* = 424.2599. $[M+H]^+$, calculated for $[C_{25}H_{33}N_3O_3+H]^+$: *m/z* = 424.2595. Adducts: 446 $[M+Na]^+$, 869 $[2M+Na]^+$. $[\alpha]_{589.3}^{20\,C}$ = -0.55°.

Homomorphosin E (5): HRMS: *m/z* = 410.2446. $[M+H]^+$, calculated for $[C_{24}H_{31}N_3O_3+H]^+$: *m/z* = 410.2438. Adducts: 432 $[M+Na]^+$, 841 $[2M+Na]^+$. $[\alpha]_{589.3}^{20\,C}$ = -0.66°.

Homomorphosin F (6): HRMS: *m/z* = 370.2128. $[M+H]^+$, calculated for $[C_{20}H_{19}N_3O_2+H]^+$: *m/z* = 370.2125. Adducts: none. $[\alpha]_{589.3}^{20\,C}$ = -0.01°.

L-valyl-L-tryptophan anhydride (7): HRMS: *m/z* = 286.1548. $[M+H]^+$, calculated for $[C_{16}H_{19}N_3O_2+H]^+$: *m/z* = 286.1550. Adducts: 308 $[M+Na]^+$, 571 $[2M+H]^+$, 593 $[2M+Na]^+$. $[\alpha]_{589.3}^{20\,C}$ = -0.14°.

^{1}H NMR (499.9 MHz, DMSO-d_6, 25 °C, 2.50 ppm): δ 10.82 (s, 1H), 7.95 (s, 1H), 7.85 (s, 1H), 7.58 (d, *J* = 7.8 Hz, 1H), 7.27 (d, *J* = 8.1 Hz, 1H), 7.06 (d, *J* = 2.1 Hz, 1H), 7.00 (t, *J* = 7.5 Hz, 1H), 6.92 (t, *J* = 7.4 Hz, 1H), 4.12 (t, *J* = 4.4 Hz, 1H), 3.47 (dd, *J* = 3.6, 2.1, 1.6 Hz, 1H), 3.19 (dd, *J* = 14.4, 5.0 Hz, 1H), 3.06 (dd, *J* = 14.4, 4.5 Hz, 1H), 1.63 (sept-d, *J* = 6.9, 4.0 Hz, 1H), 0.59 (d, *J* = 7.0 Hz, 1H), 0.17 (d, *J* = 6.8 Hz, 1H).

^{13}C NMR (125.7 MHz, DMSO-d_6, 25 °C, 39.5 ppm): δ 166.8, 166.2, 135.5, 127.8, 124.2, 120.4, 118.6, 118.0, 110.8, 108.5, 59, 54.9, 30.7, 28.4, 28.4, 18, 15.8.

4-Methoxy-6-(4-phenyl-1,3-butadienyl)-2*H*-pyran-2-one (8): HRMS: *m/z* = 255.1018. $[M+H]^+$, calculated for $[C_{16}H_{14}O_3+H]^+$: *m/z* = 255.1016. Adducts: 277 $[M+Na]^+$, 531 $[2M+Na]^+$.

^{1}H NMR (499.9 MHz, DMSO-d_6, 25 °C, 2.50 ppm): δ 7.55 (d, J = 7.4 Hz, 2H), 7.38 (t, J = 7.5 Hz, 2H), 7.30 (t, J = 7.3 Hz, 1H), 7.13 (mult, 2H), 7.01 (d, J = 14.8 Hz, 1H), 6.44 (d, J = 14.6 Hz, 1H), 6.31 (d, J = 2.1 Hz, 1H), 5.63 (d, J = 2.1 Hz, 1H), 3.83 (s, 3H).

^{13}C NMR (125.7 MHz, DMSO-d_6, 25 °C, 39.5 ppm): 170.7, 162.3, 157.7, 137.4, 136.1, 134.0, 128.5, 128.3, 127.2, 126.6, 122.5, 100.8, 88.3, 56.1

3-Methyl-4-Methoxy-6-(4-phenyl-1,3-butadienyl)-2*H*-pyran-2-one (9): HRMS: *m/z* = 269.1171. $[M+H]^+$, calculated for $[C_{17}H_{16}O_3+H]^+$: *m/z* = 269.1172. Adducts: 291 $[M+Na]^+$, 559 $[2M+Na]^+$.

^{1}H NMR (499.9 MHz, DMSO-d_6, 25 °C, 2.50 ppm): δ 7.56 (d, J = 7.4 Hz, 2H), 7.38 (t, J = 7.6 Hz, 2H), 7.30 (t, J = 7.3 Hz, 1H), 7.15 (mult, 2H), 7.00 (d, J = 14.6 Hz, 1H), 6.72 (s, 1H), 6.46 (d, J = 14.5 Hz, 1H), 3.92 (s, 3H), 1.82 (s, 3H).

^{13}C NMR (125.7 MHz, DMSO-d_6, 25 °C, 39.5 ppm): 165.9 , 163.3, 156.7, 137.4, 136.4, 134.5, 128.8, 128.5, 127.4, 126.9, 123.0, 100.8, 96.9, 56.6, 8.8

Q-20547-E (10): HRMS: *m/z* = 645.2821. $[M+H]^+$, calculated for $[C_{37}H_{36}N_6O_5+H]^+$: *m/z* = 645.2820. Adducts: 667 $[M+Na]^+$. $[\alpha]_{589.3}^{20\,C}$ = -0.86°.

^{1}H NMR (499.9 MHz, DMSO-d_6, 25 °C, 2.50 ppm): 8.91 (1H, s), 8.05 (1H, s), 7.96 (1H, s), 7.73 (1H, m), 7.54 (1H, m), 7.27 (1H, m), 7.24b (1H, m), 7.24a (1H, m), 7.21 (1H, m), 7.18 (1H, m), 7.15b (1H, m), 7.15a (1H, m), 7.07 (1H, m), 6.93 (1H, m), 6.70 (1H, s), 6.50 (1H, m), 6.47 (1H, m), 5.97 (1H, s), 5.09 (1H, s), 4.35 (1H, t, 4.6), 3.94 (1H, s), 3.80 (1H, m), 3.78 (1H, m), 3.08 (1H, m), 2.97 (1H, m), 2.73 (1H, m), 2.67 (1H, m), 2.32 (1H, m), 2.25 (1H, m), 2.03 (1H, t, 12.0), 0.92 (3H, d, 6.0), 0.73 (3H, d, 6.4).

^{13}C NMR (125.7 MHz, DMSO-d_6, 25 °C, 39.5 ppm): 167.8 (2C), 165.8, 164.7, 161.9, 150.6, 141.0, 137.0, 131.2, 130.4, 129.3, 129.1, 129.0, 128, 126.6, 126.3 (2C), 124.7, 124.5, 123.9, 117.6, 115.6, 108.7, 76.7, 76.6, 59.3, 58.5, 57.7, 57.4, 57.2, 55.1, 36.3, 35.9, 35, 28.7, 18, 16.3

Acknowledgement

We thank the Danish Instrument Center for NMR Spectroscopy of Biological Macromolecules for 800 MHz NMR time.

References

(1) Samson, R. A.; Noonim, P.; Meijer, M.; Houbraken, J.; Frisvad, J. C.; Varga, J. *Stud. Mycol.* **2007**, *59*, 129–145.

(2) Steiman, R.; Guiraud, P.; Sage, L.; Seigle-Murandi, F. *Syst. Appl. Microbiol.* **1995**, *17*, 620–624.

(3) Hendrickx, M.; Beguin, H.; Detandt, M. *Mycoses* **2012**, *55*, 148–155.

(4) Schuster, E.; Dunn-Coleman, N.; Frisvad, J. C.; Van Dijck, P. W. M. *Appl. Microbiol. Biotechnol.* **2002**, *59*, 426–435.

(5) Frisvad, J. C.; Larsen, T. O.; Thrane, U.; Meijer, M.; Varga, J.; Samson, R. a; Nielsen, K. F. *PLoS One* **2011**, *6*, e23496.

(6) Nielsen, K. F.; Mogensen, J. M.; Johansen, M.; Larsen, T. O.; Frisvad, J. C. *Anal. Bioanal. Chem.* **2009**, *395*, 1225–1242.

(7) Keller, N. P.; Turner, G.; Bennett, J. W. *Nat. Rev. Microbiol.* **2005**, *3*, 937–947.

(8) Newman, D. J.; Cragg, G. M. *J. Nat. Prod.* **2012**, *75*, 311–335.

(9) Petersen, L. M.; Hoeck, C.; Frisvad, J. C.; Gotfredsen, C. H.; Larsen, T. O. *Molecules* **2014**, *19*, 10898–10921.

(10) Shiono, Y.; Akiyama, K.; Hayashi, H. *Biosci. Biotechnol. Biochem.* **2000**, *64*, 103–110.

(11) Hayashi, H.; Asabu, Y.; Murao, S.; Arai, M. *Biosci. Biotechnol. Biochem.* **1995**, *59*, 246–250.

(12) Murao, S.; Hayashi, H.; Takiuchi, K.; Arai, M. *Agric. Biol. Chem.* **1988**, *52*, 886–886.

(13) Hayashi, H.; Takiuchi, K.; Murao, S.; Arai, M. *Agric. Biol. Chem.* **1988**, *52*, 2131–2133.

(14) Varga, J.; Frisvad, J. C.; Kocsubé, S.; Brankovics, B.; Tóth, B.; Szigeti, G.; Samson, R. A. *Stud. Mycol.* **2011**, *69*, 1–17.

(15) Pedras, M. S. C.; Smith, K. C.; Taylor, J. L. *Phytochemistry* **1998**, *49*, 1575–1577.

(16) Marfey, P. *Carlsberg Res. Commun.* **1984**, *49*, 591–596.

(17) Andersen, M. R.; Nielsen, J. B.; Klitgaard, A.; Petersen, L. M.; Zachariasen, M.; Hansen, T. J.; Blicher, L. H.; Gotfredsen, C. H.; Larsen, T. O.; Nielsen, K. F.; Mortensen, U. H. *Proc. Natl. Acad. Sci. U. S. A.* **2013**, *110*, E99–107.

(18) Metzger, U.; Schall, C.; Zocher, G.; Unsöld, I.; Stec, E.; Li, S.-M.; Heide, L.; Stehle, T. *Proc. Natl. Acad. Sci. U. S. A.* **2009**, *106*, 14309–14314.

(19) Guo, J.; Tan, J.; Wang, Y.; Wu, H.; Zhang, C.; Niu, X. **2011**, 28–31.

(20) Zhou, L.; Zhu, T.; Cai, S.; Gu, Q.; Li, D. **2010**, *93*, 1758–1763.

(21) Li, X.; Li, T.; Dang, H.; Wang, B. **2008**, *91*, 1888–1893.

(22) Dewick, P. M. *Medicinal Natural Products: A Biosynthetic Approach*; 3rd ed.; John Wiley & Sons, Ltd, 2009.

(23) Asai, T.; Chung, Y.-M.; Sakurai, H.; Ozeki, T.; Chang, F.-R.; Wu, Y.-C.; Yamashita, K.; Oshima, Y. *Tetrahedron* **2012**, *68*, 5817–5823.

(24) Hollenhorst, M. A.; Bumpus, S. B.; Matthews, M. L.; Bollinger, J. M.; Kelleher, N. L.; Walsh, C. T.; Pennsyl, V.; States, U. *J. Am. Chem. Soc.* **2010**, *132*, 15773–15781.

(25) Lorenz, N.; Olsovská, J.; Sulc, M.; Tudzynski, P. *Appl. Environ. Microbiol.* **2010**, *76*, 1822–1830.

(26) Udagawa, T.; Yuan, J.; Panigrahy, D.; Chang, Y. H.; Shah, J.; D'Amato, R. J. *J. Pharmacol. Exp. Ther.* **2000**, *294*, 421–427.

(27) Carić, D.; Tomisić, V.; Kveder, M.; Galić, N.; Pifat, G.; Magnus, V.; Soskić, M. *Biophys. Chem.* **2004**, *111*, 247–257.

(28) Figueroa, M.; Graf, T. N.; Ayers, S.; Adcock, A. F.; Kroll, D. J.; Yang, J.; Swanson, S. M.; Munoz-Acuna, U.; Carcache de Blanco, E. J.; Agrawal, R.; Wani, M. C.; Darveaux, B. a; Pearce, C. J.; Oberlies, N. H. *J. Antibiot. (Tokyo).* **2012**, *65*, 559–564.

(29) Furtado, A. F.; McAllister, T. A.; Cheng, K. J.; Milligan, L. P. *Can. J. Microbiol.* **1994**, *40*, 393–396.

(30) Zhu, L.; Tao, R.; Wang, Y.; Jiang, Y. **2011**, 903–910.

(31) Gao, J.; Radwan, M. M.; León, F.; Wang, X.; Jacob, M. R.; Tekwani, B. L.; Khan, S. I.; Lupien, S.; Hill, R. a; Dugan, F. M.; Cutler, H. G.; Cutler, S. J. *Med. Chem. Res.* **2012**, *21*, 3080–3086.

(32) Du, F.-Y.; Li, X.-M.; Li, C.-S.; Shang, Z.; Wang, B.-G. *Bioorg. Med. Chem. Lett.* **2012**, *22*, 4650–4653.

(33) Samson, R.A., Houbraken, J., Thrane, U., Frisvad, J.C., and Andersen, B. *Food and Indoor Fungi. CBS Laboratory Manual Series 2.*; Utrecht, The Netherlands: CBS KNAW Fungal Biodiversity Centre, 2010.

(34) Lee, I.-K.; Yun, B.-S. *J. Antibiot. (Tokyo).* **2011**, *64*, 349–359.

(35) Macura, S.; Farmer II, B. T.; Brown, L. R. **1986**, *499*, 493–499.

(36) Karplus, S.; Karplus, M. *Proc. Natl. Acad. Sci. U. S. A.* **1972**, *69*, 3204–3206.

(37) Pardi, A.; Billeter, M.; Wüthrich, K. *J. Mol. Biol.* **1984**, *180*, 741–751.

Supporting information

Spectra of homomorphosin A

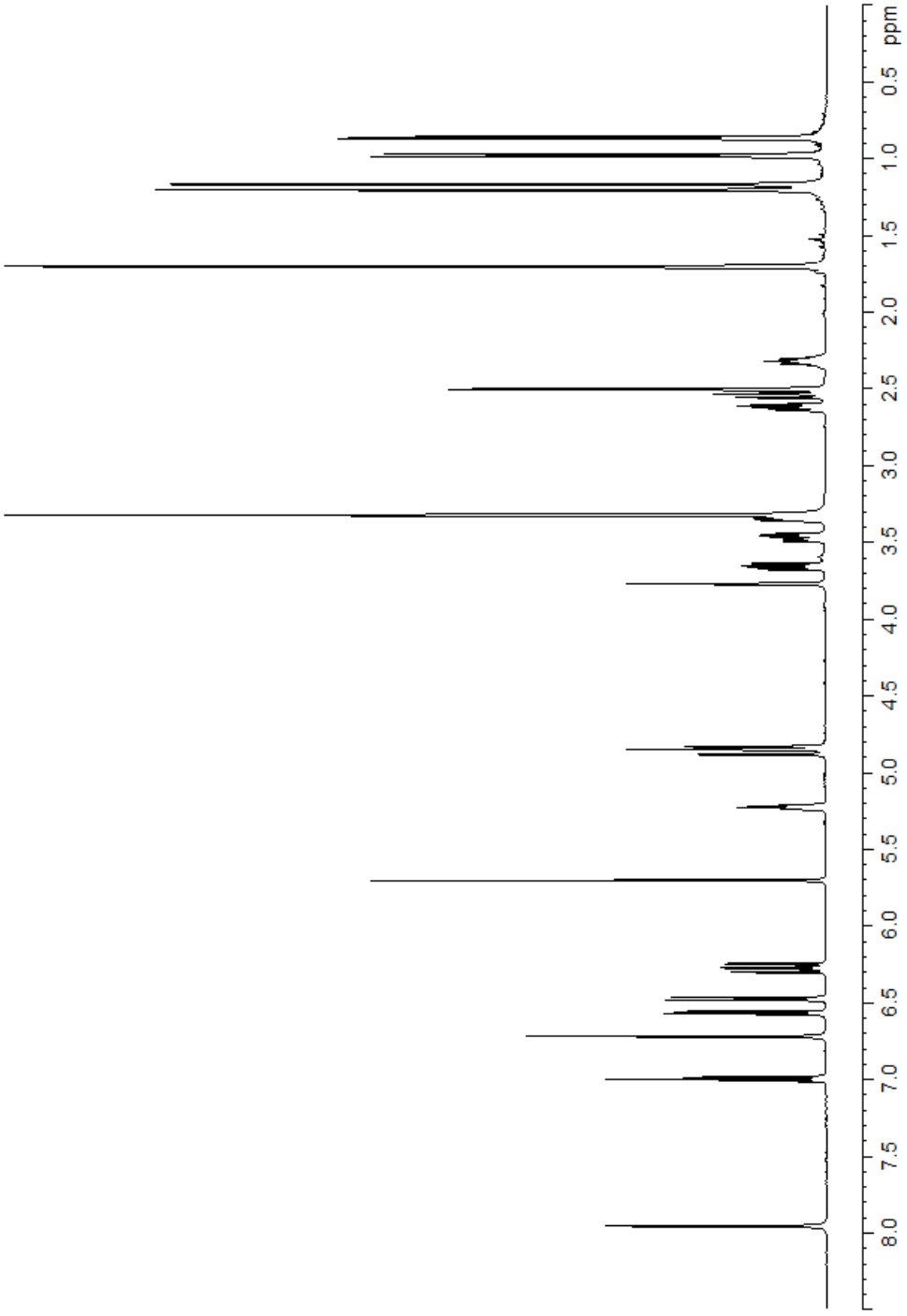

DQF-COSY

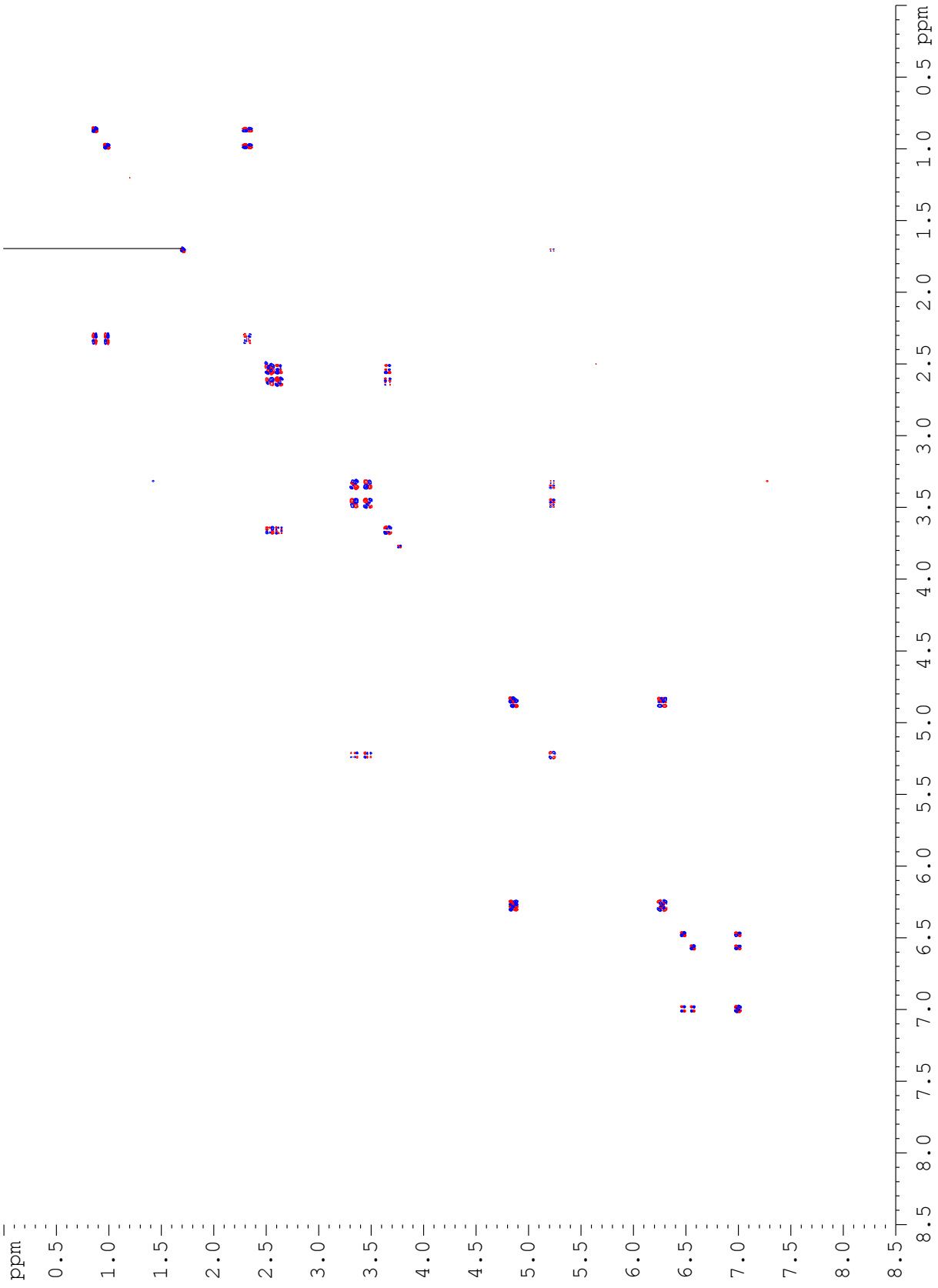

gHSQC

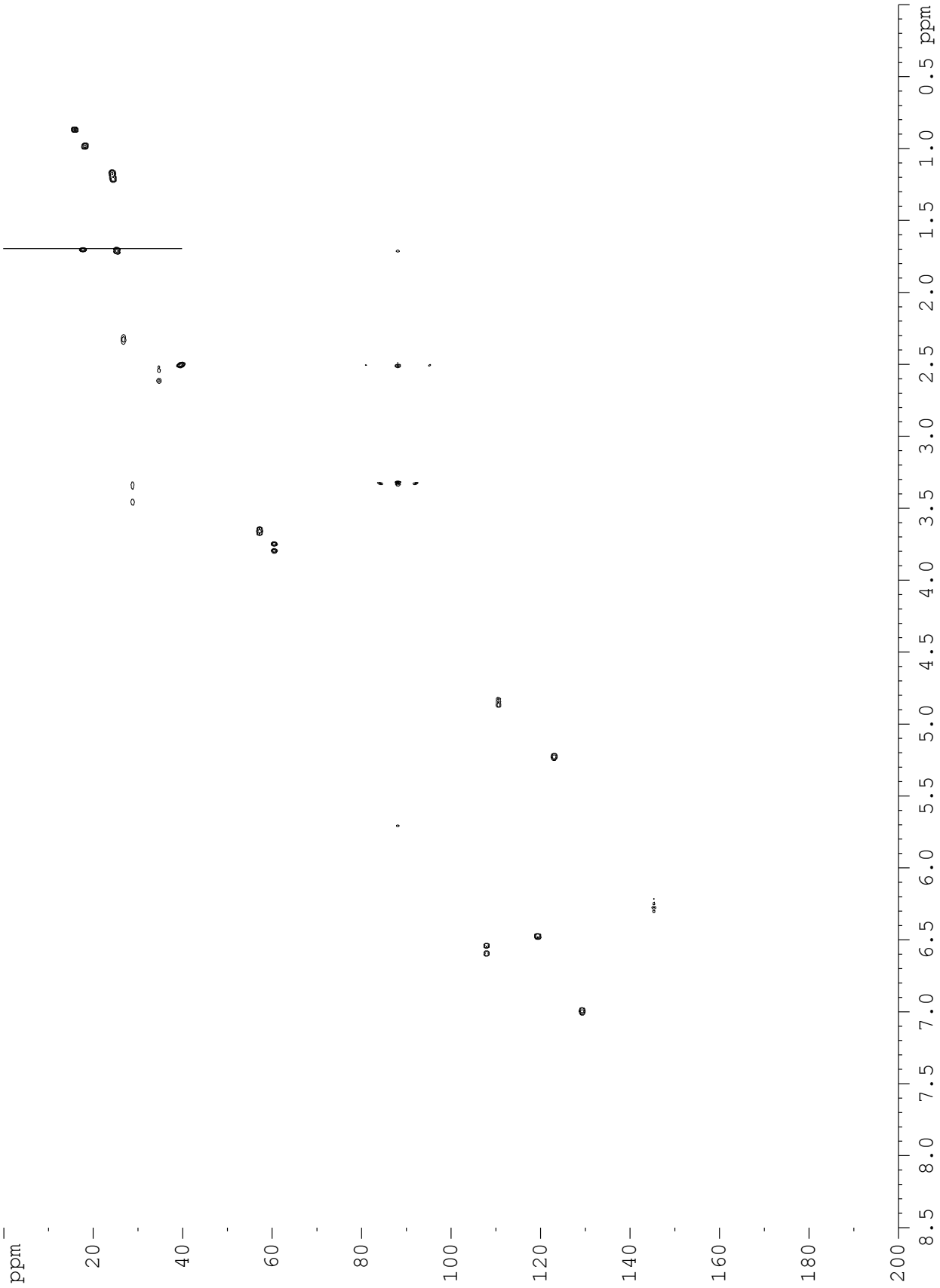
ppm
20
40
60
80
100
120
140
160
180
200
8.5
8.0
7.5
7.0
6.5
6.0
5.5
5.0
4.5
4.0
3.5
3.0
2.5
2.0
1.5
1.0
0.5
ppm

gHMBC

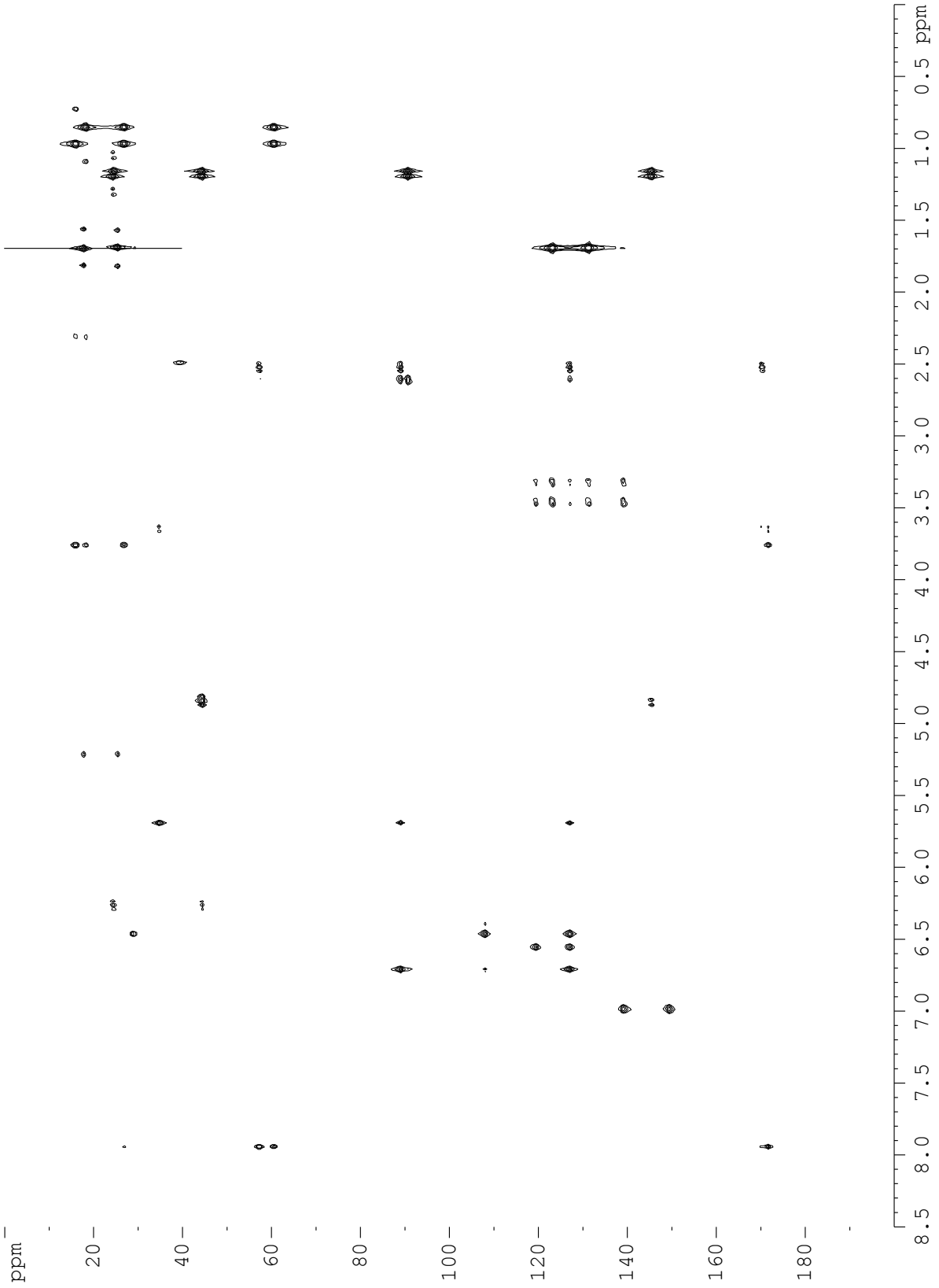
ppm
20
40
60
80
100
120
140
160
180
8.5
8.0
7.5
7.0
6.5
6.0
5.5
5.0
4.5
4.0
3.5
3.0
2.5
2.0
1.5
1.0
0.5
ppm

ROESY (150 ms)

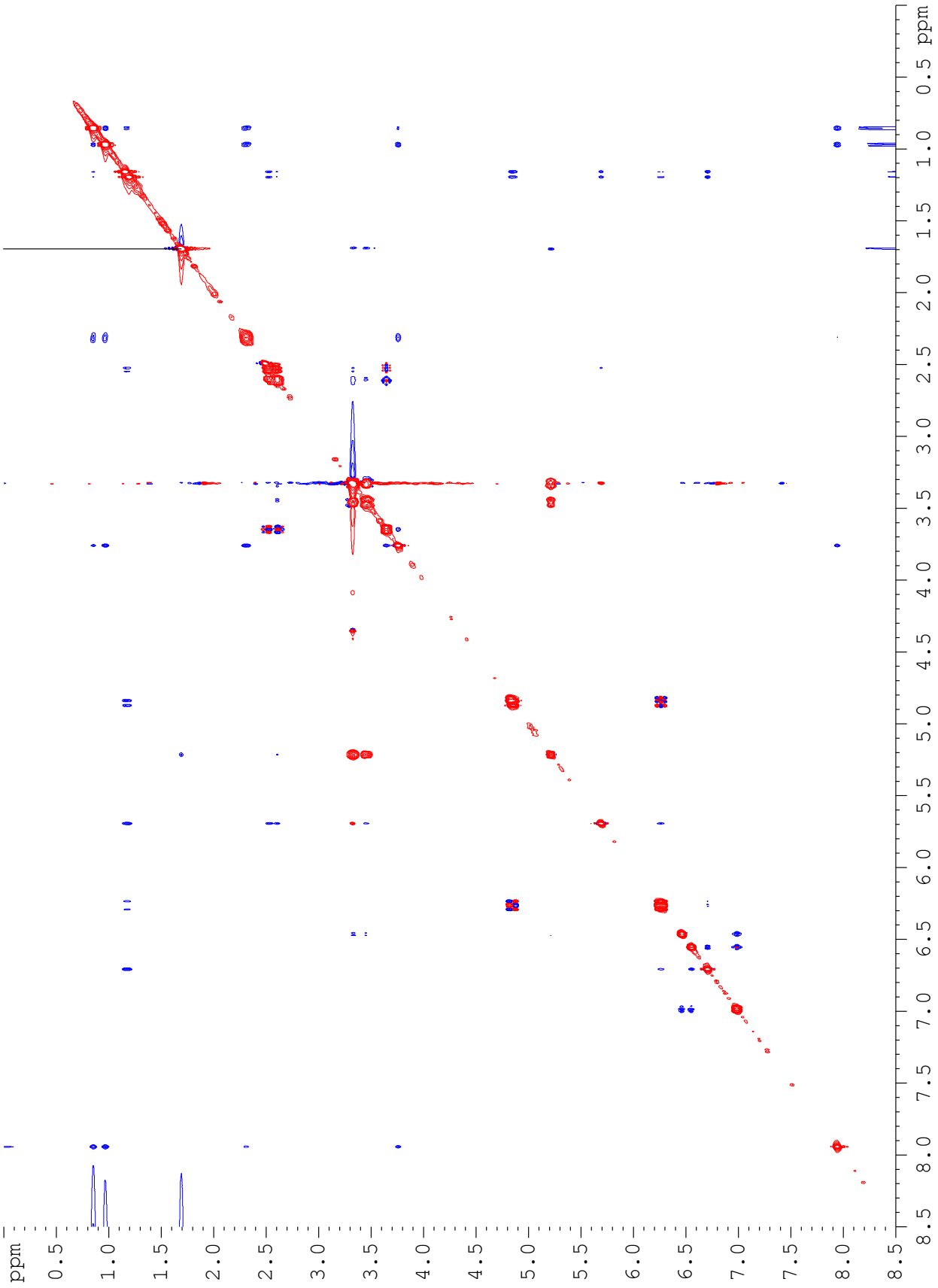

Marfey's reagents

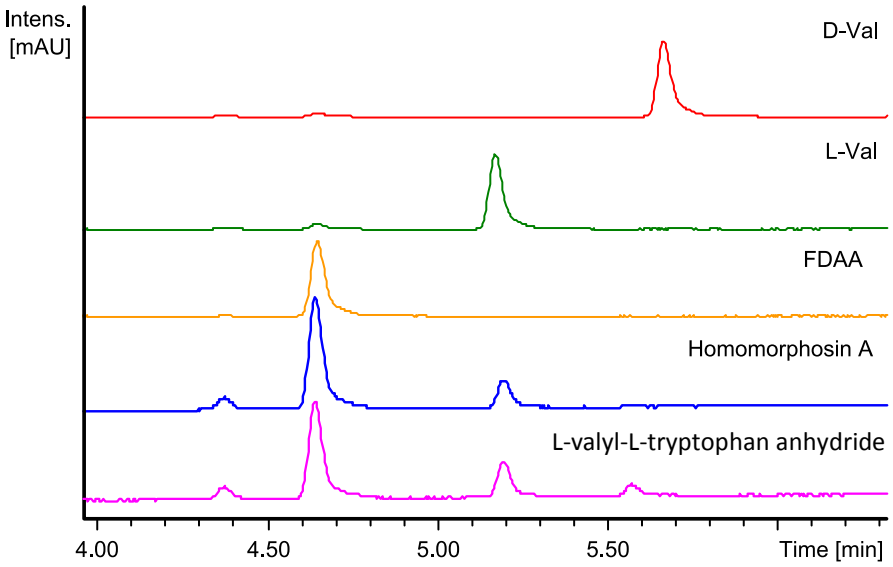

Figure S1 The retention times of the FDAA derivatives compared with retention times of the standard amino acid derivatives.UV data

UV data

1, **2**, **3** and **9** probably share a similar chromophore. This is different than the chromophore of **4**, **5** and **6** which corresponds to the absorption of an indole ring.

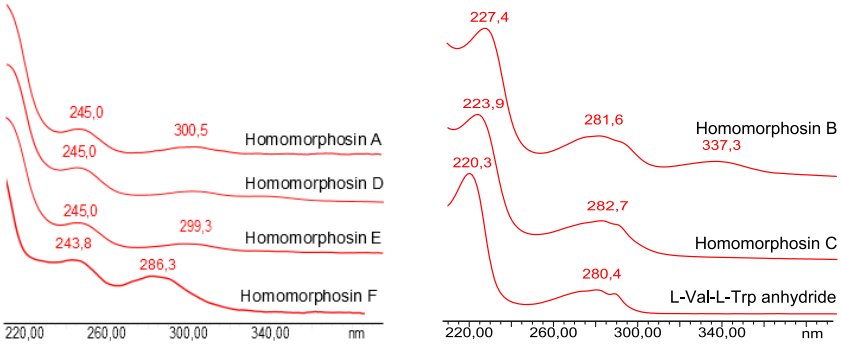

Figure S2 UV data of the homomorphosins

Stereochemistry of homomorphosin A

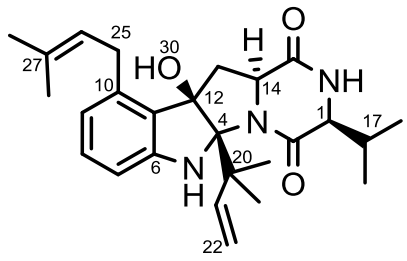

Figure S3 Numbering of homomorphosin A

Table S1. Distances of homomorphosin A from ISPA in Å. a: used as reference.

Nucleus 1	Nucleus 2	Calculated distance	Lower bound	Violation	Upper bound	Violation
16	17	2.94	3.33	0.39	4.07	
16	1	2.72	2.46		3.00	
8	7	2.48[a]	2.23		2.73	
5	21	2.88	4.18	1.3	5.11	
5	23	2.47	2.10		2.56	
9	25a	2.78	2.70		3.30	
9	26	2.79	2.71		3.31	
9	28/29	3.67	3.32		4.05	
30	23	2.29	2.38	0.09	2.91	
30	13a	2.84	1.92		2.35	0.49
30	25b	2.8	2.89	0.08	3.53	
26	28/29	2.46	2.15		2.63	
22b	23	2.26	2.07		2.53	
21	23	2.3	2.26		2.77	
21	13a	2.87	2.44		2.98	
21	30	2.77	2.96	0.19	3.62	
22b	18	3.92	3.69		4.51	
1	18	2.85	3.17	0.32	3.88	
1	19	2.29	2.25		2.75	
1	17	2.25	2.27	0.02	2.77	
25b	28/29	2.59	2.46		3.00	
25b	13b	2.18	1.88		2.30	
14	1	2.53	2.20		2.69	
17	18	2.34	2.08		2.54	
17	19	2.29	2.07		2.53	
5	7	2.61	2.39		2.92	

Table S2 Coupling *J*-constants in Hz for homomorphosin A.

Nucleus 1	Nucleus 2	Theoretical	Measured	Diff
13b	14	8.0	7.3	0.7
1	17a	2.3	2.0	0.3
13a	14	10.3	11.5	1.2

When averaging over the 364 structures from a conformational search, and only taking the structures into account which leads to increased fit iteratively over 10,000 steps, the errors are all but eliminated as seen below. This serves to show that the errors seen for a single structure is probably due to flexibility and subsequent conformational averaging.

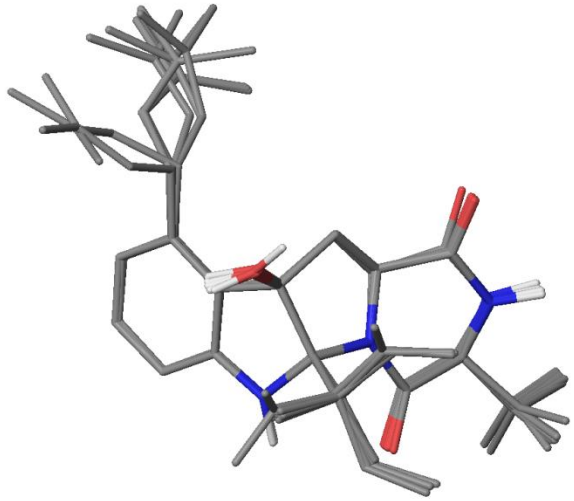

Figure S4 Superposition of the ten structures which give the lowest averaged error

Table S3 Average distances for homomorphosin A from ISPA in Å. a: used as reference.

Nucleus 1	Nucleus 2	Calculated distance	Averaged distance	Diff (Å)	Diff (%)
16	17	2.94	2.94	0.00	0.00
16	1	2.72	2.72	0.00	0.04
8	7	2.48[a]	2.48	0.00	0.00
5	21	2.88	2.88	0.00	0.00
5	23	2.44	2.48	0.04	1.52
9	25a	2.78	2.78	0.00	0.00
9	26	2.92	2.79	0.13	4.49
9	28/29	3.67	3.67	0.00	0.00
30	23	2.41	2.29	0.12	4.86

30	131	2.84	2.84	0.00	0.01
30	252	2.95	2.81	0.14	4.74
26	28/29	2.39	2.46	0.07	3.12
22b	23	2.28	2.26	0.02	0.84
21	23	2.47	2.30	0.17	7.02
21	13a	2.87	2.87	0.00	0.00
21	30	2.80	2.77	0.03	0.96
22b	18	4.30	3.92	0.38	8.75
1	18	3.05	2.85	0.20	6.61
1	19	2.58	2.30	0.29	11.05
1	17	2.53	2.25	0.28	11.02
252	28/29	2.59	2.59	0.00	0.00
25b	13b	2.26	2.18	0.08	3.59
14	1	2.46	2.53	0.07	2.96
17	18	2.30	2.34	0.04	1.60
17	19	2.30	2.29	0.01	0.48
5	7	2.66	2.61	0.05	1.89

Table S4 Average *J*-coupling constants in Hz for homomorphosin A.

Nucleus 1	**Nucleus 2**	**Theoretical**	**Measured**	**Diff**
13b	14	8.1	7.3	0.8
1	17	2.2	2.0	0.2
13a	14	10.3	11.5	1.2

Paper 4

"Formation of sclerotia and production of indoloterpenes by *Aspergillus niger* and other species in section *Nigri*"

Frisvad, J.C.; **Petersen, L. M.**; Lyhne, E. K.; Larsen, T.O.

PLoS One, **2014**, *9* (4), E94857-E94857.

OPEN ACCESS Freely available online

Formation of Sclerotia and Production of Indoloterpenes by *Aspergillus niger* and Other Species in Section *Nigri*

Jens C. Frisvad*, Lene M. Petersen, E. Kirstine Lyhne, Thomas O. Larsen

Chemodiversity Group, Department of Systems Biology, Technical University of Denmark, Lyngby, Denmark

Abstract

Several species in *Aspergillus* section *Nigri* have been reported to produce sclerotia on well-known growth media, such as Czapek yeast autolysate (CYA) agar, with sclerotia considered to be an important prerequisite for sexual development. However *Aspergillus niger sensu stricto* has not been reported to produce sclerotia, and is thought to be a purely asexual organism. Here we report, for the first time, the production of sclerotia by certain strains of *Aspergillus niger* when grown on CYA agar with raisins, or on other fruits or on rice. Up to 11 apolar indoloterpenes of the aflavinine type were detected by liquid chromatography and diode array and mass spectrometric detection where sclerotia were formed, including 10,23-dihydro-24,25-dehydroaflavinine. Sclerotium induction can thus be a way of inducing the production of new secondary metabolites from previously silent gene clusters. Cultivation of other species of the black aspergilli showed that raisins induced sclerotium formation by *A. brasiliensis*, *A. floridensis A. ibericus*, *A. luchuensis*, *A. neoniger*, *A. trinidadensis* and *A. saccharolyticus* for the first time.

Citation: Frisvad JC, Petersen LM, Lyhne EK, Larsen TO (2014) Formation of Sclerotia and Production of Indoloterpenes by *Aspergillus niger* and Other Species in Section *Nigri*. PLoS ONE 9(4): e94857. doi:10.1371/journal.pone.0094857

Editor: Kevin McCluskey, University of Missouri, United States of America

Received December 18, 2013; **Accepted** March 19, 2014; **Published** April 15, 2014

Funding: Funded by the Danish Research Agency for Technology and Production Grant 09-064967. The funders had no role in study design, data collection and analysis, decision to publish, or preparation of the manuscript.

Competing Interests: The authors have declared that no competing interests exist.

* E-mail: jcf@bio.dtu.dk

Introduction

Certain strains in several species of Aspergillus section Nigri have been reported to produce sclerotia, notably Aspergillus sclerotioniger, A. carbonarius, A. tubingensis, A. sclerotiicarbonarius, A. costaricaensis, A. ellipticus, A. japonicus, A. piperis, A. aculeatus, A. aculeatinus, A. brunneoviolaceus and A. violaceofuscus [1–9]. Some species were originally described as producers of sclerotia, for example A. heteromorphus [10]. However Al-Musallam [3] could not induce sclerotium production in this species, despite several attempts. A. indologenus (as A. aculeatus CBS 114.80) was reported as a producer of abundant sclerotia [3], but Samson et al. [6] did not observe sclerotia in that strain. Concerning Aspergillus niger, only a few strains have been reported to produce sclerotia, WB 346 [1,11–12], WB 5121 = CBS 553.65 [1], CBS 425.65 [3] and WB 4700 [13]. However these strains represent other species than Aspergillus niger sensu stricto, for example CBS 553.65 was allocated to Aspergillus costaricanesis by Samson et al. [6] and WB 346 is representative of Sterigmatocystis fusca Bain., now regarded as Aspergillus carbonarius [3], CBS 425.65 is an A. tubingensis [14] and WB 4700 is also an A. tubingensis [13]. Sclerotium-producing strains from Tübingen and other German cities, identified as A. niger [15], are probably also A. tubingensis.

Genome sequencing projects [16,17,18] have shown the presence of predicted secondary metabolite gene clusters with no known expression and some of these could code for strictly sclerotium-associated metabolites such as aflavininins, aflavarins and aflatrems in *Aspergillus flavus* sclerotia [19] Sclerotium-producing strains in section *Nigri* that have been examined produced many sclerotium-borne secondary metabolites. *Aspergillus tubingensis* NRRL 4700 was reported to produce tubingensin A & B, dihydrotubingensis A & B, 14-epi-14-hydroxy-10,23-dihydro-24,25-dehydroaflavinine, 10,23-dihydro-24,25-dehydroaflavinine and 10,23-dihydro-24,25-dehydro-21-oxo-aflavinine [20–23]. In order to induce sclerotium production in *Aspergillus carbonarius*, Raper and Fennell [1] stated that steep agar, Czapek agar containing corn steep liquor, was a most suitable medium. Indeed *A. carbonarius* produced large amounts of sclerotia containing ochratoxin A on corn kernels [24]. Al-Musallam [3] reported that *A. tubingensis* CBS 425.65 produced sclerotia only when grown on French beans, while *A. tubingensis* WB 4700 produces sclerotia freely on most media [1,13]. This shows that sclerotium production may be strain-specific, but can be induced by plants parts such as beans, corn kernels in those isolates that do not produce them on standard identification media such as those based on Czapek, malt extract or oat meal.

Sclerotial development is considered to be an important prerequisite for sexual development in *Aspergillus* section *Circumdati*, and sclerotia might also have a role in dormancy [25]. Since a sexual state has been found in species in closely related sections of *Aspergillus*, i.e. in *A. flavus*, *A. parasiticus* and *A. nomius* in *Aspergillus* section *Flavi* [26–28] and *A. muricatus* [29] in *Aspergillus* section *Circumdati* [30] the ability to induce sclerotium production could be a first step towards finding a perfect state in *Aspergillus niger*. Rajendran and Muthappa [2] showed that *Aspergillus japonicus* has a perfect state and is a homothallic species with cleistothecia formed in one or two cavities (loculi) in sclerotia. This species was named *Saitoa japonica*. Later *A. sclerotiicarbonarius* [31] and *A. tubingensis* [32] were found to be heterothallic. These species also produced cleistothecia within one or two loculi within the sclerotia [31–32].

Some strains from section *Nigri* produce sclerotia on commonly used media, so Horn et al. [32] were able to induce the perfect state in *Aspergillus tubingensis* after determining the mating types of sclerotial strains and cross them on mixed cereal medium. *A. niger* is closely related to *A. tubingensis* and is probably also heterothallic, but the lack of sclerotia in *A. niger* hinders the test of whether a perfect state can be induced in this important industrial species [33]. *A. niger* is a very common spoilage organism on grapes, dried fruits, peanuts, maize, coffee and many other plants, so we wanted to test whether any of these fruits could induce sclerotium production in *A. niger* and other species in *Aspergillus* section *Nigri*. We also hypothesized that by inducing sclerotium production we could activate silent gene clusters for fungal indolo-terpenes, and thereby find new secondary metabolites in these fungi.

Even though many secondary metabolites have been reported from *Aspergillus niger*, this species has never been reported to produce aflavinin related indoloterpenes [34]. It is known, however, that sclerotium production may be associated with increased ochratoxin A production, at least in *A. carbonarius* [24], and other sclerotium producing species such as *A. sclerotioniger* also produce ochratoxin A [5-6,8]. The species in the *A. carbonarius* clade have been reported to only produce ochratoxin A, and no aflavinines, whereas *A. tubingensis* and *A. costaricaensis* produce aflavinins in the sclerotia [6,22] and no ochratoxins. If *A. niger* produces sclerotia when induced by different fruits and other plant parts they may also produce increased amounts of ochratoxin A, which would have important consequences for food safety. Possible sclerotium production by *A. niger* and other black Aspergilli would have many biological, biotechnological and food safety consequences [33,35–42]. One paper has indicated that *A. niger* might be able to produce sclerotia, as it was found that certain poorly sporulating UV mutants of *A. niger* produced sclerotium-like structures [43]. We wanted to test our hypothesis that natural substrates for fungi might induce sclerotium production and thereby confirm that previously identified "silent" gene clusters do indeed have a functional role in *A. niger* and other species in section *Nigri*.

Materials and Methods

Media and fungi

Representatives of all species in *Aspergillus* section *Nigri* were selected with an emphasis on isolates from plants substrates, and identified to species level using a polyphasic approach [5–6,8,14,44–45]. A series of strains of *Aspergillus niger sensu stricto* and *A. tubingensis* from raisins were isolated from the medium DG18 (dichloran glycerol 18% agar) [46] on which raisins from different countries have been plated out [36]. All black aspergilli were isolated, and pure cultures were identified and accessioned in the IBT collection (Collection of fungal strains at the Department of Systems Biology, Technical University of Denmark, Lyngby, Denmark). *Aspergillus* section *Nigri* strains from other collections were also tested (Table 1 and 2). All strains were 3-point inoculated on the media Czapek yeast autolysate agar (CYA), CYA with three autoclaved black raisins (CYAR) (or other plant parts). During identification the strains were also inoculated on malt extract agar according to Blakeslee (MEA), yeast extract sucrose (YES) agar, creatine-sucrose (CREA) agar, oat-meal agar (OA), and some isolates were also inoculated on Wickerhams antibiotic test medium (WATM), and potato dextrose agar (PDA). All media were poured in 11 cm plastic Petri dishes, inoculated and incubated at 25°C for 7 days in darkness [47–48].

In the first experiments *A. niger* IBT 29019 and IBT 24631 produced sclerotia on CYA agar with scattered whole raisins. The black conidia used for inoculation were taken directly from silica gel tubes. However when conidia from colonies grown on CYA for a week at 25°C were used for inoculation, the isolates lost the ability to produce sclerotia on CYA with raisins. Since some raisins are treated with sunflower oil, CYA with 1% sunflower oil was also prepared. To possibly enhance sclerotium production in *A. niger* CYA agar was added 1 mL of biotin solution giving a final concentration of 6.4 mg biotin/L medium and raisins added as biotin induced ascoma formation in *Penicillium rubens* [49–50]. The *A. niger* strains IBT 29019, 24631 and 24634 were also inoculated on 40% and 50% white and brown rice (in water) in 200 ml Erlenmeyer flasks, on 50% corn kernels, and on 4% and 40% macerated mango or papaya in water with 2% agar added. Since the sunflower oil or biotin treatments did not induce sclerotium formation, experiments were done to compare non-frozen and frozen inoculum in the three strains of *Aspergillus niger*, as freezing of the inoculum had earlier been shown to enhance sclerotium formation in *A. aculeatus* IBT 21030. This freezing-step consistently helped inducing sclerotium production in *A. niger* IBT 29019 and IBT 24631. The black aspergilli tested were therefore pretreated by placing CYA agar slants in Eppendorf tubes with sporulating fungal strains (6 mm agar plugs, one week old) in a −18°C freezer for at least 3 weeks before inoculation on the Petri plates with and without raisins or other plant parts. In the first series of experiments *A. niger* IBT 29019, IBT 24631 and IBT 24634 were tested on a series of different substrates: CYA agar with and without raisins (of different kinds), dried mulberry, dried blueberry, dried cranberry, dried goji berry, dried apricot, dried prune, mango peel, papaya peel, dried green coffee beans, and dried kidney beans, all organically grown (Table S1 in File S1). All substrates were autoclaved for 20 min at 121°C. In the second series of experiments many strains of *A. niger* and *A. welwitchiae* were tested for sclerotium production in addition to representatives of all other known species in *Aspergillus* section *Nigri*.

Plug extraction

For standard screening three plugs were taken from one colony, by use of a 6 mm steel plug drill, close to the center of the colony, beside the raisin or other fruit, if added. If any sclerotia could be observed, the agar plugs were taken to include the sclerotia. For comparison between sclerotial extracts and agar colony extracts five plugs were taken from one colony, covering the diameter of the colony (only when HPLC-MS analysis was intended). The plugs were transferred to 2 mL vials and 750 µL methanol: dichloromethane: ethyl acetate (1:2:3 v/v/v) containing 1% formic acid was added. For HPLC-MS analysis each sample was added 40 µL chloramphenicol in ethanol (500 µg/mL) as an internal standard. The vials were placed in an ultrasonic bath (Branson 3210) for 60 minutes. The extracts were then transferred to clean vials and evaporated to dryness. This was either achieved by leaving the vials in a fume hood over night or by applying nitrogen airflow at 25–32°C. After evaporation, 500 µL MeOH was added and the samples were then ultrasonicated for 20 minutes to re-dissolve the fungal metabolites. The extracts were then filtered using a 0.45 µm polytetrafluoroethene (PTFE) filter into clean vials [51].

Sclerotium extraction

The fungi were three-point inoculated on solid CYA plates with biotin and raisins and incubated at 25°C for 7 days in the dark. Sclerotia were harvested by applying pure H_2O to the plate and carefully harvested with a Drigalski spatula. The liquid including the sclerotia and spores was filtered through sterile Miracloth and washed with pure water and ethanol. This allowed for spores to

Table 1. Production, or not, of sclerotia by *Aspergillus niger* strain IBT 29019, IBT 24631, and IBT 24634, and production of apolar indoloterpenes on Czapek yeast autolysate agar with or without added plant parts.

CYA + additional fruit/cereal grain	*Aspergillus niger* strain	Sclerotia produced	10,23-dihydro-24,25-dehydroaflavinine produced	Number of apolar indoloterpenes detected by liquid chromatography diode array detection (LC-DAD)
None	IBT 29019	-*	-	0/0
None	IBT 24631	-	-	0/0
None	IBT 24634	-	-	0/0
Raisin (CYAR)	IBT 29019	++*	+	2/2/2/**4****
Raisin (CYAR)	IBT 24631	+*	+	1/1/1/**2****
Raisin (CYAR)	IBT 24634	-	-	0/0
Mulberry	IBT 29019	++	+	2
Mulberry	IBT 24631	-	-	0
Mulberry	IBT 24634	-	-	0
Blueberry	IBT 29019	++	+	2/3
Blueberry	IBT 24631	-	-	0
Blueberry	IBT 24634	-	-	0
Cranberry	IBT 29019	++	+	2/7
Cranberry	IBT 24631	-	-	0
Cranberry	IBT 24634	-	-	0
Goji berry	IBT 29019, 24631, 24634	-	-	0
Apricot	IBT 29109	++	+	2/7
Apricot	IBT 24631	−/+***	+	0/1
Apricot	IBT 24634	-	-	0/0
Prune	IBT 29019	++	+	2/3
Prune	IBT 24631	−/+***	+	0/1
Prune	IBT 24634	-	-	0/0
Mango, 40%	IBT 29019	++	+	3/5
Mango, 40%	IBT 24631, 24634	-	-	0/0
Mango peel	IBT 29019	++	+	2
Papaya, 40% & 4%	IBT 29019	-	-	0/0
Corn	IBT 29019	-	-	0
Corn	IBT 24631	+	+	1
Corn	IBT 24634	-	-	0
White rice, 50%	IBT 29019	++	+	11/12
White rice, 50%	IBT 24631	+	+	2
White rice, 50% or 40%	IBT 24634	-	-	0
Brown rice, 50%	IBT 29019	++	+	13/13
Brown rice, 40%	IBT 29019	+	+	2/1
Brown rice, 50%	IBT 24631	+	+	1
Brown rice, 50%	IBT 24634	-	-	0

*-: no sclerotia produced, +: few scattered sclerotia, ++: many sclerotia (>10) surrounding each piece of fruit, or directly on the rice or corn.
**More indoloterpenes were detected using mass spectrometric detection than diode array detection in this case where both methods were compared. In IBT 29019 on CYAR, 4 recognizable indoloterpenes were detected using LC-mass spectrometric detection (in bold), but only two according to DAD.
***−/+: sclerotia not produced in one experiment, but produced in the other
The conidia were frozen at −18°C for three weeks before inoculation.
doi:10.1371/journal.pone.0094857.t001

pass through, while sclerotia stayed in the filter. Sclerotia were transferred to Eppendorf tubes and washed with water to remove remaining spores. After evaporation of excess H_2O, two big (diam. 4 mm) and two small steel balls (diam. 2 mm) were added to each tube. The tubes were cooled with liquid nitrogen and shaken using a frequency of 2000/min for 2×60 seconds in a sonic Micro Dismembrator U homogenizer (Sartorius). The tubes were then heated to 30°C and shaken again for 2×60 second. To each tube 40 µL chloramphenicol and 0.750 mL methanol: dichlormethane: ethyl acetate (1:2:3 v/v/v) containing 1% formic acid was added and the extracts were transferred to clean 2 mL vials. The samples were ultrasonicated (Branson 3210 sonicator) for 1 h and the extracts were then transferred to clean vials and the solvent was evaporated. The samples were re-dissolved in 500 µL MeOH,

Table 2. *Aspergillus* section *Nigri*: Production of sclerotia on CYA agar or CYA with raisins (most sclerotia were formed around the raisins on the agar surface, and few sclerotia if any on the raisins themselves, see footnotes).

Species	Isolates	Sclerotia on CYAR	Sclerotia on CYA	Predominantly sclerotial apolar metabolites and/or ochratoxin A
A. aculeatinus	CBS 121875 = IBT 29118, IBT 30576	++*	-	Indoloterpenes produced
A. aculeatus	IBT 21030, IBT 13519, IBT 32735 = IMI 240698**	++/+++*	-, ++ in sectors for IBT 21030, +++ for IMI 240698	10,23-dihydro-24,25-dehydroaflavinine, an okaramine, paspa***
A. brasiliensis	IBT 28177	++	-	10,23-dihydro-24,25-dehydroaflavinine and 4 other aflavinins No apolar sclerotial metabolites detected in other strains
A. brunneoviolaceus (*A. fijiensis*)	IBT 13989 = CBS 313.89	++	++	Paspa
A. carbonarius	IBT 21089 = NRRL 369, WB 346, IBT 31277, IBT 29172 = IBT 4916 = CBS 117.49 (on mango)	+*	-	Ochratoxin A
A. costaricaensis	IBT 23401 = CBS 115574 = ITEM 7555	+++	+	10,23-dihydro-24,25-dehydroaflavinine, aspernomine,12 other aflavinines
A. ellipticus (=*A. helicothrix*)	IBT 29172 = CBS 707.79, IBT 13963 = CBS 677.79	+	-	No apolar sclerotial metabolites detected
A. eucalypticola	IBT 29274 = CBS 122172	-	-	No apolar sclerotial metabolites detected
A. floridensis	IBT 32546 = NRRL 62478	++	-	10,23-dihydro-24,25-dehydroaflavinine
A. heteromorphus	IBT 13691 = CBS 117.55, IBT 14352 = CBS 312.89	+****	-	No apolar sclerotial metabolites detected
A. homomorphus	IBT 21893 = CBS 101889	-	-	No apolar sclerotial metabolites detected, several apolar unique extrolites are present
A. ibericus	IBT 26612 = CBS 121593	+	-	An aflavinine
A. indologenus	CBS 114.80 = IBT 3679	−/(+)*****	-	Mid-polar indoloterpenes indicate that sclerotia could be produced
A. japonicus	IBT 5718 = CBS 114.51	-	-	No apolar sclerotial metabolites detected
A. lacticoffeatus	IBT 22031 = CBS 101803	-	-	No apolar sclerotial metabolites
A. luchuensis (*A. acidus*)	IBT 24821, IBT 24825, CBS 553.65 = IBT 28612	+	-	10,23-dihydro-24,25-dehydroaflavinine, 3 other aflavinins
A. neoniger	IBT 30603, IBT 20973	++	-	10,23-dihydro-24,25-dehydroaflavinine, aspernomine, 10 other aflavinin
A. niger (the majority of strains did not produce sclerotia, see Table S2 in File S1)	IBT 24631 = CBS 133816, IBT 26389 = NRRL 599, IBT 28998, IBT 28999, IBT 29000, IBT 29001, IBT 29003, IBT 29005, IBT 29006, IBT 29007, IBT 29019 = CBS 133818, IBT 29020	++/+	-	10,23-dihydro-24,25-dehydroaflavinine, 5 other aflavinins
A. piperis	IBT 24630 = CBS 112811	+++	+++	10,23-dihydro-24,25-dehydroaflavinine, 11 other aflavinins
A. sclerotiicarbonarius	IBT 28362 = CBS 121057	++/+++	++/+++	Paspa (3 different)
A. saccharolyticus	IBT 30881, IBT 28231	++	-	Paspa (one)
A. sclerotioniger	IBT 22905	+++	+++	Ochratoxin A
A. trinidadensis	IBT 32570 = NRRL 62480	++	-	Paspa (one)
A. tubingensis (the majority of strains did not produce sclerotia, see Table S2 in File S1)	IBT 23488 = IBT 16833 = CBS 161.79 = NRRL 4700, IBT 20950, IBT 29022, IBT 29557 = CBS 122.35X, CBS 425.65, IBT 29022, IBT 31740	++/for NRRL 4700 +++	−, +++ for NRRL 4700	14-epi-14-hydroxy-10,23-dihydro-24,25-dehydroaflavinine, 10,23-dihydro-24,25-dehydroaflavinine, 10,23-dihydro-24,25-dehydro-21-oxo-aflavinine, tubingensin A & B, dehydrotubingensin A & B, aspernomine, 20 other aflavinines
A. uvarum	IBT 26606 = CBS 121591	-	-	No apolar sclerotial metabolites detected
A. vadensis	CBS 113365 = CBS 102787 = IBT 24658	-	-	No apolar sclerotial metabolites detected
A. violaceofuscus	CBS 115571 = IBT 14708	++	+	Mid-polar sclerotial metabolites detected

Table 2. Cont.

Species	Isolates	Sclerotia on CYAR	Sclerotia on CYA	Predominantly sclerotial apolar metabolites and/or ochratoxin A
A. welwitchiae (''*A. awamori*''), (further strains were tested, none produced sclerotia, see Table S2 in File S1)	CBS 139.54	-	-	No apolar sclerotial metabolites detected

*-: no sclerotia formed, +: Few scattered sclerotia (<10), ++: Several (>10) sclerotia surrounding the raisins, +++: numerous sclerotia formed all over the medium, both with and without raisins.
**Homothallic sexual state reported [2], this strain readily produced abundant sclerotia, both with and without raisins.
***Paspa is probably an indoloterpene with a paspalinine chromophore.
****In this species, sclerotia were only produced on the raisins, not on the medium.
*****Abundant sclerotia reported by Musallam [3].
Isolates not producing sclerotia in *A. brasiliensis*, *A. niger*, and *A. welwitschiae* and are listed in Table S2 in File S1. The conidia were frozen at −18°C for three weeks before inoculation.
doi:10.1371/journal.pone.0094857.t002

ultrasonicated for 20 minutes and filtered into fresh vials using 0.45 μm PTFE filters.

UHPLC-DAD analysis

The analyses of the 3 plug extracts were performed using Ultra High Performance Liquid Chromatography-diode array detection (UHPLC-DAD) as described by Frisvad and Thrane [52] as modified by Houbraken et al. [53]. UV spectra were recorded from 190 to 700 nm. For florescence detection, the excitation wavelength was 230 nm and the emission wavelength was 333 nm. This allows for a sensitive detection of extrolites with an indole chromophore, including aflavinins.

UHPLC-DAD-HRMS analysis

The analyses were performed using a Ultra High Performance Liquid Chromatograpy-UV/Vis-High Resolution Mass Spectrometer (UHPLC-DAD-HRMS) on a maXis G3 oa Qq-TOF mass spectrometer (Bruker Daltonics, Bremen, Germany) equipped with an electrospray (ESI) source and connected to an Ultimate 3000 UHPLC system (Dionex, Sunnyvale, CA). The column used was a reverse-phase Kinetex 2.6 μm C_{18}, 100×2.1 mm (Phenomenex, Torrance, CA) and the column temperature was maintained at 40°C. A linear water-acetonitrile gradient was used (both buffered with 20 mM formic acid) starting from 10% acetonitrile and increased to 100% in 10 minutes and maintaining this for 3 minutes before returning to the starting conditions in 0.1 minute and staying there for 2.4 minutes before the following run. A flow rate of 0.4 mL min^{-1} was used. HRMS was performed in ESI+ with a data acquisition range of 10 scans per second at m/z 100–1000. The MS was calibrated by use of the internal standard sodium formate, which was automatically infused prior to each run. UV spectra were collected at wavelengths from 200–700 nm. Data processing was performed using the Bruker software DataAnalysis and TargetAnalysis.

Results

Aspergillus niger and sclerotia

No strains of *Aspergillus niger sensu stricto*, tested in this study or in our earlier studies, produced sclerotia on any of the conventional media tested. The closely related sibling phylospecies *A. welwitchiae* [54], formerly called *A. awamori* [54–55] also did not produce sclerotia on any medium. Initially *A. niger* IBT 29019 and IBT 24631 produced sclerotia on a medium made with dark Californian raisins added to the medium. Interestingly sclerotia were only formed on CYA medium with whole raisins, and not on the same medium with macerated raisins. It was decided to add

Figure 1. Numerous cream-coloured sclerotia produced on CYAR agar can be seen surrounding the raisins and the usual heavy sporulation caused by black *Aspergillus niger* IBT 29019 heads. The ellipses added show the position of the raisins, which are covered with black aspergilla.
doi:10.1371/journal.pone.0094857.g001

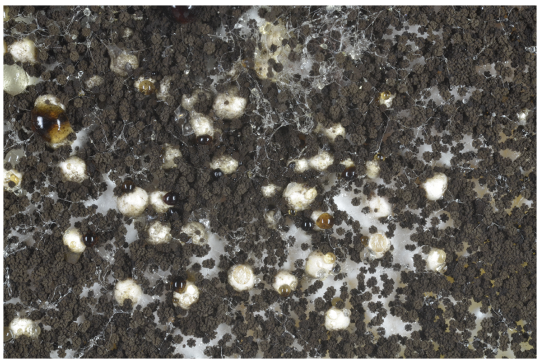

Figure 2. Approximately 41 white sclerotia can be observed on a close-up of *Aspergillus niger* IBT 29019 growing on Czapek yeast autolysate agar with raisins. Note the clear or brown exudate droplets associated with most sclerotia.
doi:10.1371/journal.pone.0094857.g002

three whole sterilized pieces of raisin on top of the CYA medium (CYAR), and the experiments were repeated with several brands of raisins from California, Turkey, Chile and Argentina (Table S1 in File S1). IBT 29019 and IBT 24631 produced sclerotia surrounding all organic and conventional dark raisins tested, but not white raisins (the latter had been treated with sulfur dioxide), and did not produce sclerotia on the control CYA agar medium. The sclerotia formed in *A. niger* (Fig. 1 and 2) were similar to those produced by *Aspergillus carbonarius* and *A. tubingensis*, i.e. large cream-coloured sclerotia, which were globose to ovoid and 500–700 μm in diameter. The strain *A. niger* IBT 24634 did not produce sclerotia under any conditions. The experiments using CYA agar with raisins were repeated several times and in nearly all cases sclerotia were formed. In few experiments sclerotia were not produced on CYA agar with whole raisins by IBT 29019, and in those cases sclerotium production could then be induced by keeping the conidia used for inoculation (conidia on agar plugs from a colony) of the media in a freezer at −18°C for at least three weeks. When this freezing step was done, sclerotium production was entirely consistent in IBT 29109 and IBT 24631.

A set of three isolates of *Aspergillus niger* (IBT 29019, IBT 24631 and IBT 24634) were first tested on the medium CYA and CYA with different pieces of whole fruits added or inoculated on whole rice (Table 1). Certain fruits stimulated sclerotium production in IBT 29019, including raisin, mulberry, blueberry, cranberry, apricot, prune, and mango peel, all placed on CYA agar, but also on 40% mango macerate in agar, and 50% white rice or 50% brown rice (rice media without added agar). Sclerotia were not formed on media with goji berries, green coffee beans, red kidney beans, black pepper, 4% or 40% papaya macerate in agar, 4% mango macerate in agar or on any of the media CYA, malt extract agar (MEA), yeast extract sucrose (YES) agar, oatmeal agar (OAT), potato dextrose agar (PDA), or Wickerhams antibiotic test medium (WATM). However regarding the latter 5 media, conidia were not frozen before inoculation, so it cannot be excluded that these media may be inducing sclerotium production if inoculated after a freeze treatment. The strain *A. niger* IBT 24631 only produced sclerotia on some of the media: CYA agar with raisins (CYAR), in some cases on CYA with prune or apricot, and on whole white or brown rice (50%). Furthermore in one case sclerotium production was seen on whole corn (50%, no agar added) in *A. niger* IBT 24631 but not in IBT 29019. Neither strain produced sclerotia on whole unpolished rice, polished rice, dried whole corn or dried kidney beans, except for the single incidences mentioned above. If produced, sclerotia were observable after 7 days of incubation, and only rarely were additional sclerotia produced after 7 days. All sclerotia produced were cream-white first, and darkening becoming beige to steel grey in age.

Strains of *Aspergillus niger* producing sclerotia and sclerotial indoloterpenes

In all cases the presence of sclerotia in *Aspergillus niger* was confirmed chemically by the presence of sclerotium associated aflavinin-type apolar indoloterpenes. Consistently, indoloterpenes of the 10,23-dihydro-24,25-dehydroaflavinine type were produced in all sclerotium containing media, but indoloterpenes were not produced in any cases on media where sclerotia were not present (Table 1). Two major indoloterpenes were produced by the strains of *A. niger* IBT 29019, and one major indoloterpene was produced by *A. niger* IBT 24631 as determined by both diode array and fluorescence detection. The total number of indoloterpenes ranged from one to 13, with highest numbers of indoloterpernes produced on brown rice (Table 2). Most of the indoloterpenes produced had an ordinary indol chromophore, but there were also apolar sclerotial metabolites with UV spectra not seen earlier, indicating that some of these had a somewhat modified chromophore but still quite similar to the normal indol chromophore. *Aspergillus niger* IBT 29019 produced 10,23-dihydro-24,25-dehydroaflavinine and two additional aflavinines, in addition to a fourth indoloterpene, which had the same formula ($C_{28}H_{39}NO$), UV spectrum and retention time as anominine (Fig. 3). On brown rice IBT 29019 produced 13 different apolar sclerotial metabolites, but most of them are as yet not structure elucidated. Anominine was formerly known as nominine [56].

Ten recently isolated strains isolated from Californian raisins produced sclerotia on CYAR, including IBT 29019 = CBS 133818, IBT 28998, IBT 28999, IBT 29000, IBT 29001, IBT 29003, IBT 29005, IBT 29006, IBT 29007 and IBT 29020 (Table 1), whereas four strains from the same raisin sample did not (IBT 29002, IBT 29004, IBT 29021, and IBT 29023) (Table S2 in File S1). One strain from black pepper, IBT 24631 = CBS 133816 could produce sclerotia on CYAR, while another strain from the

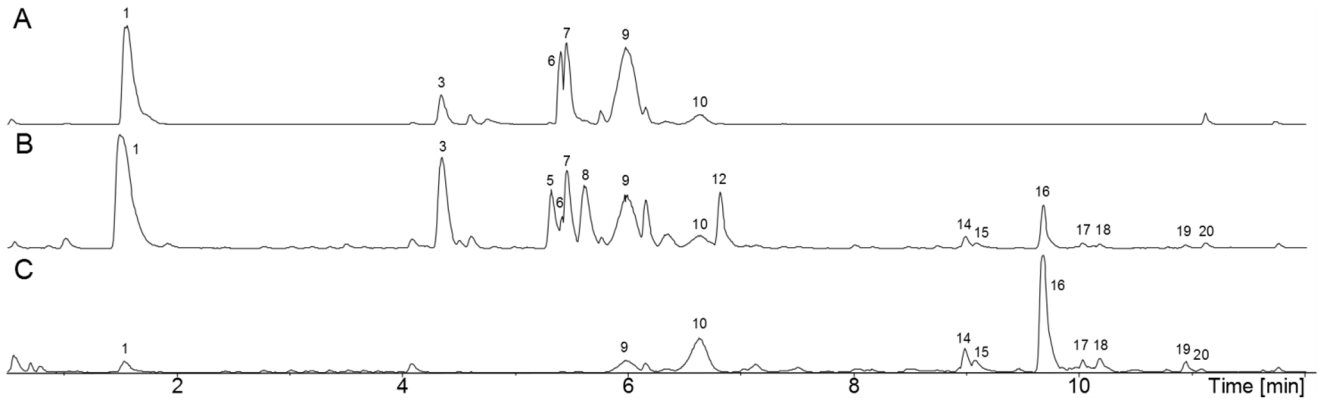

Figure 3. Ultra high performance liquid chromatography time of flight high resolution mass spectrometry electrospray ionization + base peak (UHPLC-TOF-HRMS ESI+ BP) chromatogram of *Aspergillus niger* (IBT 29019) extracts. A: Plug extraction from growing and sporulating culture with no sclerotium production (CYA agar with biotin). **B**: Plug extraction from growth with sclerotium production (CYAR with biotin). **C**: Sclerotium extraction (from CYAR with biotin). 1) Nigragillin, 2) Pyranonigrin A, 3) Fonsecin, 4) Aurasperone/nigerasperone analog, 7) Tensidol B, 11) Kotanin, 12) Flavasperone analog, 13) Rubrofusarin B, 14) Aflavinine analog, 15) Aflavinine analog, 17) Anominine, 18) 10,23-dihydro-24,25-dehydroaflavinine.

doi:10.1371/journal.pone.0094857.g003

212

same pepper sample, IBT 24634 = CBS 133817, could not. A number of culture collection strains of *A. niger* were also tested on CYAR and only 1 strain, NRRL 599, previously reported to produce high levels of citric acid formed sclerotia on CYAR, while other industrial and genome sequenced strains CBS 513.88 and NRRL 328, the culture ex type of *A. niger* NRRL 326 and other strains: CBS 139.52, CBS 119725, NRRL 363, NRRL 593, NRRL 611, NRRL 612, NRRL 2372, NRRL 3112, and NRRL 4757 did not produce sclerotia on CYAR (Table S2 in File S1).

14 strains of the sibling species of *A. niger*, *A. welwitchiae* were also tested on CYAR, and did not produce sclerotia: CBS 102.12, CBS 618.78, IBT 29098, ITEM 7097, NRRL 320, NRRL 340, NRRL 362, NRRL 372, NRRL 567, NRRL 595, NRRL 604, NRRL 2001, NRRL 4851, and NRRL 6408 (Table S2 in File S1).

All 12 *A. niger* strains producing sclerotia also produced 1–13 detectable aflavinins or related apolar indoloterpenes, including 10,23-dihydro-24,25-dehydroaflavinine (Table 2), while none of the non-sclerotium producing strains produced any aflavinin-like molecules.

In *A. niger* IBT 29019, sporulating cultures contained known *A. niger* extrolites including nigragillin, pyranonigrin A, tensidol B, kotanin and naphtho-γ-pyrones. However in the sclerotia alone, only aflavinin molecules and an indoloterpene tentatively identified as anominine were produced, with only traces of nigragillin (Fig. 3).

Strains of *Aspergillus* series *Nigri* producing sclerotia and sclerotial indoloterpenes

In *Aspergillus* series *Nigri* [44], four species did not produce sclerotia or indoloterpenes under any conditions: *A. eucalypticola*, *A. lacticoffeatus*, *A. vadensis* and *A. welwitchiae*. On the other hand *A. costaricaensis* and *A. piperis* produced sclerotia on all media at the expense of black conidiophores heads and sclerotial metabolites included 10,23-dihydro-24,25-dehydroaflavinine and 12 to 13 other apolar indoloterpenes. *A costaricaensis* also produced aspernomine [57]. Some strains of *A. tubingensis* (NRRL 4700) and *A. luchuensis* (IBT 24821, IBT 24825) produced sclerotia readily on CYA agar, while other strains of these two species needed raisins to induce sclerotium formation. The sclerotia of *A. luchuensis* formed readily on CYA tended to aggregate, they were cream coloured and very large, 800–1300 μm in diameter. The sclerotia of *A. costaricaensis* were also very large, from 1200–1800 μm, and those of *A. piperis* were yellowish to pinkish brown, 1000–1700 μm in diameter [5]. The sclerotia in *A. tubingensis* were the smallest in this series, 500–800 μm, first cream-coloured, later becoming pinkish to light brown. While sclerotium producing *A. luchuensis* produced 10,23-dihydro-24,25-dehydroaflavinine and 3 other apolar indoloterpenes, sclerotial *A. tubingensis* strains produced 10,23-dihydro-24,25-dehydroaflavinine, aspernomine and up to 19 additional apolar indoloterpenes on CYAR. We did not detect tubingensin A and B [21–22] and dehydrotubingensin A and B [23] on CYAR, but we have formerly identified these in NRRL 4700 cultures on the media CYA and YES agar. Furthermore 14-epi-14-hydroxy-10,23-dihydro-24,25-dehydroaflavinine and 10,23-dihydro-24,25-dehydro-21-oxo-aflavinine, earlier detected in *A. tubingensis* NRRL 4700 [22] were not detected on CYAR. This indicates that at least 26 different sclerotial indoloterpenes can be produced by *A. tubingensis*. In the conidial areas of *A. tubingensis* IBT 16833 (= NRRL 4700) we detected nigragillin, asperazine, and naphtho-γ-pyrones (Fig. 4). In the sclerotia, and sclerotial parts of the agar cultures (CYAR) we detected 6 aflavinins by UHPLC-TOF-HRMS and UHPLC-DAD and a compound tentatively identified as anominine. These indoloterpenes were not found in cultures with conidial heads only. It appears that the indoloterpenes and the naphtho-γ-pyrone, aurasperone B, are up-regulated in sclerotial cultures (Fig. 4).

Sclerotia were detected for the first time in *A. brasiliensis* and *A. neoniger*. *A. brasiliensis* IBT 28177 produced two detectable sclerotial indoloterpenes, while *A. neoniger* IBT 30603 and IBT 20973 produced 12 sclerotial apolar indoloterpenes on CYAR, including 10,23-dihydro-24,25-dehydroaflavinine and aspernomine (Table 2). Aspernomine was tentatively identified for the first time in *A. tubingensis*, *A. neoniger* and *A. costaricaensis*, based on comparison with aspernomine in extracts of *Aspergillus nomius* and an identical characteristic UV spectrum and retention time in all extracts of these fungi.

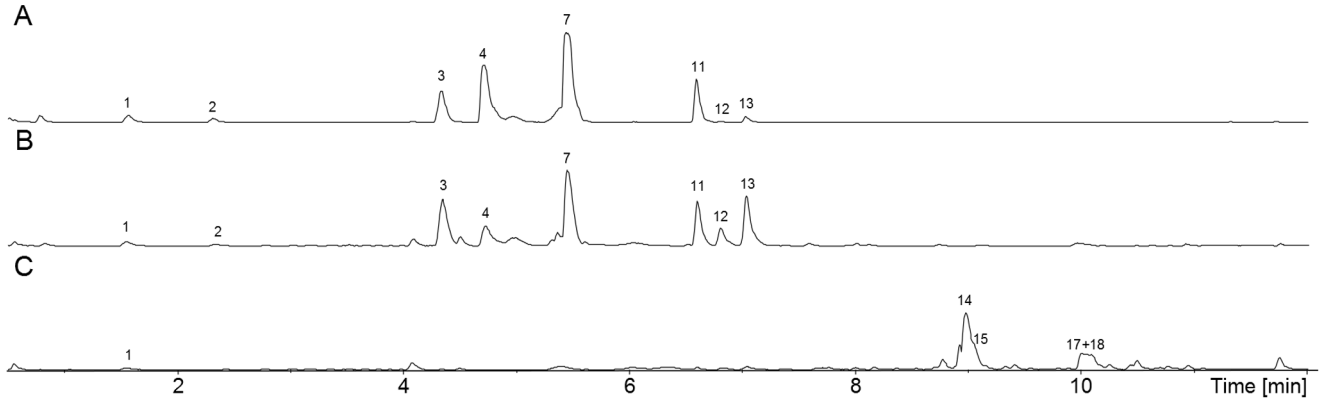

Figure 4. Ultra high performance liquid chromatography time of flight high resolution mass spectrometry electrospray ionization + base peak (UHPLC-TOF-HRMS ESI+ BP) chromatogram of *Aspergillus tubingensis* (IBT 16833 = CBS 161.79 = NRRL 4700) extracts. A: Plug extraction from colony area with no sclerotia (CYAR with biotin). **B**: Plug extraction from colony area with sclerotia (CYAR with biotin). **C**: Sclerotium extraction (from CYAR with biotin). 1) Nigragillin, 3) Fonsecin, 5) TMC-256A1, 6) Asperazine, 7) Tensidol B, 8) Fonsecin B, 9) Aurasperone C, 10) Aurasperone B, 12) Flavasperone analog, 14) Aflavinine analog, 15) Aflavinine analog, 16) Aflavinine analog, 17) Anominine, 18) 10,23-dihydro-24,25-dehydroaflavinine, 19) Aflavinine analog, 20) Aflavinine analog. From this strain TePaske et al. [20,21,22] isolated 14-epi-14-hydroxy-10,23-dihydro-24,25-dehydroaflavinine, 10,23-dihydro-24,25-dehydro-21-oxo-aflavinine, 10,23-dihydro-24,25-dehydroaflavinine, tubingensin A and B, and dehydrotubingensin A and B.
doi:10.1371/journal.pone.0094857.g004

Strains of *Aspergillus* series *Carbonaria* producing sclerotia and sclerotial indoloterpenes

In *Aspergillus* series *Carbonaria* two species, *A. sclerotiicarbonarius* and *A. sclerotioniger* produce sclerotia readily on most media. The sclerotia of *A. sclerotioniger* were 1000–1600 μm in diameter, and were yellow to red brown [5], while those of *A. sclerotiicarbonarius* were of the same colours as *A. sclerotioniger* and 600–1600 μm in diameter [7]. The sclerotia of *A. carbonarius* were cream coloured to light brown to pinkish to greyish brown in age, with a diameter of 800–1300 μm [1]. The sclerotia of *A. ibericus* were cream to light brown, and smaller than those of *A. carbonarius*: 700–1000 μm in diameter. *A. sclerotioniger* produces ochratoxin A, but not indoloterpenes on CYA or CYAR. *A. sclerotiicarbonarius* produced three indoloterpenes with a paspalinine chromophore, but none of these have been structure elucidated. Like *A. sclerotioniger*, strains of *A. carbonarius* produced ochratoxin A in the sclerotia and no indoloterpenes were detected (Table 2). While non-sclerotial strains of *A. carbonarius* can produce ochratoxin A, sclerotium production increases the ochratoxin A titre in this species [19]. In *A. ibericus* CBS 121593, CYAR induced production of sclerotia and production of one indoloterpene in those sclerotia. As is the case for *A. lacticoffeatus* and *A. niger* in series *Nigri*, no isolate has been found that produce both ochratoxin A and apolar indoloterpenes in series *Carbonaria*. This is the first report on sclerotium production and presence of an aflavinine in *A. ibericus* (Table 2).

Strains of *Aspergillus* series *Heteromorpha* producing sclerotia and sclerotial indoloterpenes

Aspergillus ellipticus and *A. heteromorphus* produced sclerotia when grown on CYAR. Both species have earlier been reported to produce sclerotia. A sclerotium producing sector of *A. ellipticus* was separated and named as a new species, *A. helicothrix*, by Al-Musallam [3]. Later research has shown that *A. ellipticus* and *A. helicothrix* are the same species [6]. We could induce sclerotium formation in *A. ellipticus* on CYAR, but we did not detect any sclerotium associated extrolites in that species. *A. heteromorphus* was originally claimed to produce sclerotia [10], but Al-Musallam [3] and Samson et al. [6] could not confirm this. We observed sclerotium production in *A. heteromorphus* CBS 101889 on CYAR. In this single case the sclerotia were only produced on the raisins and the sclerotia were the smallest observed in this study (300–500 μm) and becoming darker (steel grey) in age than those of the other species in *Aspergillus* section *Nigri*. We did not detect any sclerotium associated extrolites in this species, however (Table 2).

Strains of *Aspergillus* series *Homomorpha* producing sclerotia and sclerotial indoloterpenes

We did not detect any sclerotia in *A. homomorphus*, but we did observe sclerotia in *A. saccharolyticus* when isolates of this species (IBT 30881 and IBT 28231) grew on CYAR. The sclerotia of *A. saccharolyticus* were small, 300–500 μm in diameter and white to cream coloured. One apolar indoloterpene with a paspalinine chromophore was detected in *A. saccharolyticus* (Table 2). This is the first report on sclerotium production by *A. saccharolyticus*, as sclerotia were not reported in the original description of this species [58].

Strains of *Aspergillus* series *Aculeata* producing sclerotia and sclerotial indoloterpenes

We did not detect sclerotia in *A. indologenus* or *A. uvarum* when isolates of these species were grown on CYAR. *A. indologenus* did produce extrolites that indicate the possibility that this species may eventually produce sclerotia given the right culturing conditions as reported by Al-Musallam [3], i.e. okaramins, also produced by sclerotial *A. aculeatus* and mid-polar indol-alkaloids, in common with sclerotial *A. violaceofuscus*. Strains of three species occasionally produced sclerotia on CYA agar, but produced them regularly on CYAR: *A. aculeatinus*, *A. aculeatus* and *A. brunneoviolaceus*/*A. fijiensis* and *A. japonicus*. The sclerotia of all the species in this group were small (300–500 μm) and white to cream coloured. All species produced apolar indoloterpenes of the aflavinine or paspalinine type, but they produced different profiles of apolar indoloterpenes. The only known aflavinine identified was 10,23-dihydro-24,25-dehydroaflavinine in *A. aculeatus* and *A. japonicus*. *A. aculeatus* also produced one apolar indoloterpene of the paspalinine type and okaramins. *A. violaceofuscus* produced sclerotia, but only mid-polar indol-alkaloids were detected. *A. floridensis* and *A. trinidadensis* also produced sclerotia on CYAR. *A. floridensis* produced 10,23-dihydro-24,25-dehydroaflavinine and *A. trinidadensis* produced an apolar indoloterpene with a paspalinine chromophore (Table 2). The *extype* strain of *Saitoa japonica* (IMI 240698) [2] produced abundant sclerotia on all media, and was allocated to *Aspergillus aculeatus* based on chemotaxonomic evidence, however *S. japonica* IMI 240698 also has many similarities with *Aspergillus brunneoviolaceus*. This strain should be sequenced to allow a final identification. IMI 240698 produced three okaramins, one calbistrin, but in contrast to *A. brunneoviolaceus* it did not produce aspergillimide. After two month of incubation of *Saitoa japonica* IMI 240698 on MEA at room temperature the sclerotia were examined for ascocoma production, but these were not observed. This is the first report of sclerotium production in *A. floridensis* and *A. trinidadensis*, not reported in the original description of the two species [9].

Discussion

Aspergillus niger is one of the most important industrial microorganisms used, but is also a common contaminant of foods, so it is of high importance whether this organism can recombine or whether it is a clonal fungus. Sclerotia are necessary structures if a fungus has to produce a perfect state, at least in *Aspergillus* sections *Flavi*, *Nigri* and *Circumdati* which will produce one to several ascomata within a sclerotium [25–27,31–32,59], either homothallically or heterothallically. Even though mating-type genes have been found in *A. niger* [16,18], the absence of sclerotia in strains of *A. niger* has precluded the discovery of a perfect state in this species. We show here that addition of whole raisins or other plant parts to the medium CYA can induce sclerotium production in certain strains of *A. niger*.

Since indoloditerpenes are exclusively found in the sclerotia of *Aspergillus* sections *Nigri*, *Flavi* and *Circumdati* and since these indoloterpenes have been reported to be antiinsectan extrolites [19–23,57,60] they appear to be produced to protect sclerotia from being eaten by insects. As can be seen from the results obtained here, the sclerotia may contain a high number of indoloterpenes, many of which have been shown to be antiinsectan [60]. Sclerotium formation seems to be lost in *Aspergillus* strains cultured for a long time, but may also be lost in nature because these fungi are ever more depending on asexual conidial survival in domesticated landscapes [19,25]. Ascospore formation inside hard sclerotia in *Aspergillus* subgenus *Circumdati* is a very slow process, often taking from 3–12 month, and apparently requiring special physical and chemical factors to be initiated, irrespective of homothallism or heterothallism [2,26–29,31–33,59], and so the sexual potential of these fungi appears to be weak. This is also seen in this study: often it is only a minority of strains in the ubiquitous

species *A. niger* and *A. tubingensis* that can produce sclerotia, even after stimulation by plants parts such as seeds and fruits.

It was observed that no isolates of *A. niger* producing ochratoxin A could produce sclerotia or indoloterpenes, but more OTA producing isolates need to be examined before a conclusion on this interesting phenomenon can be made.

The first observation of a perfect state in any species of *Aspergillus* section *Nigri* was reported by Rajendran and Muthappa in 1980 [2]. In this case ascomata were found after 3 month of growth on malt extract agar. Since this fungus is homothallic, no mating partners needs to be used. It should be examined whether other sclerotium producing strains in the uniseriate black aspergilla are also homothallic. Twenty three years later Darbyshir et al. [31] succeeded to induce a perfect state in *A. sclerotiicarbonarius* and Horn et al. [32] one in *A. tubingensis*, and they used opposite mating types of naturally sclerotium producing isolates and plated these on a mixed cereal agar. Our experience has shown that cereal based media are not the most effective for sclerotium formation in species in *Aspergillus* section *Nigri*, but that the medium CYA with whole black raisins could be an ideal medium for crossing of opposite mating types of *A. niger*. It is important to note the freezing of the conidia for 3 weeks before inoculation was often necessary to induce sclerotium production on CYAR. In the initial experiments freezing was not used, and we still observed sclerotium production in *A. niger* IBT 29019. We suspect these original observations of sclerotia in *A. niger* were based on the fact that the cultures came directly from silica gel, because after several conidial transfers *A. niger* IBT 29019 failed to produce sclerotia on CYAR. The ability to produce sclerotia was restored when conidia were frozen before inoculation, so we used this treatment when testing other species for sclerotium production on CYAR. Even though sclerotium production has been reported from *A. niger* earlier [1,3,61,62], the strains reported to produce them were actually later shown to be *A. costaricaensis*, *A. tubingensis* or *A. carbonarius* [5,6,8]. Other fruits than raisins, such as blueberries, cranberries, mulberries, apricot, prune, mango were also useable for inducing sclerotium formation by *A. niger* IBT 29019 on CYA agar, while goji berries, white raisin preserved with sulfur dioxide, papaya, kidney beans, black pepper and green coffee beans were not. Whole white or brown rice also was effective for inducing sclerotium and indoloterpene production. Kjer et al. [63] recommended using whole rice in the screening for secondary metabolites in fungi, and whole rice may be a valuable addition for screening purposes to known effective media for secondary metabolite production, such as CYA agar and YES agar [64]. However, most of our experiments were done with the CYAR medium. When tested on several types and brands of black raisins, they all induced sclerotium production on CYA agar. However, macerated raisins did not induce sclerotium production, so it appears that the skin or waxy skin coating of the raisins may be the crucial factor. In grape wax oleanolic acid and octacosanoic acid are predominant [65], while in wheat leaves the wax 1-octacosanol is dominant [66] so it is not unlikely that such wax compounds, when present in high concentrations as on the surface of a fruit, are influencing sclerotium production. We tried to add sunflower oil to CYA, as this oil is often used for coating raisins to give a shiny surface, but on such a medium no sclerotia were formed. It remains to be seen what the sclerotium inducing factors are, but they appear to be based on a complicated mechanism, as some species in *Aspergillus* section *Nigri* produce sclerotia readily, while others only produce them under very specific conditions, even within the same species. Wicklow et al. [24] used whole corn kernels for inducing sclerotium formation in *A. carbonarius*, and concerning *A. niger* IBT 24631, few sclerotia were produced on whole corn kernels, but in general raisins on CYA agar is a more effective alternative. Raper and Fennell [1] induced sclerotium formation in *A. carbonarius* WB 346 by using steep agar, which is Czapek agar with 5 g/l corn steep liquor, so it appears that corn ingredients has a certain positive effect on sclerotium formation. Batista and Maia [10] also reported sclerotium production by *A. heteromorphus* on Czapek agar with 1% corn steep liquor. We tried another corn steep liquor containing medium, WATM, for inducing sclerotium formation in *A. niger* and *A. tubingensis*, but this medium did not work as well as in *Aspergillus* section *Flavi*, where it induces sclerotium formation effectively [67].

Conclusion

Adding whole autoclaved fruits or grains to an agar medium stimulates sclerotium production in some strains of many species of the black Aspergilli, notably *A. niger*, but also *A. brasiliensis*, *A. heteromorphus*, *A. ibericus*, *A. luchuensis*, *A. neoniger*, and the uniseriate black Aspergilli *A. aculeatinus*, *A. aculeatus*, *A. brunneoviolaceus*/*A. fijiensis*, *A. floridensis*, *A. japonicus*, *A. saccharolyticus*, *A. trinidadensis* and *A.violaceofuscus*. Pre-freezing of the conidium inoculum enhanced sclerotium production. Raisins also stimulated sclerotium production further in species that often produced them readily, such as some strains of *A. tubingensis* and *A. carbonarius*, and all strains of *A. costaricaensis*, *A. piperis*, *A. sclerotiicarbonarius* and *A. sclerotioniger* leaving *A. eucalypticola*, *A. lacticoffeatus*, *A. uvarum*, *A. vadensis* and *A. welwitchiae* the only species in *Aspergillus* section *Nigri* where sclerotia have not yet been detected. 10,23-dihydro-24,25-dehydroaflavinine-type apolar indoloterpenes were produced by most sclerotial species, but species related to *A. carbonarius* preferentially produced ochratoxin A in the sclerotia. The aflavinin and other apolar indoloterpene type metabolites were produced in the sclerotia only.

Supporting Information

File S1 Table S1. Table S1 is a list of fruits or seeds used to induce sclerotium production in *Aspergillus niger* strains. Table S2. Table S2 is a list of isolates in *Aspergillus brasiliensis*, *A. niger* and *A. welwitchiae* that do not produce sclerotia, even when stimulated by whole raisins in CYA agar in addition to a pre-freezing step.
(DOCX)

Acknowledgments

We thank the Danish Research Agency for Technology and Production grant 09-064967 for supporting this reseach.

Author Contributions

Conceived and designed the experiments: JCF LMP EKL TOL. Performed the experiments: JCF LMP EKL. Analyzed the data: JCF LMP TOL. Contributed reagents/materials/analysis tools: JCF LMP EKL TOL. Wrote the paper: JCF. Read and improved the draft paper: JCF LMP EKL TOL.

References

1. Raper KB, Fennell DI (1965) The genus *Aspergillus*. Baltimore, MD, USA: Williams and Wilkins. 686 p.

2. Rajendran C, Muthappa BN (1980) *Saitoa*, a new genus of Plectomycetes. Proc Indian Acad Sci (Plant Sci) 89: 185–191.

3. Al-Musallam A (1980) Revision of the black *Aspergillus* species. Baarn: Centraalbureau voor Schimmelcultures. 92 p.
4. Jarvis WR, Traquair JA (1985) Sclerotia of *Aspergillus aculeatus*. Canad J Bot 63: 1567–1571.
5. Samson RA, Houbraken JAMP, Kuijpers AFA, Frank JM, Frisvad JC (2004) New ochratoxin or sclerotium producing species in *Aspergillus* section *Nigri*. Stud Mycol 50: 45–61.
6. Samson RA, Noonim P, Meijer M, Houbraken J, Frisvad JC, et al. (2007) Diagnostic tools to identify black Aspergilli. Stud Mycol 59: 129–145.
7. Noonim P, Mahakarnchanakul W, Varga J, Frisvad JC, Samson RA (2008) Two novel species of *Aspergillus* section *Nigri* from Thai coffee beans. Int J Syst Evol Microbiol 58: 1727–1734.
8. Varga J, Frisvad JC, Kocsubé S, Brankovics B, Tóth B, et al. (2011) New and revisited species in *Aspergillus* section *Nigri*. Stud Mycol 69: 1–17.
9. Jurjević Ž, Peterson SW, Stea G, Solfrizzo M, Varga J, Hubka V, Perrone G (2012) Two novel species of *Aspergillus* section *Nigri* from indoor air. IMA Fungus 3: 159–173.
10. Batista AC, Maia H da Silva (1957) Alguns *Aspergillus* contaminantes de culturas. An Soc Biol Pernamb 15: 181–237.
11. Porter CL, Coats JH (1957) Protoplasmic connections between cells in sclerotia of certain *Aspergillus* and *Penicillium* species. Mycologia 49: 895–896.
12. Coats JH (1959) Physiological studies concerning the formation of sclerotia in *Aspergillus niger*. Diss Abstr 20: 1544–1545.
13. Rai JN, Tewari JP, Sinha AK (1967) Effect of environmental conditions on sclerotia and cleistothecia production in *Aspergillus*. Mycopathol Mycol Appl 31: 209–224.
14. Frisvad JC, Larsen TO, Thrane U, Meijer M, Varga J, et al. (2011) Fumonisin and ochratoxin production in industrial *Aspergillus niger* strains. PLOS ONE 6: e23496.
15. Peters I, Rippel-Baldes A (1949) Über das Vorkommen verschiedener Rassen von *Aspergillus niger* van Tiegh. im Boden. Arch Microbiol 14: 203–211.
16. Pel HJ de Winde JH, Archer DB, Dyer PS, Hofmann G, et al. (2007) Genome sequencing and analysis of the versatile cell factory *Aspergillus niger* CBS 513.88. Nat Biotechnol 25: 221–231.
17. Baker S (2006) *Aspergillus niger* genomics: Past, present and into the future. Med Mycol 44 Suppl 1: S17–S21.
18. Andersen MR, Salazar MP, Schaap PJ, van de Vondervoort, PJI, Culley D, et al. (2011) Comparative genomics of citric-acid producing *Aspergillus niger* ATCC 1015 versus enzyme-producing CBS 513.88. Genome Res 21: 885–897.
19. Wicklow DT (1988) Metabolites in the coevolution of fungal chemical defence systems. In: Pirozynski KA & Hawksworth DL (eds) Coevolution of fungi with plants and animals. Academic Press, London, pp. 173–201.
20. TePaske MR, Gloer JB, Wicklow DT, Dowd PF (1989a) Tubingensin A: An antiviral carbazole alkaloid from the sclerotia of *Aspergillus tubingensis*. J Org Chem 54: 4743–4746.
21. TePaske MR, Gloer JB, Wicklow DT, Dowd PF (1989b) Tubingensin B: A cytotoxic carbazole alkaloid from the sclerotia of *Aspergillus tubingensis*. Tetrahedron Lett 30: 5965–5968.
22. TePaske MR, Gloer JB, Wicklow DT, Dowd PF (1989c) Three new aflavinines from the sclerotia of *Aspergillus tubingensis*. Tetrahedron 45: 4961–4968.
23. Sings HL, Harris GH, Dombrowski AEW (2001) Dihydrocarbazole alkaloids from *Aspergillus tubingensis*. J Nat Prod 64: 836–838.
24. Wicklow DT, Dowd PF, Alfatafta AA, Gloer JB (1996) Ochratoxin A: An antiinsectan metabolite from the sclerotia of *Aspergillus carbonarius* NRRL 369. Can J Bot 42: 1100–1103.
25. Dyer PS, O'Gorman CM (2012) Sexual development and cryptic sexuality in fungi: insights from *Aspergillus* species. FEMS Microbiol Rev 36: 165–192.
26. Horn BW, Moore GG, Carbone I (2009a) Sexual reproduction in *Aspergillus flavus*. Mycologia 101: 423–429.
27. Horn BW, Moore GG, Carbone I (2009b) The sexual state of *Aspergillus parasiticus*. Mycologia 101: 275–280.
28. Horn BW, Moore GG, Carbone I (2011) Sexual reproduction in aflatoxin-producing *Aspergillus nomius*. Mycologia 103: 174–183.
29. Udagawa S, Uchiyama S, Kamiya S (1994) *Petromyces muricatus*, a new species with an *Aspergillus* anamorph. Mycotaxon 52: 207–214.
30. Frisvad JC, Samson RA (2000) *Neopetromyces* gen. nov. and an overview of teleomorphs of *Aspergillus* subg. *Circumdati*. Stud Mycol 45: 201–207.
31. Darbyshir HL, van de Vondervoort PJI, Dyer PS (2013) Discovery of sexual reproduction in the black Aspergilli. Fung Gen Rep (Suppl) 60: 290 (abstract # 687)
32. Horn BW, Olarte RA, Peterson SW, Carbone I (2013) Sexual reproduction in *Aspergillus tubingensis* from section *Nigri*. Mycologia 105: 1153–1163.
33. Kück U, Böhm J (2013) Mating type genes and cryptic sexuality as tools for genetically manipulating industrial molds. Appl Microbiol Biotechnol 97: 9609–9620.
34. Nielsen KF, Mogensen JM, Johansen M, Larsen TO, Frisvad JC (2009) Review of secondary metabolites and mycotoxins from the *Aspergillus niger* group. Anal Bioanal Chem 395: 1225–1246.
35. Mogensen JM, Nielsen KF, Frisvad JC, Samson RA Thrane U (2009) Effect of temperature and water activity on the production of fumonisin B_2 by *Aspergillus niger* and *Fusarium* species. BMC Microbiol 9: 281
36. Mogensen JM, Frisvad JC, Thrane U, and Nielsen KF (2010) Production of fumonisin B_2 and B_4 by *Aspergillus niger* on grapes and raisins. J Agric Food Chem 58: 954–958.
37. Noonim P, Mahakarnchanakul W, Frisvad JC, Samson RA (2008) Distribution of ochratoxin A-producing fungi in coffee beans (*Coffea arabica* and *Coffea robusta*) from two regions of Thailand. Int J Food Microbiol 128: 197–202.
38. Sørensen LM, Lametsch R, Andersen MR, Nielsen PV, Frisvad JC (2009) Proteome analysis of *Aspergillus niger*: Lactate added in starch-containing medium can increase production of the mycotoxin fumonisin B_2 by modifying acetyl-CoA metabolism. BMC Microbiol 9: 255.
39. Moore GG, Elliott JL, Singh R, Horn BW, Dorner JW, et al. (2013) Sexuality generates diversity in the aflatoxin gene cluster: evidence based on a global scale. PLOS Path 9: e1003574.
40. Mogensen JM, Varga J, Thrane U, Frisvad JC (2009) *Aspergillus acidus* from Puerh tea and black tea does not produce ochratoxin A and fumonisin B_2. Int J Food Microbiol 132: 141–144.
41. Noonim P, Mahakarnchanakul W, Nielsen KF, Frisvad JC, Samson RA (2009) Fumonisin B_2 production by *Aspergillus niger* from Thai coffee beans. Food Addit Contam 26: 94–100.
42. Frisvad JC, Smedsgaard J, Samson RA, Larsen TO, Thrane U (2007) Fumonisin B_2 production by *Aspergillus niger*. J Agric Food Chem 55: 9727–9732.
43. Jørgensen TR, Nielsen KF, Arentshorst M, Park J, van den Hondel C, et al. (2011) Submerged conidiation and product formation by *Aspergillus niger* at low specific growth rates are affected in aerial development mutants. Appl Environ Microbiol 77: 5270–5277.
44. Frisvad JC, Larsen TO, de Vries R, Meijer M, Houbraken J, et al. (2007) Secondary metabolite profiling, growth profiles and other tools for species recognition and important *Aspergillus* mycotoxins. Stud Mycol 59: 31–37.
45. Ferracin LM, Frisvad JC, Taniwaki MH, Iamanaka BT, Sartori D, Schaoavaloff ME, Fungaro MHP (2009) Genetic relationships among strains of the *Aspergillus niger* aggregate. Braz Arch Biol Technol 52: 241–248.
46. Hocking AD, Pitt JI (1980) Dichloran-glycerol medium for enumeration of xerophilic fungi from low-moisture foods. Appl Environ Microbiol 39: 488–492.
47. Frisvad JC, Samson RA (2004) Polyphasic taxonomy of *Penicillium* subgenus *Penicillium*. A guide to identification of food and air-borne terverticillate Penicillia and their mycotoxins. Stud Mycol 49: 1–173.
48. Nielsen ML, Nielsen JB, Rank C, Klejnstrup ML, Holm DMK, et al. (2011) A genome-wide polyketide synthase deletion library uncovers novel genetic links to polyketides and meroterpenoids in *Aspergillus nidulans*. FEMS Microbiol Lett 321: 157–166.
49. Boehm J, Hoff B, O'Gorman CM, Wolfers S, Klix V, et al. (2013) Sexual reproduction and mating-type mediated strain development in the penicillin-producing fungus *Penicillium chrysogenum*. Proc Nat Acad Sci USA 110: 1476–1481.
50. Houbraken J, Frisvad JC, Samson RA (2011) Fleming's penicillin producing strain is not *Penicillium chrysogenum* but *P. rubens*. IMA Fungus 2: 87–95.
51. Smedsgaard J (1997) Micro-scale extraction procedure for standardized screening of fungal metabolite production in cultures. J Chromatogr A 760: 264–270.
52. Frisvad JC, Thrane U (1987) Standardized High-Performance Liquid Chromatography of 182 mycotoxins and other fungal metabolites based on alkylphenone indices and UV-VIS spectra (diode-array detection). J Chromatogr 404: 195–214.
53. Houbraken J, Spierenburg H, Frisvad JC (2012) *Rasamsonia*, a new genus for thermotolerant and thermophilic *Talaromyces* and *Geosmithia* species. Antonie van Leeuwenhoek 101: 403–421.
54. Hong S-B, Lee M, Kim D-H, Varga J, Frisvad JC, et al. (2013) *Aspergillus luchuensis*, an industrially important black *Aspergillus* in East Asia. PLOS ONE 8: e63769.
55. Perrone G, Stea G, Epifani F, Varga J, Frisvad JC, et al. (2011) *Aspergillus niger* contains the cryptic phylogenetic species *A. awamori*. Fungal Biol 115: 1138–1150.
56. Bradshaw B, Etxebarria-Jardi G, Bonjoch J (2008) Polycyclic framework synthesis of anominine and tubingensin A indole diterpenes. Org Biomol Chem 6: 772–778.
57. Staub GM, Gloer JB, Wicklow DT, Down PF (1992) Aspernomine: a cytotoxic antiinsectan metabolite with a novel ring system from the sclerotia of *Aspergillus nomius*. J Amer Chem Soc 114: 1015–1017.
58. Sørensen A, Lübeck PS, Lübeck M, Nielsen KF, Ahring BK, et al. (2011) *Aspergillus saccharolyticus* sp. nov., a new black *Aspergillus* species isolated in Denmark. Int J Syst Evol Microbiol 61: 3077–3083.
59. Fennell DI, Warcup JH (1959) The ascocarps of *Aspergillus alliaceus*. Mycologia 51: 409–415.
60. Gloer JB (1995) Antiinsectan natural products from fungal sclerotia. Acc Chem Res 28: 343–350.
61. Agnihotri VP (1968) Effects of nitrogenous compounds on sclerotium formation in *Aspergillus niger*. Can J Microbiol 14: 1253–1258.
62. Agnihotri VP (1969) Some nutritional and environmental factors affecting growth and production of sclerotia by a strain of *Aspergillus niger*. Can J Microbiol 15: 835–840.
63. Kjer J, Debbab A, Aly AH, Proksch P (2010) Methods for isolation of marine-derived endophytic fungi and their bioactive secondary products. Nat Protocols 5: 479–490.
64. Frisvad JC (2012) Media and growth conditions for induction of secondary metabolite production. Meth Mol Biol 944: 47–58.
65. Mendes JAS, Prozil SO, Evtuguin DV, Lopes LPC (2013) Towards comprehensive utilization of winemaking residues: Characterization of grape

skins from red grape pomaces of variety Touriga Nacional. Ind Crop Prod 43: 25–32.

66. Myung K, Parobek AP, Godbey JA, Bowling AJ, Pence HE (2013) Interaction of organic solvents with the epicuticular wax layer of wheat leaves. J Agric Food Chem 61: 8737–8742.

67. Rank C, Klejnstrup ML, Petersen LM, Kildegaard S, Frisvad JC, Gotfredsen CH, Larsen TO (2012) Comparative chemistry of *Aspergillus oryzae* (RIB40) and *A. flavus* (NRRL 3357). Metabolites 2: 39–56.

Supplementary material

Formation of sclerotia and production of indoloterpenes by *Aspergillus niger* and other species in section *Nigri.*

Jens C. Frisvad, Lene M. Petersen, E. Kirstine Lyhne, and Thomas O. Larsen

Table S1. List of fruits or seeds used to induce sclerotium production in *Aspergillus niger* strains.

Plant part*	Type	Brand	Country of origin	Imported to
Raisins	Dark	Sun-Maid	California, USA	Denmark
Sultanas raisins	Dark, organic	Unknown	Turkey	Urtekram, Denmark
Raisins	Dark	Unknown	Turkey	Urtekram, Denmark
Raisins	Dark, organic	Unknown	Argentina	Biogan A/S, Denmark
Raisins	Dark, organic	Unknown	California, USA	Biogan A/S, Denmark
Raisins	Dark, organic	Naturata	Slovenia	Bought in Slovenia
Raisins	Dark, organic	Unknown	California, USA	Helios A/S, Denmark
Raisins	Dark, organic	Sun-Maid	California, USA	Denmark
Raisins	Dark	Frutexa	Chile	Denmark
Sultana raisins	Dark	Unknown	Unknown	X-tra, COOP, Denmark
Jumbo raisins	Dark	Delicata	Unknown	System Frugt A/S, Tilst, Denmark
Raisins (two batches)	Dark	Unknown	Turkey	Irma, COOP, Denmark
Raisins	Dark, organic	Thompson	California, USA	Irma, COOP, Denmark
Raisins	Green	Thompson	California, USA	Denmark
Raisins	Green	Unknown	Unknown	System Frugt A/S, Tilst, Denmark
Small dry apricots	Stoneless, organic	Unknown	Unknown	Biogan A/S, Denmark
Small dry prunes	Stoneless, organic	Unknown	California, USA	Helios, Denmark
Dry goji berries			China	Superfruit, Sweden then to Denmark
Dry craneberries	60%, apple juice,	Unknown	Unknown	System Frugt,

	sunflower oil			Denmark
Dry red kidney beans	organic	Unknown	Unknown	Urtekram, Denmark
Dry white mulberries	Wild-crafted and sundried	Unknown	Asia	Superfruit / Rich Nature, Denmark, batch S090225-0410-160
Dry blueberries	55%, with apple juice and sunflower oil	Unknown	USA	Superfruit, Sweden then to Denmark
Dry green coffee	Arabica	Unknown	Brazil	Denmark
Black pepper		Unknown	Indonesia	Denmark
Rice	white	Uncle Ben	USA	Denmark
Rice	Brown, long grain	Organic Cuisine	Unknown	Nordic Food Partners A/S, Denmark
Corn	Canned	Unknown	USA	Denmark
Mango	Fresh	Unknown	Brazil	Denmark
Papaya	Fresh	Unknown	Brazil	Denmark
Sunflower oil	Organic, cold-pressed	Unknown	Unknown	Produced in the Netherlands, then imported to Denmark

*All raisins were added up to 0.5% sunflower oil according to the producer. All fruits were placed as whole fruits / seeds in the same pattern as a three point inoculation of fungal colonies. The fungi were inoculated just beside the fruit parts (approximately 2 mm from the fruits). The rice was suspended in water and autoclaved. An approximately 10^7 conidia / ml suspension was used for inoculation of the rice. Pieces of mango and papaya peel (approximately 1 x 2 cm were also placed in the CYA plates in three points before inoculation. For the 4% and 40% macerated mango and papaya in agar, both fruit flesh and peel was used, but the kernel / seeds were discarded.

Table S2. *Aspergillus* section *Nigri* List of isolates in *Aspergillus brasiliensis*, *A. niger* and *A. welwitchiae* that do not produce sclerotia even when stimulated by whole raisins in CYA agar in addition to a pre-freezing step.

Species	Isolates with no sclerotia
A. brasiliensis	IBT 28083 = CBS 246.65 IBT 21946 = CBS 101740
A. niger	IBT 27878 = NRRL 328, IBT 24637, IBT 29899 = NRRL 363, IBT 29884 = NRRL 4757, IBT 29885 = NRRL 612, IBT 28099 = CBS 139.52, IBT 23540 =

	NRRL 3112, IBT 21853, IBT 23680 = IMI 041871, IBT 29887 = NRRL 611, IBT 24634 = CBS 133817, IBT 29709 = CBS 513.88, IBT 27876 = NRRL 326, IBT 24637, NRRL 2372 = IBT 29890, NRRL 328 = IBT 27878, CBS 119725 = IBT 28098, NRRL 593 = IBT 29891, IBT 29021, IBT 29023, IBT 29002, IBT 29004
A. welwitchiae ("*A. awamori*"), phylospecies	IBT 26343 = CBS 102.12; IBT 26387 = NRRL 567; IBT 26392 = NRRL 2001; IBT 3277 = CBS 618.78; IBT 28086 = ITEM 7097; IBT 28861 = NRRL 320; IBT 29098; IBT 29882 = NRRL 362; IBT 29894 = NRRL 595; IBT 29881 = NRRL 4851; IBT 29879 = NRRL 340; IBT 29888 = NRRL 6408; IBT 29890 = NRRL 372; IBT 29895 = NRRL 604

Paper 5

"Isolation, structural analyses and biological activity assays against chronic lymphocytic leukemia of two novel cytochalasins, sclerotionigrin A and B"

Petersen LM.; Bladt, T.T.; Dürr, C.; Seiffert, M.; Frisvad, J.C.; Gotfredsen, C.H.; Larsen, T.O.

Molecules, **2014**, *19*, 9786-9797

Molecules **2014**, *19*, 9786-9797; doi:10.3390/molecules19079786

OPEN ACCESS

molecules

ISSN 1420-3049
www.mdpi.com/journal/molecules

Article

Isolation, Structural Analyses and Biological Activity Assays against Chronic Lymphocytic Leukemia of Two Novel Cytochalasins — Sclerotionigrin A and B

Lene M. Petersen [1], Tanja T. Bladt [1], Claudia Dürr [2], Martina Seiffert [2], Jens C. Frisvad [1], Charlotte H. Gotfredsen [3] and Thomas O. Larsen [1,*]

[1] Technical University of Denmark, Department of Systems Biology, Søltofts Plads B221, DK-2800 Kgs. Lyngby, Denmark; E-Mails: lmape@bio.dtu.dk (L.M.P.); ttb@bio.dtu.dk (T.T.B.); jcf@bio.dtu.dk (J.C.F.)

[2] German Cancer Research Center, Molecular Genetics, Im Neuenheimer Feld 280, D-69120 Heidelberg, Germany; E-Mails: C.Duerr@dkfz-heidelberg.de (C.D.); M.Seiffert@dkfz-heidelberg.de (M.S.)

[3] Technical University of Denmark, Department of Chemistry, Kemitorvet, B201, DK-2800 Kgs. Lyngby, Denmark; E-Mail: chg@kemi.dtu.dk

***** Author to whom correspondence should be addressed; E-Mail: tol@bio.dtu.dk; Tel.: +45-4525-2632; Fax: +45-4588-4922.

Received: 21 March 2014; in revised form: 24 June 2014 / Accepted: 2 July 2014 / Published: 8 July 2014

Abstract: Two new cytochalasins, sclerotionigrin A (**1**) and B (**2**) were isolated together with the known proxiphomin (**3**) from the filamentous fungus *Aspergillus sclerotioniger*. The structures and relative stereochemistry of **1** and **2** were determined based on comparison with **3**, and from extensive 1D and 2D NMR spectroscopic analysis, supported by high resolution mass spectrometry (HRMS). Compounds **2** and **3** displayed cytotoxic activity towards chronic lymphocytic leukemia cells *in vitro*, with **3** being the most active.

Keywords: cytochalasins; apergilli; *Apsergillus sclerotioniger*; chronic lymphocytic leukemia

1. Introduction

Chronic lymphocytic leukemia (CLL) is the most common type of leukemia among adults in the Western World. CLL is considered an incurable disease and today's applied treatment strategies

primarily aim at prolonging patient survival [1,2]. Consequently discovery of compounds that act against CLL and other types of cancer cells is crucial. Numerous types of anticancer compounds have been reported in the literature [3,4], and with the increase in specific biological assays, both novel and previously described compounds might display promising novel bioactivities [5,6]. An important and diverse group of fungal anticancer compounds that have caught our interest due to their wide range of biological functions are the cytochalasans [7]. In particular this includes inhibitory activities towards lung, ovarian, and human colon cancer as well as human leukemia [8,9]. Recently, we have demonstrated that chaetoglobosin A, produced by *Penicillium aquamarinum*, selectively induces apoptosis in CLL cells with a median lethal concentration (LC_{50}) value of 2.8 μM [10]. Encouraged by this finding we searched for potential novel cytochalasan type of compounds in black aspergilli.

The only documented indication of production of cytochalasans in *Aspergillus* subgenus *Circumdati* section *Nigri* is aspergillin PZ, for which aspochalasin C or D has been suggested as precursor [11,12]. However in the sister clade *Aspergillus* subgenus *Circumdati* section *Flavipedes*, numerous cytochalasans have been reported [13–26] including aspochalasin A–D [27,28]. Also in another species of *Aspergillus* subgenus *Circumdati* section *Circumdati*, *Aspergillus elegans* several cytochalasins were found, including aspergillin PZ [29], supporting the view that aspochalasin D is a precursor of aspergillin PZ. Finally in the less closely related *Aspergillus clavatus* in *Aspergillus* subgenus *Fumigati* section *Clavati*, cytochalasin E and K have been isolated [30,31].

Here we report the target-guided isolation and structure elucidation based on UV, MS, and NMR data of the two novel cytochalasins sclerotionigrin A (**1**) and B (**2**). Compounds **1** and **2** were isolated from *Aspergillus sclerotioniger* (IBT 22905) together with the known cytochalasin proxiphomin (**3**) [32]. We have previously reported ochratoxin A, ochratoxin B and pyranonigrin A from this isolate [33].

2. Results and Discussion

The structure of compound **3** (Figure 1) was tentatively identified through UHPLC-DAD-HRMS based dereplication of the crude extract. The pseudomolecular ion, $[M+H]^+$, was recognized from the mass spectrum due to the presence of the sodiated adduct, $[M+Na]^+$ and the corresponding dimeric adducts $[2M+H]^+$ and $[2M+Na]^+$. The molecular formula $C_{29}H_{37}NO_2$ was established with an accuracy of 0.8 ppm through the monoisotopic mass of $[M+H]^+$ of *m/z* 432.2901. The formula was used for a query in Antibase2012 [34] with one resulting hit, proxiphomin (**3**). NMR data and optical rotation of **3** matched published data [32].

Figure 1. Structures of sclerotionigrin A (**1**), sclerotionigrin B (**2**) and proxiphomin (**3**).

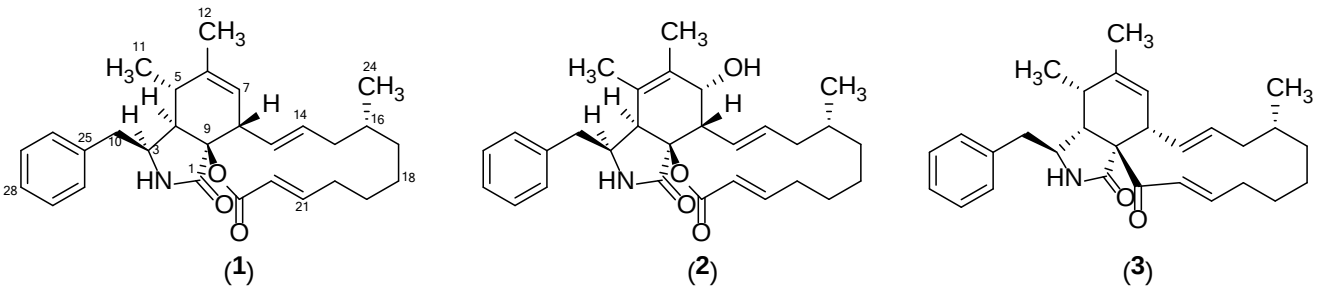

Compound **1** was purified as a yellow powder. The UV spectrum displayed an absorption maximum at 210 nm. The ESI^+ spectrum showed a distinct adduct pattern consisting of $[M+H]^+$, $[M+Na]^+$, $[2M+H]^+$ and $[2M+Na]^+$. The molecular formula $C_{29}H_{37}NO_3$ (12 double-bond equivalents) was obtained from HRMS of $[M+H]^+$ (*m/z* 448.2843) with an accuracy of 2.3 ppm. The ^{1}H-NMR spectrum revealed the presence of one amide proton, 15 methines (five which were vinylic and five aromatic), six methylenes, and three methyls (Table 1).

Table 1. NMR data for sclerotionigrin A (**1**) [†].

No.	δ_H (Integral, Mult., *J* [Hz])	δ_C	HMBC	NOESY
1	-	170.6	-	-
2	8.00 (1H, s)	-	1, 3, 4, 9	3, 10
3	3.09 (1H, td, 5.8, 3.1)	54.2	-	2, 4, 10, 11, 12, 26/30
4	2.53 (1H, dd, 4.2, 3.1)	49.1	3, 5, 6, 9	3, 10, 11, 26/30
5	2.57 (1H, m)	33.6	-	7, 8, 11
6	-	140.0	-	-
7	5.25 (1H, m)	123.6	-	5, 8, 12
8	3.15 (1H, m)	45.8	-	5, 7, 13, 14
9	-	85.4	-	-
10	2.82 (2H, m)	42.6	3, 4, 25, 26/30	3, 4, 26/30
11	0.68 (3H, d, 7.1)	12.8	4, 5, 6	3, 4, 5, 12, 26/30
12	1.65 (3H, s)	19.4	5, 6, 7	3, 7, 11
13	5.85 (1H, ddd, 14.8, 10.0, 1.2)	128.9	15	8, 15
14	5.22 (1H, m)	132.6	8	8, 15', 16
15	1.60 (1H, d, 13.5)	40.7	13, 14, 16	13, 15'
15'	2.07 (1H, dd, 13.5, 2.1)	40.7	-	14, 15, 16, 20', 24
16	1.36 (1H, m)	31.9	-	14, 15', 19'
17	0.61 (1H, m)	33.8	-	17', 18', 24
17'	1.66 (1H, m)	33.8	-	17
18	1.14 (1H, m)	25.9	-	18'
18'	1.53 (1H, m)	25.9	-	17, 18
19	1.29 (1H, m)	25.3	-	24
19'	1.68 (1H, m)	25.3	-	16, 21
20	2.23 (1H, m)	33.1	-	20', 21
20'	2.29 (1H, m)	33.1	-	15', 20, 22
21	6.96 (1H, ddd, 15.5, 8.6, 6.8)	151.7	23	19', 20, 22
22	5.65 (1H, d, 15.5)	120.6	20, 23	20', 21
23	-	163.5	-	-
24	0.84 (3H, d, 6.3)	20.0	15, 16, 17	15', 17, 19
25	-	137.8	-	-
26 [‡]	7.14 (1H, app. d, 7.5)	129.5	10, 26/30, 28	3, 4, 10, 11
27 [‡]	7.26 (1H, app. t, 7.4)	128.0	25, 29	-
28	7.18 (1H, app. t, 7.5)	126.1	26, 30	-
29 [‡]	7.26 (1H, app. t, 7.5)	128.0	25, 27	-
30 [‡]	7.14 (1H, app. d, 7.5)	129.5	10, 26/30, 28	3, 4, 10, 11

[†] ^{1}H NMR data were obtained at 500 MHz in DMSO-d_6 and ^{13}C data were obtained at 125 MHz in DMSO-d_6. ^{13}C-NMR chemical shifts were determined from HSQC and HMBC experiments; [‡] It was not possible to distinguish between No. 26 and 30 as well as No. 27 and 29.

The DQF-COSY spectrum of **1** defined four spin systems. The linking between COSY spin systems and assignments of the remaining signals and quaternary carbons were accomplished through detailed analysis of HMBC experimental data (Figure 2).

Figure 2. Important HMBC correlations connecting the four COSY spin systems (marked in bold) in **1**. The remaining HMBC correlations are found in Table 1.

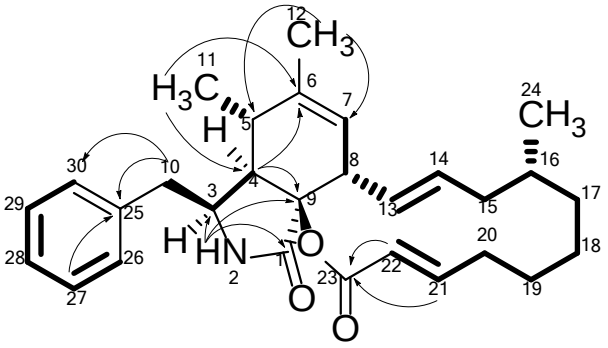

1

The HMBC correlations from the protons at δ_H 2.82 ppm (H10) and 7.26 (H27 and H29) to a quaternary carbon at δ_C 137.8 (C25), together with HMBC correlations from the protons at δ_H 7.14 (H26 and H30) to the carbon at δ_C 42.6 (C10) linked two of the spin systems belonging to the Phe moiety in **1**. The amide proton at δ_H 8.00 ppm (H2) displayed HMBC correlations to the carbons at δ_C 54.2 (C3) and 170.6 ppm (C1). Combination of these HMBC correlations established the Phe moiety of **1**, which was incorporated on the polyketide (PK) part of the molecule.

The PK part of **1** could be established through a large COSY spin system (from H7 to H22), equal to that seen in **3**. Furthermore a COSY coupling was found between the proton at δ_H 2.57 ppm (H5) and a methyl group at 0.68 ppm (H11). This part was coupled to the PK part by a weak COSY coupling between H5 and H7 identified as a ^4J alyllic coupling. The COSY spin system could furthermore be connected via HMBC correlations to the above mentioned Phe moiety as well as the PK part. The protons at δ_H 1.65 (H12) correlated to the carbons at δ_C 33.6 (C5) and 123.6 ppm (C7) where the proton at δ_H 0.68 (H11) correlated to the carbons at δ_C 49.1 (C4) and 140.0 ppm (C6). The proton at 2.53 ppm (H4) correlated to C5, C6 and the quaternary carbon at δ_C 85.4 ppm (C9). Finally the PK chain was closed via an ester bond assigned from HMBC correlations from the vinylic protons at δ_H 5.65 (H22) and 6.96 ppm (H21) to the carbonyl carbon at δ_C 163.5 ppm (C23) supported by the high chemical shift of the quaternary carbon at δ_C 85.4 ppm (C9) indicating that C9 is bound to oxygen, and a carbonyl group, similar to what is seen in several other cytochalasans [7].

This structure accounted for all the degree of unsaturation required by the formula allowing the assignment of **1** as sclerotionigrin A. The size of the vicinal coupling constants ($^3J_{HH}$) for H13/H14 and H21/H22 were rather large (14.8 and 15.5 Hz respectively) suggesting a *trans* stereochemistry. NOESY experiments enabled determination of the relative stereochemistry for most of the stereogenic centers of **1**. NOE connectivities were found between the proton at δ_H 3.09 ppm (H3), δ_H 2.53 (H4) and the methyl at δ_H 0.68 ppm (H11) placing these protons at the same side of the central ring system, which to the best of our knowledge has not been reported for other cytachalasins. Other NOE connectivities were observed between the protons at δ_H 2.57 ppm (H5), 5.25 (H7) and 3.15 (H8),

whereas no NOE connectivities could be seen from either of these to H3, H4 or H11, strongly indicating the positioning of H5, H7 and H8 on the opposite side of the central ring system compared to H3, H4 and H11. The stereocenters at C9 and C16 could not be assigned through NOESY connectivities; however being biosynthesized by the same fungus we propose that the stereochemistries at these centers are identical to those of **3**. Especially we note that the extra oxidation between C9 and C23 in other cytochalasans never leads to a change in stereochemistry at C9 [7,15]. We do however note that the optical rotation of **1** and **2** are positive as opposed to that of **3** and other similar cytochalasans [15], indicating a possible difference in stereochemistry, which could be accounted for by the change of stereochemistry at C4. Further experiments, e.g., X-ray crystallography or circular dichroism (CD) are therefore needed to clarify the absolute stereochemistry of **1**.

Compound **2** was isolated as a yellow powder, and displayed a UV absorption maximum at 212 nm and the ESI$^+$ MS adducts $[M+H]^+$, $[M+Na]^+$, $[2M+H]^+$ and $[2M+Na]^+$. The molecular formula of **2**, $C_{29}H_{37}NO_4$ was deduced from the monoisotopic mass obtained from the $[M+H]^+$ ion (*m/z* 464.2797) with an accuracy of 1.2 ppm. Examination of the NMR spectra of **2** displayed a high similarity compared to **1**. Comparison of the NMR spectra of **1** and **2** (see Tables 1 and 2, respectively) revealed that the difference between them is located in positions five, six and seven. The Phe moiety in **2** was identified through a connection of the two COSY spin systems linked by HMBC correlations as demonstrated for **1**. The COSY spin system of the PK chain terminated with a proton at δ_H 3.68 ppm (H7), indicating a binding to a hydroxyl group instead of the vinylic methine group observed for **1** at this position. This was also evident from the carbon chemical shift moving to δ_C 69.1 ppm (C7).

HMBC correlations from the three protons of the methyl group at δ_H 1.52 ppm (H12) to the carbons at δ_C 123.9 (C5), 134.2 (C6) and 69.1 (C7), combined with correlations from the protons at δ_H 1.16 ppm (H11) to the carbons at δ_C 47.1 (C4) and 123.9 ppm (C5) and 134.2 (C6) linked the Phe moiety to the spin system in the polyketide chain (Figure 3). The remaining chemical shifts in **2** matched the chemical shifts of **1** (Tables 1 and 2) and the structure of **2** was established altogether giving a classic methylated cytochalasin carbon skeleton [7].

The relative stereochemistry of **2** was established partly through NOE connectivities (Table 2) and shown to be very similar to that of **1**. Connectivities between H3 and H4 were however not confirmed in **2**, since these resonances were overlapping with the water resonance (Supplementary Figure S10). The optical rotation of **2** was positive like the optical rotation of **1**, also indicating that the two compounds have the same relative stereochemistry. The absolute stereochemistry of **2** has not yet been solved.

Biological testing of the cytotoxicity of compounds **1**–**3** towards CLL cells *in vitro* was performed using a CellTiter-Glo® assay [10]. Compound **3** displayed the strongest effects, with estimated LC_{50} values of ca. 48 µM whereas no effect was found towards healthy B-cells in concentrations <100 µM. Compounds **1** showed minor activity at a concentration of 72 µM, while **2** did not have any effect (Table 3 and Supplementary Table S2, Figures S17, S18), indicating that the novel stereochemistry in the central ring system of **1** and **2** has a negative effect on target interactions. Due to the low anticancer activities of the sclerotionigrins, no further investigations proving their exact mode of action were undertaken.

Table 2. NMR data for sclerotionigrin B (2) [†].

No.	δ_H (Integral, Mult., *J* [Hz])	δ_C	HMBC	NOESY
1	-	171.2	-	-
2	8.34 (1H, br. s)	-	3, 4, 9	3, 10'
3	3.39 (1H, m)	57.7	1, 4, 5, 9	2, 10, 10', 11, 26/30
4	3.32 (1H, m)	47.1	1, 5, 6, 9	13, 26/30
5	-	123.9	-	-
6	-	134.2	-	-
7	3.68 (1H, d, 9.7)	69.1	-	8, 12, 13
8	3.05 (1H, t, 10.0)	48.3	1, 4, 7, 9, 13, 14	7, 13, 14
9	-	83.6	-	-
10	2.55 (1H, dd, 13.0, 10.1)	42.5	3, 4, 25, 26/30	3, 10', 26/30
10'	2.92 (1H, dd, 13.0, 5.0)	42.5	3, 4, 25, 26/30	2, 3, 10, 26/30
11	1.16 (3H, s)	16.7	4, 5, 6	3, 26/30
12	1.52 (3H, s)	14.3	5, 6, 7	7
13	6.03 (1H, dd, 15.0, 11.3)	128.4	8, 15/15’	4, 7, 8, 14, 15
14	5.00 (1H, ddd, 15.0, 10.8, 3.4)	132.7	8, 15/15’	8, 13, 15, 15'
15	1.58 (1H, dt, 13.0, 11.1)	41.6	16	13, 14, 15', 16, 17'
15'	2.00 (1H, m)	41.6	-	14, 15, 16, 24
16	1.13 (1H, m)	32.5	-	15, 15', 17', 18, 24
17	0.52 (1H, m)	34.5	-	17'
17'	1.67 (1H, m)	34.5	24	15, 16, 17, 18, 24
18	0.86 (1H, m)	26.1	-	16, 17', 18'
18'	1.68 (1H, m)	26.1	20	18, 19, 21
19	1.30 (1H, m)	25.4	-	18', 19'
19'	1.73 (1H, m)	25.4	-	19
20	2.11 (1H, m)	33.4	-	20', 22
20'	2.41 (1H, m)	33.4	-	20, 21
21	6.89 (1H, ddd, 15.7, 10.8, 5.0)	151.4	20, 23	18', 20', 22
22	5.79 (1H, d, 16.1)	121.3	20, 23	20, 21
23	-	163.8	-	-
24	0.83 (3H, d, 6.6)	19.9	15, 16, 17	15', 16, 17'
25	-	137.4	-	-
26 [‡]	7.08 (1H, app. d, 7.1)	128.9	10, 28, 30	3, 4, 10, 10', 11, 27/29
27 [‡]	7.31 (1H, app. t, 7.5)	128.2	25, 29	26/30, 28
28	7.23 (1H, app. t, 7.4)	126.3	26, 30	27/29
29 [‡]	7.31(1H, app. t, 7.5)	128.2	25, 27	26/30, 28
30 [‡]	7.08 (1H, app. d, 7.1)	128.9	10, 26, 28	3, 4, 10, 10',11, 27/29

[†] ^{1}H-NMR data were obtained at 500 MHz in DMSO-d_6 and ^{13}C data were obtained at 125 MHz in DMSO-d_6. ^{13}C-NMR chemical shifts were determined from HSQC and HMBC experiments; [‡]It was not possible to distinguish between no. 26 and 30 as well as no. 27 and 29. The hydroxyl group at C7 is not observed, presumable because it overlaps with the water resonance.

Figure 3. Important HMBC correlations establishing the quaternary carbon C5 and C6 in **2**. The remaining HMBC correlations are found in Table 2. Individual COSY spin systems are marked in bold.

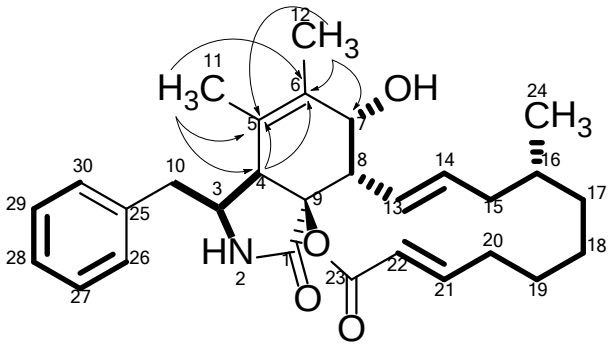

2

Table 3. Estimated LC_{50} values for compound **1**–**3**.

Compound	CLL	Healthy B-Cells
Sclerotionigrin A (**1**)	72 µM	No effect
Sclerotionigrin B (**2**)	No effect	No effect
Proxiphomin (**3**)	48 µM	No effect

3. Experimental Section

3.1. Fungal Growth and Extraction

Aspergillus sclerotioniger (IBT 22905 = CBS 115572) is from the IBT culture collection at Department of Systems Biology, Technical University of Denmark. *A. sclerotioniger* was inoculated as three point inoculations on Czapek yeast agar (CYA) on 100 plates at 25 °C for 7 days in the dark. CYA plates were prepared as described by Samson *et al.* [35]. The plates were harvested and extracted twice overnight with ethyl acetate (EtOAc) containing 1% formic acid (FA). The extracts were filtered and concentrated *in vacuo*. Work up: The combined extract was dissolved in methanol (MeOH)/ milliQ-water (water purified and deionized by a Millipore system through 0.22 µm membrane filter) (9:1) and an equal amount of heptane was added followed by separation of phases. Additional milliQ-water was added to the MeOH/water phase until a ratio of 1:1 was reached, and metabolites were extracted with dichloromethane (DCM). The phases were then concentrated separately *in vacuo*. The DCM phase was used for further fractionation.

3.2. Preparative Isolation of Cytochalasins

The extract was dry-loaded on diol resin and fractionated on a 50 g pre-packed diol column using an Isolera One automated flash purification system (Biotage, Uppsala, Sweden). The compounds were eluted using a seven step gradient of heptane-DCM-EtOAc-MeOH with a flow rate of 40 mL/min. Fractions were collected automatically (1 column volume in each fraction). The Isolera fractions were subjected to further purification on a semi-preparative HPLC Waters 600 Controller with a 996 photodiode array detector (Waters, Milford, MA, USA) on a Luna II C_{18} column 250 × 10 mm, 5 µm (Phenomenex, Torrance, CA, USA). A flowrate of 5 mL/min was used and 50% acetonitrile (ACN)

isocratic for 5 min, then to 100% in 15 min. 50 ppm trifluoroacetic acid (TFA) was added to ACN and milliQ-water. This yielded **1** (7.8 mg), **2** (2.1 mg), and **3** (1.3 mg).

Sclerotionigrin A (**1**) Yellow solid; $[\alpha]_{589.3nm}$: +4° (*c* 0.8, MeOH); UV (ACN) λ_{max}: 210 nm; HRMS *m/z* 448.2843 ($[M + H]^+$ calculated for $C_{29}H_{38}NO_3$, *m/z* 448.2853; 2.3 ppm); ^{13}C- and ^{1}H-NMR: see Table 1.

Sclerotionigrin B (**2**) Yellow solid; $[\alpha]_{589.3nm}$: +41° (*c* 0.2, MeOH); UV (ACN) λ_{max}: 212 nm; HRMS *m/z* 464.2797 ($[M + M]^+$ calculated for $C_{29}H_{38}NO_4$, *m/z* 463.2724; 1.2 ppm); ^{13}C- and ^{1}H-NMR: see Table 2.

Proxiphomin (**3**) Yellow solid; $[\alpha]_{589.3nm}$: −21° (*c* 0.1, MeOH); UV (ACN) λ_{max}: 244 nm; HRMS *m/z* 432.2901 ($[M + H]^+$ calculated for $C_{29}H_{38}NO_2$, *m/z* 432.2904; 0.8 ppm); ^{1}H-NMR (DMSO-d_6, 500 MHz): δ 0.77 (3H, d, 7.2, H11), 0.85 (3H, d, 6.7, H24), 1.13 (2H, m, H18), 1.23 (2H, m, H17), 1.38 (1H, m, H16), 1.41 (1H, m, H19), 1.56 (1H, m, H19'), 1.66 (3H, s, H12), 1.67 (1H, m, H15), 1.99 (1H, m,, H15'), 2.02 (1H, m, H20), 2.20 (1H, m, H5), 2.28 (1H, m, H20'), 2.40 (1H, dd, 13.2, 7.3, H10), 2.60 (1H, dd, 13.2, 4.9, H10'), 2.63 (1H, m, H8), 2.80 (1H, dd, 5.8, 2.6, H4), 3.25 (1H, m, H3), 5.11 (1H, ddd, 14.6, 10.3, 3.2, H14), 5.27 (1H, m, H7), 6.18 (1H, ddd, 15.2, 9.8, 1.7, H13), 6.54 (1H, ddd, 15.4, 10.2, 5.3, H21), 6.86 (1H, d, 15.5, H22), 7.10 (1H, d, 7.5, H26), 7.10 (1H, d, 7.5, H30), 7.16 (1H, d, 7.5, H28), 7.25 (1H, dd, 7.4, 1.0, H27), 7.25 (1H, dd, 7.4, 1.0, H29), 7.94 (1H, s, H2). ^{13}C-NMR (DMSO-d_6, 125 MHz) δ 12.6 (C11), 19.3 (C12), 20.8 (C24), 23.1 (C18), 25.2 (C19), 28.5 (C17), 31.1 (C20), 31.9 (C16), 33.7 (C5), 39.7 (C15), 43.1 (C10), 47.0 (C8), 47.2 (C4), 53.0 (C3), 65.7 (C9), 125.8 (C7), 126.0 (C28), 127.3 (C22), 127.9 (C27), 127.9 (C29), 129.3 (C13), 129.5 (C26), 129.5 (C30), 131.6 (C14), 136.7 (C25), 139.1 (C6), 145.7 (C21), 173.6 (C1), 196.9 (C23).

3.3. Chemical Analysis

Analysis of extracts was performed using ultra-high-performance liquid chromatography (UHPLC) UV/Vis diode array detector (DAD) high-resolution MS on a maXis 3G orthogonal acceleration quadrupole time of flight mass spectrometer (Bruker Daltonics, Bremen, Germany) equipped with an electrospray ionization (ESI) source and connected to an Ultimate 3000 UHPLC system (Dionex, Sunnyvale, CA, USA). The mass spectrometer was calibrated using sodium formate automatically infused prior to each analytical run, providing a mass accuracy below 1 ppm. Separation was achieved on a Kinetex C_{18}, 2.6 µm, 2.1 × 100 mm column (Phenomenex) with a flow rate of 0.4 mL·min^{-1} at 40 °C using a linear gradient 10% ACN in milliQ water going to 100% ACN in 10 min. Both solvents were buffered with 20 mM formic acid.

3.4. NMR and Optical Roation

One-dimensional and two-dimensional NMR experiments were acquired on a 500 MHz Varian Unity Inova (Palo Alto, CA, USA) equipped with a HCP probe. 1H, DQF-COSY, edHSQC, HMBC and NOESY experiments were acquired using standard pulse sequences. Optical rotation values were obtained on a Perkin-Elmer 241 Polarimeter at 589 nm.

3.5. CLL Cells, Cell Viability and Apoptosis Assays

Whole blood samples were obtained from healthy donors or patients that matched the standard diagnostic criteria for CLL after informed consent in accordance with the Declaration of Helsinki. All studies performed were approved by the ethics committee of the University of Ulm. Peripheral blood B cells were isolated by Ficoll density gradient followed by magnetic cell enrichment using CD19-MACS beads (Miltenyi Biotech, Bergisch Gladbach, Germany). Healthy donor B cells or CLL cells were cultured in conditioned medium of HS-5 cells, which was harvested after 3–4 days of culture and 80% confluency and depleted of HS-5 cells and debris by centrifugation. Cells were seeded in duplicates at a density of 3×10^5 cells/well in opaque-walled 96-well plates. Pure compounds were added in different concentrations and incubated for 24 h. A final concentration of 0.1% DMSO was used as negative control and 100 µM fludarabine as positive control. Cell viability was assessed using CellTiter-Glo® assay (Promega, Madison, WI, USA) according to manufacturer's protocol. Luminescence signals were recorded using a Mithras LB940 plate reader (Berthold Technologies, Bad Wildbad, Germany). Relative cell viability was calculated as described by Knudsen *et al.* [10]. All compounds were tested on the same patient cells under the same conditions. For patient data, see Supplementary Table S2, Figures S17, S18.

4. Conclusions

In summary the two new cytochalasins, sclerotionigrin A (**1**) and B (**2**) have been isolated from *A. sclerotioniger*, together with the known proxiphomin (**3**). Compound **3** displayed the strongest cytotoxic effects towards CLL, however not as promising as recently demonstrated for chaetoglobosin A [10]. This is the first report of cytochalasan production from one of the currently more than twenty-five known black *Aspergillus* species [36,37], even though cytochalasans are very common in the related yellow *Aspergillus* species such as *A. flavipes*, *A. terreus* and *A. elegans* [29,38]. Further species in *Aspergillus* section *Nigri* should be examined for cytochalasan production, as the cytochalasan related metabolite, aspergillin PZ, has also been found in this group in addition to proxiphomin, and sclerotionigrin A and B. This may be important for both drug discovery and food safety, as the black Aspergilli are common in foods.

Supplementary Materials

^{1}H, DQF-COSY, HSQC, HMBC and NOESY spectra for all three compounds, as well as bioassay results are available in the supporting information. Supplementary materials can be accessed at: http://www.mdpi.com/1420-3049/19/7/9786/s1.

Acknowledgments

The study was supported by the Danish Council for Independent Research, Technology, and Production Sciences (grant # 09-064967), and The Novo Nordic Foundation.

Author Contributions

L.M.P. isolated and elucidated the structures of the compounds and wrote the paper. T.T.B. assisted in structural elucidation. C.D. and M.S. planned and performed the anticancer bioactivity testing. J.C.F. performed comparative *Aspergillus* chemistry studies. C.H.G. assisted with structural elucidations. T.O.L. planned the study and guided structural elucidations and preparation of the manuscript.

Conflicts of Interest

The authors declare no conflict of interest.

References

1. Zenz, T.; Mertens, D.; Küppers, R.; Döhner, H.; Stilgenbauer, S. From pathogenesis to treatment of chronic lymphocytic leukaemia. *Nat. Rev. Cancer* **2010**, *10*, 37–50.
2. Burger, J.A.; Montserrat, E. Coming full circle: 70 years of chronic lymphocytic leukemia cell redistribution, from glucocorticoids to inhibitors of B-cell receptor signaling. *Blood* **2013**, *121*, 1501–1509.
3. Frisvad, J.C.; Smedsgaard, J.; Larsen, T.O.; Samson, R.A. Mycotoxins, drugs and other extrolites produced by species in *Penicillium* subgenus *Penicillium*. *Stud. Mycol.* **2004**, *49*, 201–241.
4. Bladt, T.T.; Frisvad, J.C.; Knudsen, P.B.; Larsen, T.O. Anticancer and antifungal compounds from *Aspergillus*, *Penicillium* and other filamentous fungi. *Molecules* **2013**, *18*, 11338–11376.
5. Rebacz, B.; Larsen, T.O.; Clausen, M.H.; Rønnest, M.H.; Löffler, H.; Ho, A.D.; Krämer, A. Identification of griseofulvin as an inhibitor of centrosomal clustering in a phenotype-based screen. *Cancer Res.* **2007**, *67*, 6342–6350.
6. Liao, W.-Y.; Shen, C.-N.; Lin, L.-H.; Yang, Y.-L.; Han, H.-Y.; Chen, J.-W.; Kuo, S.-C.; Wu, S.-H.; Liaw, C.-C. Asperjinone, a nor-neolignan, and terrein, a suppressor of ABCG2-expressing breast cancer cells, from thermophilic *Aspergillus terreus*. *J. Nat. Prod.* **2012**, *75*, 630–635.
7. Schümann, J.; Hertweck, C. Molecular basis of cytochalasan biosynthesis in fungi: Gene cluster analysis and evidence for the involvement of a PKS-NRPS hybrid synthase by RNA silencing. *J. Am. Chem. Soc.* **2007**, *129*, 9564–9565.
8. Wagenaar, M.M.; Corwin, J.; Strobel, G.; Clardy, J. Three new cytochalasins produced by an endophytic fungus in the genus *Rhinocladiella*. *J. Nat. Prod.* **2000**, *63*, 1692–1695.
9. Liu, R.; Gu, Q.; Zhu, W.; Cui, C.; Fan, G.; Fang, Y.; Zhu, T.; Liu, H. 10-Phenyl-[12]-cytochalasins Z7, Z8, and Z9 from the marine-derived fungus *Spicaria elegans*. *J. Nat. Prod.* **2006**, *69*, 871–875.
10. Knudsen, P.B.; Hanna, B.; Ohl, S.; Sellner, L.; Zenz, T.; Döhner, H.; Stilgenbauer, S.; Larsen, T.O.; Lichter, P.; Seiffert, M. Chaetoglobosin A preferentially induces apoptosis in chronic lymphocytic leukemia cells by targeting the cytoskeleton. *Leukemia* **2014**, *28*, 1289–1298.
11. Zhang, Y.; Wang, T.; Pei, Y.; Hua, H.; Feng, B. Aspergillin PZ, a novel isoindole-alkaloid from Aspergillus awamori. *J. Antibiot. (Tokyo)* **2002**, *55*, 693–695.

12. Canham, S.M.; Overman, L.E.; Tanis, P.S. Identification of an Unexpected 2-Oxonia[3,3]sigmatropic Rearrangement/Aldol Pathway in the Formation of Oxacyclic Rings. Total Synthesis of (+)-Aspergillin PZ. *Tetrahedron* **2011**, *67*, 9837–9843.
13. Naruse, N.; Yamamoto, S.; Yamamoto, H. β-cyanoglutamic acid, a new antifungal amino acid from a streptomycete. *J. Antibiot. (Tokyo)* **1993**, *46*, 685–686.
14. Fang, F.; Ui, H.; Shiomi, K.; Masuma, R.; Yamaguchi, Y.; Zhang, C.G.; Zhang, X.W.; Tanaka, Y.; Omura, S. Two new components of the aspochalasins produced by *Aspergillus* sp. *J. Antibiot. (Tokyo)* **1997**, *50*, 919–925.
15. Choo, S.-J.; Yun, B.-S.; Ryoo, I.-J.; Kim, Y.-H.; Bae, K.-H.; Yoo, I.-D. Aspochalasin I, a Melanogenesis Inhibitor from *Aspergillus* sp. *J. Microbiol. Biotechnol.* **2009**, *19*, 368–371.
16. Zhou, G.-X.; Wijeratne, K.E.M.; Bigelow, D.; Pierson, L.S.; VanEtten, H.D.; Gunatilaka, L.A.A. Aspochalasins I, J, and K: Three new cytotoxic cytochalasans of *Aspergillus flavipes* from the rhizosphere of Ericameria laricifolia of the Sonoran Desert. *J. Nat. Prod.* **2004**, *67*, 328–332.
17. Rochfort, S.; Ford, J.; Ovenden, S.; George, S.; Wildman, H.; Tait, R.M.; Meurer-Grimes, B.; Coxd, S.; Coatesd, J.; Rhodes, D. A novel aspochalasin with HIV-1 integrase inhibitory activity from *Aspergillus flavipes. J. Antibiot. (Tokyo)* **2005**, *58*, 279–283.
18. Liu, J.; Hu, Z.; Huang, H.; Zheng, Z.; Xu, Q. Aspochalasin U, a moderate TNF-α inhibitor from *Aspergillus* sp. *J. Antibiot. (Tokyo)* **2012**, *65*, 49–52.
19. Kohno, J.; Nonaka, N.; Nishio, M.; Ohnuki, T.; Kawano, K.; Okuda, T.; Komatsubara, S. TMC-169, a new antibiotic of the aspochalasin group produced by Aspergillus flavipes. *J. Antibiot. (Tokyo)* **1999**, *52*, 575–577.
20. Gebhardt, K.; Schimana, J.; Holitzel, A.; Dettner, K.; Draeger, S.; Beil, W.; Rheinheimer, J.; Fiedler, H.-P. Aspochalamins A-D and aspochalasin Z produced by the endosymbiotic fungus *Aspergillus niveus* LU 9574. *J. Antibiot. (Tokyo)* **2004**, *57*, 707–714.
21. Barrow, C.; Sedlock, D.; Sun, H.; Cooper, R.; Gillum, A.M. WIN 66306, a new neurokinin antagonist produced by an *Aspergillus* species: Fermentation, isolation and physico-chemical properties. *J. Antibiot. (Tokyo)* **1994**, *47*, 1182–1187.
22. Fujishima, T.; Ichikawa, M.; Ishige, H.; Yoshino, H.; Ohishi, J.; Ikegami, S. Production of cytochalasin E by Aspergillus terreus. *Hakkokogaku Kaishi–J. Soc. Ferment. Technol.* **1979**, *57*, 15–19.
23. Lin, Z.; Zhang, G.; Zhu, T.; Liu, R.; Wei, H.-J.; Gu, Q.-Q. Bioactive cytochalasins from Aspergillus flavipes, an endophytic fungus associated with the mangrove plant *Acanthus ilicifolius*. *Helv. Chim. Acta* **2009**, *92*, 1538–1544.
24. Ge, H.M.; Peng, H.; Guo, Z.K.; Cui, J.T.; Song, Y.C.; Tan, R.X. Bioactive alkaloids from the plant endophytic fungus *Aspergillus terreus. Planta Med.* **2010**, *76*, 822–824.
25. Zhang, H.-W.; Zhang, J.; Hu, S.; Zhang, Z.-J.; Zhu, C.-J.; Ng, S.W.; Tan, R.-X. Ardeemins and cytochalasins from *Aspergillus terreus* residing in *Artemisia annua*. *Planta Med.* **2010**, *76*, 1616–21.
26. Xiao, L.; Liu, H.; Wu, N.; Liu, M.; Wei, J.; Zhang, Y.; Lin, X. Characterization of the high cytochalasin E and rosellichalasin producing-*Aspergillus* sp. nov. F1 isolated from marine solar saltern in China. *World J. Microbiol. Biotechnol.* **2013**, *29*, 11–17.

27. Keller-Schierlein, W.; Kupfer, E. Metabolites of microorganisms. 186. The aspochalasins A, B, C, and D. *Helv. Chim. Acta* **1979**, *62*, 1501–1524.
28. Tomikawa, T.; Kazuo, S.; Seto, H.; Okusa, N.; Kajiura, T.; Hayakawa, Y. Structure of aspochalasin H, a new member of the aspochalasin family. *J. Antibiot. (Tokyo)* **2002**, *55*, 666–668.
29. Zheng, C.-J.; Shao, C.-L.; Wu, L.-Y.; Chen, M.; Wang, K.-L.; Zhao, D.-L.; Sun, X.-P.; Chen, G.-Y.; Wang, C.-Y. Bioactive phenylalanine derivatives and cytochalasins from the soft coral-derived fungus, *Aspergillus elegans*. *Mar. Drugs* **2013**, *11*, 2054–2068.
30. Büchi, G.; Kitaura, Y.; Yuan, S. Structure of cytochalasin E, a toxic metabolite of *Aspergillus clavatus*. *J. Am. Chem. Soc.* **1973**, *95*, 5423–5425.
31. Steyn, P.S.; van Heerden, F.R.; Rabie, C. Cytochalasin-E and cytochalasin-K, toxic metabolites from Aspergillus clavatus. *J. Am. Chem. Soc. Perkin 1* **1982**, 541–544, doi:10.1039/P19820000541.
32. Binder, M.; Tarnrn, C. Proxiphomin and Protophomin, 2 new cytochalasanes. *Helv. Chim. Acta* **1973**, *7*, 2387–2396.
33. Samson, R.; Houbraken, J.; Kuijpers, A. New ochratoxin A or sclerotium producing species in *Aspergillus* section Nigri. *Stud. Mycol.* **2004**, *2*, 45–61.
34. Laatsch, H. Antibase 2012. Available online: http://www.wiley-vch.de/stmdata/antibase.php (accessed on 1 February 2014).
35. Samson, R.A.; Houbraken, J.; Thrane, U.; Frisvad, J.C.; Andersen, B. *Food and Indoor Fungi*; CBS-KNAW Fungal Biodiversity Centre Utrecht: Utrecht, The Netherlands, 2010; pp. 372–374.
36. Varga, J.; Frisvad, J.C.; Kocsubé, S.; Brankovics, B.; Tóth, B.; Szigeti, G.; Samson, R.A. New and revisited species in *Aspergillus* section *Nigri*. *Stud. Mycol.* **2011**, *69*, 1–17.
37. Jurjević, Z.; Peterson, S.W.; Stea, G.; Solfrizzo, M.; Varga, J.; Hubka, V.; Perrone, G. Two novel species of *Aspergillus* section *Nigri* from indoor air. *IMA Fungus* **2012**, *3*, 159–173.
38. Scherlach, K.; Boettger, D.; Remme, N.; Hertweck, C. The chemistry and biology of cytochalasans. *Nat. Prod. Rep.* **2010**, *27*, 869–886.

Sample Availability: Not available.

Supplementary Material

Figure S1. ^{1}H-NMR spectrum for Sclerotionigrin A (1) at 500 MHz in DMSO-d_6.

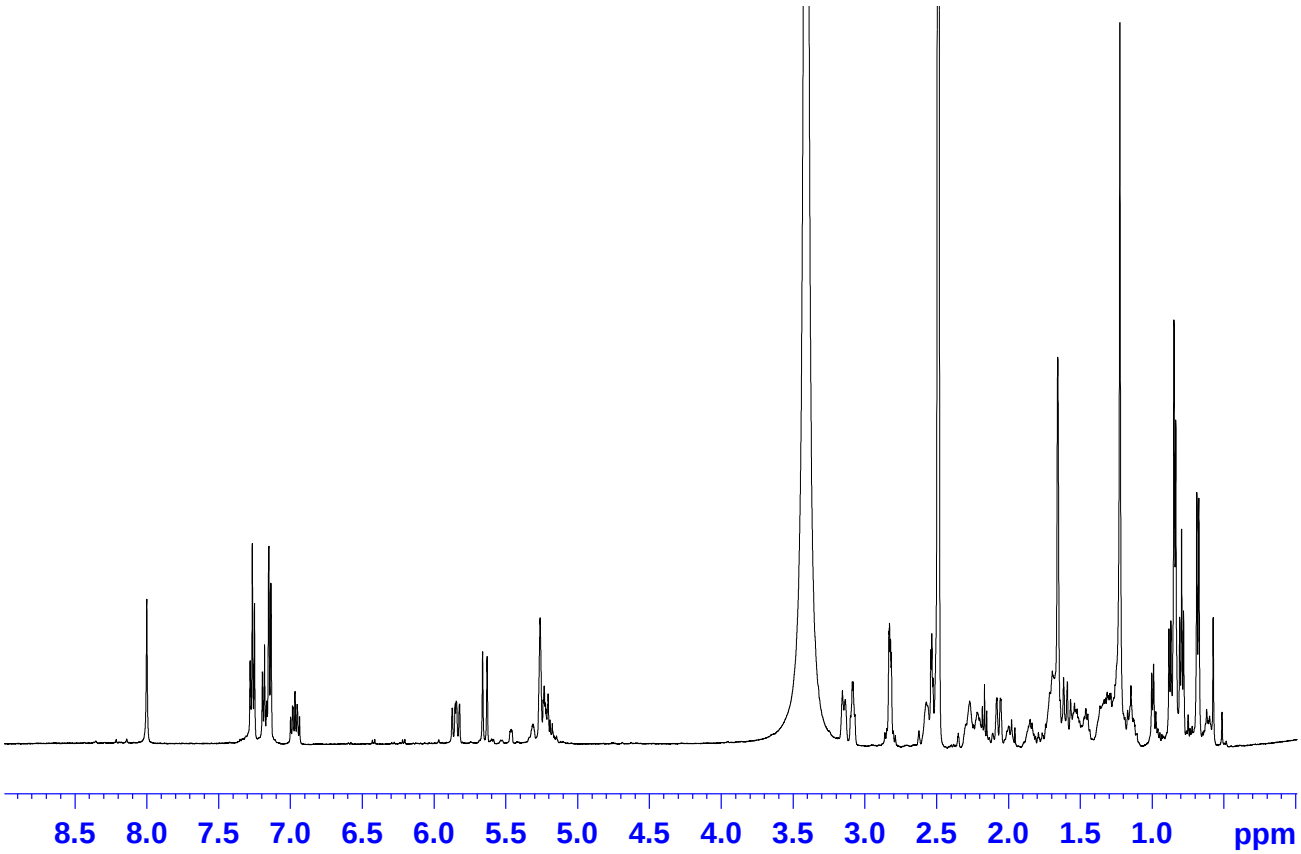

Figure S2. DQF-COSY spectrum for Sclerotionigrin A (1) in DMSO-d_6.

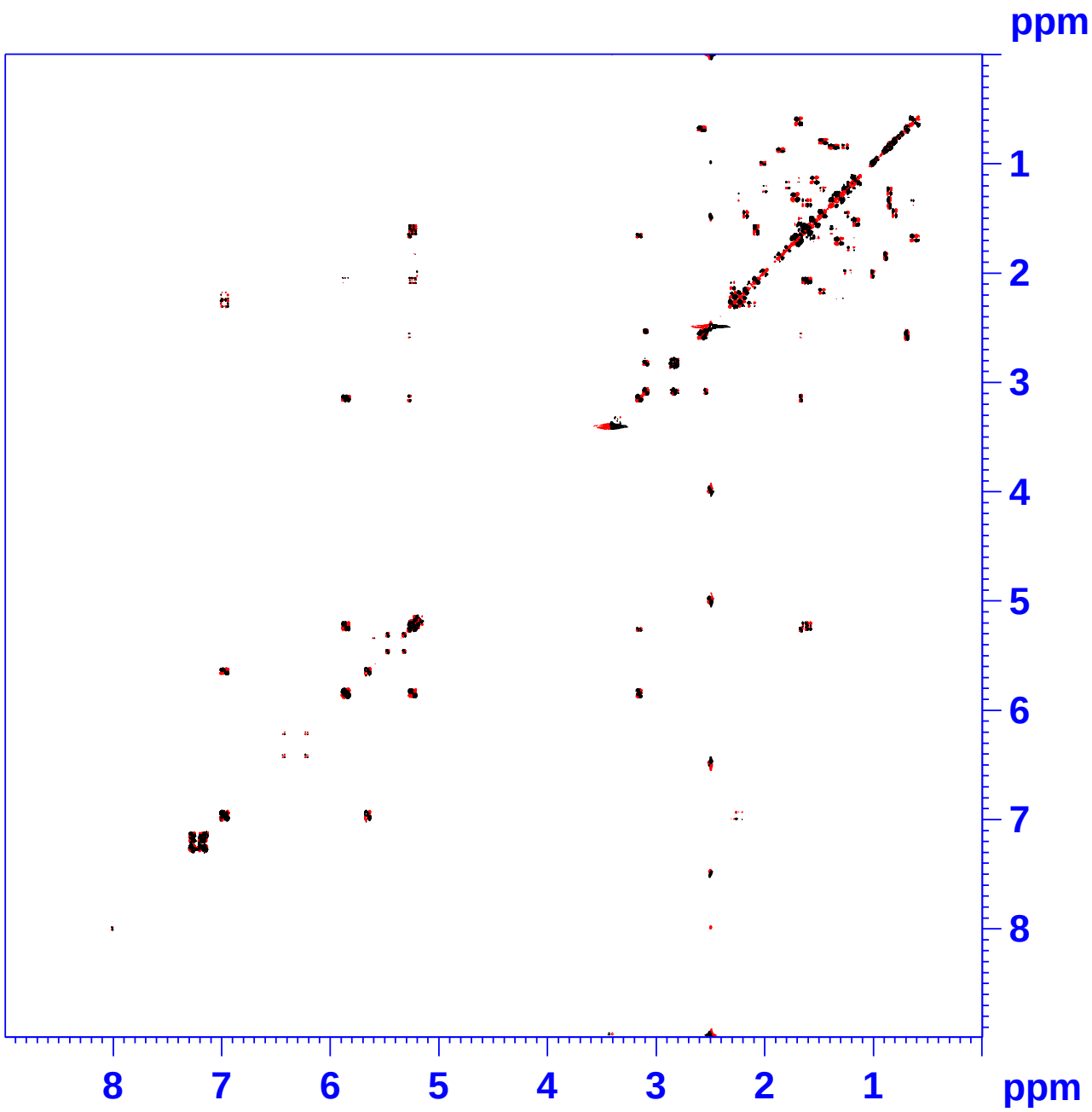

Figure S3. edHSQC spectrum for Sclerotionigrin A (1) in DMSO-d_6

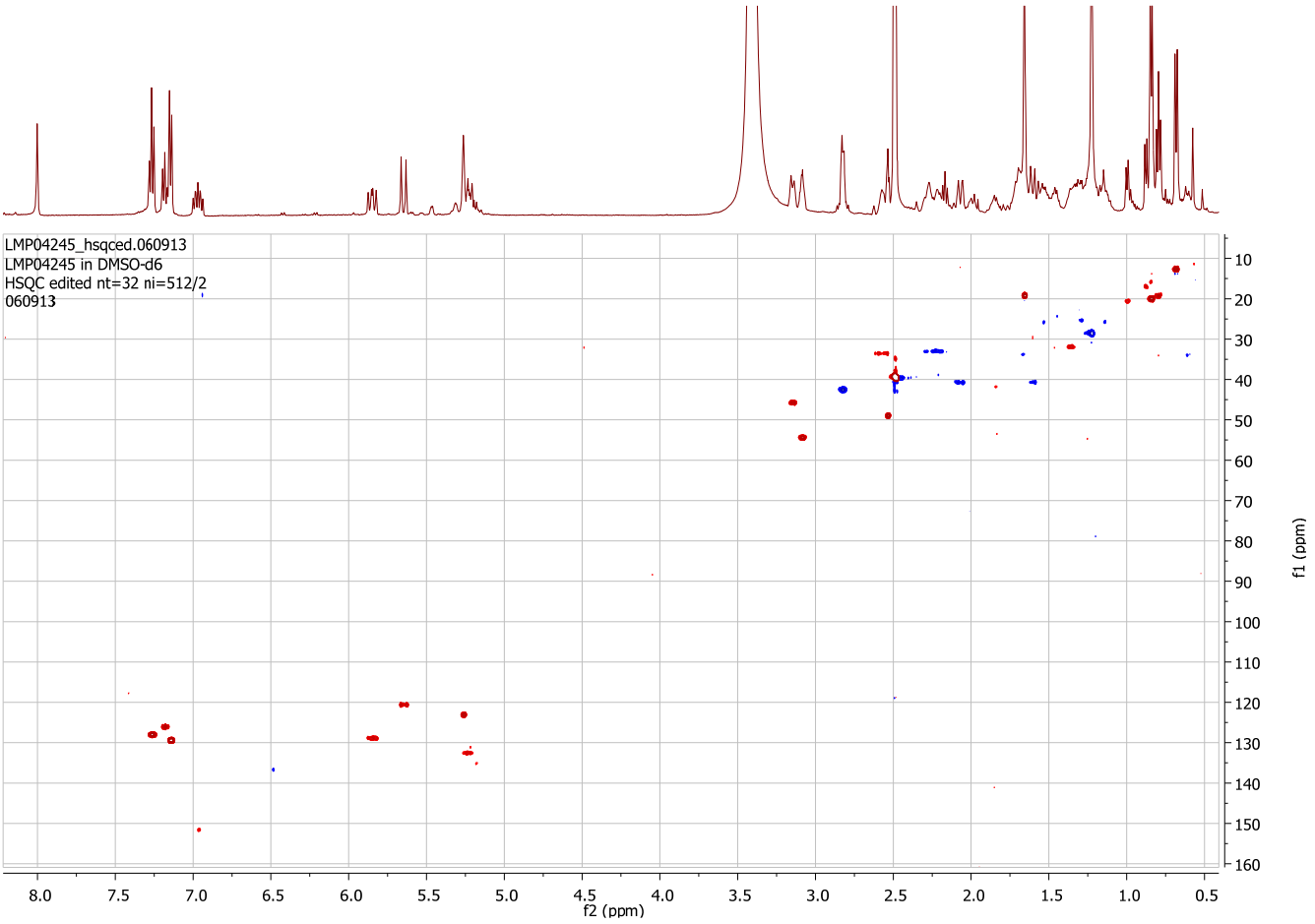

Figure S4. HMBC spectrum for Sclerotionigrin A (1) in DMSO-d_6.

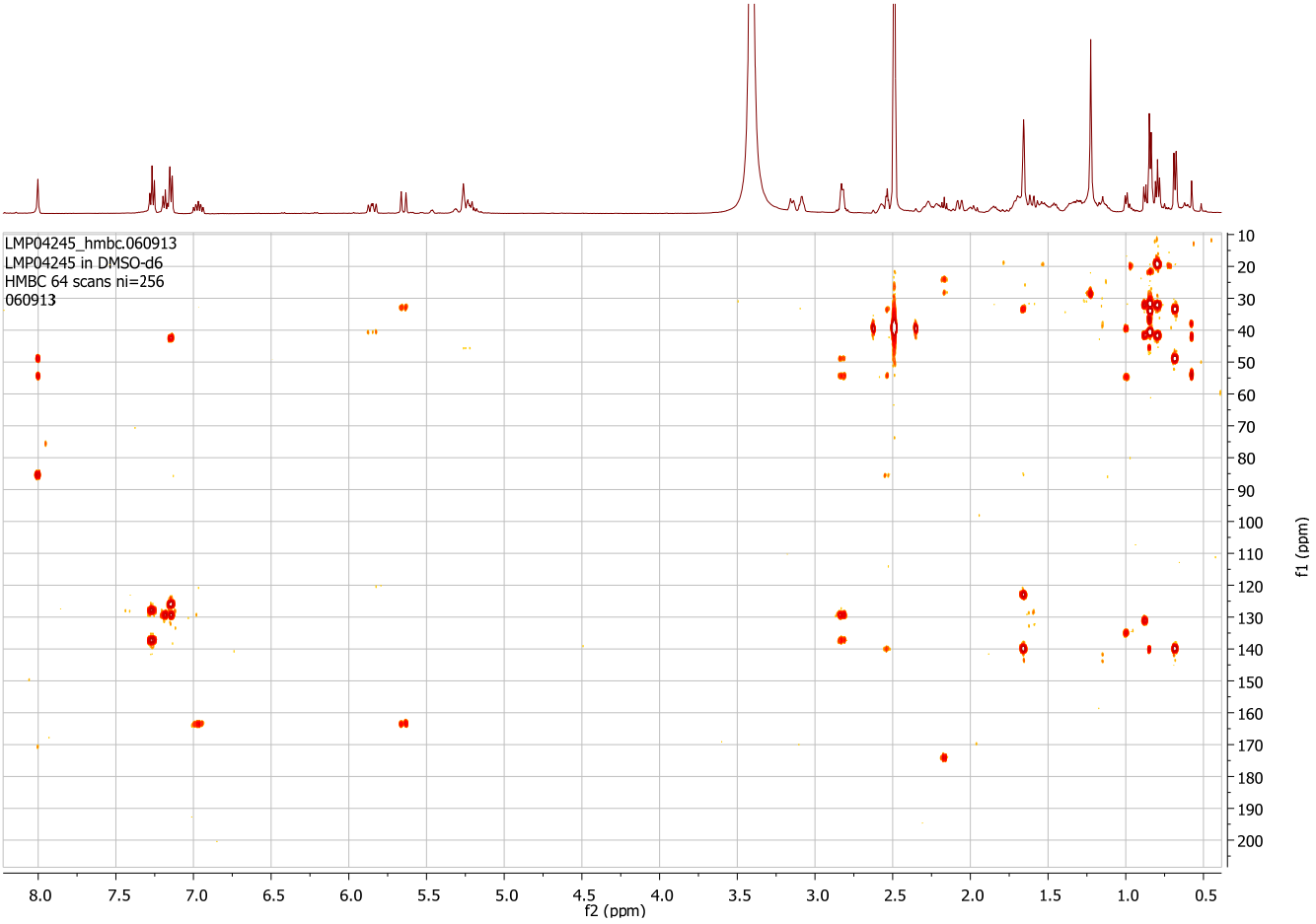

Figure S5. NOESY spectrum for Sclerotionigrin A (1) in DMSO-d_6

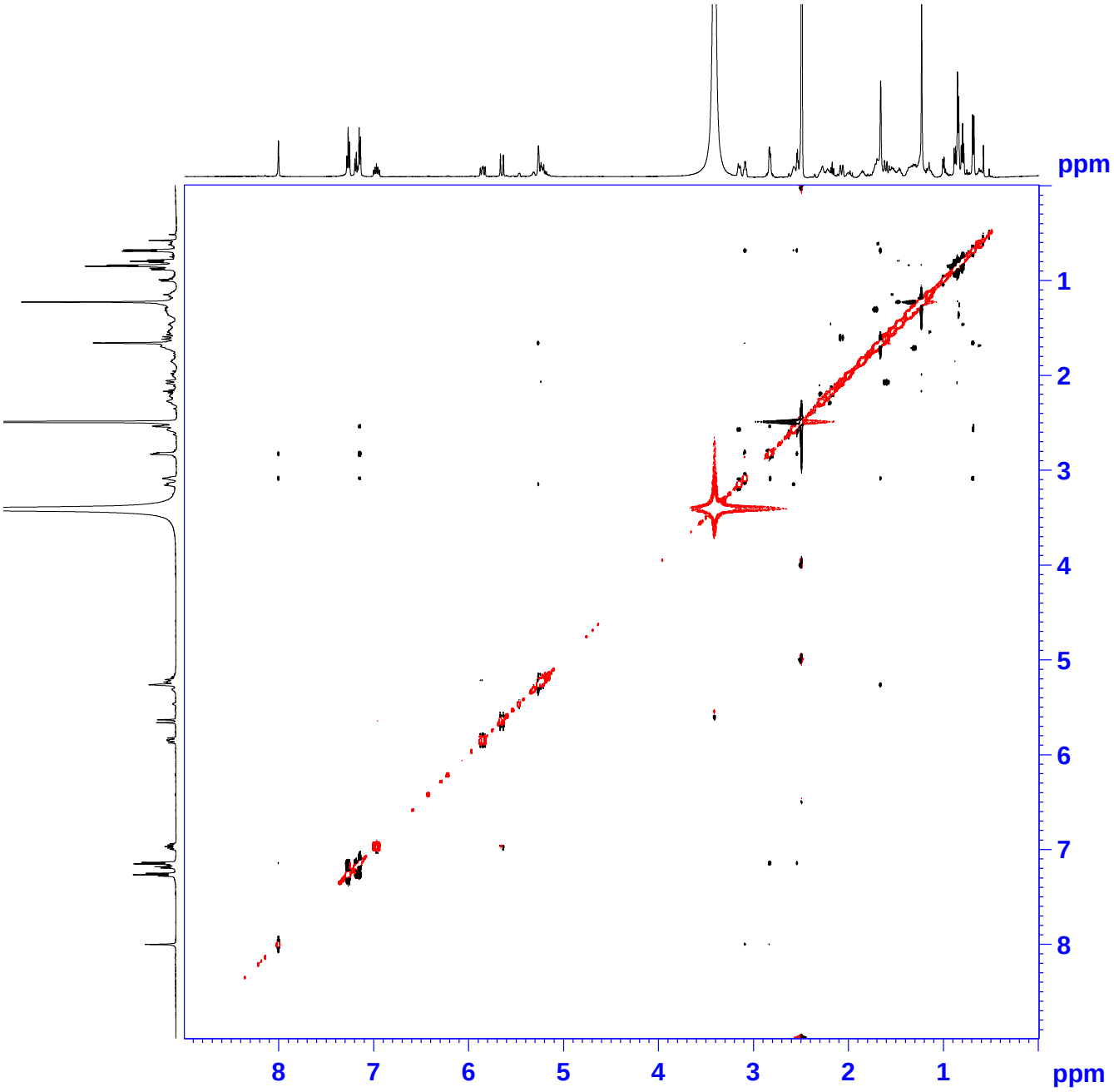

Figure S6. ^{1}H-NMR spectrum for Sclerotionigrin B (2) at 500 MHz in DMSO-d_6.

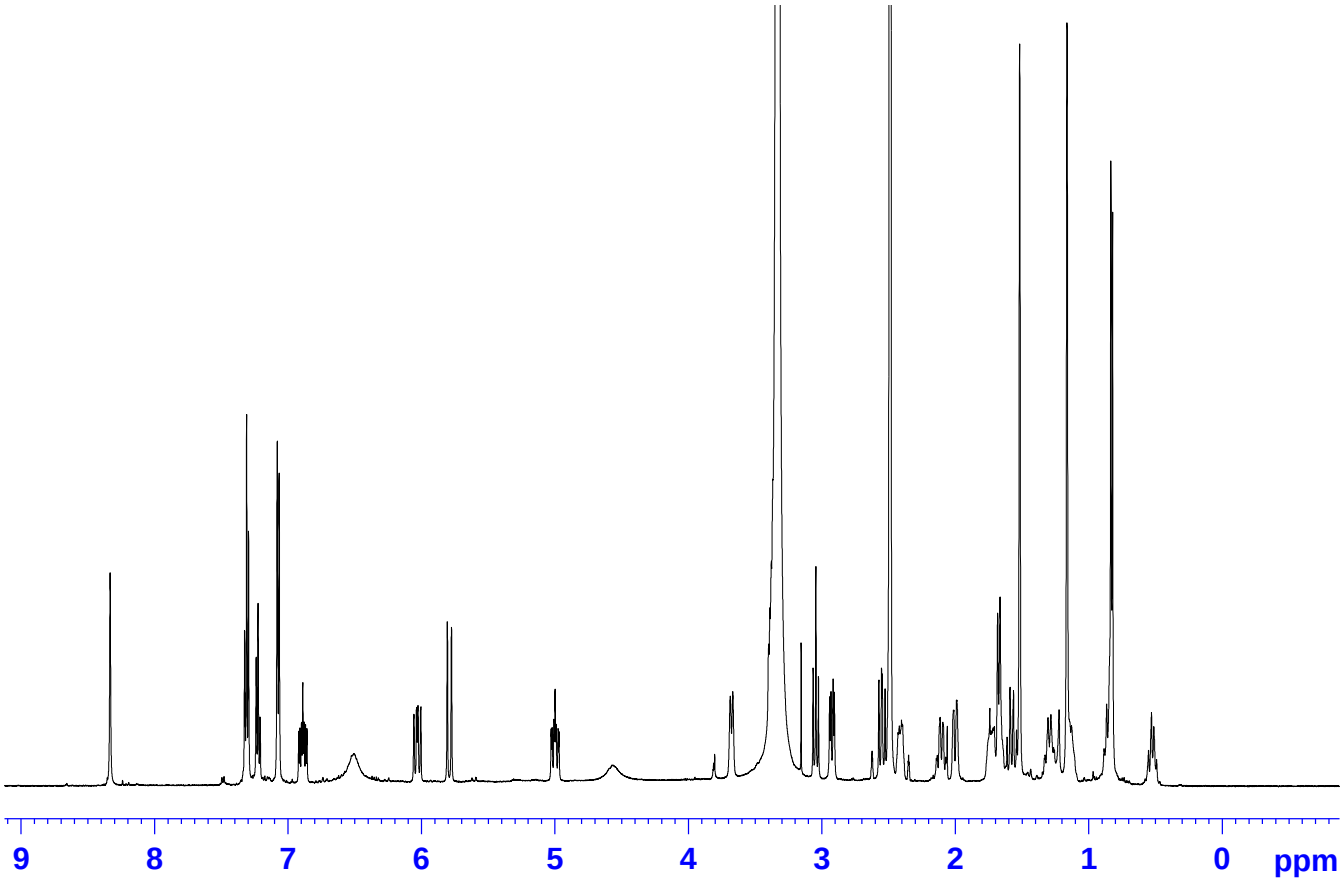

Figure S7. DQF-COSY spectrum for sclerotionigrin B (2) in DMSO-d_6.

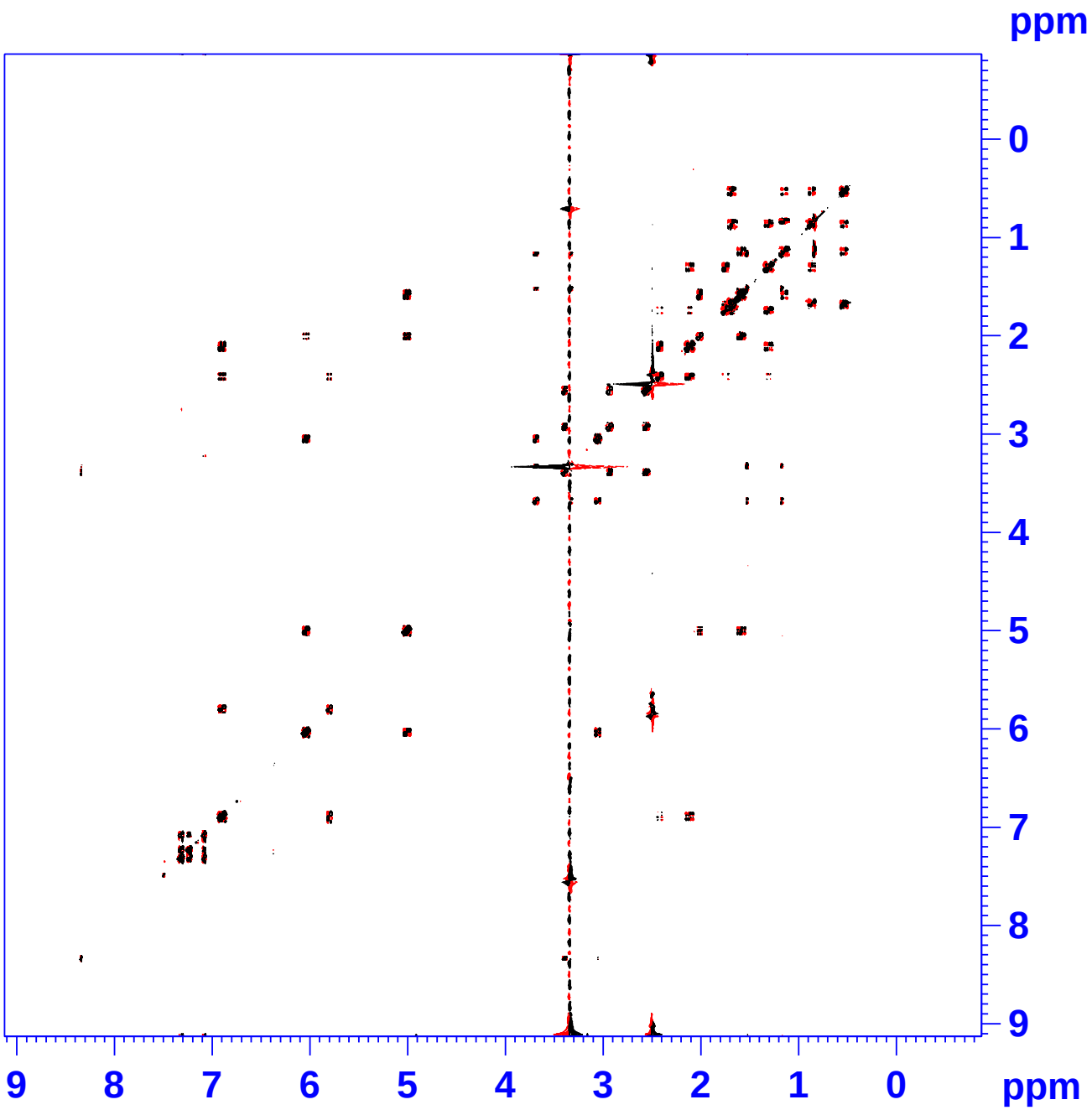

Figure S8. $_{ed}$HSQC spectrum for Sclerotionigrin B (2) in DMSO-d_6.

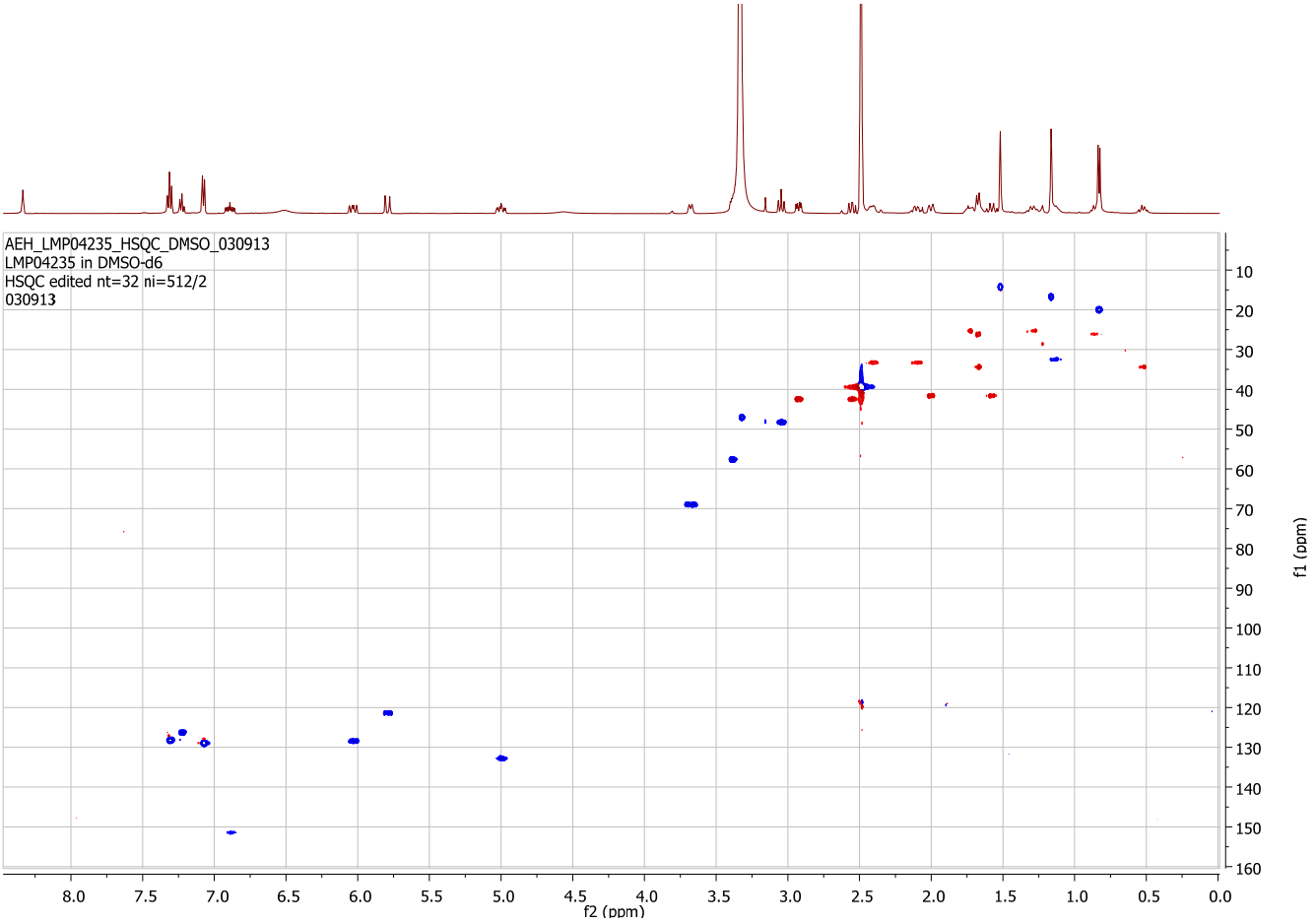

Figure S9. HMBC spectrum for Sclerotionigrin B (2) in DMSO-d_6.

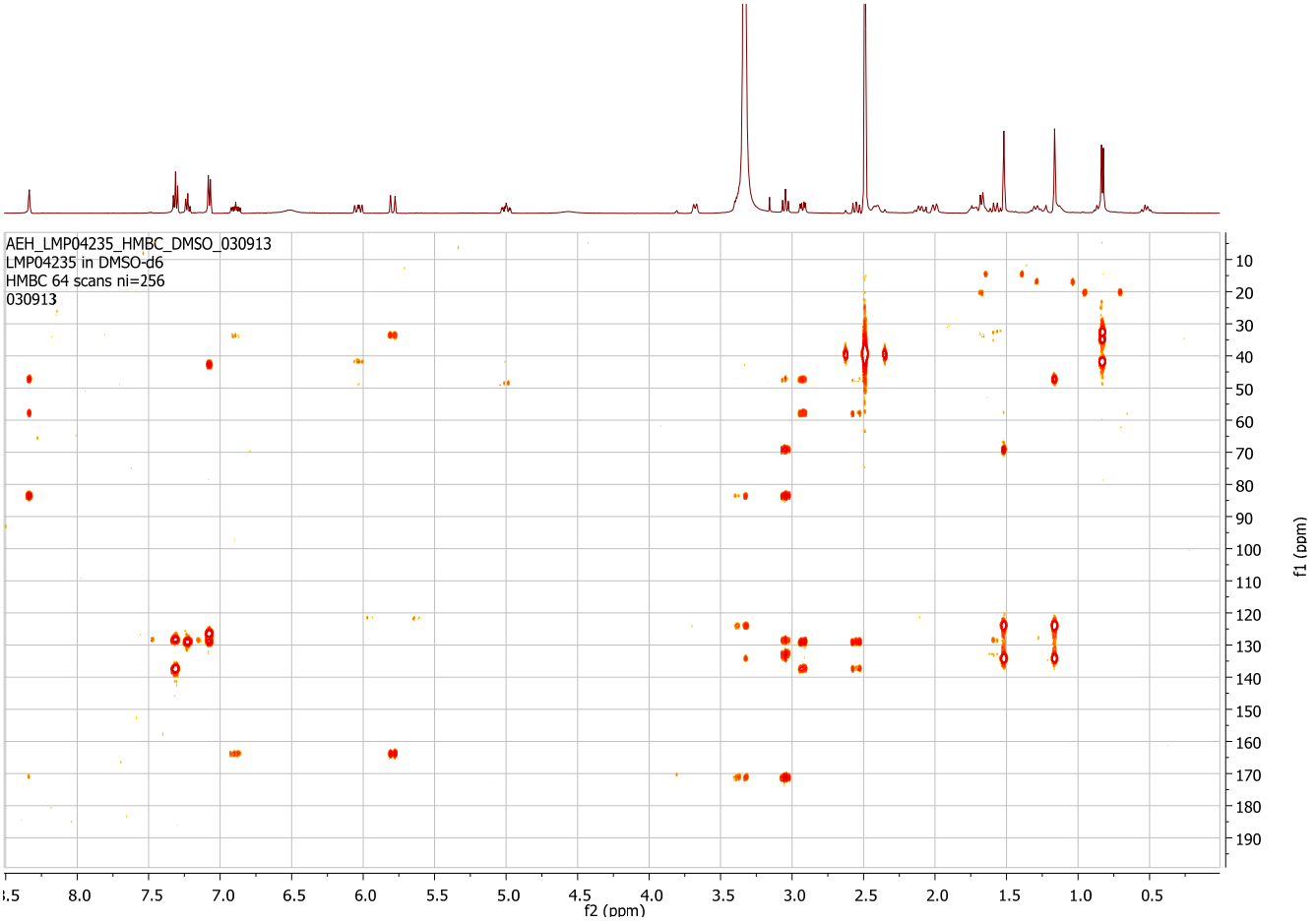

Figure S10. NOESY spectrum for Sclerotionigrin B (2) in DMSO-d_6.

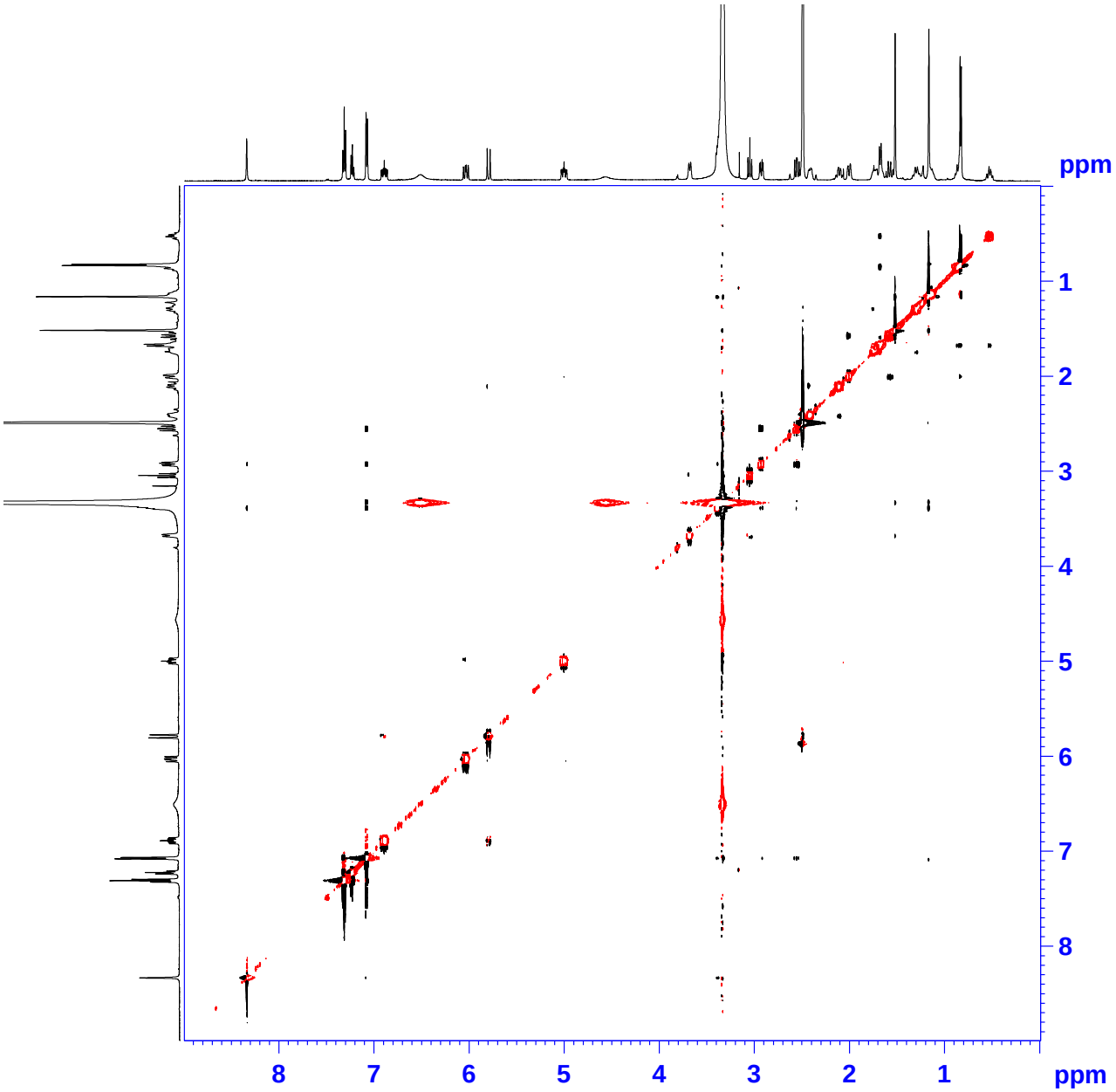

Figure S11. NMR data for proxiphomin (3).

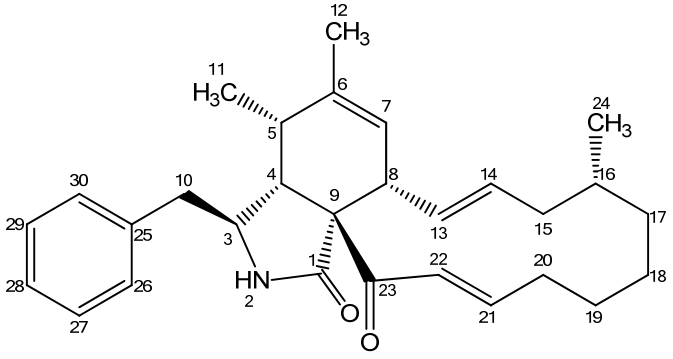

Table S1. NMR data for proxiphomin (3).

No.	δ_H (integral, mult., J [Hz])†	^{13}C-chemical shift [ppm]†	HMBC correlations	NOESY connectivities
1	-	173.6	-	-
2	7.94 (1H, s)	-	3, 4, 9	3
3	3.25 (1H, m)	53.0	-	2, 10, 10', 11, 12, 26, 30
4	2.80 (1H, dd, 5.8, 2.6)	47.2	1, 3, 5, 6, 9, 10, 23	5, 10, 10', 11, 26, 30
5	2.20 (1H, m)	33.7	1	4, 8, 11
6	-	139.1	-	-
7	5.27 (1H, m)	125.8	-	8, 12, 13
8	2.63 (1H, m)	47.0	1	7, 5, 13, 14, 22
9	-	65.7	-	-
10	2.40 (1H, dd, 13.2, 7.3)	43.1	1, 3, 4, 25, 26, 30	3, 4, 10', 26, 30
10'	2.60 (1H, dd, 13.2, 4.9)	43.1	1, 3, 4, 25, 26, 30	3, 4, 10, 26, 30
11	0.77 (3H, d, 7.2)	12.6	4, 5, 6	3, 4, 5
12	1.66 (3H, s)	19.3	5, 7	3, 7, 13
13	6.18 (1H, ddd, 15.2, 9.8, 1.7)	129.3	15	7, 8, 12, 14, 22
14	5.11 (1H, ddd, 14.6, 10.3, 3.2)	131.6	8	8, 13, 15'
15	1.67 (1H, m)	39.7	16	15'
15'	1.99 (1H, m)	39.7	16	14, 15, 16, 17 24
16	1.38 (1H, m)	31.9	-	15'
17	1.23 (2H, m)	28.5	-	15', 18
18	1.13 (2H, m)	23.1	-	17
19	1.41 (1H, m)	25.2	-	19'
19'	1.56 (1H, m)	25.2	-	19
20	2.02 (1H, m)	31.1	-	20', 21, 22
20'	2.28 (1H, m)	31.1	-	20
21	6.54 (1H, ddd, 15.4, 10.2, 5.3)	145.7	20, 23	20
22	6.86 (1H, d, 15.5)	127.3	20, 23	8, 13, 20
23	-	196.9	-	-
24	0.85 (3H, d, 6.7)	20.8	15, 16	15'
25	-	136.7	-	-
26‡	7.10 (1H, d, 7.5)	129.5	10, 28, 30	3, 4, 10, 10'
27‡	7.25 (1H, dd, 7.4, 1.0)	127.9	25, 29	
28	7.16 (1H, d, 7.5)	126.0	26, 30	
29‡	7.25 (1H, dd, 7.4, 1.0)	127.9	25, 27	
30‡	7.10 (1H, d, 7.5)	129.5	10, 26, 28	3, 4, 10, 10'

† ^{1}H-NMR data were obtained at 500 MHz in DMSO-d_6 and ^{13}C data were obtained at 125 MHz in DMSO-d_6.
‡It was not possible to distinguish between 26 and 30 as well as 27 and 29.

Figure S12. ^{1}H-NMR spectrum for proxiphomin (3) at 500 MHz in DMSO-d_6.

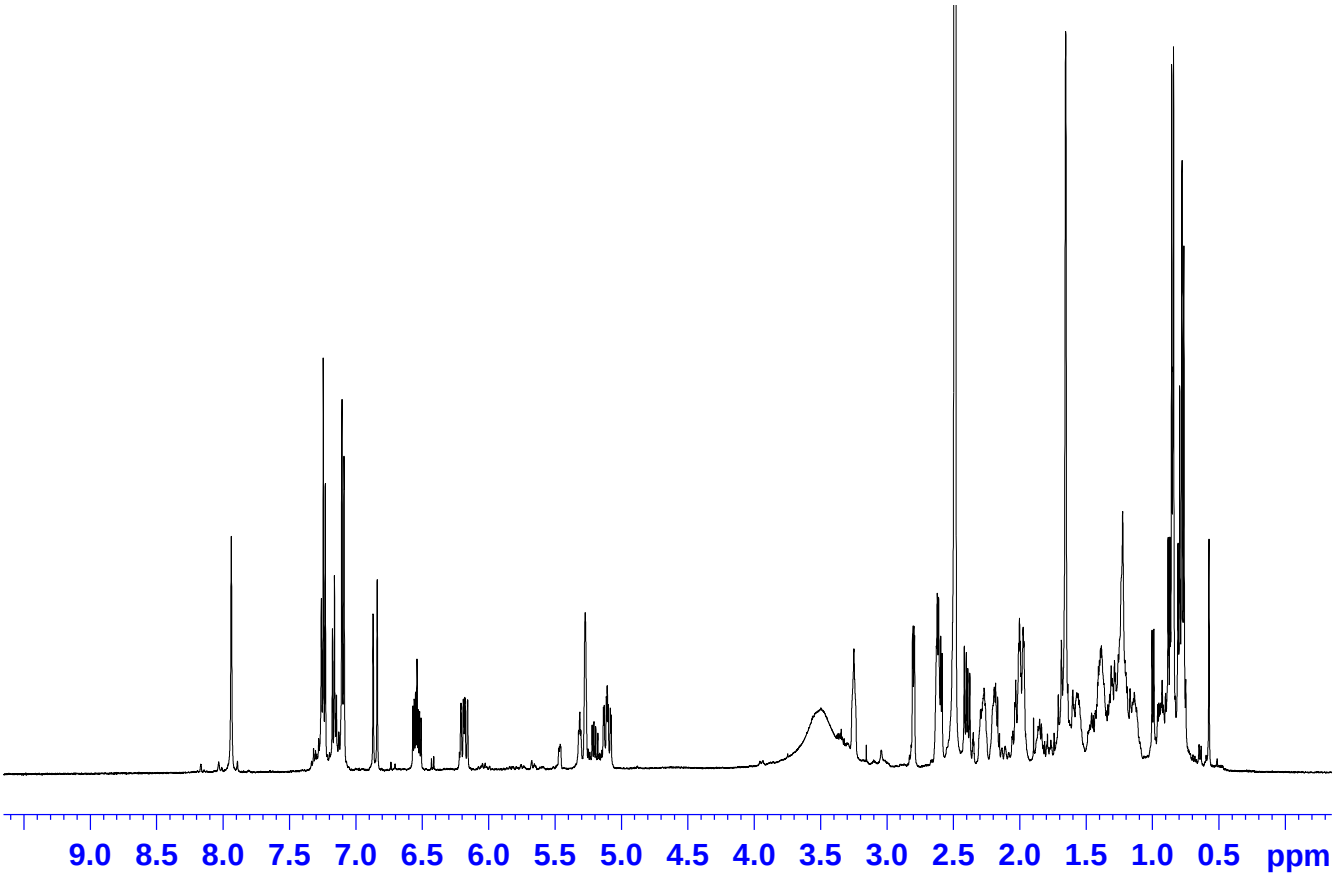

Figure S13. DQF-COSY spectrum for proxiphomin (3) in DMSO-d_6.

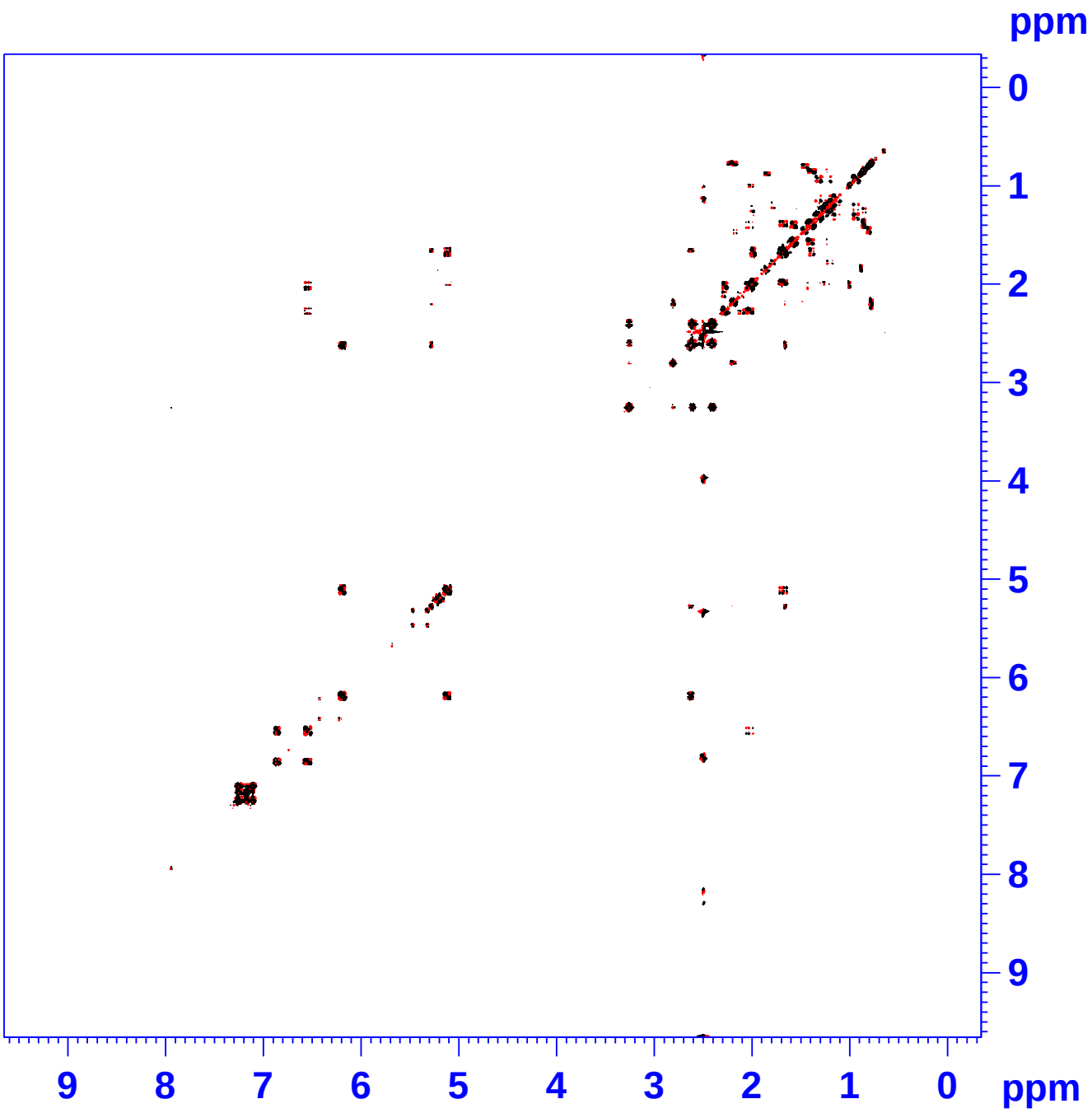

Figure S14. $_{ed}$HSQC spectrum for proxiphomin (3) in DMSO-d_6.

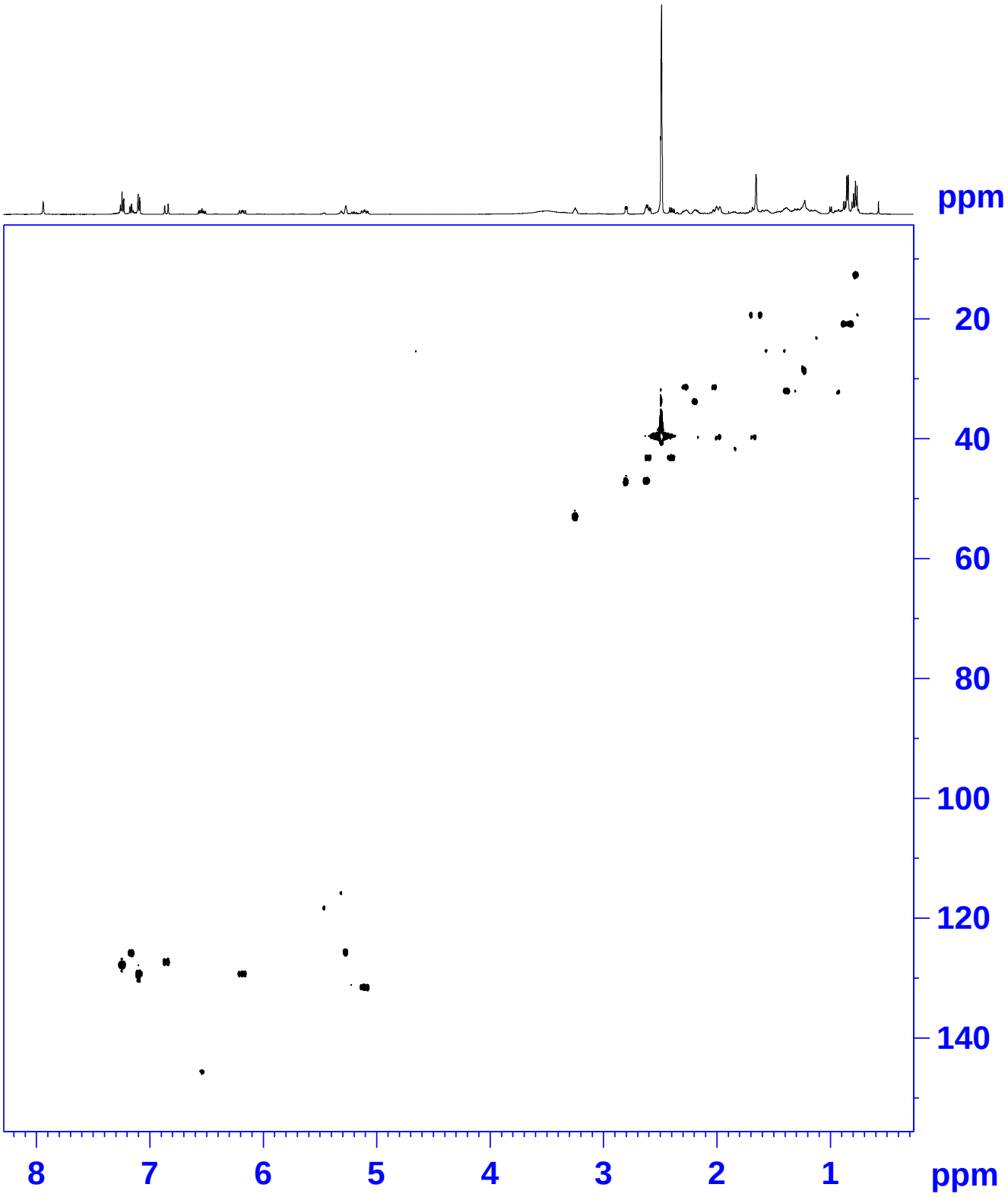

Figure S15. HMBC spectrum for proxiphomin (3) in DMSO-d_6

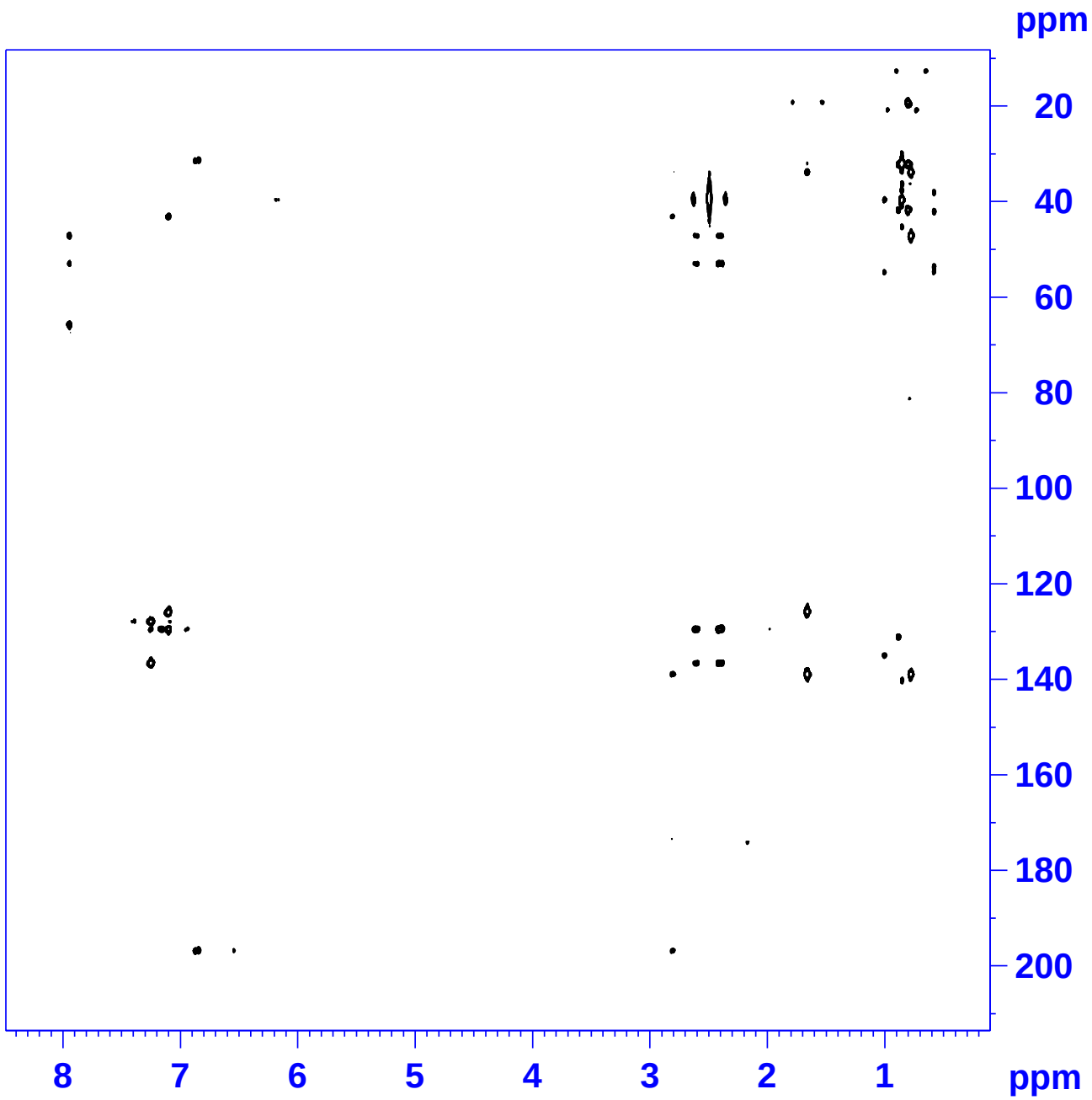

Figure S16. NOESY spectrum for proxiphomin (3) in DMSO-d_6.

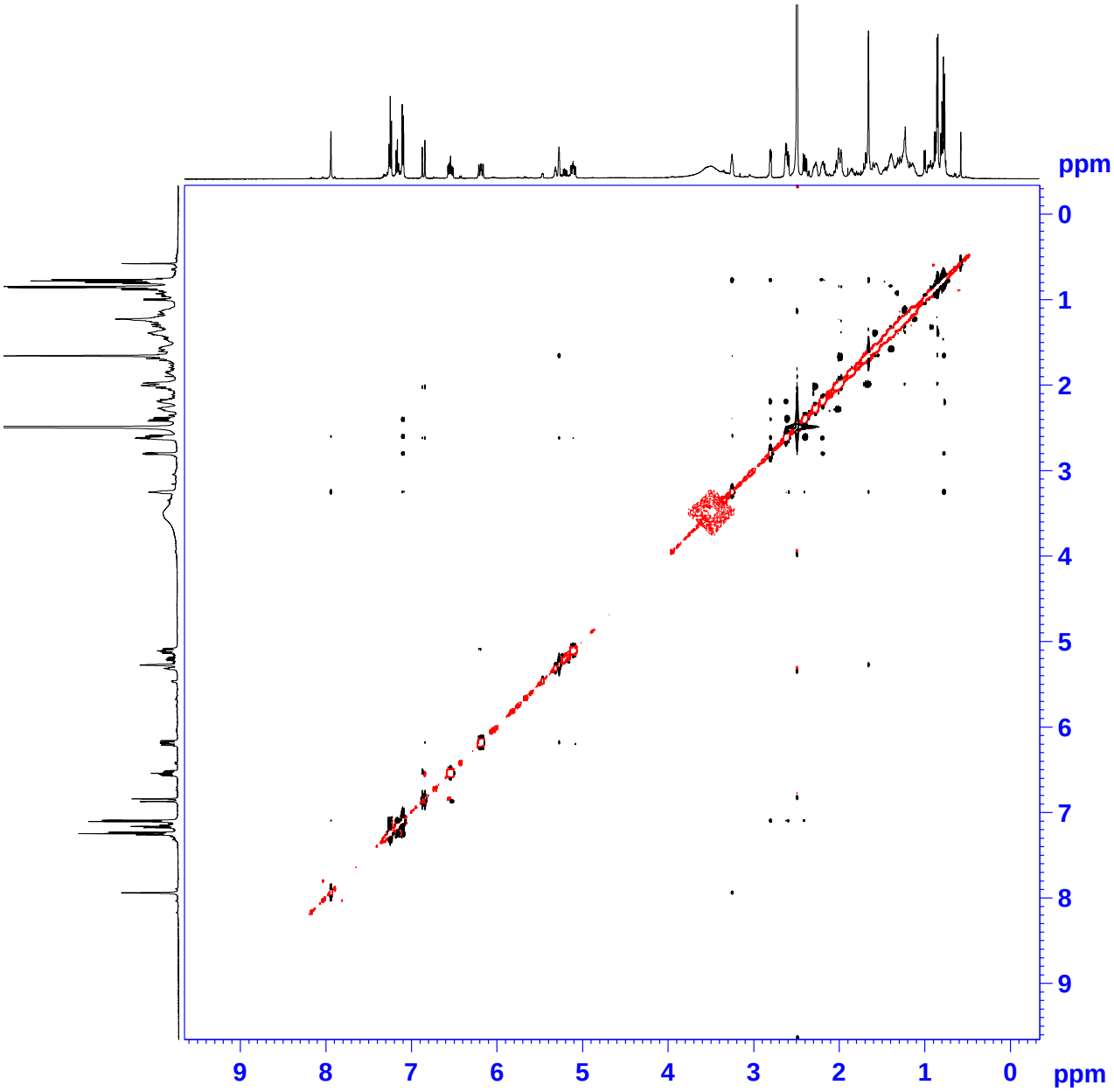

Table S2. Patient data, including age, clinical stage, IGHV mutational status and fluorescence in situ hybridization (FISH) results.

Number	Age	Binet	IGHV	FISH
1	55	A	unmutated	13q-
2	64	A	mutated	13q-
3	48	A	mutated	13q-, Tris 18
4	53	A	mutated	13q-

Mean values ± SEM of four CLL samples and three healthy donor samples are depicted.

Figure S17. Effects of 1–3 on CLL cell viabiltiy. CLL cells were treated for 24 h with increasing concentrations of 1–3 and cell viability was analyzed by CellTiter-Glo® assay. Relative cell viability is compared to DMSO control (0.1%).

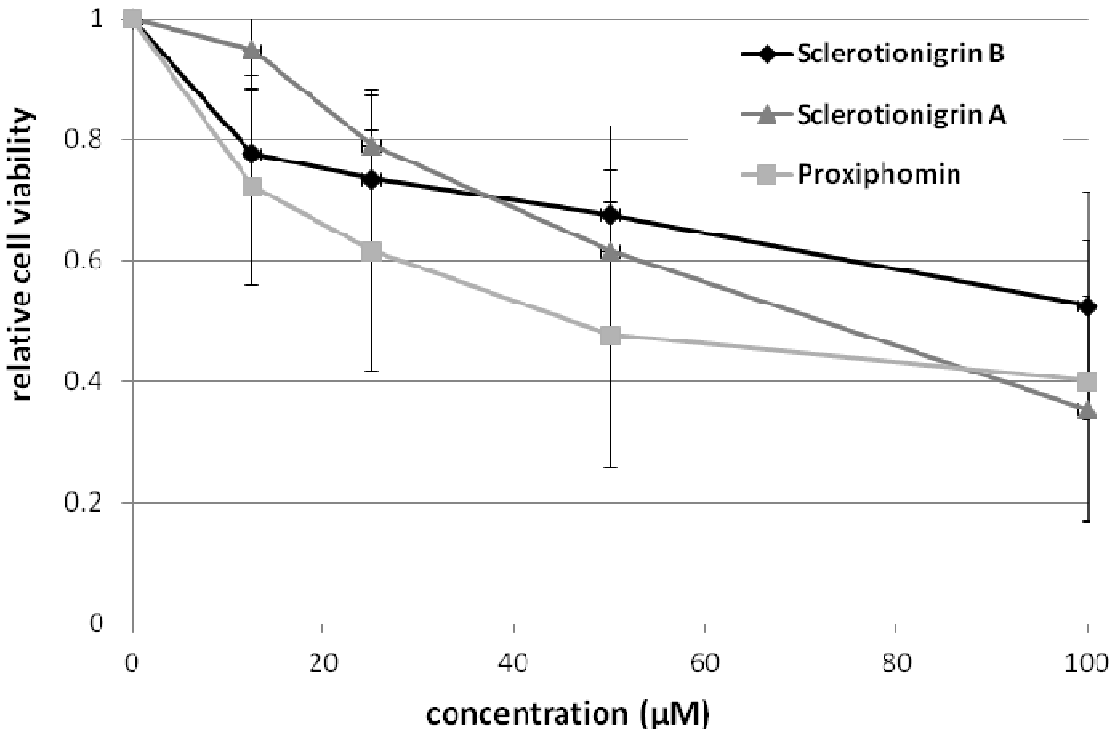

Figure S18. Effects of 1–3 on healthy B-cells cell viabiltiy. Healthy B-cells were treated for 24 h with increasing concentrations of 1–3 and cell viability was analyzed by CellTiter-Glo® assay. Relative cell viability is compared to DMSO control (0.1%).

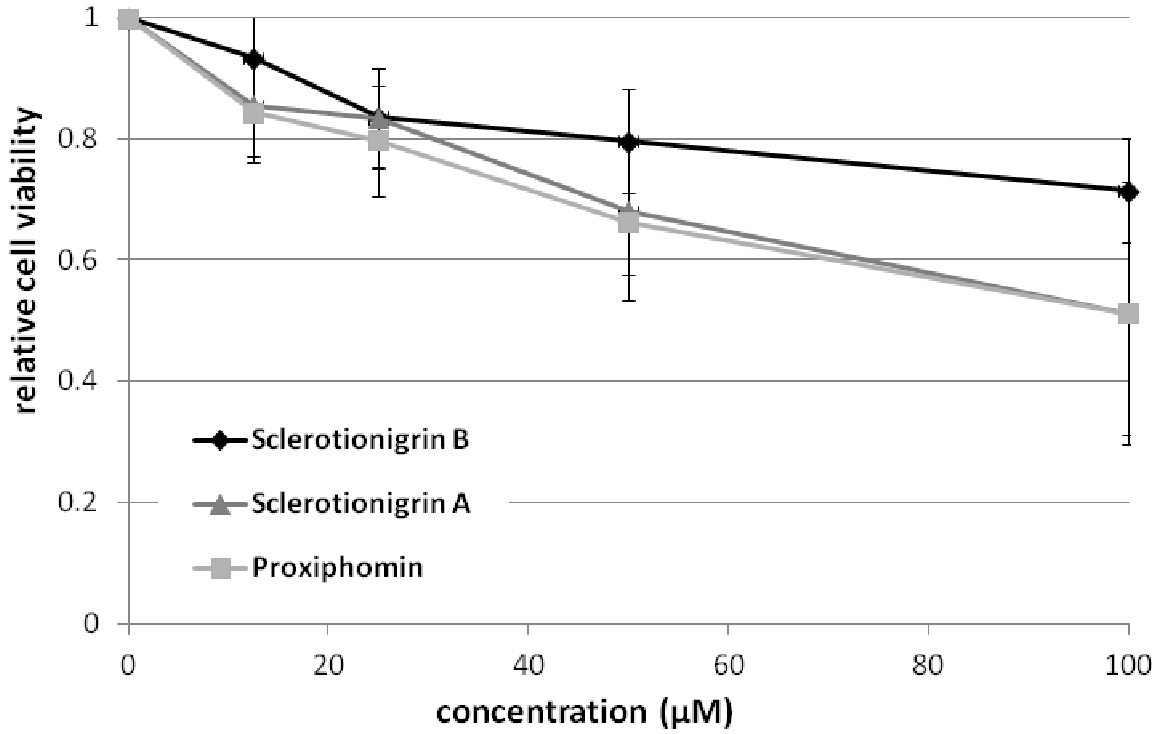

Paper 6

"Induced sclerotium formation exposes new bioactive metabolites from *Aspergillus sclerotiicarbonarius*"

Petersen, L.M.; Frisvad, J.C.; Knudsen, P.B.; Rohlfs, M.
Gotfredsen, C.H.; Larsen, T.O

Intended for publication in Journal of Antibiotics

Induced sclerotium formation exposes new bioactive metabolites from *Aspergillus sclerotiicarbonarius*

Lene M. Petersen[1], Jens C. Frisvad[1], Peter B. Knudsen[1], Marko Rohlfs[3], Charlotte H. Gotfredsen[2], Thomas O. Larsen[1*]

[1]Technical University of Denmark, Department of Systems Biology, Chemodiversity Group, Søltofts Plads B221, DK-2800 Kgs. Lyngby, Denmark

[2]Technical University of Denmark, Department of Chemistry, Kemitorvet B201, DK-2800 Kgs. Lyngby, Denmark

[3]J.F Blumenbach Institute of Zoology and Anthropology, Animal Ecology, Georg-August-University of Göttingen, BerlinerStraße 28, D- 37073 Göttingen, Germany

Correspondence: Associate professor Thomas O. Larsen, Chemodiversity Group, Department of Systems Biology, Technical University of Denmark, Soeltofts Plads B221, DK-2800 Kgs. Lyngby, Denmark. E-mail: tol@bio.dtu.dk

KEYWORDS: Antifungal agents, *Aspergillus*, sclerotia, secondary metabolites

ABSTRACT

Sclerotia are known to be fungal survival structures, and induction of sclerotia may prompt production of otherwise undiscovered metabolites. *Aspergillus sclerotiicarbonarius* (IBT 28362) was investigated under sclerotium producing conditions, which revealed a highly altered metabolic profile. Four new compounds were isolated from cultivation under sclerotium formation conditions and their structures elucidated using different analytical techniques (HRMS, UV, 1D and 2D NMR). This included sclerolizine, an alkylated and oxidized pyrrolizine, the new emindole analog emindole SC and two new carbonarins; carbonarins I and J. We have identified the three latter as true sclerotial metabolites. All metabolites were tested for antifungal and antiinsectan activity, and sclerolizine and carbonarin I displayed antifungal activity against *Candida albicans*, while all four showed antiinsectan activity. These results demonstrate induction of sclerotia as an alternative way of triggering otherwise silent biosynthetic pathways in filamentous fungi for the discovery of novel bioactive secondary metabolites.

INTRODUCTION

Natural products and their derivatives have historically been widely used as a source of therapeutic agents and amongst these are secondary metabolites (SMs) produced by filamentous fungi. In general SMs represent a wide array of structural diversity and display a broad range of biological activities, which can be utilized for pharmaceutical purposes.

The classical approach for natural product discovery has typically involved screening of crude extracts from various natural sources followed by purification and structural elucidation. With recent advances in genome sequencing projects, it has however become evident that several microorganisms have a far greater biosynthetic potential and metabolic diversity than previously assumed. In order to discover all metabolites that an organism is

capable of producing, several approaches can be taken such as the OSMAC (One Strain Many Compounds)[1], use of epi-genetic inducers[2], co-culturing experiments[3] or various methods within genome mining[2].

We have recently reported conditions triggering sclerotium production in filamentous fungi[4], where we demonstrated that under these circumstances a great alteration in the chemical profile can be acchieved[4],[5]. In this study we follow up and show that the metabolic profile of *A. sclerotiicarbonarius* (IBT 28362) is greatly altered, when sclerotia are produced, leading to the discovery of four novel compounds.

MATERIALS AND METHODS

Media. The CYA media used were prepared as described by Frisvad and Samson[6]. To trigger sclerotia production, raisins were added to the media (CYAR media) as described by Frisvad *et al.*[4]

Fungal growth and extraction. Plates were incubated at 25 °C for 7 days in the dark. For standard screening three-five plugs were taken from one colony by use of a 6 mm plug drill, covering the diameter of one colony and extracted by the micro-scale extraction method described by Smedsgaard[7]. Sclerotia were harvested and extracted as described by Frisvad *et al.*[4]

Chemical analysis of strains. Analysis was performed using reversed phase ultra-high-performance liquid chromatography (UPHLC) UV/Vis diode array detector (DAD) high-resolution time-op-flight mass spectrometer (TOFMS) on a maXis G3 orthogonal acceleration quadrupole time of flight (Q-TOF) mass spectrometer (Bruker Daltonics, Bremen, Germany) as described by Holm *et al.*[8]

Purification of metabolites. *A. sclerotiicarbonarius* (IBT 28362 = CBS 121057) was inoculated as three point inoculations on 112 plates of CYAR medium and incubated at 25 °C for 7 days in the dark. The plates were harvested and extracted twice overnight with ethyl acetate (EtOAc) with 1 % formic acid and workup was performed as described by Holm *et al.*[8] The extract was fractionated using an Isolera flash purification system (Biotage) by adsorption onto C_{18} column material and packing into a SNAP column (Biotage, Uppsala, Sweden) with C_{18} material. The extract was then fractionated using a linear gradient of ACN-water starting at 30 % ACN and increasing to 100 %. ACN used were of HPLC grade and H_2O was purified and deionized by a Millipore system through a 0.22 μm membrane filter (milliQ-water). The flow rate used was 40 mL/min, the column volume 124 mL, and fractions were collected automatically one column volume at a time.

The Isolera fractions were subjected to further purification on a semi-preparative HPLC which was either a Waters 600 Controller with a 996 photodiode array detector (Waters, Milford, MA, USA) or a Gilson 322 Controller connected to a 215 Liquid Handler, 819 Injection Module and a 172 DAD (Gilson, Middleton, WI, USA). This was achieved using a Luna II C_{18} column (250 x 10 mm, 5 μm, Phenomenex) or a Gemini C6-Phenyl 110A column (250 x 10.00 mm, 5 μm, Phenomenex). 50 ppm TFA was added to ACN of HPLC grade and milliQ-water. For choice of system, flow rate, column, gradients and yields see Table 4. Spectroscopic data for all compounds are given in the supporting information.

Table 1 Purification details for compound **1-4**

Compound name	Isolera fraction	System	Column	Flow rate	Gradient	Yield
Sclerolizine	14/15	Waters	Gemini	4 mL/min	90 % ACN isocratic for 15 min, then to 100 % ACN	13.0 mg
Emindole SC	10/15	Waters	Luna II C_{18}	5 mL/min	60-80% ACN for 18 min, then to 100 % CAN	20.3 mg
Carbonarin I	4/15	Gilson	Luna II C_{18}	5 mL/min	30-50 % ACN for 15 min, then to 100% CAN	9.6 mg
Carbonarin J	4/15	Gilson	Luna II C_{18}	5 mL/min	30-50 % ACN for 15 min, then to 100% ACN	3.9 mg

NMR and structural elucidation. ^{1}H and 2D spectra were recorded on a Varian Unity Inova-500 MHz spectrometer, while ^{13}C spectra were recorded on a Bruker Ascend 400 MHz spectrometer. Spectra were acquired using standard pulse sequences. The deuterated solvent was DMSO-d_6 and signals were referenced to the solvent signals for DMSO-d_6 at δ_H = 2.49 ppm and δ_C = 39.5 ppm. The NMR data was processed in MestReNova v.6.0.1-5391. Chemical shifts are in ppm (δ) and scalar couplings are reported in hertz (Hz). Optical rotation was measured on a Perkin Elmer 321 Polarimeter.

Antifungal susceptibility testing. All compounds were screened for antifungal activity towards *Candida albicans* in accordance with the CLSI standards, as described by Holm *et al.*[8]

***Drosophila* larval testing.** All compounds were screened for larvicidal activity towards *Drosophila melanogaster* larvae as described by Trienens *et al.*[9], but using MeOH as a solvent.

RESULTS AND DISCUSSION

The metabolic profile of *A. sclerotiicarbonarius* (IBT 28362) was investigated under conditions both with and without conditions favoring sclerotium formation. The latter was achieved using media containing raisins (CYAR), as earlier described[4]. Without presence of sclerotia, the metabolic profile (Figure 1A) displayed only few metabolites. One of the most abundant metabolites, pyranonigrin A (pyranopyrrol A) (verified with UHPLC-DAD-HRMS by comparison of retention time, monoisotopic mass for the pseudomolecular ion, adducts and UV spectrum to an authentic standard), is known from other black aspergilli[10],[11]. With formation of sclerotia, a more diverse production of secondary metabolites was observed, both in a mycelium plug extraction and by true sclerotial extraction (Figure 1B and 1C). Known black aspergilli secondary metabolites such as aurasperone B[12] and malformin C[13] were detected (verified by UHPLC-DAD-HRMS). In our previous studies we observed several aflavinines in the sclerotial extracts, and production of aurasperone B as a common trend[4], which was indeed also the case for *A. sclerotiicarbonarius.*

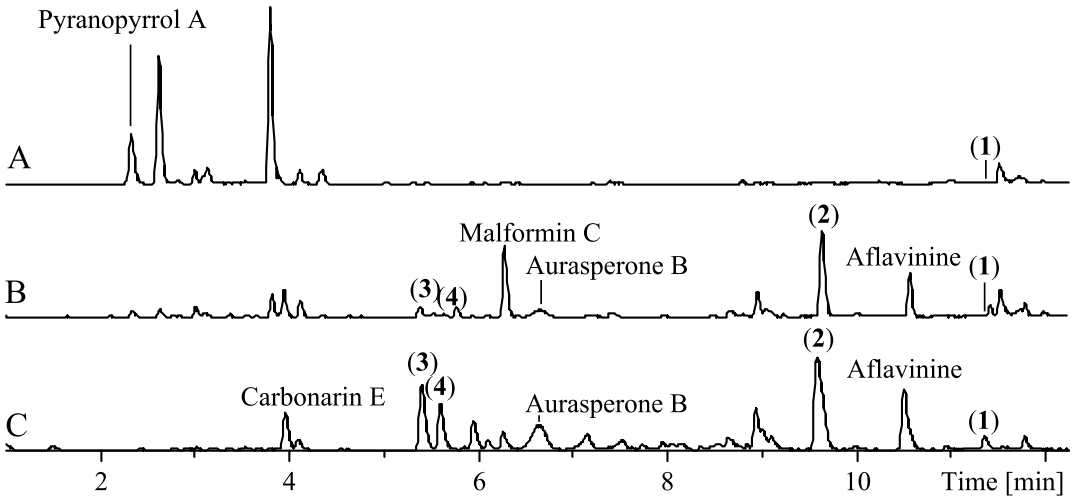

Figure 1 UHPLC-TOF-HRMS ESI+ BPC chromatogram of *Aspergillus sclerotiicarbonarius* (IBT = 28362) extractions. Scaled to RT between 1-12 minutes, intensities are to scale. A: Plug extraction from growth with no sclerotium production. B: Plug extraction from growth with sclerotium production. C: Sclerotial extraction. The extractions under sclerotium production (B + C) show the presence of the four novel compounds sclerolizine (**1**), emindole SC (**2**), carbonarin I (**3**) and carbonarin J (**4**).

From the sclerotial extract several putative unknown compounds were detected. From a larger extract cultivated under sclerotium formation conditions, these compounds were purified and their structures solved by 1D and 2D NMR spectroscopy, Figure 2 and Table 2.

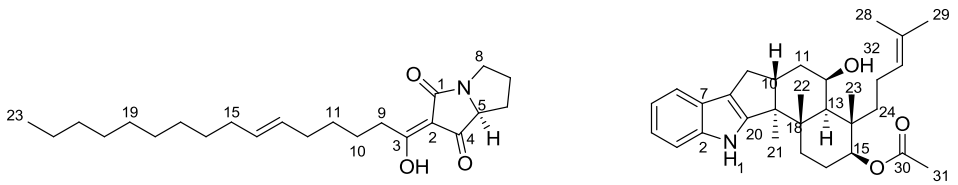

Sclerolizine (**1**)

Emindole SC (**2**)

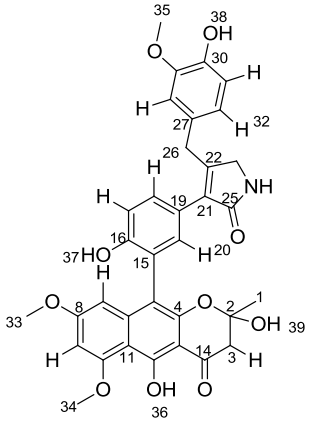

Carbonarin I (**3**)

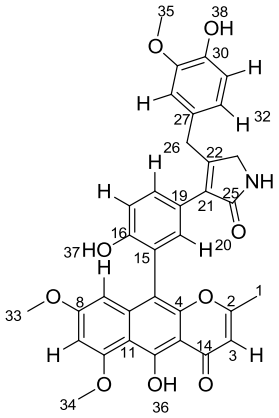

Carbonarin J (**4**)

Figure 2 Structures of the novel compounds isolated from *A. sclerotiicarbonarius*.

Table 2. ^{1}H (500 MHz) and ^{13}C (125 MHz) NMR Spectroscopic Data for compounds **1-4**.

	1		**2**		**3**		**4**	
#	δ_H (*J* in Hz)	δ_C	δ_H (*J* in Hz)	δ_C	δ_H (*J* in Hz)	δ_C	δ_H (*J* in Hz)	δ_C
1	-	175.2	10.57 (1H, s)	-	1.43 (3H, s)	26.9	2.16 (3H, s)	20.0
2	-	103.1	-	140.3	-	99.9	-	168.3
3	-	188.7	7.25 (1H, d, 7.1)	111.8	3.11	47.6	6.18 (1H, s)	106.4
3'					2.78	47.6		
4	-	194.5	6.93 (1H, t)	119.4	-	155.6	-	149.8
5	3.98 (1H, dd, 9.8, 6.6)	66.8	6.89 (1H, t)	118.4	-	110.2	-	109.2
6	1.40 (1H, m)	26.4	7.27 (1H, d, 7.1)	117.8	-	141.5	-	161.0
6'	2.01 (1H, m)	26.4						
7	1.99 (2H, m)	26.3	-	124.6	6.22 (1H, s)	97.6	6.41 (1H, d, 2.1)	96.5
8	3.09 (1H, m)	42.7	-	115.9	-	161.1	-	160.5
8'	3.52 (1H, dt, 10.9, 7.8)	42.7						
9	2.73 (2H, t, 7.5)	32.9	2.55 (1H, dd, 13.1, 6.5)	26.8	6.42 (1H, s)	95.3	6.52 (1H, d, 2.0)	96.5
9'			2.26 (1H, dd, 13.1, 11.0)	26.8				
10	1.53 (2H, m)	24.4	3.20 (1H, m)	41.9	-	161.2	-	106.7
11	1.32 (2H, m)	28.4	1.78 (1H, m)	34.7	-	106.1	-	107.4
11'			1.68 (1H, m)	34.7				
12	1.93 (2H, m)	31.5	4.14 (1H, br. s.)	66.2	-	163.4	-	161.6
13	5.34 (1H, m)	129.7	1.49 (1H, br.s)	42.6	-	102.4	-	103.2
14	5.35 (1H, m)	129.8	-	40.5	-	198.2	-	184.1
15	1.92 (2H, m)	31.5	4.68 (1H, dd, 11.2, 3.9)	75.5	-	122.5	-	120.3
16	1.27 (2H, m)	28.4	1.87 (1H, m)	23.5	-	154.9	-	154.9
16'			1.69 (1H, m)	23.5				
17	1.22 (2H, m)	28.4/21.9*	1.83 (1H, m)	32.5	7.00 (1H, dd, 8.4, 2.8)	115.3	7.07 (1H, d, 8.4)	115.6
17'			1.72 (1H, m)	32.5				
18	1.22 (2H, m)	28.4/21.9*	-	52.4	7.32 (1H, dd, 8.4, 2.1)	129.9	7.43 (1H, dd, 8.4, 2.1)	129.9
19	1.22 (2H, m)	28.4/21.9*	-	39.6	-	121.9	-	122.5
20	1.22 (2H, m)	28.4	-	151.3	7.21 (1H, dd, 4.0, 2.2)	133.4	7.27 (1H, d, 2.0)	133.2
21	1.22(2H, m)	28.4/21.9*	0.90 (3H, s)	14.2	-	130.9	-	130.9

22	1.25 (2H, m)	21.9	-	152.1	-	152.2
23	0.84 (3H, t, 6.9)	13.7	3.74 (2H, s)	47.2	3.75 (2H, s)	47.2
24			8.15 (1H, s)	-	8.12 (1H, s)	-
25			-	172.9	-	172.6
26			3.76 (2H, s)	33.2	3.76 (2H, s)	33.4
27			-	129.2	-	128.7
28			6.65 (1H, m)	112.3	6.64 (1H, m)	112.4
29			-	147.4	-	147.2
30			-	144.6	-	145.0
31			6.64 (1H, m)	115.3	6.63 (1H, d, 8.5)	115.3
32			6.51 (1H, m)	120.2	6.49 (1H, dd, 8.0, 1.6)	120.3
33			3.57 (3H, s)	55.8	3.90 (3H, s)	55.8
34			3.88 (3H, s)	54.5	3.61 (3H, s)	54.7
35			3.60 (3H, s)	54.9	3.59 (3H, s)	54.9
36			14.38 (1H, s)	-	15.09 (1H, s)	-
37			9.15 (1H, s)	-	9.36 (1H, s)	-
38			8.80 (1H, s)	-	8.81 (1H, s)	-
39			6.92 (1H, s)	-		

*Due to overlapping signals the specific carbon chemical shift could not be determined.

Structural elucidation of four new compounds. The UV spectrum of sclerolizine displayed absorption maxima at 280 nm, and the ESI+ HRMS spectrum displayed one adduct, with *m/z* = 376.2855, from which the molecular formula could be deduced to $C_{23}H_{37}NO_3$ (376.2846 calculated for $[C_{23}H_{37}NO_3 + H]^+$). The ^{1}H NMR spectra revealed the presence of one H_α proton (H5), which was found to be part of a COSY spin system with three methylene groups (C6, C7 and C8), which altogether were elucidated as the pyrrolidine ring. The remaining resonances in the ^{1}H NMR spectra belonged to a larger spin system with two overlapping protons in the double bond area, one methyl and 12 methylene groups, whereof five (H17, H18, H19, H20 and H21) where overlapping at δ_H 1.22 ppm. The linking between the two COSY spin systems and the assignment of four quaternary carbons (two carbonyls, two double bond carbons) were accomplished through detailed analysis of the HMBC spectral data (Figure 3). It is noted that there was no HMBC correlations linking the two spin systems, but to justify the chemical shifts observed, the suggested structure was the only appropriate proposal. The resonances originating from the C13-C14 double bond were very close in chemical shift leading to a second order spin system. Consequently it was not possible to accurately determine the size of the *J* coupling constant. A value of *J* could however be measured to 15.2 Hz in the second order system, suggesting a *trans* double bond. Furthermore the chemical shifts for the neighboring allylic carbons at 31.5 ppm (C12 and

C15) were also in consistence with a *trans* configuration as allylic carbons in *cis* fatty acids would be further up field, typically at values below 30 ppm[14]. The stereochemistry of the C2-C3 double bond and C5 has not been investigated, but we hypothesize that L-proline is incorporated into the molecule. Similar synthetic structures have been patented[15],[16], however to the best of our knowledgethis is the first report of an oxidized pyrrolizines from a natural source..

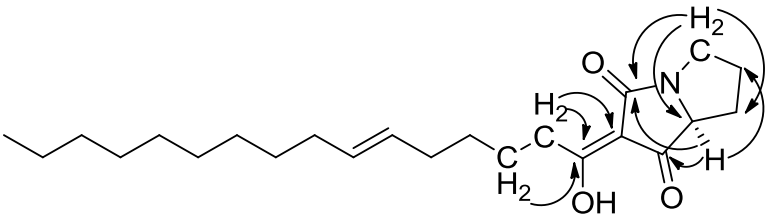

Figure 3 Key HMBC correlations of sclerolizine (**1**)

The UV spectrum of emindole SC displayed absorption maxima at 283 nm, and the ESI+ HRMS spectrum displayed one adduct, with *m/z* = 464.3164, from which the molecular formula could be deduced to $C_{30}H_{41}NO_3$ (464.3159 calculated for $[C_{30}H_{41}NO_3 + H]^+$). The backbone of emindole SC display the same skeleton as emindole SB from *Emericella striata*[17]. The main difference of emindole SC is an extra hydroxyl group (C12) and an acetylation at C15. This gives rise to additional signals in the ^{1}H NMR spectrum from the methyl group C31, and HMBC correlations to the carbonyl at δ_C 170 ppm (C30) from H15 and H31. The chemical shift of H12 is shifted downfield to δ_H 4.14 ppm, and the addition of the hydroxyl is also evident from the carbon chemical shift, which is moved downfield to δ_C 66.2 ppm. Otherwise the NMR data is very comparable to those of emindole SB[17]. NOESY experiments enabled determination of the relative stereochemistry for the stereogenic centers. NOE connectivities were found from H13 to H12, H15 and H21 placing these on the same side of the ring systems, which is also observed for other emindoles. This was further verified by strong NOESY connectivities between H10 and H22 as well as H23 and H32.

The UV spectra of carbonarin I and J displayed absorption maxima at 410 nm suggesting a highly conjugated chromophore. Analysis of the HRMS data showed *m/z* of 614.2025 and 596.1923, which was used to determine the molecular formula to $C_{34}H_{31}NO_{10}$ and $C_{34}H_{29}NO_9$ (614.2021 and 596.1915 calculated for $[C_{34}H_{31}NO_{10} + H]^+$ and $[C_{34}H_{29}NO_9 + H]^+$ respectively). Structural elucidation of the two related compounds revealed structures similar to those of carbonarin A-H, which are metabolites from *A. carbonarius*[18],[19]. Carbonarin I and J differ at C2 and C3, with a single bond in the former and a double bond in the latter. C2 has furthermore a hydroxyl group shifting the carbon chemical shift dramatically downfield to δ_C 99.9 ppm. No HMBC correlations were observed to the carbons at C6 for carbonarin I and C4, C6 or C14 for carbonarin J, wherefore these were assigned from resonances in the 1D ^{13}C carbon spectrum. The upper part of carbonarin I and J is alike (Figure 2), including two partly substituted aromatic rings and a five membered lactam ring. This part is unique for carbonarin I and J compared to other carbonarins, which show different substitution patterns in the aromatic rings. The bottom part consists of a three ring system polyketide part present in both carbonarin I and J, similar to what is seen in other naphthopyrones such as aurasperone B[12] and fonsecin B[20]. By comparison to an authentic standard, we found trace amounts of fonsecin B being produced under conditions with sclerotium formation (data not shown), why we hypothesize that fonsecin B is the likely precursor of the new carbonarins described here.

A search for carbonarin A-H in the UHPLC-UV-HRMS data from the sclerotial extract showed trace amounts of carbonarin A-D, high production of carbonarin E and F, while no carbonarin G nor H could be detected (Tentatively identified by HRMS with a mass tolerance of *m/z* +/- 0.005). An equivalent search for carbonarins in the *A. sclerotiicarbonarius* extract with no sclerotium production showed no traces of any of the carbonarins, clearly indication that this group of compounds is be related to sclerotium production.

Three of the new compounds are true sclerotial metabolites. For verification of whether the compounds are true sclerotial metabolites, extracted ion chromatograms (EICs) with a mass tolerance of +/- 0.005 were performed based on plug extraction from growth conditions with and without sclerotium formation as well as the sclerotium extraction, Table 3 and supporting information. It was here found that all metabolites (**1-4**) were present in both the sclerotial extracts and the plug extracts under sclerotium formation. In the plug extraction where no sclerotia were formed, all compounds, but sclerolizine were absent, strongly indicating that emindole SC, carbonarin I, and carbonarin J are true sclerotium metabolites.

Table 3. Presence of compound **1-4** with and without sclerotium production. Detected by Extracted Ion Chromatograms (EICs) with a mass tolerance of *m/z* +/- 0.005.

	Plug extraction CYA (No sclerotium formation)	Plug extraction CYA (Sclerotium formation)	Sclerotial extraction
Sclerolizine (**1**)	x	x	x
Emindole SC (**2**)	-	x	x
Carbonarin I (**3**)	-	x	x
Carbonarin J (**4**)	-	x	x

Bioactivities

Compounds **1-4** were tested for antifungal and insecticidal activity. The half maximal inhibitory concentrations (IC_{50}) for *Candida albicans* treated with compound 1-4 are displayed in Table 4. The IC_{50} values were calculated based on duplicate experiments carried out in at least two independent trials and annotated with their respective standard deviation. Sclerolizine and carbonarin I displayed moderate antifungal activity, with sclerolizine as the most active.

Table 4. Antifungal activities of compound **1-4** against *Candida albicans*.

Compound	Origin	IC_{50} (µM)
Sclerolizine (**1**)	*A. sclerotiicarbonarius*	8.5 ± 2.0
Emindole SC (**2**)	*A. sclerotiicarbonarius*	>100
Carbonarin I (**3**)	*A. sclerotiicarbonarius*	85.8 ± 13.1
Carbonarin J (**4**)	*A. sclerotiicarbonarius*	>100

As sclerotial compounds have often been found to possess insecticidal properties[21], all compounds were furthermore tested for larvicial activity towards *Drosophila melanogaster* larvae. The results are depicted in Figure 4. With increasing concentrations all compounds were affecting the survival of the insect larvae ($p < 0.001$), yet there was no compound-specific variation in this effect. Overall, at a concentration of 1.83 ±0.08 µmol, 50% of the larvae were found dead.

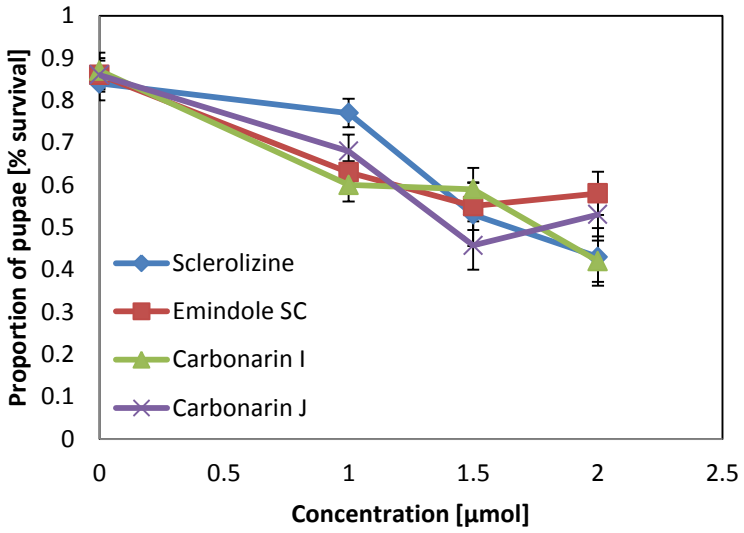

Figure 4. Mean proportional survival of *Drosophila* larvae to the pupal stage as a function of different concentrations (µmol) of the *A. sclerotiicarbonarius* new compounds in the insect's food. Error bars depict the standard error.

CONCLUSION

We here show that the chemical profile of *A. sclerotiicarbonarius* is greatly altered when cultivated under conditions favoring production of sclerotia. By cultivation of a large scale extract under these conditions we have isolated four novel secondary metabolites of mixed biosynthetic origin and elucidated their structures leading to the new compounds sclerolizine, emindole SC, carbonarin I and J. Our analysis has shown that the three latter compounds were locally restricted to the sclerotia, which indicates that these are true sclerotial metabolites.

Sclerolizine and carbonarin I displayed antifungal activity against *Candida albicans* and all four compounds antiinsectan activity. This study thus provides an alternative way of triggering silent biosynthetic pathways in filamentous fungi for the discovery of novel bioactive secondary metabolites. With the discovery of a perfect state in *Aspergillus*

sclerotiicarbonarius[22], further secondary metabolites may be discovered in the progeny of this species.

ACKNOWLEDGMENT

This work was supported by grant 09-064967 from the Danish Council for Independent Research, Technology, and Production Sciences.

Supplementary information is available at the Journal of Antibiotics's website (http://www.nature.com/ja)

REFERENCES

1. Bode, H.; Bethe, B.; Höfs, R.; Zeeck, A. Big effects from small changes: possible ways to explore nature's chemical diversity. *ChemBioChem* **2002**, *3*, 619–627.

2. Brakhage, A. A.; Schroeckh, V. Fungal secondary metabolites - strategies to activate silent gene clusters. *Fungal Genet. Biol.* **2011**, *48*, 15–22.

3. Schroeckh, V.; Scherlach, K.; Nützmann, H. W.; Shelest, E.; Schmidt-Heck, W.; Schuemann, J.; Martin, K.; Hertweck, C.; Brakhage, A. A. Intimate bacterial-fungal interaction triggers biosynthesis of archetypal polyketides in *Aspergillus nidulans*. *Proc. Natl. Acad. Sci. U. S. A.* **2009**, *106*, 14558–14563.

4. Frisvad, J. C.; Petersen, L. M.; Lyhne, E. K.; Larsen, T. O. Formation of sclerotia and production of indoloterpenes by *Aspergillus niger* and other species in section *Nigri*. *PLoS One* **2014**, *9*, e94857.

5. Petersen, L. M.; Hoeck, C.; Frisvad, J. C.; Gotfredsen, C. H.; Larsen, T. O. Dereplication guided discovery of secondary metabolites of mixed biosynthetic origin from *Aspergillus aculeatus*. *Molecules* **2014**, *19*, 10898–10921.

6. Samson, R. A.; Houbraken, J.; Thrane, U.; Frisvad, J. C.; Andersen, B. *Food and Indoor Fungi*; CBS-KNAW Fungal Biodiversity Centre: Utrecht (NL), 2010.

7. Smedsgaard, J. Micro-scale extraction procedure for standardized screening of fungal metabolite production in cultures. *J. Chromatogr. A* **1997**, *760*, 264–270.

8. Holm, D. K.; Petersen, L. M.; Klitgaard, A.; Knudsen, P. B.; Jarczynska, Z. D.; Nielsen, K. F.; Gotfredsen, C. H.; Larsen, T. O.; Mortensen, U. H. Molecular and chemical characterization of the biosynthesis of the 6-MSA derived meroterpenoid yanuthone D in *Aspergillus niger*. *Chem. Biol.* **2014**, *21*, 519–529.

9. Trienens, M.; Rohlfs, M. Experimental evolution of defense against a competitive mold confers reduced sensitivity to fungal toxins but no increased resistance in Drosophila larvae. *BMC Evol. Biol.* **2011**, *11*, 1–10.

10. Hiort, J.; Maksimenka, K.; Reichert, M.; Perović-Ottstadt, S.; Lin, W. H.; Wray, V.; Steube, K.; Schaumann, K.; Weber, H.; Proksch, P.; Ebel, R.; Müller, W. E. G.; Bringmann, G. New natural products from the sponge-derived fungus *Aspergillus niger*. *J. Nat. Prod.* **2004**, *67*, 1532–1543.

11. Nielsen, K. F.; Mogensen, J. M.; Johansen, M.; Larsen, T. O.; Frisvad, J. C. Review of secondary metabolites and mycotoxins from the *Aspergillus niger* group. *Anal. Bioanal. Chem.* **2009**, *395*, 1225–1242.

12. Tanaka, H.; Wang, P.-L.; Yamada, O.; Tamura, L. T. Yellow Pigments of *Aspergillus niger* and *Asp. awamori*. Part I Isolation of Aurasperone A and related pigments. *Agric. Biol. Chem.* **1966**, *30*, 107–113.

13. Varoglu, M.; Crews, P. Biosynthetically diverse compounds from a saltwater culture of sponge-derived *Aspergillus niger*. *J. Nat. Prod.* **2000**, *63*, 41–43.

14. Gunstone, F. D.; Polard, M. R.; Scrimgeour, C. M.; Vedanayagam, H. S. Fatty acids. Part 50. 13C nuclear magnetic resonance studies of olefinic fatty acids and esters. *Chem. Phys. Lipids* **1977**, *18*, 115–129.

15. Laufer, S.; Striegel, H. G. EP0763036B1: Annelierte pyrrolderivate und deren anwendung in der pharmazie 1995.

16. Laufer, S.; Striegel, H. G.; Dannhardt, G. US005939415A: Annellated pyrrole derivatives and their use in pharmacology 1999.

17. Nozawa, K.; Nakajima, S.; Kawai, K.-I.; Udagawa, S.-I. Isolation and structures of indoloditerpenes, possible biosynthetic intermediates to the tremorgenic mycotoxin, paxilline, from *Emericella striata*. *J. Chem. Soc. Perkin Trans. 1* **1988**, 2607–2610.

18. Alfatafta, A. A.; Dowd, P. F.; Gloer, J. B.; Wicklow, D. T. US005519052A: New pure carbonarin derivatives - are insecticides active against *Coleoptera* and *Lepidoptera* 1996.

19. Alfatafta, A. A.; Dowd, P. F.; Gloer, J. B.; Wicklow, D. T. US005672621A: New carbonarin compounds - useful for controlling insects 1997.

20. Priestap, H. A. New naphthopyrones from *Aspergillus fonsecaeus*. *Tetrahedron* **1984**, *40*, 3617–3624.

21. Gloer, J. B. Antiinsectan natural products from fungal sclerotia. *Acc. Chem. Res.* **1995**, *28*, 343–350.

22. Darbyshir, H. L.; van de Vondervoort, P. J. I.; Dyer, P. S. Discovery of sexual reproduction in the black Aspergilli. **2013**, Fung Gen Rep (Suppl) 60: 290 (abstract # 687).

S 1. Extrated Ion Chromatograms of compounds **1-4**

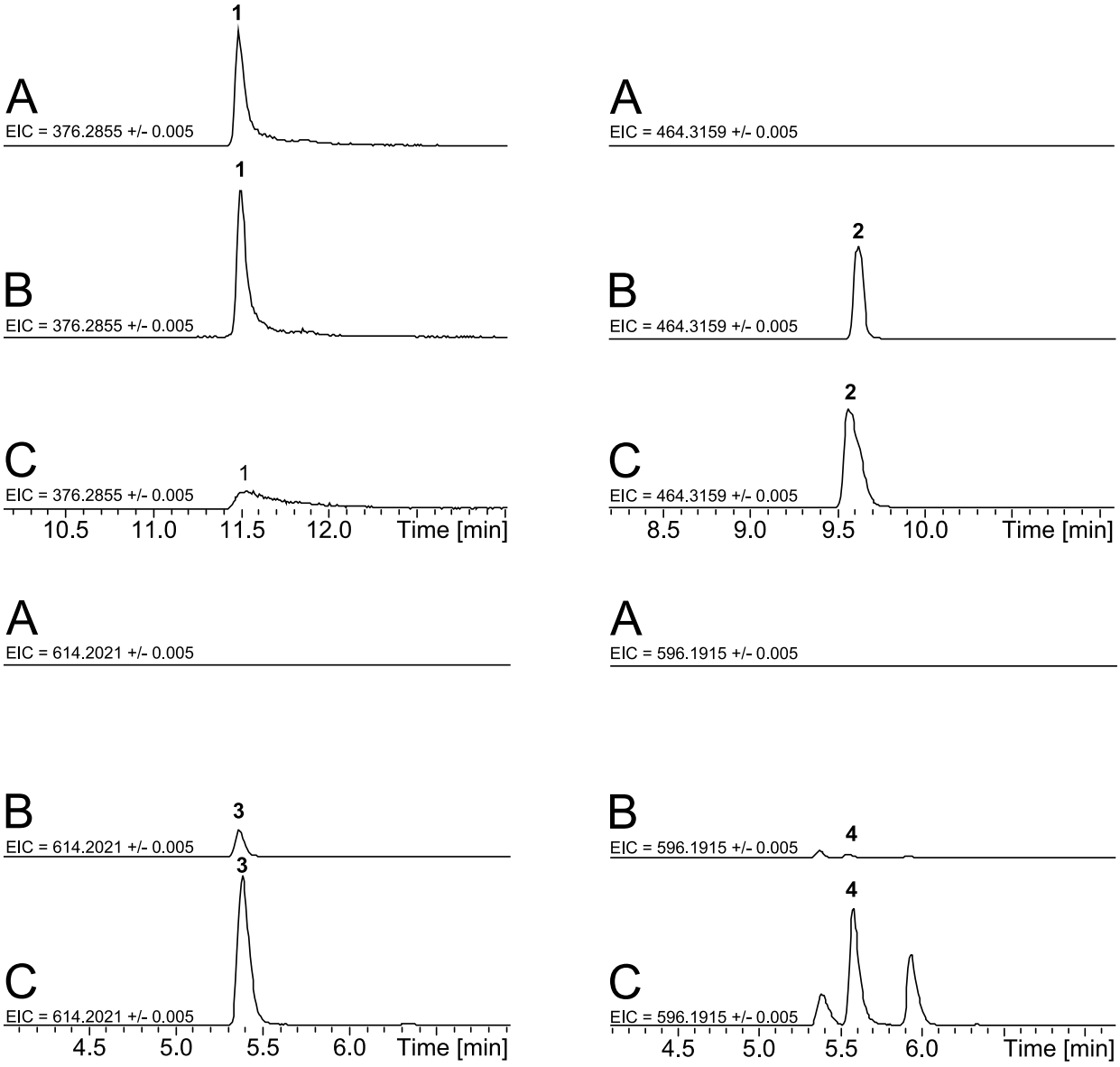

Extracted Ion Chromatograms to check the presence of compound **1-4** with and without sclerotia production. Detected by Extracted Ion Chromatograms (EICs) with a *m/z* of 376.2846, 464.3159, 614.2021, and 596.1915 respectively with a tolerance of *m/z* +/- 0.005. **A**: Plug extraction from growth with no sclerotia production. **B**: Plug extraction from growth with sclerotia production. **C**: Sclerotia extraction. Scaled to relevant RT for each compound; intensities are to scale.

S 2. UV spectra of compounds **1-4**

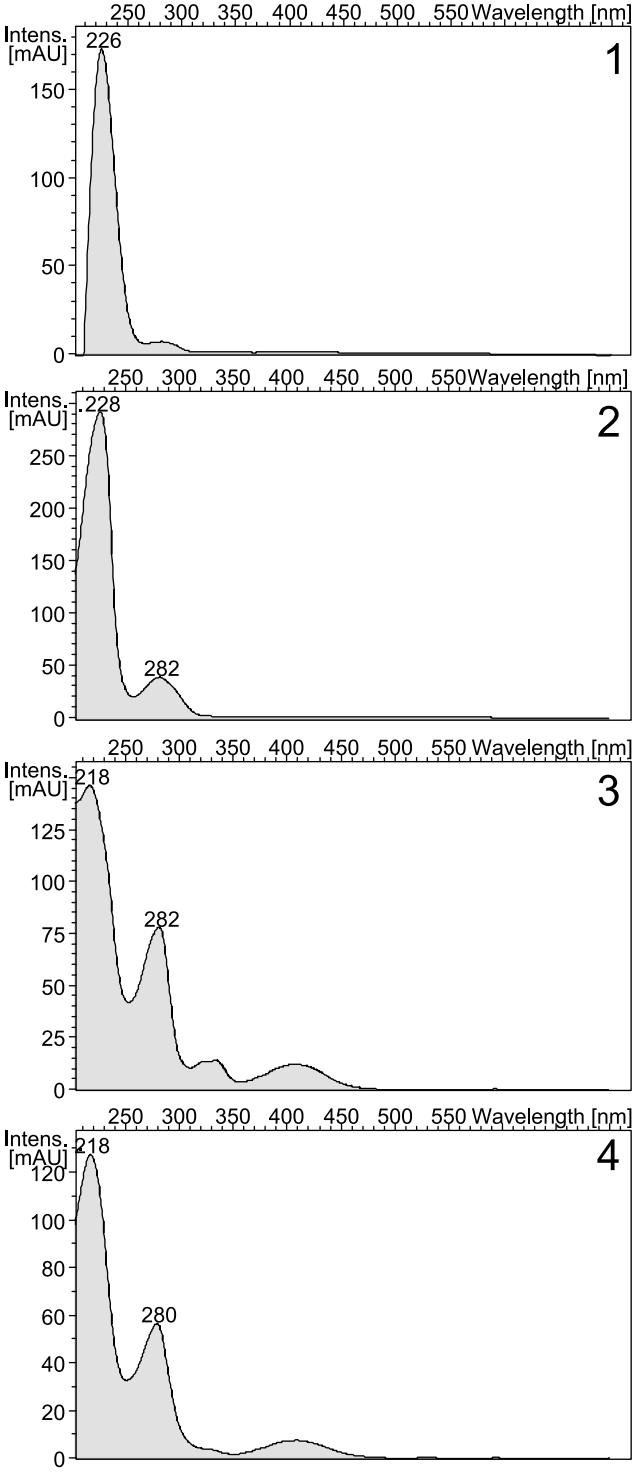

S 3. Spectroscopic data for sclerolizine (**1**)

HRESIMS: $[M+H]^+$ = 376.2855, calculated for $[C_{23}H_{37}NO_3+H]^+$ = 376.2846, $[\alpha]_{587}^{20} = -14.12$

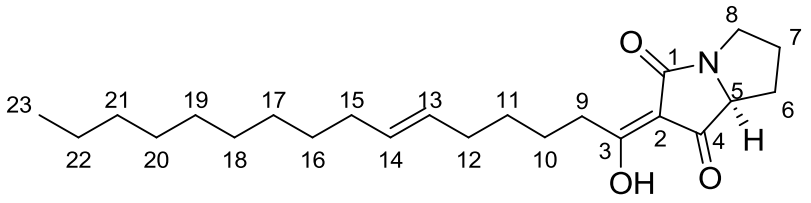

Atom assignment	^{1}H-chemical shift [ppm]/ (integral, mult., *J* [Hz])	^{13}C-chemical shift [ppm]	HMBC correlations
1	-	175.2	
2	-	103.1	
3	-	188.7	
4	-	194.5	
5	3.98 (1H, dd, 9.8, 6.6)	66.8	1, 4, 7
6	1.40 (1H, m)	26.4	4, 5, 7
6'	2.01 (1H, m)	26.4	5, 7, 8
7	1.99 (2H, m)	26.3	5, 6
8	3.09 (1H, m)	42.7	1, 5, 6
8'	3.52 (1H, dt, 10.9, 7.8)	42.7	1, 5, 6
9	2.73 (2H, t, 7.5)	32.9	2, 3, 10, 11
10	1.53 (2H, m)	24.4	3, 9, 11, 12
11	1.32 (2H, m)	28.4	9, 10, 12, 13
12	1.93 (2H, m)	31.5	10
13	5.34 (1H, dd, 15.2, 5.2)	129.7	14, 15
14	5.35 (1H, dd, 15.2, 5.2)	129.8	13, 15
15	1.92 (2H, m)	31.5	16/17/18/19/20/21**, 14
16	1.27 (2H, m)	28.4	16/17/18/19/20/21**
17	1.22 (2H, m)	28.4/21.9*	22, 23, 16/17/18/19/20/21**
18	1.22 (2H, m)	28.4/21.9*	22, 23, 16/17/18/19/20/21**
19	1.22 (2H, m)	28.4/21.9*	22, 23, 16/17/18/19/20/21**
20	1.22 (2H, m)	28.4	22, 23, 16/17/18/19/20/21**
21	1.22(2H, m)	28.4/21.9*	22, 23, 16/17/18/19/20/21**
22	1.25 (2H, m)	21.9	20, 21, 23
23	0.84 (3H, t, 6.9)	13.7	21, 22

*Due to overlapping signals the specific carbon chemical shift could not be determined

**Due to many carbon chemical shifts at C_δ = 28.4 ppm, this HMBC correlation could not be unambiguously assigned.

S 4. ^{1}H NMR (500 MHz, DMSO-d_6 spectrum) of the new compound sclerolizine (**1**)

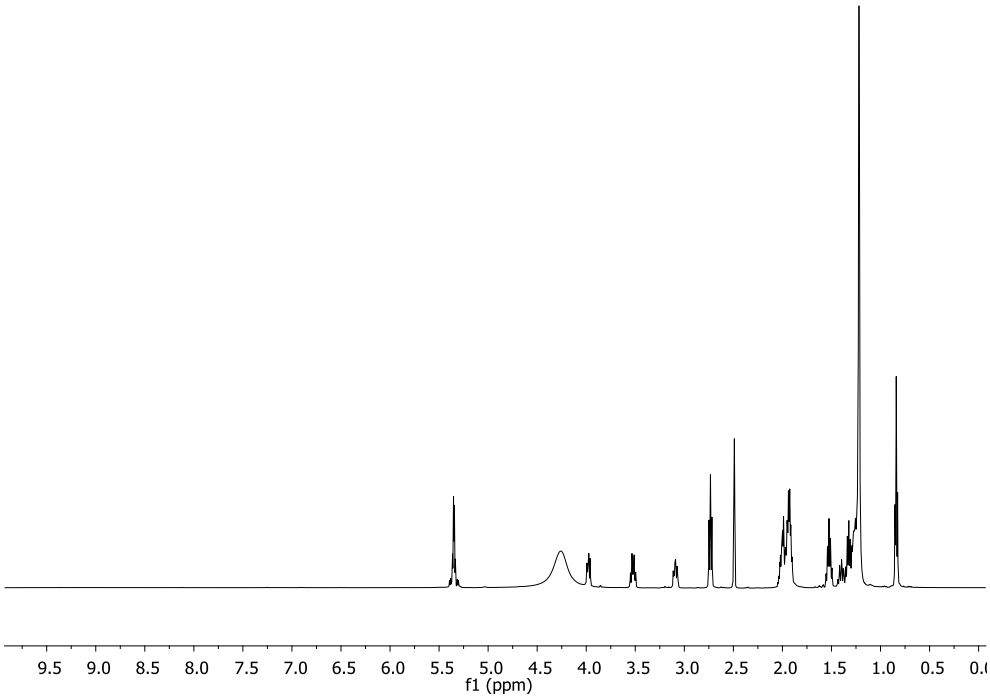

S 5. DQF-COSY spectrum of the new compound sclerolizine (**1**)

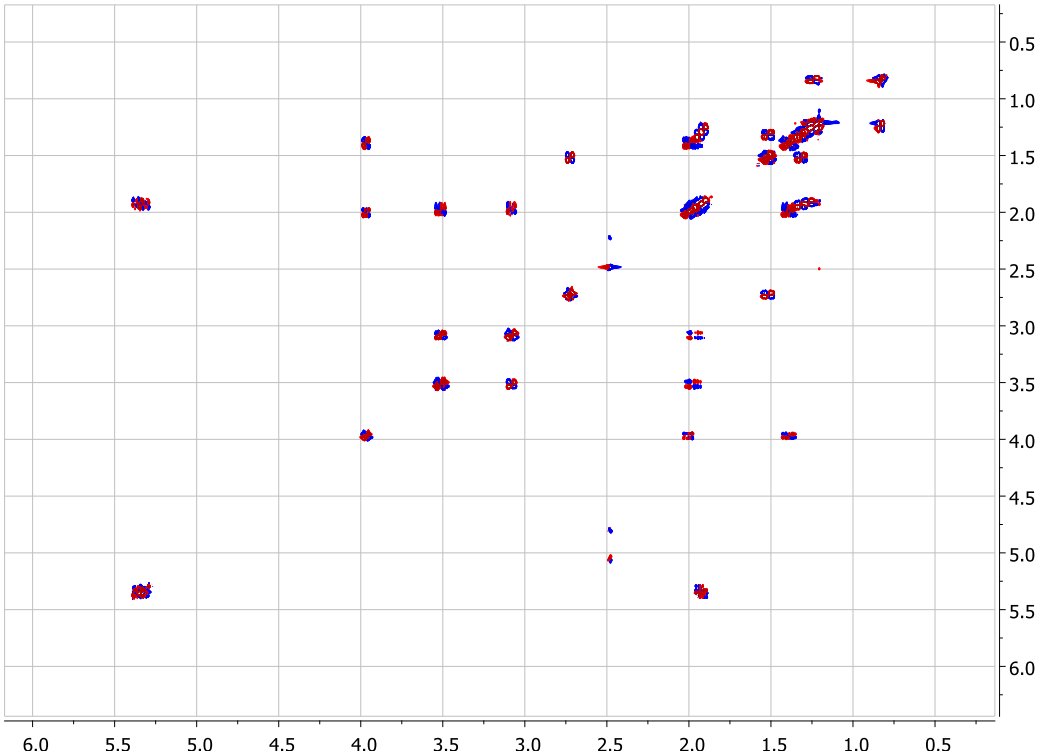

S 6. HSQC spectrum of the new compound sclerolizine (**1**)

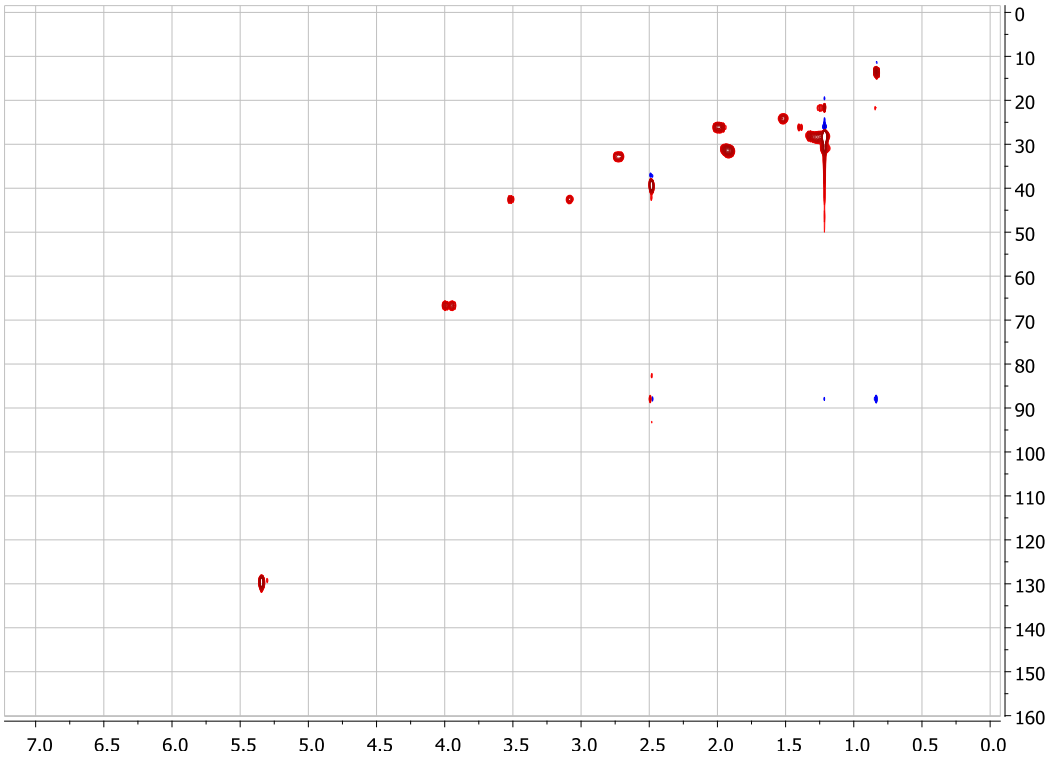

S 7. HMBC spectrum of the new compound sclerolizine (**1**)

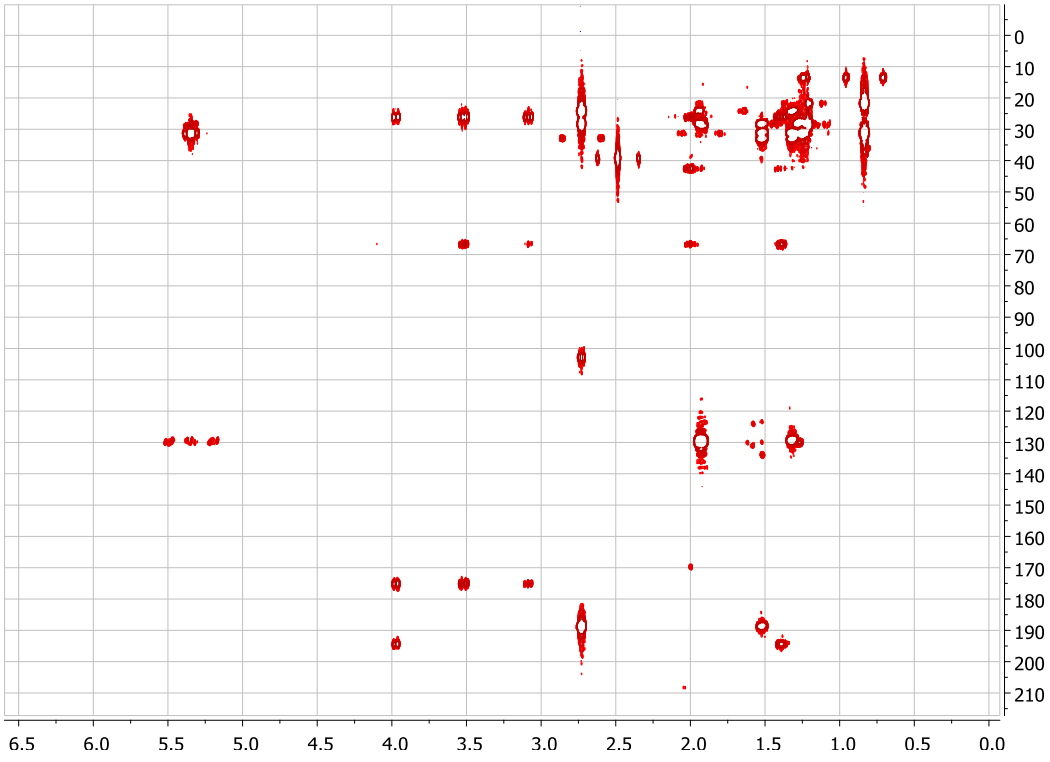

S 8. Spectroscopic data for emindole SC (**2**)

HRESIMS: $[M+H]^+$ = 464.3159, calculated for $[C_{30}H_{41}NO_3+H]^+$ = 464.3159, $[\alpha]_{587}^{20} = 1.23$

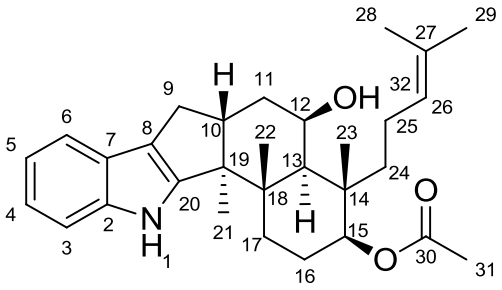

Atom assignment	^{1}H-chemical shift [ppm]/ (integral, mult., *J* [Hz])	^{13}C-chemical shift [ppm]	HMBC correlations	NOESY
1	10.57 (1H, s)	-	2, 7, 8, 20	3, 17
2	-	140.3	-	
3	7.25 (1H, d, 7.1)	111.8	5, 7	1, 4
4	6.93 (1H, t)	119.4	2, 6	3
5	6.89 (1H, t)	118.4	3, 7	6
6	7.27 (1H, d, 7.1)	117.8	2, 4, 8	5
7	-	124.6	-	
8	-	115.9	-	
9	2.55 (1H, dd, 13.1, 6.5)	26.8	8, 10, 18, 20	9',10
9'	2.26 (1H, dd, 13.1, 11.0)	26.8	8, 10, 11/11', 20	9,10,21
10	3.20 (1H, m)	41.9	9/9', 11/11', 12, 18, 19, 21	9,9',22
11	1.78 (1H, m)	34.7	18	12
11'	1.68 (1H, m)	34.7	12, 13, 18	12
12	4.14 (1H, br. s.)	66.2	10, 19	11,11',13
13	1.49 (1H, br.s)	42.6	12, 14, 15, 18	12,15,21
14	-	40.5	-	
15	4.68 (1H, dd, 11.2, 3.9)	75.5	14,16/16',17/17',23,24/24',30	13,16'
16	1.87 (1H, m)	23.5	15	
16'	1.69 (1H, m)	23.5	14, 15, 18, 19, 22	15
17	1.83 (1H, m)	32.5	13, 15, 16/16', 19, 22	1
17'	1.72 (1H, m)	32.5	14, 15, 19	21
18	-	52.4	-	
19	-	39.6	-	
20	-	151.3	-	
21	0.90 (3H, s)	14.2	10, 18, 19, 20	9',13,17'
22	1.33 (3H, s)	20.5	13, 17/17', 18, 19	10
23	1.26 (3H, s)	19.3	13, 14, 15, 24/24'	32
24	1.54 (1H, m)	37.5	-	
24'	1.22 (1H, m)	37.5	-	
25	1.93 (1H, m)	21.0	26, 27	26

25'	1.76 (1H, m)	21.0	26, 27	26
26	5.04 (1H, t, 7.0)	124.6	24/24' 25/25', 28, 29	24',25,25',28,29
27	-	130.6	-	
28	1.53 (3H, s)	17.4	26, 27	26
29	1.64 (3H, s)	25.4	24/24', 26, 27, 28	26
30	-	170.0	-	
31	2.01 (3H, s)	20.7	15, 30	
32	4.42 (1H, br.s)	-	12, 13	23

S 9. ^{1}H NMR (500 MHz, DMSO-d_6 spectrum) of the new compound emindole SC (**2**)

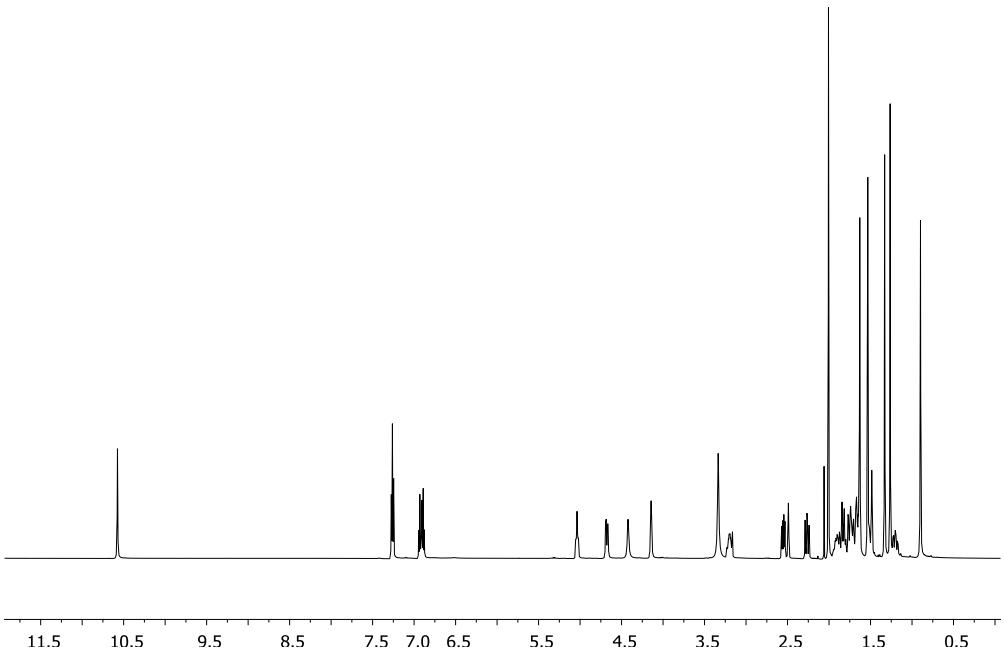

S 10. DQF-COSY spectrum of the new compound emindole SC (**2**)

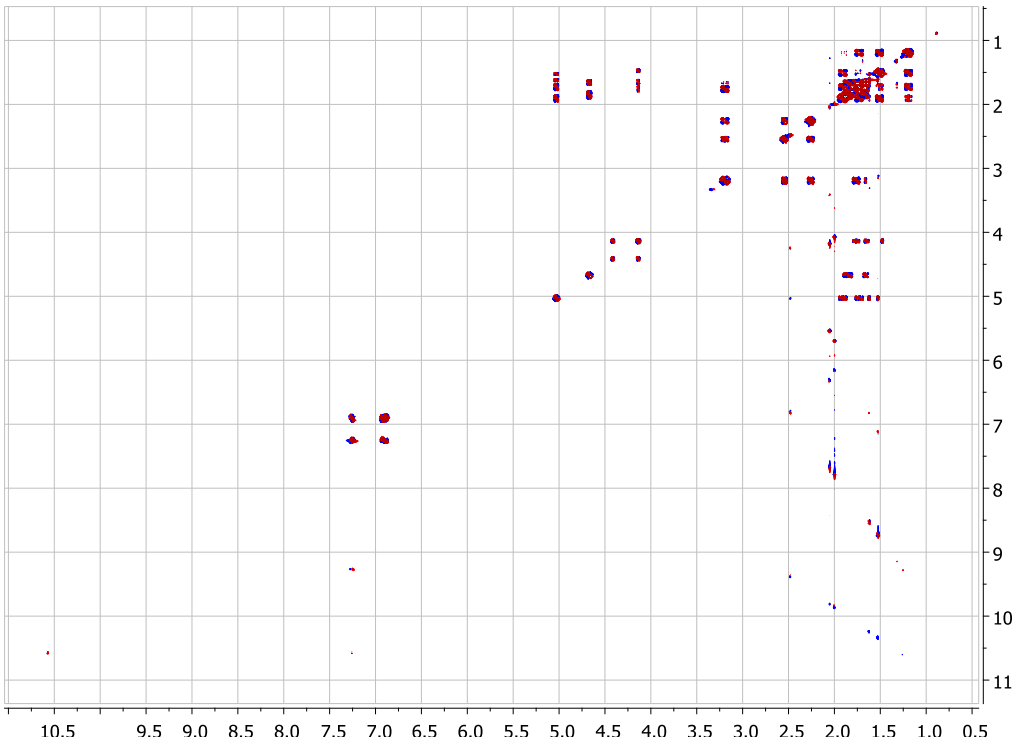

S 11. Ed-HSQC spectrum of the new compound emindole SC (**2**)

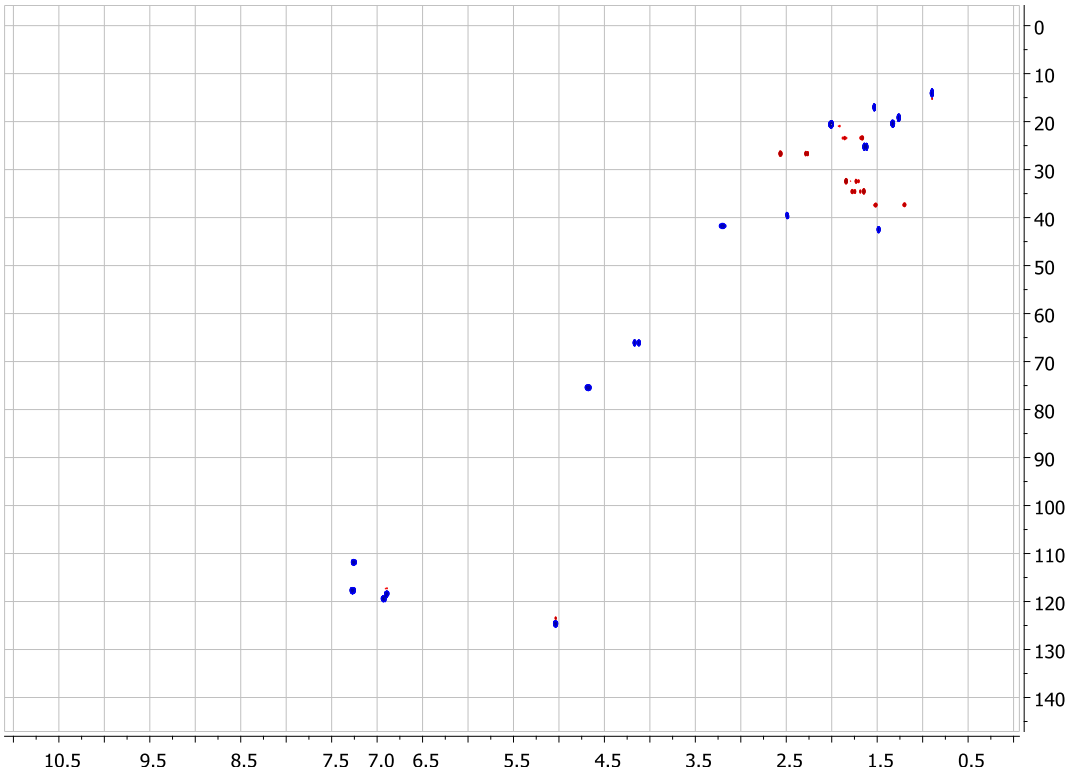

S 12. HMBC spectrum of the new compound emindole SC (**2**)

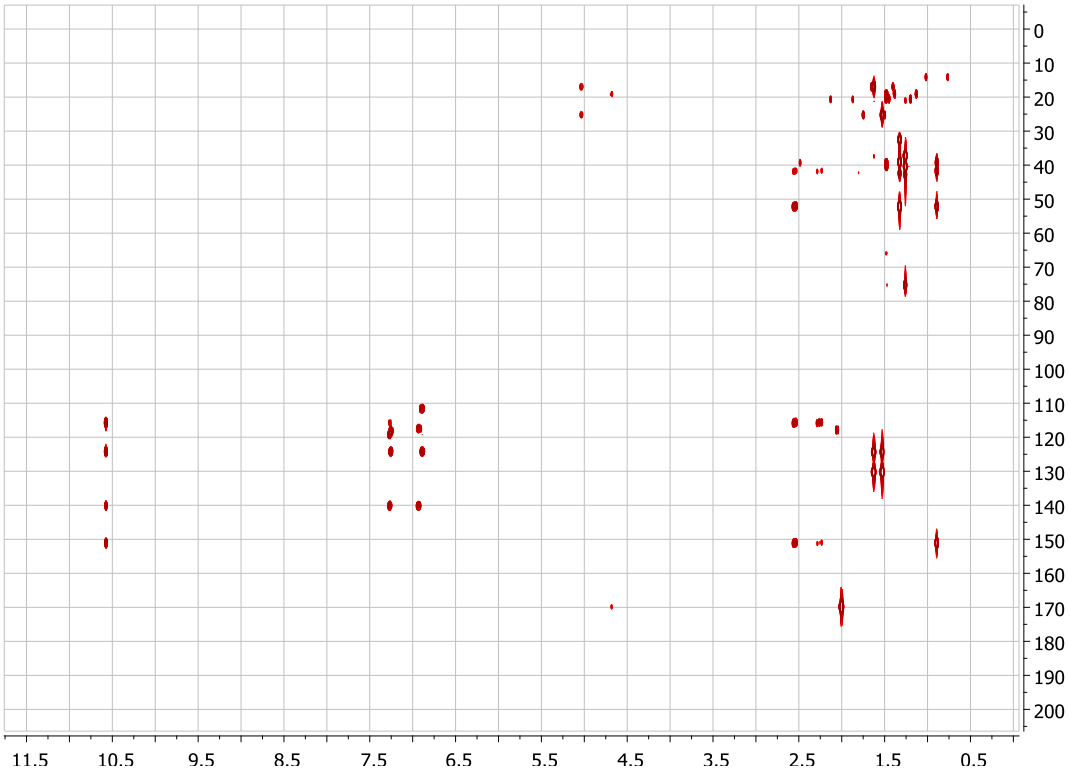

S 13. Spectroscopic data for carbonarin I (**3**)

HRESIMS: $[M+H]^+$ = 614.2025, calculated for $[C_{34}H_{31}NO_{10}+H]^+$ = 614.2021, $[\alpha]_{587}^{20} = -14.58$

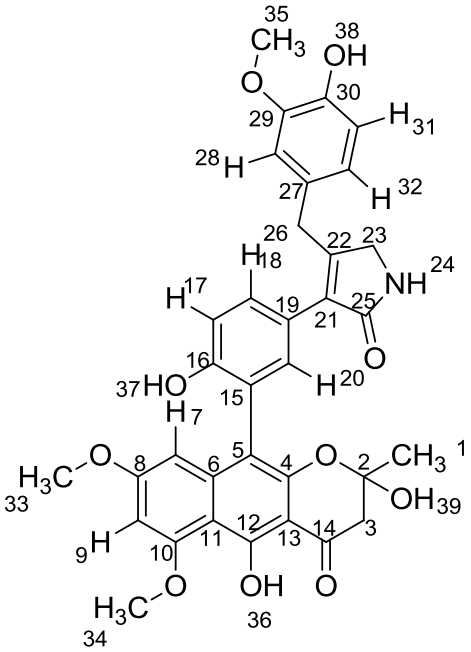

Atom assignment	^{1}H-chemical shift [ppm]/ (integral, mult., *J* [Hz])	^{13}C-chemical shift [ppm]	HMBC correlations	NOESY
1	1.43 (3H, s)	26.9	2, 3/3', 14	
2	-	99.9	-	
3	3.11	47.6	1, 2, 14	3'
3'	2.78	47.6	1, 2, 14	3
4	-	155.6	-	
5	-	110.2	-	
6	-	141.5	-	
7	6.22 (1H, s)	97.6	5, 8/10, 9, 11	33
8	-	161.1	-	
9	6.42 (1H, s)	95.3	7, 8/10, 11	33, 34
10	-	161.2	-	
11	-	106.1	-	
12	-	163.4	-	
13	-	102.4	-	
14	-	198.2	-	
15	-	122.5	-	
16	-	154.9	-	
17	7.00 (1H, dd, 8.4, 2.8)	115.3	15, 16, 19	18
18	7.32 (1H, dd, 8.4, 2.1)	129.9	16, 20, 21	17
19	-	121.9	-	
20	7.21 (1H, dd, 4.0, 2.2)	133.4	5, 16, 18, 21	

21	-	130.9	-	
22	-	152.1	-	
23	3.74 (2H, s)	47.2	21, 22	24
24	8.15 (1H, s)	-	21, 22, 23, 25	23
25	-	172.9	-	
26	3.76 (2H, s)	33.2	21, 22, 23, 28, 32	
27	-	129.2	-	
28	6.65 (1H, m)	112.3	26, 30, 32	
29	-	147.4	-	
30	-	144.6	-	
31	6.64 (1H, m)	115.3	27, 29	32
32	6.51 (1H, m)	120.2	26, 28, 30	31
33	3.57 (3H, s)	55.8	8	7, 9
34	3.88 (3H, s)	54.5	10	9
35	3.60 (3H, s)	54.9	29	
36	14.38 (1H, s)	-	11, 12, 13, 14	
37	9.15 (1H, s)	-	15, 16, 17	
38	8.80 (1H, s)	-	-	
39	6.92 (1H, s)	-	2, 3, 4	

S 14. ^{1}H NMR (500 MHz, DMSO-d_6 spectrum) of the new compound carbonarin I (**3**)

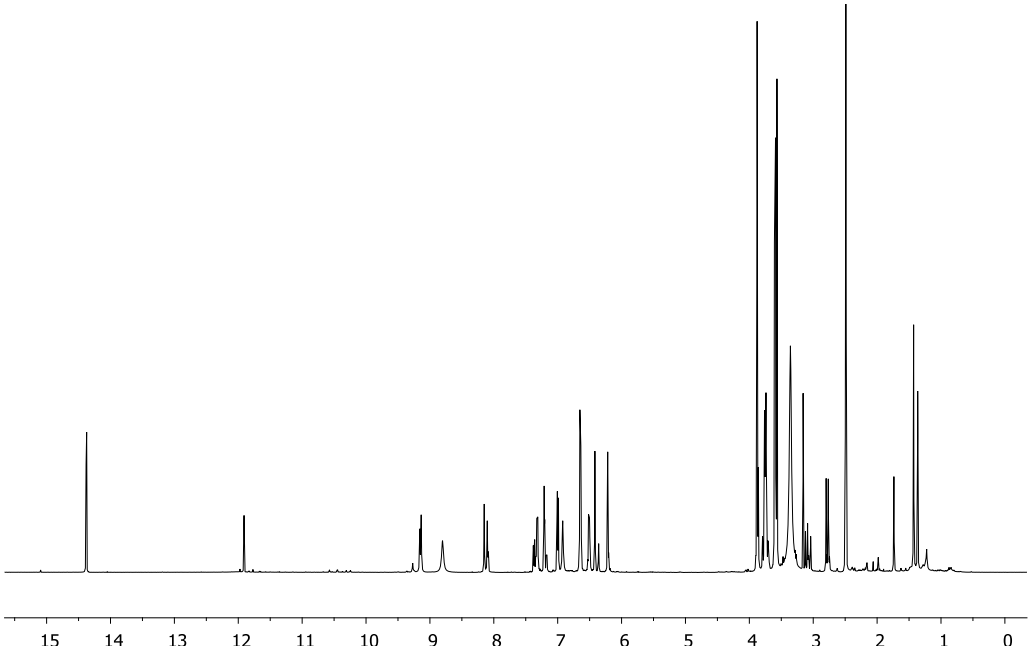

S 15. DQF-COSY spectrum of the new compound carbonarin I (**3**)

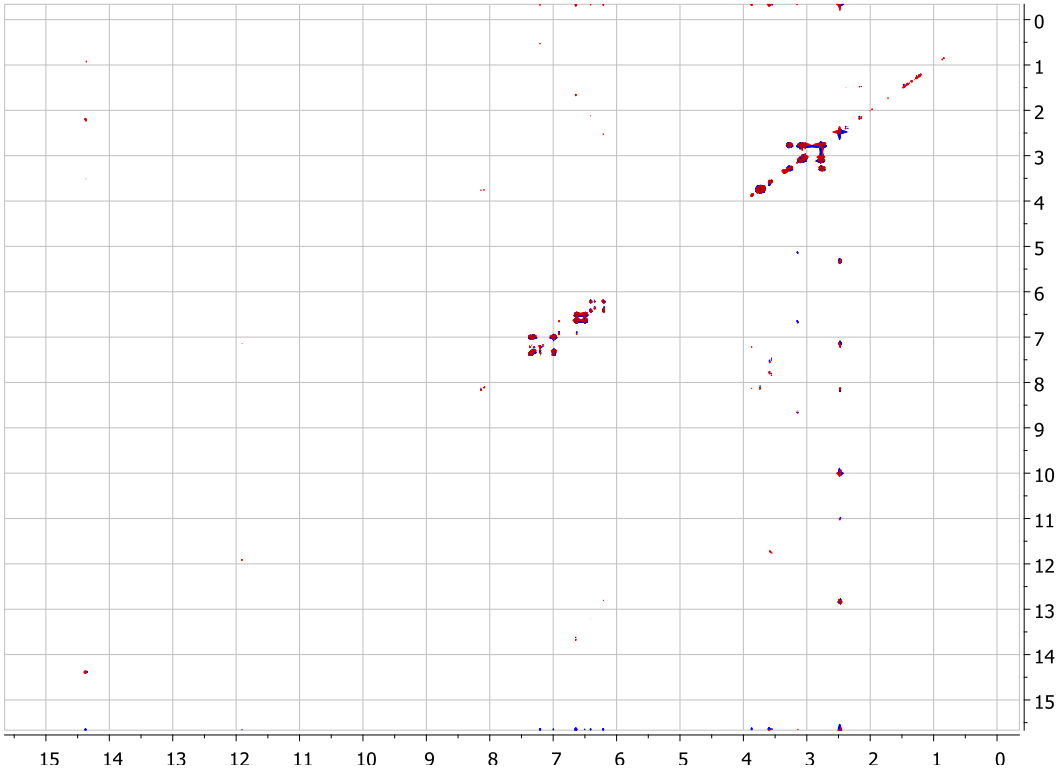

S 16. HSQC spectrum of the new compound carbonarin I (**3**)

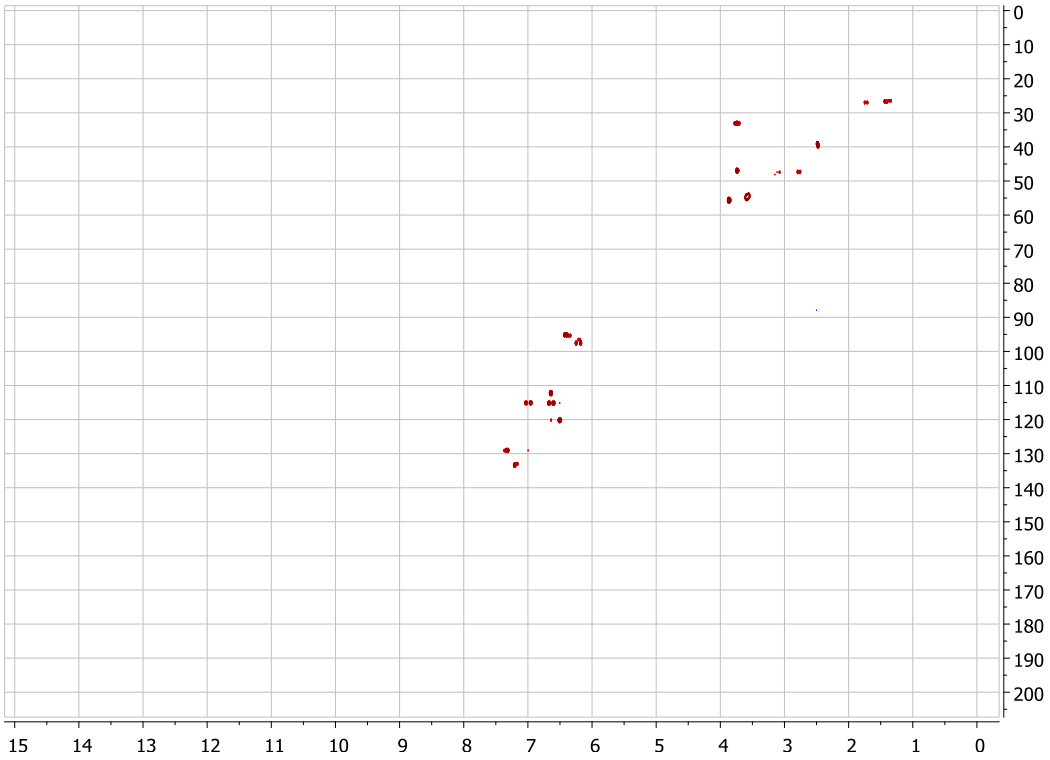

S 17. HMBC spectrum of the new compound carbonarin I (**3**)

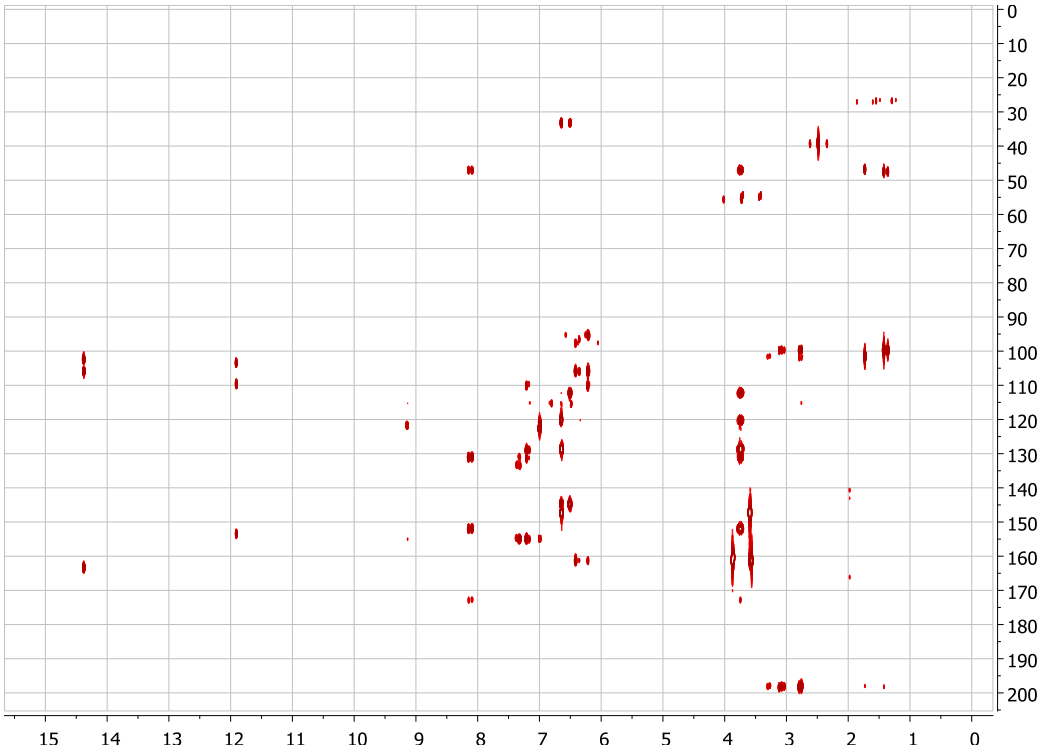

S 18. Spectroscopic data for carbonarin J (**4**)

HRESIMS: $[M+H]^+$ = 596.1923, calculated for $[C_{34}H_{29}NO_9+H]^+$ = 596.1915, $[\alpha]_{587}^{20} = -41.20$

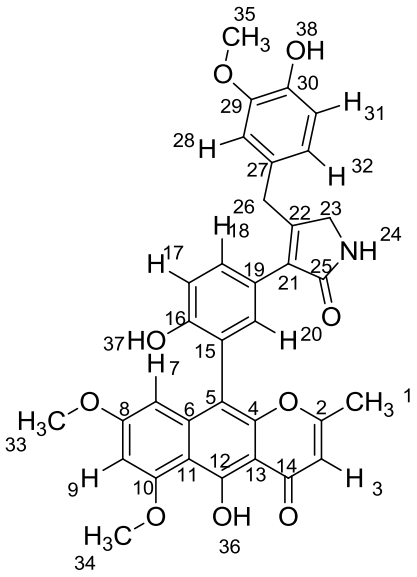

Atom assignment	^{1}H-chemical shift [ppm]/ (integral, mult., *J* [Hz])	^{13}C-chemical shift [ppm]	HMBC correlations	NOESY
1	2.16 (3H, s)	20.0	2, 3	3
2	-	168.3	-	
3	6.18 (1H, s)	106.4	1, 2, 13	1
4	-	149.8	-	
5	-	109.2	-	
6	-	161.0	-	
7	6.41 (1H, d, 2.1)	96.5	5, 9, 11	
8	-	160.5	-	
9	6.52 (1H, d, 2.0)	96.5	7, 10, 11	
10	-	106.7	-	
11	-	107.4	-	
12	-	161.6	-	
13	-	103.2	-	
14	-	184.1	-	
15	-	120.3	-	
16	-	154.9	-	
17	7.07 (1H, d, 8.4)	115.6	15, 16, 19	18, 37
18	7.43 (1H, dd, 8.4, 2.1)	129.9	15, 16, 20, 21	17
19	-	122.5	-	
20	7.27 (1H, d, 2.0)	133.2	5, 15, 21	
21	-	130.9	-	
22	-	152.2	-	
23	3.75 (2H, s)	47.2	21, 22, 25	24
24	8.12 (1H, s)	-	21, 22, 23, 25	23

25	-	172.6	-	
26	3.76 (2H, s)	33.4	23, 27, 28, 32	28
27	-	128.7	-	
28	6.64 (1H, m)	112.4	26, 30, 32	26, 35
29	-	147.2	-	
30	-	145.0	-	
31	6.63 (1H, d, 8.5)	115.3	27, 29, 30	38
32	6.49 (1H, dd, 8.0, 1.6)	120.3	26, 28, 30	
33	3.90 (3H, s)	55.8	8	34
34	3.61 (3H, s)	54.7	10	33
35	3.59 (3H, s)	54.9	29	28
36	15.09 (1H, s)	-	11, 12, 13	
37	9.36 (1H, s)	-	15, 16, 17	17
38	8.81 (1H, s)	-	29, 30, 31	31

S 19. ^{1}H NMR (500 MHz, DMSO-d_6 spectrum) of the new compound carbonarin J (**4**)

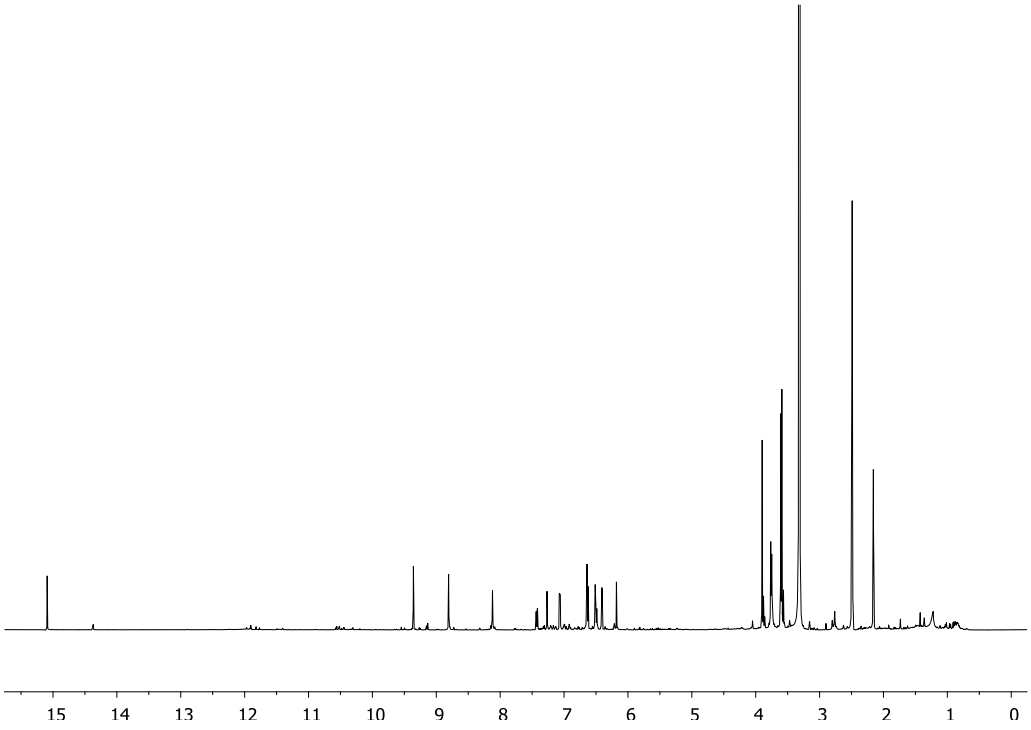

S 20. DQF-COSY spectrum of the new compound carbonarin J (**4**)

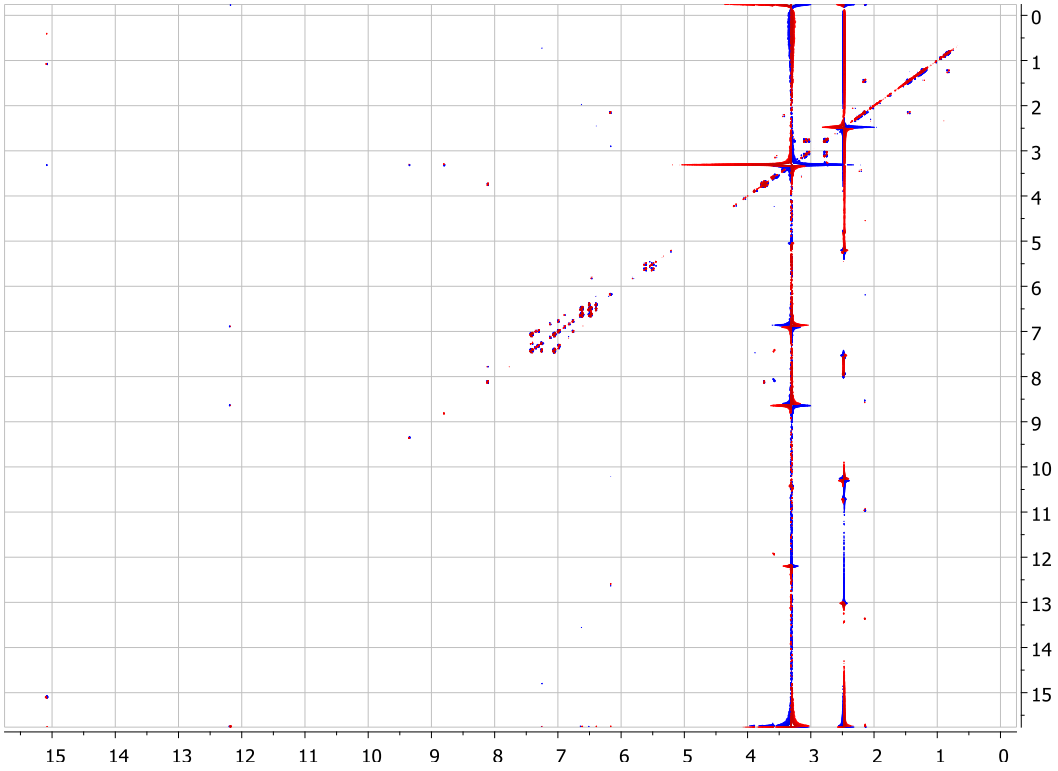

S 21. Ed-HSQC spectrum of the new compound carbonarin J (**4**)

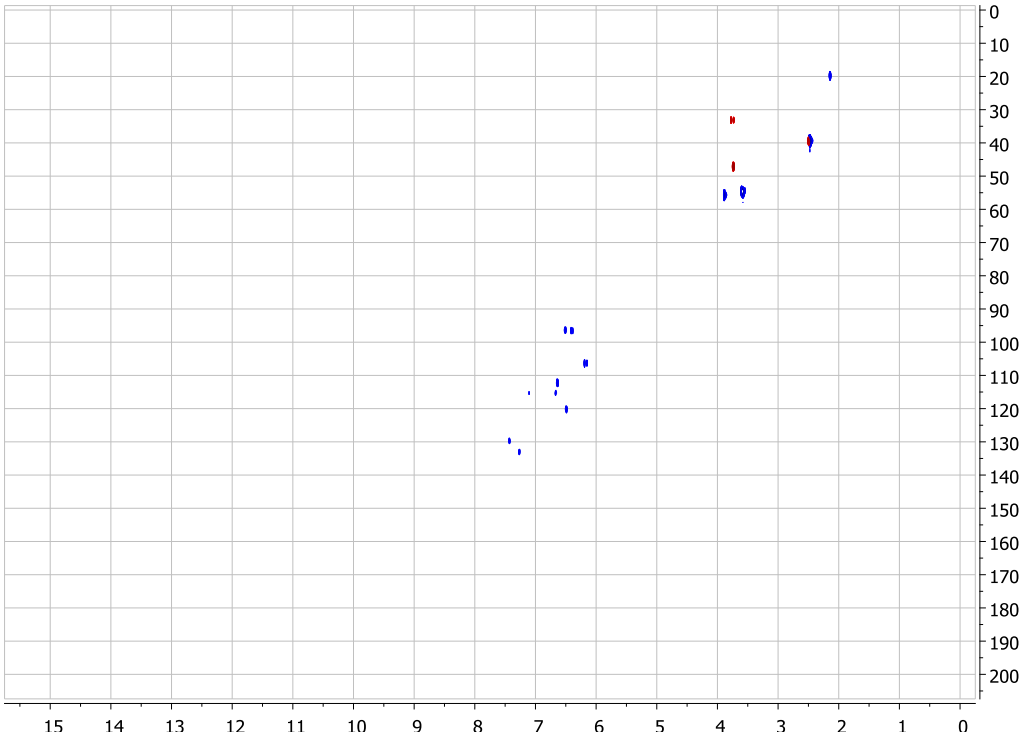

S 22. HMBC spectrum of the new compound carbonarin J (**4**)

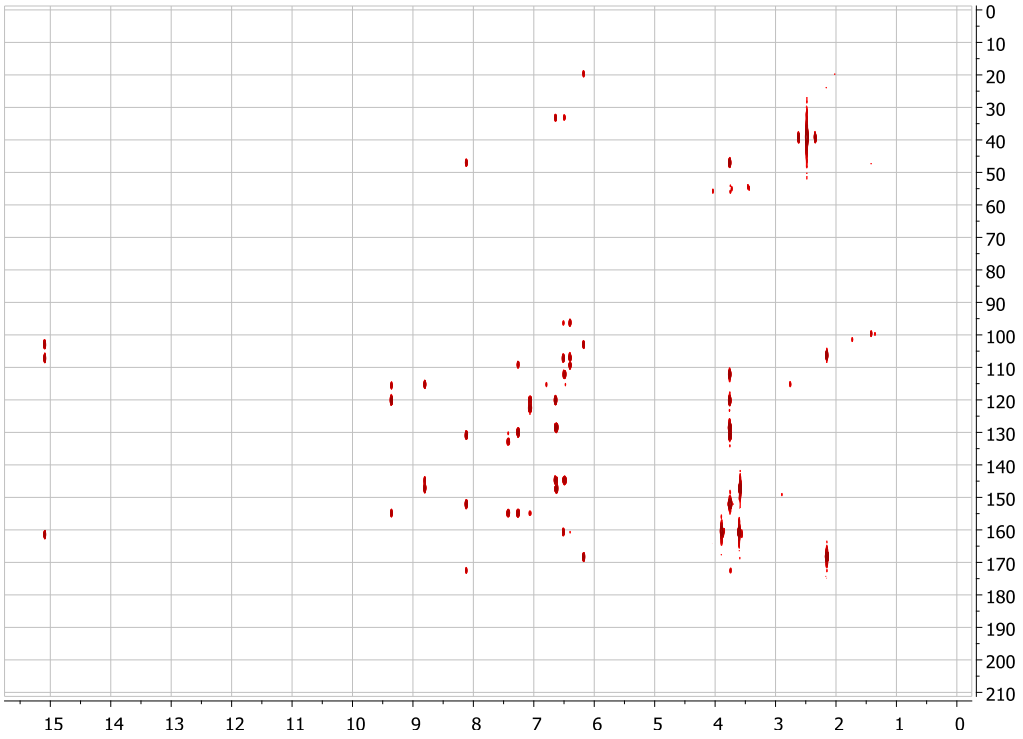

Paper 7

"Comparative Chemistry of *Aspergillus oryzae* (RIB40) and *A. flavus* (NRRL 3357)"

Rank, C.; Klejnstrup, M.L.; **Petersen, L.M.**; Kildgaard, S.; Frisvad, J.C.; Gotfredsen, C.H.; Larsen, T.O.

Metabolites, **2012**, *2* (1), 39-56

Metabolites **2012**, *2*, 39-56; doi:10.3390/metabo2010039

OPEN ACCESS

metabolites

ISSN 2218-1989
www.mdpi.com/journal/metabolites/

Article

Comparative Chemistry of *Aspergillus oryzae* (RIB40) and *A. flavus* (NRRL 3357)

Christian Rank [1,†], Marie Louise Klejnstrup [1,†], Lene Maj Petersen [1], Sara Kildgaard [1], Jens Christian Frisvad [1], Charlotte Held Gotfredsen [2] and Thomas Ostenfeld Larsen [1,*]

[1] Department of Systems Biology, Center for Microbial Biotechnology, Technical University of Denmark, Søltofts Plads B221, DK-2800 Kgs. Lyngby, Denmark;
E-Mails: christian.rank@gmail.com (C.R.); marlk@bio.dtu.dk (M.L.K.); lmape@bio.dtu.dk (L.M.P.); sarakildgaard@hotmail.com (S.K.); jcf@bio.dtu.dk (J.C.F.)

[2] Department of Chemistry, Technical University of Denmark, Kemitorvet B201, DK-2800 Kgs. Lyngby, Denmark; E-Mail: chg@kemi.dtu.dk

† These authors contributed equally to this work.

* Author to whom correspondence should be addressed; E-Mail: tol@bio.dtu.dk;
Tel.: +45-4525-2632; Fax: +45-4588-4148.

Received: 18 November 2011; in revised form: 14 December 2011 / Accepted: 22 December 2011 / Published: 5 January 2012

Abstract: *Aspergillus oryzae* and *A. flavus* are important species in industrial biotechnology and food safety and have been some of the first aspergilli to be fully genome sequenced. Bioinformatic analysis has revealed 99.5% gene homology between the two species pointing towards a large coherence in the secondary metabolite production. In this study we report on the first comparison of secondary metabolite production between the full genome sequenced strains of *A. oryzae* (RIB40) and *A. flavus* (NRRL 3357). Surprisingly, the overall chemical profiles of the two strains were mostly very different across 15 growth conditions. Contrary to previous studies we found the aflatrem precursor 13-desoxypaxilline to be a major metabolite from *A. oryzae* under certain growth conditions. For the first time, we additionally report *A. oryzae* to produce parasiticolide A and two new analogues hereof, along with four new alkaloids related to the *A. flavus* metabolites ditryptophenalines and miyakamides. Generally the secondary metabolite capability of *A. oryzae* presents several novel end products likely to result from the domestication process from *A. flavus*.

Keywords: *Aspergillus oryzae*; (RIB40); *Aspergillus flavus*; (NRRL 3357); parasiticolide; ditryptoleucine; oryzamide

1. Introduction

Aspergillus oryzae is one of industry's most used "workhorses" and has been used for centuries in food fermentation for the production of e.g., sake, soy sauce and other traditional Asian foods [1]. *A. oryzae* is also a widely used organism for production of amylase, lipases and proteases and more recently also for heterologous expression of secondary metabolite genes and non-fungal proteins [2–4]. For many years, *A. oryzae* has been suspected to be a domesticated form of *A. flavus*, a plant and mammalian pathogenic saprophyte, capable of producing some of the most carcinogenic compounds known: the aflatoxins. Genetic work and subsequent genome sequencing of strains of both species have verified the tight link between the species [1,5–8].

The relationship of the two species has resulted in extensive screening of the toxic potential of *A. oryzae*, but no genuine evidence of aflatoxin production in validated *A. oryzae* isolates has ever been shown. Other important toxins, known from *A. flavus*, have on the other hand been shown in *A. oryzae*: 3-Nitropropionic acid [9] and cyclopiazonic acid (CPA) [10] along with kojic acid [11,12] (Figure 1). Additional metabolites previously reported from *A. oryzae* are asperfuran [13], sporogen AO1 [14,15], maltoryzine [16], and aspergillomarasmine A [17,18]. Aspirochlorine has been found in *A. flavus*, *A. oryzae* and *A. tamarii* [19–23] (Figure 1). For reviews on the safety and taxonomy of *A. oryzae*, see [7,24–26].

Figure 1. Known compounds from *Aspergillus flavus* or *A. oryzae.*

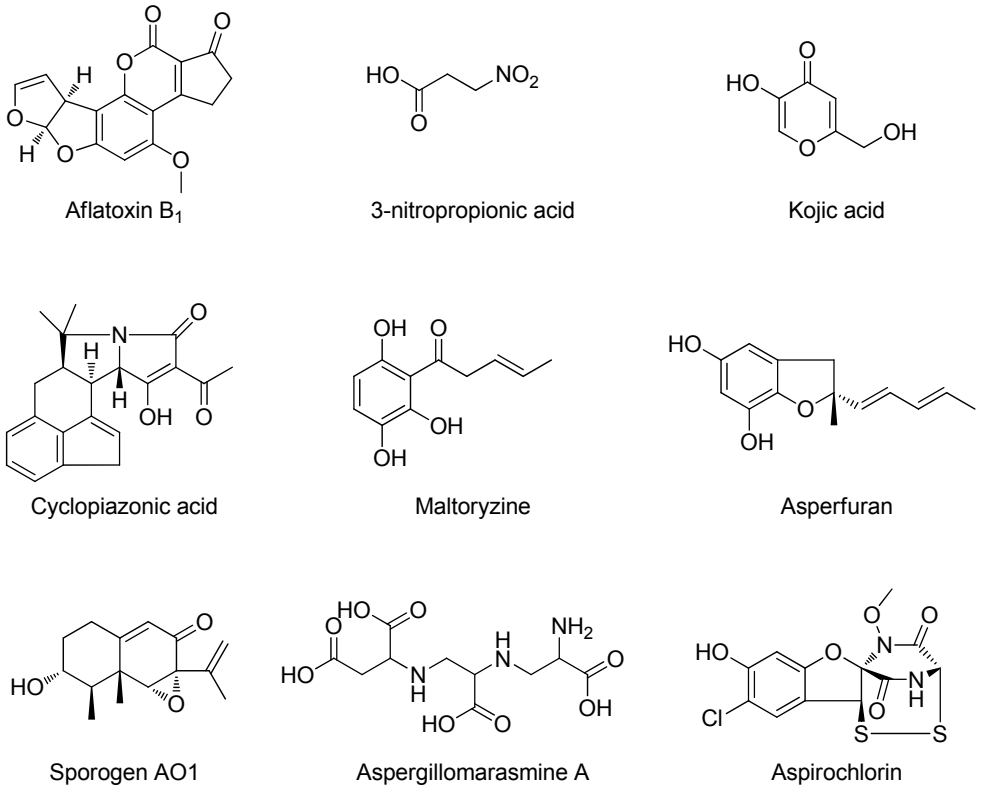

The few predicted differences between the genomes of *A. oryzae* and *A. flavus* (ca. 99.5% genome homology and 98% at the protein level for RIB40/ATCC 42149 and NRRL 3357 [27]), could lead one to expect *A. oryzae* to produce most of the metabolites found in *A. flavus* [1,28–31], but published metabolic data indicates a very low chemical correlation [32]. It is with reference to the established genetic heritage of *A. oryzae* from *A. flavus* remarkable that maltoryzine, sporogen AO1, asperfuran and aspergillomarasmine A have never been unambigously identified in *A. flavus*. Though research on *A. flavus* chemistry has focused primarily on toxic compounds, one would expect that these metabolites should be part of its chemical potential as they are for the domesticated *A. oryzae*. The preliminary bioinformatic studies in conjunction with the genome sequencing shows roughly the same number of predicted genes: 32 Polyketide synthases (PKSs) and 28 non-ribosomal synthases (NRPSs) for *A. flavus* and 32 PKSs and 27 NRPSs for *A. oryzae* with 2 NRPSs apparently unique for each strain [33]. The exclusiveness of these genes in terms of end product has yet to be verified chemically.

Most of the predicted genes for secondary metabolites of *A. oryzae* (or *A. flavus*) have not been mapped to specific metabolic products, despite the genome sequencing of RIB40 in 2005 [27]. Only genes of the most important toxins: Aflatoxin [31,34,35], CPA [36,37] and aflatrem [38] have been fully annotated in both species, which leaves much to be explored. The full chemical potential of either species is unknown and epigenetic modifiers [39–43] may be necessary, alongside with the use of different growth conditions to aid triggering the full potential of secondary metabolite expression in these two closely related species.

The aim of the current work has been to perform an initial comparative investigation of the chemistry from the two genome sequenced strains of *A. oryzae* (RIB40) and *A. flavus* (NRRL 3357), in order to get further insights into possible homologies and differences in secondary metabolite production for these two important species.

2. Results and Discussion

2.1. De-Replication of A. oryzae RIB40

For the analysis of *A. oryzae* RIB40 chemistry, we investigated a series of solid media (YES, YESBEE, DRYES, CYA, CYAS, CY20, CY40, DUL, GAK, GMMS, MEA, OAT, PDA, TGY, WATM (see Methods and Materials for explanation) cultivations with micro-scale extractions [44,45] and subsequently analyzed with HPLC-DAD-MS for selection of optimal conditions. The different media were tested on a collection of *A. oryzae* (RIB40, IBT 28103) and *A. flavus* (NRRL 3357, IBT 23106, IBT 3642) and these strains were cultivated at 25 °C in the dark for 7 and 14 days. The media screening for *A. oryzae* and *A. flavus* indicated the greatest chemodiversity and metabolite production from CYA, YES and WATM agar for our purpose.

The comparison of the secondary metabolite profiles of the two strains, NRRL 3357 and RIB40, exposed a surprisingly high degree of chemical difference on all media as illustrated in Figure 2 and Table 1 for the WATM medium. The major metabolite repetitions between the two genome sequenced strains were merely kojic acid and ergosterol, like a number of minor metabolites (not analyzed here) seemed to be shared between the two strains. Altogether, this is in sharp contrast to the high gene homology, particularly for the secondary metabolite genes.

Figure 2. ESI+ BPC chromatogram of 7 day micro scale extract from WATM, bottom: *A. oryzae* RIB40, top: *A. flavus* NRRL 3357. Besides kojic acid (shown in box) and analogues in the beginning of chromatogram and ergosterol in the end (not shown), there are very few identical compounds between the genetically almost identical strains. Note that aspirochlorine is only detectable in negative ionization, and therefore not visible in this chromatogram.

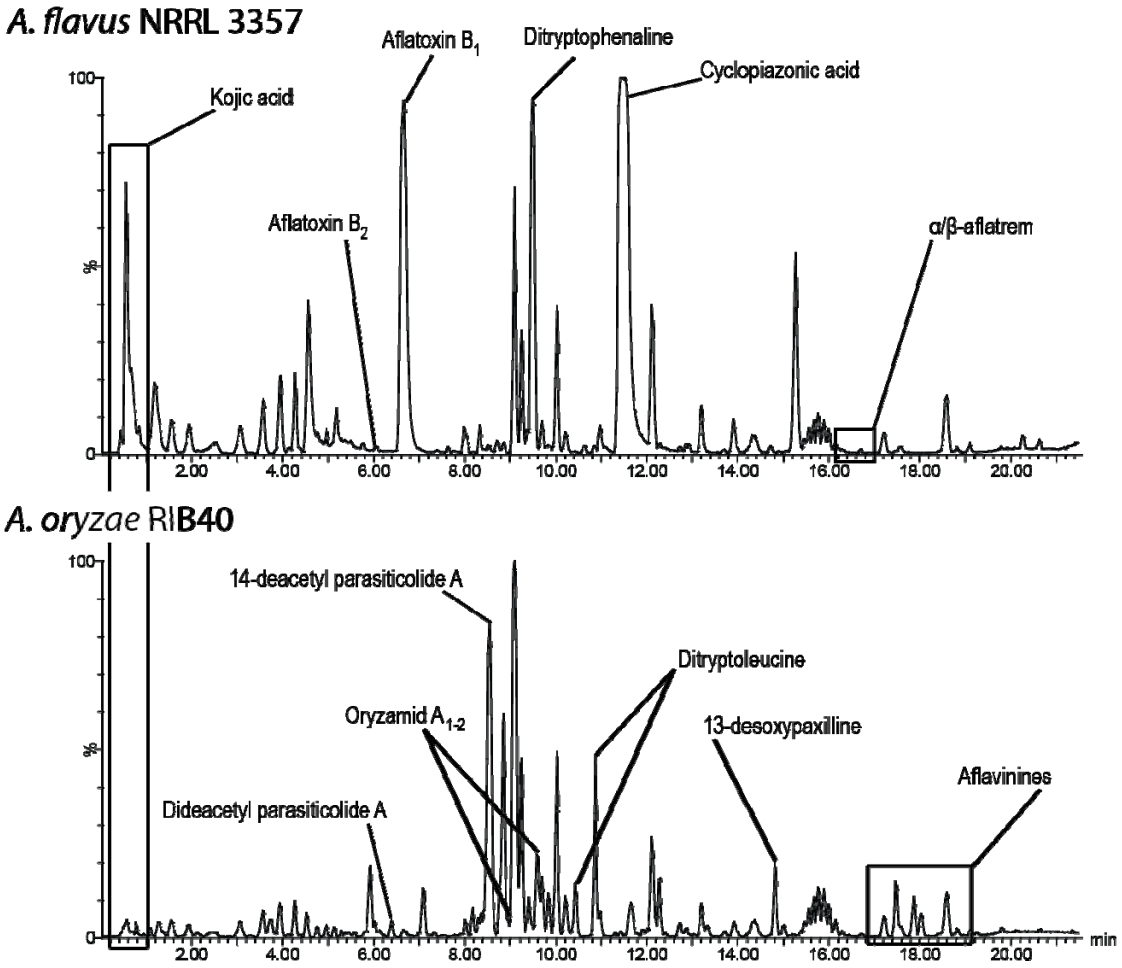

Table 1. LC-MS de-replication of some of the important secondary metabolite pathways from the two full genome sequenced siblings, *A. flavus* (NRRL 3357) and *A. oryzae* (RIB40). Based on 7 day fermentation on solid WATM agar in the dark. (+) indicates the presence of these types of compounds in *A. flavus* based on UV spectroscopic analysis. * New compounds reported here for the first time.

Metabolite	***A. flavus* NRRL 3357**	***A. oryzae* RIB40**
Kojic acid	+	+
Aflatoxin	+	-
Aflavinines	(+)	+
Aflatrem	+	13-desoxypaxilline
Miyakamides	(+)	Oryzamides *
Aspirochlorine	-	+
Cyclopiazonic acid	+	-
Ditryptophenaline	+	Ditryptoleucine *
Parasiticolide A	-	14-deacetyl parasiticolide A *

Known metabolites to *A. oryzae* were de-replicated and we found that the RIB40 strain did not produce detectable levels (LC-MS) of CPA (as also noted by Tokuoka *et al.* [36]), asperfuran, sporogen AO1, maltoryzine or aspergillomarasmine under these growth conditions. It did, however, produce kojic acid and aspirochlorine and a series of potentially new metabolites of which some were isolated, structurally characterized and reported here.

2.2. New Metabolites to A. oryzae RIB40

During fermentation of the chemically potent RIB40 strain, we have been interested in the tremorgenic compounds, allegedly coupled to fungal sclerotia [46–54] and whether these could be found in *A. oryzae* as they have been in *A. flavus*. The RIB40 strain produces large and abundant sclerotia, especially on WATM agar, a fact not widely announced in literature although sclerotia have been observed in *A. oryzae* sporadically [55–57]. No sclerotia were observable after 14 days on YES agar, but although these metabolites are often characterized as sclerotial metabolites, there is not a strict correlation between the biosynthesis of these metabolites and the formation of sclerotia, as also noted by Wilson [58], and this extract was used for the described isolations.

Here, we report the discovery of the aflatrem precursor 13-desoxypaxilline (13-dehydroxypaxilline) in *A. oryzae* RIB40, originally isolated from *Penicillium paxilli* [59–63]. Aflatrem is known from *A. flavus* and was discovered by Wilson and Wilson in 1964 [64] and structure elucidated by Gallagher *et al.* in 1978 and 1980 [65,66]. 13-desoxypaxilline was present in YES, CYA, OAT and WATM agar 7 day old micro-scale extracts. From the 14 days old YES 200 plate extract used for isolation, 13-desoxypaxilline was recovered as an intermediate metabolite. LC-MS, LC-MS/MS and NMR data analysis (Supplementary Material) confirmed the structure. Naturally the prospect of finding aflatrem itself was investigated, though no apparent peak was visible in HPLC-DAD data files. The use of a LC-MS/MS method further confirmed 13-desoxypaxilline as an end-product of *A. oryzae* RIB40 for the above cultivation conditions, since none of the proposed intermediate steps towards aflatrem could be detected (LC-MS/MS) and only one sample (WATM, 7d) showed traces of paspaline, a precursor for 13-desoxypaxilline (Figure 3).

Figure 3. The final steps in the proposed biosynthesis of aflatrem (in *A. flavus*). *A. oryzae* RIB40 biosynthesis stops at 13-desoxypaxilline [38].

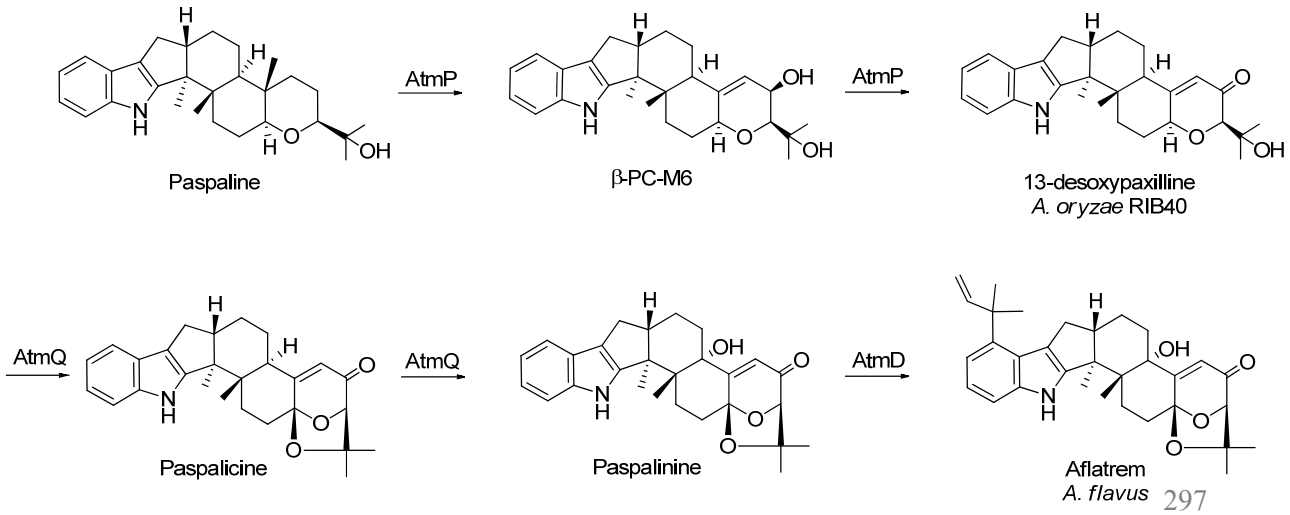

A second extract was made from 100 plates of a 14-day old *A. oryzae* RIB40 culture grown on WATM agar with abundant sclerotia formation to validate the findings from the YES extract. The analysis of the WATM extract showed 13-desoxypaxilline as a major metabolite alongside other sclerotium-related metabolites, such as aflavinines (based on UV-data not shown). The discovery of 13-desoxypaxilline as the apparent end-product of *A. oryzae* RIB40 is in agreement with the analysis of Nicholson *et al.* [38], who showed that a frameshift mutation in the *atmQ* gene presumably accounts for 13-desoxypaxilline not being converted into paspalicine and paspalinine. This mutation is therefore likely responsible for terminating the aflatrem biosynthesis in RIB40 prematurely, short of the acetal ring closure, C-13 hydroxylation and isoprene attachment. Nicholson *et al.* [38] demonstrated that AtmQ is a multifunctional cytochrome P450 monooxygenase likely to catalyze the several oxidative steps needed for biosynthesis of the acetal ring present in the structures of paspalicine, paspalinine and aflatrem, altogether pointing towards a more complex biosynthesis than shown here. Contrary to our discovery, Nicholson *et al.* did not find the aflatrem gene cluster of RIB40 to be transcribed during their fermentations [38].

The isolated 13-desoxypaxilline is a member of the paspalitrem tremorgens, a widely distributed group of metabolites that have been isolated from several genera: *Penicillium*, *Eupenicillium*, *Claviceps*, *Emericella*, *Aspergillus* and *Phomopsis* [67–69]. Besides the tremorgenic activity in animals, these metabolites have been shown to be insecticides [68], which is believed to be their ecological function together with aflatoxin and CPA for protection of the sclerotia against fungivorous insects [46,47].

In addition to 13-desoxypaxilline, two new analogues of parasiticolide A were also isolated and are here reported for the first time. The metabolites showed to be dide- and 14-deacetoxy analogues, and are most likely precursors to the sesquiterpene parasiticolide A (= astellolide A) (see Figure 4). The metabolites were present in CYA, YES and WATM extracts and isolated from the same 14 day old YES extract as 13-desoxypaxilline, and the dide- and 14-deacetyl analogues were also found in the sclerotia enriched WATM extract. Again the metabolites were analyzed using LC-MS and NMR. Several different extraction procedures were tested to verify the correctness of the compounds as genuine metabolites and not as *in vitro* degraded parasiticolide A products, but all samples showed only dide- and 14-deacetyl parasiticolide A and no traceable (LC-MS) levels of parasiticolide A itself, even with different non-acidic extractions. Parasiticolide A have been isolated from *A. flavus* var. *columnaris* (FKI-0739) once [71] and was originally isolated and characterized from *A. parasiticus* (IFO 4082) [72,73] and later also from a mutant of *Emericella variecolor* (= *A. stellatus* Curzi) [74]. Recently parasiticolides have been detected in the newly described species *A. arachidicola* (CBS 117610) and *A. minisclerotigenes* (CBS 117635) [75]. There have to our knowledge not been published any toxic studies on the parasiticolides, but the related peniopholides from the fungus *Peniophora polygonia* have been reported to have antifungal properties [76].

Figure 4. Structures of dide- and 14-deacetyl parasiticolide A and parasiticolide A.

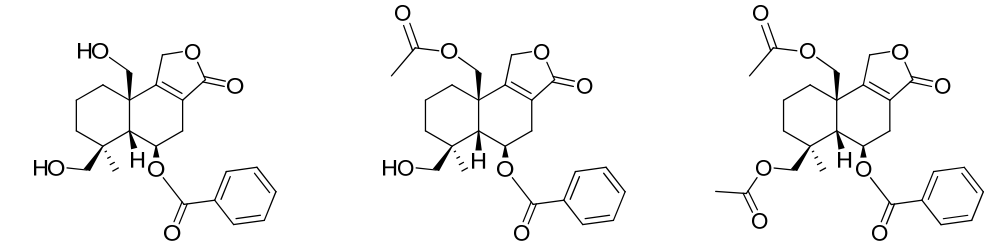

In our observations parasiticolides are more often detectable metabolites of *A. oryzae* than of *A. flavus* under the same fermentation conditions, suggesting that the pathway is partly silenced for *A. flavus* and may need epigenetic modification to be expressed under otherwise normal growth conditions. It is interesting that parasiticolide A is scarcely observed in *A. flavus*, when it is an important product of *A. oryzae* and also of *A. parasiticus*. As for 13-desoxypaxilline, dide- and 14-deacetyl parasiticolide A are almost certainly products of a prematurely ended biosynthesis, here parasiticolide A. We also isolated and elucidated a third parasiticolide A analogue; a formyl variant of parasiticolide A, but it was not possible to exclude the possibility of in vitro chemistry due to the formic acid added during the ethyl acetate extraction, so the correctness of this metabolite remains tentative. (Hamasaki *et al.* used benzene to extract parasiticolide A [77]). All paraciticolide analogues were structure elucidated by NMR and shift values correlated with the published data for parasiticolide A, except for the missing signals of the acetate units and their minor influence on the chemical shifts values of adjacent protons and carbons (See Supplementary Material for NMR data).

To further verify these observations, a MS/MS method was used to analyze several different microscale extracts of RIB40 for parasiticolide A itself. Trace amounts of parasiticolide A was found under these conditions and compared to an isolate of *A. parasiticus* (IBT 4387) capable of producing parasiticolide A. In the *A. parasiticus* isolate no dide- or 14-deacetyl parasiticolide A could be measured, indicating a complete transformation into the end-product (Figure 4). The small amount of parasiticolide A in RIB40 (roughly 1:1.000 ratio compared to 14-acetyl parasiticolide A, presuming the same response factor) might be the result of spontaneous acetylation involving the first acetylating enzyme. When the gene cluster of this metabolite is mapped, it is likely that the gene responsible for the last (specific) acetylation will be found to be mutated. Except for the section *Nidulantes* member *Emericella variecolor*, all other producers of these metabolites have been members of section *Flavi*. No indication points to these metabolites being part of the previously mentioned sclerotium metabolites since they are not found in selective sclerotium extracts, but are found for example in *A. arachidicola*, which is not known to produce sclerotia.

Four new *A. flavus* related NRPS compounds were also isolated from *A. oryzae* RIB40 and characterized based on standard interpretation of ^{1}H, COSY, HMQC and HMBC NMR data (see Supplementary Material). The compounds showed to be two isomeric metabolites named ditryptoleucine related to the ditryptophenalines [78–81] and the two indole-enamides named oryzamides $A_{1\text{-}2}$ (*cis*- and *trans*-forms) structurally similar to the antibiotic miyakamide $B_{1\text{-}2}$ [71] (Figure 5).

Figure 5. Structure of the new *A. oryzae* metabolites: Ditryptoleucine and oryzamide A_{1-2}.

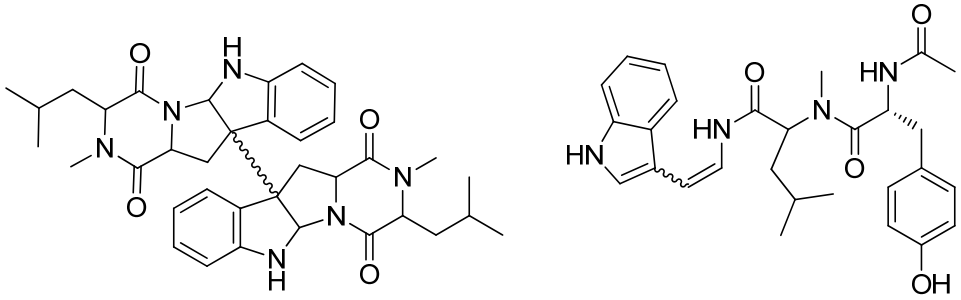

Ditryptoleucine Oryzamide A_{1-2}

It proved difficult to unambiguously isolate the *cis*- and *trans*-isomer of oryzamide A in a pure form due to isomerization around the double bond. Due to this the structure elucidation has been performed on mixtures of compounds. It is evident from the structure elucidation that oryzamides A_{1-2} only differ in the configuration around the double bond of the enamine as evident from the size of the coupling constant. Marfey analysis of the amino acid derived compounds only established the presence of L-tyrosine in the oryzamides. NMR structural data on the trans isomer (A_1) is present in the supporting material.

Intriguingly, these *A. oryzae* metabolites have apparently exchanged phenylalanine with leucine compared to the similar *A. flavus* metabolites, indicating either a common trait in the domestication process or a coupling between the two pathways. The diketopiperazine ditryptoleucine was isolated in two variants with ^{1}H-NMR shifts varying around the C-C dimeric bond, but with the same base structure. This unspecific dimerization is in line with previously isolated compounds. A hybrid between the ditryptophenaline and ditryptoleucine was isolated from an *Aspergillus* sp. as WIN 64745, with both a phenylalanine and leucine moiety, but with no *N*-methylation [79]. These compounds were tested and proved antagonistic against substance P at the NK1 receptor [82]. The oryzamides A_{1-2} are variants of the miyakamides B_{1-2} [71]. The exchanged phenylalanine has been substituted with leucine between a tryptophan and a tyrosine in the oryzamides. However this exchange of phenylalanine and leucine has often been found for compounds produced within the same species. *Penicillium polonicum* (= *P. fructigenum*) [83-85] produces both fructigenine A = puberuline = rugulosuvine A, containing phenylalanine and fructigenine B = verrucofortine, containing leucine. We could also detect two slightly later eluting compounds in the *A. oryzae* RIB40 extracts likely to be two further indole-enamides having phenylalanine incorporated instead of tyrosine as evident from LC-DAD-MS analysis (data not shown) as also seen for the miyakamides [71].

3. Experimental

General procedures and methods for analysis are described in [43,44,86].

Mass spectrometric analysis was performed using a Agilent HP 1100 liquid chromatograph with a DAD system (Waldbronn, Germany) on a LCT oaTOF mass spectrometer (Micromass, Manchester, UK) with a Z-spray ESI source and a LockSpray probe. For general procedures see [87]; method 1 for

LC-DAD-TOF was used in this study. All solvents used were HPLC grade from Sigma-Aldrich (St. Louis, MO, USA).

3.1. Fungal Material and Fermentation

A. oryzae RIB40 (IBT28103); *A. flavus* NRRL3357 (IBT3696), (IBT15934), NRRL 13462; *A. parvisclerotigenus* IBT16807 and *A. minisclerotigenes* IBT13353 were obtained from the IBT Culture Collection at DTU Systems Biology, Technical University of Denmark. The RIB40 isolate used for isolation of 13-dehydroxypaxilline was cultured for 14 days at 25 °C in the dark on 200 Petri dishes with Yeast Extract Sucrose agar (YES). All strains were grown for 1 week at 25 °C on YES, Czapek Yeast Autolysate (CYA), Wickerhams Antibiotic Test Medium (WATM) agar [88], YESBEE [89] (YES+50 g Bee pollen Type III, granulate, Sigma, P-8753, pr. 1 L medium), DRYES (Dichloran rose Bengal chloramphenicol agar), AFPA (*Aspergillus flavus*, *A. parasiticus* agar), CYAS (CYA + 50 g NaCl pr. 1 L medium), CY20 (CYA + 170 g sucrose pr. 1 L), CY40 (CYA with added 370 g sucrose pr. 1 L medium), DUL (Dulaney's medium for Penicillin), GAK (Potato-carrot agar), GMMS (Glucose minimal media (GMM) + 2% sorbitol), MEA (Malt extract agar), OAT (Oat meal agar), PDA (Potato-dextrose agar). For medium formulations see Samson *et al.* [90].

3.2. Extraction and Isolation of Pure Compounds

13-Desoxypaxilline. The plates were homogenized using a Stomacher and 100 mL EtOAc with 1% HCO_2H pr. 10 plates. The extract was filtered and dried down on a freeze drier. The crude extract was separated on a KP-C18-HS 60 g SNAP column using a Biotage Isolera One (Biotage, Uppsala, Sweden), resulting in a 22 mg fraction. The fraction was segmented with a 10 g ISOL Diol column, using 12 steps of stepwise Heptane-dichloromethane-EtOAc-MeOH. 13-desoxypaxilline was predominant in a 100% EtOAc fraction (6 mg), and purified on a Waters HPLC W600/996PDA (Milford, MA, USA) and a RP column (Phenomenex Luna C18(2), 250 × 10 mm, 5 µm, Torrance, CA, USA) using a gradient of 80% MeCN (H_2O–Milli-Q (Millipore, MA, USA)) to 90% over 10 min. with 50 ppm TFA added to the solvents. The collection was concentrated on a rotary evaporator (Büchi V-855/ R-215, Flawil, Switzerland) and dried under N_2 to yield 0.5 mg of white, amorphous 13-desoxypaxilline.

Dideacetyl-, 14-deacetyl-, and 18-formyl parasiticolide A. From the same fermentation described for 13-desoxypaxilline a more polar, 90 mg fraction was fractionated with a 10 g ISOL Diol column, using 12 steps of stepwise Heptane-dichloromethane-EtOAc-MeOH. The parasiticolide A-analogues were predominant in a 100% EtOAc fraction (10 mg), and purified on a Waters HPLC W600/996PDA (Milford, MA, USA) and a RP column (Phenomenex Luna C18(2), 250 × 10 mm, 5 µm, Torrance, CA, USA) using a gradient of 72% MeCN (H_2O–Milli-Q (Millipore, MA, USA)) to 87% over 15 min. with 50 ppm TFA. The collection was concentrated on a rotary evaporator (Büchi V-855/R-215) and dried under N_2 to yield 0.3, 1.0 and 0.8 mg of white, amorphous di-, 14-deactyl- and 18-formyl parasiticolide A, respectively. See Supplemental Material for NMR data.

Ditryptoleucine. 400 plates of *A. oryzae* RIB40 were cultured on YES medium. The plates were homogenized using a Stomacher and 100 mL EtOAc pr. 10 plates. The extract was filtered and dried

down on a freeze drier. The crude extract were separated into three phases by dissolving it in 9:1 MeOH:H_2O–Milli-Q and extracted into a heptan phase and afterwards a DCM phase. The DCM phase was separated on a KP-C18-HS SNAP column using a Biotage Isolera One (Biotage, Uppsala, Sweden) using a gradient of 10% MeOH (H_2O–Milli-Q (Millipore, MA, USA)) to 100% over 15 CVs (column volumes) resulting in a 402 mg fraction. The fraction was further separated on another KP-C18-HS SNAP column using a Biotage Isolera One (Biotage, Uppsala, Sweden) using a gradient of 10% MeOH (H_2O–Milli-Q (Millipore, Ma, USA)) to 25% over 2 CVs, 25% MeOH to 50% over 8 CVs and 50% to 100% over 4 CVs resulting in a 60.1 mg fraction. The fraction was fractionated on a LH-20 column using 100% MeOH. The ditryptoleucines were present in the earlier fractions and were purified on a Waters HPLC W600/996PDA (Milford, MA, USA) using a RP column (Phenomenex Luna C18(2), 250 × 10 mm, 5 µm, Torrance, CA, USA) using a gradient of 50% MeCN (H_2O–Milli-Q (Millipore, MA, USA)) to 100% over 20 min. with 50 ppm TFA and a flow of 4 mL/min. The collections were concentrated on a rotary evaporator (Büchi V-855/R-215) and dried under N_2 to yield 4.0 mg of the two isomers. See Supplemental Data for NMR data.

Oryzamides A_{1-2}. The remaining broth from the fermentation described for ditryptoleucine was extracted with EtOAc + 1% HCO_2H for 24 h. The extract was filtered and dried down on a freeze drier. The crude extract were separated into three phases by dissolving it in 9:1 MeOH:H_2O–Milli-Q and extracted into a heptan phase and afterwards a DCM phase. The DCM phase was separated on a KP-C18-HS SNAP column using a Biotage Isolera One (Biotage, Uppsala, Sweden) using a gradient of 10% MeOH (H_2O–Milli-Q (Millipore, MA, USA)) to 100% over 15 CVs (column volumes) resulting in a 654 mg fraction. The fraction was fractionated with a 10 g ISOL Diol column, using 13 steps of stepwise Hexane-dichloromethane-EtOAc-MeOH. The miyakamides were predominant in the 40:60 DCM:EtOAc and 20:80 DCM:EtOAc fractions (43.8 mg), and purified on a Waters HPLC W600/996PDA (Milford, MA, USA) and a RP column (Phenomenex Luna C18(2), 250 × 10 mm, 5µm, Torrance, CA, USA) using a gradient of 45% MeCN (H_2O–Milli-Q (Millipore, MA, USA)) to 62% over 15 min. with 50 ppm TFA. The collection was concentrated on a rotarvap (Büchi V-855/ R-215) and dried down under N_2 to yield 4.0 and 2.0 mg of oryzamide A_1 and A_2, respectively. See Supplemental Data for NMR data.

3.3. Marfeys Method

100 µg of each peptide was hydrolysed with 200 µL 6 M HCl at 110 °C for 20 h. To the hydrolysis products (or 50 µL (2.5 µmol) solutions of standard D- and L-amino acids) was added 50 µL water, 20 µL 1 M $NaHCO_3$ solution and 100 µL 1% FDAA in acetone, followed by reaction at 40 °C for 1 h. The reaction mixture was removed from the heat, neutralized with 10 µL 2 M HCl and the solution was diluted with 820 µL MeOH to a total volume of 1 mL. The FDAA derivatives were analysed by UHPLC-DAD on a Dionex Ultimate 3000 RS DAD equipped with a Kinetex C18 column (2.6 µm, 150 × 2.10mm, Phenomenex). The analyses were run with a gradient elution of MeCN/H_2O–Mili-Q (Millipore, MA,USA) added 50 ppm TFA from 15 to 100% MeCN over 7 min (60 °C, 0.8 mL/min). The retention times of the FDAA derivatives were compared to retention times of the standard amino acid derivatives.

3.4. Selective Extraction of Sclerotium Metabolites

The selective extraction of sclerotia from IBT 15934, NRRL 13462, IBT 16807 and IBT 13353 was made from harvested sclerotia of a 7 day old cultivation on WATM and CYA agar (25 °C in dark). The sclerotia were washed several times with Milli-Q (Millipore, Millford, USA) 0.22 µm H_2O and dried. The sclerotia were transferred to a 2 mL Eppendorf tube together with three stainless steel balls (2 × 1 mm and 1 × 5 mm) and frozen with liquid N_2 before mechanical crushed. The pulverized sclerotia were suspended in 1mL methanol and transferred to a 2 mL vial with 1 mL of 1:2:3 methanol:dichloromethane:ethylacetate and left for evaporation overnight in a fume hood. The dried extract was resolved in 1 mL methanol in ultrasonicated for 10 min and then filtered with a 0.45 µm PTFE filter to a clean vial for analysis.

3.5. HPLC-DAD-TOF Method

Mass was measured using a Agilent HP 1100 liquid chromatograph with a DAD system (Waldbronn, Germany) on a LCT oaTOF mass spectrometer (Micromass, Manchester, UK) with a Z-spray ESI source and a LockSpray probe. For general procedures see [86], method 1.

3.6. NMR Instrumentation

NMR spectra were recorded on a Varian Unity Inova 500 MHz spectrometer equipped with a 5 mm probe using standard pulse sequences. The signals of the residual solvent protons and solvent carbons were used as internal references (δ_H 2.50 and δ_C 39.5 ppm for DMSO). In cases where higher field was needed the NMR spectra were recorded on a Bruker Avance 800-MHz spectrometer equipped with a 5-mm TCI Cryoprobe at the Danish Instrument Center for NMR Spectroscopy of Biological Macromolecules.

3.7. MS/MS Method Used for Aflatrem and Parasiticolide Screening

Liquid chromatography was performed on an Agilent (Torrence, CA, USA) 1100 HPLC system coupled to a triple-quadropole mass spectrometer (Waters-Micromass, Manchester, UK) with a Z-spray ESI operated in positive mode source using a flow of 700 L/h nitrogen desolvated at 350 °C. The hexapole was held at 50 V. The system was controlled by MassLynx v4.1 (Waters-Micromass). Nitrogen was used as collision gas, and the MS operated in MRM mode (dwell time = 100 ms) with the parameters listed in Table 2. Extracts of 2 µL were injected and separated on a Phenomenex Gemini C_6-phenyl, 3 µm, 2 × 50 mm column with a flow of 0.3 µL/min. Water contained 20 mM ammonium formate. Oven temperature 40 °C. Two different methods were applied to the aflatrem- and parasiticolide screen: Aflatrem inlet method: Linearly gradient from 50 to 100% MeCN over 5 min, increased to 0.5 µL/min over 1.5 min. The column was washed additionally 1.5 min with 100% MeCN at 0.5 µL/min, followed by a return to 50% MeCN over 2.5 min and kept at this level for another 1 min with a linearly decrease in flow to 0.3 µL/min, prior to the next sample. Standards used for analysis of this pathway were from Sigma-Aldrich Aldrich (St. Louis, MO, USA). Parasiticolides: linearly gradient from 20 to 90% MeCN over 15 min, increased to 0.5µL/min from 90 to 100% MeCN in additional 1 min. The column was washed from 2 min with 100% MeCN at 0.5 µL/min, followed by a return to

20% MeCN over 1.5 min and kept at this level for another 3.5 min with a linearly decrease in flow to 0.3 µL/min, before the next sample. Standards were internal standards from other extracts of the known parasiticolide A producer *A. parasiticus*: IBT 4387 (= CBS 260.67) and IBT 11863 (= CBS 115.37).

Table 2. MS/MS method including scan event, retention times, transition ions and the cone and collision energies used.

Compound	Scan event	RT (min)	Ion type	Transition (*m*/*z*) [a]	Cone (V)	Collision energy (eV)
Paxilline	1	4.0	Quantifier	436 → 130	25	30
			Qualifier	436 → 182	25	30
Paspalinine	2	4.3	Quantifier	434 → 130	25	20
			Qualifier	434 → 376	25	20
13-desoxypaxilline	3	4.8	Quantifier	420 → 182	25	30
			Qualifier	420 → 130	25	30
Aflatrem	4	5.2	Quantifier	502 → 198	25	20
			Qualifier	502 → 445	25	20
Paspaline	5	5.5	Quantifier	422 → 130	25	20
			Qualifier	422 → 275	25	20
Dideacetyl-parasiticolide A	1	7.0	Quantifier	387 → 217	30	40
			Qualifier	387 → 189	30	40
14-deacetyl parasiticolide A	2	8.7	Quantifier	429 → 217	30	40
			Qualifier	429 → 189	30	40
Parasiticolide A	3	10.4	Quantifier	488 → 229	30	30
			Qualifier	488 → 247	30	30

[a] All transitions were made from $[M+H]^+$, except for paraciticolide A: $[M+NH_4]^+$.

4. Conclusions

The tremorgenic 13-desoxypaxilline has been isolated from *A. oryzae* RIB40 and verified under several different growth conditions contrary to previous studies. We believe that 13-desoxypaxilline is the end-product of the aflatrem biosynthesis for the RIB40 strain since no aflatrem could be detected in any fermentation using LC-MS/MS as detection.

The new metabolites dide- and 14-deacetyl parasiticolide A were also found as genuine products from the RIB40 strain and the compounds were present in multiple fermentations, however parasiticolide A was only detected in trace amounts using a LC-MS/MS method. This indicates a defective acetylation of the 14-deacetyl parasiticolide A and the small amount of parasiticolide A in RIB40 could be the result of spontaneous acetylation in the cell cytosol. The mono-deacetylated analogue detected in both *A. flavus* and *A. oryzae* had same retention times, suggesting a selective acetylation.

The new NRPS compounds ditryptoleucine and oryzamides A_{1-2} appear to be natural variants of known *A. flavus* metabolites. They share the exchange of a phenylalanine for a leucine, although they are believed to originate from two unrelated pathways.

Altogether, our findings contribute to understanding why the overall chemical profiles of *A. oryzae* (RIB40) and *A. flavus* (NRRL 3357) appear quite different since some of the end-products usually seen in *A. flavus* are apparently not reached in *A. oryzae*. Whether the different chemical profiles are merely

the result of different regulation that can be overcome by the use of epigenetic modifiers or are a result of genuine mutations remains to be settled. *A. oryzae* RIB40 is clearly a chemically potent strain, and as more of its chemistry is unfolded we believe that most of the biosynthetic pathways of *A. flavus* will be found to be more or less functional. Future research will reveal whether the many different *A. oryzae* strains that are used as industrial workhorses are as chemically potent as the RIB40 strain.

Supplementary Materials

Supplementary materials can be accessed at: http://www.mdpi.com/2218-1989/2/1/39/s1.

Acknowledgments

This work was funded by the Danish Research Agency for Technology and Production (Grant: 09-064967). We thank the Danish Instrument Center for NMR Spectroscopy of Biological Macromolecules at the Carlsberg Laboratory for 800 MHz NMR time.

Conflict of Interest

The authors declare no conflict of interest.

References and Notes

1. Machida, M.; Yamada, O.; Gomi, K. Genomics of *Aspergillus oryzae*: Learning from the history of koji mold and exploration of its future. *DNA Res.* **2008**, *15*, 173–183.
2. Punt, P.J.; Biezen, N.V.; Conesa, A.; Albers, A.; Mangnus, J.; van den Hondel, C. Filamentous fungi as cell factories for heterologous protein production. *Trends Biotechnol.* **2002**, *20*, 200–206.
3. Meyer, V. Genetic engineering of filamentous fungi—Progress, obstacles and future trends. *Biotechnol. Adv.* **2008**, *26*, 177–185.
4. Fisch, K.M.; Bakeer, W.; Yakasai, A.A.; Song, Z.; Pedrick, J.; Wasil, Z.; Bailey, A.M.; Lazarus, C.M.; Simpson, T.J.; Cox, R.J. Rational domain swaps decipher programming in fungal highly reducing polyketide synthases and resurrect an extinct metabolite. *J. Am. Chem. Soc.* **2011**, *133*, 16335–16641.
5. Geiser, D.M.; Pitt, J.I.; Taylor, J.W. Cryptic speciation and recombination in the aflatoxin-producing fungus *Aspergillus flavus*. *Proc. Natl. Acad. Sci. USA* **1998**, *95*, 388–393.
6. Geiser, D.M.; Dorner, J.W.; Horn, B.W.; Taylor, J.W. The phylogenetics of mycotoxin and sclerotium production in *Aspergillus flavus* and *Aspergillus oryzae*. *Fungal Genet. Biol.* **2000**, *31*, 169–179.
7. Abe, K.; Gomi, K.; Hasegawa, F.; Machida, M. Impact of *Aspergillus oryzae* genomics on industrial production of metabolites. *Mycopathologia* **2006**, *162*, 143–153.
8. Kobayashi, T.; Abe, K.; Asai, K.; Gomi, K.; Juvvadi, P.R.; Kato, M.; Kitamoto, K.; Takeuchi, M.; Machida M. Genomics of *Aspergillus oryzae*. *Biosci. Biotechnol. Biochem.* **2007**, *71*, 646–670.
9. Iwasaki, T.; Kosikowski, F.V. Production of beta-nitropropionic acid in foods. *J. Food Sci.* **1973**, *38*, 1162–1165.

10. Orth, R. Mycotoxins of *Aspergillus oryzae* strains for use in food-industry as starters and enzyme producing molds. *Annales de la Nutrition et de l'Alimentation* **1977**, *31*, 617–624.
11. Manabe, M; Tanaka, K.; Goto, T.; Matsuura, S. Production capabilities of kojic acid and aflatixin by koji mold. In *Toxigenic Fungi—Their Toxins and Health Hazards*; Kurata, H., Ueno, Y., Eds.; Elsevier: Amsterdam, The Netherlands, 1984; Volume 7, pp. 4–14.
12. Bentley, R. From miso, sake and shoyu to cosmetics: A century of science for kojic acid. *Nat. Prod. Rep.* **2006**, *23*, 1046–1062.
13. Pfefferle, W.; Anke, H.; Bross, M.; Steffan, B.; Vianden, R.; Steglich, W. Asperfuran, a novel antifungal metabolite from *Aspergillus oryzae*. *J. Antibiot.* **1990**, *43*, 648–654.
14. Tanaka, S.; Wada, K.; Katayama, M.; Marumo, S. Isolation of sporogen AO1, a sporogenic substance, from *Aspergillus oryzae*. *Agric. Biol. Chem.* **1984**, *48*, 3189–3191.
15. Tanaka, S.; Wada, K.; Marumo, S.; Hattori, H. Structure of sporogen AO1, a sporogenic substance of *Aspergillus oryzae*. *Tetrahedron Lett.* **1984**, *25*, 5907–5910.
16. Iizuka, H.; Iida, M. Maltoryzine, a new toxic metabolite produced by a strain of *Aspergillus oryzae* var. *microsporus* isolated from poisonous malt sprout. *Nature* **1962**, *196*, 681–682.
17. Barbier, M.; Vetter, W.; Bogdanov, D.; Lederer, E. Synthese und eigenschafgen eines analogen des lycomarasmins und der aspergillomarasmine. *Annalen der Chemie-Justus Liebig* **1963**, *668*, 132.
18. Robert, M.; Barbier, M.; Lederer, E.; Roux, L.; Bieman, K.; Vetter, W. Two new natural phytotoxins—Aspergillomarasmines A and B and their identity to lycomarasmine and its derivatives. *Bulletin de la Societe Chimique de France* **1962**, 187–188.
19. Monti, F.; Ripamonti, F.; Hawser, S.P.; Islam, K. Aspirochlorine: A highly selective and potent inhibitor of fungal protein synthesis. *J. Antibiot.* **1999**, *52*, 311–318.
20. Sakata, K.; Masago, H.; Sakurai, A.; Takahashi, N. Isolation of aspirochlorine (=antibiotic A30641) posessing a novel dithiodiketopiperazine structure from *Aspergillus flavus*. *Tetrahedron Lett.* **1982**, *23*, 2095–2098.
21. Sakata, K.; Kuwatsuka, T.; Sakurai, A.; Takahashi, N.; Tamura, G. Isolation of aspirochlorine (=antibiotic A30641) as a true anti-microbial constituent of the antibiotic, oryzachlorin, from *Aspergillus oryzae*. *Agric. Biol. Chem.* **1983**, *47*, 2673–2674.
22. Sakata, K.; Maruyama, M.; Uzawa, J.; Sakurai, A.; Lu, H.S.M.; Clardy, J. Structural revision of aspirochlorine (=antibiotic A30641), a novel epidithiopiperazine-2,5-dione produced by *Aspergillus* spp. *Tetrahedron Lett.* **1987**, *28*, 5607–5610.
23. Klausmeyer, P.; McCloud, T.G.; Tucker, K.D.; Cardellina, J.H.; Shoemaker, R.H. Aspirochlorine class compounds from *Aspergillus flavus* inhibit azole-resistant *Candida albicans*. *J. Nat. Prod.* **2005**, *68*, 1300–1302.
24. Barbesgaard, P.; Heldt-Hansen, H.P.; Diderichsen, B. On the safety of *Aspergillus oryzae*: A review. *Appl. Microbiol. Biotechnol.* **1992**, *36*, 569–572.
25. Tanaka, K.; Goto, T.; Manabe, M.; Matsuura, S. Traditional Japanese fermented foods free from mycotoxin contamination. *Jpn. Agric. Res. Quart.* **2002**, *36*, 45–50.
26. Varga, J.; Frisvad, J.C.; Samson, R.A. Two new aflatoxin producing species, and an overview of *Aspergillus* section Flavi. *Stud. Mycol.* **2011**, *69*, 57–80.

27. Rokas, A.; Payne, G.; Fedorova, N.D.; Baker, S.E.; Machida, M.; Yu, J.; Georgianna, D.R.; Dean, R.A.; Bhatnagar, D.; Cleveland, T.E. What can comparative genomics tell us about species concepts in the genus *Aspergillus*? *Stud. Mycol.* **2007**, *59*, 11–17.
28. Machida, M.; Asai, K.; Sano, M.; Tanaka, T.; Kumagai. T.; Terai., G.; Kusumoto, K.-I.; Arima, T.; Akita, O.; Kashiwagi, Y.; *et al.* Genome sequencing and analysis of *Aspergillus oryzae*. *Nature* **2005**, *438*, 1157–1161.
29. Machida, M.; Terabayashi, Y.; Sano, M.; Yamane, N.; Tamano, K.; Payne, G.A.; Yu, J.; Cleveland, T.E.; Nierman, W.C. Genomics of industrial aspergilli and comparison with toxigenic relatives. *Food Addit. Contam. Part A* **2008**, *25*, 1147–1151.
30. Payne, G.A.; Nierman, W.C.; Wortman, J.R.; Pritchard, B.L.; Brown, D.; Dean, R.A.; Bhatnagar, D.; Cleveland, T.E.; Machida, M.; Yu, J. Whole genome comparison of *Aspergillus flavus* and *A. oryzae*. *Med. Mycol.* **2006**, *44*, S9–S11.
31. Yu, J.; Payne, G.A.; Nierman, W.C.; Machida, M.; Bennett, J.W.; Campbell, B.C.; Robens, J.F.; Bhatnagar, D.; Dean, R.A.; Cleveland, T.E. *Aspergillus flavus* genomics as a tool for studying the mechanism of aflatoxin formation. *Food Addit. Contam. Part A* **2008**, *25*, 1152–1157.
32. Laatsch, H. AntiBase 2010. Available online: http://www.wiley-vch.de/stmdata/antibase2010.php (accessed on 27 December 2011).
33. Cleveland, T.E.; Yu, J.; Fedorova, N.; Bhatnagar, D.; Payne, G.A.; Nierman, W.C.; Bennett, J.W. Potential of *Aspergillus flavus* genomics for applications in biotechnology. *Trends Biotechnol.* **2009**, *27*, 151–157.
34. Lee, Y.-H.; Tominaga, M.; Hayashi, R.; Sakamoto, K.; Yamada, O.; Akita, O. *Aspergillus oryzae* strains with a large deletion of the aflatoxin biosynthetic homologous gene cluster differentiated by chromosomal breakage. *Appl. Microbiol. Biotechnol.* **2006**, *72*, 339–345.
35. Tominaga, M.; Lee, Y.H.; Hayashi, R.; Suzuki, Y.; Yamada, O.; Sakamoto, K.; Gotoh, K.; Akita, O. Molecular analysis of an inactive aflatoxin biosynthesis gene cluster in *Aspergillus oryzae* RIB strains. *Appl. Environ. Microbiol.* **2006**, *72*, 484–490.
36. Tokuoka, M.; Seshime, Y.; Fujii, I.; Kitamoto, K.; Takahashi, T.; Koyama, Y. Identification of a novel polyketide synthase-nonribosomal peptide synthetase (PKS-NRPS) gene required for the biosynthesis of cyclopiazonic acid in *Aspergillus oryzae*. *Fungal Genet. Biol.* **2008**, *45*, 1608–1615.
37. Chang, P.-K.; Horn, B.W.; Dorner, J.W. Clustered genes involved in cyclopiazonic acid production are next to the aflatoxin biosynthesis gene cluster in *Aspergillus flavus*. *Fungal Genet. Biol.* **2009**, *46*, 176–182.
38. Nicholson, M.J.; Koulman, A.; Monahan, B.J.; Pritchard, B.L.; Payne, G.A.; Scott, B. Identification of two aflatrem biosynthetic gene loci in *Aspergillus flavus* and metabolic engineering in *Penicillium paxilli* to elucidate gene function. *Appl. Environ. Microbiol.* **2009**, *75*, 7469–7481.
39. Shwab, E.K.; Bok, J.W.; Tribus, M.; Galehr, J.; Graessle, S.; Keller, N.P. Histone deacetylase activity regulates chemical diversity in *Aspergillus*. *Eukaryot. Cell* **2007**, *6*, 1656–1664.
40. Shwab, E.K.; Keller, N.P. Regulation of secondary metabolite production in filamentous ascomycetes. *Mycol. Res.* **2008**, *112*, 225–230.
41. Williams, R.B.; Henrikson, J.C.; Hoover, A.R.; Lee, A.E.; Cichewicz, R.H. Epigenetic remodeling of the fungal secondary metabolome. *Org. Biomol. Chem.* **2008**, *6*, 1895–1897.

42. Henrikson, J.C.; Hoover, A.R.; Joyner, P.M.; Cichewicz, R.H. A chemical epigenetics approach for engineering the in situ biosynthesis of a cryptic natural product from *Aspergillus niger*. *Org. Biomol. Chem.* **2009**, *7*, 435–438.
43. Yakasai, A.A.; Davison, J.; Wasil, Z.; Halo, L.M.; Butts, C.P.; Lazarus, C.M.; Bailey, A.M.; Simpson, T.J.; Cox, R.J. Nongenetic reprogramming of a fungal highly reducing polyketide synthase. *J. Am. Chem. Soc.* **2011**, *133*, 10990–10998.
44. Frisvad, J.C.; Thrane, U. Standardized high-performance liquid-chromatography of 182 mycotoxins and other fungal metabolites based on alkylphenone retention indexes and UV-Vis spectra (Diode-Array Detection). *J. Chromatogr. A* **1987**, *404*, 195–214.
45. Smedsgaard, J. Micro-scale extraction procedure for standardized screening of fungal metabolite production in cultures. *J. Chromatogr. A* **1997**, *760*, 264–270.
46. Wicklow, D.T.; Cole, R.J. Tremorgenic indole metabolites and aflatoxins in sclerotia of *Aspergillus flavus*—An evolutionary perspective. *Can. J. Bot.* **1982**, *60*, 525–528.
47. Gloer, J.B.; Tepaske, M.R.; Sima, J.S.; Wicklow, D.T.; Dowd, P.F. Antiinsectan aflavinine derivatives from the sclerotia of *Aspergillus flavus*. *J. Org. Chem.* **1988**, *53*, 5457–5460.
48. Gloer, J.B.; Rinderknecht, B.L.; Wicklow, D.T.; Dowd, P.F. Nominine—A new insecticidal indole diterpene from the sclerotia of *Aspergillus nomius*. *J. Org. Chem.* **1989**, *54*, 2530–2532.
49. Staub, G.M.; Gloer, J.B.; Wicklow, D.T.; Dowd, P.F. Aspernomine—A cytotoxic antiinsectan metabolite with a novel ring-system from the sclerotia of *Aspergillus nomius*. *J. Am. Chem. Soc.* **1992**, *114*, 1015–1017.
50. Staub, G.M.; Gloer, K.B.; Gloer, J.B.; Wicklow, D.T.; Dowd, P.F. New paspalinine derivatives with antiinsectan activity from the sclerotia of *Aspergillus nomius*. *Tetrahedron Lett.* **1993**, *34*, 2569–2572.
51. Tepaske, M.R.; Gloer, J.B.; Wicklow, D.T.; Dowd, P.F. The structure of tubingensin B—A cytotoxic carbazole alkaloid from the sclerotia of *Aspergillus tubingensis*. *Tetrahedron Lett.* **1989**, *30*, 5965–5968.
52. Tepaske, M.R.; Gloer, J.B.; Wicklow, D.T.; Dowd, P.F. 3 new aflavinines from the sclerotia of *Aspergillus tubingensis*. *Tetrahedron* **1989**, *45*, 4961–4968.
53. Tepaske, M.R.; Gloer, J.B.; Wicklow, D.T.; Dowd, P.F. Aflavazole—A new antiinsectan carbazole metabolite from the sclerotia of *Aspergillus flavus*. *J. Org. Chem.* **1990**, *55*, 5299–5301.
54. Tepaske, M.R.; Gloer, J.B.; Wicklow, D.T.; Dowd, P.F. Aflavarin and beta-aflatrem—New anti-insectan metabolites from the sclerotia of *Aspergillus flavus*. *J. Nat. Prod.* **1992**, *55*, 1080–1086.
55. Raper, K.B.; Fennell, D.I. *The genus Aspergillus*; Williams & Wilkins: Baltimore, MD, USA, 1965.
56. Wicklow, D.T.; Mcalpin, C.E.; Yeoh, Q.L. Diversity of *Aspergillus oryzae* genotypes (RFLP) isolated from traditional soy sauce production within Malaysia and Southeast Asia. *Mycoscience* **2007**, *48*, 373–380.
57. Jin, F.J.; Takahashi, T.; Utsushikawa, M.; Furukido, T.; Nishida, M.; Ogawa, M.; Tokuoka, M.; Koyama Y. A trial of minimization of chromosome 7 in *Aspergillus oryzae* by multiple chromosomal deletions. *Mol. Genet. Genomics* **2010**, *283*, 1–12.
58. Wilson, B.J. Toxins other than aflatoxins produced by *Aspergillus flavus*. *Bacteriol. Rev.* **1966**, *30*, 478–484.

59. Springer, J.P.; Clardy, J.C.; Wells, J.M.; Cole, R.J.; Kirksey, J.W. Structure of paxilline, a tremorgenic metabolite of *Penicillium paxilli* Bainier. *Tetrahedron Lett.* **1975**, 2531–2534.
60. Longland, C.L.; Dyer, J.L.; Michelangeli, F. The mycotoxin paxilline inhibits the cerebellar inositol 1,4, 5-trisphosphate receptor. *Eur. J. Pharmacol.* **2000**, *408*, 219–225.
61. Bilmen, J.G.; Wootton, L.L.; Michelangeli, F. The mechanism of inhibition of the sarco/ endoplasmic reticulum Ca2+ ATPase by paxilline. *Arch. Biochem. Biophys.* **2002**, *406*, 55–64.
62. Sabater-Vilar, M.; Nijmeijer, S.; Fink-Gremmels, J. Genotoxicity assessment of five tremorgenic mycotoxins (fumitremorgen B, paxilline, penitrem A, verruculogen, and verrucosidin) produced by molds isolated from fermented meats. *J. Food Protec.* **2003**, *66*, 2123–2129.
63. Sheehan, J.J.; Benedetti, B.L.; Barth, A.L. Anticonvulsant effects of the BK-channel antagonist paxilline. *Epilepsia* **2009**, *50*, 711–720.
64. Wilson, B.J.; Wilson, C.H. Toxin from *Aspergillus flavus*—Production on food materials of substance causing tremors in mice. *Science* **1964**, *144*, 177–178.
65. Gallagher, R.T.; Wilson, B.J. Aflatrem, the tremorgenic mycotoxin from *Aspergillus flavus*. *Mycopathologia* **1978**, *66*, 183–185.
66. Gallagher, R.T.; Clardy, J.C.; Wilson, B.J. Aflatrem, a tremorgenic toxin from *Aspergillus flavus*. *Tetrahedron Lett.* **1980**, *21*, 239–242.
67. Cole, R.J.; Dorner, J.W.; Springer, J.P.; Cox, R.H. Indole metabolites from a strain of *Aspergillus flavus*. *J. Agric. Food Chem.* **1981**, *29*, 293–295.
68. Steyn, P.S.; Vleggaar, R. Tremorgenic mycotoxins. *Fortschritte der Chemie Organischer Naturstoffe* **1985**, *48*, 1–80.
69. Bills, G.F.; Giacobbe, R.A.; Lee, S.H.; Peláez, F.; Tkacz, J.S. Tremorgenic mycotoxins, paspalitrem A and C, from a tropical *Phomopsis*. *Mycol. Res.* **1992**, *96*, 977–983.
70. Laakso, J.A.; Gloer, J.B.; Wicklow, D.T.; Dowd, P.F. A new penitrem analog with antiinsectan activity from the sclerotia of *Aspergillus sulphureus*. *J. Agric. Food Chem.* **1993**, *41*, 973–975.
71. Shiomi, K.; Hatae, K.; Yamaguchi, Y.; Masuma, R.; Tomoda, H.; Kobayashi, S.; Omura, S. New antibiotics miyakamides produced by a fungus. *J. Antibiot.* **2002**, *55*, 952–961.
72. Fukuyama, K.; Kawai, H.; Tsukihara, T.; Tsukihara, K.; Katsube, Y.; Hamasaki, T.; Hatsuda, Y.; Kuwano, H. Structure-analysis of a bromo derivative of parasiticolide A by X-ray-diffraction method. *Bull. Chem. Soc. Jpn*. **1975**, *48*, 2949–2950.
73. Ishikawa, Y.; Morimoto, K.; Hamasaki, T. Flavoglaucin, a metabolite of *Eurotium chevalieri*, its antioxidation and synergism with tocopherol. *J. Am. Oil Chem. Soc.* **1984**, *61*, 1864–1868.
74. Gould, R.O.; Simpson, T.J.; Walkinshaw, M.D. Isolation and X-ray crystal structures of astellolides A and B, sesquiterpenoid metabolites of *Aspergillus variecolor*. *Tetrahedron Lett.* **1981**, *22*, 1047–1050.
75. Pildain, M.B.; Frisvad, J.C.; Vaamonde, G.; Cabral, D.; Varga, J.; Samson, R.A. Two novel aflatoxin-producing *Aspergillus* species from Argentinean peanuts. *Int. J. Syst. Evol. Microbiol.* **2008**, *58*, 725–735.
76. Ayer, W.A.; Trifonov, L.S. Drimane sesquiterpene lactones from *Peniophora polygonia*. *J. Nat. Prod.* **1992**, *55*, 1454–1461.
77. Hamasaki, T.; Kuwano, H.; Isono, K.; Hatsuda, Y.; Fukuyama, K.; Tsukihara, T.; Katsube, Y. New metabolite, parasiticolide A, from *Aspergillus parasiticus*. *Agric. Biol. Chem.* **1975**, *39*, 749–751.

78. Springer, J.P.; Buchi, G.; Kobbe, B.; Demain, A.L.; Clardy, J.C. The structure of ditryptophenaline—New metabolite of *Aspergillus flavus*. *Tetrahedron Lett.* **1997**, *27*, 2403–2406.
79. Barrow, C.J.; Cai, P.; Snyder, J.K.; Sedlock, D.M.; Sun, H.H.; Cooper, R. WIN 64821, a new competitive antagonist to substance-P, isolated from an *Aspergillus* species—Structure determination and solution conformation. *J. Org. Chem.* **1993**, *58*, 6016–6021.
80. Oleynek, J.J.; Sedlock, D.M.; Barrow, C.J.; Appell, K.C.; Casiano, F.; Haycock, D.; Ward, S.J.; Kaplita, P.; Gillum, A.M. WIN-64821, a novel neurokinin antagonist produced by an *Aspergillus* sp .2. Biological-activity. *J. Antibiot.* **1994**, *47*, 391–398.
81. Barrow, C.J.; Sedlock, D.M. 1′-(2-Phenyl-ethylene)-ditryptophenaline, a new dimeric diketopiperazine from *Aspergillus flavus*. *J. Nat. Prod.* **1994**, *57*, 1239–1244.
82. Movassaghi, M.; Schmidt, M.; Ashenhurst, J. Concise total synthesis of (+)-WIN 64821 and (−)-ditryptophenaline. *Angew. Chem. Int. Ed. Engl.* **2008**, *47*, 1485–1487.
83. Arai, K.; Kimura, K.; Mushiroda, T.; Yamamoto, Y. Structures of fructigenines A and B, new alkaloids isolated from *Penicillium fructigenum* Takeuchi. *Chem. Pharm. Bull.* **1989**, *37*, 2937–2939.
84. Frisvad, J.C.; Samson, R.A. Polyphasic taxonomy of *Penicillium* subgenus *Penicillium*. A guide to identification of the food and air-borne terverticillate Penicillia and their mycotoxins. *Stud. Mycol.* **2004**, *49*, 1–173.
85. Frisvad, J.C.; Smedsgaard, J.; Larsen, T.O.; Samson, R.A. Mycotoxins, drugs and other extrolites produced by species in *Penicillium* subgenus *Penicillium*. *Stud. Mycol.* **2004**, **49**, 201–241.
86. Frisvad, J.C.; Skouboe, P.; Samson, R.A. Taxonomic comparison of three different groups of aflatoxin producers and a new efficient producer of aflatoxin B1, sterigmatocystin and 3-*O*-methylsterigmatocystin, *Aspergillus rambellii* sp nov. *Syst. Appl. Microbiol.* **2005**, *28*, 442–453.
87. Nielsen, K.F.; Mogensen, J.M.; Johansen, M.; Larsen, T.O.; Frisvad, J.C. Review of secondary metabolites and mycotoxins from the *Aspergillus niger* group. *Anal. Bioanal. Chem.* **2009**, *395*, 1225-1242.
88. Raper, K.B.; Thom, C. *Manual of the Penicillia*; Williams and Wilkins: Baltimore, MD, USA, 1949.
89. Medina, A.; Gonzalez, G.; Saez, J.M. Bee pollen, a substrate that stimulates ochratoxin A production by *Aspergillus ochraceus*. *Syst. Appl. Microbiol.* **2004**, *27*, 261–267.
90. Samson, R.A.; Hoekstra, E.S.; Frisvad, J.C. *Introduction to Food- and Airborne Fungi*. **7**; Centraalbureau voor Schimmelcultures: Utrecht, The Netherlands, 2004.

Supplementary Material

Comparative chemistry of *Aspergillus oryzae* (RIB40) and *A. flavus* (NRRL 3357)

Christian Rank [1,†], Marie Louise Klejnstrup [1,†], Lene Maj Petersen [1], Sara Kildgaard [1], Jens Christian Frisvad [1], Charlotte Held Gotfredsen [2] and Thomas Ostenfeld Larsen [1,*]

13-Desoxypaxilline

HRESIMS: *m/z* = 420.2551 $[M+H]^+$, calculated for $[C_{27}H_{33}NO_3+H]^+$: 420.2533.

NMR spectra were acquired in DMSO-d_6 on a Bruker Avance 800 MHz spectrometer using standard pulse sequences. ^{1}H-NMR (799.30 MHz, DMSO-d_6, 25 °C, 2.50 ppm): 0.88 (3H, s, H-23), 1.00 (3H, s, H-25), 1.16 (3H, s, H-29), 1.20 (3H, s, H-28), 1.52 (1H, ddd, *J* = 25.4, 12.8, 4.4 Hz, H-14a), 1.60 (1H, m, H-14b), 1.65 (1H, m, H-15a), 1.74 (1H, d, *J* = 12.2 Hz, H-15b), 1.81 (1H, ddd, *J* = 17.9, 13.8, 4.2 Hz, H-6a), 1.98 (1H, ddd, *J* = 13.8, 13.6, 4.2 Hz, H-5a), 2.07 (1H, m, H-5b), 2.22 (1H, m, H-6b), 2.32 (1H, dd, *J* = 12.8, 11.0 Hz, H-17a), 2.53 (1H, m, H-13), 2.62 (1H, dd, *J* = 12.8, 6.3 Hz, H-17b), 2.71 (1H, m, H-16), 3.74 (1H, d, *J* = 1.6 Hz, H-9), 4.34 (1H, br. s, 27-OH), 4.41 (1H, m, H-7), 5.73 (1H, s, H-11), 6.91 (1H, dd, *J* = 7.6, 7.6 Hz, H-21), 6.95 (1H, dd, *J* = 7.6, 7.6 Hz, H-22), 7.27 (1H, d, *J* = 7.6 Hz, H-23), 7.28 (1H, d, *J* = 7.6 Hz, H-20), 10.76 (1H, s, N-H).

^{13}C-NMR (201.00, DMSO-d_6, 25 °C, 39.5 ppm): 14.4 (C-25), 15.4 (C-26), 23.5 (C-15), 24.8 (C-14), 25.5 (C-28), 25.7 (C-29), 26.7 (C-17), 29.5 (C-6), 30.7 (C-5), 41.6 (C-13), 48.5 (C-16), 49.2 (C-3), 49.8 (C-4), 70.7 (C-27), 74.0 (C-7), 82.4 (C-9), 111.6 (C-23), 115.8 (C-18), 117.5 (C-20), 118.1 (C-21), 119.2 (C-22), 120.7 (C-11), 124.4 (C-19), 140.2 (C-24), 150.4 (C-2), 168.6 (C-12), 196.1 (C-10).

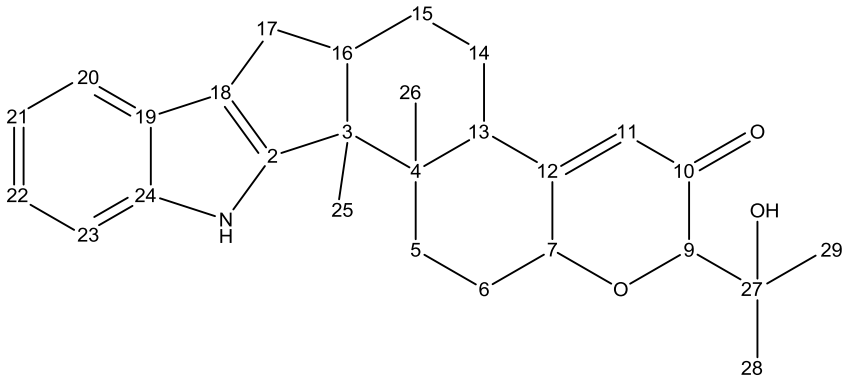

14-Deacetyl parasiticolide A

All NMR spectra of parasiticolide A analogues were acquired in DMSO-d_6 on a Varian Unity Inova 500 MHz spectrometer with 4 mm gHX Nano probe and with a spin rate of 2 kHz for all samples, using standard pulse sequences. The spectra were referenced to this solvent with resonances δ_H = 2.50 and δ_C = 39.5.

HRESIMS: *m/z* = 429.1901 $[M+H]^+$, calculated for $[C_{24}H_{28}O_7+H]^+$: 429.1908.

^{1}H-NMR (499.87 MHz, DMSO-d_6, 25 °C, 2.50 ppm): 0.96 (1H, td, *J* = 13.6, 3.7 Hz, H-3a), 1.01 (3H, s, H-13), 1.36 (1H, td, *J* = 13.3, 3.3 Hz, H-1a), 1.45 (1H, m, H-2a), 1.63 (1H, m, H-2b), 1.91 (1H, s, H-5), 1.97 (1H, m, H-3b), 2.08 (3H, s, H-17), 2.11 (1H, d, *J* = 13.2, H-1b), 2.36 (1H, d, *J* = 19.0 Hz, H-7a), 2.76 (1H, ddt, *J* = 19.0, 6.0, 3.1 Hz, H-7b), 3.14 (1H, d, *J* = 10.6, H-14a), 3.61 (1H, d, *J* = 10.6 Hz, H-14b), 4.67 (1H, d, *J* = 11.0 Hz, H-15a), 4.80 (1H, d, *J* = 11.0, H-15b), 4.96 (2H, m, H-11), 5.83 (1H, d, *J* = 6.0 Hz, H-6), 7.52 (2H, m, H-4′/6′), 7.67 (1H, tt, *J* = 7.3, 1.2 Hz, H-5′), 7.97 (2H, m, H-3′/7′).

^{13}C-NMR (125.70 MHz, DMSO-d_6, 25 °C, 39.5 ppm): 17.3 (C-2), 20.6 (C-17), 28.2 (C-7), 30.7 (C-1), 34.6 (C-3), 39.4 (C-4), 39.8 (C-10), 52.5 (C-5), 62.9 (C-14), 65.4 (C-15), 66.5 (C-6), 71.1 (C-11), 121.2 (C-8), 128.7 (4′/6′), 129.3 (3′/7′), 129.8 (C-2′), 133.5 (5′), 165.6 (C-1′), 166.8 (C-9), 170.5 (C-16), 173.2 (C-12).

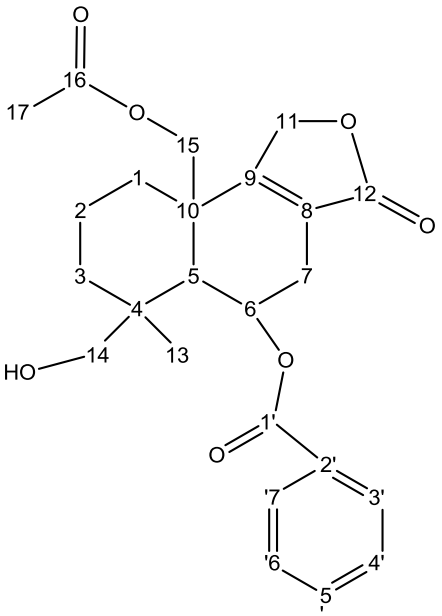

Dideacetyl parasiticolide A

HRESIMS: *m/z* = 387.1817 $[M+H]^+$, calculated for $[C_{22}H_{26}O_6+H]^+$: 387.1802.

^{1}H-NMR (499.87 MHz, DMSO-d_6, 25 °C, 2.50 ppm): 0.91 (1H, ddd, *J* = 13.4, 13.4, 3.7 Hz, H-3a), 0.99 (3H, s, H-13), 1.17 (1H, dd, *J* = 12.9, 3.5 Hz, H-1a), 1.42 (1H, m, H-2a), 1.65 (1H, m, H-2b), 1.81 (1H, s, H-5), 1.97 (1H, d, *J* = 13.4 Hz, H-3b), 2.28 (1H, d, *J* = 12.9 Hz, H-1b), 2.31 (1H, d, *J* = 19.3 Hz, H-7a), 2.73 (1H, m, H-7b), 3.09 (1H, dd, *J* = 10.5, 5.3 Hz), 3.60 (1H, dd, *J* = 10.5, 5.3 Hz, H-14b), 4.07 (1H, m, H-15a), 4.12 (1H, m, H-15b), 4.42 (1H, dd, *J* = 5.3, 5.3 Hz, 14-OH), 4.86 (1H, dd, *J* = 17.5, 2.0 Hz, H-11a), 5.06 (1H, dt, *J* = 17.5, 2.5 Hz, H-11b), 5.10 (1H, dd, *J* = 5.2, 5.2 Hz, 15-OH), 5.80 (1H, d, *J* = 5.8 Hz, H-6), 7.55 (2H, m, H-4′/6′), 7.67 (1H, m, H-5′), 7.90 (2H, m, H-3′/7′).

^{13}C-NMR (125.70 MHz, DMSO-d_6, 25 °C, 39.5 ppm): 17.6 (C-2), 27.3 (C-13), 28.5 (C-7), 30.5 (C-1), 34.9 (C-3), 39.4 (C-4), 42.9 (C-10), 52.7 (C-5), 62.4 (C-15), 63.1 (C-14), 66.9 (C-6), 72.0 (C-11), 119.5 (C-8), 128.9 (C-4′/6′), 129.0 (C-3′/7′), 129.8 (C-2′), 133.5 (C-5′), 165.7 (C-1′), 169.4 (C-9), 173.6 (C-12).

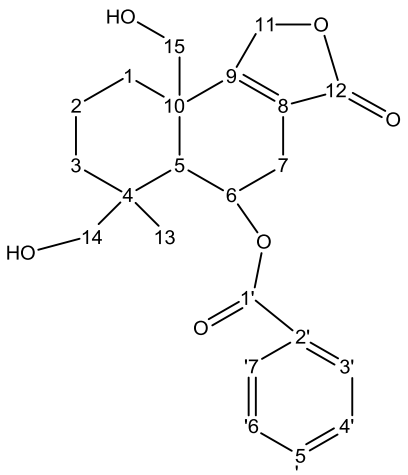

18-Formyl parasiticolide A

HRESIMS: *m/z* = 457.1889 $[M+H]^+$, calculated for $[C_{25}H_{28}O_8+H]^+$: 457.1857.

^{1}H-NMR (499.87 MHz, DMSO-d_6, 25 °C, 2.50 ppm): 1.10 (3H, s, H-13), 1.18 (1H, ddd, *J* = 13.7, 13.7, 3.3 Hz, H-3a), 1.43 (1H, ddd, *J* = 13.2, 13.2, 2.9 Hz, H-1a), 1.51 (1H, m, H-2a), 1.71 (1H, m, H-2b), 1.82 (1H, d, *J* = 13.7 Hz, H-3a), 2.06 (1H, s, H-5), 2.09 (3H, s, H-17), 2.16 (1H, d, *J* = 13.2 Hz, H-1b), 2.43 (1H, d, *J* = 19.3 Hz, H-7a), 2.80 (1H, m, H-7b), 3.99 (1H, d, *J* = 11.0 Hz, H-14a), 4.36 (1H, d, *J* = 11.0 Hz, H-14b), 4.71 (1H, d, *J* = 10.8 Hz, H-15a), 4.78 (1H, d, *J* = 10.8 Hz, H-15b), 4.98 (2H, m, H-11), 5.83 (1H, d, *J* = 5.6 Hz, H-6), 7.52 (2H, dd, *J* = 7.6, 7.6 Hz, H-4′/6′), 7.68 (1H, dd, *J* = 7.6, 7.6 Hz, H-5′), 7.98 (2H, d, *J* = 7.6 Hz, H-3′/7′), 8.06 (1H, s, H-18).

^{13}C-NMR (125.70 MHz, DMSO-d_6, 25 °C, 39.5 ppm): 16.9 (C-2), 20.5 (C-17), 26.6 (C-13), 27.9 (C-7), 30.5 (C-1), 35.4 (C-3), 36.9 (C-4), 39.6 (C-10), 52.1 (C-5), 65.0 (C-14), 65.1 (C-15), 66.5 (C-6), 71.1 (C-11), 121.0 (C-8), 128.6 (C-4′/6′), 129.0 (C-3′/7′), 129.2 (C-2′), 133.4 (C-5′), 161.6 (C-18), 165.1 (C-1′), 165.9 (C-9), 170.1 (C-16), 172.8 (C-12).

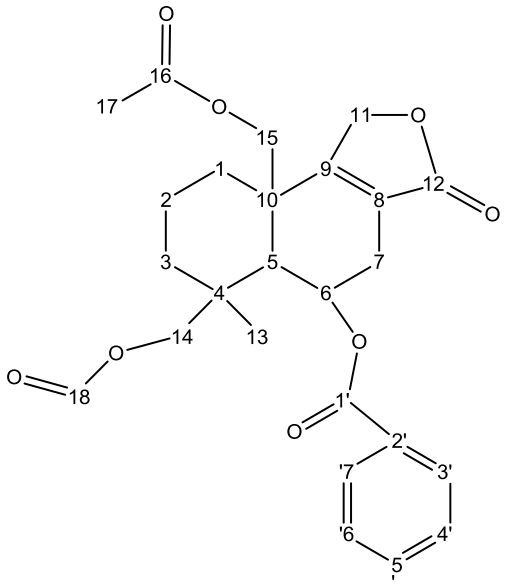

Ditryptoleucine A

HRESIMS: *m/z* = 625.3472 $[M+H]^+$, calculated for $[C_{36}H_{44}N_6O_4+H]^+$: 625.3497.

^{1}H-NMR (499.87 MHz, DMSO-d_6, 25 °C, 2.50 ppm): 0.81 (6H, d, *J* = 6.4 Hz, H-21), 0.83 (6H, d, *J* = 6.4 Hz, H-20), 1.42 (H2, m, H-18a), 1.48 (H2, m, H-18b), 1.58 (H2, m, H-19), 2.44 (H4, m, H-11), 2.80 (H6, s, H-17), 3.76 (H2, dd, *J* = 10.4, 3.8 Hz, H-12), 3.81 (H2, dd, *J* = 7.9, 6.0 Hz, H-15), 5.09 (H2, m, H-2), 6.61 (H2, d, *J* = 7.8, H-5), 6.66 (H2, t, *J* = 7.5, H-7), 6.68 (H2, s, H-3), 7.05 (H2, t, 7.8, H-6), 7.23 (H2, d, *J* = 7.8, H-8).

^{13}C-NMR (125.70 MHz, DMSO-d_6, 25 °C, 39.5 ppm): 21.9 (C-20), 22.6 (C-21), 23.7 (C-19), 31.8 (C-17), 36.1 (C-11), 39.4 (C-18), 56.7 (C-12), 57.9 (C-10), 61.6 (C-15), 76.7 (C-2), 108.7 (C-5), 117.2 (C-7), 124.6 (C-8), 126.7 (C-9), 129.0 (C-6), 150.9 (C-4), 165.0 (C-16), 166.1 (C-13).

Ditryptoleucine B

^{1}H-NMR (499.87 MHz, DMSO-d_6, 25 °C, 2.50 ppm): 0.81 (6H, d, *J* = 6.1 Hz, H-21), 0.83 (6H, d, *J* = 6.2 Hz, H-20), 1.42 (H2, m, H-18), 1.49 (H2, m, H-19), 2.45 (H2, dd, *J* = 13.5, 4.7, H-11a), 2.75 (H6, s, H-17), 3.13 (H2, m, H-11b), 3.33 (H2, s, H-2), 3.82 (H2, t, *J* = 6.9 Hz, H-15), 4.23 (H2, m, H-12), 6.58 (H2, d, *J* = 7.5, H-5), 6.65 (H2, t, *J* = 7.1, H-7), 6.70 (H2, s, H-3), 7.01 (H2, t, 7.2, H-6), 7.37 (H2, d, *J* = 7.1, H-8).

^{13}C-NMR (125.70 MHz, DMSO-d_6, 25 °C, 39.5 ppm): 21.5 (C-21), 22.5 (C-20), 23.6 (C-19), 31.6 (C-17), 37.0 (C-11), 38.0 (C-18), 55.3 (C-12), 60.8 (C-10), 61.7 (C-15), 76.3 (C-2), 108.5 (C-5), 117.4 (C-7), 124.0 (C-8), 130.2 (C-9), 128.3 (C-6), 149.6 (C-4) 166.9 (C-16), 166.6 (C-13).

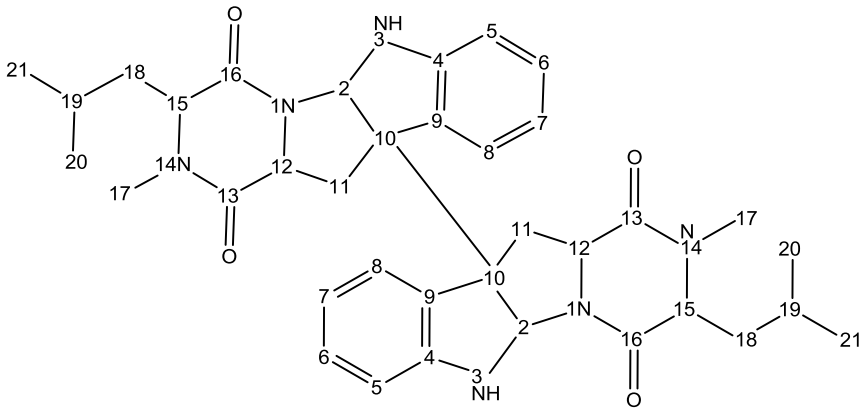

Oryzamide A$_1$

HRESIMS: *m/z* = 491.26526 $[M+H]^+$, calculated for $[C_{28}H_{34}N_4O_4+H]^+$: 491.26525.

^{1}H-NMR (499.87 MHz, DMSO-d_6, 25 °C, 2.50 ppm): 0.83 (3H, d, *J* = 6.5 Hz, H-5′), 0.88 (3H, d, *J* = 6.6 J, H-5′), 1.36 (1H, m, H-4′), 1.59 (2H, m, H-3′), 1.77 (3H, s, H-2‴), 2.67 (1H, m, H-3″), 2.83 (1H, m, H-3″), 2.87 (3H, s, N-CH), 4.76 (1H, m, H-2″), 5.02 (1H, m, H-2′), 6.47 (1H, d, *J* = 14.8, H-2), 6.61 (2H, d, *J* = 8.4 Hz, H-6″/8″), 7.01 (2H, d, *J* = 8.4 Hz, H-5″/9″), 7.05 (1H, m, H-8), 7.10

(1H, m, H-7), 7.26 (1H, m, H-1), 7.36 (1H, m, H-6), 7.41 (1H, s, H-4), 7.62 (1H, d, *J* = 7.9 Hz, H-9), 8.24 (1H, d, *J* = 8.0 Hz, 2″-NH), 9.16 (1H, s, 7″-OH), 9.84 (1H, d, *J* = 9.8 Hz, 1-NH), 11.11 (1H, s, 4-NH).

^{13}C-NMR (125.70 MHz, DMSO-d_6, 25 °C, 39.5 ppm): 21.6 (C-5′), 22.0 (C-2‴), 22.7 (C-5′), 24.1 (C-4′), 30.9 (C-N), 36.2 (C-3″), 36.9 (C-3′), 50.5 (C-2″), 54.2 (C-2′), 106.4 (C-2), 111.4 (C-3), 111.5 (C-6),114.6 (C-6″/8″), 118.5 (C-9), 118.8 (C-8), 119.2 (C-1), 121.1 (C-7), 123.1 (C-4), 125.0 (C-10), 127.4 (C-4″), 129.7 (C-5″/9″), 136.9 (C-5), 156.0 (C-7″), 167.7 (C-1′), 168.8 (C-1‴), 172.3 (C-1″).

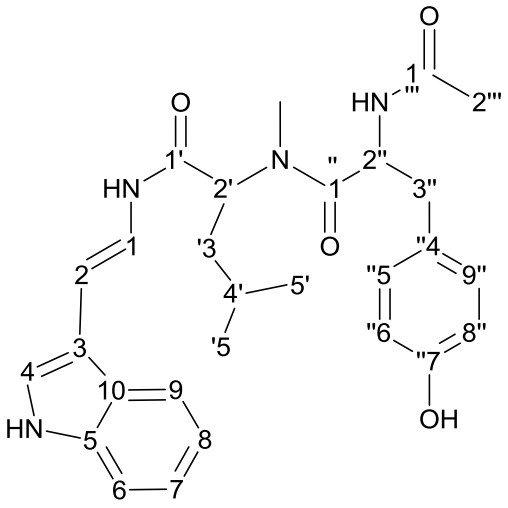

Paper 8

"Accurate prediction of secondary metabolite gene clusters in filamentous fungi"

Andersen, M.R.; Nielsen, J.B.; Klitgaard, A.; **Petersen, L.M**.; Zachariasen, M.; Hansen, T.J.; Blicher, L.H.; Gotfredsen, C.H.; Larsen, T.O.; Nielsen, K.F.; Mortensen, U.H.

Proceedings of the National Academy of Sciences of the United States of America, **2013**, *110* (1), E99–E107

Accurate prediction of secondary metabolite gene clusters in filamentous fungi

Mikael R. Andersen[a,1], Jakob B. Nielsen[a], Andreas Klitgaard[a], Lene M. Petersen[a], Mia Zachariasen[a], Tilde J. Hansen[a], Lene H. Blicher[b], Charlotte H. Gotfredsen[c], Thomas O. Larsen[a], Kristian F. Nielsen[a], and Uffe H. Mortensen[a]

[a]Center for Microbial Biotechnology, Department of Systems Biology, [b]DTU Multi-Assay Core, Department of Systems Biology, and [c]Department of Chemistry, Technical University of Denmark, DK-2800 Kongens Lyngby, Denmark

Edited by Jerrold Meinwald, Cornell University, Ithaca, NY, and approved November 19, 2012 (received for review August 20, 2012)

Biosynthetic pathways of secondary metabolites from fungi are currently subject to an intense effort to elucidate the genetic basis for these compounds due to their large potential within pharmaceutics and synthetic biochemistry. The preferred method is methodical gene deletions to identify supporting enzymes for key synthases one cluster at a time. In this study, we design and apply a DNA expression array for *Aspergillus nidulans* in combination with legacy data to form a comprehensive gene expression compendium. We apply a guilt-by-association–based analysis to predict the extent of the biosynthetic clusters for the 58 synthases active in our set of experimental conditions. A comparison with legacy data shows the method to be accurate in 13 of 16 known clusters and nearly accurate for the remaining 3 clusters. Furthermore, we apply a data clustering approach, which identifies cross-chemistry between physically separate gene clusters (superclusters), and validate this both with legacy data and experimentally by prediction and verification of a supercluster consisting of the synthase AN1242 and the prenyltransferase AN11080, as well as identification of the product compound nidulanin A. We have used *A. nidulans* for our method development and validation due to the wealth of available biochemical data, but the method can be applied to any fungus with a sequenced and assembled genome, thus supporting further secondary metabolite pathway elucidation in the fungal kingdom.

aspergilli | natural products | secondary metabolism | polyketide synthases

No other group of biochemical compounds holds as much promise for drug development as the secondary (nongrowth associated) metabolites (SMs). A review from 2012 (1) found that for small-molecule pharmaceuticals, 68% of the anticancer agents and 52% of the antiinfective agents are natural products, or derived from natural products. The fact that SMs are often synthesized as polymer backbones that are subsequently diversified greatly via the actions of tailoring enzymes sets the stage for combinatorial biochemistry (2), because their biosynthesis is modular.

Major groups of SMs include polyketides (PKs) consisting of $-CH_2-(C=O)-$ units, ribosomal and nonribosomomal peptides (NRPs), and terpenoids made from C_5 isoprene units. These polymer backbones are, with the exception of ribosomal peptides, made by synthases or synthetases and are modified by a plethora of tailoring enzymes, including (de)hydratases, oxygenases, hydrolases, methylases, and others.

In fungi, these biosynthetic genes of secondary metabolism are organized in discrete clusters around the synthase genes. Although quite accurate algorithms are available for identification of possible SM biosynthetic genes, particularly PK synthases (PKSs), NRP synthetases (NRPSs), and dimethylallyl tryptophan synthases (DMATSs) (3, 4), the assignment and prediction of the members of the individual clusters solely from the genome sequence have not been accurate. Relevant protein domains can be predicted for some of the genes (e.g., cytochrome P450 genes) (5); however, genes in identified clusters often have unknown functions, which makes predicting their inclusion impossible. Furthermore, SM gene clusters often colocalize on the chromosomes (6), which makes separation of clusters solely based on gene function predictions difficult.

The efficient elucidation of the biosynthetic genes for each SM cluster has thus so far been based on laborious single gene deletion of each of the putative members and chemical profiling of the SMs of the deletion strains. This effort has been especially noticeable in the model fungus *Aspergillus nidulans*, which is presently the fungal species with the largest number ($n = 25$) of characterized SM synthases/synthetases, due to a massive effort by several groups (7–30). In recent studies, this fungus has also been shown to have cross-chemistry between gene clusters on separate chromosomes (8, 30). Although these reactions are highly interesting for combinatorial chemistry, the identification of gene clusters involved in cross-chemistry is cumbersome because it involves combinatorial deletion of SM synthetic genes, thus greatly increasing the potential number of candidates.

In this study, we propose a general "omics"-based method for the accurate determination of fungal SM gene cluster members. The method is based on an annotated genome sequence and a catalog of gene expression, a set of information that is readily available for many fungal species and can easily be generated for more. To develop, benchmark, and validate this algorithm, we have used *A. nidulans* as a model organism, which is especially well-suited for this purpose due to the above-stated wealth of information. The algorithm is proven to be very powerful in identifying gene cluster members. We furthermore report an extension of the algorithm, which is proven to be successful in identifying cross-chemistry between gene clusters.

Results

Analysis of SMs *A. nidulans* on Complex Solid Medium Identifies 42 Compounds. Initially, we evaluated the production of SMs on four different solid media [oatmeal agar (OTA), yeast extract sucrose (YES), Czapek yeast autolysate (CYA), and CYA with 50 g/L NaCl sucrose (CYAS); *Materials and Methods*] at 4, 8, and 10 d. The object of this was to identify a selection of media that (*i*) gave as many produced SMs as possible, (*ii*) showed one or more SMs unique to each medium, and (*iii*) had SMs that were only produced on two of the selected media.

Author contributions: M.R.A., J.B.N., L.M.P., C.H.G., T.O.L., K.F.N., and U.H.M. designed research; M.R.A., J.B.N., A.K., L.M.P., M.Z., T.J.H., L.H.B., C.H.G., and K.F.N. performed research; M.R.A. and K.F.N. contributed new reagents/analytic tools; M.R.A., J.B.N., A.K., L.M.P., T.J.H., C.H.G., T.O.L., K.F.N., and U.H.M. analyzed data; and M.R.A., J.B.N., A.K., L.M.P., C.H.G., K.F.N., and U.H.M. wrote the paper.

The authors declare no conflict of interest.

This article is a PNAS Direct Submission.

Data deposition: The gene expression data, gene expression microarray data description, and legacy gene expression data reported in this paper are available from the Gene Expression Omnibus (GEO) database, www.ncbi.nlm.nih.gov/geo (accession nos. GSE39993, GPL15899, GSE12859 and GSE7295).

[1]To whom correspondence should be addressed. E-mail: mr@bio.dtu.dk.

See Author Summary on page 24 (volume 110, number 1).

This article contains supporting information online at www.pnas.org/lookup/suppl/doi:10.1073/pnas.1205532110/-/DCSupplemental.

These characteristics should allow us to have as many active gene clusters as possible, as well as ensuring unique production profiles for as many SM gene clusters as possible.

From this initial analysis, we selected the YES, CYA, and CYAS media for transcriptional profiling. On these media, we were able to separate and detect 59 unique SMs, of which we could name 42 by comparison with our extensive in-house library of microbial metabolites (31) and the AntiBase 2010 natural products database. The production profile of the compounds satisfied the three criteria listed above (Fig. 1, Fig. S1, and Dataset S1).

Generation of a Diverse Gene Expression Compendium for *A. nidulans*. Samples were taken for transcriptional profiling from plates cultivated in parallel to those of the SM profiling above. RNA was purified, prepared for labeling, and hybridized to custom-designed Agilent Technologies arrays based on version 5 of the *A. nidulans* annotation (32).

The produced data were combined with previously published microarray data from *A. nidulans* bioreactor cultivations (33, 34) to form a microarray compendium spanning a diverse set of conditions, comprising 44 samples in total. The set includes four strains of *A. nidulans*. Four different growth media are included: three complex media (see above) and one minimal medium. Medium variations include five different defined carbon sources (ethanol, glycerol, xylose, glucose, and sucrose), as well as yeast extract. The combined compendium of expression data is available in Dataset S2.

Correlation-Based Identification of Gene Clusters. To identify gene clusters efficiently around SM synthases, we developed a gene clustering score (CS) based on the Pearson product-moment correlation coefficient. Our CS gives a numerical value for correlation of the expression profile of a given gene with the expression profiles of the three immediate neighbor genes on either side. Only positive correlation is considered. Values for the CS are available in Dataset S2.

Statistical simulation of the distribution of CS on the given dataset showed that CS values ≥2.13 corresponded to a false-positive rate of 0.05 (Fig. S2). Therefore, CS ≥ 2.13 was used as a guideline for identifying the extent of gene clusters.

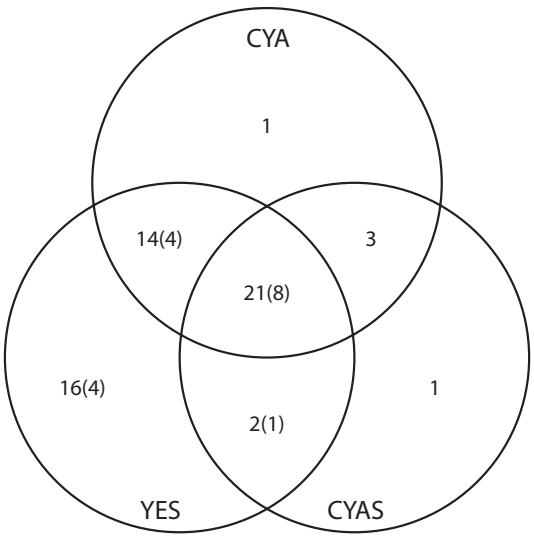

Fig. 1. Venn diagram of SMs found on three different solid media. The number of different metabolites is sorted according to which media the metabolites have been identified on. The number of metabolites unable to be confidently identified are noted in parentheses. Details can be found in Dataset S1, and the chemical structures are illustrated in Fig. S1.

Prediction of the Extent of 51 Gene Clusters. Evaluation of the size of the clusters around SM genes was performed using a precomputed list of 66 putative PKSs, NRPSs, and DMATSs from the secondary metabolite unique regions finder (SMURF) algorithm (3) based on the *A. nidulans* FGSC A4 gene set (35). In addition to these 66 genes, we added one prenyltransferase gene found in the primary literature (30) and three diterpene synthase (DTS) genes predicted by Bromann et al. (25), resulting in 70 putative biosynthetic genes. All 25 experimentally verified PKSs, NRPSs, DTSs, and prenyltransferases were found to be included in this list (Tables 1–3).

For each of the 70 biosynthetic genes, we examined the genes nearby for high CS values and inspected the expression profiles of the genes manually for additional validation and refinement. Apart from 12 genes that were silent under the conditions tested (Table S1), this allowed prediction of the sizes of gene clusters around 58 biosynthetic genes organized in 51 clusters and counting of a total of 254 genes included in the clusters (an example is shown in Fig. 2). The fact that we can map expression for 58 of the 70 biosynthetic genes (a large proportion of the gene clusters) is surprising, considering that many, or even the majority, of the gene clusters are reported to be silent under standard laboratory conditions (13, 14, 20, 36–38). An example of a cluster previously described as silent but identified here is the *inpAB* cluster (39). However, those cultivation experiments were conducted on liquid minimal medium and not on solid complex media, where we find that the expression from most of these genes is most pronounced. We therefore see the large number of active clusters as a confirmation of adequate diversity of the cultivation conditions in our microarray compendium.

Next, we investigated how our cluster predictions matched those published in the literature. This comparison demonstrated that our algorithm generally predicts gene clusters with excellent accuracy. Specifically, we accurately predict the extent of 11 of the 16 known gene clusters (Tables 1–3). In two of the remaining 5 gene clusters, the difference is due to artifacts. For the gene sterigmatocystin cluster (Fig. 2), the difference of 24 genes relative to 25 genes is caused by differences in the current gene annotation compared with the original paper from 1996 (17). Changes in gene calling are also the reason for discrepancy in the terrequinone cluster, where our legacy microarray data only contain data for 3 of the 5 genes, thus impairing the prediction. For the three remaining cases, the 2 gene clusters involved in meroterpenoid (austinol and dehydroaustinol) biosynthesis and the aspyridone cluster, the divergence seems to be biological. For the austinol/dehydroaustinol double-cluster system, we predict 3 extra genes in one cluster (around AN8383) and 2 extra genes in the other cluster (around AN9259) in addition to genes identified by Lo et al. (30). We individually deleted the 3 extra genes (AN8375, AN8376, and AN8380) in the AN8383 cluster; however, apart from differences in the austinol/dehydroaustinol ratio, we could only confirm the results of Lo et al. (30) of these genes not being essential for austinol/dehydroaustinol biosynthesis (Fig. S3). Because the size of most of the clusters was accurately predicted by our algorithm, we speculate that some or all of the extra genes are involved in biosynthesis of derivatives of austinol/dehydroaustinol. In agreement with this scenario, it is not uncommon that newly detected compounds are linked to known PKS pathways. For example, shamixanthones and arugusins were recently discovered to be products derived from the monodictyphenone cluster (8, 11), and this cluster has been redefined several times (9, 10). For the remaining case, the *apdG* gene of the aspyridone cluster (20), misprediction of the cluster members is due to a complete divergence between the transcription profiles of *apdG* and the remainder of the gene cluster. In general, we conclude that the use of

Table 1. Prediction of PKS gene clusters

GeneID	Gene	Compound (if known)	Cluster size		Medium	Ref(s).
			Predicted	Known		
AN0150	*mdpG*	Monodictyphenone/emodin	12	12	Solid	(7–10)
AN7903		Violaceol I and II	12	?	Solid	(11)
AN6448	*pkbA*		8	?	Solid	(24)
AN7084			8		Solid	
AN8209	*wA*	Green conidial pigment	6	?	Solid	
AN7909	*orsA*	Orsellinic acid/F9975/violaceols	5	5	Solid	(11–14)
AN1784			4		Solid	
AN9005			4		Solid	
AN6000	*aptA*	Asperthecin	3	3	Solid	(15)
AN6431			3		Solid	
AN11191			2		Solid	
AN7489			1		Solid	
AN3273			1		Solid	
AN2547	*easB*	Emericellamide	4	4	Both	(16)
AN3230	*pkfA*	Orsellinaldehydes	6	?	Both	(24)
AN7071	*pkgA*	Alternariol/isocoumarins	7	?	Both	(24)
AN7825	*stcA*	Sterigmatocystin	24*	25	Both	(17–19)
AN7815	*stcJ*	Sterigmatocystin	24*	25	Both	(17–19)
AN8383	*ausA*	Austinol	7	4	Both	(11, 24, 30)
AN2032	*pkhA*	Unknown	10	?	Liquid	(24)
AN2035	*pkhB*	Unknown	10	?	Liquid	(24)
AN8412	*adpA*	Aspyridone	7†	8	Liquid	(20)
AN6791			1		Liquid	
AN8910			1		Liquid	

This table contains predicted PKSs as well as PKS-like genes (AN7489 and AN7815) and a PKS/hybrid gene (AN8412). The medium column describes under which type of medium (liquid, solid, or both) the cluster is expressed. For gene clusters with identified functions and gene members, the number of identified cluster members is given as well as references to the original papers. Further details on the cluster members and the expression profiles of the individual clusters may be found in Dataset S2 and Fig. S4. Chemical structures of all compounds may be found in Fig. S1.

*Difference seemingly due to the current gene calling diverging from the original paper from 1996 (17).

†Algorithm was not able to predict the inclusion of *apdG*, the outmost gene hypothesized to be a part of the cluster (20). The expression profile of *apdG* diverges from the rest of the cluster.

CS values in combination with inspection of the expression profiles is a very effective tool to predict the extent of gene clusters, because the borders of 13 of 16 clusters were accurately predicted (when predictions were adjusted to compensate for the two artifacts discussed above) and there was near-accurate prediction of all 16 clusters.

Diverse Gene Expression Compendium Is Important for Accurate Prediction. To evaluate the compendium size needed for accurate predictions, we used principal component analysis (PCA) on our matrix of expression values (Dataset S2). Greater than 95% of the variation within the set can be described in the first three principal components. This suggests that a theoretical lower limit for this type of analysis would be three arrays if one could select conditions with a near-perfect difference in expression levels, ideally high, medium, and low expression for all genes, and with a maximum difference between all clusters and their surrounding genes. This would be nearly impossible to achieve for all clusters. However, if one is only interested in a single or a few gene clusters of interest, and has the appropriate prior knowledge, it should be possible to select three to five conditions and achieve accurate predictions. Very informative studies have been performed with two conditions, but the boundaries of the cluster can be difficult to determine (e.g., ref. 25).

To test how much it was possible to reduce our dataset, we used an unsupervised PCA-based analysis for incremental reduction of the dataset. In this, we found (unsurprisingly) that our biological replicate samples contain the smallest amount of unique information. Ten of 44 samples can be removed with only an approximately 10% loss in the data variation, and 25 of 44 samples (all replicates) can be removed with less than a 35% loss in data variation. The time sample series on a solid medium presented in this study were not reduced from the set until all biological replicates were reduced. We conclude that in selection of samples for cluster elucidation, one should sample as diversely as possible. Biological replicates are not cost-effective unless already available from prior studies.

Clustering of Synthase Expression Profiles Identifies Superclusters. Recent work has identified two cases of cross-chemistry between clusters located on separate chromosomes. The production of austinol and derived compounds (the meroterpenoid pathway) has been shown to be dependent on two separate clusters (11, 30), and the biosynthesis of prenyl xanthones is dependent on three separate clusters (8). We were interested in seeing whether this is a general phenomenon and whether such cross-chromosomal "superclusters" could be detected using our expression data.

A full gene-to-gene comparison of expression profiles between all predicted NRPSs, PKSs, DTSs, and prenyl transferases found in the array data was conducted, and the genes were clustered (Fig. 3). This clustering is not based directly on the expression profiles, because expression index variation from silent conditions distorts clustering. Instead, we clustered on the basis of a Spearman-based score of similarity to the expression profiles of the other synthases, which effectively eliminates noise.

The method is efficient for clustering the synthases and transferases according to shared products. Seven of eight sets of genes

Table 2. Prediction of NRPS gene clusters

GeneID	Gene	Compound (if known)	Cluster size		Medium	Source
			Predicted	Known		
AN9226			18		Solid	
AN6444			8		Solid	
AN4827			7		Solid	
AN8105			8		Solid	
AN8513	*tdiA*	Terrequinone A	3*	5	Solid	(21, 22)
AN1242	*nlsA*	Nidulanin A	3		Solid	This study
AN6961			2		Solid	
AN0016			1		Solid	
AN10486			1		Solid	
AN7884			14		Both	
AN3495	*inpA*	Unknown	7	7	Both	(25, 39)
AN3496	*inpB*	Unknown	7	7	Both	(25, 39)
AN2545	*easA*	Emericellamide	4	4	Both	(16)
AN2621	*acvA/pcbAB*	Penicillin G	3	3	Both	(25, 27, 28)
AN3396	*mica*	Microperfuranone	3	3†	Both	(29)
AN2924			2		Both	
AN10576	*ivoA*	*N*-acetyl-6-hydroxytryptophan	2	2	Both	(23, 26)
AN0607	*sidC*	Siderophores	1	1	Both	(55)
AN10297			1		Both	
AN5318			1		Both	
AN1680			1		Liquid	
AN2064			1		Liquid	
AN9129			1		Liquid	
AN9291			1		Liquid	

This table contains predicted NRPSs as well as NRPS-like genes (AN3396, AN5318, and AN9291). The medium column describes under which type of medium (liquid, solid, or both) the cluster is expressed. For gene clusters with identified functions and gene members, the number of identified cluster members is given as well as references to the original papers. Further details on the cluster members and the expression profiles of the individual clusters may be found in Dataset S2, and Fig. S4. Chemical structures of all compounds may be found in Fig. S1.
*Extent of the gene cluster is predicted correctly. The difference is due to the absence of two of the genes on the legacy microarray data, which removes them from the prediction.
†Yeh et al. (29), who examined this cluster, found increased transcription of the two extra genes we predict, but they found them to be nonessential for microperfuranone production.

predicted to be in the same biosynthetic clusters by the method above are found to cluster together in this representation. The exception is AN2032 and AN2035, which do not cocluster due to very low signals from the AN2032 probes on the microarray. Furthermore, the clustering is accurate in terms of cross-chemistry. In examining the two examples of cross-chemistry between gene clusters, it is found that these are predicted correctly. The meroterpenoid pathway includes the PKS AN8383 and the DMATS AN9259, which are illustrated to colocate in Fig. 3. The other example is the prenylxanthone biosynthetic pathway, which includes

Table 3. Prediction of gene clusters around prenyltransferases and diterpene synthases

GeneID	Type	Gene	Compound (if known)	Cluster size		Medium	Source
				Predicted	Known		
AN11194	DMATS			18		Solid	
AN11202	DMATS			18		Solid	
AN9259	DMATS			12	10	Both	(30)
AN8514	DMATS	*tdiB*	Terrequinone A	3*	5	Solid	(21, 22)
AN11080	DMATS	*nptA*	Nidulanin A	1		Both	This study
AN10289	DMATS			1		Solid	
AN6784	DMATS	*xptA*	Variecoxanthone A	1	1	Solid	(8–10)
AN1594	DTS		Ent-pimara-8(14),15-diene	9	9	Solid	(25)
AN3252	DTS			7		Solid	
AN9314	DTS			2		Solid	

This table contains predicted DMATSs, functionally prenyltransferases, and three DTSs predicted by Bromann et al. (25). The medium column describes on which type of medium (liquid, solid, or both) the cluster is expressed. For gene clusters with identified functions and gene members, the number of identified cluster members is given as well as references to the original papers. Further details on the cluster members and the expression profiles of the individual clusters may be found in Dataset S2, and Fig. S4. Chemical structures of all compounds may be found in Fig. S1.
*Extent of the gene cluster is predicted correctly. The difference is due to the absence of two of the genes on the legacy microarray data, which removes them from the prediction.

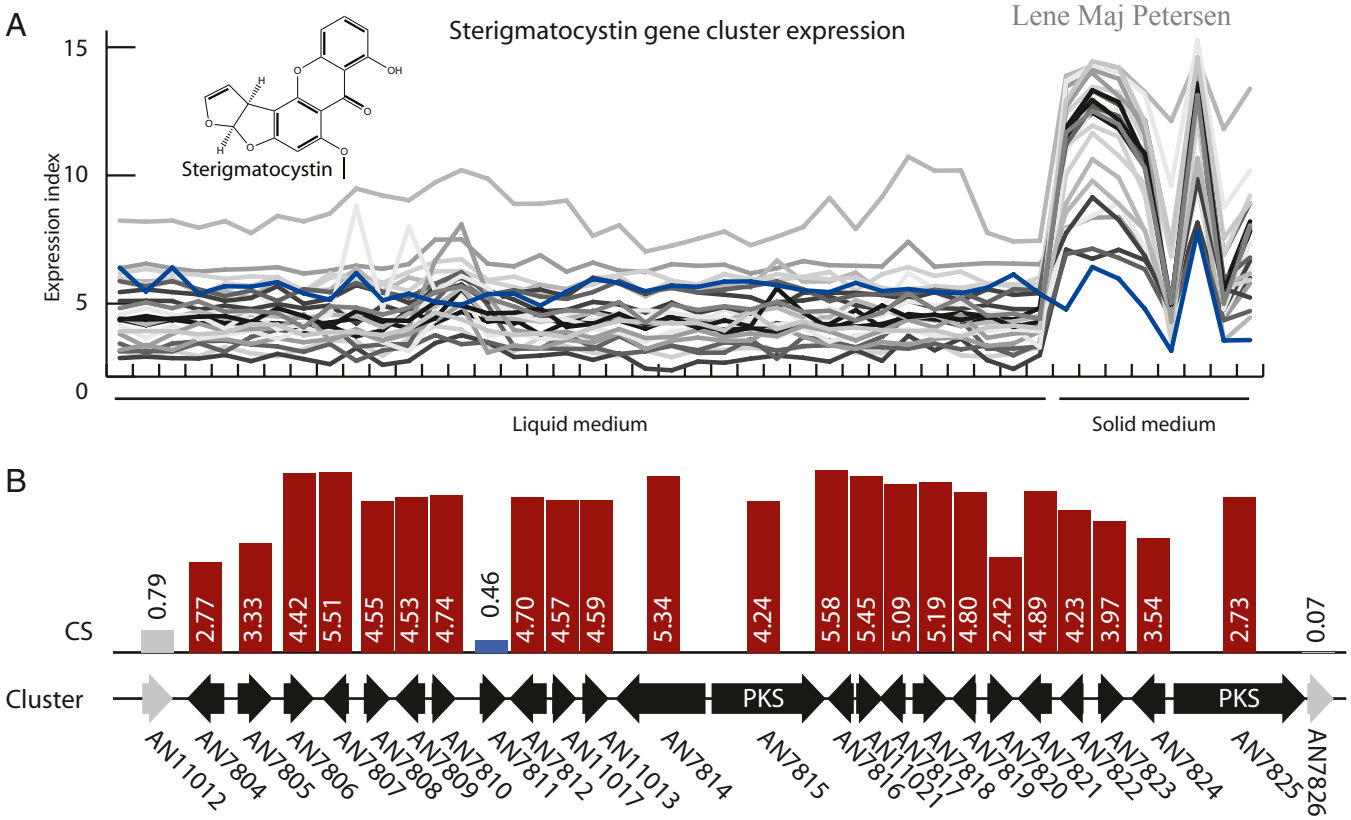

Fig. 2. Identification of the sterigmatocystin biosynthetic cluster. (*A*) Gene expression profiles across 44 experiments for the 24 genes (marked in black in *B*) predicted to be in the sterigmatocystin biosynthetic cluster (liquid and solid cultures are marked for reference). The expression profile of AN7811(*stcO*) is marked in blue. (*B*) Illustration of the values of the gene CS for the 24 genes and the two immediate neighbors. Genes included in the predicted cluster are marked in black. AN7811(*stcO*) did not have a CS above the used cutoff of 2.13 denoting clustering but was added due to the similarity of the expression profile, as shown in blue. The predicted extent of the cluster corresponds with the cluster as originally described by Brown et al. (17), when correcting for the fact that the gene models have changed since then. Full data for all predicted clusters may be found in Dataset S2.

the PKS AN0150 and the DMATS AN6784. These two genes are also found close to each other in Fig. 3.

We further use the maximum separation distance of two genes in the same biosynthetic cluster in the heat map of Fig. 3 as a cutoff distance for cross-chemistry. This allowed the genes to be sorted into seven larger superclusters. Details on the expression profiles of the individual clusters in each supercluster can be found in Fig. S4. Although we cannot directly separate tight coregulation from cross-chemistry with this method, the presence of these superclusters consisting of individual clusters with similar expression profiles suggests a larger extent of cross-chemistry in *A. nidulans* than what has been reported to date. To test the predictive power of this clustering further, we performed a gene deletion study within supercluster 5, which contains clusters located on six of the eight chromosomes.

Identification of the Chemical Structure of Nidulanin A Confirms Prediction of Cross-Chemistry Between NRPS AN1242 (NlsA) and Prenyltransferase AN11080 (NptA). To test the hypothesis of superclusters and whether the analysis above could be used to elucidate cross-chemistry, we constructed a deletion mutant of the NRPS AN1242 and evaluated the SMs found in the mutant relative to a reference strain. Four related compounds (compounds 1–4) were found to be absent in the ΔAN1242 strain (Fig. S5). MS isotope patterns as well as tandem MS (MS/MS) analysis showed compound 1 to have the molecular formula $C_{34}H_{45}N_5O_5$, with compounds 2 and 3 likely being oxygenated forms with one and two extra oxygen molecules, respectively. Compounds 1–3 all seem to be prenylated, as shown by spontaneous loss of a prenyl-like fragment, C_5H_8, in a small fraction of the ions during MS analysis. Compound 4 has a molecular formula of (1)-C5H8, suggesting it to be the unprenylated precursor of compound 1.

We thus isolated and elucidated the structure of compound 1, henceforth called nidulanin A, based on NMR spectroscopy. The stereochemistry of compound 1 was examined using Marfey's method (40) and was supported by bioinformatic analysis of the protein domains of AN1242 (*SI Text*). Altogether, nidulanin A is proposed to be a tetracyclopeptide with the sequence -L-Phe-L-Kyn-L-Val-D-Val- and an isoprene unit *N*-linked to the amino group of L-kynurenine (Fig. 4).

Because no prenyltransferase genes are found near AN1242, cross-chemistry catalyzed by an *N*-prenylating DMATS is a likely assumption. Examination of supercluster 5 in Fig. 3, where the NRPS AN1242 is found, shows AN11080 to be the DMATS with the expression profile most similar to AN1242. Gene deletion of AN11080 and subsequent ultra-high-performance liquid chromatography (UHPLC) high-resolution MS (HRMS) analysis of the ΔAN11080 strain show that the deprenylated compound 4, but none of the three prenylated forms, is present, thus confirming that nidulanin A and the two oxygenated forms (compounds 3 and 4) are synthesized by cross-chemistry between AN1242 (now NlsA) on chromosome VIII and AN11080 (now NptA) on chromosome V (Fig. S5).

Furthermore, we note that the masses corresponding to compound 3 (nidulanin A + O) and compound 4 (nidulanin A + O_2) are not found in the reference strain or in the ΔAN11080 strain. This suggests that compounds 3 and 4 are oxidized after the prenylation step.

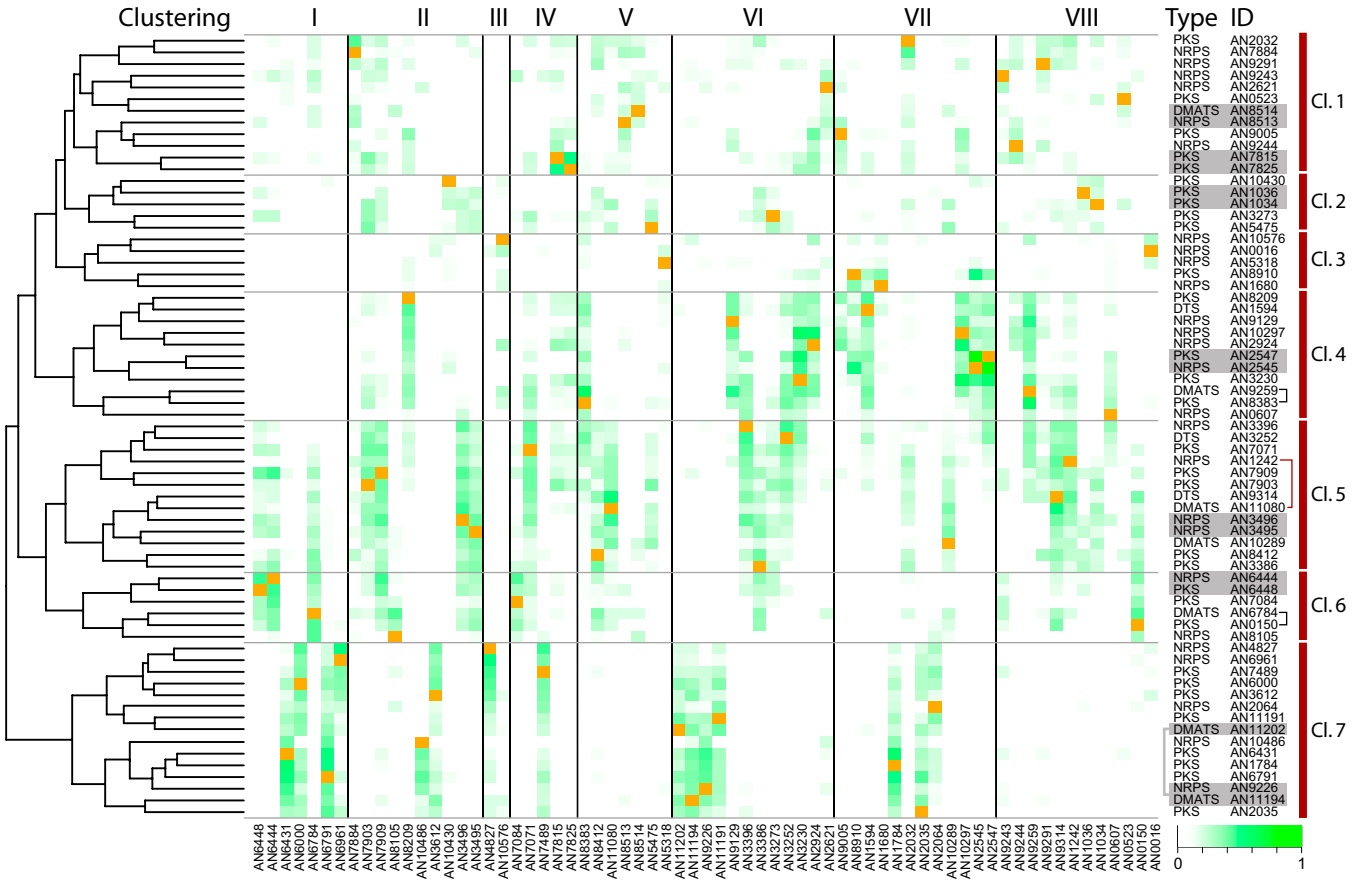

Fig. 3. Cross-chromosomal clustering. Matrix diagram of the correlation between 67 predicted and known biosynthetic genes. Each square in the matrix shows the compounded squared Spearman correlation coefficient for comparison of the expression profile of the genes color-coded from 0 (white) to 1 (green). Genes are sorted horizontally according to their location on the chromosomes (marked in orange) and vertically according to their scores (*Left*, marked with a dendrogram). (*Right*) Genes located in the same clusters are highlighted with a gray box, which is connected with a gray bracket in one case. Genes with known cross-chemistry are marked with a black bracket. An example of cross-chemistry found in this study is marked with a red bracket. Seven putative superclusters are marked. Further details of the clusters may be found in Fig. S4.

Discussion

In this study, we present a method for fungal SM cluster estimation based on similarity of expression profiles for neighboring genes. For the given organism *A. nidulans*, comparison with legacy data has verified the method to be highly accurate and effective for a large proportion of the gene clusters.

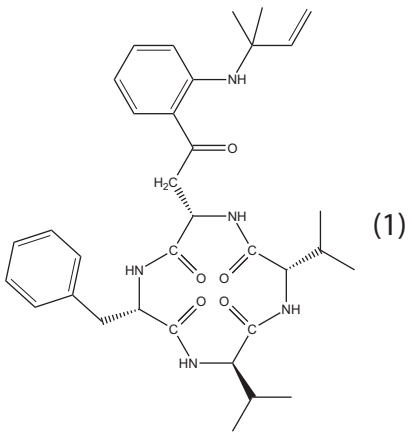

Nidulanin A

Fig. 4. Proposed absolute structure of nidulanin A. Details on the structural elucidation are available in *SI Text*.

It is clear from our results that the composition of the gene expression compendium has a significant effect on cluster predictions. We show here that it is important with a diverse set of samples, including both liquid and agar cultures as well as minimal medium and complex medium. This is in accordance with previous observations (11, 13, 14, 20, 36) stating that at a given set of conditions, only a fraction of the clusters are active. A reduction analysis of our own data has further shown that the inclusion of biological replicates in the dataset does not improve the analysis as much as inclusion of more unique samples. A diverse set of conditions should remedy regulation at the transcriptional level as well as chromatin-level regulation, which has been shown to have significant effects in fungi (13, 41). Another factor of importance is the quality of genome annotation. Erroneous gene calls inside clusters decrease the value of the CS for genes within a distance of three genes. Furthermore, problems with gene calls can affect expression profiling if a nontranscribed region is included in the gene cluster. However, neither of these seems to be a problem in the data presented here. Including the expression profiles of seven genes in the calculation of the CS also increases the robustness of the method toward erroneous gene calls.

The stated robustness of the CS has the disadvantage that the CS alone performs poorly for clusters with four or fewer genes,

because the maximum value of CS for n genes is $n - 1$. However, in the cases of small clusters, the clustering can still be predicted from the transcription profiles, as shown in this study.

In some cases, we also see that cluster calling based on expression profiles outperforms the combination of gene KO and metabolomics. If a given detected metabolite is not the end product of the biosynthetic pathway, gene deletions will only identify a part of an SM cluster as being relevant for that metabolite, thus missing genes. An example of this is seen in the emodin/monodictyphenone cluster (PKS AN0150), where a subset of the genes is only required for some of the metabolites, resulting in a two-step elucidation of the gene cluster (7, 8). The CS method correctly calls the full cluster.

One aspect of the method is the ability to identify gene clusters simply from identifying groups of genes with high CS values, and not using a seeding set of synthases as was done in this case. This allows the unbiased identification of gene clusters throughout the entire genome. Although we see a surprising amount of these clusters (Dataset S2) not limited to the predicted SM synthases, we have not evaluated these in this study, because data for appropriate benchmarking is not available. However, we believe that there is great potential for biological discoveries to be made here, both in terms of promoter and chromatin-based transcriptional regulation.

The final extension of the algorithm is its ability to identify biosynthetic superclusters scattered across different chromosomes. Although this is a recently reported phenomenon (8), we believe that this is a common phenomenon, at least in *A. nidulans* and possibly in fungi in general. It is important to note that our method does not allow one to discriminate between tight coregulation and cross-chemistry between two distant clusters. It is therefore most efficient in cases in which it is evident that a given gene cluster does not hold all enzymatic activities required to synthesize the associated compound. In those cases, the use of a diverse transcription catalog, such as the one applied here, is a powerful strategy for identifying cross-chemistry, as shown for the NRPS AN1242 and the assisting prenyltransferase AN11080 in the synthesis of nidulanin A and derived compounds.

In summary, this study provides (*i*) an updated gene expression DNA array for *A. nidulans*, (*ii*) a wealth of information advancing the cluster elucidation in the model fungus *A. nidulans*, (*iii*) a powerful tool for prediction of SM cluster gene members in fungi, (*iv*) a proven methodology for prediction of SM gene cluster cross-chemistry, and (*v*) a proposed structure for the compound nidulanin A.

Materials and Methods

Strains. *A. nidulans* FGSC A4 was used for all transcriptomic experiments in this study. Furthermore, legacy data using the FGSC A4, *A. nidulans* AR16msaGP74 (expressing the *msaS* gene from *Penicillium griseofulvum*) (34), *A. nidulans* AR1phk6msaGP74 (expressing the *msaS* gene from *P. griseofulvum* and overexpressing the *A. nidulans xpkA*) (34), and *A. nidulans* AR1phkGP74 (overexpressing the *A. nidulans xpkA*) (33), were applied.

The *A. nidulans* FGSC A4 stock culture was maintained on CYA agar at 4 °C. *A. nidulans* strain IBT 29539 (*veA1*, *argB2*, *pyrG89*, and *nkuA*Δ) was used for all gene deletions. Gene deletion strains (see below) are available from the IBT fungal collection as *A. nidulans* IBT 32029, (AN1242Δ::*AfpyrG*, *veA1*, *argB2*, *pyrG89*, and *nkuA*Δ) and *A. nidulans* IBT 32030, (AN11080Δ::*AfpyrG*, *veA1*, *argB2*, *pyrG89*, and *nkuA*Δ). For chemical analyses, *A. nidulans* IBT 28738 (*veA1*, *argB2*, *pyrG89*, and *nkuA-trS*::*AfpyrG*) was used as reference strain.

Metabolite Profiling Analysis. *A. nidulans* strains were inoculated on CYA agar, OTA, YES agar, and CYAS agar (42). All strains were three-point inoculated on these media and incubated at 32 °C in darkness for 4, 8, or 10 d, after which three to five plugs (6-mm diameter) along the diameter of the fungal colony were cut out and extracted (43).

Samples were subsequently analyzed by UHPLC-UV/vis diode array detector (DAD)-HRMS on a maXis G3 quadrupole time-of-flight mass spectrometer (Bruker Daltonics) equipped with an electrospray injection (ESI) source. The mass spectrometer was connected to an Ultimate 3000 UHPLC system (Dionex). Separation of 1-μL samples was performed at 40 °C on a 100-mm × 2.1-mm inner diameter (ID), 2.6-μm Kinetex C_{18} column (Phenomenex) using a linear water-acetonitrile gradient (both buffered with 20 mM formic acid) at a flow rate of 0.4 mL/min starting from 10% (vol/vol) acetonitrile and increased to 100% acetonitrile in 10 min, keeping this for 3 min. HRMS was performed in ESI^+ with a data acquisition range of 10 scans per second at *m/z* 100–1,000. The mass spectrometer was calibrated using sodium formate automatically infused before each analytical run, providing a mass accuracy better than 1.5 ppm. Compounds were detected as their $[M + H]^+$ ion ± 0.002 Da, often with their $[M + NH_4]^+$ and/or $[M + Na]^+$ ion used as a qualifier ion with the same narrow mass range. SMs with a peak areas >10,000 counts (random noise peaks of approximately 300 counts) were integrated and identified by comparison with approximately 900 authentic standards available from previous studies (31, 44) and dereplicated against the approximately 18,000 fungal metabolites listed in AntiBase 2010 by ultraviolet-visible (UV/Vis) spectra, retention time, adduct pattern, and high-resolution data (<1.5 ppm mass accuracy and isotope fit better than 40 using SigmaFit; Bruker Daltonics) (31, 45).

Array Design. Initial probe design was done using OligoWiz 2.0 software (46) from the coding sequences of predicted genes from the genome sequence of *A. nidulans* FGSC A4 (35), using version 5 of the *A. nidulans* gene annotation, downloaded from the *Aspergillus* Genome Database (32).

For each gene, a maximum of three nonoverlapping, perfect-match 60-mer probes was calculated using the OligoWiz standard scoring of cross-hybridization, melting temperature, folding, position preference, and low complexity. A position preference for the probes was included in the computations. Pruning of the probe sequences was done by removing duplicate probe sequences.

Also included on the chip were 1,407 standard controls designed by Agilent Technologies. Details of the array are available from the National Center for Biotechnology Information Gene Expression Omnibus (accession no. GPL15899).

Microarray Gene Expression Profiling. ***Mycelium harvest and RNA purification.*** Whole colonies from three-stab agar plates were sampled for transcriptional analysis by scraping the mycelium off the agar with a scalpel and transferring the agar directly into a 50-mL Falcon tube containing approximately 15 mL of liquid nitrogen. Care was taken to transfer a minimum of agar to the Falcon tube. The liquid nitrogen was allowed to evaporate before capping the lid and recooling the tube in liquid nitrogen before storing the tube at −80 °C until use for RNA purification.

For RNA purification, 40–50 mg of frozen mycelium was placed in a 2-mL microcentrifuge tube precooled in liquid nitrogen containing three steel balls (two balls with a diameter of 2 mm and one ball with a diameter of 5 mm). The tubes were then shaken in a Retsch Mixer Mill at 5 °C for 10 min until the mycelium was ground to a powder. Total RNA was isolated from the powder using the Qiagen RNeasy Mini Kit according to the protocol for isolation of total RNA from plant and fungi, including the optional use of the QiaShredder column. Quality of the purified RNA was verified using a NanoDrop ND-1000 spectrophotometer and an Agilent 2100 Bioanalyzer (Agilent Technologies).

Microarray hybridization. A total of 150 ng in 1.5-μL total RNA was labeled according to the One Color Labeling for Expression Analysis, Quick Amp Low Input (QALI) manual, version 6.5, from Agilent Technologies. Yield and specific activity were determined on the ND-1000 spectrophotometer and verified on a Qubit 2.0 fluorometer (Invitrogen). A total of 1.65 μg of labeled cRNA was fragmented at 60 °C on a heating block, and the cRNA was prepared for hybridization according to the QALI protocol. A 100-μL sample was loaded on a 4 × 44 Agilent Gasket Slide situated in a hybridization chamber (both from Agilent Technologies). The 4 × 44 array was placed on top of the Gasket Slide. The array was hybridized at 65 °C for 17 h in an Agilent Technologies hybridization oven. The array was washed following the QALI protocol and scanned in a G2505C Agilent Technologies Micro Array Scanner.

Analysis of transcriptome data. The raw array signal was processed by first removing the background noise using the normexp method, and signals between arrays were made comparable using the quantiles normalization method as implemented in the Limma package (47). Multiple probe signals per gene were summarized into a gene-level expression index using Tukey's medianpolish, as performed in the last step of the robust multiarray average (RMA) processing method (48). The data are available from the Gene Expression Omnibus database (accession no. GSE39993).

The generated data from the Agilent Technologies arrays were combined with legacy Affymetrix data (accession nos. GSE12859 and GSE7295) using the qspline normalization method (46) to combine the two normalized sets of data to one microarray catalog with expression indices in comparable ranges.

Calculation of the Gene CS. The CS is calculated for each individual gene along the chromosomes according to the following equation:

$$CS_{\pm 3} = \sum_{i=-3}^{3} \left(\frac{s_{0,i} + \|s_{0,i}\|}{2} \right)^2 + \sum_{i=1}^{3} \left(\frac{s_{0,i} + \|s_{0,i}\|}{2} \right)^2, \quad [1]$$

where $s_{0,i}$ is the Spearman coefficient for the expression indices of the gene in question and the gene located i genes away in a positive or negative direction relative to the chromosomal coordinate of the gene. The absolute term is added to set inverse correlations to 0. The CS assigned to a specific gene is the average of the CS for the liquid cultures and the CS for the solid cultures to adjust for background expression levels. Genes located less than four genes away from the ends of the supercontigs are assigned a CS of 0. All calculations were performed in the R software suite v. 2.14.0 (49), using the Bioconductor package (50, 51) for handling of array data. An adaptable R script for calculation of the CS is available on request.

Generation of Random Values for Evaluation of CS Significance. To estimate significance levels of the CS, a random set of scores was generated by selecting six genes at random as simulated neighbors for each of the 10,411 genes in the dataset. Examining this random distribution showed 95% of the population to have a CS <2.13 (Fig. S2). This value was used to have a false discovery rate of 0.05. All calculations were performed in R (49).

Identification of Gene Clusters. Gene clusters were defined around each NRPS, PKS, and DMATS by examination of the transcription profile of all surrounding genes with a CS ≥2.13 as well as three flanking genes in either direction. All genes with similar expression profiles were included in the cluster.

PCA-Based Analysis of Dataset Variation. PCA analysis was performed on the data of Dataset S2 using the prcomp-function of R (49). For stepwise reduction of the dataset, all principal components were calculated in each iteration and a sample was eliminated based on the one that had the largest contribution to the last principal component (i.e., with the smallest amount of unique information).

Generation of *A. nidulans* Gene Deletion Mutants. The genetic transformation experiments were performed with *A. nidulans* strain IBT 29539 [*veA1*, *argB2*, *pyrG89*, and *nkuA*Δ as described by Nielsen et al. (52)]. Fusion PCR-based bipartite gene targeting of substrates using the AF*pyrG* marker for selection and deletion of AN1242 was performed as described by Nielsen et al. (52), with the exception that all PCR assays were performed with the PfuX7 DNA polymerase (53). The deletion construct for AN11080 was assembled by uracil-specific excision reagent (USER) cloning. Specifically, sequences upstream and downstream of the gene to be deleted were amplified by PCR using primers containing a uracil residue (Table S2). The two PCR fragments were simultaneously inserted into the *Pac*I/Nt.*Bbv*CI USER cassette of pU20002A by USER cloning (54, 55). As a result, AF*pyrG* is now flanked by the two PCR fragments to complete the gene targeting substrate. The gene targeting substrate was released from the resulting vector pU20002A-AN11080 by digestion with *Swa*I. All restriction enzymes are from New England Biolabs. Primer sequences for deletion of the targeted genes and verification of strains are listed in Table S2. In addition, internal AF*pyrG* primers were used in combination with the check primers listed in Table S2 for confirmation of correct integration of DNA substrates (52). Transformants and AF*pyrG* pop-out recombinant strains were rigorously tested for correct insertions as well as for the presence of heterokaryons by touchdown spore-PCR analysis on conidia with an initial denaturation at 98 °C for 20 min.

MS/MS-Based Characterization of Compounds 1–4. Analysis was performed as stated above for the UHPLC-DAD-HRMS but in MS/MS mode, where analysis of the target mass and 6 *m/z* units up (to maintain isotopic pattern) was performed both via a targeted MS/MS list for the target compounds of interest and by the data-dependent MS/MS mode with an exclusion list, such that the same compound was selected several times. MS/MS fragmentation energy was varied from 18 to 55 eV.

Isolation and Structural Elucidation of Nidulanin A. Two hundred plates of minimal medium were inoculated with *A. nidulans*, from which SMs were extracted and nidulanin A was isolated in pure form. One-dimensional and 2D NMR spectra were recorded on a Bruker Daltonics Avance 800-MHz spectrometer with a 5-mm TCI Cryoprobe at the Danish Instrument Centre for NMR Spectroscopy of Biological Macromolecules at Carlsberg Laboratory. Stereoisometry of the amino acids was elucidated using Marfey's method (40). Details are provided in *SI Text*, Table S3, and Figs. S6–S8.

NRPS protein domains were predicted to identify adenylation domains and epimerase domains (56). Adenylation-domain specificities were predicted using NRPSpredictor (57). Details are provided in *SI Text*.

ACKNOWLEDGMENTS. We thank Peter Dmitrov, who treated the raw microarray data. We acknowledge Laurent Gautier for good scientific discussion of experimental design for microarray experiments, Marie-Louise Klejnstrup for assistance in retrieving MS data, and Dorte Koefoed Holm and Francesca Ambri for analysis of the austinol gene deletion mutants. We also thank the Danish Instrument Center for NMR Spectroscopy of Biological Macromolecules for NMR time. This work was supported by the Danish Research Agency for Technology and Production Grants 09-064967 and FI 2136-08-0023.

1. Newman DJ, Cragg GM (2012) Natural products as sources of new drugs over the 30 years from 1981 to 2010. *J Nat Prod* 75(3):311–335.
2. Liu T, Chiang YM, Somoza AD, Oakley BR, Wang CC (2011) Engineering of an "unnatural" natural product by swapping polyketide synthase domains in Aspergillus nidulans. *J Am Chem Soc* 133(34):13314–13316.
3. Khaldi N, et al. (2010) SMURF: Genomic mapping of fungal secondary metabolite clusters. *Fungal Genet Biol* 47(9):736–741.
4. Medema MH, et al. (2011) antiSMASH: Rapid identification, annotation and analysis of secondary metabolite biosynthesis gene clusters in bacterial and fungal genome sequences. *Nucleic Acids Res* 39(Web server issue):W339–W346.
5. Kelly DE, Krasevec N, Mullins J, Nelson DR (2009) The CYPome (Cytochrome P450 complement) of Aspergillus nidulans. *Fungal Genet Biol* 46(Suppl 1):S53–S61.
6. Palmer JM, Keller NP (2010) Secondary metabolism in fungi: Does chromosomal location matter? *Curr Opin Microbiol* 13(4):431–436.
7. Chiang YM, et al. (2010) Characterization of the Aspergillus nidulans monodictyphenone gene cluster. *Appl Environ Microbiol* 76(7):2067–2074.
8. Sanchez JF, et al. (2011) Genome-based deletion analysis reveals the prenyl xanthone biosynthesis pathway in Aspergillus nidulans. *J Am Chem Soc* 133(11):4010–4017.
9. Simpson TJ (2012) Genetic and biosynthetic studies of the fungal prenylated xanthone shamixanthone and related metabolites in Aspergillus spp. revisited. *ChemBioChem* 13(11):1680–1688.
10. Schätzle MA, Husain SM, Ferlaino S, Müller M (2012) Tautomers of anthrahydroquinones: Enzymatic reduction and implications for chrysophanol, monodictyphenone, and related xanthone biosyntheses. *J Am Chem Soc* 134(36):14742–14745.
11. Nielsen ML, et al. (2011) A genome-wide polyketide synthase deletion library uncovers novel genetic links to polyketides and meroterpenoids in Aspergillus nidulans. *FEMS Microbiol Lett* 321(2):157–166.
12. Sanchez JF, et al. (2010) Molecular genetic analysis of the orsellinic acid/F9775 gene cluster of Aspergillus nidulans. *Mol Biosyst* 6(3):587–593.
13. Bok JW, et al. (2009) Chromatin-level regulation of biosynthetic gene clusters. *Nat Chem Biol* 5(7):462–464.
14. Schroeckh V, et al. (2009) Intimate bacterial-fungal interaction triggers biosynthesis of archetypal polyketides in Aspergillus nidulans. *Proc Natl Acad Sci USA* 106(34):14558–14563.
15. Szewczyk E, et al. (2008) Identification and characterization of the asperthecin gene cluster of Aspergillus nidulans. *Appl Environ Microbiol* 74(24):7607–7612.
16. Chiang YM, et al. (2008) Molecular genetic mining of the Aspergillus secondary metabolome: Discovery of the emericellamide biosynthetic pathway. *Chem Biol* 15(6):527–532.
17. Brown DW, et al. (1996) Twenty-five coregulated transcripts define a sterigmatocystin gene cluster in Aspergillus nidulans. *Proc Natl Acad Sci USA* 93(4):1418–1422.
18. Kelkar HS, Keller NP, Adams TH (1996) Aspergillus nidulans stcP encodes an O-methyltransferase that is required for sterigmatocystin biosynthesis. *Appl Environ Microbiol* 62(11):4296–4298.
19. Keller NP, Watanabe CM, Kelkar HS, Adams TH, Townsend CA (2000) Requirement of monooxygenase-mediated steps for sterigmatocystin biosynthesis by Aspergillus nidulans. *Appl Environ Microbiol* 66(1):359–362.
20. Bergmann S, et al. (2007) Genomics-driven discovery of PKS-NRPS hybrid metabolites from Aspergillus nidulans. *Nat Chem Biol* 3(4):213–217.
21. Bouhired S, Weber M, Kempf-Sontag A, Keller NP, Hoffmeister D (2007) Accurate prediction of the Aspergillus nidulans terrequinone gene cluster boundaries using the transcriptional regulator LaeA. *Fungal Genet Biol* 44(11):1134–1145.
22. Schneider P, Weber M, Hoffmeister D (2008) The Aspergillus nidulans enzyme TdiB catalyzes prenyltransfer to the precursor of bioactive asterriquinones. *Fungal Genet Biol* 45(3):302–309.
23. Clutterbuck AJ (1969) A mutational analysis of conidial development in Aspergillus nidulans. *Genetics* 63(2):317–327.
24. Ahuja M, et al. (2012) Illuminating the diversity of aromatic polyketide synthases in Aspergillus nidulans. *J Am Chem Soc* 134(19):8212–8221.
25. Bromann K, et al. (2012) Identification and characterization of a novel diterpene gene cluster in Aspergillus nidulans. *PLoS ONE* 7(4):e35450.

26. Birse CE, Clutterbuck AJ (1990) N-acetyl-6-hydroxytryptophan oxidase, a developmentally controlled phenol oxidase from Aspergillus nidulans. *J Gen Microbiol* 136(9):1725–1730.
27. MacCabe AP, et al. (1991) Delta-(L-alpha-aminoadipyl)-L-cysteinyl-D-valine synthetase from Aspergillus nidulans. Molecular characterization of the acvA gene encoding the first enzyme of the penicillin biosynthetic pathway. *J Biol Chem* 266(19):12646–12654.
28. Martin JF (1992) Clusters of genes for the biosynthesis of antibiotics: regulatory genes and overproduction of pharmaceuticals. *J Ind Microbiol* 9(2):73–90.
29. Yeh HH, et al. (2012) Molecular genetic analysis reveals that a nonribosomal peptide synthetase-like (NRPS-like) gene in Aspergillus nidulans is responsible for microperfuranone biosynthesis. *Appl Microbiol Biotechnol* 96(3):739–748.
30. Lo H-C, et al. (2012) Two separate gene clusters encode the biosynthetic pathway for the meroterpenoids austinol and dehydroaustinol in Aspergillus nidulans. *J Am Chem Soc* 134(10):4709–4720.
31. Nielsen KF, Månsson M, Rank C, Frisvad JC, Larsen TO (2011) Dereplication of microbial natural products by LC-DAD-TOFMS. *J Nat Prod* 74(11):2338–2348.
32. Arnaud MB, et al. (2010) The Aspergillus Genome Database, a curated comparative genomics resource for gene, protein and sequence information for the Aspergillus research community. *Nucleic Acids Res* 38(Database issue):D420–D427.
33. Panagiotou G, et al. (2008) Systems analysis unfolds the relationship between the phosphoketolase pathway and growth in Aspergillus nidulans. *PLoS ONE* 3(12):e3847.
34. Panagiotou G, et al. (2009) Studies of the production of fungal polyketides in Aspergillus nidulans by using systems biology tools. *Appl Environ Microbiol* 75(7): 2212–2220.
35. Galagan JE, et al. (2005) Sequencing of Aspergillus nidulans and comparative analysis with A. fumigatus and A. oryzae. *Nature* 438(7071):1105–1115.
36. Brakhage AA, et al. (2008) Activation of fungal silent gene clusters: A new avenue to drug discovery. *Prog Drug Res* 66(1):3–12.
37. Bok JW, et al. (2006) Genomic mining for Aspergillus natural products. *Chem Biol* 13 (1):31–37.
38. Cullen D (2007) The genome of an industrial workhorse. *Nat Biotechnol* 25(2): 189–190.
39. Bergmann S, et al. (2010) Activation of a silent fungal polyketide biosynthesis pathway through regulatory cross talk with a cryptic nonribosomal peptide synthetase gene cluster. *Appl Environ Microbiol* 76(24):8143–8149.
40. Marfey P (1984) Determination of D- amino acids. II. Use of a bifunctional reagent, 1,5-di-fluoro-2,4-dinitrobenzene. *Carlsberg Res Commun* 49(6):591–596.
41. Nützmann HW, et al. (2011) Bacteria-induced natural product formation in the fungus Aspergillus nidulans requires Saga/Ada-mediated histone acetylation. *Proc Natl Acad Sci USA* 108(34):14282–14287.
42. Frisvad JC, Samson R (2004) Polyphasic taxonomy of Penicillium subgenus Penicillium. A guide to identification of the food and air-borne terverticillate Penicillia and their mycotoxins. *Stud Mycol* 49:1–173.
43. Smedsgaard J (1997) Micro-scale extraction procedure for standardized screening of fungal metabolite production in cultures. *J Chromatogr A* 760(2):264–270.
44. Nielsen KF, Smedsgaard J (2003) Fungal metabolite screening: Database of 474 mycotoxins and fungal metabolites for dereplication by standardised liquid chromatography-UV-mass spectrometry methodology. *J Chromatogr A* 1002(1-2): 111–136.
45. Månsson M, et al. (2010) Explorative solid-phase extraction (E-SPE) for accelerated microbial natural product discovery, dereplication, and purification. *J Nat Prod* 73(6): 1126–1132.
46. Workman C, et al. (2002) A new non-linear normalization method for reducing variability in DNA microarray experiments. *Genome Biol* 3(9):research0048.
47. Smyth GK (2005) *Limma: Linear models for microarray data* (Springer, New York), pp 397–420.
48. Irizarry RA, et al. (2003) Summaries of Affymetrix GeneChip probe level data. *Nucleic Acids Res* 31(4):e15.
49. R Development Core Team (2007) *R: A Language and Environment for Statistical Computing* (R Foundation for Statistical Computing, Vienna, Austria), Available at www.R-project.org.
50. Gentleman RC, et al. (2004) Bioconductor: Open software development for computational biology and bioinformatics. *Genome Biol* 5(10):R80.
51. Nielsen ML, Albertsen L, Lettier G, Nielsen JB, Mortensen UH (2006) Efficient PCR-based gene targeting with a recyclable marker for Aspergillus nidulans. *Fungal Genet Biol* 43(1):54–64.
52. Nielsen JB, Nielsen ML, Mortensen UH (2008) Transient disruption of non-homologous end-joining facilitates targeted genome manipulations in the filamentous fungus Aspergillus nidulans. *Fungal Genet Biol* 45(3):165–170.
53. Nørholm MH (2010) A mutant Pfu DNA polymerase designed for advanced uracil-excision DNA engineering. *BMC Biotechnol* 10:21.
54. Hansen BG, et al. (2011) Versatile enzyme expression and characterization system for Aspergillus nidulans, with the Penicillium brevicompactum polyketide synthase gene from the mycophenolic acid gene cluster as a test case. *Appl Environ Microbiol* 77(9): 3044–3051.
55. Eisendle M, Oberegger H, Zadra I, Haas H (2003) The siderophore system is essential for viability of Aspergillus nidulans: Functional analysis of two genes encoding l-ornithine N 5-monooxygenase (sidA) and a non-ribosomal peptide synthetase (sidC). *Mol Microbiol* 49(2):359–375.
56. Bachmann BO, Ravel J (2009) Chapter 8. Methods for in silico prediction of microbial polyketide and nonribosomal peptide biosynthetic pathways from DNA sequence data. *Methods Enzymol* 458:181–217.
57. Rausch C, Weber T, Kohlbacher O, Wohlleben W, Huson DH (2005) Specificity prediction of adenylation domains in nonribosomal peptide synthetases (NRPS) using transductive support vector machines (TSVMs). *Nucleic Acids Res* 33(18):5799–5808.

Supporting Information

Andersen et al. 10.1073/pnas.1205532110

SI Materials and Methods

Fungal Growth, Extraction, and Isolation of Nidulanin A. *Aspergillus nidulans* (IBT 22600) was inoculated as three-point stabs on 200 plates of MM and incubated in the dark at 30 °C for 7 d. The fungi were harvested and extracted twice overnight with EtOAc. The extract was filtered and concentrated in vacuo. The combined extract was dissolved in 100 mL of MeOH and H_2O (9:1), and 100 mL of heptane was added after the phases were separated. Eighty milliliters of H_2O was added to the MeOH/H_2O phase, and metabolites were then extracted with 5 × 100 mL of dichloromethane (DCM). The phases were then concentrated separately in vacuo. The DCM phase (0.2021 g) was absorbed onto diol column material and dried before packing into a 10-g SNAP column [coefficient of variation (CV) = 15 mL; Biotage] with diol material. The extract was then fractionated on an Isolera flash purification system (Biotage) using seven steps of heptane-DCM-EtOAc-MeOH. A flow rate of 20 mL·min^{-1} was used, and fractions were automatically collected with 2 × 2 CVs for each step. Solvents used were of HPLC grade, and H_2O was milliQ-water (purified and deionized using a Millipore system through a 0.22-μm membrane filter). Two of the Isolera fractions were subjected to further purification on separate runs on semipreparative HPLC (Waters 600 Controller with a 996-photodiode array detector). This was achieved using a Luna II C_{18} column (250 mm × 10 mm, 5 μm; Phenomenex). A linear water-MeCN gradient was used starting with 15% MeCN and increasing to 100% over 20 min using a flow rate of 4 mL·min^{-1}. MeCN was of HPLC grade, and H_2O was milliQ-water (purified and deionized using the Millipore system through a 0.22-μm membrane filter); both were added to 50 ppm of TFA. The fractions obtained from the separate runs were pooled, and a final purification using the same method yielded 1.5 mg of nidulanin A.

Marfey's Method. Stereoisometry of the amino acids was elucidated using Marfey's method (1). One hundred micrograms of the peptide was hydrolyzed with 200 μL of 6 M HCl at 110 °C for 20 h. To the hydrolysis product (or 2.5 μmol of standard D- and L-amino acids) was added 50 μL of water, 20 μL of 1 M $NaHCO_3$ solution, and 100 μL of 1% 1-fluoro-2-4-dinitrophenyl-5-L-alanine amide (FDAA) in acetone, followed by reaction at 40 °C for 1 h. The reaction mixture was removed from the heat and neutralized with 10 μL of 2 M HCl, and the solution was diluted with 820 μL of MeOH to a total volume of 1 mL. The retention times of the FDAA derivatives were compared with retention times of the standard amino acid derivatives.

Analysis. Analysis was performed using ultra-high-performance liquid chromatography (UPHLC) UV/Vis diode array detector (DAD) high-resolution MS (HRMS) on a maXis G3 orthogonal acceleration (OA) quadrupole–quadrupole time of flight (QQ-TOF) mass spectrometer (Bruker Daltonics) equipped with an electrospray injection (ESI) source and connected to an Ultimate 3000 UHPLC system (Dionex). The column used was a reverse-phase Kinetex 2.6-μm C_{18}, 100 mm × 2.1 mm (Phenomenex), and the column temperature was maintained at 40 °C. A linear water-acetonitrile gradient was used (both solvents were buffered with 20 mM formic acid) starting from 10% (vol/vol) MeCN and increased to 100% in 10 min, maintaining this rate for 3 min before returning to the starting conditions in 0.1 min and staying there for 2.4 min before the following run. A flow rate of 0.4 mL·min^{-1} was used. HRMS was performed in ESI$^+$ with a data acquisition range of 10 scans per second at *m/z* 100–1,000. The mass spectrometer was calibrated using bruker daltonics high precision calibration (HPC) by means of the use of the internal standard sodium formate, which was automatically infused before each run. UV spectra were collected at wavelengths from 200 to 700 nm. Data processing was performed using DataAnalysis software (Bruker Daltonics). HRMS analysis of nidulanin A was measured to 604.3497 Da corresponding to a molecular formula of $C_{34}H_{45}N_5O_5$ (deviation of −0.6 ppm).

NMR. The 1D and 2D spectra were recorded on a Bruker Daltonics Avance 800-MHz spectrometer equipped with a 5-mm TCI Cryoprobe at the Danish Instrument Centre for NMR Spectroscopy of Biological Macromolecules at Carlsberg Laboratory. Spectra were acquired using standard pulse sequences, and a 1H spectrum, as well as COSY, NOESY, heteronuclear single quantum coherence (HSQC), and heteronuclear multiple bond correlation (HMBC) spectra, were acquired. The deuterated solvent was acetonitrile-d_3, and signals were referenced by solvent signals for acetonitrile-d_3 at δ_H = 1.94 ppm and δ_C = 1.32/118.26 ppm. The NMR data were processed using Topspin 3.1 (Bruker Daltonics). Chemical shifts are reported in parts per million (δ), and scalar couplings are reported in hertz. The sizes of the *J* coupling constants reported in the tables are the experimentally measured values from the spectra. There are minor variations in the measurements, which may be explained by the uncertainty of *J*. NMR data for nidulanin A are presented in Table S3, and the structure is shown in Fig. S6.

Protein Domain Predictions. Nonribosomal peptide synthase (NRPS) protein domains were predicted using the analysis tool of Bachmann and Ravel (2) with the standard settings. Only domains with significant *P* values ($P < 0.05$) were included in the analysis. Adenylation domain specificities were predicted using NRPSpredictor (3).

Structural Elucidation. The 1H NMR spectrum of nidulanin A displayed four resonances at δ_H 8.16, 7.91, 7.64, and 7.51 ppm, which were identified as amide protons indicative of a nonribosomal peptide type of compound. For each resonance, a COSY correlation to a proton further up-field in the α-proton area could be observed. This coupled each of the amide protons to Hα protons at resonances of δ_H 4.82, 3.92, 4.56, and 3.85 ppm, respectively. Investigation of the NOESY connectivities allowed for assembling of the peptide backbone, which revealed a cyclical tetrapeptide as illustrated in Fig. S7.

The two protons at δ_H 7.64 and 4.56 ppm were part of a larger spin system with correlations to a couple of diastereotopic protons at δ_H 3.02 [1H, doublet of doublets (dd), 14.4, 8.0] and 2.82 (1H, dd, 14.3, 7.5) ppm, as well as five aromatic protons at δ_H 7.14 [1H, multiplet (m)], 7.21 (2H, m), and 7.22 (2H, m). HMBC correlations from the diastereotopic pair as well as the aromatic protons revealed a quaternary carbon with a carbon chemical shift of 137.5 ppm. This information, put together, led to the amino acid phenylalanine. The protons at δ_H 7.91 and 3.92 ppm, as well as the protons at δ_H 7.51 and 3.85 ppm, had very similar spin systems. In both spin systems, a single proton appeared (δ_H 1.93 and 1.96, both multiplets), as well as two methyl groups as doublets (δ_H 0.71/0.78 ppm and 0.84/0.79 ppm). In both cases, the amino acid could be established as valine. Elucidation of the final part of the structure showed that this was not one of the standard proteinogenic amino acids. For this final part, three different spin systems, as well as two

isolated methyl groups, were present, which could be linked together by HMBC correlations as well as NOESY connectivities. The first spin system consisted of the amide proton at δ_H 8.16 ppm, the H_α proton at 4.82 ppm, and a diastereotopic pair of protons at δ_H 3.63 (1H, dd, 17.7, 9.7) and 3.09 (1H, dd, 17.6, 4.9) ppm. The second spin system consisted of four aromatic protons at δ_H 7.79 (1H, dd, 8.2, 1.5), 7.28 [1H, doublet of doublets of doublets (ddd), 8.6, 7.0, 1.5], 6.81 (1H, dd, 8.7, 0.7), and 6.57 (1H, ddd, 8.6, 7.0, 1.1) ppm, whereas the third and final spin system contained three protons located in the double-bond area at δ_H 5.95 (1H, dd, 17.6, 10.7), 5.13 (1H, dd, 10.7, 1.0), and 5.15 (1H, dd, 17.6, 1.0) ppm. The latter was shown to be connected to the two methyl groups at δ_H 1.39 [3H, singlet (s)] and 1.38 (3H, s) ppm, and the presence of a quaternary carbon at δ_C 53.7 ppm linked this part as an isoprene unit. The entire residue and key HMBC correlations for the structural elucidation of this part are shown in Fig. S8. The residue contains the amino acid L-kynurenine, which is an intermediate in the tryptophan degradation pathway. In this structure, L-kynurenine has been further modified, because the aforementioned isoprene unit has been incorporated onto the amine located at the aromatic ring.

To establish the stereochemistry of nidulanin A, Marfey's analysis (1) was performed. This technique enables one to determine the absolute configuration of amino acids in peptides (1). The analysis showed the phenylalanine residue present was L-phenylalanine, whereas the analysis for valine showed equal amounts of L- and D-valine.

We used bioinformatics prediction algorithms to identify the stereochemistry of the added amino acids further. Both NRPS protein domain predictions and adenylation domain specificity predictors identify four adenylation domains, corresponding to the four amino acids of the cyclopeptide. By comparison of predictions and the known sequence, the specificity and sequence of the adenylation domains were assigned as predicted to Phe-Kyn-Val-Val. The last two adenylation domains give similar predictions, further supporting both to be specific for valine.

The structure with the proposed absolute chemistry is given in Fig. 4. The absolute configuration of the kynurenine, as well as the order of the L- and D-valine, which is based solely on the bioinformatic studies, has not been verified chemically.

1. Marfey P (1984) Determination of D-amino acids. II. Use of a bifunctional reagent,1,5-difluoro-2,4-dinitrobenzene. *Carlsberg Res Commun* 49:591.
2. Bachmann BO, Ravel J (2009) Chapter 8. Methods for in silico prediction of microbial polyketide and nonribosomal peptide biosynthetic pathways from DNA sequence data. *Methods Enzymol* 458:181–217.
3. Rausch C, Weber T, Kohlbacher O, Wohlleben W, Huson DH (2005) Specificity prediction of adenylation domains in nonribosomal peptide synthetases (NRPS) using transductive support vector machines (TSVMs). *Nucleic Acids Res* 33(18): 5799–5808.

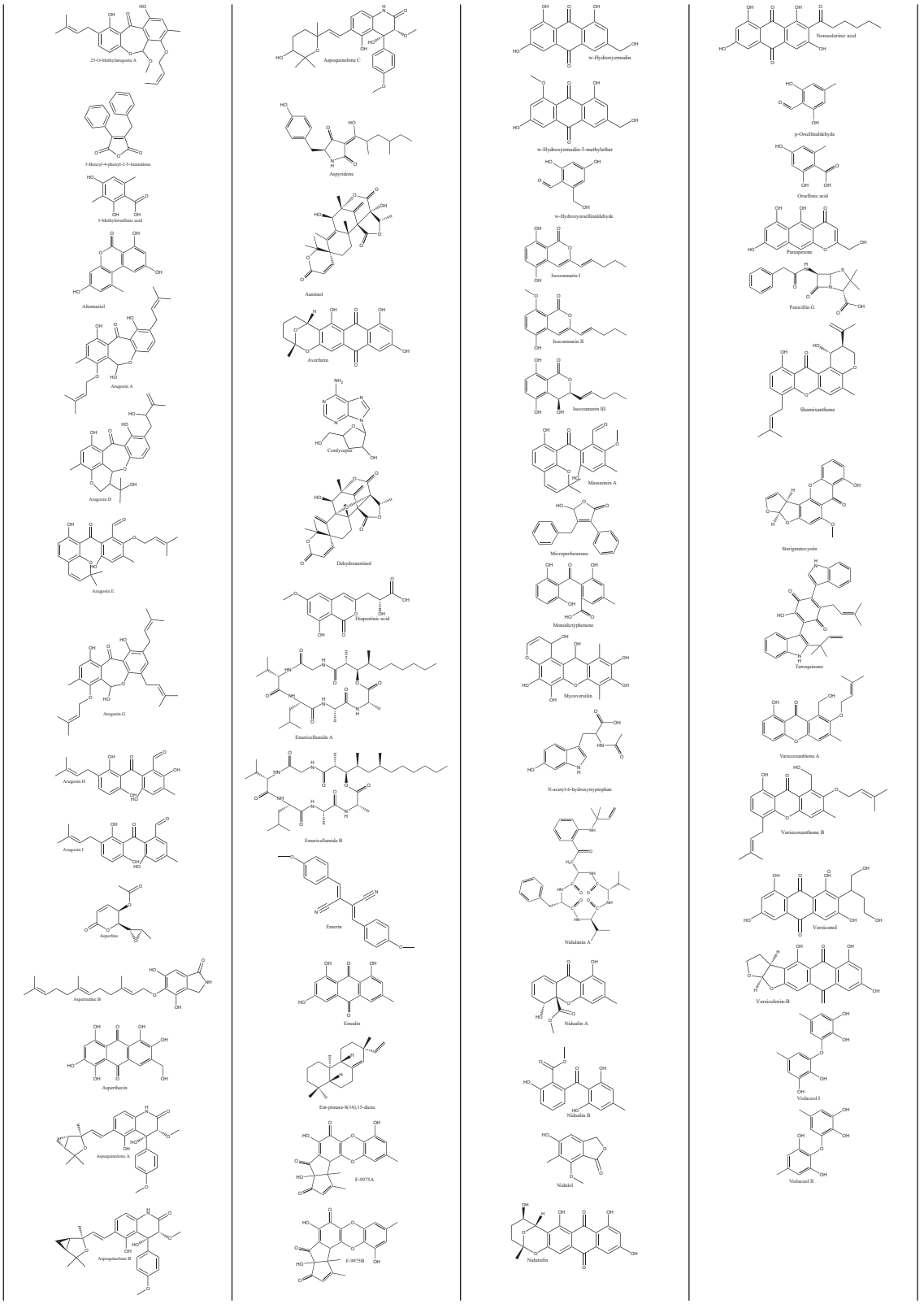

Fig. S1. Chemical structures of secondary metabolites. Structures are shown in alphabetical order in columns from left to right.

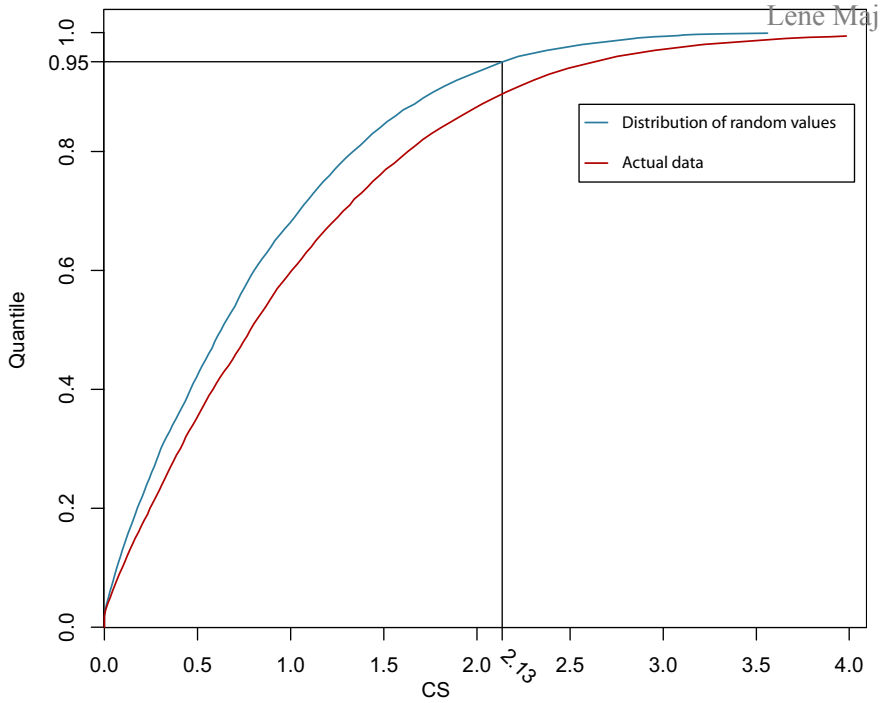

Fig. S2. Quantile plot of clustering scores (CSs). The gray line plots the quantile for a given value of the CS based on a random combination of genes (*Materials and Methods*). Ninety-five percent of the values attained are 2.13 or below (as shown). The red line is a plot of the quantiles of actual values for the genes, as can be found in Dataset S2.

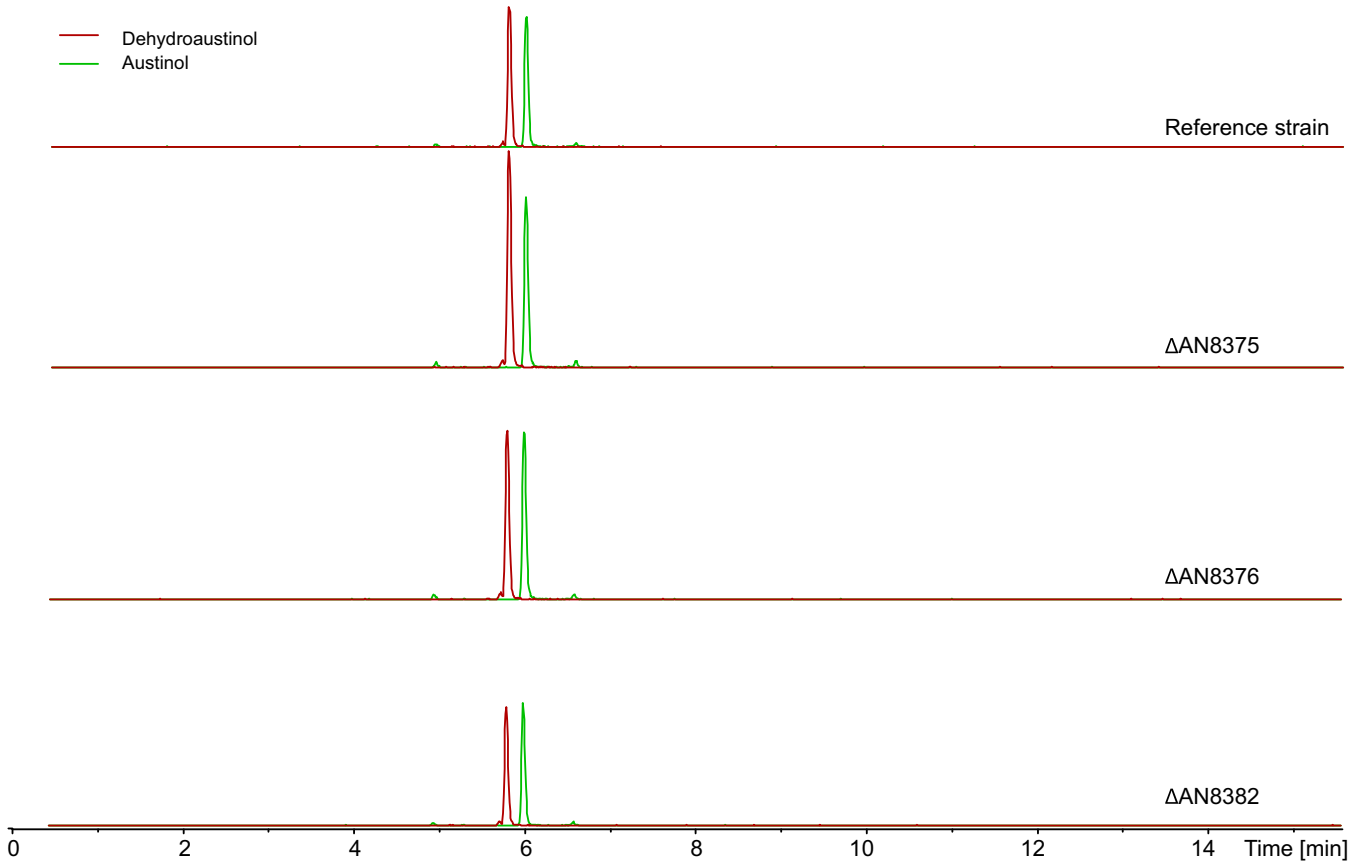

Fig. S3. Extracted ion chromatograms (EICs) for austinol and dehydroaustinol (mass tolerance ± 0.005 Da) from UHPLC-DAD-HRMS of chemical extractions from the reference strain and the ΔAN8375, ΔAN8376 and ΔAN8382 strains. DAD, diode array detector.

Fig. S4. Overview of the gene expression profiles for all predicted members of the biosynthetic gene clusters (Tables 1–3 and Dataset S2). The *y* axis indicates the gene expression index on a $\log_2$ scale, and the *x* axis represents the 44 experimental conditions included in the microarray compendium. The biosynthetic clusters are sorted into the Superclusters indicated in Fig. 3.

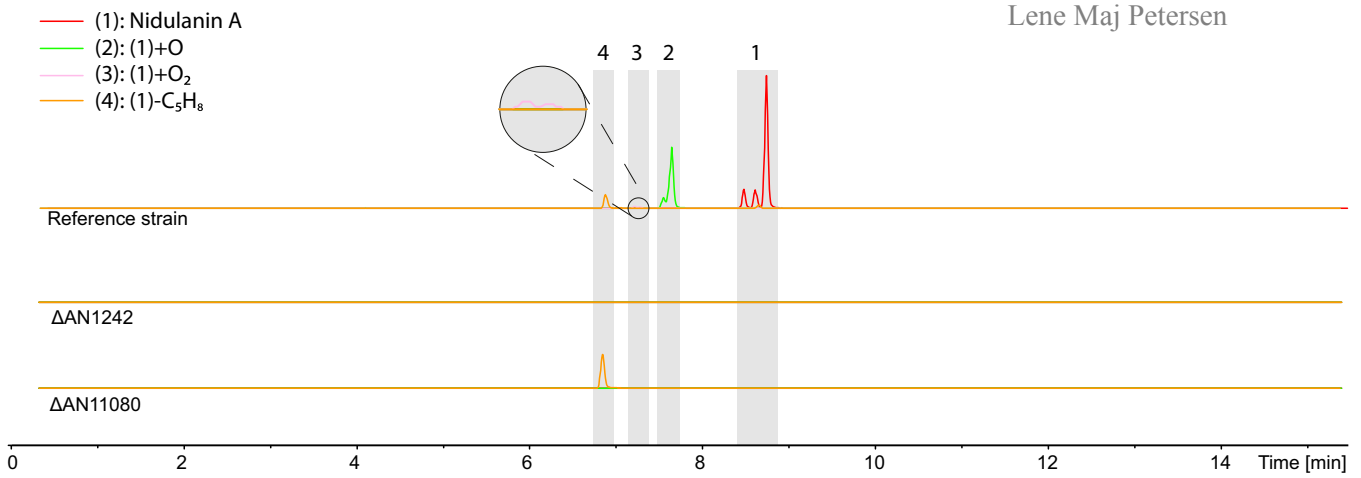

Fig. S5. Extracted ion chromatograms (EICs) for compounds 1–4. Mass tolerance ± 0.005 Da from UHPLC-DAD-HRMS of chemical extractions from the reference strain and ΔAN1242 and ΔAN11080 strains. DAD, diode array detector.

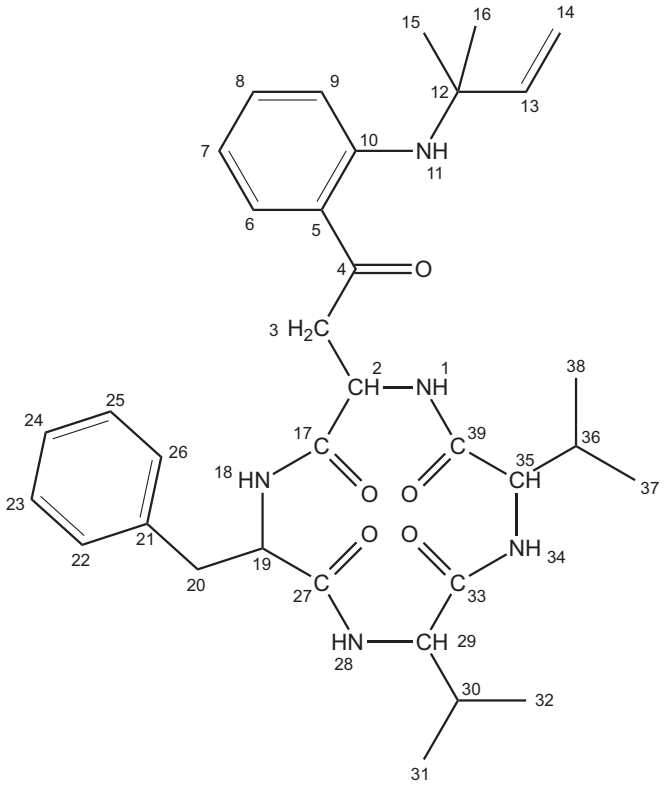

Fig. S6. Structure of nidulanin A, including numbering of individual atoms.

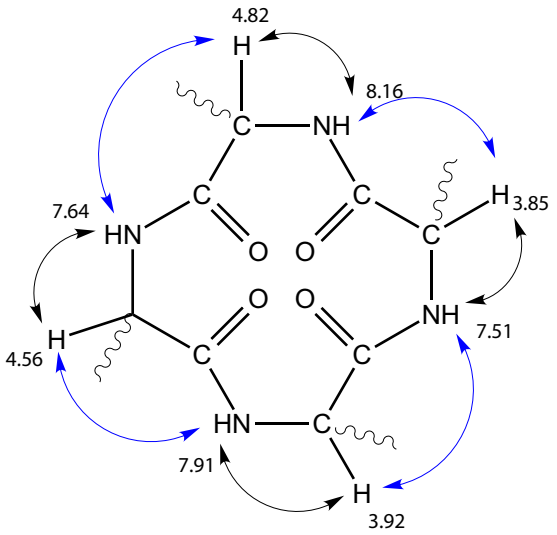

Fig. S7. COSY (black) and NOESY (blue) connectivities lead to the cyclical tetrapeptide.

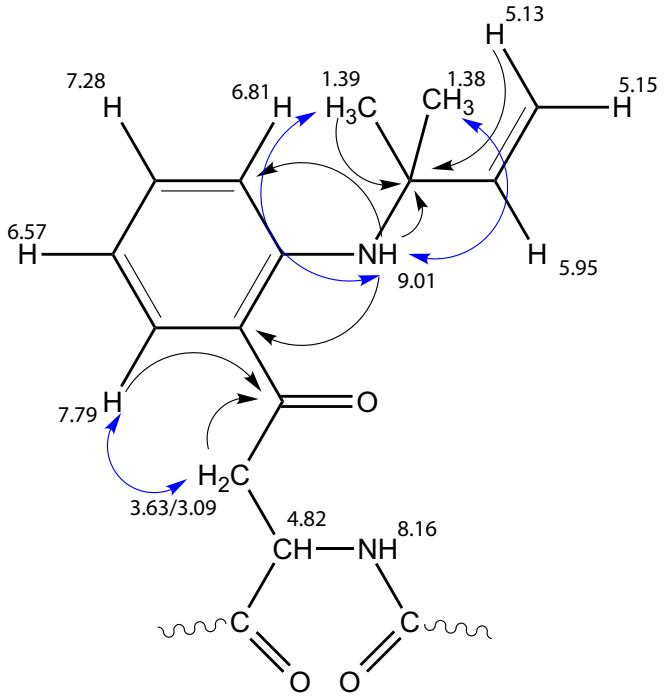

Fig. S8. Key HMBC (black) correlations and NOESY (blue) connectivities link the different spin systems.

Table S1. List of predicted biosynthetic genes where low expression indices with low variation across the 44 conditions were found

GeneID	Type	Gene name	Compound (if known)	Gene no.	Known	Refs.
AN0523	PKS				4	(1)
AN1034	PKS	*afoE*	Asperfuranone	5	7	(2, 3)
AN1036	PKS	*afoG*	Asperfuranone	5	7	(2, 3)
AN10430	PKS					
AN3273	PKS					
AN3386	PKS					
AN3612	PKS					
AN5475	PKS					
AN6961	NRPS					
AN9243	NRPS					
AN9244	NRPS					
AN6810	DTS					

These genes are assumed to be silent in all 44 conditions. DTS, diterpene synthase; NRPS, nonribosomal peptide synthase; PKS, polyketide synthase.

1. Bromann K, et al. (2012) Identification and characterization of a novel diterpene gene cluster in Aspergillus nidulans. *PLoS ONE* 7(4):e35450.
2. Chiang YM, et al. (2008) Molecular genetic mining of the Aspergillus secondary metabolome: Discovery of the emericellamide biosynthetic pathway. *Chem Biol* 15(6):527–532.
3. Bergmann S, et al. (2010) Activation of a silent fungal polyketide biosynthesis pathway through regulatory cross talk with a cryptic nonribosomal peptide synthetase gene cluster. *Appl Environ Microbiol* 76(24):8143–8149.

Table S2. Primer sequences

Primer name	Sequence
AN1242-DL-Up-F	GAGATCGTCGATGGAGTGGCG
AN1242-DL-Up-Rad	gatccccgggaattgccatgCTGCGAGGCACATCATGTTGCC
AN1242-DL-Dw-Fad	aattccagctgaccaccatgGGGTCTGGGTACGCGGGTTTG
AN1242-DL-Dw-R	GATGTGTAGGCGCGACATGGG
AN1242-CHK-Up-F	CCGTCATCATCGTTATAGCC
AN1242-CHK-Dw-R	GCACCCGCTATCACATAC
AN1242-GAPCHK-F	GGCATTATGTGAGCTGTCGTG
AN1242-GAPCHK-R	GATGGAGGGCTTGGTCTTGG
AN1242-INTCHK-R	GATCGAGACGGGTCGTTTAGG
AN11080-DL-Up-FU	GGGTTTAAUGGCAGGTACCAATAATGA
AN11080-DL-Up-RU	GGACTTAAUAGATATACGAGTATGCGG
AN11080-DL-Dw-FU	GGCATTAAUAGTGCCTGATAACTCTGC
AN11080-DL-Dw-RU	GGTCTTAAUGTTGAATCCCTCTGCCTT
AN11080-CHK-Up-F	GGACGGCCCATATTCAGA
AN11080-CHK-Dw-R	AATAAGCTGTAGCGGCGA

Table S3. NMR data for nidulanin A in acetonitrile-d_3

Atom assignment	1H-chemical shift, ppm/J coupling constants, Hz	^{13}C-chemical shift, ppm	HMBC correlations	NOE connectivities
1	8.16 (1H, d, 9.2)	—	—	2, 3, 3′, 35
2	4.82 (1H, ddd, 8.6, 7.0, 1.5)	48.2	—	1, 3, 3′, 18
3	3.63 (1H, dd, 17.7, 9.7)	50.0	2, 4, 17	1, 2, 3′, 6
3′	3.09 (1H, dd, 17.6, 4.9)	50.0	4	1, 2, 3, 6
4	—	198.9	—	—
5	—	116.6	—	—
6	7.79 (1H, dd, 8.2, 1.5)	131.8	4, 8, 10	3, 3′, 7
7	6.57 (1H, ddd, 8.6, 7.0, 1.1)	114.3	5, 9	6
8	7.28 (1H, ddd, 8.6, 7.0, 1.5)	134.0	6, 10	—
9	6.81 (1H, dd, 8.7, 0.7)	114.9	5, 7	15, 16
10	—	148.7	—	—
11	9.01 (1H, s)	—	5, 9, 12	15, 16
12	—	53.7	—	—
13	5.95 (1H, dd, 17.6, 10.7)	145.0	—	14, 14′
14	5.13 (1H, dd, 10.7, 1.0)	113.3	12	13
14′	5.15 (1H, dd, 17.6, 1.0)	113.3	12, 13	13
15	1.39 (3H, s)	27.8	12, 13, 16	9, 11
16	1.38 (3H, s)	27.5	12, 13, 15	9, 11
17	—	172.1	—	—
18	7.64 (1H, d, 8.4)	—	—	2, 19, 20, 20′
19	4.56 (1H, q, 8.0)	53.7	—	18, 28, 20, 20′
20	3.02 (1H, dd, 14.4, 8.0)	*	19, 21, 22/26	18, 19, 20′
20′	2.82 (1H, dd, 14.3, 7.5)	*	19, 21, 22/26, 27	18, 19, 20
21	—	137.5	—	—
22	7.22 (1H, m)	128.0	23/25	—
23	7.21 (1H, m)	127.7	21	—
24	7.14 (1H, m)	126.4	—	—
25	7.21 (1H, m)	127.7	21	—
26	7.22 (1H, m)	128.0	23/25	—
27	—	172.7	—	—
28	7.91 (1H, d, 9.2)	—	—	19, 29, 30, 31
29	3.92 (1H, d, 9.5)	59.1	27, 33	28, 30, 31, 32, 34
30	1.93 (1H, m)	26.3	—	28, 29, 31, 32
31	0.71 (3H, d, 6.6)	18.1	29, 30, 32	28, 29, 30
32	0.78 (3H, d, 6.6)	18.9	29, 30, 31	29, 30
33	—	172.2	172.6	—
34	7.51 (1H, d, 9.6)	—	—	29, 36
35	3.85 (1H, dd, 9.8, 10.7)	59.4	33, 39	1, 36, 37, 38
36	1.96 (1H, m)	26.9	—	34, 35, 37, 38
37	0.84 (3H, d, 6.7)	18.1	35, 36, 38	35, 36
38	0.79 (3H, d, 6.6)	18.9	35, 36, 37	35, 36
39	—	172.1	—	—

1H NMR spectrum and 2D spectra were recorded at with a Bruker Daltonics Avance 800 MHz spectrometer at Carlsberg Laboratory. Signals were referenced to the solvent signals for acetonitrile-d_3 at δ_H = 1.94 ppm and δ_C = 1.32/118.26 ppm. There are minor variations in the measurements which may be explained by the uncertainty of *J*. d, doublet; dd, doublet of doublet; ddd, doublet of doublets of doublets; m, multiplet; q, quartet; s, singlet.
*Cannot be unambiguously assigned.

Dataset S1. Overview of UHPLC-DAD-HRMS analysis of chemical extractions from the reference strain on three solid media after 4, 8, or 10 d (4d, 8d, and 10d, respectively)

Dataset S1

Values given are extracted ion chromatogram peak areas. DAD, diode array detector.

Dataset S2. Gene expression indices from 44 experimental conditions sorted according to chromosomal coordinates

Dataset S2

Locus names and annotation from the *Aspergillus* Genome Database (www.ASPGD.org) are given where available. Clustering scores and cluster members are given.

Paper 9

"Molecular and chemical characterization of the biosynthesis of the 6-MSA derived meroterpenoid yanuthone D in *Aspergillus niger*"

Holm, D.K.; **Petersen L.M. (Joint 1st author)**; Klitgaard, A.; Knudsen, P.B.; Jarczynska, Z.D.; Nielsen, K.F.; Gotfredsen, C.H.; Larsen, T.O.; Mortensen, U.H.

Chemistry & Biology, **2014**, *21*, 519-529.

Chemistry & Biology
Article

CellPress

Molecular and Chemical Characterization of the Biosynthesis of the 6-MSA-Derived Meroterpenoid Yanuthone D in *Aspergillus niger*

Dorte K. Holm,[1,6] Lene M. Petersen,[2,6] Andreas Klitgaard,[3] Peter B. Knudsen,[5] Zofia D. Jarczynska,[1] Kristian F. Nielsen,[3] Charlotte H. Gotfredsen,[4] Thomas O. Larsen,[2,*] and Uffe H. Mortensen[1,*]
[1]Eukaryotic Molecular Cell Biology Group, Department of Systems Biology, Center for Microbial Biotechnology, Soltofts Plads, Building 223, Technical University of Denmark, 2800 Kongens Lyngby, Denmark
[2]Chemodiversity Group, Department of Systems Biology, Center for Microbial Biotechnology, Soltofts Plads, Building 221, Technical University of Denmark, 2800 Kongens Lyngby, Denmark
[3]Metabolic Signaling and Regulation Group, Department of Systems Biology, Center for Microbial Biotechnology, Soltofts Plads, Building 221, Technical University of Denmark, 2800 Kongens Lyngby, Denmark
[4]Department of Chemistry, Kemitorvet, Building 201, Technical University of Denmark, 2800 Kongens Lyngby, Denmark
[5]Fungal Physiology and Biotechnology Group, Department of Systems Biology, Center for Microbial Biotechnology, Soltofts Plads, Building 223, Technical University of Denmark, 2800 Kongens Lyngby, Denmark
[6]These authors contributed equally to this work
*Correspondence: tol@bio.dtu.dk (T.O.L.), um@bio.dtu.dk (U.H.M.)
http://dx.doi.org/10.1016/j.chembiol.2014.01.013

SUMMARY

Secondary metabolites in filamentous fungi constitute a rich source of bioactive molecules. We have deduced the genetic and biosynthetic pathway of the antibiotic yanuthone D from *Aspergillus niger*. Our analyses show that yanuthone D is a meroterpenoid derived from the polyketide 6-methylsalicylic acid (6-MSA). Yanuthone D formation depends on a cluster composed of ten genes including *yanA* and *yanI*, which encode a 6-MSA polyketide synthase and a previously undescribed O-mevalon transferase, respectively. In addition, several branching points in the pathway were discovered, revealing five yanuthones (F, G, H, I, and J). Furthermore, we have identified another compound (yanuthone X_1) that defines a class of yanuthones that depend on several enzymatic activities encoded by genes in the *yan* cluster but that are not derived from 6-MSA.

INTRODUCTION

Fungal polyketides (PKs) comprise a large and complex group of metabolites with a wide range of bioactivities. Hence, the group includes compounds that are used by fungi as pigments for UV-light protection, in intra- and interspecies signaling, and in chemical warfare against competitors (Williams et al., 1989). Many PKs are mycotoxins that are harmful to human health, e.g., patulin and the highly carcinogenic aflatoxins (Olsen et al., 1988). On the other hand, several PKs have a great medical potential, e.g., cholesterol-lowering statins (Endo et al., 1976), the antimicrobial and immunosuppressive mycophenolic acid (Bentley, 2000), the acetyl-coenzyme A acetyltransferase-inhibiting pyripyropenes (Frisvad et al., 2009), and the farnesyltransferase inhibiting andrastins (Rho et al., 1998). Although more than 6,000 different PKs have been isolated and characterized (AntiBase 2012), these compounds are likely only the tip of the iceberg. For example, for each fungus analyzed, only a small part of its full repertoire of PKs genes appears to be produced under laboratory conditions (Pel et al., 2007; Andersen et al., 2013). In agreement with this view, genome sequencing of several fungal species have uncovered far more genes for PKs production than can be accounted for by the number of compounds that they are actually known to produce. Hence, the chemical space of PKs is far from fully known, and many new drugs and mycotoxins await discovery.

The fungal genome sequencing projects have demonstrated that genes necessary for production of individual PKs often cluster around the gene encoding the polyketide synthase (PKS), which delivers the first intermediate in a given PK pathway. Although this is helpful for pathway elucidation, compounds produced by orphan gene clusters (Gross, 2007) can still not be easily predicted by bioinformatic tools (for review, see Cox, 2007 and Hertweck, 2009). This is because most fungal PKs are produced by type I iterative PKSs whose products are notoriously difficult to predict. Moreover, the specificities and the order of actions of the tailoring enzymes that modify the PK released from the PKS further complicate prediction of the end products. To elucidate the biochemical pathway of an orphan gene cluster, it is therefore necessary to create gene cluster mutations and/or to genetically reconstitute the pathway in a heterologous host. Subsequent analytical and structural chemistry analyses of the compounds that are present in the reference strain but not in the mutant strains and of compounds that accumulate in the mutant strains but are absent or present in minute amounts in the reference strain may deliver insights that can be used for pathway elucidation.

Aspergillus niger is an industrially important filamentous fungus, which has obtained GRAS status for use in several industrial processes and is used for production of organic acids and enzymes. Importantly, when the full genome sequence of *A. niger* was examined, a gene cluster resembling the fumonisin gene

A

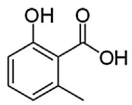

6-MSA

B

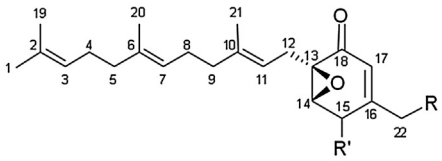

Compound	R	R'
Yanuthone A	OAc	⁻OH, ····H
Yanuthone B	OAc	=O
Yanuthone C	OH	⁻OAc , ····H
Yanuthone D (1)	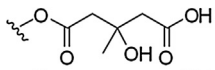	=O
Yanuthone E (2)	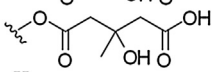	⁻OH, ····H
7-deacetoxyyanuthone A (3)	H	⁻OH, ····H
22-deacetylyanuthone A (6)	OH	⁻OH, ····H

Figure 1. Chemical Structures of 6-MSA and Previously Described Yanuthones

(A) Chemical structure of 6-MSA.

(B) Chemical structures of previously described yanuthones: yanuthones A–E, 7-deacetoxyyanuthone A, and 22-deacetylyanuthone A (Bugni et al., 2000; Li et al., 2003).

cluster from *Gibberella moniliformis* was surprisingly identified, suggesting that this well-characterized fungus has the genetic potential to produce the carcinogenic fumonisins (Baker, 2006). This possibility was later confirmed by genetic and chemical analyses (Pel et al., 2007; Frisvad et al., 2007). The fact that the *A. niger* genome contains several orphan gene clusters for production of secondary metabolites (Fisch et al., 2009) raises the question of whether it can produce other bioactive PKs that could be harmful, or perhaps beneficial, to human health. To this end, one silent cluster in *A. niger* was recently activated by expression of a transcription factor-encoding gene, which was embedded in the cluster. The resulting strain produced six azaphilone compounds, and further studies uncovered substantial new insights into the biosynthesis of this class of compounds (Zabala et al., 2012). It is interesting to note that among the 33 predicted PKS and PKS-like genes in *A. niger*, one encodes a putative PKS, which is phylogenetically close to fungal 6-methylsalicylic acid (6-MSA) synthases (Fisch et al., 2009). Importantly, the model PK 6-MSA (Wattanachaisaereekul et al., 2008) (Figure 1A) is known to be the precursor to, for example, the mycotoxin patulin (Beck et al., 1990) produced by many *Aspergillus* and *Penicillium* species, substantiating the possibility that this gene could be the source of yet another unknown bioactive PK in *A. niger*. Importantly, none of these 6-MSA-derived compounds have been observed in *A. niger* (Nielsen et al., 2009). We therefore investigated whether *A. niger* has the potential to produce 6-MSA or 6-MSA-derived compounds.

Known yanuthones constitute a group of compounds that are derived from a six-membered methylated ring (the C_7 core scaffold) with three side chains: one sesquiterpene and two varying side chains (-R and R') (Figure 1B). In this study we demonstrate that in *A. niger*, 6-MSA is the precursor for formation of yanuthone D, which is an antibiotic against *Candida albicans*, methicillin-resistant *Staphylococcus aureus* (MRSA), and vancomycin-resistant *Enterococcus* (Bugni et al., 2000). We also show that yanuthone D is in fact a complex meroterpenoid synthesized by a pathway where 6-MSA is decarboxylated, heavily oxidized, and fused to a sesquiterpene and a mevalon moiety (the di-acid of mevalonic acid). This is surprising, because yanuthones have been hypothesized to originate from the shikimate pathway (Bugni et al., 2000).

RESULTS

A. niger PKS48 Encodes a 6-MSA Synthase

To investigate the possibility that the *A. niger* gene PKS48/ASPNIDRAFT_44965 encodes a 6-MSA synthase, we transferred the gene to *A. nidulans*, which has not been shown to produce 6-MSA and which does not contain a close homolog to known 6-MSA PKSs. To ensure a high expression level on a defined medium, the PKS48 gene was integrated into a well characterized integration site, *IS1* (Hansen et al., 2011), under control of the strong constitutive promoter *PgpdA*. As expected, the metabolite profile obtained with an *Aspergillus nidulans* reference strain (IBT 29539) did not show any indications of 6-MSA when analyzed by ultra-high-performance liquid chromatography (UPHLC)-UV-visible diode array detector (DAD)-high-resolution time-of-flight mass spectrometry (TOFMS) (Figure 2A). In contrast, the metabolite profile of the strain expressing PKS48 showed the presence of a prominent new peak, which had the same retention time as an authentic 6-MSA standard and displayed the same adducts and monoisotopic mass for the pseudomolecular ion. We therefore conclude that PKS48 encodes a 6-MSA synthase.

Production of Yanuthones D and E Is Eliminated by Deletion of PKS48

The fact that 6-MSA has not previously been reported from *A. niger* prompted us to investigate whether this compound could be a precursor to a known secondary metabolite produced by this fungus. We therefore cultivated an *A. niger* reference strain (KB1001) and an *A. niger* PKS48Δ strain on four different solid media (minimal medium [MM], CYA, YES, and MEA) that are known to trigger the production of a wide range of metabolites (Nielsen et al., 2011). The resulting UHPLC-DAD-TOFMS metabolite profiles were almost identical (Figure S1 available online), showing that the PKS48Δ mutation did not induce a global response on the secondary metabolism. However, on YES and MM media, we identified two compounds that were produced by KB1001, but not by the PKS48Δ strain (Figures 2B and 2C; Table S1). UHPLC separation with UV-visible and

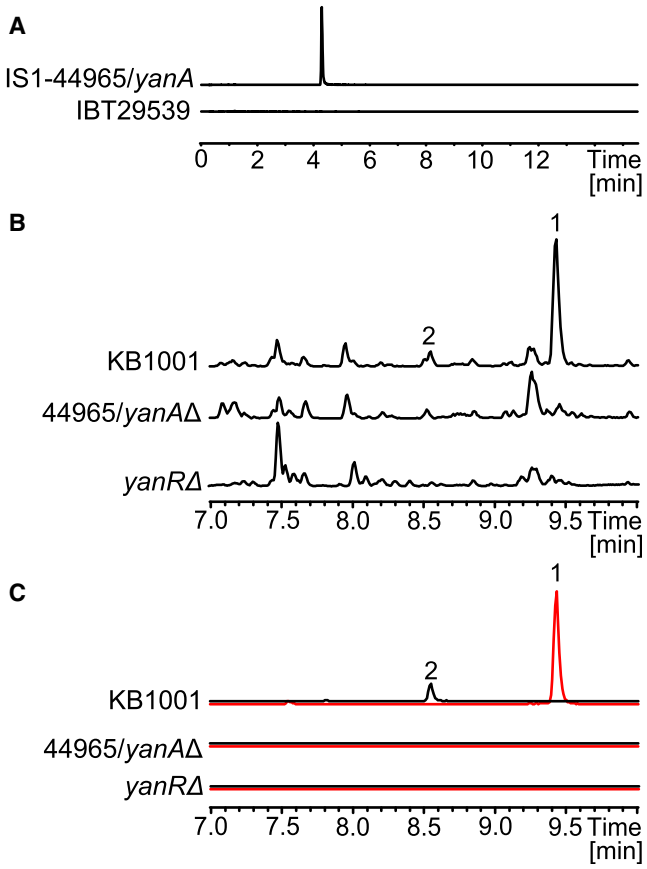

Figure 2. Extracted Ion Chromatograms

(A) Extracted ion chromatogram (EIC, *m/z* 153.0546 ± 0.005) of an *A. nidulans* reference strain (IBT 29539) and a 6-MSA producing strain (IS*1*-44965/*yanA*).

(B) Base peak chromatograms (BPC) *m/z* 100-1,000 of the *A. niger* reference (KB1001), *yanA*Δ, and *yanR*Δ strains.

(C) EICs of yanuthone D (**1**) 503.2640 ± 0.005 (red) and yanuthone E (**2**) 505.2791 ± 0.005 (black) for KB1001, *yanA*Δ, and *yanR*Δ.

All chromatograms are to scale.

high-resolution MS detection as well as MS/MS suggested that the two compounds were yanuthones D and E. This was confirmed by isolation of the compounds, nuclear magnetic resonance (NMR) spectroscopy, and circular dichroism (CD) (Tables S3 and S4). Hence, production of yanuthones D and E appears to be based on the use of 6-MSA as a key precursor. In this scenario, one carbon must be eliminated from C_8-based 6-MSA to form the C_7 core scaffold of yanuthones D and E.

Yanuthones Constitute a Complex Group of Compounds That Appear to Originate from Different Precursors

In addition to yanuthones D and E, *A. niger* has previously been reported to produce yanuthones A, B, and C, 1-hydroxyyanuthone A, 1-hydroxyyanuthone C, and 22-deacetylyanuthone A (Bugni et al., 2000), and 7-deacetoxyyanuthone A has been reported from the genus *Penicillium* (Li et al., 2003) (Figure 1B). We thus examined the extracted ion chromatograms from the UHPLC-DAD-TOFMS profiles obtained by KB1001 for the presence of these metabolites. In extracts obtained after cultivation on MM, YES, and CYA media, this analysis identified trace amounts of a compound (yanuthone X_1) with a mass and elemental composition corresponding to the yanuthone isomers A and C. The nature of this compound was further investigated by MS/MS, and its fragmentation pattern was similar to the pattern of other yanuthones, showing characteristics such as loss of a sesquiterpene chain. Moreover, the UV-visible spectrum of the compound was similar to spectra obtained for yanuthones D and E, substantiating that this compound was a yanuthone. Surprisingly, when the UHPLC-DAD-TOFMS metabolite profiles obtained with the PKS48Δ strain were examined for the presence of this yanuthone, it was still present. This observation strongly suggested that some yanuthones are produced independently of PKS48.

Fully Labeled $^{13}C_8$-6-MSA Is Incorporated into Yanuthones D and E In Vivo

The fact that some yanuthones could be produced independently of PKS48, combined with the fact that yanuthones have been proposed to originate from the shikimate pathway, raised the possibility that the absence of yanuthones D and E in the PKS48 deletion strain potentially could be the result of an indirect effect. To investigate this possibility, we fed fully labeled $^{13}C_8$-6-MSA to KB1001 and the PKS48Δ strain at different time points during growth (24, 48, and 72 hr; see Experimental Procedures). The addition of $^{13}C_8$-6-MSA did not seem to adversely affect the growth rate, and the morphologies of the colonies of the two strains were identical (Figure S2). This indicates that the amounts of $^{13}C_8$-6-MSA added (2-10 μg/ml) did not significantly influence strain fitness. Metabolites were then extracted from the plates and analyzed by UHPLC-DAD-TOFMS. For both strains, $^{13}C_8$-6-MSA was incorporated into yanuthones D and E, resulting in a mass shift of 7.023 Da. This is in agreement with the scenario described above, where one carbon atom must be eliminated from 6-MSA in the biosynthetic processing toward yanuthones D and E. Moreover, the MS-based metabolite profiles also showed that $^{13}C_8$-6-MSA was exclusively incorporated into compounds related to yanuthones. These compounds are only present in tiny amounts and are likely intermediates or analogs of yanuthone D or E, because they share the same UV chromophore and because their masses corresponded to water loss(es) or gain from yanuthone D or E. Based on these results, we named the 6-MSA synthase (encoded by PKS48/ASPNIDRAFT_44965) YanA (*yan*uthone) and the corresponding gene *yanA.* On the other hand, no labeled yanuthone X_1 was observed in KB1001 as well as in the PKS48 deletion strain after addition of $^{13}C_8$-6-MSA (mass spectra are shown in Figure S3), confirming our finding that yanuthone X_1 is formed in the absence of PKS48. Hence, we conclude that 6-MSA is not the precursor of yanuthone X_1.

The *yan* Gene Cluster Comprises Ten Genes

To determine whether *yanA* defines a gene cluster for a biosynthetic pathway toward yanuthones D and E, ten genes up- and downstream of *yanA* were annotated using FGeneSH (Softberry) and AUGUSTUS software (Stanke and Morgenstern, 2005). Subsequently, these twenty putative genes were examined using the NCBI Conserved Domain Database (Marchler-Bauer et al., 2011) for open reading frames (ORFs) encoding activities that are typically employed for the modification of PKs. Based on these

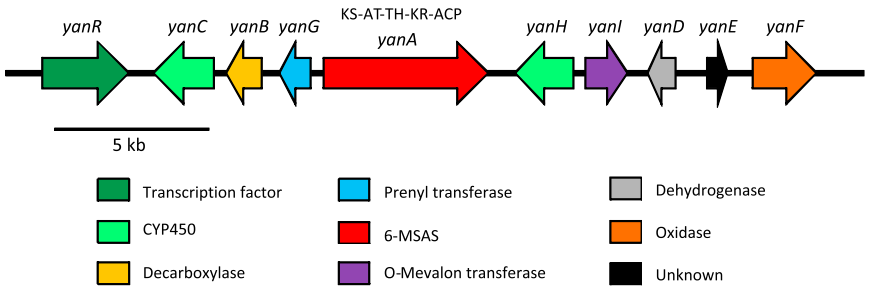

Figure 3. The Proposed *yan* Cluster

The *yanA* 6-MSA synthase-encoding gene is flanked by nine cluster genes (*yanB*, *yanC yanD*, *yanE*, *yanF*, *yanG*, *yanH*, *yanI*, and *yanR*) whose products contain all necessary activities for conversion of 6-MSA into yanuthone D.

analyses, eight additional genes could potentially belong to the *yanA* cluster, including genes encoding a transcription factor (TF), a prenyl transferase, an O-acyltransferase, a decarboxylase, two oxidases, two cytochrome P450s (CYP450s), and a dehydrogenase (Figure 3; Table S2). Together with *yanA* and 192604 (a gene with no known homologs), these eight genes form a cluster of ten genes that are not interrupted by any of the remaining eleven genes included in the analysis. The fact that one of the ten genes in this cluster (44961) putatively encodes a TF raised the possibility that expression of the genes involved in yanuthones D and E production is controlled by this TF. In agreement with this view, deletion of 44961 resulted in a strain that did not produce these two yanuthones (Figures 2B and 2C). To further delineate the *yanA* gene cluster, we determined the expression levels of the ten cluster genes as well as of four flanking genes by RT-quantitative PCR (qPCR) in a 44961Δ strain and KB1001. When the two data sets were compared, we found, as expected, that expression from 44961 is eliminated in the 44961Δ strain where the entire gene is deleted (Figure S4). More importantly, the analysis demonstrated that expression from the other nine genes in the cluster was significantly downregulated in the 44961Δ strain as compared to KB1001 (p value < 0.05). Specifically, the expression was reduced more than 10-fold for seven of the genes, including *yanA*. Expression of the remaining two genes, 54844 and 44964, was expressed at a level corresponding to 20% and 11%, respectively, of the level obtained with KB1001. In contrast, expression levels from the four flanking genes were not significantly different from KB1001 (Figure S4). Next, we individually deleted the remaining eight genes in the proposed *yan* gene cluster, which encode putative activities for PK modification. None of the resulting strains, including 192604Δ, produced yanuthone D, indicating that all genes belong to the *yan* cluster (Table S1). As a control, the four additional genes flanking this cluster were also individually deleted, but all these four strains produced yanuthone D. Based on these analyses and the results from the RT-qPCR, we propose that the *yan* gene cluster is composed by 10 genes, *yanA*, *yanB*, *yanC*, *yanD*, *yanE*, *yanF*, *yanG*, *yanH*, *yanI*, and *yanR*, where *yanR* encodes a TF that regulates the gene cluster (Figure 3; Table S2). Finally, all ten genes were simultaneously deleted in one strain. When $^{13}C_8$-6-MSA was fed to this strain, no labeled metabolites were detected, showing that all 6-MSA-derived yanuthones depend on this gene cluster (see above).

YanF Converts Yanuthone E into Yanuthone D

As the first step toward elucidating the order of reaction steps in the pathway toward yanuthones D and E, we asked whether yanuthones D and E are two different end products or whether one is an intermediate in the pathway toward production of the other. To this end, we note that individual deletion of genes in the *yan* gene cluster generally resulted in loss of production of both yanuthones D and E on YES medium. The only exception is the *yanF*Δ strain, which produced substantial amounts of yanuthone E (**2**), but no yanuthone D (**1**) (Figure 4). These findings suggest that YanF converts yanuthone E into yanuthone D, which is the true end product of the pathway. Interestingly, the *yanF*Δ strain produced a new and unknown compound, which was not detected in KB1001. Elucidation of its structure revealed a yanuthone E analog with a hydroxylation at C-2 at the expense of the first double bond (between C-2 and C-3) in the sesquiterpene moiety (Table S4). This compound was named yanuthone J (**9**).

m-Cresol and Toluquinol Are Intermediates of the Yanuthone D Biosynthesis

Deletion of *yanB*, *yanC*, *yanD*, *yanE*, and *yanG* did not produce any detectable intermediates, and the phenotype of these mutations therefore does not link any of the genes to specific reaction steps in the pathway toward formation of yanuthone D. However, one of the five putative enzymes, YanC, has a defined homolog, PatI, in the *Aspergillus clavatus* patulin biosynthesis pathway (Artigot et al., 2009) where it catalyzes the oxidation of *m*-cresol into toluquinol, suggesting that toluquinol and *m*-cresol are also likely intermediates in the yanuthone biosynthesis. To test this hypothesis, we fed *m*-cresol and toluquinol to the *yanA*Δ strain. Analysis of the metabolite profiles of the two strains indeed showed that addition of *m*-cresol or toluquinol restored production of yanuthones D and E in the *yanA*Δ strain (Figure 5).

In an attempt to further elucidate the role of the five enzymes, the corresponding genes were inserted into plasmid pDHX2 (Figure S5) and individually expressed in the *A. nidulans* strain harboring the *yanA* gene. No new compounds were produced in these *IS1-yanA* strains expressing *yanC*, *yanD*, *yanE*, and *yanG*, despite the fact that 6-MSA was produced in high amounts (Figure S6). Similarly, in the strain expressing *yanB*, no new product was observed, but in this case 6-MSA was absent, indicating that 6-MSA is a substrate for YanB.

Deletion of *yanI* and *yanH* Reveals Key Intermediates in the Biosynthesis of Yanuthone D

In contrast to the *yanB*Δ-*E*Δ and *yanG*Δ strains, new products were observed in the *yanH*Δ and *yanI*Δ strains. Deletion of *yanH* resulted in a strain where the most prominent compound accumulating is 7-deacetoxyyanuthone A (**3**) (NMR data in Table S4). Interestingly, we also identified two compounds in this strain (Figure 4). Isolation and structure elucidation revealed two C-1 oxidized yanuthone derivatives, which we named

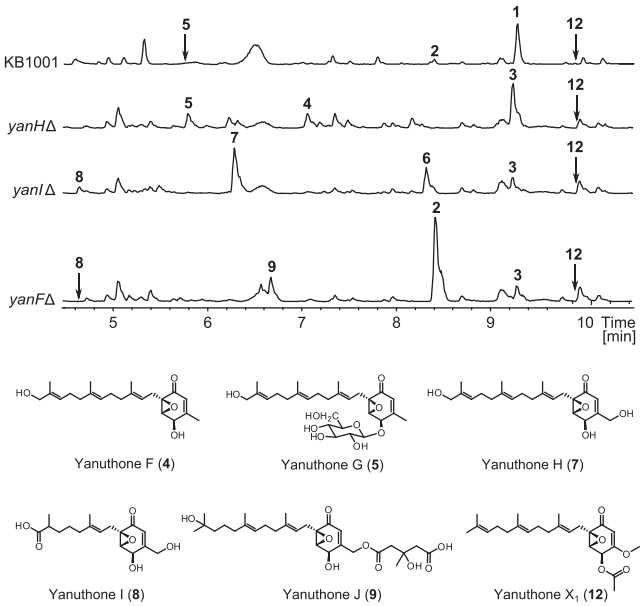

Figure 4. BPC *m/z* 100–1,000 of Reference Strain KB1001, *yanH*Δ, *yanI*Δ, and *yanF*Δ

All NMR-elucidated compounds are shown for comparison of intensity and relative retention times. Below are structures of the yanuthones identified in this study. The structures of yanuthone D (**1**), yanuthone E (**2**), 7-deacetoxyyanuthone A (**3**), and 22-deacetylyanuthone A (**6**) are shown in Figure 1.

yanuthone F (**4**) and yanuthone G (**5**) (NMR data in Table S4). Yanuthone G (**5**) is a glycosylated version of yanuthone F (**4**), which can also be detected in trace amounts in KB1001 (Table S1). Deletion of *yanI* resulted in a strain producing the known compounds 7-deacetoxyyanuthone A (**3**) and 22-deacetylyanuthone A (**6**) (NMR data in Table S4; Figure 1B). Importantly, the latter compound corresponds to yanuthone E (**2**) without the mevalon moiety. In addition, two compounds were produced. The structures were elucidated by NMR spectroscopy, revealing that one, which we named yanuthone H (**7**), is very similar to 22-deacetylyanuthone A (**6**), but with a hydroxyl group at C-1 (Figure 4; Table S4). The other compound, which we named yanuthone I (**8**), is a modification of 22-deacetylyanuthone A (**6**) with a shorter and oxidized terpene (NMR data in Table S4). We note that yanuthone I (**8**) was also detected in trace amounts in KB1001 (Table S1).

Determination of the Yanuthone X_1 Structure

As mentioned above, yanuthone X_1 (**12**) has an elemental composition corresponding to yanuthone A and C but was biosynthesized from another precursor than yanuthone D and E. We therefore isolated and elucidated the structure (Figure 4; Table S4). This analysis confirmed that yanuthone X_1 (**12**) does not have the same C_7 core scaffold but instead has a C_6 core with a methoxygroup directly attached to the six-membered ring at the expense of a methyl group (Figure 4). Despite the fact that yanuthone X_1 (**12**) and yanuthones D and E employ different precursors, they share common features like the epoxide and the sesquiterpene side chain, and we therefore hypothesized that they share common enzymatic steps during their biosynthesis. In agreement with this, examination of the metabolite profiles obtained with the *yan* gene deletion strains revealed that yanuthone X_1 (**12**) was absent in the *yanC*, *yanD*, *yanE*, and *yanG* deletion strains (Table S1). In contrast, yanuthone X_1 (**12**) is produced in larger amounts in the *yanA*Δ strain, which cannot produce 6-MSA.

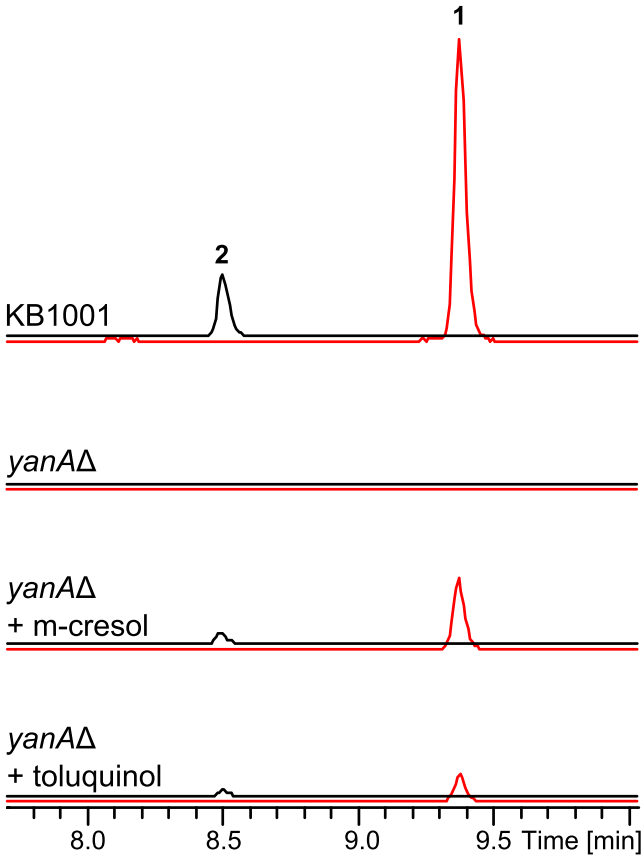

Figure 5. Feeding with Unlabeled *m*-cresol and Toluquinol

Shown are EICs of yanuthone D (**1**) 503.2640 ± 0.005 (red) and yanuthone E (**2**) 505.2791 ± 0.005 (black) for KB1001 and the *yanA*Δ strain with and without feeding. Chromatograms are to scale.

Antifungal Activity of Yanuthones

Yanuthones have earlier been reported to display antimicrobial activity (Bugni et al., 2000), and we therefore tested all ten yanuthones presented in this study for antifungal activity toward *C. albicans* (Table 1). Among these compounds, our analysis identified yanuthone D as the most toxic species in agreement with the fact that it represents the most likely end point of the pathway. Among the remaining yanuthones, three other species, yanuthone G, yanuthone H, and 22-deacetylyanuthone A, exhibited antimicrobial activity. In these cases, IC_{50} values were ~5- to 10-fold higher than the IC_{50} value determined for yanuthone D.

DISCUSSION

Elucidation of the Biosynthetic Route from 6-MSA toward Yanuthone D

We have used a combination of bioinformatics, genetic tools, chemical analyses, and feeding experiments to investigate

Table 1. The Half-Maximal Inhibitory Concentration for *C. albicans* Treated with a Small Library of Yanuthones

Compound	Origin	Isolate	IC_{50} (μM)
Yanuthone D	*A. niger*	KB1001	3.3 ± 0.5
Yanuthone E	*A. niger*	KB1001	>100
Yanuthone F	*A. niger*	*yanHΔ*	>100
Yanuthone G	*A. niger*	*yanHΔ*	38.8 ± 5.1
Yanuthone H	*A. niger*	*yanIΔ*	24.5 ± 1.1
Yanuthone I	*A. niger*	*yanIΔ*	>100
Yanuthone J	*A. niger*	*yanFΔ*	>100
7-deacetoxyyanuthone A	*A. niger*	KB1001	>100
22-deacetylyanuthone A	*A. niger*	KB1001	19.4 ± 1.8
Yanuthone X_1	*A. niger*	KB1001	>100

The IC_{50} values were calculated based on duplicate experiments carried out in three independent trials and annotated with their respective SD.

whether 6-MSA is produced and whether it is used for production of toxic secondary metabolites in *A. niger*. Our work demonstrates that 6-MSA is synthesized by the YanA PKS and then subsequently modified into the antimicrobial end product yanuthone D. This is intriguing because yanuthones have previously been suggested to originate from shikimic acid (Bugni et al., 2000). Yanuthones have previously been observed on YES agar (Klitgaard et al., 2014; Nielsen et al., 2009) and a mixture of yeast, beef, and casein extract (Bugni et al., 2000). In this study yanuthones were detected on solid YES and MM medium, but not on solid CYA or MEA medium, and yanuthone synthesis is therefore conditionally induced. To this end, we find that yanuthone D is not produced in liquid YES and MM medium, in agreement with the fact that secondary metabolism is generally turned off in submerged cultures (González, 2012; Schachtschabel et al., 2013).

We have also shown that *yanA* defines a gene cluster of ten members: *yanA*, *yanB*, *yanC*, *yanD*, *yanE*, *yanF*, *yanG*, *yanH*, *yanI*, and *yanR*, which is regulated by YanR. In agreement with this, YanR is homologous to Zn_2Cys_6 transcription factors that are commonly involved in regulation of secondary metabolite production. The fact that deletion of *yanR* completely abolished production of yanuthone D suggests that YanR acts as an activator of the *yan* cluster. Additionally, analyses of strains where the remaining genes in the *yan* cluster were individually deleted have allowed us to isolate and characterize the full structures of three intermediates. Based on these compounds, we propose the entire pathway for yanuthone D formation including addition of a sesquiterpene and a mevalon to the core polyketide moiety at different stages of the biosynthesis (Figure 6).

In our model, the last intermediate in the pathway is yanuthone E (**2**), which is converted into the end product yanuthone D (**1**) by oxidation of the hydroxyl group at C-15 in a process catalyzed by YanF. The fact that yanuthone E (**2**) is present in KB1001 indicates that it may act as a reservoir for rapid conversion into the more potent antibiotic compound yanuthone D. Yanuthone E (**2**) is likely formed from 22-deacetylyanuthone A (**6**) by attachment of mevalon to the hydroxyl group at C-22. Because 22-deacetylyanuthone A (**6**), but not yanuthone E (**2**), accumulates in the *yanIΔ* strain, we propose that YanI, a putative O-acyltransferase, catalyzes this step. Intriguingly, YanI therefore appears to be an O-mevalon transferase, an activity, which, to the best of our knowledge, has not previously been described in the literature. Next, we propose that 22-deacetylyanuthone A (**6**) is formed by hydroxylation of C-22 of 7-deacetylyanuthone A (**3**). In agreement with this view, 7-deacetylyanuthone A (**3**), but not 22-deacetoxyyanuthone A (**6**), accumulates in the absence of YanH.

Unfortunately we did not detect any intermediates leading from 6-MSA to 7-deacetoxyyanuthone A (**3**) in any of the deletion strains in *A. niger*. The remaining tentative steps in the pathway were therefore deduced from bioinformatics and feeding experiments. First, analyses of patulin formation in *Aspergillus flocco-sus* (previously identified as *Aspergillus terreus*; Jens C. Frisvad, personal communication) and in *A. clavatus* have shown that it requires decarboxylation of 6-MSA into *m*-cresol (Artigot et al., 2009; Puel et al., 2010). This step is catalyzed by 6-MSA decarboxylase (Light, 1969), which has been proposed to be encoded by *patG* (Puel et al., 2010). *m*-Cresol is then converted into gentisyl alcohol in two consecutive hydroxylation steps catalyzed by the two cytochrome P450s CYP619C3 (PatH) and CYP619C2 (PatI). However, CYP619C2 may also act directly on *m*-cresol to form the co-metabolite toluquinol, which is not an intermediate toward patulin. When we inspected the *yan* gene cluster for similar activities, we found a putative 6-MSA decarboxylase (YanB) and CYP619C2 (YanC), but not CYP619C3. These observations suggest that *m*-cresol and toluquinol are intermediates in yanuthone D formation. We present two lines of evidence in support of this view. First, our feeding experiments demonstrate that both compounds can be converted into yanuthone D. Second, heterologous expression of *yanA* in *A. nidulans* leads to production of 6-MSA. This compound disappears if the strain also expresses *yanB*, indicating that 6-MSA is a substrate for the putative 6-MSA decarboxylase YanB. Together these results strongly suggest that *m*-cresol is formed directly from 6-MSA by a decarboxylation reaction, which is most likely catalyzed by YanB. This reaction explains how C_8-based 6-MSA can serve as the building block for the C_7-based core unit of yanuthones. Moreover, the analyses show that toluquinol is an intermediate in the production of yanuthone D and that it is formed from *m*-cresol in a process most likely catalyzed by the putative cytochrome P450 encoded by *yanC*. Conversion of toluquinol into 7-deacetylyanuthone A (**3**) requires epoxidation and prenylation. Based on the fact that prenylated toluquinol is never observed in KB1001 or mutant strains, we propose that epoxidation precedes prenylation. In this scenario, toluquinol is epoxidated into (**10**), which is in equilibrium with the tautomer (**11**). This compound (**11**) is then prenylated to form 7-deacetylyanuthone A (**3**) as a sesquiterpene moiety is attached to C-13 of (**11**). The latter reaction is likely catalyzed by YanG, a putative prenyltransferase. This is supported by the observation that yanuthone D (**1**) and all detectable intermediates, including 7-deacetoxyyanuthone A (**3**), were absent in the *yanG*Δ strain. The identity of the gene products(s) responsible for epoxidation of toluquinol is less clear. Among the putative activities encoded by the genes in the *yan* cluster, which have not been assigned to any reaction step during the analyses above, we note the presence of a putative dehydrogenase (YanD) and one with an unknown activity and with no obvious homologs (YanE) as judged by BLAST

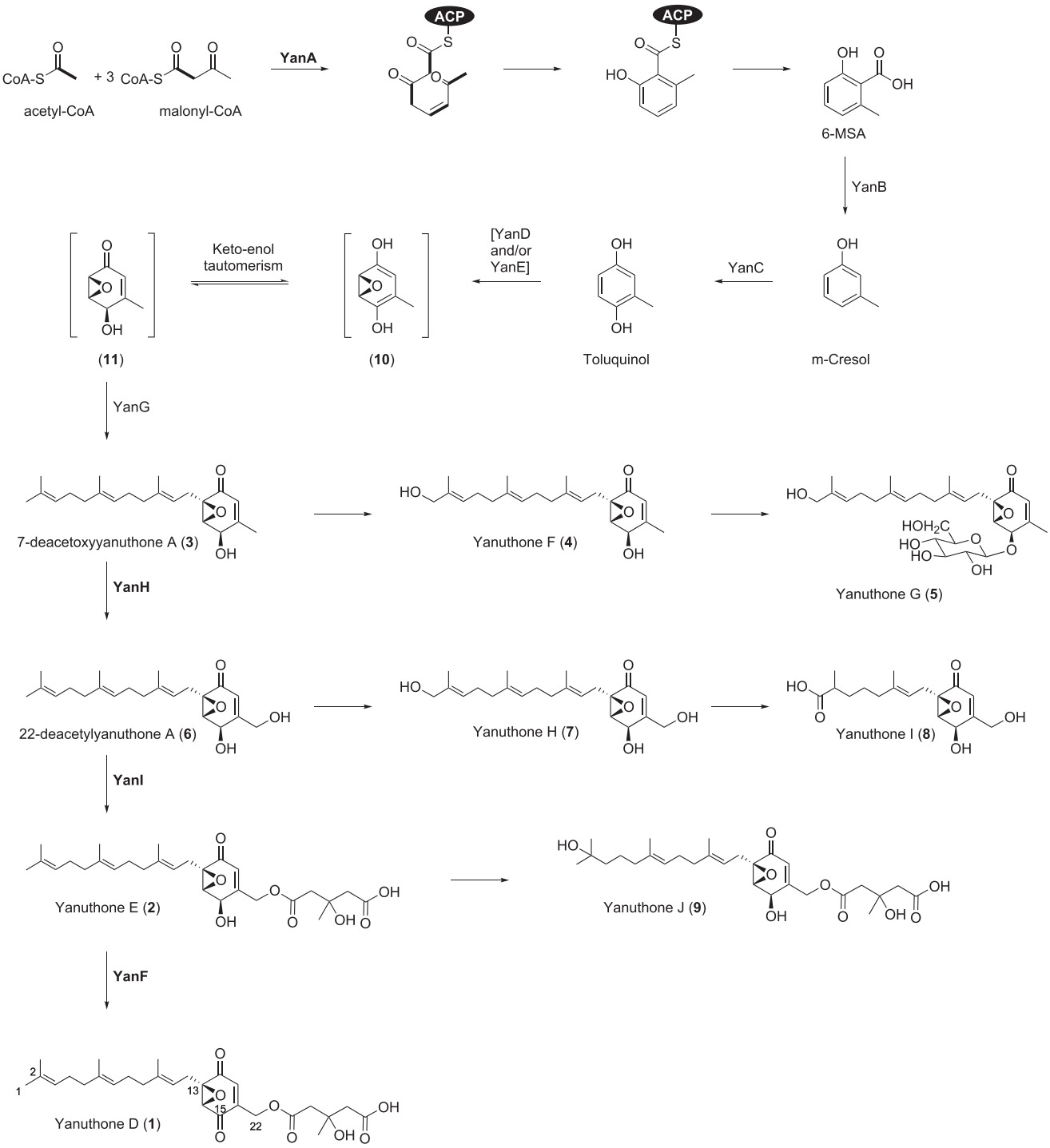

Figure 6. Proposed Biosynthesis of yanuthone D

Structures and enzymatic activities in brackets are hypothesized, activities in plain text have been proposed from bioinformatics, and activities in bold have been experimentally verified.

analysis of the GenBank database (Altschul et al., 1990). We hypothesize that one or both of these enzymes catalyze epoxidation. The fact that neither 6-MSA, *m*-cresol, toluquinol, nor any other intermediates were detected in the *yanB*Δ, *yanC*Δ, *yanD*Δ, and *yanE*Δ strains suggests that these small, aromatic compounds must be rapidly degraded or converted into other compound(s), or they may be incorporated into insoluble material, e.g., the cell wall.

Accumulation of Intermediates in the Yanuthone D Pathway Triggers Formation of Novel Yanuthones

Disruption of the biosynthetic pathway toward yanuthone D results in formation of three branch points in the pathway toward yanuthone D: at yanuthone E (**2**), at 7-deacetoxyyanuthone A (**3**), and at 22-deacetylyanuthone A (**6**). In addition to yanuthone E (**2**), yanuthone J (**9**) accumulates in the *yanF*Δ strain. Similarly, yanuthone F (**4**) accumulates in addition to 7-deacetoxyyanuthone A (**3**) in the *yanH*Δ strain, and yanuthone H (**7**) accumulates in addition to 22-deacetylyanuthone A (**6**) in the *yanI*Δ strain. In all cases, the sesquiterpenes of the accumulated intermediates in the main pathway are oxidized at C-1 or C-2. Because hydroxylation is a known detoxification mode, we speculate that the abnormally high amount of potentially toxic intermediates 7-deacetoxyyanuthone A (**3**), 22-deacetylyanuthone A (**6**), and yanuthone E (**2**) triggers the cell to initiate phase I type of detoxification processes in which the toxic intermediates are hydroxylated. This hypothesis is supported by the fact that there is no obvious assignment of an enzyme with this activity, encoded by the *yan* gene cluster, and by the fact that one of the intermediates, 22-deacetylyanuthone, is toxic to *C. albicans*.

An additional variant of yanuthone F (**4**) was identified in the *yanH*Δ strain, in which yanuthone F (**4**) is glycosylated at the hydroxyl group at C-15 to form yanuthone G (**5**). The glucose moiety of yanuthone G (**5**) is intriguing because sugar moieties are rare in fungal secondary metabolites, and the fact that yanuthone G (**5**) is detected in KB1001 shows that it is a naturally occurring compound (Figure 4; Table S1). Because yanuthone G (**5**) production is upregulated in *yanH*Δ, we suggest that glycosylation poses a second (phase II conjugation) type of mechanism for further detoxification of possible toxic intermediates.

The branch point at 22-deacetylyanuthone A (**6**) revealed a novel compound yanuthone I (**8**), which is identical to 22-deacetylyanuthone A (**6**) and yanuthone H (**7**) but with a shorter and oxidized sesquiterpene chain. A similar modification has been observed in the biosynthetic pathway for production of mycophenolic acid (Regueira et al., 2011). Here it was proposed to occur by oxidative cleavage between C-4 and C-5 of the sesquiterpene chain. Alternatively, it could occur by terminal oxidation of a geranyl side chain.

Yanuthone X_1 Defines a Novel Class of Yanuthones

Because yanuthones are based on a C_7 scaffold, they were previously proposed to originate from shikimic acid (Bugni et al., 2000). However, in our study we demonstrate that yanuthones D and E originate from the C_8 polyketide precursor 6-MSA, which is decarboxylated to form the C_7 core of the yanuthone structure. In contrast, the novel yanuthone X_1 (**12**) has a C_6 core scaffold that does not originate from 6-MSA and does not require decarboxylation by YanB. Based on this we define two classes of yanuthones: those that are based on the polyketide 6-MSA, class I, and those that are based on the yet unknown precursor leading to the formation of yanuthone X_1 (**12**), class II. The two classes of yanuthones share several enzymatic steps. First we note that the sesquiterpene side chain in yanuthone X_1 (**12**) is likely attached by YanG, as is the case for yanuthone D. Second, it depends on enzyme activities of YanC, YanD, and YanE, but not of YanB. Together this suggests that the precursor is a small aromatic compound similar to 6-MSA but lacking the carboxylic acid. Importantly, the main difference between yanuthone D and yanuthone X_1 (**12**) are the groups attached to C-16. In the case of yanuthone X_1 (**12**), this position is oxidized, whereas in yanuthones D and E there is a carbon-carbon bond that originates from the methyl group of 6-MSA. Consequently, yanuthone X_1 (**12**) cannot be mevalonated by YanI.

246

SIGNIFICANCE

This study has identified a cluster of 10 genes, which is responsible for production of antimicrobial yanuthone D in *A. niger*. We show that yanuthone D is based on the polyketide 6-MSA and not on shikimic acid as previously suggested, and we have proposed a detailed genetic and biochemical pathway for converting 6-MSA into yanuthone D. Interestingly, we have revealed that yanuthone X_1, although similar in structure, is not derived from 6-MSA, but the yet unknown precursor to yanuthone X_1 does employ several enzymes encoded by the *yan* cluster. An important finding in the elucidation of the biosynthesis is the identification of *yanI* encoding an O-mevalon transferase, which represents a different enzymatic activity. We have discovered that the pathway toward yanuthone D branches when intermediates accumulate, because three intermediates are hydroxylated. Two of the hydroxylated compounds are further modified by oxidative cleavage of the sesquiterpene and glycosylation, respectively, resulting in five yanuthones. The discovery of a glycosylated compound, yanuthone G, is intriguing because glycosylated compounds are very rare in fungal secondary metabolism. We successfully employed an interdisciplinary approach for solving the biosynthetic pathway: applying gene deletions, heterologous gene expression, UHPLC-DAD-MS, MS/MS, structural elucidation by NMR spectroscopy and CD, and feeding experiments with ^{13}C-labeled and unlabeled metabolites. Together, our analyses have cast insights into understanding the complexity of fungal secondary metabolism.

EXPERIMENTAL PROCEDURES

Strains and Media

The strain IBT 29539 was used for strain constructions in *A. nidulans*. ATCC1015-derived strain KB1001 was used for strain constructions in *A. niger*. All fungal strains prepared in the present work (Table S5) have been deposited in the IBT Culture Collection at the Department of Systems Biology, Technical University of Denmark, Kongens Lyngby, Denmark. *Escherichia coli* strain DH5α was used for propagating plasmids, except *E. coli* ccdB survival2 cells (Invitrogen), which were used for plasmids carrying the *ccdB* gene.

MM for *A. nidulans* was made as described by Cove (1966), but with 1% glucose, 10 mM $NaNO_3$, and 2% agar. MM for *A. niger* was prepared as described by Chiang et al. (2011). YES, MEA, and CYA were prepared as described by Frisvad and Samson (Samson et al., 2010). When necessary, media were supplemented with 4 mM L-arginine, 10 mM uridine, 10 mM uracil, and/or 100 μg/ml hygromycin B (InvivoGen). Luria-Bertani (LB) medium was used for cultivation of *E. coli* strains and consisted of 10 g/l tryptone (Bacto), 5 g/l yeast extract (Bacto), and 10 g/l NaCl (pH 7.0). When necessary, LB was supplemented with 100 μg/ml ampicillin.

For batch cultivation the medium contained 20 g/l D-glucose-$^{13}C_6$ (99 atom % ^{13}C; Sigma-Aldrich) or D-glucose, 7.3 g/l $(NH_4)_2SO_4$, 1.5 g/l KH_2PO_4, 1.0 g/l $MgSO_4 \cdot 7\ H_2O$, 1.0 g/l NaCl, 0.1 g/l $CaCl_2$, 0.1 ml of Antifoam 204

(Sigma), and 1 ml/l trace element solution. Trace element solution contained 0.4 g/l $CuSO_4 \cdot 5\ H_2O$, 0.04 g/l $Na_2B_2O_7 \cdot 10\ H_2O$, 0.8 g/l $FeSO_4 \cdot 7\ H_2O$, 0.8 g/l $MnSO_4 \cdot H_2O$, 0.8 g/l $Na_2MoO_4 \cdot 2\ H_2O$, and 8.0 g/l $ZnSO_4 \cdot 7\ H_2O$.

Construction of Basic Vectors for Strain Construction

All primers are listed in Table S6. The PfuX7 polymerase (Nørholm, 2010) was used in all PCRs. Fragments were assembled via uracil-excision fusion (Geu-Flores et al., 2007) into a compatible vector.

pDH56 and pDH57 are designed for integration of novel genes into the *IS1* site of *A. nidulans*. In pDH56, the AsiSI/Nb.BtsI uracil-excision cassette of CMBU1111 (Hansen et al., 2011) is modified into a *ccdB-cm*^{R} AsiSI/Nb.BtsI uracil-excision cassette. Unlike with CMBU1111, new fragments can be introduced into this cassette and cloned in *ccdA*-deficient *E. coli* strains like DH5α without generating background because false positives resulting from incomplete digestion of the USER cassette are eliminated (Bernard and Couturier, 1992). Specifically, the suicide gene *ccdB* and the chloramphenicol resistance gene *cm*^{R} (*ccdB-cm*^{R}) construct was PCR amplified (using primers 84 and 85) from pDONR (Invitrogen) and inserted into CMBU1111 by uracil-excision cloning in a manner that reconstituted the original uracil excision cassette on either side of the insert. pDH57 was constructed from pDH56 by removing an undesirable Nb.BtsI nicking site located in the *amp*^{R} gene. pDH56 was PCR amplified in two pieces (81 + 76 and 75 + 80). 75 and 76 were designed to introduce a silent mutation into the Nb.BtsI recognition site. Fragments were assembled via uracil-excision cloning, and correct clones were verified by sequencing. The gene targeting substrate for insertion of the 6-MSA synthase gene *yanA* was made by amplifying the synthase gene *yanA* (PKS48/ASPNIDRAFT_44965) from IBT 29539 genomic DNA (primers 1 and 2) and inserted into pDH57, yielding pDH57-*yanA*.

The pDHX2 vector is AMA1-based and designed for episomal gene expression. pDHX2 was constructed by USER fusion of five fragments: (1) *E. coli* origin of replication (*ori*^{R}) and the *E. coli* ampicillin resistance gene (*amp*^{R}); (2) the 5′ half of AMA1; (3) the 3′ half of AMA1; (4) 0.5 kb of the P*gpdA* promoter, an AsiSI/Nb.BtsI USER cassette containing *ccdB* and *cm*^{R}, and the TtrpC terminator; and (5) the *A. fumigatus pyrG* selection marker (Figure S5). Fragment 1 was amplified from pDH57 (primers 77 + 78); fragments 2, 3, and 5 were amplified from pDEL2 (primers 86 + 89, 87 + 88, and 82 + 83) (Nielsen et al., 2008); and fragment 4 was amplified from pDH57 (primers 79 + 80). Fragments were assembled as described by Geu-Flores et al. (2007) using equal molar amounts of purified PCR product, and correct clones were verified by restriction digestion. Plasmids for episomal heterologous expression of cluster genes were constructed by PCR amplification of ORFs using primers 3–12 pairwise. Genes were inserted into AsiSI/Nb.BtsI-digested pDHX2 as described by Nour-Eldin et al. (2006), resulting in pDHX2-*yanB*, pDHX2-*yanC*, pDHX2-*yanD*, and pDHX2-*yanE*. Plasmids were verified by sequencing.

Plasmids carrying gene targeting substrates for gene deletion in *A. niger* were constructed by PCR amplification of upstream (US) and downstream (DS) targeting sequences along with the *hph* marker, conferring resistance to hygromycin B. US and DS targeting sequences were generated using the primers 17–72, and *hph* was amplified from pCB1003 (McCluskey et al., 2010) using primers 13 + 14. The three fragments were assembled into the CMBU0020 vector (Hansen et al., 2011).

Strain Construction

Protoplasting and gene-targeting procedures were performed as described previously for *A. nidulans* (Johnstone et al., 1985; Nielsen et al., 2006) and *A. niger* (Chiang et al., 2011). NotI-linearized pDH57-*yanA* was transformed into IBT 29539. Transformants were verified by diagnostic PCR as described by Hansen et al. (2011).

Strains for episomal expression of cluster genes were constructed by transforming the IS1-yanA strain with circular plasmids (pDHX2-*yanB*, pDHX2-*yanC*, pDHX2-*yanD*, and pDHX2-*yanE*) using *pyrG* as a selectable marker.

A. niger deletion strains were constructed by transforming KB1001 with bipartite gene targeting substrates. The substrates were generated by PCR amplification of the US::*hph*::DS cassettes of the CMBU0020-based plasmids using primers GENE_US-FW+73 and 74+GENE_DS-RV. Deletion strains were selected on 100 μg/ml hygromycin B and verified by diagnostic PCR.

RNA Extraction and RT-qPCR

RNA isolation from the *A. niger* strains and subsequent quantitative RT-PCRs were done as previously described by Hansen et al. (2011) except that biomass for RNA isolation was prepared with a Tissue-Lyser LT (QIAGEN) by treating samples for 1 min at 45 MHz. The *A. niger* histone 3-encoding gene, *hhtA* (ASPNIDRAFT_52637) and gamma-actin-encoding gene *actA* (ASPNIDRAFT_200483) were used as internal standards for normalization of expression levels. All primers used for quantitative RT-PCR are shown in Table S6 (primers 90–121). The relative expression levels were approximated based on $2^{\Delta\Delta c(t)}$, with $\Delta\Delta c(t) = \Delta c(t)_{(normalized)} - \Delta c(t)_{(calibrator)}$, where $\Delta c(t)_{(normalized)} = \Delta c(t)_{(target\ gene)} - \Delta c(t)_{(actA\ or\ hhtA)}$.The calibrator c(t) values are those from the *A. niger* reference strain KB1001. Statistical analysis of RT-qPCR results was performed as a Student's t test, and the error bars indicate the SD.

Chemical Analysis of Strains

Unless otherwise stated, strains were cultivated on solid MM media and incubated at 37°C for 5 days. Extraction of metabolites was performed as described by Smedsgaard (1997). 6-MSA was purchased from (Apin Chemicals). Analysis was performed using UPHLC-DAD-TOFMS on a maXis 3G orthogonal acceleration quadrupole time-of-flight mass spectrometer (Bruker Daltonics) equipped with an electrospray ionization (ESI) source and connected to an Ultimate 3000 UHPLC system (Dionex). The column used was a reverse-phase Kinetex 2.6 μm C_{18}, 100 mm × 2.1 mm (Phenomenex), and the column temperature was maintained at 40°C. A linear water-acetonitrile (liquid chromatography-mass spectrometry grade) gradient was used (both solvents were buffered with 20 mM formic acid) starting from 10% (v/v) acetonitrile and increased to 100% in 10 min, maintaining this rate for 3 min before returning to the starting conditions in 0.1 min and staying there for 2.4 min before the following run. A flow rate of 0.4 ml•min^{-1} was used. TOFMS was performed in ESI+ with a data acquisition range of 10 scans per second at *m/z* 100–1,000. The TOFMS was calibrated using Bruker Daltonics high precision calibration algorithm by means of the use of the internal standard sodium formate, which was automatically infused before each run. This provided a mass accuracy of better than 1.5 ppm in MS mode. UV-visible spectra were collected at wavelengths from 200 to 700 nm. Data processing was performed using DataAnalysis 4.0 and Target Analysis 1.2 software (Bruker Daltonics) (Klitgaard et al., 2014). Tandem MS was performed with fragmentation energies from 18 to 55 eV.

Preparative Isolation of Selected Metabolites

The fungal strains were cultivated on 10-200 YES plates at 30°C for 5 days. For details about each extraction, see Table S3. Extracts were filtered and concentrated in vacuo. The combined extract was dissolved in 9:1 methanol (MeOH):H_2O, and 1:1 heptane was added, resulting in two phases. To the MeOH/H_2O phase H_2O was added to a ratio of 1:1, and metabolites were extracted with dichlormethane (DCM). The phases were concentrated separately in vacuo. The DCM phase was adsorbed onto diol column material and dried before packing into a SNAP column (Biotage) with diol material. The extract was fractionated on an Isolera flash purification system (Biotage) using seven steps of heptane-DCM-EtOAc-MeOH. Solvents were of HPLC grade, and H_2O was purified and deionized by a Millipore system through a 0.22 μm membrane filter.

The Isolera fractions were subjected to further purification on a semipreparative high-performance liquid chromatography (HPLC), which was either a Waters 600 controller with a 996 photodiode array detector (Waters) or a Gilson 322 controller connected to a 215 Liquid Handler, 819 Injection Module, and a 172 DAD (Gilson). This was achieved using a Luna II C_{18} column (250 × 10 mm, 5 μm; Phenomenex) or a Gemini C6-Phenyl 110A column (250 × 10.00 mm, 5 μm; Phenomenex). 50 ppm TFA was added to acetonitrile of HPLC grade and Milli-Q water. For choice of system, flow rate, column, gradients, and yields, see Table S3.

NMR and Structural Elucidation

The 1D and 2D spectra were recorded on a Unity Inova-500 MHz spectrometer (Varian). Spectra were acquired using standard pulse sequences, and ^{1}H, double quantum filtered-correlated spectroscopy, nuclear Overhauser effect spectroscopy, heteronuclear single quantum coherence, and heteronuclear multiple bond correlation spectra were acquired. The deuterated solvent

was acetonitrile-d_3, and signals were referenced by solvent signals for acetonitrile-d_3 at δ_H = 1.94 ppm and δ_C = 1.32/118.26 ppm. The NMR data was processed in Bruker Topspin 3.1 or ACD NMR Workbook. Chemical shifts are reported in ppm (δ) and scalar couplings in hertz. The sizes of the *J* coupling constants reported in the tables are experimentally measured values from the spectra. There are minor variations in the measurements that may be explained by the uncertainty of *J*. Descriptions of the structural elucidations are shown in Table S4.

CD spectra were obtained from a J-710 spectropolarimeter (Jasco). The methanol dissolved samples (1 mg/3 ml) were analyzed in 0.2 cm optical path length cells at 20°C, and the spectra were recorded from 200 to 500 nm. Optical rotation was measured on a PerkinElmer 321 Polarimeter.

Production and Purification of Fully Labeled ^{13}C-6-MSA

Because fully labeled $^{13}C_8$-6-MSA was not commercially available, it was produced in-house from the 6-MSA-producing strain by batch cultivation. Spores propagated on CYA media plates for 7 days at 30°C were harvested with 10 ml of 0.9% NaCl through Mira cloth. The spores were washed twice with 0.9% NaCl. The batch fermentation was initiated by inoculation of $2 \cdot 10^9$ spores/l. A Sartorious 1 l bioreactor (Satorious) with a working volume of 0.8 l equipped with two Rushton six-blade disc turbines was used. The pH electrode (Mettler) was calibrated according to manufacturer standard procedures. The bioreactor was sparged with sterile atmospheric air, and off-gas concentrations of oxygen and carbon dioxide were measured with a Prima Pro Process Mass Spectrometer (Thermo-Fischer Scientific). Temperature was maintained at 30°C, and pH was controlled by addition of 2 M NaOH and H_2SO_4. Start conditions were pH: 3.0, stir rate: 100 rpm, and air flow: 0.1 volume of air per volume of liquid per minute (vvm). These conditions were changed linearly in 720 min to pH: 5.0, stir rate: 800 rpm, and air flow: 1 vvm. The strain was cultivated until glucose was depleted, as measured by glucose test strips (Machery-Nagel), and the culture had entered stationary phase as monitored by off-gas CO_2 concentration.

The entire volume of the reactor was harvested, and the biomass was removed by filtration through a Whatman 1 qualitative paper filter followed by centrifugation at 8,000 × *g* for 20 min to remove fine sediments. The 6-MSA was then recovered from the supernatant by liquid-liquid extraction using ethyl acetate with 0.5% formic acid.

The organic extract then dried in vacuo to give a crude extract that was redissolved in 20 ml of ethyl acetate and dry loaded onto 3 g of Sepra ZT C18 (Phenomenex) resin prior to packing into a 25 g SNAP column (Biotage) with 22 g of pure resin in the base. The crude extract was fractionated on an Isolera flask purification system (Biotage) using an water-acetonitrile gradient starting at 15:85 going to 100% acetonitrile in 23 min at a flow rate of 25 ml min^{-1} and kept at that level for 4 min. Fractions were collected using UV detection at 210 and 254 nm, resulting in a total of 15 fractions, of which 3 were pooled and analyzed. 6-MSA concentration was assessed using a Dionex Ultimate 3000 UHPLC coupled with a ultimate 3000 RS diode array detector (Dionex) equipped with a Poroshell 120 phenyl hexyl 2.1 × 100 mm, 2.7 μm (Agilent) column. Finally, purity (98.7%) was analyzed by UHPLC-TOFMS (Figure S3A).

Feeding Experiments

Solid YES plates were prepared using a 6 mm plug drill to make a well in the middle of the agar. 25-100 μl of spore suspension was added to the well, and plates were incubated at 30°C for 5 days. 100 μg of ^{13}C-6-MSA, *m*-cresol, and toluquinol (ortoluquinol) was added to the plates after 24, 48, and 72 hr, respectively. Agar plugs were taken both as reported previously (Smedsgaard, 1997) and also separately from the center, the middle, and the rim of the colony, respectively, to verify diffusion and absorption of the 6-MSA and the location of yanuthone production. Samples were analyzed as described in "Chemical Analysis of Strains."

Antifungal Susceptibility Testing

All compounds were screened for antifungal activity toward *C. albicans* in accordance with the CLSI standards using RPMI 1640 medium adjusted to pH 7 with 0.165 M MOPS buffer (CLSI, 2012). Inoculum was prepared to a final concentration of approximately 2.5×10^3 cells per ml. Inoculated media were seeded into 96-well microtiter plates in aliquots of 200 μl using a Hamilton STAR liquid handling workstation with an integrated Thermo Cytomat shaking incubator and Biotek Synergy Mx microplate reader. The pure compounds were dissolved in Me_2SO and applied at 100 to 5 μM (1% Me_2SO per well). The plates were incubated at 35°C at 1,200 rpm shaking with a 2 mm amplitude. Optical density was recorded every hour for 20 hr. Endpoint optical densities from compound screens were normalized to the negative controls, and susceptibility was evaluated as the percentage of reduction in optical density. All bioactive compounds were tested in duplicate in three independent trials to ensure reproducibility and to evaluate potency of the compound toward the target organism. The half-maximal inhibitory concentration (IC_{50}) was extrapolated from compound specific dilution sequences and annotated as the average concentration for which 50% inhibition plus minus the SD was observed.

SUPPLEMENTAL INFORMATION

Supplemental information includes six figures and six tables and can be found with this article online at http://dx.doi.org/10.1016/j.chembiol.2014.01.013.

ACKNOWLEDGMENTS

We kindly acknowledge Kenneth S. Bruno (Pacific Northwest National Laboratory, Richland, WA) for providing the KB1001 strain and Solveig Kallesøe (University of Copenhagen) for obtaining CD data. We also acknowledge Diana C. Anyaogu for assisting with the RT-qPCR analysis. The study was supported by grant 09-064967 from the Danish Council for Independent Research, Technology, and Production Sciences.

Received: October 18, 2013
Revised: January 14, 2014
Accepted: January 29, 2014
Published: March 27, 2014

REFERENCES

Altschul, S.F., Gish, W., Miller, W., Myers, E.W., and Lipman, D.J. (1990). Basic local alignment search tool. J. Mol. Biol. *215*, 403–410.

Andersen, M.R., Nielsen, J.B., Klitgaard, A., Petersen, L.M., Zachariasen, M., Hansen, T.J., Blicher, L.H., Gotfredsen, C.H., Larsen, T.O., Nielsen, K.F., and Mortensen, U.H. (2013). Accurate prediction of secondary metabolite gene clusters in filamentous fungi. Proc. Natl. Acad. Sci. USA *110*, E99–E107.

Artigot, M.P., Loiseau, N., Laffitte, J., Mas-Reguieg, L., Tadrist, S., Oswald, I.P., and Puel, O. (2009). Molecular cloning and functional characterization of two CYP619 cytochrome P450s involved in biosynthesis of patulin in Aspergillus clavatus. Microbiology *155*, 1738–1747.

Baker, S.E. (2006). Aspergillus niger genomics: past, present and into the future. Med. Mycol. *44* (*Suppl 1*), S17–S21.

Beck, J., Ripka, S., Siegner, A., Schiltz, E., and Schweizer, E. (1990). The multifunctional 6-methylsalicylic acid synthase gene of *Penicillium patulum*. Its gene structure relative to that of other polyketide synthases. Eur. J. Biochem. *192*, 487–498.

Bentley, R. (2000). Mycophenolic acid: a one hundred year odyssey from antibiotic to immunosuppressant. Chem. Rev. *100*, 3801–3826.

Bernard, P., and Couturier, M. (1992). Cell killing by the F plasmid CcdB protein involves poisoning of DNA-topoisomerase II complexes. J. Mol. Biol. *226*, 735–745.

Bugni, T.S., Abbanat, D., Bernan, V.S., Maiese, W.M., Greenstein, M., Van Wagoner, R.M., and Ireland, C.M. (2000). Yanuthones: novel metabolites from a marine isolate of Aspergillus niger. J. Org. Chem. *65*, 7195–7200.

Chiang, Y.-M., Meyer, K.M., Praseuth, M., Baker, S.E., Bruno, K.S., and Wang, C.C.C. (2011). Characterization of a polyketide synthase in Aspergillus niger whose product is a precursor for both dihydroxynaphthalene (DHN) melanin and naphtho-γ-pyrone. Fungal Genet. Biol. *48*, 430–437.

CLSI (Clinical and Laboratory Standards Institute) (2012). Reference methods for broth dilution antifungal susceptibility testing of yeasts. CLSI document M27-S4, Fourth International Supplement. (Wayne, PA: Clinical and Laboratory Standards Institute).

Cove, D.J. (1966). The induction and repression of nitrate reductase in the fungus Aspergillus nidulans. Biochim. Biophys. Acta *113*, 51–56.

Cox, R.J. (2007). Polyketides, proteins and genes in fungi: programmed nano-machines begin to reveal their secrets. Org. Biomol. Chem. *5*, 2010–2026.

Endo, A., Kuroda, M., and Tsujita, Y. (1976). ML-236A, ML-236B, and ML-236C, new inhibitors of cholesterogenesis produced by *Penicillium citrinium*. J. Antibiot. (Tokyo) *29*, 1346–1348.

Fisch, K.M., Gillaspy, A.F., Gipson, M., Henrikson, J.C., Hoover, A.R., Jackson, L., Najar, F.Z., Wägele, H., and Cichewicz, R.H. (2009). Chemical induction of silent biosynthetic pathway transcription in Aspergillus niger. J. Ind. Microbiol. Biotechnol. *36*, 1199–1213.

Frisvad, J.C., Smedsgaard, J., Samson, R.A., Larsen, T.O., and Thrane, U. (2007). Fumonisin B2 production by Aspergillus niger. J. Agric. Food Chem. *55*, 9727–9732.

Frisvad, J.C., Rank, C., Nielsen, K.F., and Larsen, T.O. (2009). Metabolomics of Aspergillus fumigatus. Med. Mycol. *47* (*Suppl 1*), S53–S71.

Geu-Flores, F., Nour-Eldin, H.H., Nielsen, M.T., and Halkier, B.A. (2007). USER fusion: a rapid and efficient method for simultaneous fusion and cloning of multiple PCR products. Nucleic Acids Res. *35*, e55.

González, J.B. (2012). Solid-state fermentation: physiology of solid medium, its molecular basis and applications. Process Biochem. *47*, 175–185.

Gross, H. (2007). Strategies to unravel the function of orphan biosynthesis pathways: recent examples and future prospects. Appl. Microbiol. Biotechnol. *75*, 267–277.

Hansen, B.G., Salomonsen, B., Nielsen, M.T., Nielsen, J.B., Hansen, N.B., Nielsen, K.F., Regueira, T.B., Nielsen, J., Patil, K.R., and Mortensen, U.H. (2011). Versatile enzyme expression and characterization system for Aspergillus nidulans, with the Penicillium brevicompactum polyketide synthase gene from the mycophenolic acid gene cluster as a test case. Appl. Environ. Microbiol. *77*, 3044–3051.

Hertweck, C. (2009). The biosynthetic logic of polyketide diversity. Angew. Chem. Int. Ed. Engl. *48*, 4688–4716.

Johnstone, I.L., Hughes, S.G., and Clutterbuck, A.J. (1985). Cloning an Aspergillus nidulans developmental gene by transformation. EMBO J. *4*, 1307–1311.

Klitgaard, A., Iversen, A., Andersen, M.R., Larsen, T.O., Frisvad, J.C., and Nielsen, K.F. (2014). Aggressive dereplication using UHPLC-DAD-QTOF: screening extracts for up to 3000 fungal secondary metabolites. Anal. Bioanal. Chem. Published online January 18, 2014. http://dx.doi.org/10.1007/s00216-013-7582-x.

Li, X., Choi, H.D., Kang, J.S., Lee, C.O., and Son, B.W. (2003). New polyoxygenated farnesylcyclohexenones, deacetoxyyanuthone A and its hydro derivative from the marine-derived fungus *Penicillium sp*. J. Nat. Prod. *66*, 1499–1500.

Light, R.J. (1969). 6-methylsalicylic acid decarboxylase from *Penicillium patulum*. Biochim. Biophys. Acta *191*, 430–438.

Marchler-Bauer, A., Lu, S., Anderson, J.B., Chitsaz, F., Derbyshire, M.K., DeWeese-Scott, C., Fong, J.H., Geer, L.Y., Geer, R.C., Gonzales, N.R., et al. (2011). CDD: a Conserved Domain Database for the functional annotation of proteins. Nucleic Acids Res. *39* (Database issue), D225–D229.

McCluskey, K., Wiest, A., and Plamann, M. (2010). The Fungal Genetics Stock Center: a repository for 50 years of fungal genetics research. J. Biosci. *35*, 119–126.

Nielsen, M.L., Albertsen, L., Lettier, G., Nielsen, J.B., and Mortensen, U.H. (2006). Efficient PCR-based gene targeting with a recyclable marker for Aspergillus nidulans. Fungal Genet. Biol. *43*, 54–64.

Nielsen, J.B., Nielsen, M.L., and Mortensen, U.H. (2008). Transient disruption of non-homologous end-joining facilitates targeted genome manipulations in the filamentous fungus Aspergillus nidulans. Fungal Genet. Biol. *45*, 165–170.

Nielsen, K.F., Mogensen, J.M., Johansen, M., Larsen, T.O., and Frisvad, J.C. (2009). Review of secondary metabolites and mycotoxins from the Aspergillus niger group. Anal. Bioanal. Chem. *395*, 1225–1242.

Nielsen, M.L., Nielsen, J.B., Rank, C., Klejnstrup, M.L., Holm, D.K., Brogaard, K.H., Hansen, B.G., Frisvad, J.C., Larsen, T.O., and Mortensen, U.H. (2011). A genome-wide polyketide synthase deletion library uncovers novel genetic links to polyketides and meroterpenoids in Aspergillus nidulans. FEMS Microbiol. Lett. *321*, 157–166.

Nørholm, M.H.H. (2010). A mutant Pfu DNA polymerase designed for advanced uracil-excision DNA engineering. BMC Biotechnol. *10*, 21.

Nour-Eldin, H.H., Hansen, B.G., Nørholm, M.H.H., Jensen, J.K., and Halkier, B.A. (2006). Advancing uracil-excision based cloning towards an ideal technique for cloning PCR fragments. Nucleic Acids Res. *34*, e122.

Olsen, J.H., Dragsted, L., and Autrup, H. (1988). Cancer risk and occupational exposure to aflatoxins in Denmark. Br. J. Cancer *58*, 392–396.

Pel, H.J., de Winde, J.H., Archer, D.B., Dyer, P.S., Hofmann, G., Schaap, P.J., Turner, G., de Vries, R.P., Albang, R., Albermann, K., et al. (2007). Genome sequencing and analysis of the versatile cell factory Aspergillus niger CBS 513.88. Nat. Biotechnol. *25*, 221–231.

Puel, O., Galtier, P., and Oswald, I.P. (2010). Biosynthesis and toxicological effects of patulin. Toxins (Basel) *2*, 613–631.

Regueira, T.B., Kildegaard, K.R., Hansen, B.G., Mortensen, U.H., Hertweck, C., and Nielsen, J. (2011). Molecular basis for mycophenolic acid biosynthesis in Penicillium brevicompactum. Appl. Environ. Microbiol. *77*, 3035–3043.

Rho, M.C., Toyoshima, M., Hayashi, M., Uchida, R., Shiomi, K., Komiyama, K., and Omura, S. (1998). Enhancement of drug accumulation by andrastin A produced by Penicillium sp. FO-3929 in vincristine-resistant KB cells. J. Antibiot. (Tokyo) *51*, 68–72.

Samson, R.A., Houbraken, J., Thrane, U., Frisvad, J.C., and Andersen, B. (2010). Food and Indoor Fungi. CBS Laboratory Manual Series 2. (Utrecht, The Netherlands: CBS KNAW Fungal Biodiversity Centre).

Schachtschabel, D., Arentshorst, M., Nitsche, B.M., Morris, S., Nielsen, K.F., van den Hondel, C.A.M., Klis, F.M., and Ram, A.F.J. (2013). The transcriptional repressor TupA in Aspergillus niger is involved in controlling gene expression related to cell wall biosynthesis, development, and nitrogen source availability. PLoS One *8*, e78102.

Smedsgaard, J. (1997). Micro-scale extraction procedure for standardized screening of fungal metabolite production in cultures. J. Chromatogr. A *760*, 264–270.

Stanke, M., and Morgenstern, B. (2005). AUGUSTUS: a web server for gene prediction in eukaryotes that allows user-defined constraints. Nucleic Acids Res. *33* (Web Server issue), W465–W467.

Wattanachaisaereekul, S., Lantz, A.E., Nielsen, M.L., and Nielsen, J. (2008). Production of the polyketide 6-MSA in yeast engineered for increased malonyl-CoA supply. Metab. Eng. *10*, 246–254.

Williams, D.H., Stone, M.J., Hauck, P.R., and Rahman, S.K. (1989). Why are secondary metabolites (natural products) biosynthesized? J. Nat. Prod. *52*, 1189–1208.

Zabala, A.O., Xu, W., Chooi, Y.-H., and Tang, Y. (2012). Characterization of a silent azaphilone gene cluster from Aspergillus niger ATCC 1015 reveals a hydroxylation-mediated pyran-ring formation. Chem. Biol. *19*, 1049–1059.

SUPPORTING INFORMATION

Figures:

Tables:

Figure S1, related to Figure 2. BPC of *yanA*Δ strain relative to the reference KB1001, cultivated on MM (**A**), YES (**B**), CYA (**C**), and MEA (**D**) for 5 days at 30°C.

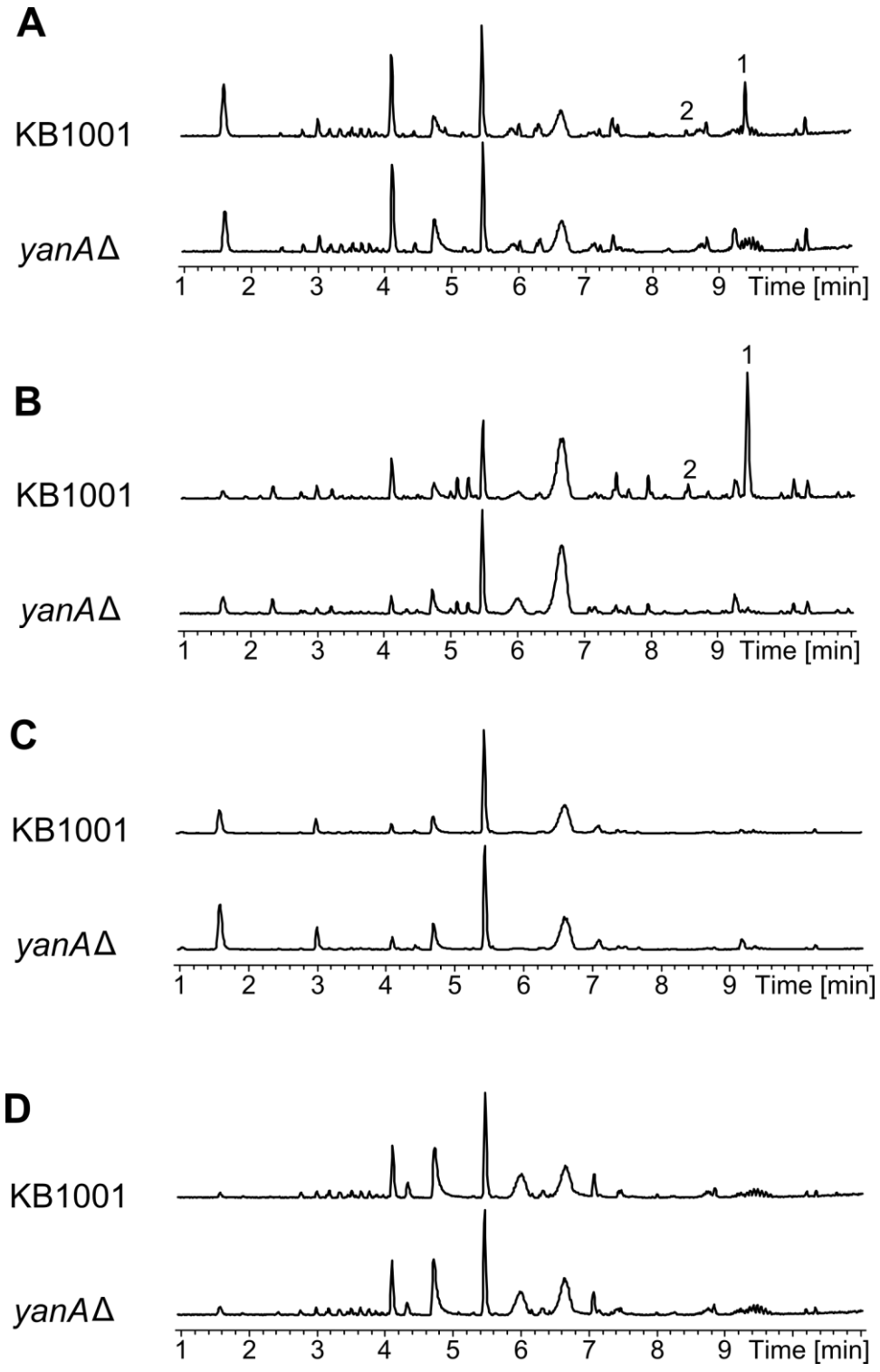

Figure S2, related to Figure 2. The morphology of *A. niger* KB1001 is identical with and without addition of $^{13}C_8$-6-MSA. The figure shows the top and bottom of KB1001 cultivated on YES medium for 5 days at 30 °C.

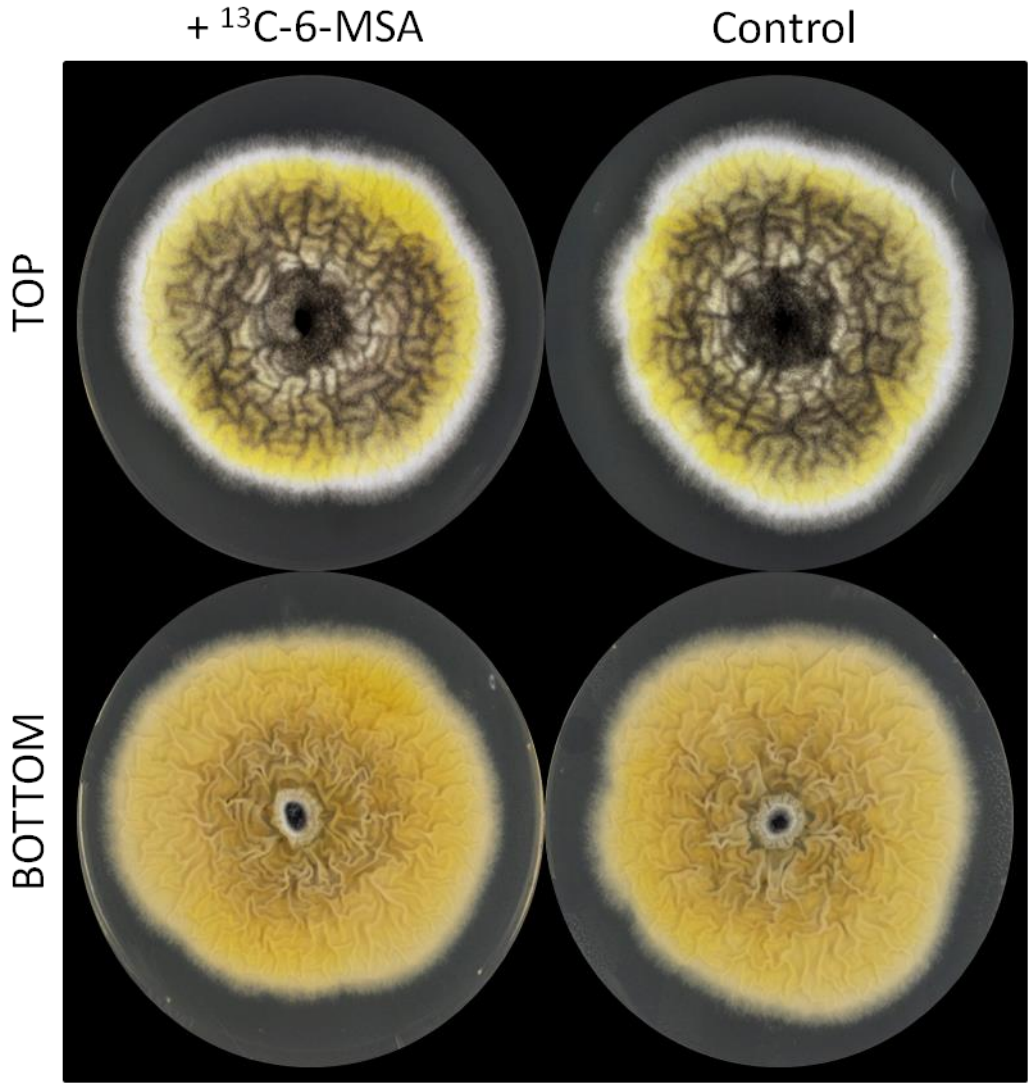

Figure S3, related to Figure 2. Positive electrospray **(**ESI+) mass spectrum of: **(A)** uniformly labeled $^{13}C_8$-6-methylsalicylic acid, **(B)** unlabeled and labeled yanuthone D**, (C)** unlabeled and labeled yanuthone E, and **(D)** unlabelled yanuthone X_1. The calculated shift from $^{12}C_7$ to $^{13}C_7$ is 7.0234 Da.

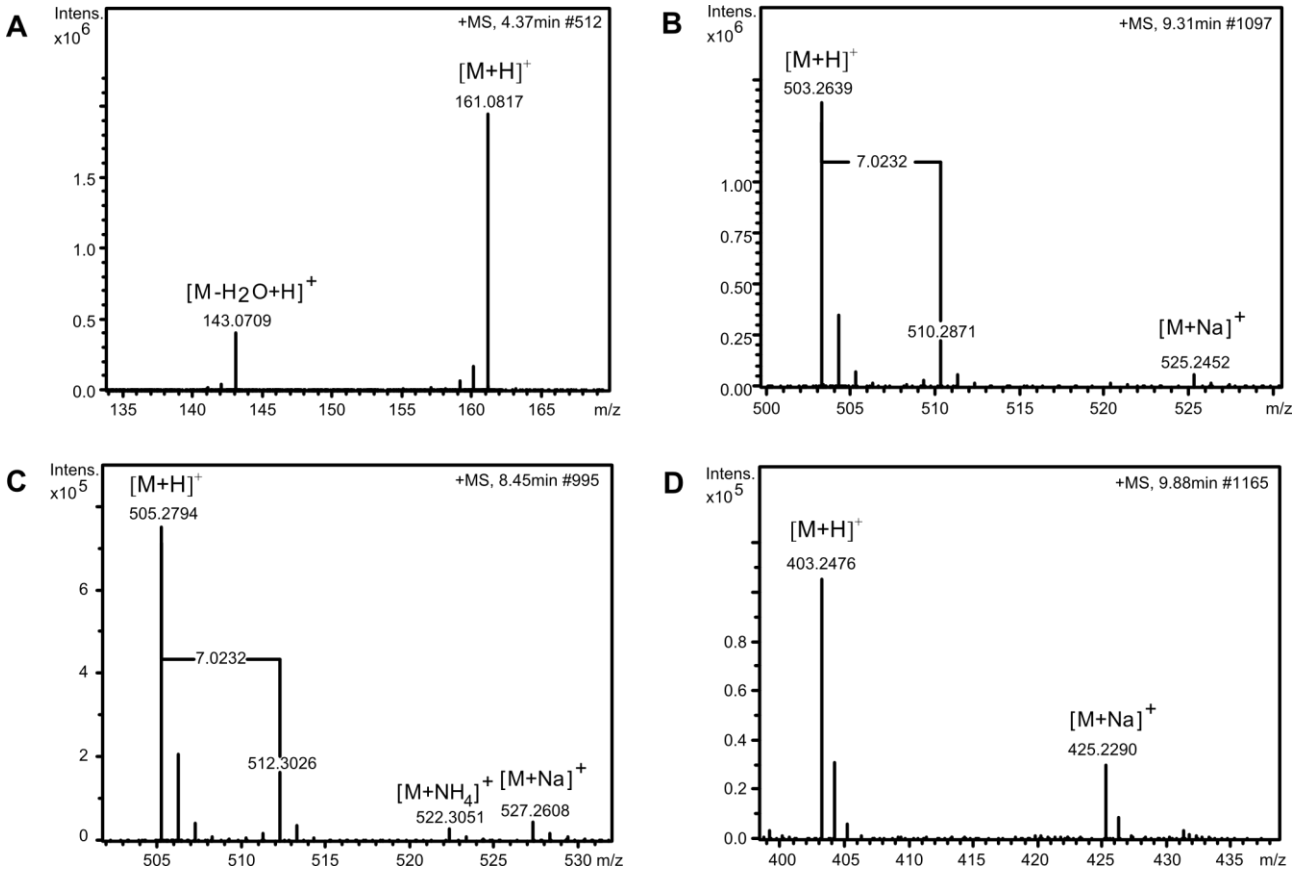

Figure S4, related to Figure 3. RT-qPCR expression analysis of *yanA* and 13 flanking genes in a *yanR*Δ (44961Δ) strain and a reference strain, KB1001. **A**. Absolute expression levels ($(\Delta c(t))^{-1}$ values) in KB1001 (grey bar) compared to the TFΔ strain (blue/red bar). Red bars indicate significant down-regulation (p-value <0.05), blue bars indicate non-significant changes (p-value >0.05). Error bars indicate the standard deviation (SD). Values are normalized to expression of *hhtA*. **B**. Relative expression levels (fold change, $2^{\Delta\Delta c(t)}$ values) of *yan* cluster genes (except *yanR*, which is deleted) in the TFΔ strain relative to KB1001. Error bars indicate the standard deviation (SD). Expression levels are individually normalized to expression of *actA* and *hhtA*, as indicated.

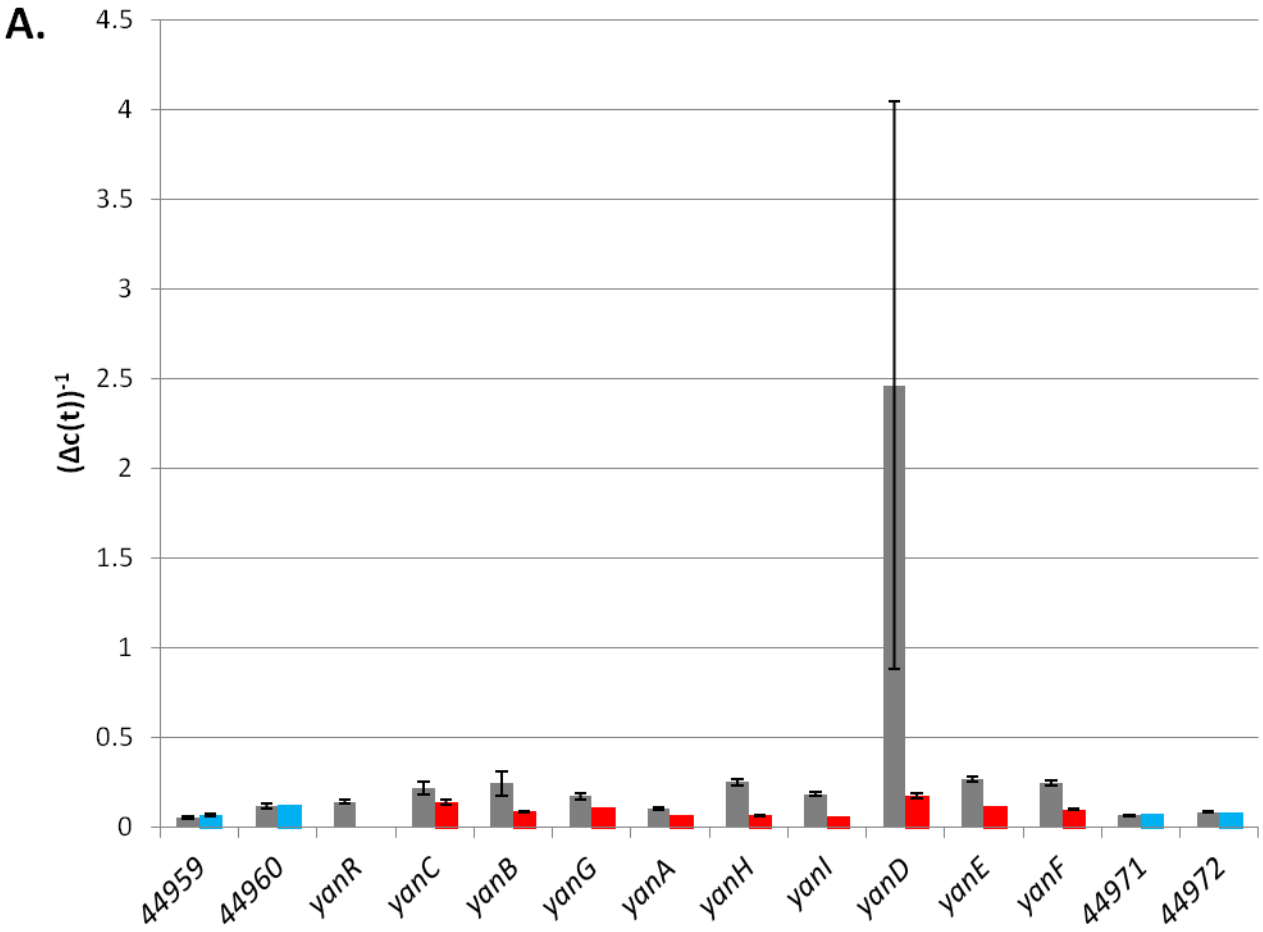
A.
4.5
4
3.5
3
2.5
2
1.5
1
0.5
0
(Δc(t))-1
44959
44960
yanR
yanC
yanB
yanG
yanA
yanH
yanI
yanD
yanE
yanF
44971
44972

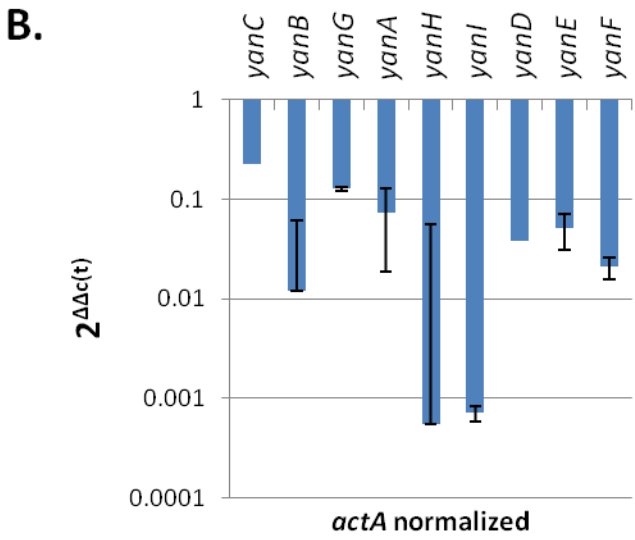
B.
yanC
yanB
yanG
yanA
yanH
yanI
yanD
yanE
yanF
1
0.1
0.01
0.001
0.0001
2ΔΔc(t)
actA normalized

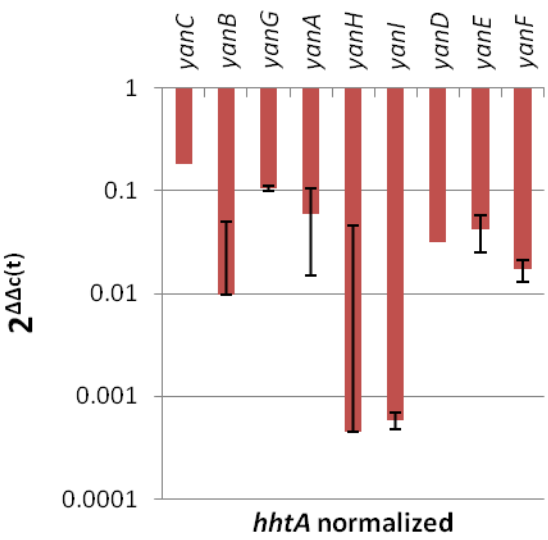
yanC
yanB
yanG
yanA
yanH
yanI
yanD
yanE
yanF
1
0.1
0.01
0.001
0.0001
2ΔΔc(t)
hhtA normalized

Figure S5, related to Figure 2. (**A)** Gene deletion in *A. niger*. The ORF is replaced by the selectable hygromycin B phosphatase (*hph*) gene. Not to scale. (**B)** pDHX2 vector used for expression of all cluster genes in the *A. nidulans* IS*1-yanA* strain. The vector contains the AMA1 sequence for autonomous replication in *Aspergillus* and the *pyrG* gene for selection.

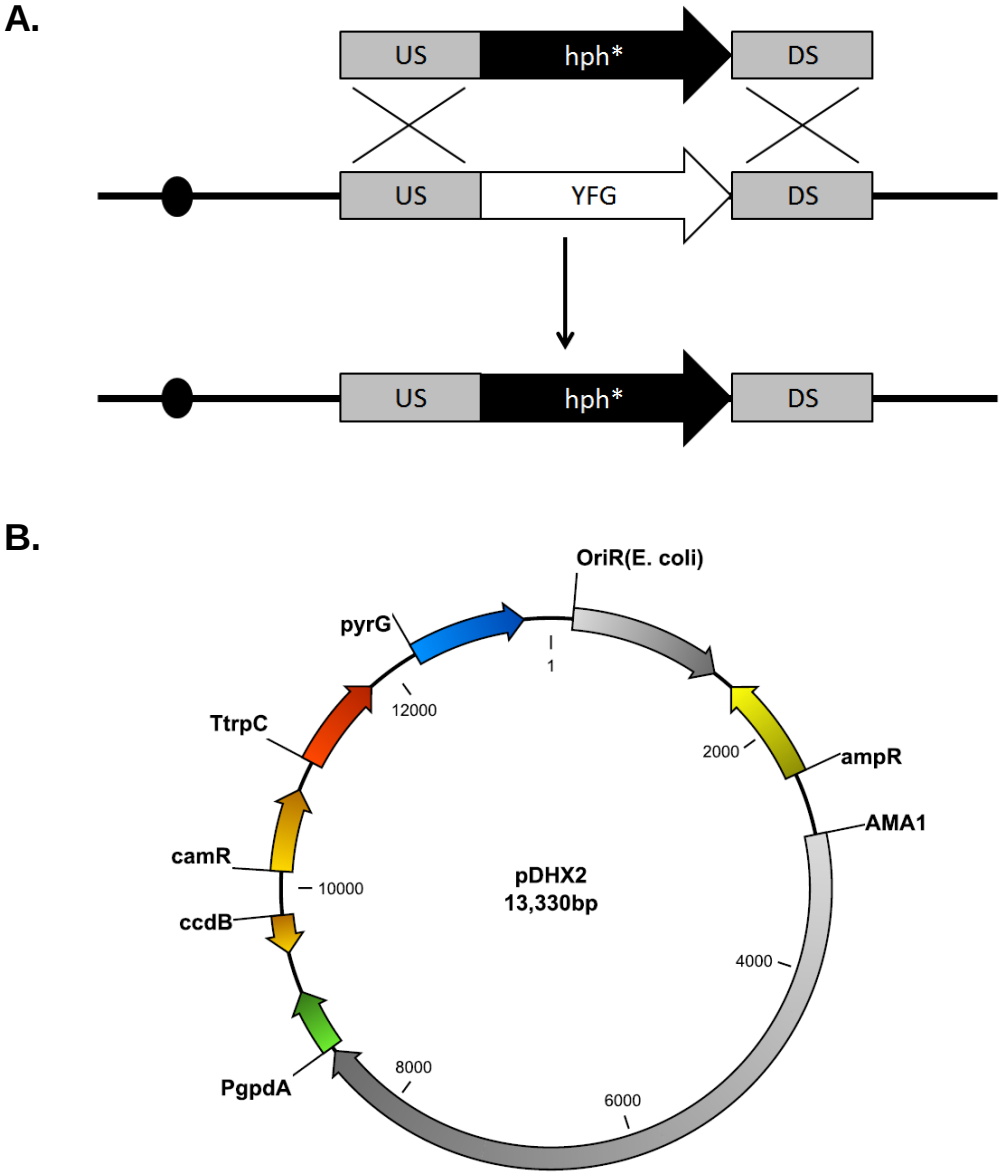

Figure S6, related to Figure 5. Base peak chromatogram (ESI+) of the five strains that express putative cluster genes *yanB*, *yanC*, *yanD*, *yanE*, and *yanG* in the *A. nidulans* IS*1*-*yanA* strain (6-MSA producing reference strain). All strains, except Oex-*yanB* still produce 6-MSA. IS = internal standard: chloroamphenicol, A = austinol, DHA = dehydroaustinol. Chromatograms are to scale.

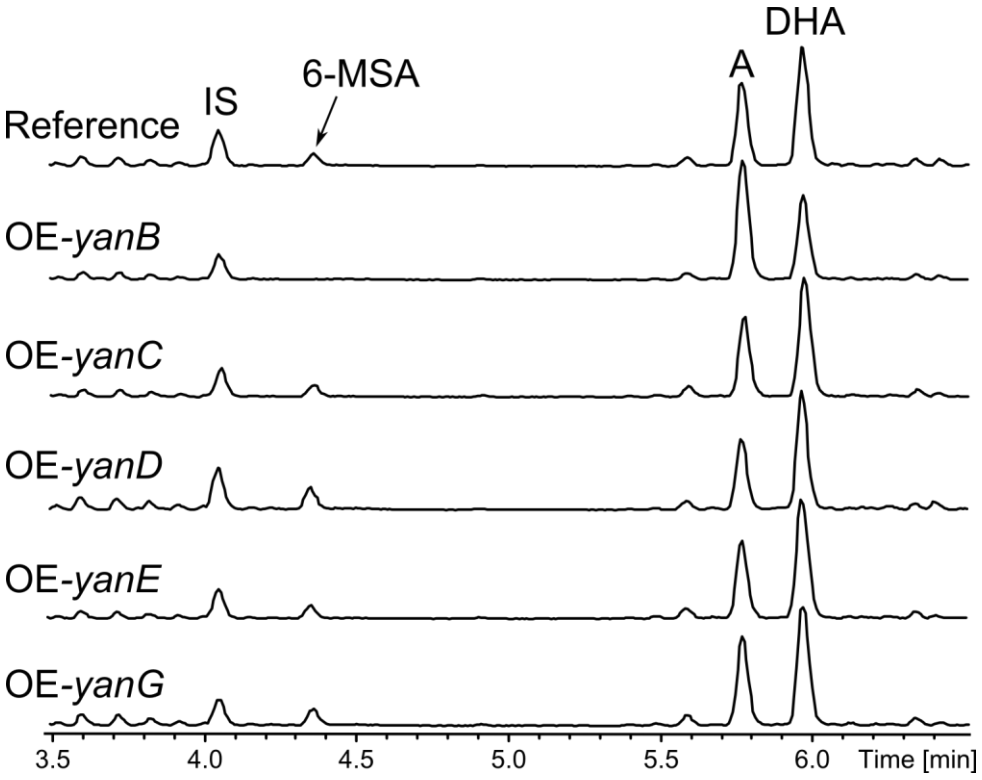

Table S1, related to Figures 2 and 4. Detection of metabolites in the deletion and overexpression strains using extracted ion chromatograms of $[M+H]^+ \pm 0.005$.

	6-MSA	Yanuthone D (**1**)	Yanuthone E (**2**)	7-deacetoxyyanuthone A (**3**)	Yanuthone F (**4**)	Yanuthone G (**5**)	22-deacetylyanutone A (**6**)	Yanuthone H (**7**)	Yanuthone I (**8**)	Yanuthone J (**9**)	Yanuthone X_1 (**12**)
KB1001	-	+	+	-	-	+	-	-	+	-	+
OE-*yanA*	+	-	-	-	-	-	-	-	-	-	-
*yanA*Δ	-	-	-	-	-	-	-	-	-	-	+
*yanB*Δ	-	-	-	-	-	+	-	-	+	-	+
*yanC*Δ	-	-	-	-	-	-	-	-	-	-	-
*yanD*Δ	-	-	-	-	-	-	-	-	-	-	-
*yanE*Δ	-	-	-	-	-	-	-	-	-	-	-
*yanF*Δ	-	-	+	+	-	-	-	-	+	+	+
*yanG*Δ	-	-	-	-	-	-	-	-	-	-	-
*yanH*Δ	-	-	-	+	+	+	-	-	-	-	+
*yanI*Δ	-	-	-	+	-	-	+	+	+	-	+
*yanR*Δ	-	-	-	+	-	+	-	-	-	-	+

Table S2, related to Figure 3. Overview of genes and proposed activities of the *yan* cluster.

Locus (ASPNIDRAFT_)	**Gene name**	**Predicted functional domains (CDD)**	**Proposed activity**
44959	-	No conservation	-
44960	-	Glyoxalase	-
44961	*yanR*	Fungal transcription factor	Transcription factor
54844	*yanC*	CYP450	*m*-Cresol hydroxylase
44963	*yanB*	Amidohydrolase, decarboxylase	6-MSA decarboxylase
44964	*yanG*	UbiA-like prenyltransferase	Prenyltransferase
44965	*yanA*	Polyketide synthase	6-MSA synthase
193092	*yanH*	CYP450	Cytochrome P450
44967	*yanI*	Membrane bound O-acyl transferase	O-Mevalon transferase
127904	*yanD*	Short-chain dehydrogenase	Dehydrogenase
192604	*yanE*	No conservation	-
44970	*yanF*	FAD/FMN-containing dehydrogenases	Oxidase
44971	-	No conservation	-
44972	-	No conservation	-

Table S3, related to Figure 4. Purification of metabolites

Compound name	Strain	Number of plates	Extraction	Isolera fractionation	Purification	Yield
Yanuthone D (**1**)	*A. niger* KB1001	200	EtOAc + 1 % FA	50g diol, 40 mL·min^{-1}, CV = 66 mL, auto fractionation, 15 fractions	Waters, Luna II C_{18}, 4 mL·min^{-1}, 40-100% ACN over 20 min.	4.5 mg
Yanuthone E (**2**)	*A. niger* KB1001	200	EtOAc + 1 % FA	50g diol, 40 mL·min^{-1}, CV = 66 mL, auto fractionation, 15 fractions	Gilson, Luna II C_{18}, 5 mL·min^{-1}, 40-100% ACN over 20 min.	2.9 mg
7-deacetoxy Yanuthone A (**3**)	*A. niger* KB1001	200	EtOAc + 1 % FA	50g diol, 40 mL·min^{-1}, CV = 66 mL, auto fractionation, 15 fractions	Waters, Luna II C_{18}, 4 mL·min^{-1}, 40-100% ACN over 20 min.	9.3 mg
Yanuthone F (**4**)	*yanH*Δ	100	EtOAc	25g diol, 25 mL·min^{-1}, CV = 33 mL, auto fractionation, 10 fractions	Gilson, Luna II C_{18}, 5 mL·min^{-1}, 30-80% ACN over 18 min. Waters, gemini, 5 mL·min^{-1}, 40-65% ACN over 20 min	1.8 mg
Yanuthone G (**5**)	*yanH*Δ	100	EtOAc	25g diol, 25 mL·min^{-1}, CV = 33 mL, auto fractionation, 10 fractions	Gilson, Luna II C_{18}, 5 mL·min^{-1}, 30-80% ACN over 18 min. Waters, gemini, 5 mL·min^{-1}, 30-40% ACN over 20 min, to 45% for 2 min.	4.0 mg
22-deacetylyanu-thone A (**6**)	*yanI*Δ	100	EtOAc	25g diol, 25 mL·min^{-1}, CV = 33 mL, auto fractionation, 12 fractions	Gilson, Luna II C_{18}, 5 mL·min^{-1}, 20-90% ACN over 17 min. Waters, Luna II C_{18}, 5 mL·min^{-1}, 30-100% ACN over 20 min.	7.3 mg
Yanuthone H (**7**)	*yanI*Δ	100	EtOAc	25g diol, 25 mL·min^{-1}, CV = 33 mL, auto fractionation, 12 fractions	Gilson, Luna II C_{18}, 5 mL·min^{-1}, 30-60% ACN over 16 min.	9.8 mg
Yanuthone I **(8)**	*yanI*Δ	100	EtOAc	25g diol, 25 mL·min^{-1}, CV = 33 mL, auto fractionation, 12 fractions	Waters, Luna II C_{18}, 5 mL·min^{-1}, 30-60% ACN over 16 min.	4.7 mg
Yanuthone J **(9)**	*yanF*Δ	150	EtOAc + 1 % FA	25g diol, 25 mL·min^{-1}, CV = 33 mL, auto fractionation, 15 fractions	Waters, Luna II C_{18}, 4 mL·min^{-1}, 20-100% ACN over 20 min.	1.5 mg
Yanuthone X_1 (**12**)	*A. niger* KB1001	200	EtOAc + 1 % FA	50g diol, 40 mL·min^{-1}, CV = 66 mL, auto fractionation, 15 fractions	Waters, gemini, 4 mL·min^{-1}, 90 % ACN isocratic for 15 min, then to 100 % ACN for 5 min.	1.5 mg

Table S4, related to Figure 6. Spectroscopic data

The structural elucidation of the compounds showed several similar features in the ^{1}H as well as 2D spectra comparable to those reported for the known yanuthones(Bugni *et al.*, 2000; Li *et al.*, 2003). All compounds except yanuthone I displayed 8H overlapping resonances at δ_H 1.93-2.11 ppm in the ^{1}H spectrum corresponding to the four methylene groups H4, H5, H8 and H9 in the sesquiterpene moiety. Other common resonances were from the diastereotopic pair H-12/H-12' and 3 methyl groups (H-19, H-20 and H-21) around δ_H 1.60 ppm, whereof H-20 and H-21 were overlapping. In the HMBC spectrum a correlation to the quaternary C-18 around δ_C 194 ppm was seen and all compounds also had two carbons around 60 ppm (one quaternary, one methine) being the carbons in the epoxide ring.

The compounds however differed greatly in the moiety attached to C-16. Yanuthone D, yanuthone E and yanuthone J all displayed two methylene groups around δ_C 45 ppm, a methyl group around δ_C 28 ppm, two carbonyls around δ_C 171 ppm and another quaternary carbon around δ_C 70 ppm for the mevalonic acid part. 7-deacetoxyanuthone A, yanuthone F and yanuthone G all had a methyl group attached at C-16 while yanuthone H, yanuthone I and 22-deacetylyanuthone A had a further hydroxy group at C-22. The hydroxylation in this position was indicated by a significant shift downfield of H-22/C-22.

Some structures had a further modification being a hydroxy group at either C-1 or C-2. The compounds yanuthone F, G and H all had a hydroxy group at C-1, shifting C-1 and H-1 significantly downfield. Yanuthone J had the hydroxy group attached at C-2 which shifted the resonances for C-2 and H-2 downfield, and due to the lack of the double bond in those structures, the resonance for H-3 was no longer observed in the double bond area but at δ_H 1.35 ppm. Yanuthone I differed in this part of the structure with fewer resonances due to the shorter terpene chain.

The ^{1}H NMR spectrum for yanuthone G stood out from the rest due to several resonances between 3-5 ppm. Elucidation of the structure revealed a sugar moiety attached to the hydroxy group at C-15. The presence of this hexose unit gave rise to the additional resonances observed.

The NMR data for yanuthone X_1 displayed the same resonances for the sesquiterpene part of the molecule, but the methoxy group attached to C-16 is different for all other reported yanuthones, and was obvious from the chemical shift of C-16 which gave rise to a resonance at δ_C 168.3 ppm, which is considerable further downfield than in the other structures. Furthermore C-17 was affected shifting upfield to δ_C 100.3 ppm. NMR data for all compounds can be found in invidual tabs in this file.

The stereochemistry of the compounds was investigated by circular dichroism (CD) and optical rotation. The CD data for yanuthone D, E and 7-deacetoxyyanuthone A showed that the positive and negative cotton effects were identical to those previously reported for these compounds (Bugni et al., 2000).

Table S4, related to Figure 6. Spectroscopic data. *Continued*

Yanuthone D

HRESIMS: *m/z* = 503.2640 $[M + H]^+$, calculated for $[C_{28}H_{38}O_8+H]^+$: 503.2639. $[\alpha]_{587}^{20} = 32.4°$
CD_{MeOH}: $[\theta]_{213}$ = 12.4263, $[\theta]_{230}$ = -7.8722, $[\theta]_{240}$ = 1.1769, $[\theta]_{260}$ = -4.0282, $[\theta]_{298}$ = 0.7690

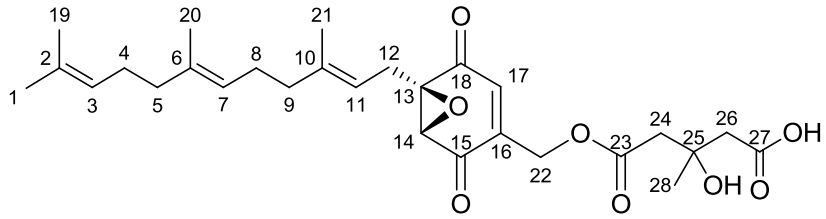

NMR data for yanuthone D

Atom assignment	^{1}H-chemical shift [ppm]/ J coupling constants [Hz]	^{13}C-chemical shift [ppm]	HMBC correlations	NOESY connectivities
1	1.59 (3H, s)	17.1	2, 19	-
2	-	132.1	-	-
3	5.10 (1H, m)	125.0	1, 19	19
4	2.06 (2H, m)	27.3	2, 3, 5/9	20
5	1.97 (2H, m)	40.2	3/7, 6, 4/8,20	20
6	-	136.4	-	-
7	5.09 (1H, m)	124.9	5/9, 8, 20	9
8	2.09 (2H, m)	27.0	5/9, 6, 7, 10	20, 21
9	1.99 (2H, m)	40.1	7, 8, 10, 11, 21	7, 11
10	-	141.0	-	-
11	5.03 (1H, t, 1.5)	116.4	9, 12, 21	9, 12, 12', 14
12	2.66 (1H, m)	25.6	10, 11, 13, 14, 15/18	11, 12', 14, 21
12'	2.76 (1H, m)	25.6	10, 11, 13, 14, 15/18	11, 12, 14, 21
13	-	63.0	-	-
14	3.68 (1H, s)	58.6	12, 13, 15/18, 16, 22	11, 12, 12', 21
15	-	193.2	-	-
16	-	143.9	-	-
17	6.58 (1H, t, 1.5)	133.1	13, 15/18, 22	22, 22', 24, 28
18	-	193.2	-	-
19	1.66 (3H, s)	25.7	1, 2, 3	3, 4
20	1.591 (3H, s)	16.1	5, 6, 7	5, 8
21	1.63 (3H, s)	16.2	9, 10, 11	8, 12, 12', 14
22	4.84 (1H, dd, 16.1, 1.5)	60.2	15/18, 16, 17, 23	17
22'	4.89 (1H, dd, 16.1, 1.5)	60.2	15/18, 16, 17, 23	17
23	-	171.2	-	-
24	2.69 (2H, m)	45.6	23, 26	17, 28
25	-	70.0	-	-
26	2.64 (1H, m)	45.1	24, 25, 28	28
26'	2.57 (1H, m)	45.1	27	-
27	-	173.1	-	-
28	1.33 (3H, s)	27.6	24, 25	17, 24, 26

Table S4, related to Figure 6. Spectroscopic data. *Continued*

Yanuthone E

HRESIMS: *m/z* = 505.2791 $[M + H]^+$, calculated for $[C_{28}H_{40}O_8+H]^+$: 505.2789. $[\alpha]_{587}^{20} = 11.7°$
CD_{MeOH}: $[\theta]_{209}$ = 2.1815, $[\theta]_{241}$ = -12.3941, $[\theta]_{340}$ = 7.4622

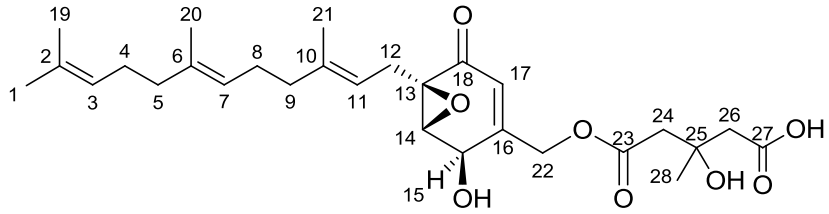

NMR data for yanuthone E

Atom assignment	^{1}H-chemical shift [ppm]/ J coupling constants [Hz]	^{13}C-chemical shift [ppm]	HMBC correlations	NOESY connectivities
1	1.58 (3H, s)	17.7	2, 3, 19	-
2	-	131.8	-	-
3	5.07 (1H, m)	124.9	1, 4, 5, 19	4, 5, 19
4	2.02 (2H, m)	27.2	2, 6	3
5	1.96 (2H, m)	40.3	3/7, 4, 6, 20,	3, 7
6	-	135.8	-	-
7	5.06 (1H, t, 6.4)	124.9	5/9, 8, 20	5, 9, 20
8	2.06 (2H, m)	27.2	5/9, 6, 7, 10	-
9	1.99 (2H, m)	40.3	6, 7, 8, 11, 21	7, 11
10	-	139.9	-	-
11	5.04 (1H, t, 7.2)	117.7	9, 12, 13, 21	9, 12, 12’, 14
12	2.67 (1H, m)	26.6	10, 11, 13, 14, 18	11, 12’, 14
12’	2.42 (1H, m)	26.6	10, 11, 13, 14, 18	11, 12, 14
13	-	61.3	-	-
14	3.64 (1H, d, 2.8)	60.1	12/12’, 13, 15, 16, 22/22’,	11, 12, 12’ 15
15	4.68 (1H, br. s)	65.8	16, 17	14
16	-	154.6	-	-
17	5.86 (1H, q, 1.4)	121.6	13, 15, 16, 22, 22’	22, 22’, 24
18	-	194.8	-	-
19	1.66 (3H, s)	25.6	1, 2, 3	3
20	1.581 (3H, s)	16.0	5, 6, 7	7
21	1.62 (3H, s)	16.3	9, 10, 11	-
22	4.82 (1H, d, 16.1)	63.6	15, 16, 17, 18, 23	17, 22’
22’	4.76 (1H, d, 16.1)	63.6	15, 16, 17, 18, 23	17, 22
23	-	171.4	-	-
24	2.69 (2H, m)	45.8	23, 25, 26, 28	17
25	-	70.2	-	-
26	2.59 (2H, m)	45.4	24, 25, 27, 28	-
27	-	173.5	-	-
28	1.33 (3H, s)	27.7	25, 26	-

Table S4, related to Figure 6. Spectroscopic data. *Continued*

Yanuthone J

HRESIMS: *m/z* = 523.2907 $[M + H]^+$, calculated for $[C_{28}H_{42}O_9+H]^+$: 523.2901 $[\alpha]_{587}^{20} = 3.6°$

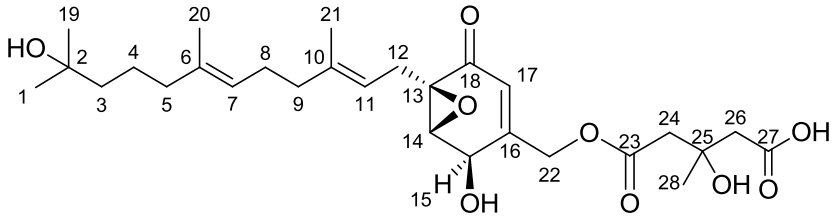

NMR data for yanuthone J

Atom assignment	^{1}H-chemical shift [ppm]/ J coupling constants [Hz]	^{13}C-chemical shift [ppm]	HMBC correlations
1	1.28 (3H, m)	29.7	-
2	-	70.9	-
3	1.35 (2H, m)	44.0	4, 19
4	1.43 (2H, m)	23.1	-
5	1.93 (2H, m)	40.5	3, 4, 6, 7, 11, 20
6	-	136.3	-
7	5.08 (1H, tq, 6.3, 1.0)	124.4	-
8	2.09 (2H, m)	26.7	6, 7, 9, 10
9	2.02 (2H, m)	40.3	7, 8, 10, 11, 21
10	-	139.6	-
11	5.03 (1H, tq, 6.3, 1.0)	117.5	-
12	2.45 (1H, m)	26.5	10, 11, 13, (18)
12’	2.68 (1H, m)	26.5	10, 11, 13
13	-	61.1	-
14	3.63 (1H, d, 2.8)	59.9	13, 15, 16
15	4.69 (1H, m)	65.7	-
16	-	154.7	-
17	5.86 (1H, q, 1.5)	121.5	13, 15, 22
18	-	(194.2)	-
19	1.12 (3H, s)	29.2	1, 2, 3
20	1.58 (3H, s)	15.9	5, 6, 7
21	1.62 (3H, s)	16.2	9, 10, 11
22	4.83 (1H, d, 16.0)	63.6	16, 17, 23
22’	4.76 (1H, d, 16.0)	63.6	16, 17, 23
23	-	171.2	-
24	2.681 (2H, m)	43.7	23, 25, 26, 28
25	-	70.9	-
26	2.61 (2H, m)	45.1	24, 25, 27, 28
27	-	173.6	-
28	1.33 (3H, s)	27.5	25, 26

Table S4, related to Figure 6. Spectroscopic data. *Continued*

7-deacetoxyyanuthone A

HRESIMS: *m/z* = 345.2434 $[M + H]^+$, calculated for $[C_{22}H_{32}O_3+H]^+$: 345.2424 $[\alpha]_{587}^{20} = 20.0°$
CD_{MeOH}: $[\theta]_{206}$ = -13.6324, $[\theta]_{242}$ = -25.0218, $[\theta]_{335}$ = 16.7472

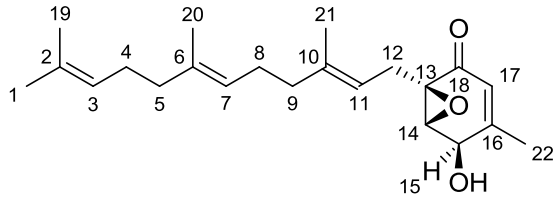

NMR data for 7-deacetoxyyanuthone A

Atom assignment	**^{1}H-chemical shift [ppm]/ J coupling constants [Hz]**
1	1.67 (3H, d 1.0)
2	-
3	5.10 (1H, m)
4	2.07-1.90 (2H, m)
5	2.07-1.90 (2H, m)
6	-
7	5.09 (1H, m)
8	2.07-1.90 (2H, m)
9	2.07-1.90 (2H, m)
10	-
11	5.05 (1H, m)
12	2.72 (1H, dd, 15.2, 7.9)
12’	2.39 (1H, dd, 15.2, 6.7)
13	-
14	3.62 (1H, d, 2.89)
15	4.49 (1H, br. s)
16	-
17	5.70 (1H, p, 1.5)
18	-
19	1.60 (3H, s)
20	1.59 (3H, s)
21	1.64 (3H, s)
22	2.07-1.90 (3H, m)

Table S4, related to Figure 6. Spectroscopic data. *Continued*

Yanuthone F

HRESIMS: *m/z* = 361.2373 [M + H]$^+$, calculated for [$C_{22}H_{32}O_4$+H]$^+$: 361.2373 $[\alpha]_{587}^{20} = 14.2°$

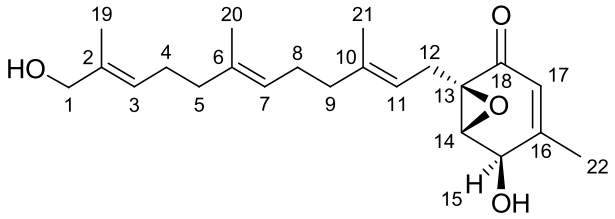

NMR data for yanuthone F

Atom assignment	^{1}H-chemical shift [ppm]/ J coupling constants [Hz]	^{13}C-chemical shift [ppm]	HMBC correlations	NOESY connectivities
1	3.84 (2H, br. s)	68.3	2, 3, 19	3, 5
2	-	136.2	-	-
3	5.33 (1H, tq, 7.4, 1.5)	125.3	1, 19	1, 4, 5
4	2.11 (2H, m)	26.8	2, 5, 6	3, 7
5	1.99 (2H, m)	40.1	2/6, 4/8, 20	1, 3, 7
6	-	136.2	-	-
7	5.09 (1H, tq, 6.9, 1.1)	124.9	4/8, 5/9, 20	4, 5, 8, 9
8	2.07 (2H, m)	26.8	6, 5/9, 10	7
9	2.01 (2H, m)	40.1	6, 8/12, 10, 21	7, 11, 14
10	-	139.7	-	-
11	5.04 (1H, tq, 7.3, 1.2)	118.0	8/12, 9, 21	9, 12, 12', 14
12	2.70 (1H, dd, 15.1, 8.1)	27.0	10, 11, 13	11, 12', 14
12'	2.37 (1H, m)	27.0	10, 11, 13, 18	11, 12, 14
13	-	61.4	-	-
14	3.60 (1H, d, 2.7)	60.2	13, 15, 16	9, 11, 12, 12', 15
15	4.48 (1H, m)	67.6	16, 17	14, 22
16	-	158.8	-	-
17	5.68 (1H, m)	123.2	13, 15, 22	22
18	-	194.9	-	-
19	1.59 (3H, s)	13.5	1, 2, 3, 4	-
20	1.591 (3H, s)	16.1	5, 6, 7	-
21	1.62 (3H, s)	16.1	6, 10, 11, 13	-
22	1.92 (2H, br. s)	20.0	15, 16	15, 17

Table S4, related to Figure 6. Spectroscopic data. *Continued*

Yanuthone G

HRESIMS: *m/z* = 523.2917 $[M + H]^+$, calculated for $[C_{28}H_{42}O_9+H]^+$: 523.2901. $[\alpha]_{587}^{20} = 19.6°$

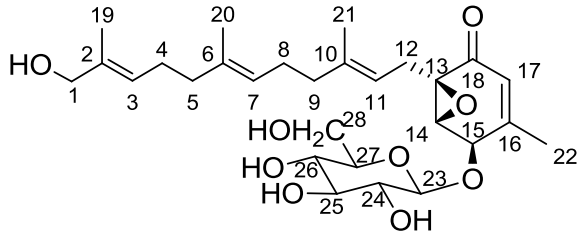

NMR data for yanuthone G

Atom assignment	^{1}H-chemical shift [ppm]/ J coupling constants [Hz]	^{13}C-chemical shift [ppm]	HMBC correlations	NOESY connectivities
1	3.86 (2H, s)	68.2	2, 3, 19	3, 19
2	-	135.9	-	-
3	5.34 (1H, t, 6.3)	125.2	1, 4, 5, 19	1
4	2.10 (2H, m)	26.8	2/6, 3, 5	5, 20
5	1.99 (2H, m)	40.0	2/6, 4/8, 7, 20	4, 7
6	-	135.9	-	-
7	5.10 (1H, t, 6.3)	124.9	4/8, 5/9, 20	5, 9
8	2.06 (2H, m)	26.9	5/9, 6, 10	9, 20, 21
9	2.02 (2H, m)	40.0	6, 8/12, 10, 11, 21	7, 8, 11, 14
10	-	139.7	-	-
11	5.04 (1H, t, 6.7)	117.9	8/12, 9, 21	9, 12, 12’, 14, 15
12	2.67 (1H, m)	26.9	10, 11, 13, 18	11, 14, 21
12'	2.37 (1H, dd, 14.8, 6.2)	26.9	10, 11, 13, 18	11, 14, 21
13	-	61.3	-	-
14	3.82 (1H, br. s)	59.7	15, 16	9, 11, 12, 12’, 15, 17, 21
15	4.59 (1H, m)	76.2	23	11, 14, 17
16	-	157.0	-	-
17	5.71 (1H, br. s)	123.9	13, 15, 22	14, 15, 27
18	-	194.4	-	-
19	1.591 (3H, s)	13.7	1, 2, 3	1
20	1.59 (3H, s)	15.9	5, 6, 7	4, 8
21	1.62 (3H, s)	16.3	9, 10, 11	8, 12, 12’, 14
22	1.97 (3H, m)	20.1	15, 16	26, 27
23	4.56 (1H, m)	105.7	16	24, 25, 26, 27, 28, 28’
24	3.25 (1H, br. s)	74.6	23, 26/27	23, 25, 26, 27
25	3.37 (1H, m)	77.2	-	23, 24, 26, 27, 28, 28’
26	3.35 (1H, m)	71.2	-	22, 23, 24, 25, 27, 28, 28’
27	3.35 (1H, m)	77.2	-	17, 22, 23, 24, 25, 26, 28, 28’
28	6.77 (1H, d, 10.7)	62.6	-	23, 25, 26, 27, 28’
28’	3.66 (1H, d, 10.7)	62.6	-	23, 25, 26, 27, 28

Table S4, related to Figure 6. Spectroscopic data. *Continued*

22-deacetylyanuthone A

HRESIMS: *m/z* = 361.2372 $[M + H]^+$, calculated for $[C_{22}H_{32}O_4+H]^+$: 361.2373 $[\alpha]_{587}^{20} = 30.6°$

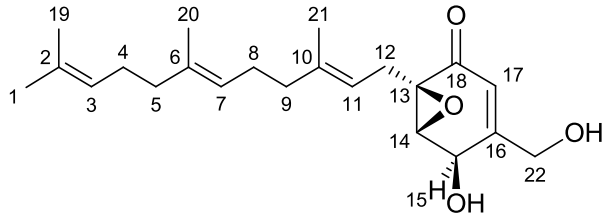

NMR data for 22-deacetylyanuthone A

Atom assignment	^{1}H-chemical shift [ppm]/ J coupling constants [Hz]	^{13}C-chemical shift [ppm]	HMBC correlations	NOESY connectivities
1	1.66 (3H, s)	25.8	2, 3, 19	-
2	-	132.0	-	-
3	5.10 (1H, m)	124.9	1, 4, 5, 19	4, 5, 19
4	2.07 (2H, m)	26.8	2, 5, 6	3, 5, 19, 20
5	1.98 (2H, m)	40.1	4/8, 6, 3/7, 20	3, 4, 7
6	-	136.0	-	
7	5.10 (1H, m)	124.9	4/8, 5/9, 20	8, 5/9, 20
8	2.09 (2H, m)	26.8	5/9, 6, 7, 10	7, 9, 20, 21
9	2.03 (2H, m)	40.1	7, 10, 11, 13, 8/12, 21	7, 8, 11
10	-	140.2	-	-
11	5.05 (1H, ddd, 7.93, 6.71, 1.22)	118.0	9, 8/12, 13, 21	9, 12, 12', 14, 21
12	2.70 (1H, dd, 15.3, 7.9)	26.8	10, 13, 17, 18	11, 12', 14, 21
12'	2.42 (1H, dd, 15.3, 6.7)	26.8	10, 13, 17, 18	11, 12, 14, 21
13	-	61.6	-	-
14	3.62 (1H, d, 2.8)	60.2	12,15, 16, 22	11, 12, 12', 15
15	4.64 (1H, m)	66.2	13, 16, 17, 18	14, 22, 22'
16	-	160.8	-	-
17	5.87 (1H, q, 1.73)	119.7	15, 16, 22	22, 22'
18	-	195.1	-	-
19	1.601 (3H, s)	17.7	1, 2, 3	3, 4
20	1.60 (3H, s)	15.9	5, 6, 7	4, 7, 8
21	1.63 (3H, s)	16.2	8/12, 9, 10, 11, 13	8, 11, 12, 12'
22	4.27 (1H, m)	62.0	15	15, 17
22'	4.21 (1H, m)	62.0	-	15, 17

Table S4, related to Figure 6. Spectroscopic data. *Continued*

Yanuthone H

HRESIMS: *m/z* = 377.2332 $[M + H]^+$, calculated for $[C_{22}H_{32}O_5+H]^+$: 377.2322. $[\alpha]_{587}^{20} = 27.7°$

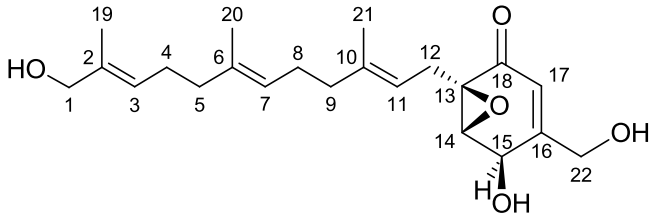

NMR data for yanuthone H

Atom assignment	^{1}H-chemical shift [ppm]/ J coupling constants [Hz]	^{13}C-chemical shift [ppm]	HMBC correlations	NOESY connectivities
1	3.85 (2H, s)	68.3	2, 3, 4, 19	3
2	-	136.0	-	-
3	5.34 (1H, m)	125.4	1, 4, 5, 19	1, 5
4	2.11 (2H, m)	26.8	3, 5, 6	-
5	1.99 (2H, m)	40.1	4/8, 6, 7, 12, 20	3
6	-	135.9	-	-
7	5.10 (1H, t, 6.4)	124.9	4/8, 5/9, 20	9
8	2.07 (2H, m)	26.8	5/9, 7, 10	-
9	2.02 (2H, m)	40.1	7, 10, 11, 8/12, 21	7, 11
10	-	139.8	-	-
11	5.05 (1H, t, 6.8)	118.0	8/12, 21	9, 12, 12', 14
12	2.71 (1H, dd, 15.1, 8.3)	26.8	10, 11, 13, 18	11, 12', 14
12'	2.40 (1H, dd, 15.1, 6.8)	26.8	20, 11, 13, 18	11, 12, 14
13	-	60.9	-	-
14	3.62 (1H, d, 2.9)	60.4	12, 13, 15, 16	11, 12, 12' 15
15	4.64 (1H, br. s)	66.1	16, 17	14, 16, 17
16	-	160.6	-	15
17	5.87 (1H, d, 1.5)	119.7	13, 15, 16	15, 22, 22'
18	-	194.9	-	-
19	1.601 (3H, s)	13.5	1, 2	-
20	1.60 (3H, s)	16.1	5/8, 7	-
21	1.63 (3H, s)	16.2	8/12, 10, 11	-
22	4.27 (1H, d, 17.6)	62.0	15, 16, 17, 18	17, 22'
22'	4.21 (1H, m)	62.0	15, 16, 17, 18	17, 22

Table S4, related to Figure 6. Spectroscopic data. *Continued*

Yanuthone I

HRESIMS: *m/z* = 325.1635 [M + H]$^+$, calculated for [$C_{17}H_{24}O_6$+H]$^+$: 325.1646. $[\alpha]_{587}^{20} = 21.1°$

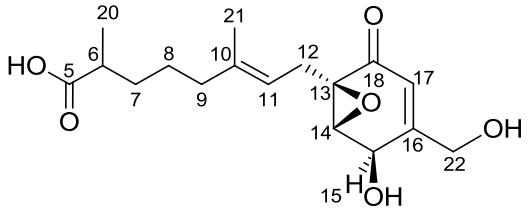

NMR data for yanuthone I

Atom assignment	^{1}H-chemical shift [ppm]/ J coupling constants [Hz]	^{13}C-chemical shift [ppm]	HMBC correlations	NOESY connectivities
5	-	177.4	-	-
6	2.28 (1H, m)	38.2	5, 7/7', 8, 20	7, 7', 8, 20
7	1.48 (1H, m)	32.5	5, 6, 8, 20	6, 7', 8, 9, 20
7'	1.26 (1H, m)	32.5	5, 6, 8, 20	6, 7, 8, 9, 21
8	1.32 (2H, m)	24.5	7/7', 9, 10	6, 7, 7', 9, 11, 20
9	1.92 (2H, t, 7.1)	38.7	7/7', 8, 10, 11, 21	7, 7', 8, 11, 14
10	-	137.9	-	-
11	5.00 (1H, t, 7.1)	116.9	9, 12/12', 13, 21	8, 9, 12, 12', 14
12	2.63 (1H, dd, 15.1, 7.9)	25.7	10, 11, 13, 14, 17, 18	12', 14, 17, 21
12'	2.32 (1H, m)	25.7	9, 10, 11, 13, 14, 17, 18	12, 14, 17, 21
13	-	60.0	-	-
14	3.59 (1H, d, 2.4)	59.1	12/12', 13/22/22', 15, 16	9, 11, 12, 12', 15, 17, 21
15	4.61 (1H, br. S)	64.3	16, 17	14, 22'
16	-	162.2	-	-
17	5.82 (1H, d, 1.6)	117.4	13/22/22', 14, 15, 16, 18	22'
18	-	193.7	-	-
20	1.02 (3H, d, 6.7)	16.7	5, 6, 7	6, 7, 7', 8
21	1.56 (3H, s)	15.6	9, 10, 11, 12/12', 13	7', 9, 12, 12', 14
22	4.21 (1H, d, 18.5)	60.0	15, 16, 17, 18	22'
22'	4.09 (1H, d, 18.5)	60.0	15, 16, 17, 18	15, 17, 22
-COOH	12.01 (1H, br. s)	-		

Table S4, related to Figure 6. Spectroscopic data. *Continued*

Yanuthone X_1

HRESIMS: *m/z* = 403.2482 $[M + H]^+$, calculated for $[C_{17}H_{24}O_6+H]^+$: 403.2479 $[\alpha]_{587}^{20} = 2.5°$

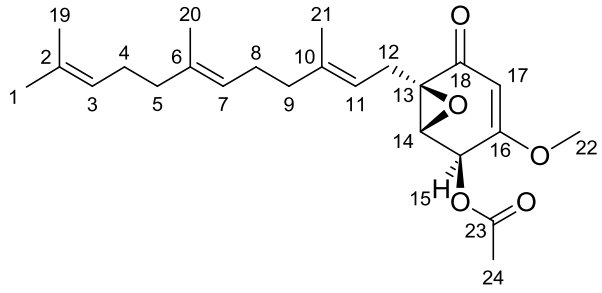

NMR data for yanuthone X_1

Atom assignment	^{1}H-chemical shift [ppm]/ J coupling constants [Hz]	^{13}C-chemical shift [ppm]	HMBC correlations	NOESY correlations
1	1.66 (3H, s)	25.6	2, 3, 19	3
2	-	132.2	-	-
3	5.08 (1H, m)	125.0	5	1, 4/5
4	2.05 (2H, m)	27.6	3, 5, 6	3, 5
5	2.00 (2H, m)	40.3	6, 4/8, 7, 11	3, 4
6	-	135.6	-	-
7	5.08 (1H, m)	125.0	5/9, 20	-
8	2.07 (2H, m)	27.6	5/9, 6, 7	9
9	1.95 (2H, m)	40.3	7, 8, 10, 11, 21	8, 11
10	-	139.8	-	-
11	5.01 (1H, t, 7.3)	117.5	9, 21	9, 12, 12’
12	2.78 (1H, dd, 15.3, 8.2)	26.2	10, 11, 13, 14	11, 12’
12’	2.45 (1H, dd, 15.3, 6.7)	26.2	10, 11, 13, 14, 18	11, 12
13	-	60.5	-	-
14	3.59 (1H, d, 3.1)	56.3	15, 16	15
15	5.95 (1H, d, 3.1)	66.6	16	14
16	-	168.3	-	-
17	5.30 (1H, s)	100.3	13, 15, 16	22
18	-	193.7	-	-
19	1.57 (3H, s)	17.6	1, 2, 3	-
20	1.571 (3H, s)	15.8	5, 6	-
21	1.61 (3H, s)	16.3	9, 10, 11	-
22	3.67 (3H, s)	57.4	16	17
23	-	170.7	-	-
24	2.14 (3H, s)	20.6	23	-

Table S5, related to Figures 2, 3, and 4. Fungal strains.

Name	Organism	Genotype
IBT 29539	*A. nidulans*	*argB2*, *pyrG89*, *veA1*, *nkuA*Δ
OE-*yanA*	*A. nidulans*	*argB2*, *pyrG89*, *veA1*, *nkuA*Δ S1::P*gpdA*::*yanA*::T*trpC*::*argB*
OE-*yanG*	*A. nidulans*	*argB2*, *pyrG89*, *veA1*, *nkuA*Δ IS1::P*gpdA*::*yanA*::T*trpC*::*argB*, pDHX2::*yanG*
OE-*yanC*	*A. nidulans*	*argB2*, *pyrG89*, *veA1*, *nkuA*Δ IS1::P*gpdA*::*yanA*::T*trpC*::*argB*, pDHX2::*yanC*
OE-*yanB*	*A. nidulans*	*argB2*, *pyrG89*, *veA1*, *nkuA*Δ IS1::P*gpdA*::*yanA*::T*trpC*::*argB*, pDHX2::*yanB*
OE-*yanD*	*A. nidulans*	*argB2*, *pyrG89*, *veA1*, *nkuA*Δ IS1::P*gpdA*::*yanA*::T*trpC*::*argB*, pDHX2::*yanD*
OE-*yanE*	*A. nidulans*	*argB2*, *pyrG89*, *veA1*, *nkuA*Δ IS1::P*gpdA*::*yanA*::T*trpC*::*argB*, pDHX2::*yanE*
KB1001	*A. niger*	*pyrG*Δ *kusA*::*AFpyrG*
*yanA*Δ	*A. niger*	*pyrG*Δ *kusA*::*AFpyrG yanA*Δ
*yanG*Δ	*A. niger*	*pyrG*Δ *kusA*::*AFpyrG yanG*Δ
*yanI*Δ	*A. niger*	*pyrG*Δ *kusA*::*AFpyrG yanI*Δ
*yanC*Δ	*A. niger*	*pyrG*Δ *kusA*::*AFpyrG yanC*Δ
*yanB*Δ	*A. niger*	*pyrG*Δ *kusA*::*AFpyrG yanB*Δ
*yanH*Δ	*A. niger*	*pyrG*Δ *kusA*::*AFpyrG yanH*Δ
*yanD*Δ	*A. niger*	*pyrG*Δ *kusA*::*AFpyrG yanD*Δ
*yanE*Δ	*A. niger*	*pyrG*Δ *kusA*::*AFpyrG yanE*Δ
*yanF*Δ	*A. niger*	*pyrG*Δ *kusA*::*AFpyrG yanF*Δ
*yanR*Δ	*A. niger*	*pyrG*Δ *kusA*::*AFpyrG yanR*Δ
44959Δ	*A. niger*	*pyrG*Δ *kusA*::*AFpyrG* ASPNI_DRAFT44959Δ
44960Δ	*A. niger*	*pyrG*Δ *kusA*::*AFpyrG* ASPNI_DRAFT44960Δ
44971Δ	*A. niger*	*pyrG*Δ *kusA*::*AFpyrG* ASPNI_DRAFT44971Δ
44972Δ	*A. niger*	*pyrG*Δ *kusA*::*AFpyrG* ASPNI_DRAFT44972Δ
ClusterΔ	*A. niger*	*pyrG*Δ *kusA*::*AFpyrG* ASPNI_DRAFT44958-44972Δ

Table S6, related to Figures 2, 3, and 4. Primers used in the study. See details in experimental section.

#	Primer name	Sequence 5'→ 3'
1	44965-fw	AGAGCGAUATGCCAGGCCTTGTACAC
2	44965-rv	TCTGCGAUTTAAGCATCCAGCTCCTTTGT
3	44963_ORF_FW	AGAGCGAUATGGACCGTATCGACGTACACC
4	44963_ORF_RV	TCTGCGAUCTAGGTACTATAAGTATGAACACGAGACTG
5	44964_ORF_FW	AGAGCGAUATGTCTACTACTAAGCGCTCGGTAAC
6	44964_ORF_RV	TCTGCGAUCTAGTATACTTTCATGGGTGCGTGA
7	54844_ORF_FW	AGAGCGAUCGGGCTAGACTTTCTCTTCCTAAG
8	54844_ORF_RV	TCTGCGAUATGGCGCTTGTTCATCTGACT
9	127904_ORF_FW	AGAGCGAUATGGTCAAGTTTTTTCAGCCCA
10	127904_ORF_RV	TCTGCGAUCTAACGGAACTGGGGAGGAA
11	192604_ORF_FW	AGAGCGAUTACTTTGCGACTACCTGCCATG
12	192604_ORF_RV	TCTGCGAUCTACTCCGACTTTTCACCTTTGG
13	hph-1003-Fw	AGCCCAATAUGCTAGTGGAGGTCAACACATCA
14	hph-1003-Rv	ATTACCTAGUCGGTCGGCATCTACTCTATT
15	44965-chk-usF	CAGTTGACTAGACTAGGAACGGTCA
16	44965-chk-dsR	AACGACCATGATGCTTGTTCAG
17	44965_US-FW	GGGTTTAAUATGACTCCACATCATCTTCCACAC
18	44965_US-RV	ATATTGGGCUGATGGTGTGTACAAGGCCTGG
19	44965_DS-FW	ACTAGGTAAUGACTGTTATGCATTGAATTTGAGC
20	44965_DS-RV	GGTCTTAAUAGATCCTGACGCTCATATCTGCT
21	44964_US-FW	GGGTTTAAUGGTCTTTCCGACACGTAAGTCTG
22	44964_US-RV	ATATTGGGCUTGGACCTCAATGGCCGCT
23	44964_DS-FW	ACTAGGTAAUGCGAGTATGAAGAAGGTGGATGA
24	44964_DS-RV	GGTCTTAAUATTCAGGGTCTTGAGATTGGC
25	44963_US-FW	GGGTTTAAUAAGTCCTCCCACGTCGGAG
26	44963_US-RV	ATATTGGGCUAGAATCTAAACCTTGTCTCTTCGCT
27	44963_DS-FW	ACTAGGTAAUGAACGTTTGATTGGTAATGGATGT
28	44963_DS-RV	GGTCTTAAUTCATCCACCTTCTTCATACTCGC
29	54844_US-FW	GGGTTTAAUGTAGAATAACAGCTACCTCGAATTTGA
30	54844_US-RV	ATATTGGGCUACGTGGTGCGTAAGCAGACAT
31	54844_DS-FW	ACTAGGTAAUCCTGCTGAATAAACACGAAGG
32	54844_DS-RV	GGTCTTAAUATGGACCGTATCGACGTACACC
33	44960_US-FW	GGGTTTAAUTGAGTACCTATCCACTCTTCCTGG
34	44960_US-RV	ATATTGGGCUGATGGAGTGTGAAGCCAATGAG
35	44960_DS-FW	ACTAGGTAAUTCATTCTAAAATTGGCGTCTTCA
36	44960_DS-RV	GGTCTTAAUCTACTGCCGCCGTCACTATCTA
37	193092_US-FW	GGGTTTAAUCATCGACATCTCTCTGCCCAT
38	193092_US-RV	ATATTGGGCUGAAAGCTGGTTGGAAGTATAAGTGG
39	193092_DS-FW	ACTAGGTAAUTGTGCAGCGGTATTGACTTCA

40	193092_DS-RV	GGTCTTAAUCACGGAGTTATTTTCCACGCT
41	44967_US-FW	GGGTTTAAUCGTTGGCATGACAGTCTTCAA
42	44967_US-RV	ATATTGGGCUGTCTGCCATCACAACCAGTTTG
43	44967_DS-FW	ACTAGGTAAUAGCCATGTTGCCAGACACAGT
44	44967_DS-RV	GGTCTTAAUACTACCATCTCGTAACCGTCCTAG
45	127904_US-FW	GGGTTTAAUGACCGACTCTACACTACCGTTCC
46	127904_US-RV	ATATTGGGCUATTGAACTGGTAAACATGCCATG
47	127904_DS-FW	ACTAGGTAAUTAGCCCTAGGACGGTTACGAG
48	127904_DS-RV	GGTCTTAAUAACCAACTTTGTTCCATTCTATCG
49	192604_US-FW	GGGTTTAAUGACACATCGTATTGATGACGACC
50	192604_US-RV	ATATTGGGCUCATGGCAGGTAGTCGCAAAG
51	192604_DS-FW	ACTAGGTAAUAAGAGAATACGGAACACATTGACC
52	192604_DS-RV	GGTCTTAAUCGGTCCAACAGTGAGGGTCT
53	44970_US-FW	GGGTTTAAUCGTTGATAATTCCAATTCCAATTC
54	44970_US-RV	ATATTGGGCUCGTCGAAGATGACCTGATTTG
55	44970_DS-FW	ACTAGGTAAUCGGGTTATCACTGTATCAATATCG
56	44970_DS-RV	GGTCTTAAUGCTACTACTATGCCGACTGCGT
57	44971_US-FW	GGGTTTAAUGGCCACACCTCAAGTTTGTATG
58	44971_US-RV	ATATTGGGCUCGGGATTGGAGTGCTCTAGTT
59	44971_DS-FW	ACTAGGTAAUGTTGGCTGAGAGTCAGGGTTAG
60	44971_DS-RV	GGTCTTAAUCCATTAGCTTCGGAACACTGG
61	44959_US-FW	GGGTTTAAUCCTTGTATTCATATCAATTGCGA
62	44959_US-RV	ATATTGGGCUATGTGACAATGAAGAATGGTACG
63	44959_DS-FW	ACTAGGTAAUGGAAAGGATGTTCCAAACAGTT
64	44959_DS-RV	GGTCTTAAUCTTTGTTGATTACTAGTCGTAATCATATG
65	44961_US-FW	GGGTTTAAUTGTCATGTTGTATCGGAGTGTTTAG
66	44961_US-RV	ATATTGGGCUTGTAGCACAAGTGTCTCACTAGTAAATAG
67	44961_DS-FW	ACTAGGTAAUGATTGGAAGTATCCCACAGTCTG
68	44961_DS-RV	GGTCTTAAUGAGAACACCGATCTCCGACGTGGGA
69	44972_US-FW	GGGTTTAAUGACGCAGTCGGCATAGTAGTAG
70	44972_US-RV	ATATTGGGCUGGAGAAGTGGTCAAACTTGTTTCA
71	44972_DS-FW	ACTAGGTAAUACAGGTGATTAAGATGCAAGGCT
72	44972_DS-RV	GGTCTTAAUCTTGCATCATCCGTAATTATGCT
73	Upst-HygR-N	CTGCTGCTCCATACAAGCCAACC
74	Dwst-1003HygF-N	GACATTGGGGAGTTCAGCGAGAG
75	ampR_PM_FW	AGCGCTACAUAATTCTCTTACTGTCATGCCATCC
76	ampR_PM_RV	ATGTAGCGCUGCCATAACCATGAGTGATAACACTG
77	ori_coli_FW	ATCCCCACUACCGCATTAAGACCTCAGCG
78	ampR_RV	AGCTGCTUCGTCGATTAAACCCTCAGCG
79	p71_prom-ter_short_usF	AGCCCAATAUTAAGCTCCCTAATTGGCCC
80	p71_prom-ter_dsR	ATTACCTAGUGGGCGCTTACACAGTACA
81	argB_FW	ACTAGGTAAUATCGCGTGCATTCCGCGGT

82	pyrG_FW_C1	ACTAGGTAAUATGACATGATTACGAATTCGAGCT
83	pyrG_RV_G16	AGTGGGGAUGCCTCAATTGTGCTAGCTGC
84	ccdB-camR-fw	AGAGCGAUCGCAGAAGCCTACTCGCTATTGTCCTCA
85	ccdB-camR-rv	TCTGCGAUCGCTCTTGCGCCGAATAAATACCTGT
86	AMA1_FW	AAGCAGCUGACGGCCAGTGCCAAGCT
87	AMA1_RV	ATATTGGGCUGGAAACAGCTATGACCATGAGATCT
88	AMA-3'-Fw	ACCCCAAUGGAAACGGTGAGAGTCCAGTG
89	AMA-5'-Rv	ATTGGGGUACTAACATAGCCATCAAATGCC
90	ANIG-actA-qFw	GTATGCAGAAGGAGATCACTGCTCT
91	ANIG-actA-qRv	GAGGGACCGCTCTCGTCGT
92	ANIG-hhtA-qFw	CTTCCAGCGTCTTGTCCGTG
93	ANIG-hhtA-qRv	GCTGGATGTCCTTGGACTGGAT
94	44959-qFw	GGCAAAGTTCTAGTCATCGACGA
95	44959-qRv	CATATATCCCAGAGGCGGACAC
96	44960-qFw	GATAGAGGAGATGAGGAAGAGAGGCT
97	44960-qRv	CCTTGGGTACCATTCACAGTCAG
98	44961-qFw	ACATGGACCACCGAGTAGCGT
99	44961-qRv	TAGGGTGTGCGAGAATATCACTTG
100	54844-qFw	CGATGAAGATGGCAATCCCAT
101	54844-qRv	CTATGGCATCGCATACTGAGAAAGA
102	44963-qFw	GCGAGGAGGTAGAAAAGGCAAT
103	44963-qRv	TGAACACGAGACTGGAGTACGGA
104	44964-qFw	TCTTCTGGATACTGGGAATTGGAG
105	44964-qRv	GCGTGATGCACCCTCAACA
106	44965-qFw	TTGTCTGTCAAGGAGGACGAGATT
107	44965-qRv	CTTCACCAAATGCTGCACAGTC
108	193092-qFw	ATCACGGCAAAGAGAGCCAAGT
109	193092-qRv	GAACTGTGGCACGACCATGTC
110	44967-qFw	TGCTGGCTGCTAAGGATTGATG
111	44967-qRv	ATGTTCCAACGCAATGAACAAC
112	127904-qFw	ATGAGCAACATGCTCCCACTACAT
113	127904-qRv	CAGTGATGGTCTTATCCGCCAG
114	192604-qFw	GCCTAATCCTGGGCATCGTG
115	192604-qRv	CTGTGCTCCCCGATCTGCA
116	44970-qFw	TCTCAGGGTGTCCATCTTCCGT
117	44970-qRv	CGACACGAAATAGGCATCATTCT
118	44971-qFw	ATCTACTCCGGCTCCTGCGAT
119	44971-qRv	ACTCGCAAACAACTTCATTGCTC
120	44972-qFw	AGGTGACTCGAACTGGTATGCTG
121	44972-qRv	CAGAATATACTCGATATGATCGCCTC

Paper 10

"Characterization of four new antifungal yanuthones from *Aspergillus niger*"

Petersen, L.M.; Holm, D.K.; Klitgaard, A.; Knudsen, P.B.; Nielsen, K.F.; Gotfredsen, C.H.; Mortensen, U.H.; Larsen, T.O.

Journal of Antibiotics, **2014**, In Press.

Characterization of four new antifungal yanuthones from *Aspergillus niger*

Lene M. Petersen[1,6], Dorte K. Holm[2,6], Peter B. Knudsen[3], Kristian F. Nielsen[4], Charlotte H. Gotfredsen[5], Uffe H. Mortensen[2], Thomas O. Larsen[1]

[1]Chemodiversity Group, Department of Systems Biology, Technical University of Denmark, Soeltofts Plads B221, DK-2800 Kgs. Lyngby, Denmark
[2]Eukaryotic Molecular Cell Biology Group, Department of Systems Biology, Technical University of Denmark, Soeltofts Plads B223, DK-2800 Kgs. Lyngby, Denmark
[3]Fungal Physiology and Biotechnology Group, Department of Systems Biology, Technical University of Denmark, Soeltofts Plads B223, DK-2800 Kgs. Lyngby, Denmark
[4]Metabolic Signaling and Regulation Group, Department of Systems Biology, Technical University of Denmark, Soeltofts Plads B223, DK-2800 Kgs. Lyngby, Denmark
[5]Department of Chemistry, Kemitorvet, Building 201, Technical University of Denmark, DK-2800 Kgs. Lyngby, Denmark

[6]These authors have contributed equally to this work

Correspondence: Associate professor Thomas O. Larsen, Chemodiversity Group, Department of Systems Biology, Technical University of Denmark, Soeltofts Plads B221, DK-2800 Kgs. Lyngby, Denmark.
E-mail: tol@bio.dtu.dk

Running head: Antifungal yanuthones from *Aspergillus niger*

ABSTRACT

Four new yanuthone analogs (**1-4**) were isolated from the filamentous fungus *Aspergillus niger*. The structures of the new compounds were elucidated on the basis of UHPLC-DAD-HRMS data and 1D and 2D NMR spectroscopy. Labeling studies with $^{13}C_8$-6-methylsalicylic acid identified three class I yanuthones originating from the polyketide 6-methylsalicylic acid (yanuthone K, L and M (**1-3**)) and a class II yanuthone, which was named yanuthone X_2 (**4**). The four new compounds were tested towards the pathogenic yeast *Candida albicans* and all displayed antifungal activity. Yanuthone X_2 represents the first example of a bioactive class II yanuthone, demonstrating the pharmaceutical potential of this class.

Keywords: Antifungal agents/Aspergillus/meroterpenoid/polyketide/yanuthone

INTRODUCTION

The black fungus *Aspergillus niger* is a significant contaminant of food and feeds and a widely used cell factory for production of citric acid and bulk enzymes.[1,2] In this context it is important to note that *A. niger* is known to produce more than 100 secondary metabolites,[3] including not only mycotoxins such as ochratoxin A and fumonisins,[3,4,5,6,7,8] but also medically relevant compounds such as asperpyrone B and yanuthones targeting *Candida albicans*.[9,10] Recently, access to the full genome of *A. niger*[11,12] has provided a platform that allows for linking genes to specific secondary metabolites. To this end, we have recently reported the characterization of the biosynthetic pathway towards antimicrobial yanuthone D in *A. niger*.[13]

The core structure of yanuthones constitutes an epoxylated six-membered ring, which may be further decorated with different side chains: one sesquiterpene (at C13) and varying side chains (at C15 and C16), see Figure 1. The core structure may be derived from at least two different precursors, which lead to formation of two classes of yanuthones. Class I yanuthones are derived from the polyketide 6-methylsalicylic acid (6-MSA), which due to a decarboxylation event during yanuthone formation, delivers a six-membered methylated ring (a C_7 scaffold) to the yanuthones. Class II yanuthones contains a C_6 core scaffold derived from an unknown precursor.[13] The additional methyl group in class I yanuthones controls what type of decoration is possible at C16. Despite derivation of the two classes of yanuthones from different precursors, they share downstream enzymatic activities toward product maturation. So far, 15 class I yanuthones and a single class II yanuthone have been described in the literature of which only yanuthone D, a class I yanuthone, has displayed strong antimicrobial activity.[9,13,14]

These observations prompted us to investigate whether additional yanuthones exist in *A. niger* and whether such new compounds display antimicrobial activity. *C. albicans* accounts for the highest source of fungal infections worldwide,[15] which is why it is of great interest to find new drug candidates. Here we report the structures of four new yanuthones and their bioactivities towards *C. albicans*.

MATERIALS AND METHODS

Strains, media and feeding experiments. The strains used for this study were the *A. niger* ATCC1015-derived KB1001[16] and the *yanA*Δ strain (6-MSA PKS deleted).[13] Solid plates with YES

media were prepared as described by Frisvad and Samson[17], and feeding experiments with fully labelled $^{13}C_8$-6-MSA were carried out as described by Holm *et al.*[13]

Chemical analysis of strains. Strains were cultivated on solid YES media at 25 °C for 5-7 days in the dark. Extraction of metabolites was performed as described by Smedsgaard.[18] Analysis was performed using reversed phase ultra-high-performance liquid chromatography (UPHLC) UV/Vis diode array detector (DAD) high-resolution time-of-flight mass spectrometer (TOFMS) on a maXis G3 orthogonal acceleration quadrupole time of flight (Q-TOF) mass spectrometer (Bruker Daltonics, Bremen) as described by Holm *et al.*[13]

Preparative isolation of selected metabolites. *A. niger* (KB1001) was cultivated on 200 plates of YES medium at 30 °C for 5 days in the dark. Extraction, workup and fractionation were performed as described by Holm *et al.*[13] Final purification was completed on a semi-preparative HPLC system, which was a Waters 600 Controller with a Waters 996 photodiode array detector. This was achieved using a Luna II C_{18} column (250 x 10 mm, 5 µm, Phenomenex) and a flow rate of 4 $mL \cdot min^{-1}$. Solvents used were acetonitrile (ACN) of HPLC grade and milliQ-water, both with 50 ppm trifluoroacetic acid. For the isolation of yanuthone L, M and X_2 a gradient of 40-100 % ACN in 20 min was used, yielding 2.0, 1.5 and 1.2 mg, respectively. For isolation of yanuthone K an isocratic run with 90 % ACN for 15 min was used, yielding 6.7 mg.

NMR and structural elucidation. The 1D and 2D spectra were recorded on a Varian Unity Inova-500 MHz spectrometer. Spectra were acquired using standard pulse sequences, and ^1H spectra as well as DQF-COSY, NOESY, HSQC and HMBC spectra were acquired. The deuterated solvent was acetonitrile-d_3 and signals were referenced by solvent signals for acetonitrile-d_3 at δ_H = 1.94 ppm and

δ_C = 1.32/118.26 ppm. Chemical shifts are reported in ppm (δ) and scalar couplings in hertz (Hz). The sizes of the *J* coupling constants reported in the tables are the experimentally measured values from the spectra. There are minor variations in the measurements which may be explained by the uncertainty of *J*. NMR data for all compounds including ^{1}H and 2D spectra are found in supporting information. Optical rotation was measured on a Perkin Elmer 321 Polarimeter.

Antifungal susceptibility testing. All compounds were screened for antifungal activity towards *Candida albicans* (IBT 654) in accordance with the CLSI standards, as described by Holm *et al.*[13]

RESULTS AND DISCUSSION

Identification and structural elucidation of four new yanuthones

Inspired by our previous discovery of six new yanuthones in *A. niger*,[13] the *A. niger* strain KB1001 was cultivated on YES, and a large extract was scrutinized for compounds that could potentially be new yanuthones. The UHPLC-DAD-HRMS analysis tentatively identified four yanuthone related structures. Their UV spectra as well as chemical compositions indicated coherence to the previously identified structures.[9,13,14] The four compounds were purified and their structures elucidated from the HRMS data, UV data and 1D and 2D NMR experiments (see Table 1, Table 2 and further details in the supporting information).

All structures contain a six-membered ring containing an epoxide, which define the core structure of yanuthones, but vary in their side chains, see Figure 1. Importantly, three of the compounds (yanuthones K-M (**1**-**3**)) contain a C_7 core associated with class I yanuthones, whereas the remaining

yanuthone X_2 (**4**) contains a C_6 core scaffold characteristic for class II yanuthone, hence representing the second compound of this class.

All four yanuthones showed several similar features in the ^1H as well as 2D spectra. All displayed eight overlapping proton resonances at δ_H 1.41-2.08 ppm in the ^1H spectrum, corresponding to the four methylene groups at C4, C5, C8 and C9, present in all structures. Other common resonances were seen for the diastereotopic pair H12/H12' and the 3 methyl groups (H19, H20 and H21) around δ_H 1.60 ppm, of which H20 and H21 were overlapping. Moreover, all four yanuthones showed HMBC correlations to a quaternary carbon (C18) around δ_C 194 ppm as well as two carbons around δ_C 60 ppm (one quaternary, one methine) being the carbons in the epoxide ring.

The moiety attached to C15 varied, with yanuthone K-M having an acetoxy group attached (as also seen for yanuthone C [9]), while yanuthone X_2 had a hydroxyl group (as seen in yanuthone A and E [9]). The structures also showed variance regarding the group attached to C16. Yanuthone K-M had a methyl group, while yanuthone X_2 differed in having a methoxy group attached at the C16 position. This was obvious from the chemical shift of C16, which gave rise to a resonance at δ_C 172.6 ppm, considerably further downfield than in the other structures (yanuthone K-M). Furthermore, C17 was affected, shifting upfield to δ_C 98.8 ppm. As expected, the chemical shifts of the core structure of yanuthone K-M are very similar, whereas yanuthone X_2 differs especially around position C16.

The attached terpene chain also varied in the four structures. Yanuthone K and X_2 proved to contain a non-modified sesquiterpene. Yanuthone L and M also contain a sesquiterpene chain, but this is oxidized at C1 and C2, respectively.

NOESY experiments enabled determination of the stereogenic centers of **1**-**4** to be similar to the previously described yanuthones. For all four yanuthones the NOESY data showed a strong correlation between H14 and H15 (see supporting information), suggesting these protons to be on the same side of the six-membered ring. This was further supported by the optical rotation measured, which was comparable to those reported for other yanuthones, altogether strongly indicating the absolute stereochemistry of C13, C14 and C15 is similar to other yanuthones.

Labeling studies confirm that yanuthones K-M are class I yanuthones, and yanuthone X_2 is a class II yanuthone

In previous work it was demonstrated that yanuthone D, unlike the highly similar compound yanuthone X_1, is biosynthesized from 6-MSA.[13] To prove that yanuthones K, L, and M truly are class I yanuthones and that yanuthone X_2 is a class II yanuthone, the *A. niger* strain (KB1001) and a 6-MSA synthase deletion strain (*yanA*Δ)[13] were analyzed for the presence of the four new yanuthones. This experiment revealed that neither yanuthone K, L nor M were present in *yanA*Δ (data not shown) suggesting that these three compounds are class I compounds, biosynthesized using 6-MSA as precursor. In contrast, yanuthone X_2 was still present in the *yanA*Δ strain, indicating that it is indeed a class II yanuthone. To further verify this, fully labeled $^{13}C_8$-MSA was fed to *yanA*Δ and KB1001. Yanuthone L was not produced under the given conditions in this experiment, but the data confirmed that 6-MSA was indeed incorporated into yanuthone K and M, verifying 6-MSA as the precursor (Figure 2). In contrast, no $^{13}C_8$-6-MSA was incorporated into yanuthone X_2, which is in agreement with this compound being a class II yanuthone.

Yanuthones K-M and X_2 display antifungal activity

Some of the yanuthones have earlier been reported to display antimicrobial activity[9], and in our previous study we reported that several of the yanuthones showed antifungal activity towards *C. albicans*, with yanuthone D being the most active with an IC_{50} value of 3.3 µM.[13] We therefore tested the four new yanuthones identified in this study for antifungal activity towards *C. albicans*, see Table 3. All three class I yanuthones showed antifungal activity in this assay. The strongest activities were observed with yanuthones K and L, which resulted in IC_{50} values that were 5-fold higher than that obtained with yanuthone D. The weakest activity was obtained with yanuthones M, which was 20-fold higher than the value obtained with yanuthone D. Importantly; yanuthone X_2 also displayed an antimicrobial effect. With an IC_{50} value 15-fold higher than that of yanuthone D, it represents the first example of a bioactive class II yanuthone. This result demonstrates that there may be a pharmaceutical potential for this class of yanuthones.

Comparison of all class I yanuthone structures to their corresponding antifungal activities revealed some structure-activity relationship (SAR) features that may be relevant for potency towards *C. albicans*. Firstly, yanuthone D (IC_{50} = 3.3 µM) and yanuthone E (IC_{50} > 100 µM) only differ by the functional group at C15. In this case, a shift from of a ketone to a hydroxyl at this position is sufficient to eliminate the antimicrobial effect of the most bioactive yanuthone (see Figure 3). Inspection of the other compounds revealed that the functional group at C15 does have a significant impact on the potency, as O-glycosylation increases antifungal activity (yanuthone G compared to yanuthone F), and

O-acetylation at C15 also increases antifungal activity compared to hydroxylation (yanuthone K and L compared to 7-deacetoxyanuthone A[i] and yanuthone F, respectively).

Secondly, hydroxylation of C22 appears to increase antifungal activity. This is seen in yanuthone H (IC_{50} = 24.5 µM) compared to yanuthone F (IC_{50} > 100 µM) as well as in 22-deacetylyanuthone A (IC_{50} = 19.4 µM) compared to 7-deacetoxyyanuthone A (IC_{50} > 100 µM) (Figure 3). In both cases, the structures differ only by the C22 hydroxylation.

Lastly, two features seem to decrease antifungal activity: chain shortening of the sesquiterpene and hydroxylation of C2. Chain shortening of the sesquiterpene of yanuthone I (IC_{50} > 100 µM) decreased antifungal activity compared to yanuthone H (IC_{50} = 24.5 µM), which contains an intact C_{15} sesquiterpene (Figure 3). However, this could also be connected to the level of oxidation, and not the chain length alone. Hydroxylation of C2 also seems to decrease the activity, as yanuthone M (IC_{50} = 77.5 µM) is less active than yanuthone K (IC_{50} = 17.5 µM) (Figure 3). It is unclear how O-mevalonation at C22 affects the activity as both 7-deacetoxyyanuthone A (non-mevalonated) and yanuthone E (mevalonated) have IC_{50}-values above 100 µM, and thus the activities were too low to be measured in this assay. The same goes for hydroxylation at C1, where 7-deacetoxyyanuthone A (non-hydroxylated) and yanuthone F (hydroxylated) have IC_{50}-values above 100 µM. Based on the above correlation between structures and antifungal activities, we propose that antifungal activity of class I yanuthones may increase by combining 1) oxidation of the hydroxyl group at C15 with hydroxylation of C22, or 2) O-acetylation of C15 with hydroxylation of C22.

[i] 7-deacetoxyyanuthone A was named by Li *et al.* using another numbering system for the yanuthones than the originally suggested by Bugni *et al.* According to the latter numbering system, which has also been used here, the appropriate name for 7-deacetoxyyanuthone A would have been 22-deacetoxyyanothone A.

For class II yanuthones, the picture is different. In contrast to class I yanuthones, O-acetylation at C15 appears to reduce antifungal activity compared to hydroxylation (Figure 3). As class II yanuthones lack the C22 carbon and have a methoxy group attached to C16 instead, there may be interplay between the side groups, which may explain this difference. Since yanuthone X_2, but not yanuthone E, shows antimicrobial bioactivity, it would be of great interest to synthesize a class II yanuthone with a ketone at C15, to investigate whether this compound shows a stronger biological effect than yanuthone D.

In summary a large scale cultivation of *A. niger* has led to the discovery of four new yanuthones, which were all characterized by 1D and 2D NMR spectroscopy. Labeling studies with $^{13}C_8$-6-MSA and comparison of the chemical profile of the *A. niger* strain (KB1001) and a 6-MSA synthase gene deletion strain (*yanA*Δ) revealed three class I yanuthones (yanuthone K-M) originating from 6-MSA and one class II yanuthone (yanuthone X_2) originating from a yet unknown precursor. These results were in agreement with their elucidated structures, with yanuthone K-M containing a C_7 core scaffold and yanuthone X_2 a C_6 core scaffold.

Furthermore, we have tested the antifungal activity of the new yanuthones towards the pathogenic yeast *C. albicans* and found that all were active. This not only shed light on the structure-activity relationships, that are relevant for the potency towards *C. albicans*, but also demonstrated the possible pharmaceutical potential of the class II yanuthones, as yanuthone X_2 represents the first example of a bioactive class II yanuthone.

ACKNOWLEDGMENTS

The study was supported by grant 09-064967 from the Danish Council for Independent Research, Technology, and Production Sciences.

Supplementary information is available at the Journal of Antibiotics's website (http://www.nature.com/ja).

REFERENCES

1. Schuster, E., Dunn-Coleman, N. S., Frisvad, J. C. & Van Dijck, P. W. M. On the safety of Aspergillus niger - a review. *Appl. Microbiol. Biotechnol.* **59,** 426–435 (2002).

2. Perrone, G. *et al.* Biodiversity of Aspergillus species in some important agricultural products. *Stud. Mycol.* **59,** 53–66 (2007).

3. Nielsen, K. F., Mogensen, J. M., Johansen, M., Larsen, T. O. & Frisvad, J. C. Review of secondary metabolites and mycotoxins from the *Aspergillus niger* group. *Anal. Bioanal. Chem.* **395,** 1225–1242 (2009).

4. Frisvad, J. C., Smedsgaard, J., Samson, R. A., Larsen, T. O. & Thrane, U. Fumonisin B2 Production by *Aspergillus niger*. *J. Agric. Food Chem.* **55,** 9727–9732 (2007).

5. Mogensen, J. M., Frisvad, J. C., Thrane, U. & Nielsen, K. F. Production of Fumonisin B2 and B4 by *Aspergillus niger* on grapes and raisins. *J. Agric. Food Chem.* **58,** 954–958 (2010).

6. Noonim, P., Mahakarnchanakul, W., Nielsen, K. F., Frisvad, J. C. & Samson, R. A. Fumonisin B2 production by *Aspergillus niger* in Thai coffee beans. *Food Addit. Contam.* **26,** 94–100 (2009).

7. Mogensen, J. M., Larsen, T. O. & Nielsen, K. F. Widespread occurrence of the mycotoxin fumonisin B2 in wine. *J. Agric. Food Chem.* **58,** 4853–4857 (2010).

8. Knudsen, P. B., Mogensen, J. M., Larsen, T. O. & Nielsen, K. F. Occurrence of fumonisins B(2) and B(4) in retail raisins. *J. Agric. Food Chem.* **59,** 772–776 (2011).

9. Bugni, T. S. *et al.* Yanuthones: novel metabolites from a marine isolate of Aspergillus niger. *J. Org. Chem.* **65,** 7195–7200 (2000).

10. Song, Y. C. *et al.* Endophytic naphthopyrone metabolites are co-inhibitors of xanthine oxidase, SW1116 cell and some microbial growths. *FEMS Microbiol. Lett.* **241,** 67–72 (2004).

11. Baker, S. E. *Aspergillus niger* genomics: past, present and into the future. *Med. Mycol.* **44,** 17–21 (2006).

12. Pel, H. J. *et al.* Genome sequencing and analysis of the versatile cell factory *Aspergillus niger* CBS 513.88. *Nat. Biotechnol.* **25,** 221–231 (2007).

13. Holm, D. K. *et al.* Molecular and chemical characterization of the biosynthesis of the 6-MSA derived meroterpenoid yanuthone D in *Aspergillus niger*. *Chem. Biol.* **21,** 519–529 (2014).

14. Li, X., Choi, H. D., Kang, J. S., Lee, C.-O. & Son, B. W. New polyoxygenated farnesylcyclohexenones, deacetoxyyanuthone A and its hydro derivative from the marine-derived fungus Penicillium sp. *J. Nat. Prod.* **66,** 1499–1500 (2003).

15. Richards, M. & Edwards, J. Nosocomial infections in combined medical-surgical intensive care units in the United States. *Infect. Control Hosp. Epidemiol.* **21,** 510–515 (2000).

16. Chiang, Y.-M. *et al.* Characterization of a polyketide synthase in *Aspergillus niger* whose product is a precursor for both dihydroxynaphthalene (DHN) melanin and naphtho-γ-pyrone. *Fungal Genet. Biol.* **48,** 430–437 (2011).

17. Samson, R. A., Houbraken, J., Thrane, U., Frisvad, J. C. & Andersen, B. *Food and indoor fungi*. CBS KNAW Fungal Biodiversity Centre: Utrecht (NL) (2010).

18. Smedsgaard, J. Micro-scale extraction procedure for standardized screening of fungal metabolite production in cultures. *J. Chromatogr. A* **760,** 264–270 (1997).

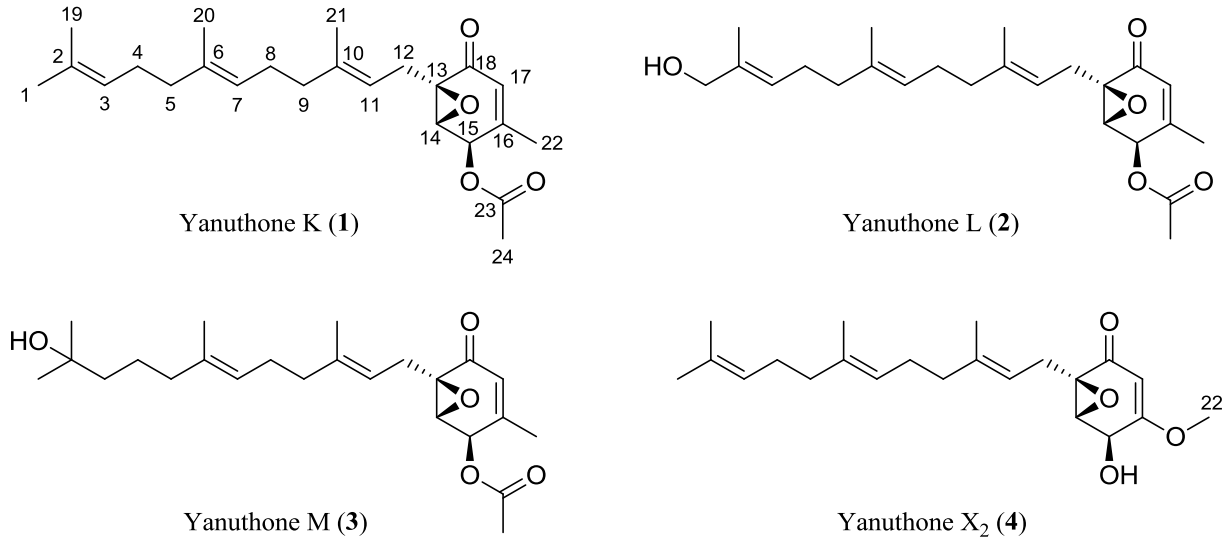

Figure 1. Structures of the four new compounds yanuthone K-M and X_2.

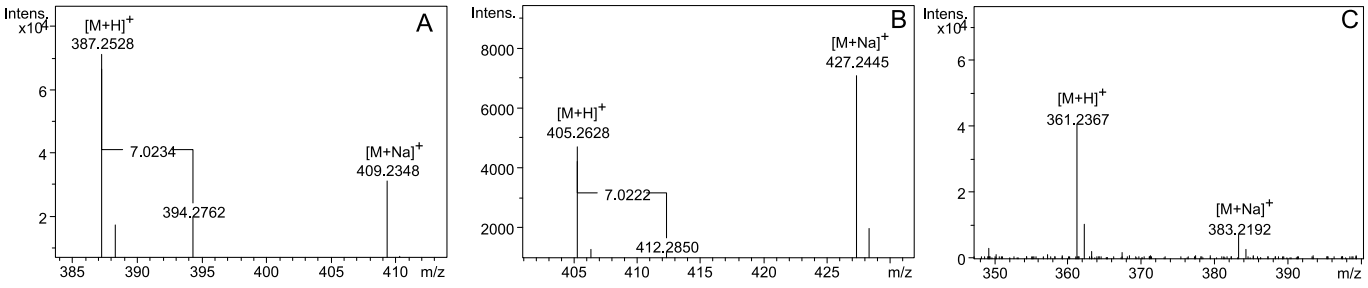

Figure 2. Positive electrospray (ESI^+) mass spectrum of: (A) Unlabeled and labeled yanuthone K (**1**), (B) Unlabeled and labeled yanuthone M (**3**), and (C) unlabeled yanuthone X_2 (**3**). The calculated shift from $^{12}C_7$ to $^{13}C_7$ is 7.0234 Da.

Class I yanuthones

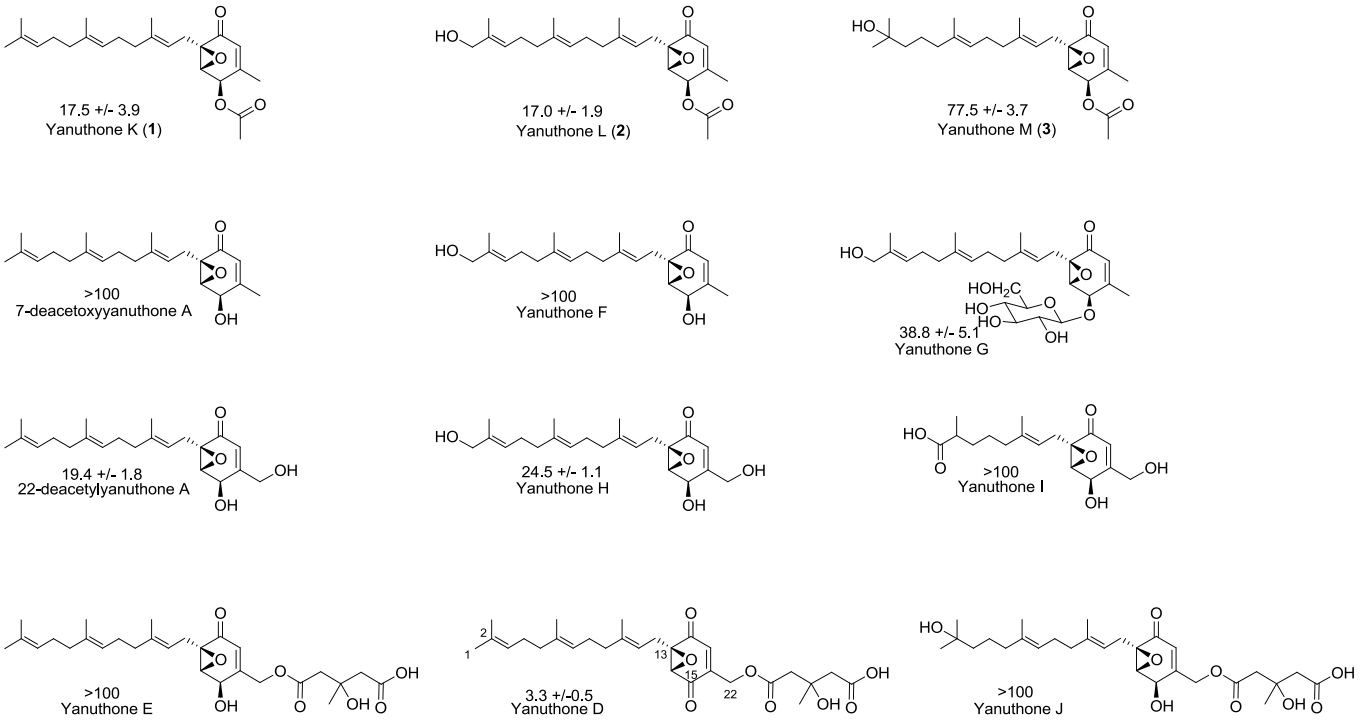

Class II yanuthones

Figure 3. Overview of class I and II yanuthones as well as their IC_{50} [µM] towards *Candida albicans*.

Table 1. ^{1}H NMR chemical shift [ppm], integral, multiplicity and *J* coupling constants [Hz] for yanuthone K-M and X_2. Spectra were referenced by solvent signals for CD_3CN at δ_H = 1.94 ppm and δ_C = 1.32, 118.26 ppm.

Atom #	Yanuthone K (**1**)	Yanuthone L (**2**)	Yanuthone M (**3**)	Yanuthone X_2 (**4**)
1	1.65 (3H, s)	3.84 (2H, s)	1.11 (3H, m)	1.66 (3H, d, 0.9)
2	-	-	-	-
3	5.08 (1H, m)	5.32 (1H, tq, 7.0, 1.4)	1.34 (2H, m)	5.09 (1H, m)
4	2.02 (2H, m)	2.08 (2H, m)	1.41 (2H, m)	2.05 (2H, m)
5	1.94 (2H, m)	1.99 (2H, m)	1.93 (2H, m)	1.95 (2H, m)
6	-	-	-	-
7	5.07 (1H, m)	5.09 (1H, tq, 7.0, 1.3)	5.08 (1H, m)	5.08 (1H, m)
8	2.06 (1H, m)	2.07 (2H, m)	2.07 (2H, m)	2.07 (2H, m)
8’	2.00 (1H, m)			
9	-	1.991 (2H, m)	2.00 (2H, m)	1.99 (2H, m)
10	-	-	-	-
11	5.01 (1H, m)	5.01 (1H, m)	5.02 (1H, m)	5.04 (1H, m)
12	2.69 (1H, dd, 15.3, 8.1)	2.69 (1H, dd, 15.6, 8.2)	2.69 (1H, dd, 15.4, 8.1)	2.74 (1H, dd, 15.0, 8.1)
12’	2.45 (1H, dd, 15.4, 6.7)	2.45 (1H, dd, 15.5, 6.7)	2.45 (1H, dd, 15.4, 6.7)	2.36 (1H, dd, 15.0, 6.6)
13	-	-	-	-
14	3.65 (1H, d, 2.6)	3.66 (1H, d, 2.6)	3.66 (1H, d, 2.6)	3.58 (1H, d, 3.1)
15	5.80 (1H, m)	5.80 (1H, m)	5.81 (1H, m)	4.58 (1H, d, 2.9)
16	-	-	-	-
17	5.81 (1H, m)	5.81(1H, m)	5.82 (1H, m)	5.18 (1H, s)
18	-	-	-	-
19	1.59 (3H, s)	1.591 (3H, s)	1.11 (3H, s)	1.59 (3H, s)
20	1.58 (3H, s)	1.59 (3H, s)	1.57 (3H, s)	1.58 (3H, s)
21	1.62 (3H, s)	1.62 (3H, s)	1.62 (3H, s)	1.62 (3H, s)
22	1.84 (3H, s)	1.84 (3H, t, 1.22)	1.85 (3H, m)	3.69 (3H, s)
23	-	-	-	
24	2.16 (3H, s)	2.16 (3H, s)	2.16 (3H, s)	

Table 2. ^{13}C NMR chemical shifts [ppm] for yanuthone K-M and X_2. Spectra were referenced by solvent signals for CD_3CN at δ_H = 1.94 ppm and δ_C = 1.32, 118.26 ppm.

Atom #	**1**	**2**	**3**	**4**
1	25.7	68.1	29.2	25.8
2	132.0	136.1	70.7	132.1
3	125.1	125.1	43.9	124.9
4	27.5	26.8	23.2	27.3
5	40.4	40.0	40.5	40.4
6	136.1	135.9	136.4	136.0
7	125.1	124.7	124.7	124.8
8	27.4	26.8	26.9	27.3
9	40.4	40.0	40.3	40.4
10	140.4	140.1	140.3	139.7
11	117.6	117.4	117.3	118.1
12	26.5	26.4	26.3	27.1
13	61.0	61.0	60.8	61.1
14	57.2	57.1	57.2	58.9
15	69.6	69.4	69.5	65.9
16	153.9	153.8	153.7	172.6
17	125.2	124.9	124.9	98.8
18	194.1	194.1	194.2	194.4
19	17.6	13.6	29.2	17.7
20	16.0	15.8	15.8	16.2
21	16.2	16.4	16.3	16.4
22	19.8	19.6	19.6	57.1
23	171.2	171.4	171.0	
24	20.8	20.8	20.8	

Table 3. The half maximal inhibitory concentration (IC_{50}) for *Candida albicans* treated with a small library of yanuthones isolated from *Aspergillus niger* KB1001. The IC_{50} values were calculated based on duplicate experiments carried out in three independent trials and annotated with their respective standard deviation.

Compound	**IC_{50} (µM)**
Yanuthone K (**1**)	17.5 ± 3.9
Yanuthone L (**2**)	17.0 ± 1.9
Yanuthone M (**3**)	77.5 ± 3.7
Yanuthone X_2 (**4**)	51.7 ± 4.7

Contents

S 1. Spectroscopic data for yanuthone K (**1**)

HRESIMS: *m/z* = 387.2531 $[M + H]^+$, calculated for $[C_{24}H_{34}O_4+H]^+$: 387.2530.
$[\alpha]_{587}^{20} = 42.7°$ (MeOH)

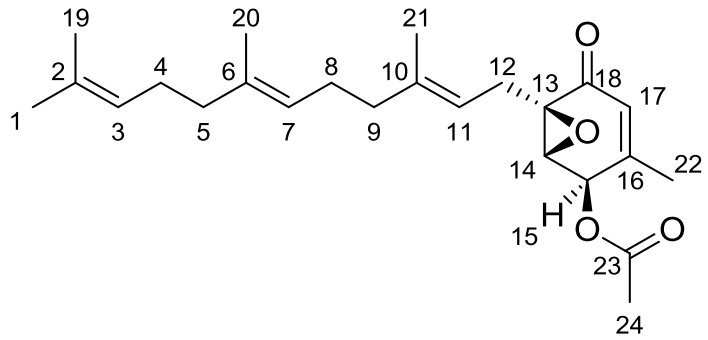

Atom assignment	^{1}H-chemical shift [ppm] (integral, mult., *J* [Hz])	^{13}C-chemical shift [ppm]	HMBC correlations	NOESY connectivities
1	1.65 (3H, s)	25.7	2, 3, 19	3
2	-	132.0	-	-
3	5.08 (1H, m)	125.1	1, 19	1, 4
4	2.02 (2H, m)	27.5	2	3
5	1.94 (2H, m)	40.4	3, 4, 6, 20	7
6	-	136.1	-	-
7	5.07 (1H, m)	125.1	4/8, 5/9, 20	5, 8, 9
8	2.06 (2H, m)	27.4	5/9, 6, 7, 10	7
9	2.00 (2H, m)	40.4	7, 8, 10, 11, 21	7, 11
10	-	140.4	-	-
11	5.01 (1H, m)	117.6	9, 12/12', 13, 21	9, 12, 12', 14
12	2.69 (1H, dd, 15.3, 8.1)	26.5	10**,** 11**,** 13, 14, 18	11, 12', 14, 21
12'	2.45 (1H, dd, 15.4, 6.7)	26.5	10**,** 11**,** 13, 14, 18	11, 12, 14, 21
13	-	61.0	-	-
14	3.65 (1H, d, 2.6)	57.2	12/12', 13, 15, 16 22	11, 12, 12', 15
15	5.80 (1H, m)	69.6	13, 14, 16, 22, 23	14, 22
16	-	153.9	-	-
17	5.81 (1H, m)	125.2	13, 15, 16, 22	-
18	-	194.1	-	-
19	1.59 (3H, s)	17.6	1, 2, 3	-
20	1.58 (3H, s)	16.0	5, 6, 7	-
21	1.62 (3H, s)	16.2	9, 10, 11	12, 12'
22	1.84 (3H, s)	19.8	15, 16, 17	15
23	-	171.2	-	-
24	2.16 (3H, s)	20.8	15, 23	-

S 2. Spectroscopic data for yanuthone L (**2**)

HRESIMS: *m/z* = 403.2482 $[M + H]^+$, calculated for $[C_{24}H_{34}O_5+H]^+$: 403.2484.
$[\alpha]_{587}^{20} = 15.0°$ (MeOH)

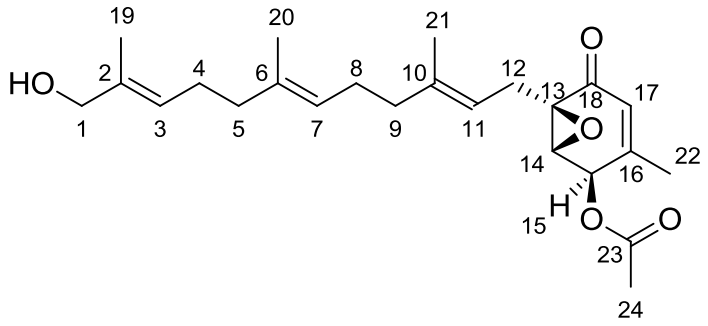

Atom assignment	^{1}H-chemical shift [ppm] (integral, mult., *J* [Hz])	^{13}C-chemical shift [ppm]	HMBC correlations	NOESY connectivities
1	3.84 (2H, s)	68.1	2, 3, 19	3, 4, 19
2	-	136.1	-	-
3	5.32 (1H, tq, 7.0, 1.4)	125.1	1, 4, 19	1, 4
4	2.08 (2H, m)	26.8	3, 5, 6, 19	1, 3
5	1.99 (2H, m)	40.0	4, 6, 7	7
6	-	135.9	-	-
7	5.09 (1H, tq, 7.0, 1.3)	124.7	5, 9, 20	5, 8, 9
8	2.07 (2H, m)	26.8	6, 9	7, 11, 21
9	1.991 (2H, m)	40.0	8, 10, 11, 21	7, 11, 14
10	-	140.1	-	-
11	5.01 (1H, m)	117.4	9, 21	8, 9, 12, 12’, 14
12	2.69 (1H, dd, 15.6, 8.2)	26.4	10, 11, 13, 14, 18	11, 12’, 14, 21
12’	2.45 (1H, dd, 15.5, 6.7)	26.4	10, 11, 13, 14, 18	11, 12, 14, 21
13	-	61.0	-	-
14	3.66 (1H, d, 2.6)	57.1	15, 16	9, 11, 12, 12’, 15, 17, 21
15	5.80 (1H, m)	69.4	13, 22, 23	14, 22
16	-	153.8	-	-
17	5.81(1H, m)	124.9	13, 15, 22	14, 22
18	-	194.1	-	-
19	1.591 (3H, s)	13.6	1, 3, 19	1
20	1.59 (3H, s)	15.8	5, 6	-
21	1.62 (3H, s)	16.4	9, 10, 11	8, 12, 12’, 14,
22	1.84 (3H, t, 1.22)	19.6	15, 16, 17	15, 17
23	-	171.4	-	-
24	2.16 (3H, s)	20.8	23	-

S 3. Spectroscopic data for yanuthone M (**3**)

HRESIMS: *m/z* = 405.2636 $[M + H]^+$, calculated for $[C_{24}H_{36}O_5+H]^+$: 405.2635.
$[\alpha]_{587}^{20} = 10.8°$ (MeOH)

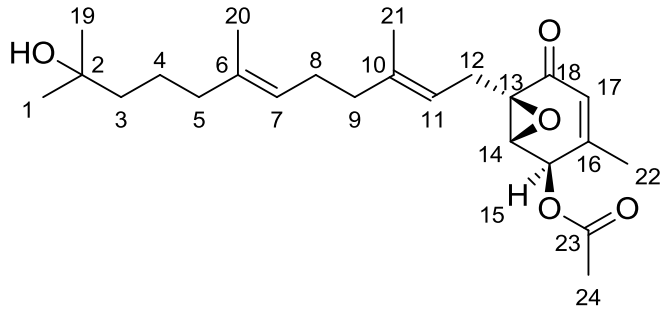

Atom assignment	^{1}H-chemical shift [ppm] (integral, mult., *J* [Hz])	^{13}C-chemical shift [ppm]	HMBC correlations	NOESY connectivities
1	1.11 (3H, m)	29.2	2, 3, 19	3, 4
2	-	70.7	-	-
3	1.34 (2H, m)	43.9	-	1, 19
4	1.41 (2H, m)	23.2	-	1, 19
5	1.93 (2H, m)	40.5	3, 4, 6	7
6	-	136.4	-	-
7	5.08 (1H, m)	124.7	-	5, 8, 9
8	2.07 (2H, m)	26.9	5/9, 6, 7	7
9	2.00 (2H, m)	40.3	7, 8, 10, 11, 12, 21	7, 11
10	-	140.3	-	-
11	5.02 (1H, m)	117.3	-	9, 12, 12’
12	2.69 (1H, dd, 15.4, 8.1)	26.3	10, 11, 13	11, 12, 21
12’	2.45 (1H, dd, 15.4, 6.7)	26.3	10, 11, 13	11, 12’
13	-	60.8	-	-
14	3.66 (1H, d, 2.6)	57.2	16	15
15	5.81 (1H, m)	69.5	-	14, 22
16	-	153.7	-	-
17	5.82 (1H, m)	124.9	-	-
18	-	(194.2)	-	-
19	1.11 (3H, s)	29.2	2, 3, 1	3, 4
20	1.57 (3H, s)	15.8	5, 6, 7	-
21	1.62 (3H, s)	16.3	9, 10, 11	12
22	1.85 (3H, m)	19.6	15, 16, 17	15
23	-	171.0	-	-
24	2.16 (3H, s)	20.8	23	-

S 4. Spectroscopic data for yanuthone X_2 (**4**)

HRESIMS: *m/z* = 361.2373 $[M + H]^+$, calculated for $[C_{22}H_{32}O_4+H]^+$: 361.2373.
$[\alpha]_{587}^{20} = 3.6°$ (MeOH)

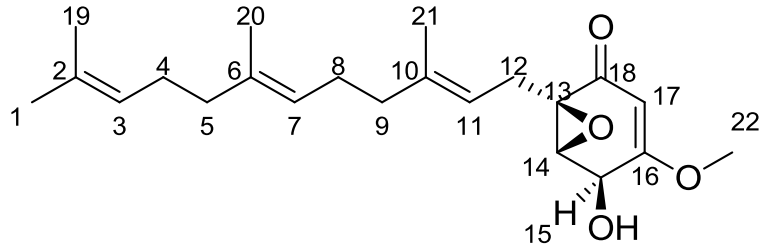

Atom assignment	^{1}H-chemical shift [ppm] (integral, mult., *J* [Hz])	^{13}C-chemical shift [ppm]	HMBC correlations	NOESY connectivities
1	1.66 (3H, d, 0.9)	25.8	2, 3, 19	-
2	-	132.1	-	-
3	5.09 (1H, m)	124.9	5	4/5
4	2.05 (2H, m)	27.3	2	3, 5
5	1.95 (2H, m)	40.4	3, 4/8, 6	3, 4
6	-	136.0	-	-
7	5.08 (1H, m)	124.8	5/9, 20	-
8	2.07 (2H, m)	27.3	6, 7, 10	9
9	1.99 (2H, m)	40.4	8/12, 10, 11, 21,	8, 11
10	-	139.7	-	-
11	5.04 (1H, m)	118.1	9, 21	9, 12, 12’
12	2.74 (1H, dd, 15.0, 8.1)	27.1	10, 11, 13, 14	11, 12’, 14, 21
12’	2.36 (1H, dd, 15.0, 6.6)	27.1	10, 11, 13, 14	11, 12, 14, 21
13	-	61.1	-	-
14	3.58 (1H, d, 3.1)	58.9	15, 16	12, 12’, 15
15	4.58 (1H, d, 2.9)	65.9	16	14
16	-	172.6	-	-
17	5.18 (1H, s)	98.8	13, 15, 16	22
18	-	194.4	-	-
19	1.59 (3H, s)	17.7	1, 2, 3	-
20	1.58 (3H, s)	16.2	5, 6, 7	-
21	1.62 (3H, s)	16.4	9, 10, 11	12, 12’
22	3.69 (3H, s)	57.1	16	17

S 5. ^{1}H NMR spectrum for yanuthone K (**1**) at 500 MHz in acetonitrile-d_3

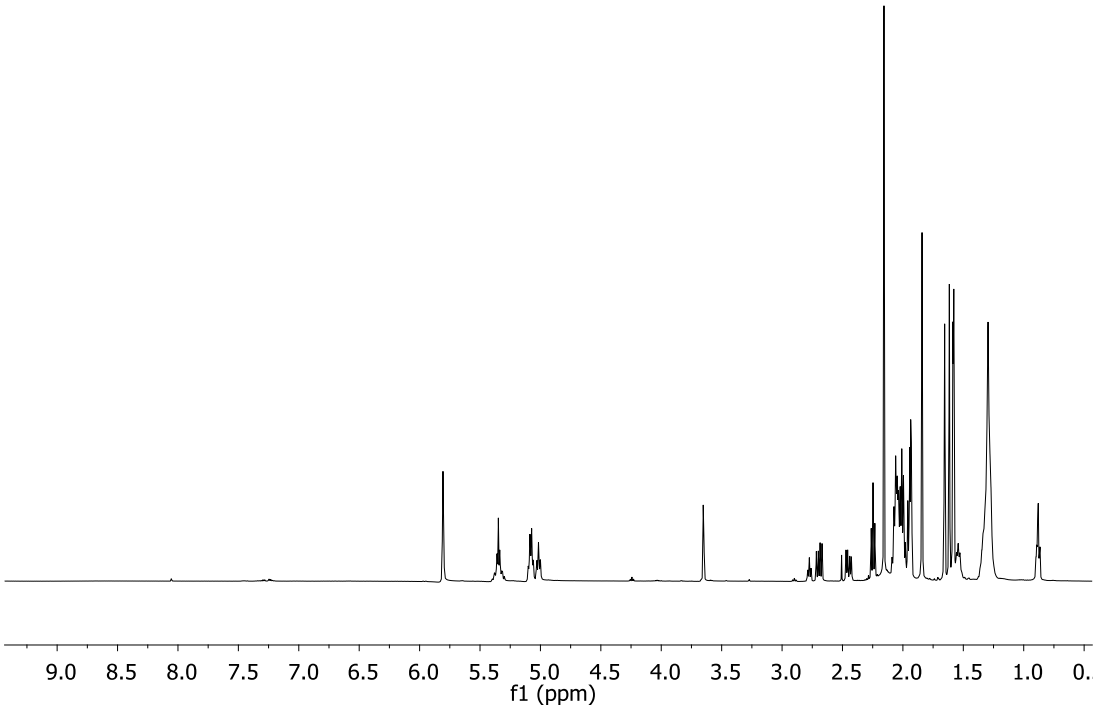

S 6. DQF-COSY spectrum for yanuthone K (**1**) in acetonitrile-d_3

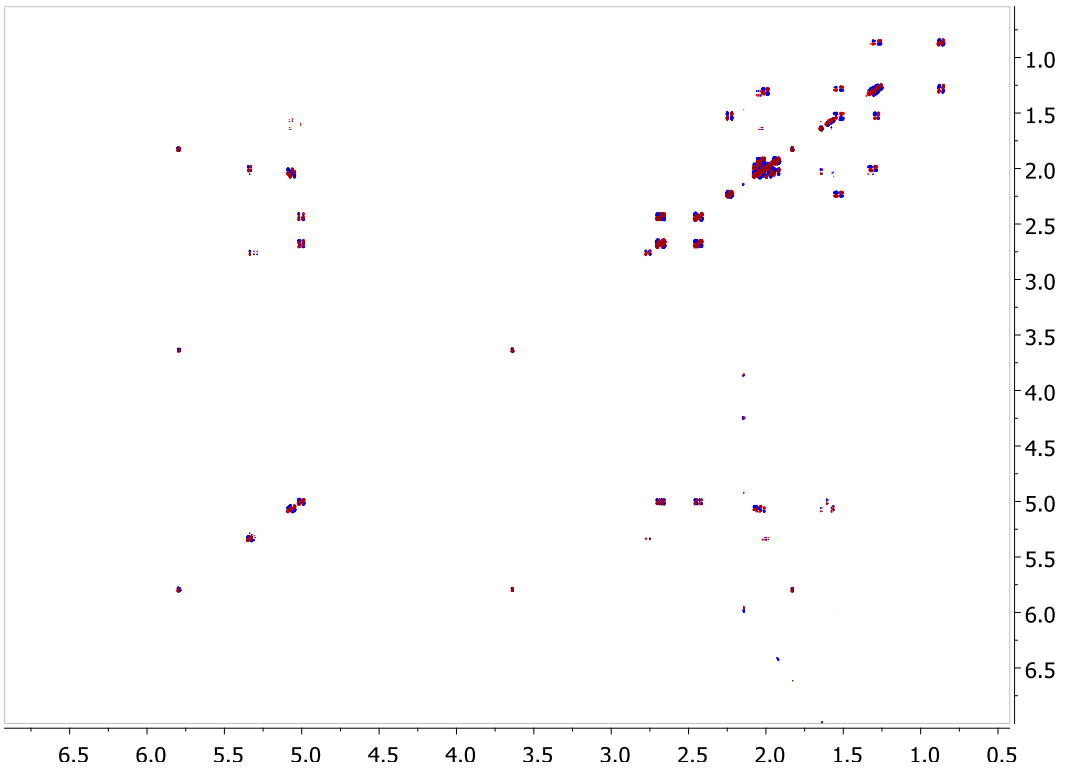

S 7. HSQC spectrum for yanuthone K (**1**) in acetonitrile-d_3

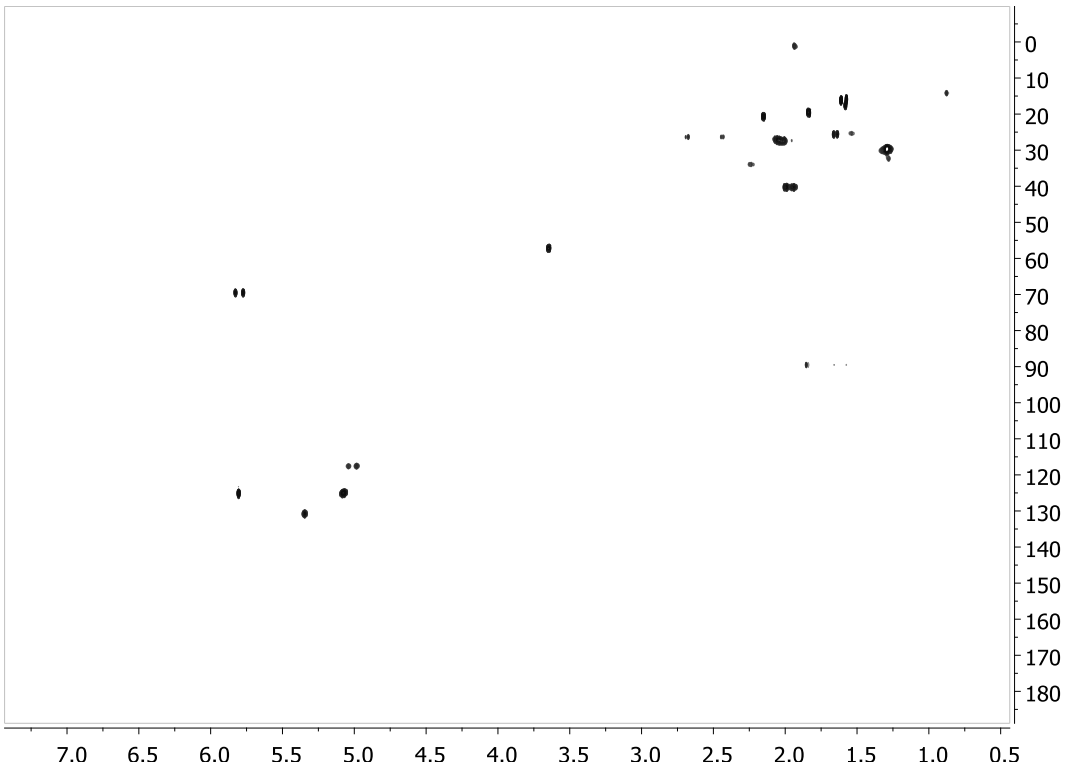

S 8. HMBC spectrum for yanuthone K (**1**) in acetonitrile-d_3

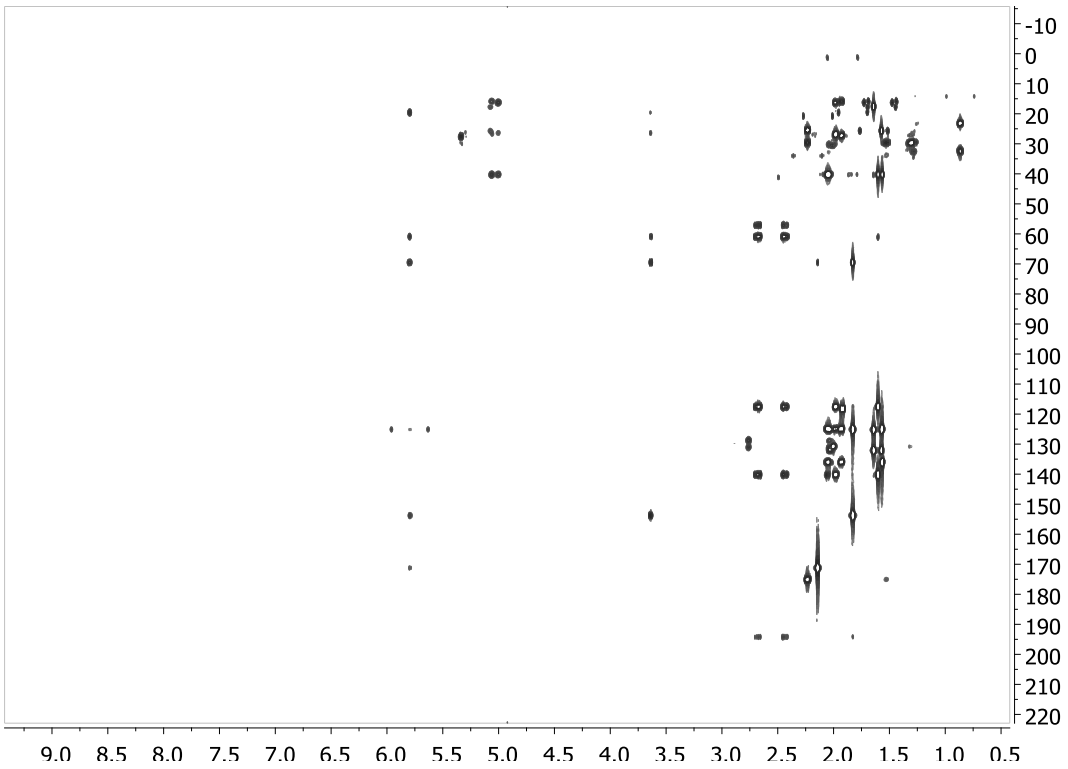

S 9. NOESY spectrum for yanuthone K (**1**) in acetonitrile-d_3

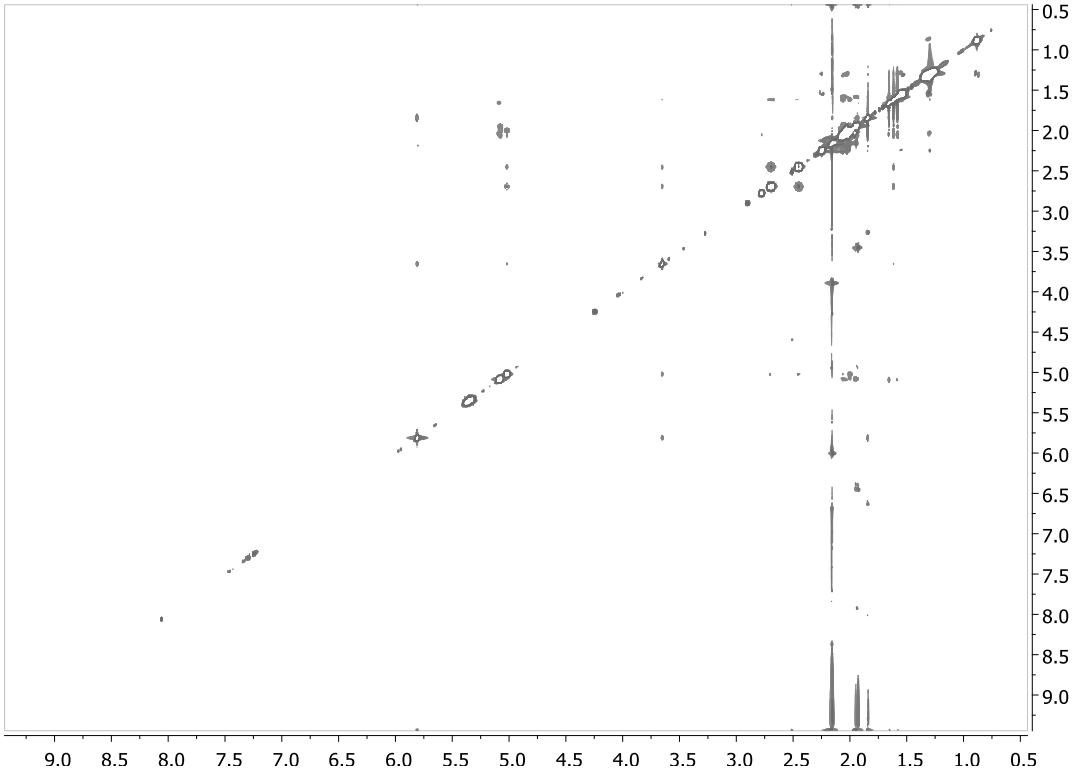

S 10. ^{1}H NMR spectrum for yanuthone L (2) at 500 MHz in acetonitrile-d_3

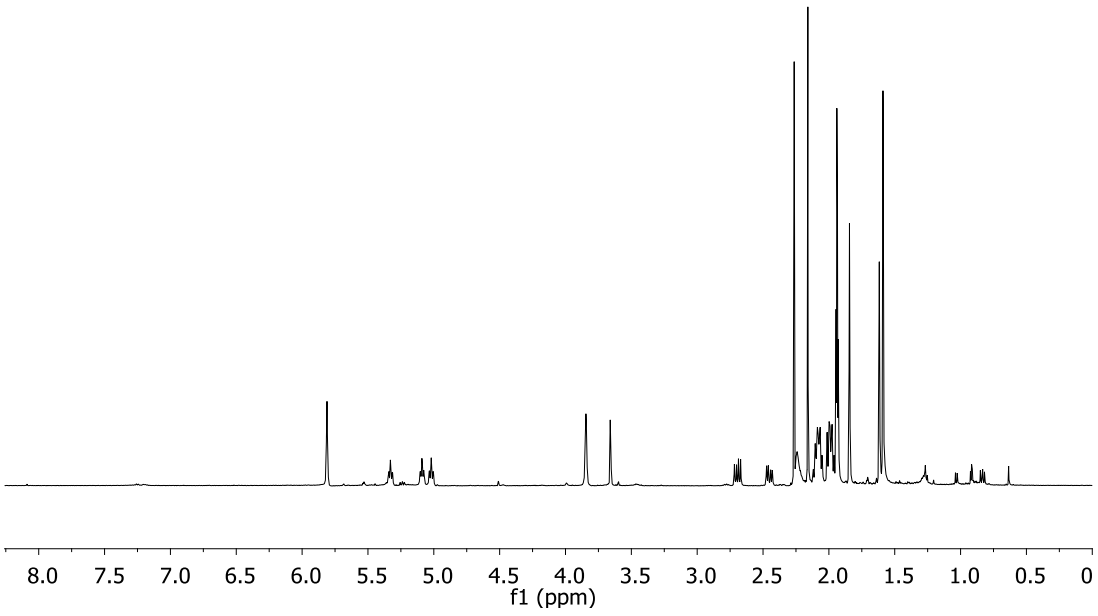

S 11. DQF-COSY spectrum for yanuthone L (**2**) in acetonitrile-d_3

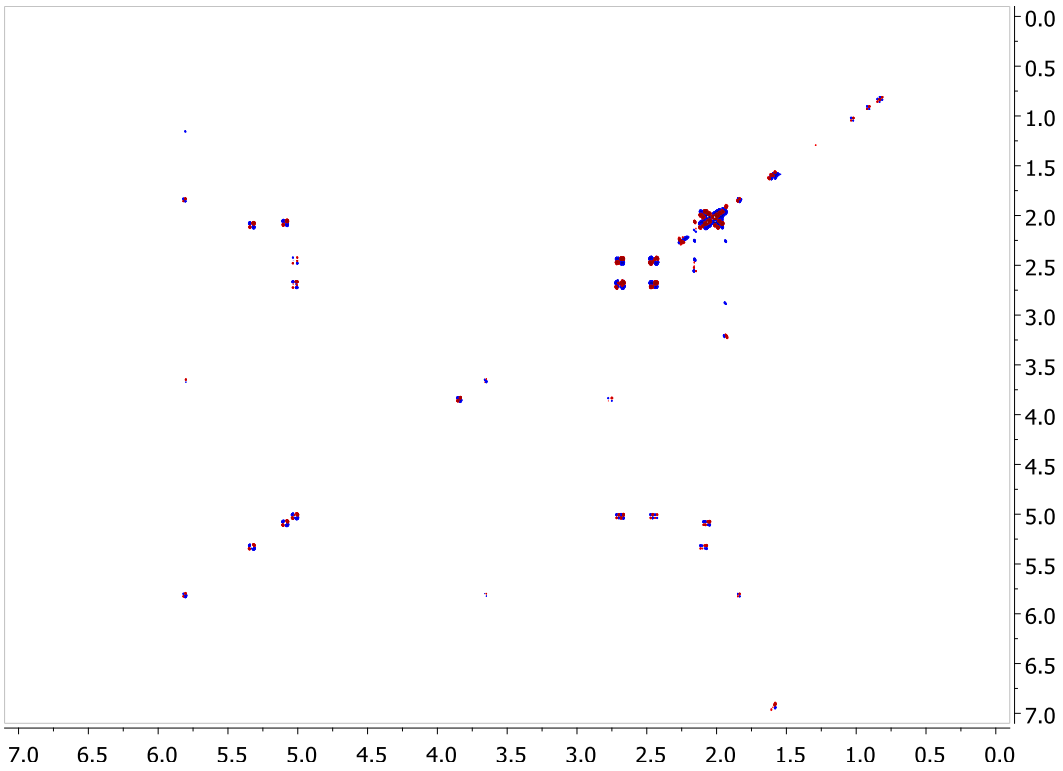

S 12. HSQC spectrum for yanuthone L (**2**) in acetonitrile-d_3

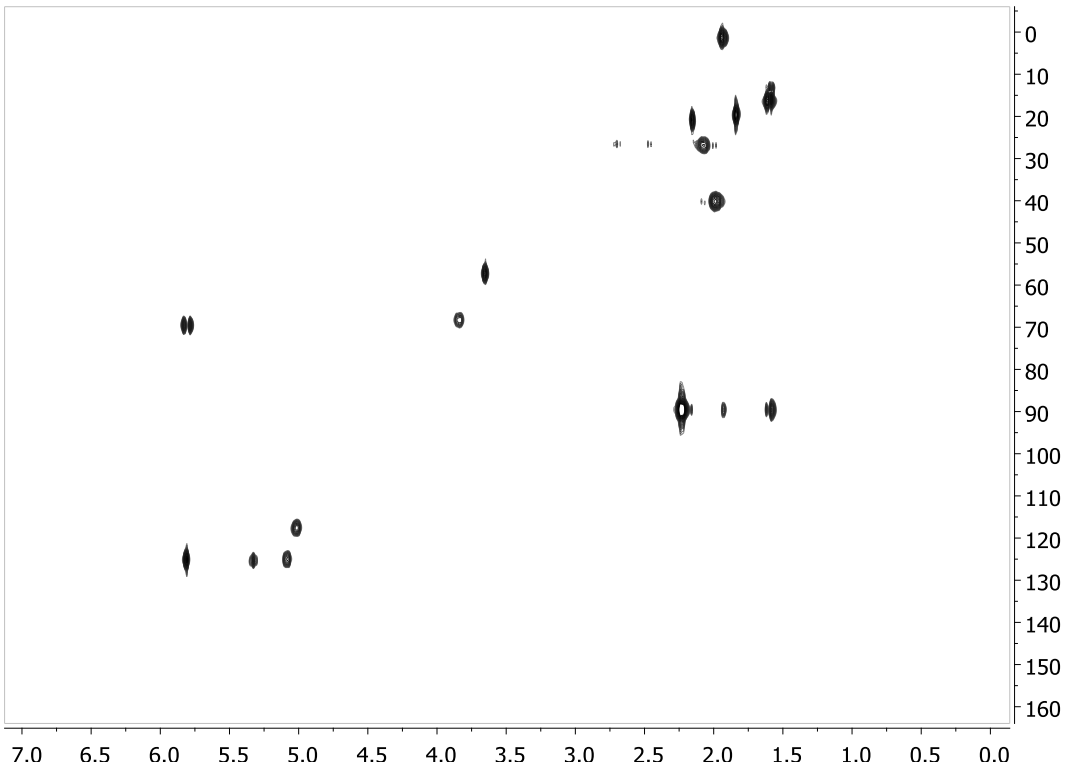

S 13. HMBC spectrum for yanuthone L (**2**) in acetonitrile-d_3

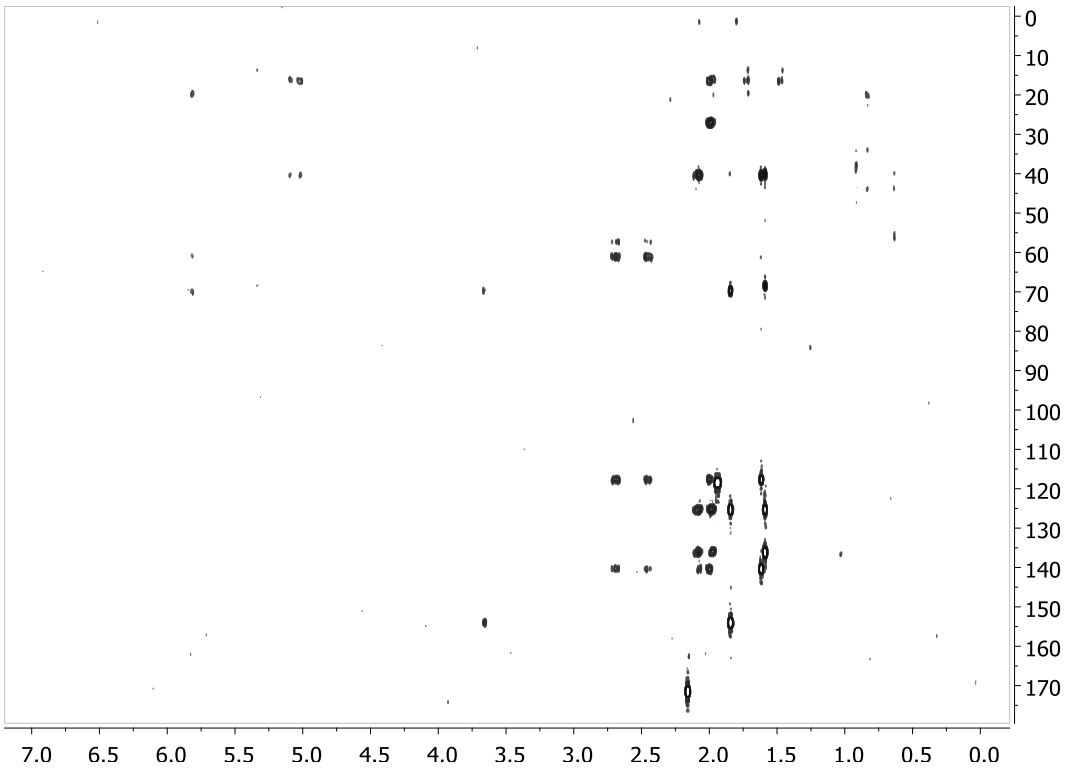

S 14. NOESY spectrum for yanuthone L (2) in acetonitrile-d_3

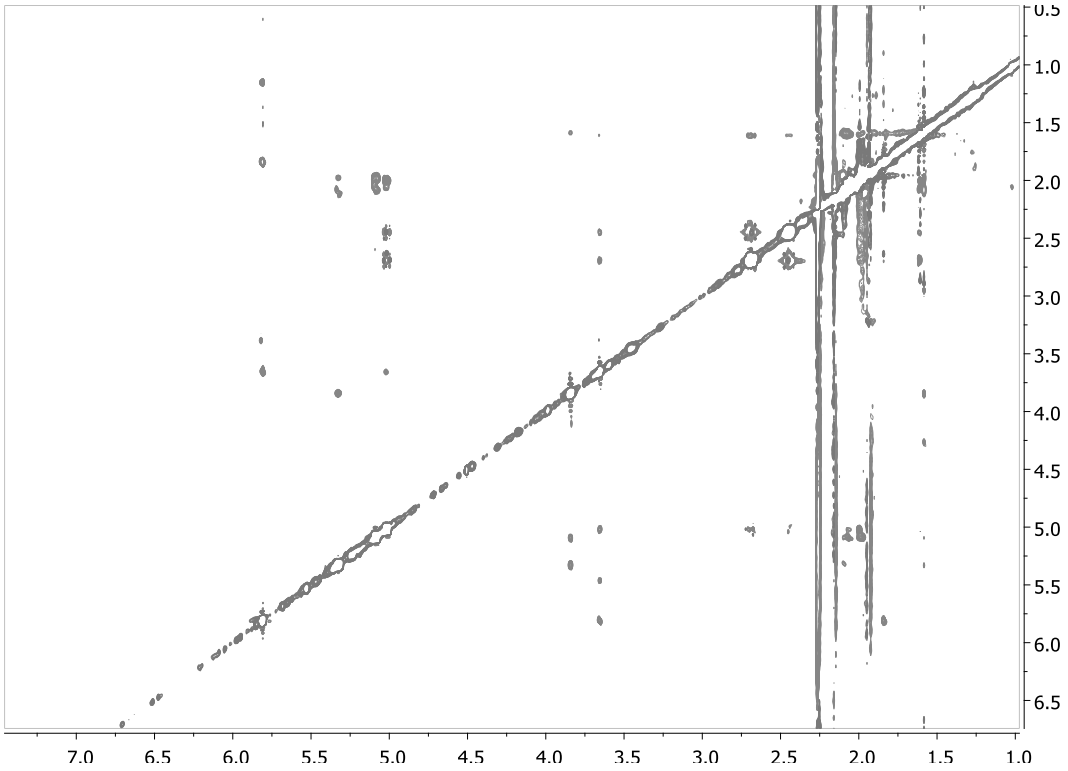

S 15. ^{1}H NMR spectrum for yanuthone M (**3**) at 500 MHz in acetonitrile-d_3

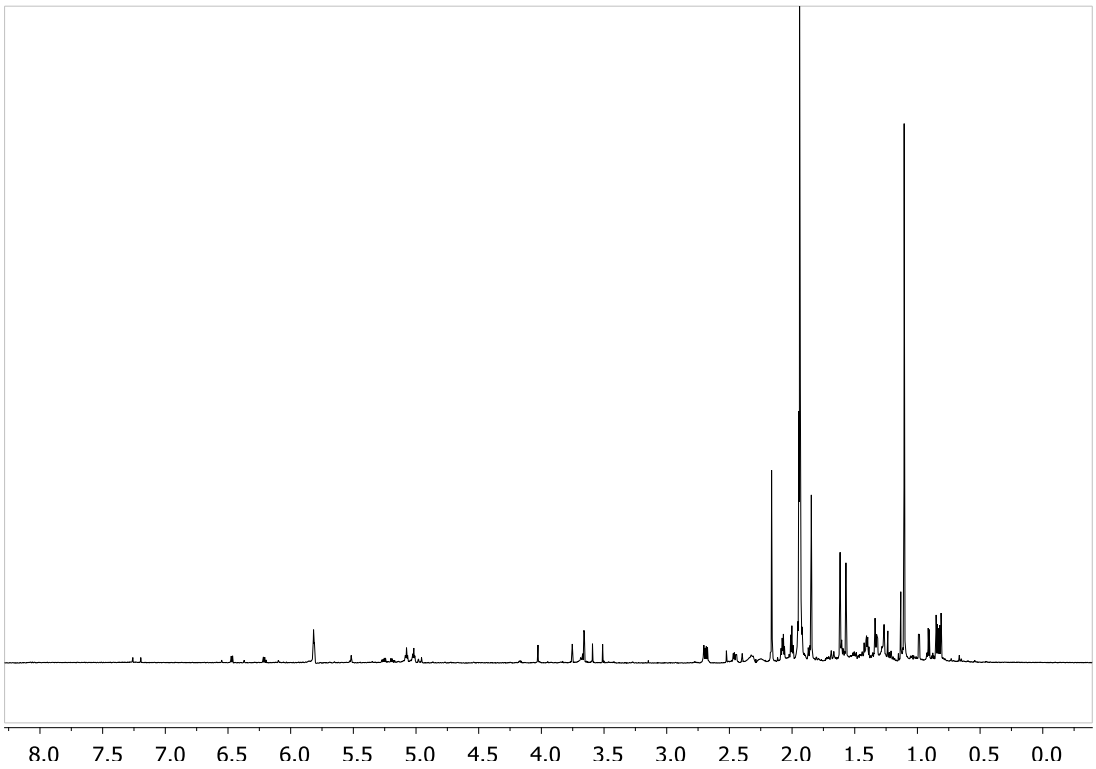

S 16. DQF-COSY spectrum for yanuthone M (**3**) in acetonitrile-d_3

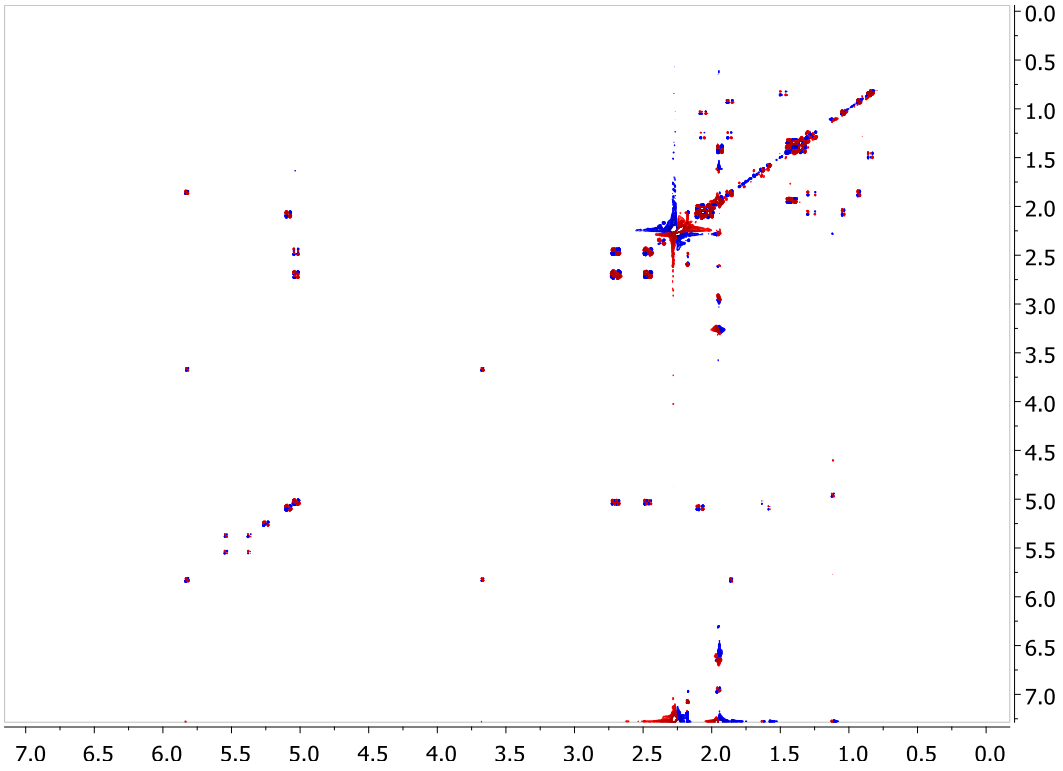

S 17. HSQC spectrum for yanuthone M (**3**) in acetonitrile-d_3

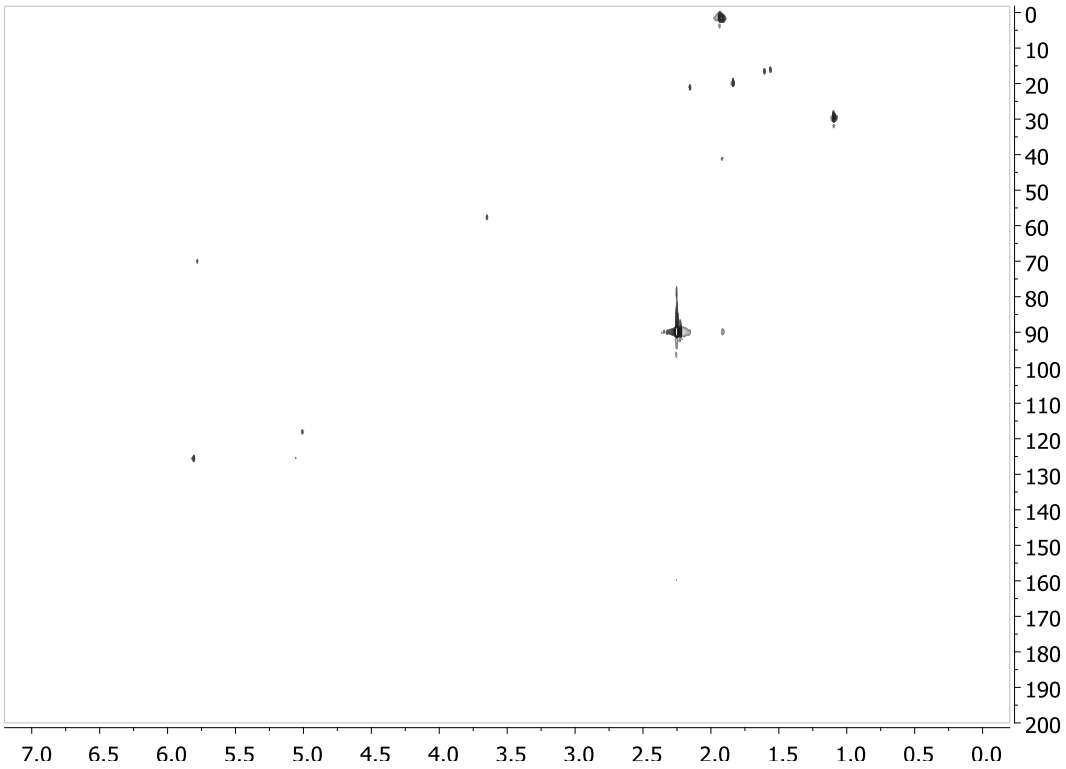

S 18. HMBC spectrum for yanuthone M (**3**) in acetonitrile-d_3

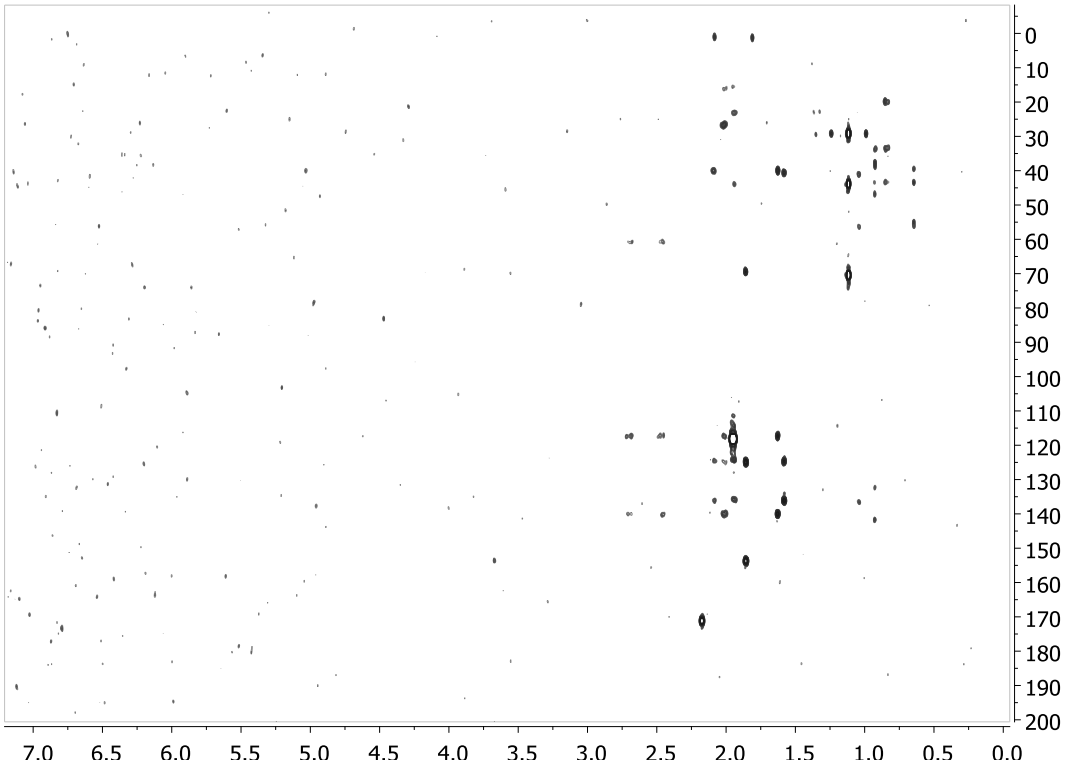

S 19. NOESY spectrum for yanuthone M (3) in acetonitrile-d_3

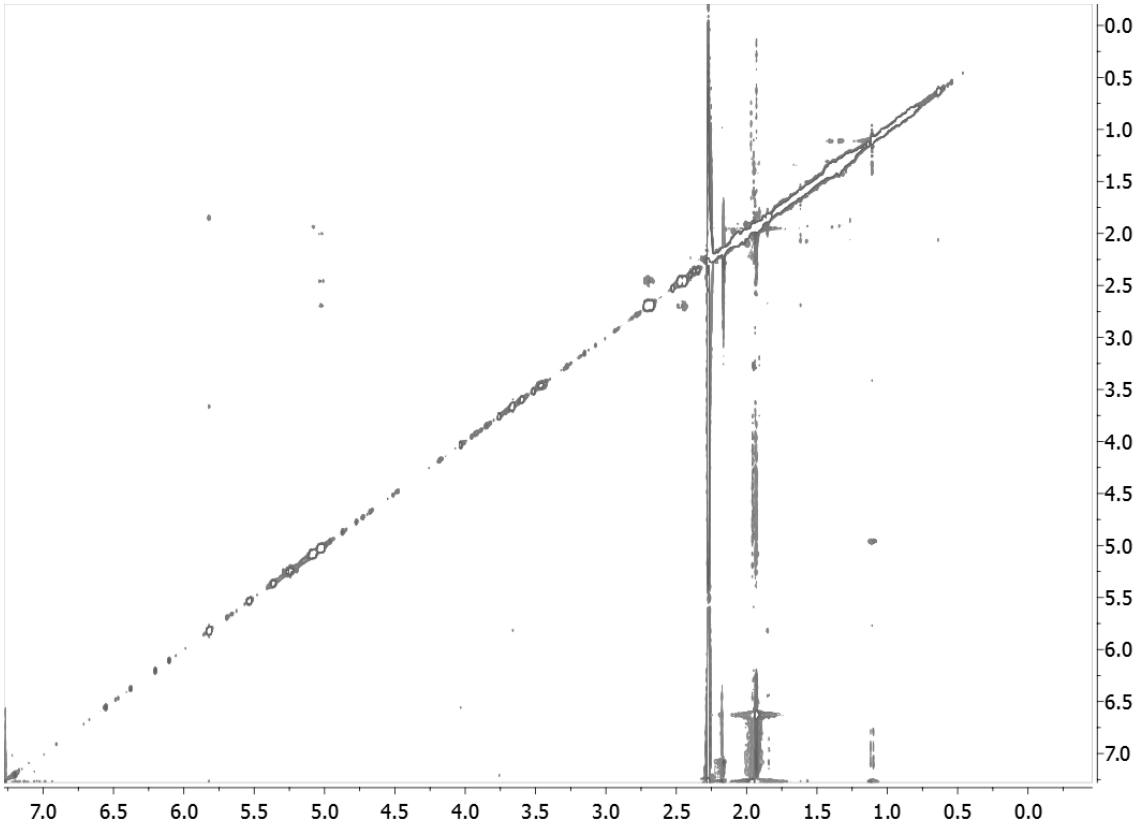

S 20. ^{1}H NMR spectrum for yanuthone X_2 (**4**) at 500 MHz in acetonitrile-d_3

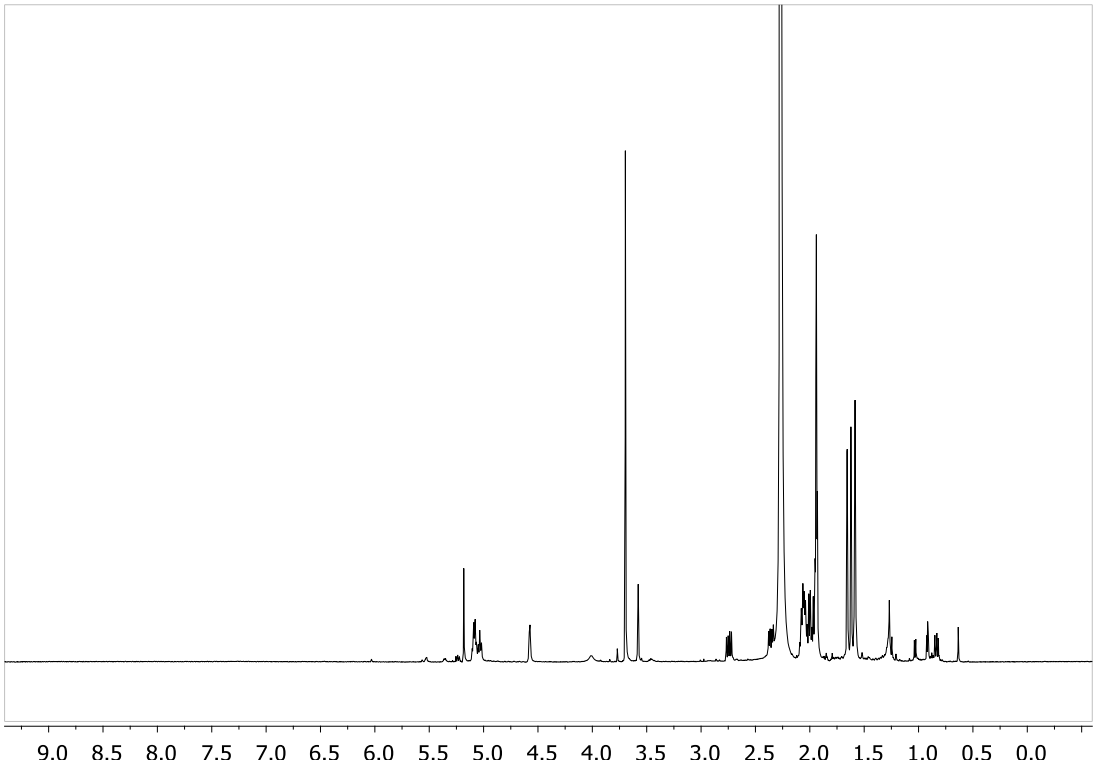

S 21. DQF-COSY spectrum for yanuthone X_2 (**4**) in acetonitrile-d_3

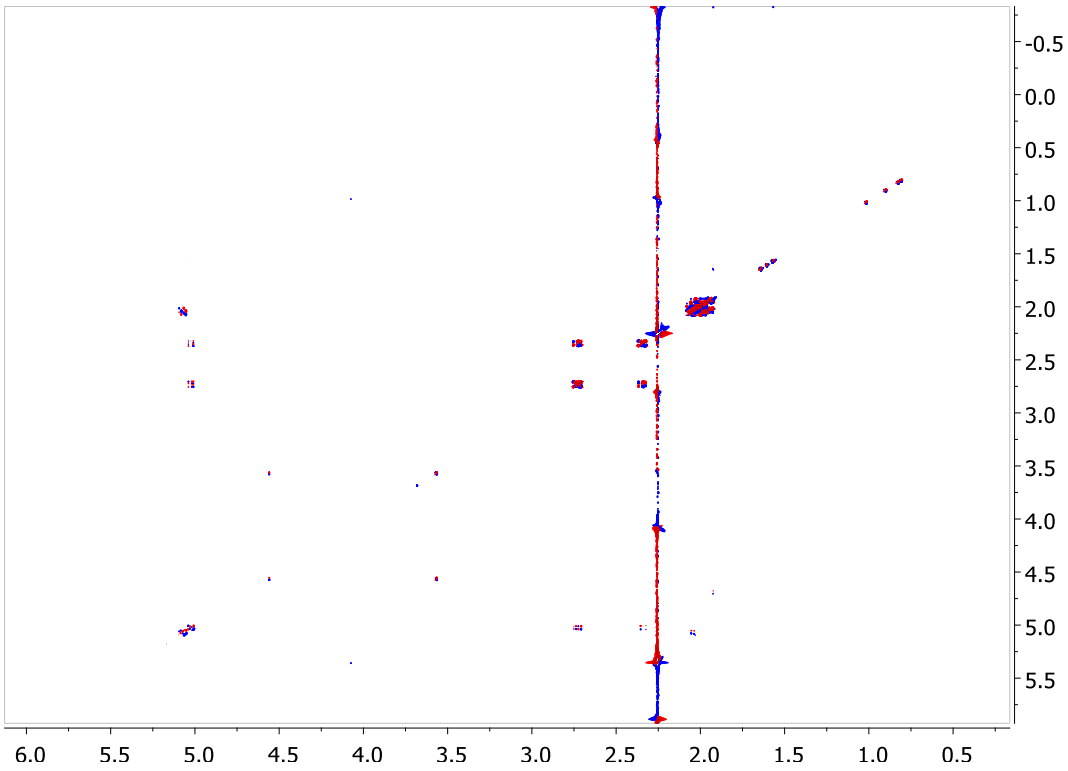

S 22. HSQC spectrum for yanuthone X_2 (**4**) in acetonitrile-d_3

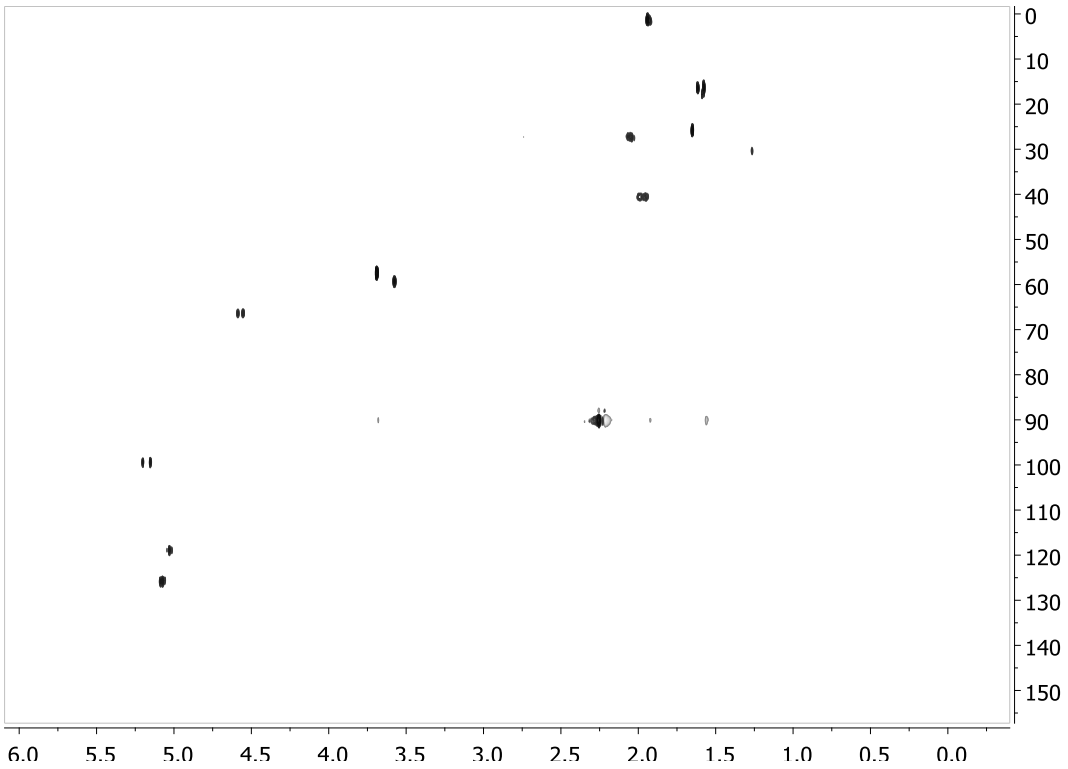

S 23. HMBC spectrum for yanuthone X_2 (**4**) in acetonitrile-d_3

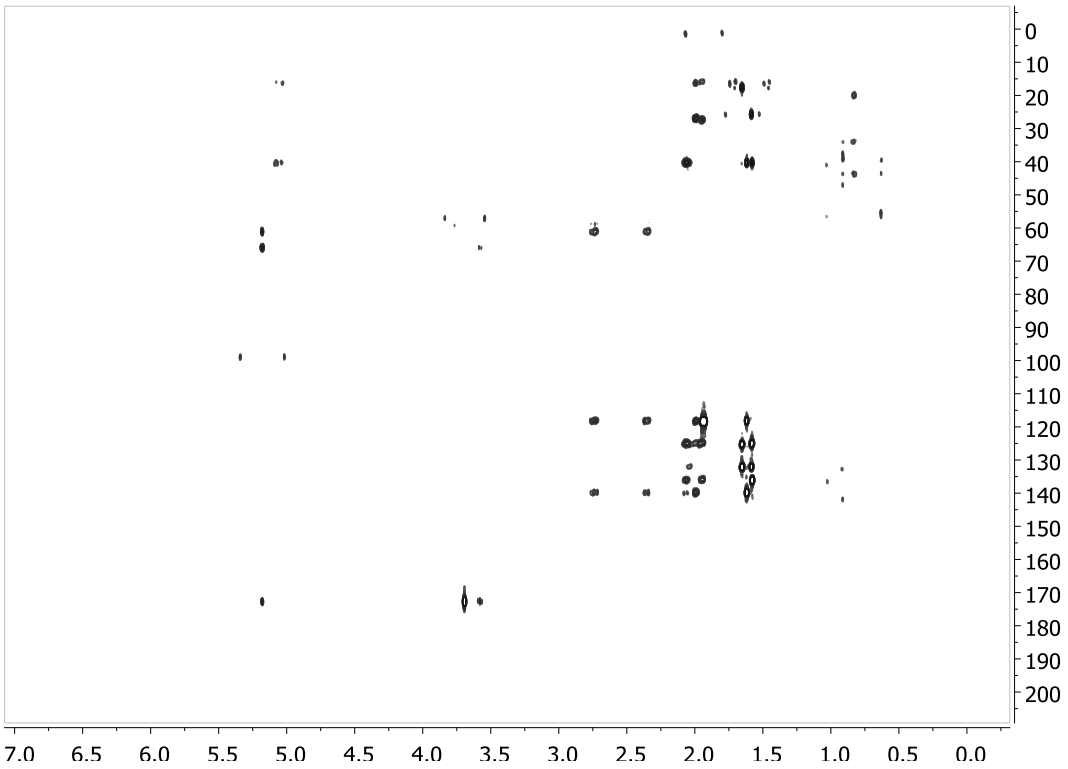

S 24. NOESY spectrum for yanuthone X_2 (4) in acetonitrile-d_3

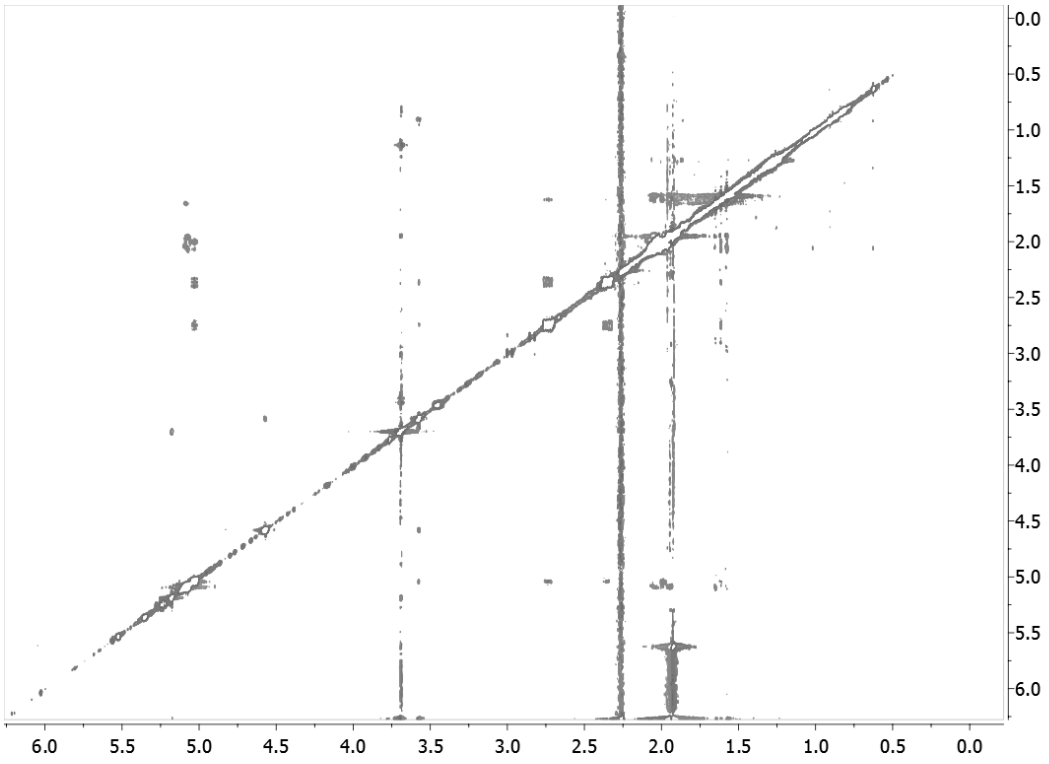

S 25. UV spectra for yanuthone K-M and X_2

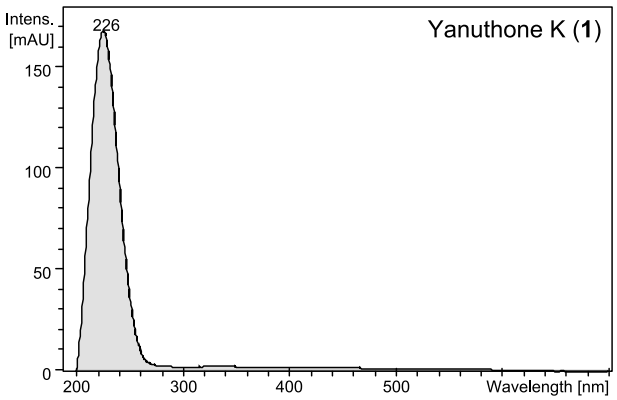

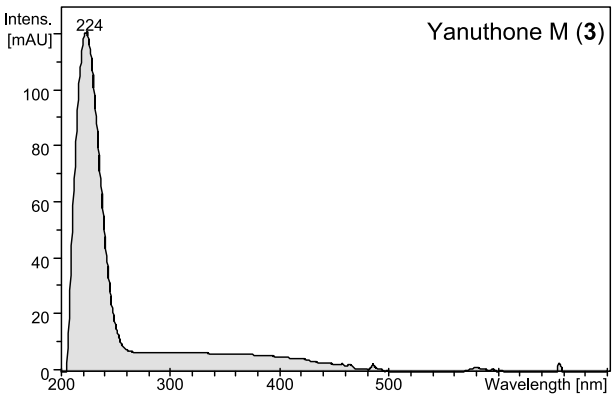

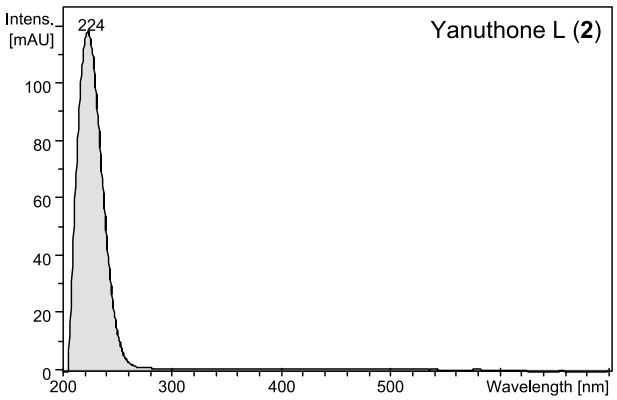

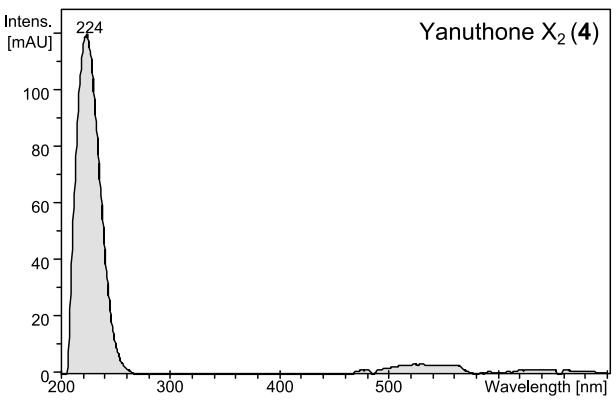

Paper 11

"Investigation of a 6-MSA synthase gene cluster in *Aspergillus aculeatus* reveals 6-MSA derived aculins A-B and non-6-MSA derived pyrrolidinones"

Petersen L.M.; Holm, D.K.; Gotfredsen, C.H.; Mortensen, U.H.; Larsen, T.O.

Intended for publication in Chemistry & Biology

Investigation of a 6-MSA synthase gene cluster in *Aspergillus aculeatus* reveals 6-MSA derived aculins A-B and non-6-MSA derived pyrrolidinones.

Lene M. Petersen[†,1], Dorte K. Holm[†,2], Charlotte H. Gotfredsen[3], Uffe H. Mortensen[2], Thomas O. Larsen[1,*]

Affiliation:

[1]Chemodiversity group, Eukaryotic Biotechnology, Department of Systems Biology, Søltofts Plads, Building 221, Technical University of Denmark, 2800 Kgs. Lyngby, Denmark.

[2]Eukaryotic Molecular Cell Biology group, Eukaryotic Biotechnology, Department of Systems Biology, Søltofts Plads, Building 223, Technical University of Denmark, 2800 Kgs. Lyngby, Denmark.

[3]Department of Chemistry, Kemitorvet, Building 201, Technical University of Denmark, 2800 Kgs. Lyngby, Denmark.

†These authors have contributed equally to this work.

***Corresponding author:**
Thomas O. Larsen, Technical University of Denmark, Department of Systems Biology
Eukaryotic Biotechnology, Building 221
2800 Kgs. Lyngby, Denmark
Email: tol@bio.dtu.dk
Phone: +45 45252632
Fax: +45 45884922

ABSTRACT

Aspergillus aculeatus is a filamentous fungus, belonging to the *Aspergillus* clade *Nigri*, and is an industrial workhorse used for enzyme production. Recently we have reported a number of secondary metabolites from this fungus [1], however, its genetic potential for production of secondary metabolites is vast. In this study we have identified a 6-methylsalicylic acid (6-MSA) synthase from *A. aculeatus*, and verified its functionality by episomal expression in *A. aculeatus* and heterologous expression in *A. nidulans*. Furthermore, we have over-expressed a transcription factor, embedded in the gene cluster, and found that it activated a biosynthetic cluster responsible for production of two pyrrolidinones, which were found to be diastereomers of RKB-3384B. Feeding studies with fully ^{13}C-labeled 6-MSA dismisses that 6-MSA is incorporated into the two pyrrolidinones, instead, 6-MSA is incorporated into three other novel compounds, which we have named aculins A and B, and epi-aculine A. Based on NMR data and bioinformatic studies we propose the structures of the compounds as well as a biosynthetic pathway leading to formation of aculins from 6-MSA.

INTRODUCTION

Aspergillus aculeatus is a filamentous fungus belonging to the group of black Aspergilli. *A. aculeatus* was recently sequenced by the DOE Joint Genome Institute (JGI), but no genes have yet been linked to production of metabolites. *A. aculeatus* is a known producer of several important secondary metabolites including the antiinsectan okaramines [2], the toxic secalonic acids [3] and recently we have reported production of the antifungal compounds calbistrins as well as several novel compounds including aculenes A-D with yet unknown activities [1].

Analysis of the published genome sequence revealed that *A. aculeatus* contains a gene with high similarity to 6-MSA synthases. No 6-MSA or obvious 6-MSA-derived compounds have been

detected in wildtype extracts of *A. aculeatus*, so it is possible that 6-MSA is highly modified into the final metabolite as it is the case for both yanuthone D [4], terreic acid [5], and patulin [6].

As no genetic techniques exist for *A. aculeatus*, we have used an AMA1-based episomal expression platform for gene expression. AMA1-containing plasmids allow for autonomous replication in many different Aspergilli [7,8] why this is a quick and efficient tool for expressing genes in organisms for which no available genetic techniques are available. Furthermore, the transformation efficiency with autonomous plasmids is much higher than integrating linear substrates [7] why it is also an efficient mean for gene expression in organisms that protoplast or transform very poorly.

In this study we have shown that the putative 6-MSA synthase is in fact a 6-MSA synthase, by heterologous expression of the gene in the model fungus *Aspergillus nidulans*. Furthermore, we have used the AMA1-based expression platform in *A. aculeatus* for expression of a transcription factor embedded in the 6-MSA gene cluster. This approach activated a biosynthetic cluster with unknown relation to the 6-MSA gene cluster, which is responsible for production of two diastereomers of RKB-3384B. Furthermore, labelling studies have identified three compounds originating from 6-MSA, which are likely related to the gene cluster. We propose the structures of the compounds and suggest a possible biosynthetic pathway from 6-MSA.

RESULTS AND DISCUSSION

Heterologous expression of a putative 6-MSA synthase verifies production of 6-MSA.

A BLAST analysis of the ASPACDRAFT_1904397 gene on all genomes in the Aspergillus Genome Database (AspGD) revealed a high similarity to fungal 6-methylsalicylic acid (6-MSA) synthases (data not shown). To verify that the gene indeed encodes a 6-MSA synthase the gene was

integrated into the defined and characterized locus *IS1* of *A. nidulans*, which is a site that has previously been used for successful expression of PKS genes [4][9]. This approach is useful in this study, as *A. nidulans* is known not to produce 6-MSA, and does not contain any PKSs with homology to 6-MSA synthases. The metabolite profile of the strain was analyzed by UHPLC-DAD-TOFMS, and a new compound was indeed produced compared to the reference (Figure 1). Dereplication of the compound and comparison to an authentic standard of 6-MSA verified that the compound was 6-MSA (**1**), confirming that ASPACDRAFT_1904397 encodes a 6-MSA synthase.

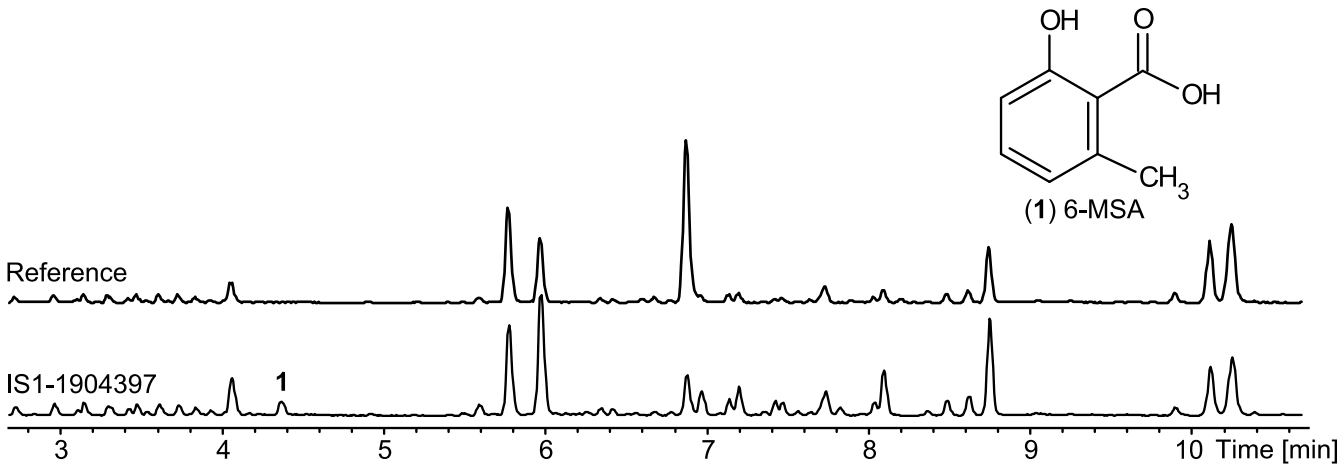

Figure 1. BPC of the *A. nidulans* strain expressing the putative 6-MSA synthase 1904397 compared to an *A. nidulans* reference.

Expression of the 6-MSA synthase in *A. aculeatus* results in accumulation of 6-MSA.

Having confirmed that *A. aculeatus* contained a 6-MSA synthase, wildtype extracts were scrutinized for the presence of 6-MSA. As no 6-MSA was detected in any wildtype extracts of *A. aculeatus*, we hypothesized that either the 6-MSA synthase gene was silenced or that all produced 6-MSA was modified into a different compound by a number of tailoring enzymes. Based on this hypothesis, over-expression of the 6-MSA synthase might result in production of 6-MSA or another compound, or in production of higher amounts of a compound that was also produced by the

wildtype strain. Accordingly, the 6-MSA synthase was expressed in *A. aculeatus* from the plasmid pDHX3, carrying the *hph* selection marker. Correct transformants were cultivated on solid minimal medium with hygromycin B and subjected to metabolite profile analysis by UHPLC-DAD-TOFMS. Data analysis verified that the strain produced 6-MSA (Figure 2). However, there was no significant change in the rest of the metabolite profile (Figure 2). The fact that the *A. aculeatus* pDHX3-6-MSAS strain produced 6-MSA rather than a biosynthetic end product, indicated that no tailoring enzymes in the biosynthetic pathway (if any) were expressed, and that the entire proposed 6-MSA cluster was silent under the applied laboratory conditions.

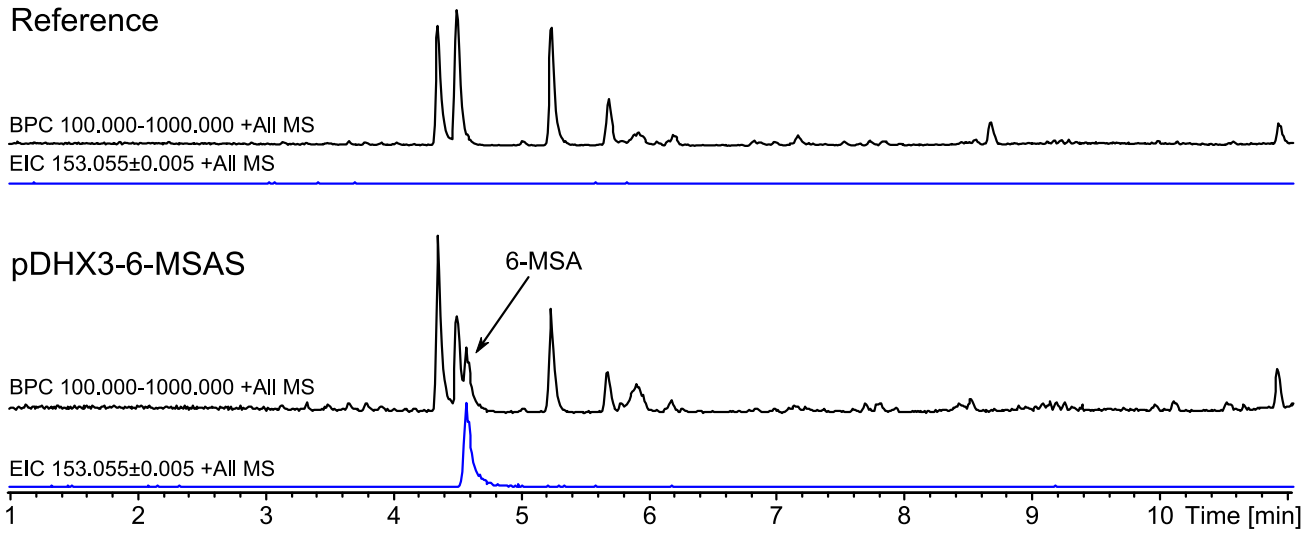

Figure 2. BPC and EIC (153.055±0.005) for *A. aculeatus* reference and pDHX3-6-MSAS over-expression strain.

Over-expression of a transcription factor from the proposed 6-MSA cluster results in up-regulation of two compounds.

Examination of the predicted gene cluster revealed that a putative transcription factor (TF) was located immediately downstream of the 6-MSA synthase gene, indicating that this could be a

regulator of the 6-MSA gene cluster. The TF was expressed from the expression platform pDHX2 (pDHX2-TF), cultivated on minimal and YES media, and analyzed by UHPLC-DAD-TOFMS. Examination of the metabolite profiles revealed up-regulation of production of two compounds on minimal medium, (**2**) and (**3**), which were not present in the reference (Figure 3).

The two compounds, (**2**) and (**3**), were produced by both the reference strain and pDHX2-TF when cultivated on YES, indicating that the biosynthesis of these compounds is normally active when cultivated on YES medium, but not on minimal medium. In general, cultivation on YES medium did not result in detectable changes in the metabolite profile (Figure 3). One explanation for this result might be that the plasmid is lost when proper selection is not maintained; YES provides all nutrients, including uridine, whereas minimal medium does not. Another explanation is that the TF is already highly expressed during cultivation on YES, why over-expression does not affect production of the compounds.

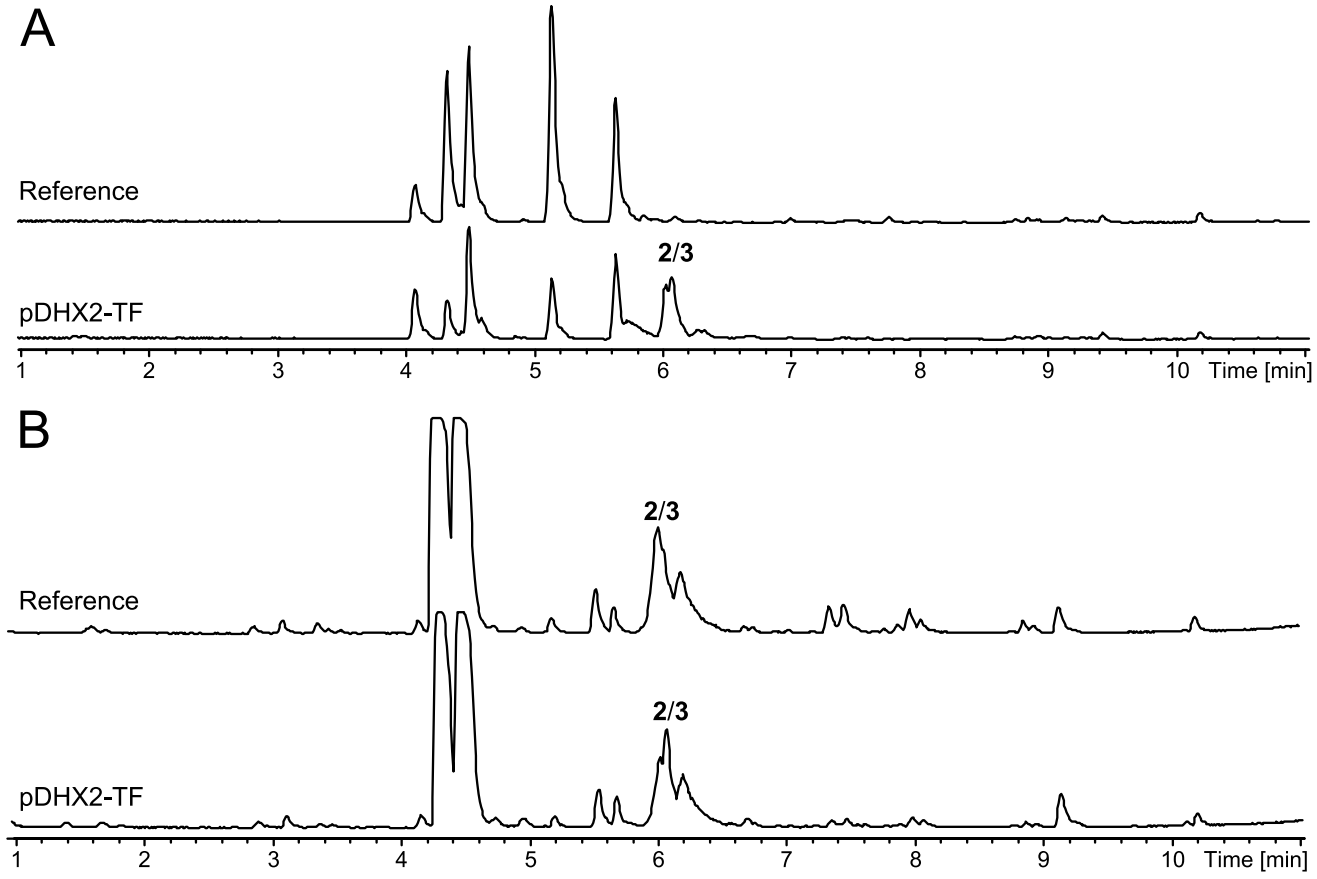

Figure 3. BPC of *A. aculeatus* expressing putative transcription factor from plasmid (pDHX2-TF) compared to a reference, cultivated on minimal medium (**A**) and YES (**B**).

Elucidation of the structures revealed two diastereomers, of the patented compound RKB-3384B [10] (Figure 4). NMR data is available in supplementary Tables S1 and S2.

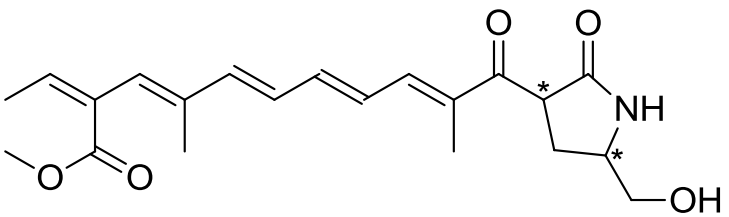

RKB-3384B (**2**)/(**3**)

Figure 4. Structure of the diastereomers of RKB-3384B (**2**)/(**3**). Stereocenters are marked with *.

The structures of (**2**) and (**3**), which differ only by their stereochemistry, are surprising, as it is not obvious how they were derived from 6-MSA, if at all. The backbone have previously been observed e.g. in lucilactaene produced by a *Fusarium sp*. [11], epolactaene from a marine *Penicilium sp*. [12] and fusarin C from *Fusarium moniliforme* [13]. All of these compounds contain the long hydrocarbon chain observed in (**2**) and (**3**), but differs in the attached moiety. Lucilactaene contains two fused five-membered rings, epolactaene a single five-membered lactam entailing an epoxide, and the fusarins display different structural features. Labeling studies have shown that the backbone chain of fusarins is of polyketide origin [14], and both labeling and genetic studies provided insight into the 5-membered ring structures, which originate from a C_4-unit [15]. Assuming that (**2**) and (**3**) entail the same polyketide chain, the 5-membered ring must consist of a nitrogen-containing C_3 unit e.g. serine, and the connection to 6-MSA is not obvious.

The pyrrolidinones is not bioactive against cancer cells. Some of the compounds that are structurally similar to (**2**) and (**3**) have been reported as bioactive; Lucilactaene as a cell cycle inhibitor in p53-transfected cancer cell [11], epolactaene as a neuritogenic compound in human neuroblastoma cells [12], and fusarin C as a mutagen [13]. This prompted us to investigate the bioactivity. (**2**) was tested in a CellTiter-Glo® assay [16] (Figure S2), but was found to be inactive.

Fully labeled 6-MSA is incorporated into three compounds, but not the pyrrolidinones.

To test whether 6-MSA was indeed incorporated into (**2**) and (**3**) we fed fully labeled 6-MSA ($^{13}C_8$-6-MSA) to the TF expressing strain (Figure 5).

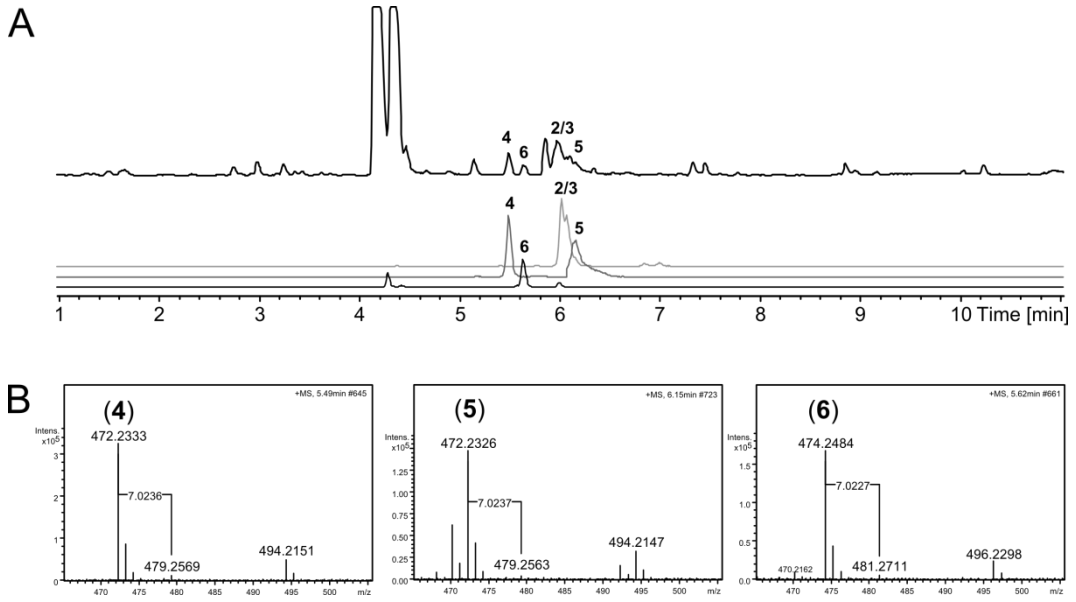

Figure 5 A. BPC (black) of pDHX2-TF on YES+$^{13}C_8$-6-MSA, EIC 374.1963±0.005 (light grey), EIC 472.2333 ± 0.005 (dark grey), EIC 474.2484 ± 0.005 (black). **B.** Mass spectra of compounds (**4**), (**5**), and (**6**).

Careful inspection of the metabolite profile revealed a mass shift of 7.023 Da for three compounds: (**4**) and (**5**), and (**6**) (Figure 5). The fact that a mass shift equivalent of seven ^{13}C atoms, and not the eight ^{13}C atoms that are present in $^{13}C_8$-6-MSA, suggests that one carbon atom is eliminated from 6-MSA during modification into the end products. A mass shift of 7.023 Da was also observed in feeding studies of the yanuthone D biosynthesis, where one carbon atom is eliminated from 6-MSA by decarboxylation [4].

Interestingly, but not surprisingly, 6-MSA was not incorporated into (**2**) and (**3**) (Figure S1). Thus (**2**) and (**3**) do not origin from 6-MSA although production of the two compounds appeared to be activated by expression of the TF. It is surprising that a putative TF, located immediately downstream of a 6-MSA synthase, controls expression of two compounds, which do not depend on 6-MSA. Similarly, the three compounds that do contain 6-MSA, are not controlled by the putative TF in a simple manner, if at all. Thus, the mode of action for the putative TF is not clear. We have

named the gene encoding the TF *arnR*, and the corresponding gene product ArnR, to underline that the TF positively controls expression of genes involved with formation of (**2**) and (**3**), but does not seem to regulate the genes that are part of the 6-MSA gene cluster.

Structure elucidation of degradation products lead to identification of three novel compounds.

To elucidate the structures of (**4**), (**5**), and (**6**) a large scale cultivation was prepared. Purification of the compounds proved challenging as the compounds were unstable even under mild conditions. Apparently, (**4**) and (**5**) were degraded to a small acid (**7**)/(**8**) and aculene A (**9**), a compound that we have previously characterized from *A. aculeatus* [1]. Likewise (**6**) was degraded to aculene B and (**7**)/(**8**), and the same trend has previously been observed for other *A. aculeatus* metabolites, the acucalbistrins A-B [1]. Although impossible to isolate (**4**), (**5**), and (**6**), the structures of the degradation products were solved, see Figure 6.

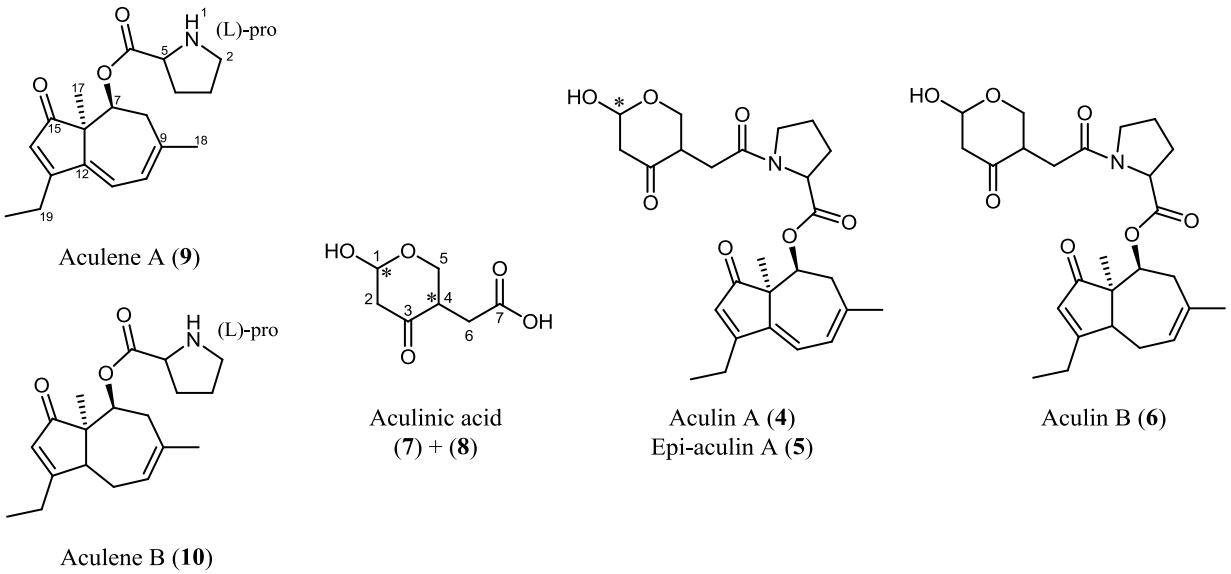

Figure 6. Structures of the degradation products of (**4**) (aculene A (**9**) and (**7**) + (**8**)) and the suggested structure of (**4**), (**5**) and (**6**).

The resonances observed from aculene A (see table S3) were comparable to those reported earlier [1]. The small acid (**7**)/(**8**) gave rise to two set of signals probably due to hemiacetal opening and closing at C1. This leads to different stereocenters at C1, resulting in diastereomers and justifying the observed shifts (see Tables S4 and S5). Database searches in Scifinder [17] and Antibase [18] did not provide the structures of (**7**)/(**8**) or any compounds with incorporation of (**7**)/(**8**). The calculated mass of the suggested structure (**4**) is 471.2257 Da, corresponding to a *m/z* of $[M+H]^+$ of 472.2330, which matches the observed *m/z* for compounds (**4**) and (**5**). We therefore suggest that the two structures are the same, and only differ at the stereocenters in (**7**) and (**8**). The *m/z* of (**6**) is 2 Da higher than (**4**) and (**5**), why we suggest the same structure, but with incorporation of aculene B rather than aculene A (see Figure 6), similar to what we have proposed for the acu-calbistrins A and B [1]. The degradation products of (**6**) have not been confirmed by NMR experiments, but have been verified by UHPLC-DAD-HRMS data. We have named the new compounds aculin A (**4**) , epi-aculin A (**5**) and aculin B (**6**). Accordingly, the small acid that is incorporated into the three aculins was named aculinic acid (**7**)/(**8**).

The biosynthetic pathway from 6-MSA to aculin A.

The 6-MSA synthase gene and surrounding genes are depicted in Figure 7. We define the *acu* gene cluster as the genes *acuA*-*acuI* spanning 23.6 kb with no disruption from unrelated genes.

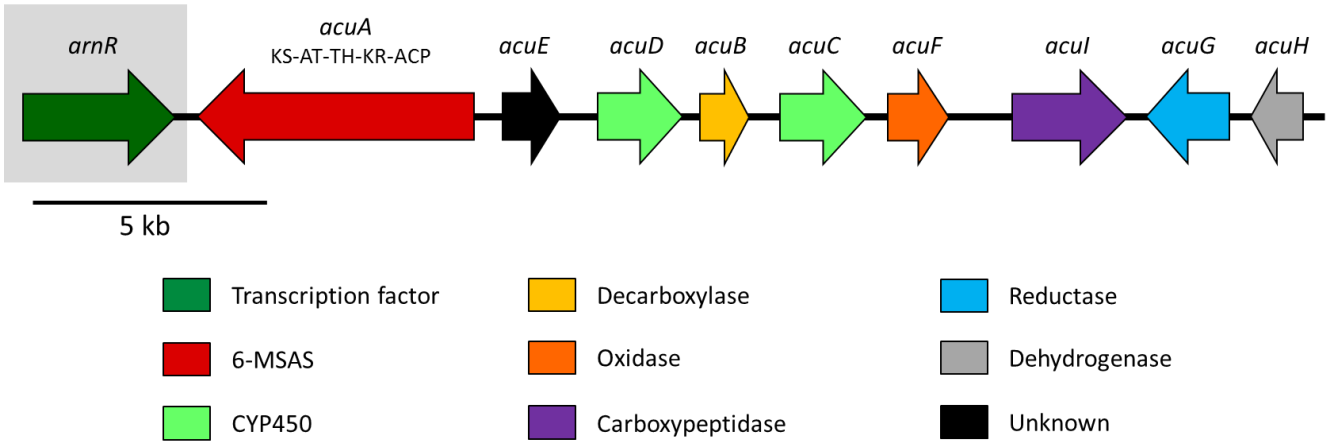

Figure 7. The *acuA* 6-MSA synthase encoding gene is flanked by eight genes which we define as the *acu* gene cluster. The *arnR* TF is not part of the *acu* cluster, but is located immediately upstream of *acuA*.

Table 1. Overview of genes and proposed activities of the *acu* cluster

Gene name	**Locus (ASPACDRAFT_)**	**Proposed biosynthetic activity**	**Note**
-	1904392	-	Predicted ATPase
arnR	123491	Transcriptional activator of RKB-3384B cluster (unknown)	Predicted fungal transcription factor
acuA	1904397	6-MSA synthase	Confirmed 6-MSA synthase (this study)
acuE	1904400	Oxidase	No homology to known activities, but homologous to YanE (E-value 1.91E-38)
acuD	32595	m-hydroxybenzyl alcohol hydroxylase	Predicted CYP450, PatI homolog (*A. clavatus*)
acuB	45672	Decarboxylase	6-MSA decarboxylase homolog (*P. expansum*)
acuC	45673	m-cresol methyl hydroxylase	Predicted CYP450, PatH homolog (*A. clavatus*)
acuF	geneX	Baeyer-Villiger oxidation	No homology to known activities. Gene predicted by AUGUSTUS and FGeneSH
acuI	1904405	Attachment of aculinic acid to aculene A	Predicted carboxypeptidase
acuG	80410	Reductase	Predicted oxidoreductase.
acuH	geneY	Dehydrogenase	Predicted dehydrogenase. Gene predicted by AUGUSTUS and FGeneSH
-	80411	-	Predicted siderophore iron transporter
-	123500	-	No homology to known activities

Utilizing knowledge of the two other 6-MSA derived pathways towards yanuthone D [4] and patulin [19], as well as the predicted activities encoded by the *acu* cluster (Table 1), allows us to propose a biosynthetic pathway from 6-MSA (**1**) towards aculin A (**4**), see Figure 8. We suggest that after formation of 6-MSA by the AcuA PKS, 6-MSA is decarboxylated to *m*-cresol, followed by oxidations to *m*-hydroxybenzyl alcohol, and subsequently to gentisyl alcohol, as is described for the patulin and yanuthone D biosynthetic pathways [6][19][4]. In our model the AcuB decarboxylase converts 6-MSA to *m*-cresol as a first step. Subsequently, oxidation of *m*-cresol to *m*-hydroxybenzyl alcohol and oxidation of *m*-hydroxybenzyl alcohol to gentisyl alcohol is catalyzed by AcuC and AcuD, which are homologs of PatI and PatH from the patulin pathway in *A. clavatus*. Gentisyl alcohol is then oxidized to (**11)** by AcuE, which is homologous to YanE from the *yan* cluster in *A. niger*. In the yanuthone biosynthesis it was proposed that YanE, along with another enzyme, YanD, catalyzes formation of the epoxide on the core aromatic moiety [4]. Thus it is likely that the one gene (YanE/AcuE) can catalyze hydroxylation of the aromatic ring. The aromatic system is opened via oxidation by a Baeyer-Villiger type of oxidation; however, there is no gene in the cluster that has homology to any known Baeyer-Villiger oxidase. We therefore suggest that the product of a cluster gene encoding an unknown activity, AcuF, may be responsible for this step. In this scenario, the carboxylic acid at C1 of (**12**) is subsequently reduced to an aldehyde by AcuG to form (**13**). Subsequently, a hemiacetal is formed, as suggested for the patulin biosynthetic pathway [20] and AcuH, a putative dehydrogenase, then reduces the double bond between C4 and C6. Finally, keto-enol tautomerism results in formation of aculinic acid (**7**)/(**8**), which exist as two diastereomers (both R/S configuration at C1) due to the non-enzymatic hemiacetal formation.

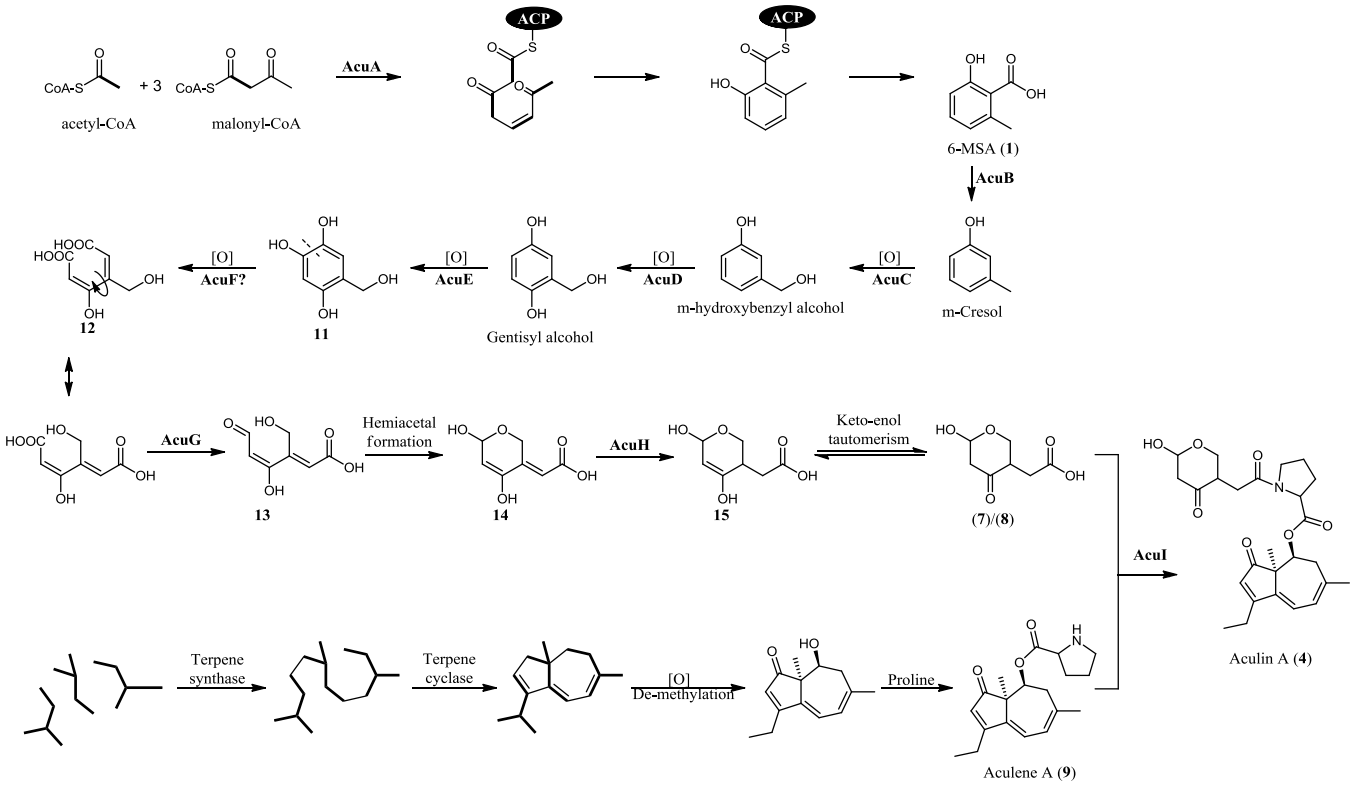

Figure 8. Proposed biosynthetic pathway of aculin A (**4**).

We propose the biosynthesis of the aculene A moiety to originate from the terpene pathway. We have earlier suggested this fourteen carbon moeity to originate from three isoprene units with the loss of one carbon atom at C9 [1]. The proposed sesquiterpene skeleton is also seen in the compound lasidiol angelate from *Lasiantheae fruticosa* [21], however with a isopropenyl moeity instead of the ethyl group, resulting in a C_{15} carbon skeleton. In this scenario the demethylation occurs at C19, as illustrated in Figure 8. Linking of (**7**)/(**8**) to (**9**) could be achieved by AcuI, which is predicted as a carboxypeptidase. The expected activity for a carboxypeptidase is cleavage of the terminal amino acid in the C-terminal of a peptide, however, the similarity to this enzymatic activity could also be indicative of a general affinity towards amino acids. Thus we propose that AcuI could be involved with attachment of an amino acid (in this case proline) to aculinic acid (**7**)/(**8**) to form (epi-)aculins A and B (**5**)/(**4**)/(**6**).

ACKNOWLEDGMENTS

We kindly acknowledge Kenneth S. Bruno (Pacific Northwest National Laboratory, Richland, WA) for providing the KB1042 strain. Kristian F. Nielsen and Peter B. Knudsen (Technical University of Denmark) are acknowledged for providing fully labeled 6-MSA. This study was supported by grant 09-064967 from the Danish Council for Independent Research, Technology, and Production Sciences.

MATERIALS AND METHODS

Strains and media. The *A. nidulans* strain IBT29539 (*argB2, pyrG89, veA1, nkuA*Δ) [22] was used for heterologous expression of 6-MSAS (AcuA). *A. aculeatus* ATCC16872-derived strain KB1042 (*pyr*$^{-}$) was used as reference and for expression of AcuA and ArnR. KB1042 was kindly provided by Kenneth S. Bruno (Pacific Northwest National Laboratory, Richland, WA, USA). *Escherichia coli* strain DH5α was used for cloning. Minimal media (MM) contained 1% glucose, 10 mM NaNO3, 1x salt solution [23] and 2% agar for solid media. MM was supplemented with 10 mM uridine, 10 mM uracil, 4 mM L-arginine, 100 µg/ml hygromycin B (Invivogen, San Diego, CA, USA) when necessary.

Heterologous expression of 6-MSAS in *A. nidulans*. AcuA from *A. aculeatus* ATCC16872 (ASPACDRAFT_1904397) was expressed heterologously in *A. nidulans*, using the expression platform developed in [9]. The 6-MSAS gene was PCR amplified using primers 6MSAS_ORF_FW (5'-AGAGCGAUATGCCTCACTTCTCCTCTGCC-3') and 6MSAS_ORF_RV (5'-TCTGCGAUGGTTAGAGATCTGATTAGCGGG-3'). Protoplasting, gene-targeting procedures and verification of strains were as described previously [4][24].

Expression of 6-MSAS and TF in *A. aculeatus*. 6-MSAS (ASPACDRAFT_1904397) and TF (ASPACDRAFT_123491) were expressed in *A. aculeatus*, using the AMA1-based expression platforms pDHX2 and pDHX3. pDHX2 is described in [4]. pDHX3 was constructed exactly as pDHX2, except *hph* was PCR amplified from pCB1003 [25] using primers hph-pX-Fw (5'-ACTAGGTAAUGCTAGTGGAGGTCAACACATCA-3') and hph-pX-Rv (5'-AGTGGGGAUCGGTCGGCATCTACTCTATT -3') and inserted instead of *pyrG*. The 6-MSAS gene was PCR amplified as described above, and the TF was PCR amplified using primers TF_ORF_FW (5'-AGAGCGAUAAGCCATGTTCTCCACCTTCTC-3') and TF_ORF_RV (5'-TCTGCGAUTGTGACGGGACCCTAGATGAC-3'). Protoplasting and transformation procedures were carried out as described previously [24]. Transformants were selected on MM without uracil and uridine (for strains carrying pDHX2) or MM with hygromycin B (for strains carrying pDHX3).

Chemical analysis of strains. Unless otherwise stated strains were inoculated as a three point inoculation on solid MM media and incubated at 37 °C for 5 days. Extraction of metabolites was performed as described in [26]. 6-MSA was purchased from (Apin Chemicals, Oxon, UK). Analysis was performed using ultra-high-performance liquid chromatography (UPHLC) UV/Vis diode array detector (DAD) high-resolution MS (TOFMS) on a maXis 3G orthogonal acceleration quadrupole time of flight mass spectrometer (Bruker Daltonics, Bremen, Germany) equipped with an electrospray ionization (ESI) source and connected to an Ultimate 3000 UHPLC system (Dionex, Sunnyvale, USA). The column used was a reverse-phase Kinetex 2.6-μmC_{18}, 100 mm × 2.1mm (Phenomenex, Torrance, CA), and the column temperature was maintained at 40 °C. A linear water-acetonitrile (LCMS-grade) gradient was used (both solvents were buffered with 20 mM formic acid) starting from 10% (vol/vol) acetonitrile and increased to 100% in 10min, maintaining this rate for 3 min before returning to the starting conditions in 0.1 min and staying there for 2.4 min before the following run. A flow rate of 0.4 $mL \cdot min^{-1}$ was used. TOFMS was performed in ESI+ with a

data acquisition range of 10 scans per second at m/z 100–1000. The TOFMS was calibrated using Bruker Daltonics high precision calibration algorithm (HPC) by means of the use of the internal standard sodium formate, which was automatically infused before each run. This provided a mass accuracy of better than 1.5 ppm in MS mode. UV/VIS spectra were collected at wavelengths from 200 to 700 nm. Data processing was performed using DataAnalysis 1.2 and Target Analysis4.0 software (Bruker Daltonics).

Feeding experiments. Feeding experiments were carried out exactly as described in [4] on solid YES plates. Fully labeled 6-MSA ($^{13}C_8$-6-MSA) was kindly provided by Kristian F. Nielsen (Technical University of Denmark), described in [4].

Preparative isolation of selected metabolites. *A. aculeatus* OeX-TF2 was cultivated on solid MM and incubated at 30°C for five days. The plates were harvested and extracted twice overnight with ethyl acetate (EtOAc) with 1 % formic acid. The extract was filtered and concentrated *in vacuo*. The combined extract was dissolved in methanol (MeOH) and H_2O (9:1), and an equal amount of heptane was added where after the phases were separated. To the MeOH/H_2O phase H_2O was added to a ratio of 1:1, and metabolites were then extracted with dichlormethane (DCM). The phases were then concentrated separately in vacuo.

The DCM phase was subjected to further purification on a semi-preparative HPLC, a Waters 600 Controller with a 996 photodiode array detector (Waters, Milford, MA, USA). This was achieved using a Luna II C_{18} column (250 x 10 mm, 5 µm, Phenomenex), a flowrate of 4 mL/min and a isocratic run at 40 % acetonitrile for 18 minutes. 50 ppm TFA was added to acetonitrile of HPLC grade and milliQ-water. This yielded 4.4 mg of (**2**) and 5.0 mg of (**3**).

In another run using a Luna II C_{18} column (250 x 10 mm, 5 μm, Phenomenex), a flowrate of 5 mL/min and a gradient going from 34% acetonitrile to 45 % in 25 minutes was used, yielding 2.7 mg of a mixture of (**4**), (**7**), (**8**) and (**9**).

NMR and structural elucidation. The 1D and 2D spectra were recorded on a Unity Inova-500 MHz spectrometer (Varian, Palo Alto, CA, USA). Spectra were acquired using standard pulse sequences and ^{1}H spectra as well as DQF-COSY, NOESY, HSQC and HMBC spectra were acquired. The deuterated solvent was DMSO-d_6 and signals were referenced by solvent signals for DMSO-d_6 at δ_H = 2.49 ppm and δ_C = 39.5 ppm. The NMR data was processed in Bruker Topspin 3.1. Chemical shifts are reported in ppm (δ) and scalar couplings in hertz (Hz). The sizes of the *J* coupling constants reported in the tables are the experimentally measured values from the spectra. There are minor variations in the measurements which may be explained by the uncertainty of *J*. NMR data for the compounds are found in the Supporting Information.

REFERENCES

1. Petersen, L. M.; Hoeck, C.; Frisvad, J. C.; Gotfredsen, C. H.; Larsen, T. O. Dereplication guided discovery of secondary metabolites of mixed biosynthetic origin from *Aspergillus aculeatus*. *Molecules* **2014**, *19*, 10898–10921.

2. Hayashi, H.; Furutsuka, K.; Shiono, Y. Okaramines H and I, new okaramine congeners, from *Aspergillus aculeatus* . *J. Nat. Prod.* **1999**, *62*, 315–317.

3. Andersen, R.; Buechi, G.; Kobbe, B.; Demain, A. L. Secalonic acids D and F are toxic metabolites of *Aspergillus aculeatus*. *J. Org. Chem.* **1977**, *42*, 352–353.

4. Holm, D. K.; Petersen, L. M.; Klitgaard, A.; Knudsen, P. B.; Jarczynska, Z. D.; Nielsen, K. F.; Gotfredsen, C. H.; Larsen, T. O.; Mortensen, U. H. Molecular and chemical characterization of the biosynthesis of the 6-MSA derived meroterpenoid yanuthone D in *Aspergillus niger*. *Chem. Biol.* **2014**, *21*, 519–529.

5. Read, G.; Vining, L. The biosynthesis of terreic acid. *Chem. Commun.* **1968**, 935–937.

6. Artigot, M. P.; Loiseau, N.; Laffitte, J.; Mas-Reguieg, L.; Tadrist, S.; Oswald, I. P.; Puel, O. Molecular cloning and functional characterization of two CYP619 cytochrome P450s involved in biosynthesis of patulin in *Aspergillus clavatus*. *Microbiology* **2009**, *155*, 1738–1747.

7. Gems, D.; Johnstone, I. L.; Clutterbuck, A. J. An autonomously replicating plasmid transforms *Aspergillus nidulans* at high frequency. *Gene* **1991**, *98*, 61–67.

8. Aleksenko, A.; Clutterbuck, A. J. The plasmid replicator AMA1 in *Aspergillus nidulans* is an inverted duplication of a low-copy-number dispersed genomic repeat. *Mol. Microbiol.* **1996**, *19*, 565–574.

9. Hansen, B. G.; Salomonsen, B.; Nielsen, M. T.; Nielsen, J. B.; Hansen, N. B.; Nielsen, K. F.; Regueira, T. B.; Nielsen, J.; Patil, K. R.; Mortensen, U. H. Versatile enzyme expression and characterization system for *Aspergillus nidulans*, with the *Penicillium brevicompactum* polyketide synthase gene from the mycophenolic acid gene cluster as a test case. *Appl. Environ. Microbiol.* **2011**, *77*, 3044–3051.

10. Nagata, H.; Kakeya, H.; Konno, H.; Kanazawa, S. JP2002322149-A ; JP4870276-B2: RKB-3384 analogs from *Aspergillus* species, and pharmaceuticals containing them.

11. Kakeya, H.; Kageyama, S.; Nie, L.; Onose, R.; Okada, G.; Beppu, T.; Norbury, C. J.; Osada, H. Lucilactaene, a new cell cycle inhibitor in p53-transfected cancer cells, produced by a *Fusarium* sp. *J. Antibiot. (Tokyo).* **2001**, *54*, 850–854.

12. Kakeya, H.; Takahashi, I.; Okada, G.; Isono, K.; Osada, H. Epolactaene, a novel neuritogenic compound in human neuroblastoma cells, produced by a marine fungus. *J. Antibiot. (Tokyo).* **1995**, *48*, 733–735.

13. Gelderblom, W.; Marasas, W.; Steyn, P.; PG, T.; Van der Merwe, K. J.; Rooyen, P.; Vleggaar, R.; Wessels, P. L. Structure elucidation of fusarin C, a mutagen produced by *Fusarium moniliforme*. *J. Chem. Soc., Chem.Commun.* **1984**, 122–124.

14. Steyn, P.; Vleggaar, R. Biosynthetic studies on the fusarins, metabolites of *Fusarium moniliforme*. *J. Chem. Soc. Chem. Commun.* **1985**, 1189–1191.

15. Song, Z.; Cox, R. J.; Lazarus, C. M.; Simpson, T. J. Fusarin C biosynthesis in *Fusarium moniliforme* and *Fusarium venenatum*. *ChemBioChem* **2004**, *5*, 1196–1203.

16. Bladt, T. T.; Dürr, C.; Knudsen, P. B.; Kildgaard, S.; Frisvad, J. C.; Gotfredsen, C. H.; Seiffert, M.; Larsen, T. O. Bio-activity and dereplication-based discovery of ophiobolins and other fungal secondary metabolites targeting leukemia cells. *Molecules* **2013**, *18*, 14629–14650.

17. Scifinder. https://scifinder.cas.org/scifinder/view/scifinder/scifinderExplore.jsf (Accessed on 1 August 2014).

18. Laatsch, H. Antibase 2012. http://www.wiley-vch.de/stmdata/antibase.php (Accessed on 1 August 2014).

19. Puel, O.; Galtier, P.; Oswald, I. P. Biosynthesis and toxicological effects of patulin. *Toxins (Basel).* **2010**, *2*, 613–631.

20. Herbert, R. B. *The Biosynthesis of Secondary Metabolites*; 1st ed.; Chapman and Hall Ltd: New York, 1981; pp. 34–37.

21. Wiemer, D. F.; Ales, D. C. Lasidiol angelate: an ant repellent sesquiterpenoid from *Lasiantheae fruticosa*. *J. Org. Chem.* **1981**, 5449–5450.

22. Nielsen, J. B.; Nielsen, M. L.; Mortensen, U. H. Transient disruption of non-homologous end-joining facilitates targeted genome manipulations in the filamentous fungus *Aspergillus nidulans*. *Fungal Genet. Biol.* **2008**, *45*, 165–170.

23. Cove, D. J. The induction and repression of nitrate reductase in the fungus *Aspergillus nidulans*. *Biochim. Biophys. Acta* **1966**, *113*, 51–56.

24. Nielsen, M. L.; Albertsen, L.; Lettier, G.; Nielsen, J. B.; Mortensen, U. H. Efficient PCR-based gene targeting with a recyclable marker for *Aspergillus nidulans*. *Fungal Genet. Biol.* **2006**, *43*, 54–64.

25. McCluskey, K.; Wiest, a.; Plamann, M. The Fungal Genetics Stock Center: a repository for 50 years of fungal genetics research. *J. Biosci.* **2010**, *35*, 119–126.

26. Smedsgaard, J. Micro-scale extraction procedure for standardized screening of fungal metabolite production in cultures. *J. Chromatogr. A* **1997**, *760*, 264–270.

Investigation of a 6-MSA synthase gene cluster in *Aspergillus aculeatus* reveals 6-MSA derived aculins A-B and non-6-MSA derived pyrrolidinones.

Lene M. Petersen, Dorte K. Holm, Charlotte H. Gotfredsen, Uffe H. Mortensen, and Thomas O. Larsen.

SUPPORTING INFORMATION

Figures:

Tables:

Figure S1. Mass spectra of compounds (**2**), (**3**), (**4**), (**5**), and (**6**), cultivated on YES or YES + ^{13}C-6-MSA.

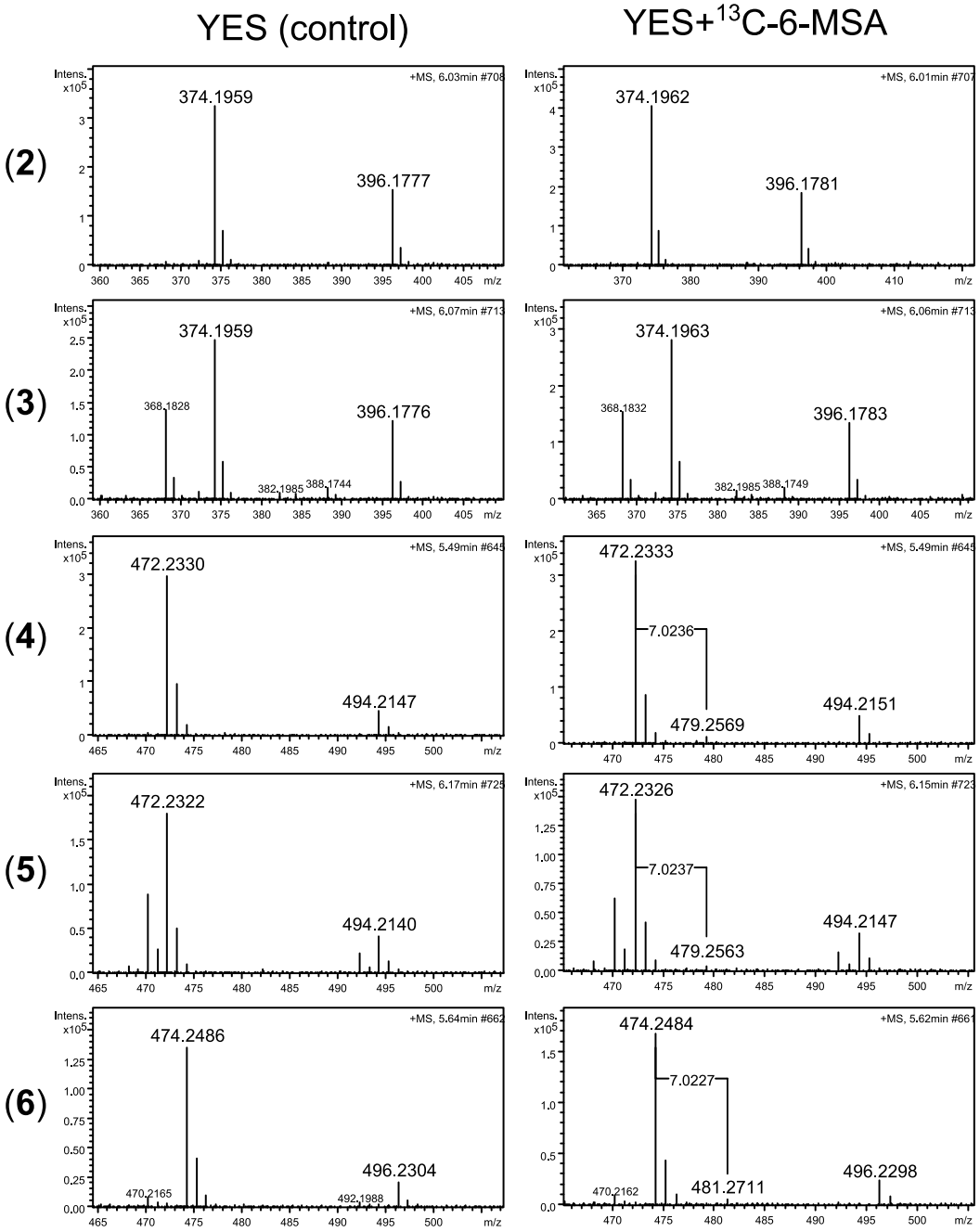

Figure S2. Effect of increasing concentrations of (**1**) on CLL cell viability in a CellTiter-Glo® assay. The relative cell viability is compared to DMSO control (1 %).

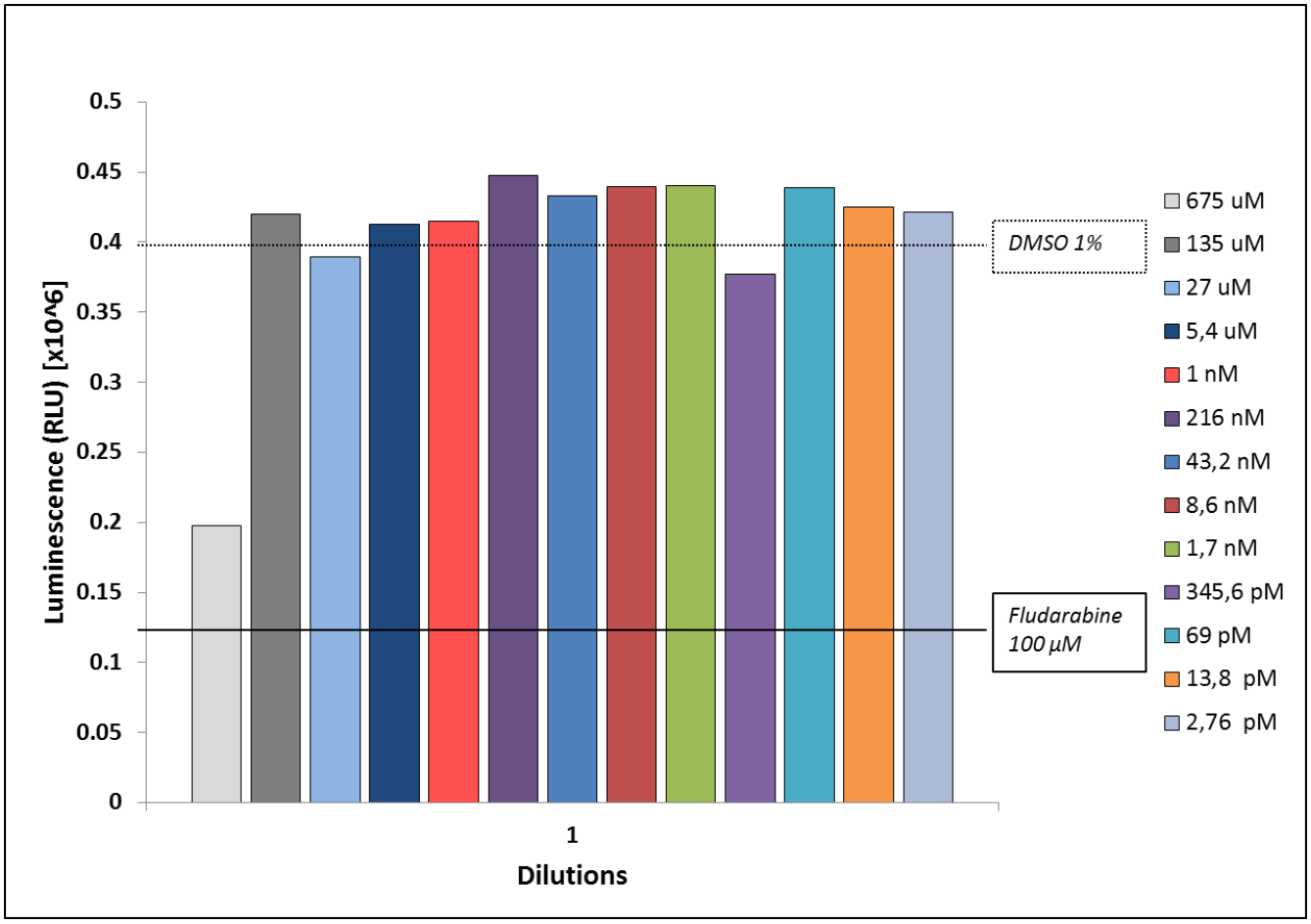

Table S1. NMR Data for (**1**) (500 MHz, DMSO-d_6). Signals were referenced by solvent signals for DMSO-d_6 at δ_H = 2.49 ppm and δ_C = 39.5 ppm.

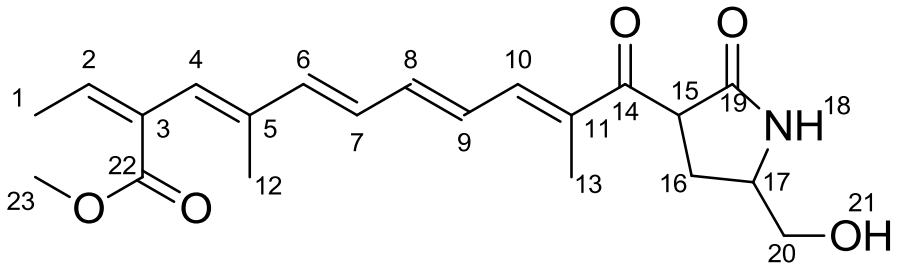

No.	^{1}H-chemical shift [ppm] (integral, mult., *J* [Hz])	^{13}C-chemical shift [ppm]	HMBC correlations	H2BC correlations	NOE connectivities
1	1.71 (dd 7.2, 1.0)	15.4	2, 3, 22	2	2, 4
2	6.88 (m)	139.9	1, 4, 22	1	1
3	-	129.8	-	-	
4	6.22 (s)	126.8	6, 12, 22	-	1, 6, 12
5	-	137.5	-	-	
6	6.69 (d 15.4)	140.0	4, 5, 8, 9, 12	7	4, 7
7	6.60 (m)	128.8	5, 8	6	6, 12
8	6.83	141.0	10	7/9	6, 7
9	6.831 (m)	128.9	7	8	
10	7.38 (m)	141.3	8, 13, 14	9	9, 15
11	-	134.4	-	-	
12	1.64 (s)	13.8	4, 5	4	4, 7
13	1.85 (s)	11.6	10, 11, 14	10	
14	-	197.8	-	-	
15	4.39 (m)	47.5	14, 16/16', 19	16/16'	16'
16	2.33 (m)	27.3	14, 15, 17, 20	15, 17	16', 20
16'	1.92 (m)	27.3	-	15, 17	15, 16, 20
17	3.54 (m)	53.6	16/16'	16/16',20	
18	7.84 (d 10)	-	15, 16/16',19, 20	-	20, 20'
19	-	173.0	-	-	
20	3.35 (m)	64.4	16/16'	17	16/16', 18
21	-	-	-	-	
22	-	166.3	-	-	
23	3.66 (s)	51.6	22	-	

Table S2. NMR Data for (**2**) (500 MHz, DMSO-d_6). Signals were referenced by solvent signals for DMSO-d_6 at δ_H = 2.49 ppm and δ_C = 39.5 ppm.

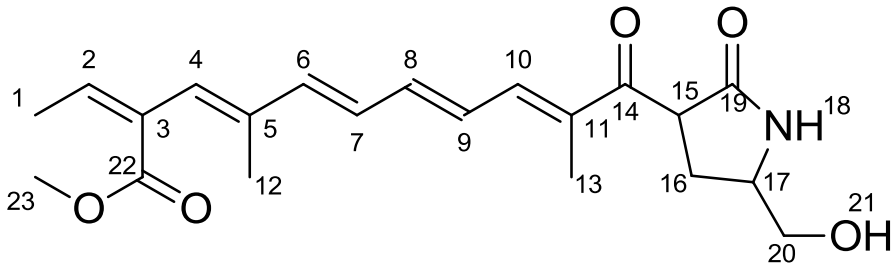

No.	^{1}H-chemical shift [ppm] (integral, mult., *J* [Hz])	^{13}C-chemical shift [ppm]	HMBC correlations
1	1.71 (1H, m)	14.3	2, 3, 4, 22
2	6.87 (1H, m)	139.2	1, 3, 22
3	-	125.0	-
4	6.84 (1H, m)	128.5	22
5	-	136.7	-
6	6.69 (dd, 15.1, 2.5)	140.0	3, 5, 12
7	6.57 (1H, m)	137.9	5
8	7.04 (1H, m)	123.3	-
9	6.47 (1H, m)	123.7	8, 14
10	7.83 (1H, m)	135.1	13
11	-	140.0	-
12	1.63 (3H, m)	13.2	3, 5
13	1.85 (3H, s)	10.8	10, 11, 14
14	-	199.8	-
15	4.50 (1H, m)	47.3	14, 16/16', 19
16	2.35	26.6	14
16'	1.92	26.6	14
17	3.55 (1H, m)	63.5	15, 16/16', 20
18	7.89 (1H, m)	-	15, 16, 17
19	-	172.2	-
20	3.36 (2H, m)	52.9	-
21	-	-	-
22	-	166.3	-
23	3.65 (3H, s)	50.9	22

Table S3. NMR Data for the aculene A part of aculin A (500 MHz, DMSO-d_6). Signals were referenced by solvent signals for DMSO-d_6 at δ_H = 2.49 ppm and δ_C = 39.5 ppm.

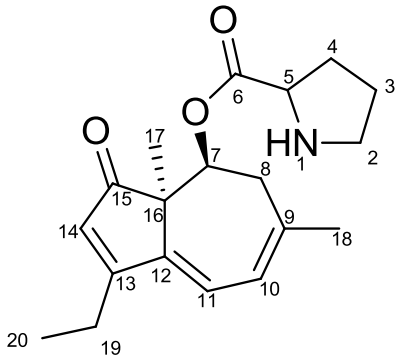

No.	^{1}H-chemical shift [ppm] (integral, mult., *J* [Hz])	^{13}C-chemical shift [ppm]	HMBC correlations
1	-	-	-
2	3.15 (1H, m)	45.1	-
2'	3.09 (1H, m)	45.1	-
3	1.83 (1H, m)	22.3	5
3'	1.68 (1H, td, 14.3, 7.6)	22.3	4,5
4	1.94 (1H, m)	27.6	2,6
4'	1.46 (1H, dt, 20.1, 7.2)	27.6	2,3,5,6
5	4.22 (1H, t, 7.8)	58.4	6
6	-	168.2	
7	5.33 (1H, dd, 4.3, 2.4)	72.9	-
8	2.82 (1H, br.d., 20)	36.5	10
8'	2.55 (1H, m)	36.5	7,9,10,16
9	-	141.7	
10	5.97 (1H, d, 7.3)	120.2	8,12,18
11	6.24 (1H, d, 7.4)	118.8	12,13,16
12	-	142.4	
13	-	175.3	
14	6.02 (1H, s)	125.3	12,13,15,16,19
15	-	205.8	
16	-	51.9	
17	0.96 (3H, s)	17.9	7,12,15,16
18	1.85 (3H, s)	27.1	8,9,10
19	2.54 (2H, m)	20.2	13,14,20
20	1.16 (3H, t, 7.4)	12.0	13,19
-OH	-	-	-

Table S4 (upper) and S5 (lower). NMR Data for aculinic acid (500 MHz, DMSO-d_6). Signals were referenced by solvent signals for DMSO-d_6 at δ_H = 2.49 ppm and δ_C = 39.5 ppm.

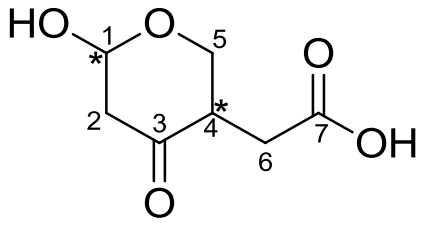

No.	^{1}H-chemical shift [ppm] (integral, mult., *J* [Hz])	^{13}C-chemical shift [ppm]	HMBC correlations	NOESY connectivities
1	5.49 (1H, br. D., 3.9)	93.4	5	2,2’
2	2.20 (1H, m)	47.6	4,5,3	1
2’	2.77 (1H, m)	47.6	3,5	1,4
3	-	205.8	-	
4	2.95 (1H, dt, 13.0, 6.8)	46.3	-	2’,5,5’,6,6’
5	3.77 (1H, m)	62.1	1,3	4,5’,6
5’	3.87 (1H, dd, 10.7, 7.0)	62.1	1,3	4,5,6
6	2.02 (1H, dd, 17.0, 6.0)	29.2	3,4,5,7	4,5,5’,6’
6’	2.49 (1H, m)	29.2	3,4,5,7	4,6
7	-	172.8	-	

No.	^{1}H-chemical shift [ppm] (integral, mult., *J* [Hz])	^{13}C-chemical shift [ppm]	HMBC correlations	NOESY connectivities
1	4.85 (1H, dd, 7.4, 3.7)	94.8	-	2,5
2	2.45 (2H, m)	49.1	5	1
3	-	205.8	-	
4	2.77 (1H, m)	45.6	5	5,5’
5	3.34 (1H, m)	63.8	1	1,4
5’	4.05 (1H, dd, 11.3, 6.7)	63.8	3	4
6	2.14 (1H, dd, 17.0, 6.3)	29.4	4,7	
6’	2.44 (1H, m)	29.4	3,4,7	
7	-	172.8	-	

Table S6. Genes and gene products predicted by AUGUSTUS [1] and FGeneSH (Softberry).

>acuF atggagagagcaatcagcacgacgcccatcctcgaccaagcgctcacatgcgtgcagtcatacaaagctcttgcggcaaccgtccaagagctcgccagcc cggagctacaacgcagcatcgaagagggccttgcgcagtttctaactcacatgcccgagttcaacatcttggtcaacgccgtcgaacccccgcacacgtcgt gggactacctcctgcgcaacgacgccagccaacgcggggagatgaccatgctcctcatggagctgcagtgtgagatcgaccagatggccttcgcgatccg ccaagcgatgcagcagcagcaccccgaagccgaacccctgagcaacaacagccgcctcgtcgacgcgtggacagagaacctgcgcagcgtggaggac cacacggtgtggcgcctggccttctggcggcgcgaccatgcggtgcacacgacctacccaaccaccaatccgctggtcaaccagtccttctacttcgcgatc cgcaacgagctcggcctcgacgtctccacgcagttccgcgagtgcatccgccgcgccatcacacaggaatgcccaaccatcaccgcgcggccggccctcc accgccgactagtcgatctagtcgtccagcgccggcgattctggaacttccagcgccgcatccgcggactcagcaaggacgccgtgctctgggggcggga cgcgttagcaccgccacattttgccccgggggacgagcgcttcacctgtccgttctgcttcttcgacctccccgtcgcggcctaccggactccgcgcgcgtgg acggaccacgtgatgagcgacctggagggctacgtctgcctgtacgagacgtgctcctccacccggtcctggcccgagacctgtccgcatgcctgcacctc cttcggcgcctggtttaccgccatggccggcagcttcgccgagggcgtcgagtggtgcagccacgcctttgcctgtgacggccgccggctggaggaggtcc accgcccgcgctgcgccgcacctgctgtccggttggacagtgtctgtccgctgtgtggaagggagccggccgtcgaggagacggagctgcgcatggcgg acgcggcggaccccctgcaggatgatgaccagaaccgcgcgaaggccaggctgttactgtcgcatattgccggccatctggaggtgatcacgccgatggc gtttacctggaataccgatcggaatgccctcgatccggatcggcggctgttttgggggggacattgggtcaccgggggggtgctggagggtcggcgtga
>AcuF MERAISTTPILDQALTCVQSYKALAATVQELASPELQRSIEEGLAQFLTHMPEFNILVNAVEPPHTSW DYLLRNDASQRGEMTMLLMELQCEIDQMAFAIRQAMQQQHPEAEPLSNNSRLVDAWTENLRSVE DHTVWRLAFWRRDHAVHTTYPTTNPLVNQSFYFAIRNELGLDVSTQFRECIRRAITQECPTITARPA LHRRLVDLVVQRRRFWNFQRRIRGLSKDAVLWGRDALAPPHFAPGDERFTCPFCFFDLPVAAYRTP RAWTDHVMSDLEGYVCLYETCSSTRSWPETCPHACTSFGAWFTAMAGSFAEGVEWCSHAFACDG RRLEEVHRPRCAAPAVRLDSVCPLCGREPAVEETELRMADAADPLQDDDQNRAKARLLLSHIAGH LEVITPMAFTWNTDRNALDPDRRLFWGDIGSPGGAGGSA
>acuH Atgcactttcgtactgtgaacaccccggctaggctgcagtttatctcacggtttgtcctccagccactccgtccgctgctgcactataaggatcacacgatccgg acggcggcggaggcggggctagacgtggcggagctggcggtggggcccgcgttcgtcgtggcgcgggggtatttcaccttgcggcaagcggataccag ctcggcggagagtcgcgatcccacaaagcaacagcagctgtgggagaagacgttggagtggctggggatgaccgaggagcaggggcactttag
>AcuH MHFRTVNTPARLQFISRFVLQPLRPLLHYKDHTIRTAAEAGLDVAELAVGPAFVVARGYFTLRQAD TSSAESRDPTKQQQLWEKTLEWLGMTEEQGAL

1. Stanke, M.; Morgenstern, B. AUGUSTUS: a web server for gene prediction in eukaryotes that allows user-defined constraints. *Nucleic Acids Res.* **2005**, *33*, 465–467.

Paper 12

"Reconstitution of the cytochalasin gene cluster from *Aspergillus clavatus* in *Aspergillus nidulans*"

Draft

Reconstitution of the cytochalasin gene cluster from *Aspergillus clavatus* in *Aspergillus nidulans*

ABSTRACT: Reconstitution of gene clusters has the potential to provide access to the chemical diversity encoded in the genomes of otherwise unculturable filamentous fungi. Cytochalasins constitute a group of fungal secondary metabolites with diverse structures and bioactivities, e.g. cytochalasins produced by *A. clavatus*. In this work the cytochalasin gene cluster was reconstituted in the model organism *A. nidulans* by transformation associated recombination (TAR), resulting in production of cytochalasin K.

1. Introduction

1.1 Biosynthesis of cytochalasins

Cytochalasans constitute a class of polyketide-non-ribosomal peptide (PK-NRP) hybrids containing a highly reduced PK backbone and an amino acid. Characteristic for the cytochalasans is their tricyclic core consisting of a macrocycle fused to a bicyclic lactam (isoindolone) system. The macrocycle origins from the reduced PK part and can be fused to the isoindolone system by a cyclic ketone, a lactone or a cyclic carbonate. The cytochalasans are classified based on the amino acid incorporated into the PK backbone. The name origins from Greek and refers to the best known property of the cytochalasans: Kytos (cell) and chalasis (relaxation) refers to the capping of actin filaments [1][2]. The group displays a wide range of biological functions. This is exemplified by the earliest reported cytochalasin A and B [3][4] which can repress glucose transport in human erythrocyte membrane [5] and cytochalasin E, which have been reported to show inhibitory activities towards ovarian, and human colon cancer [6] and possess strong anti-angiogenic activities [7]. A subclass of the cytochalasans is the cytochalasins, distinguishing by having the amino acid phenylalanine. The structures of cytochalasins E and K from *Aspergillus clavatus* are depicted in Figure 1.

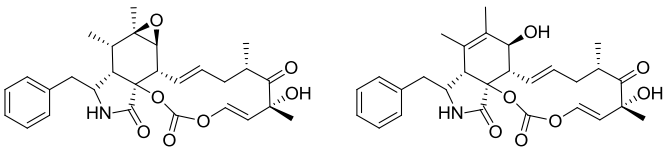

Figure 1 Structures of cytochalasins E and K from *A. clavatus*

Due to the wide range of biological functions of cytochalasins, as well as their interesting and complex structures, their biosynthesis has been a topic of particular interest. Isotope labeling studies have revealed that the cytochalasans origin from malonyl building blocks as well as amino acids [8][9], suggesting the mixed biosynthetic pathway. The genetic and molecular basis of cytochalasin biosynthesis have been studied by Hertweck and co-workers for chaetoglobosin A from *Penicillium expansum* [10] and by Tang and co-

workers for cytochalasin E and K from *A. clavatus* [11][12]. The biosynthetic genes responsible for cytochalasin production in *A. clavatus* are depicted in Figure 2. The genes *ccsA-ccsG* and *ccsR* comprises the *ccs* biosynthetic gene cluster spanning 29,819 kb of DNA.

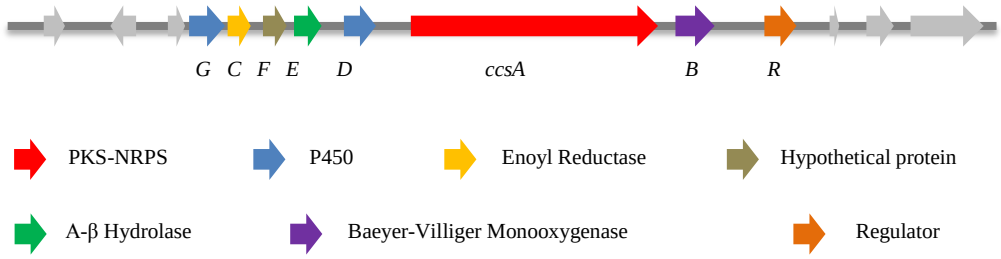

Figure 2 Organization of the *ccs* gene cluster in the genome of *A. clavatus* NRRL 1. Adapted from [11].

In Table 1 an overview of the genes from the *ccs* cluster is given, including locus, size and function of the gene, as well as a brief description of the role in the biosynthesis towards cytochalasin K.

Table 1 Overview of genes and functions in the *ccs* gene cluster. Adapted from [11].

Gene	Gene locus (ACLA_)	Gene size(bp)	Function	Biosynthetic description
ccsR	078640	1593	Transcription regulator	Encodes a transcription factor. Cytochalasin pathway specific regulator, upregulates the production
ccsA	078660	12374	PKS-NRPS hybrid	Formation of the PK-NRP backbone
ccsB	078650	1967	Baeyer-Villiger monooxygenase	Oxidizes, forming the cyclic carbonate in the macrocycle
ccsC	078700	1154	Enoyl reductase	Functional enoyl reductase, facilitating CcsA
ccsD	078670	1598	P450 epoxidase	Introduces the epoxide
ccsE	078680	1381	Esterase	Converts cytochalasin E to K
ccsF	078690	1190	Unknown	Unknown. Perhaps post-PKS-NRPS tailoring, resistance or transport
ccsG	078710	1797	P450 monooxygenase	Oxidizes, Introduces a hydroxyl and keto group

The proposed biosynthetic pathway towards cytochalasin K is depicted in Figure 3. The first step in the biosynthetic pathway is formation of the backbone by the PK synthase-NRP synthetase (PKS-NRPS) (CcsA). The PKS has the necessary domains (KS, AT, ACP) as well as reductive domains (KR, DH, ER) and a methyltransferase (MT). However, the ER domain is believed to be inactive due to lack of a key NADPH binding motif. Another enzyme encoded by the *ccsC* gene located downstream of *ccsA*, is proposed to be carrying out the enoyl reductions. This is also seen in the lovastatin biosynthetic pathway from *A. terreus*, where an enoyl reductase encoding gene, *lovC*, facilitates the PKS *lovB*, which has an inactive ER domain[13][14]. The PKS CcsA uses malonyl-CoA as a starter unit and seven malonyl-CoAs as extender units and forms the octaketide backbone. The level of reduction varies, from unreduced carbonyls, to

alcohols, enoyls and all the way to the fully saturated alkans. Furthermore three SAM donors are used, enzymatically incorporating three methyl groups. After formation of the PK backbone the A domain of the NRPS module selects one phenylalanine molecule, which is transferred to the T domain. The C domain of the NRPS then catalyzes the condensation between the nucleophilic amino group of Phe and the electrophilic carbonyl of the octaketide chain still attached to the ACP domain of the PKS. The result is the PK-NRP chain linked to the T domain of the NRPS as illustrated in Figure 3. Release of the chain is believed to be achieved by an R domain of the NRPS, making a reductive release forming an amino-aldehyde intermediate. This reactive intermediate can do an intramolecular aldol type of condensation, followed by loss of water, forming the pentaene intermediate.

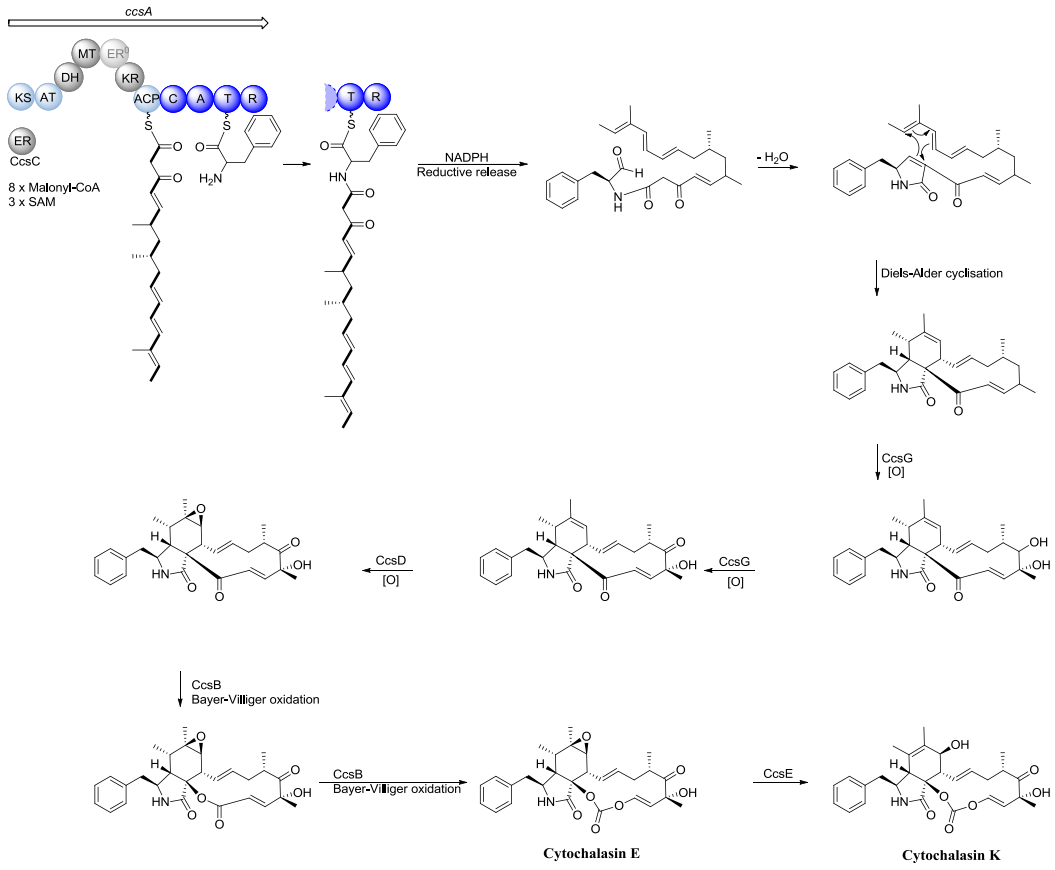

Figure 3 Proposed biosyntethis of cytochalsin E. The PKS-NRPS **CcsA** is responsible for formation of the octaketide with incorporation of phenylalanine in combination with **CcsC** a functional enoyl reductase. After release an intramolecular condensation followed by a Diels-Alder cyclisation is forming the tricycle core. The P450s **CcsG** and **CcsD** introduce a hydroxyl group, a keto group and the epoxide. Finally **CcsB**, a Bayer-Villiger oxidase, introduces two oxygens to form the carbonate moiety. **CcsE** converts cytochalasin E to cytochalasin K, while **CcsF** may be involved in a post-PKS-NRPS tailoring, resistance or transport. Adapted from [11].

In the next step a [4+2] Diels-Alder endo cycloaddition of the pentaene intermediate is responsible for forming the tricyclic core, characteristic for the cytochalasins.

To get to the structure of cytochalasin E a series of oxidations catalyzed by CcsG, CcsD and CcsB occurs. CcsG, a P450, performs two consecutive steps of oxidations, firstly introducing two hydroxyl groups, and secondly, oxidizing one of these even further to a carbonyl. Another P450, CcsD, is then mediating formation of the epoxide.

Finally, two Baeyer-Villiger oxidations catalyzed by CcsB, a Baeyer-Villiger monooxygenase, introduces two oxygens, one at a time, on each side of the carbonyl of the 11-membered ring, forming the unique vinyl carbonate moiety in cytochalasin E and K [12].

The remaining enzymes encoded by the cluster are CcsR, CcsE and CcsF. The firstmentioned, *ccsR*, encodes a transcription factor, which is a cytochalasin pathway specific regulator, found to facilitate transcription. The specific role of CcsE and CcsF have not been determined, but CcsE is believed to be involved in the conversion of cytochalasin E to cytochalasin K, while CcsF may be involved in a post-PKS-NRPS tailoring, resistance or transport.

1.2 Gene cluster reconstitution by TAR

Transformation-Associated Recombination (TAR) [15][16] is becoming a generically useful tool for reconstructing large biosynthetic gene clusters from genomic DNA (gDNA) and environmental DNA (eDNA) [17]. With TAR it is possible to explore large gene clusters (~40 kb) by reassembling them from sets of smaller overlapping fragments in *Saccharomyces cerevisiae*. This yeast is used since it has an extremely efficient DNA recombination system [15]. TAR was developed as a recombinational cloning strategy, to isolate large genomic fragments from human DNA [16][18].

TAR has been used to reassemble eDNA derived type II PKS gene cluster from *Streptomyces albus* for production of fluostatins [19]. General descriptions of how to recover large NP biosynthetic gene clusters from eDNA using TAR have been described[17] and the TAR approach has been applied to several organisms including human [16][18], mouse [20], fish [21], parasites [22] and bacteria [19].

Using the TAR approach we wanted to reconstitute the *ccs* gene cluster in *A. nidulans*.

2. Results and discussion

In this study TAR was used to reconstitute the cytochalasin gene cluster from *A. clavatus* and express it in the model organism *A. nidulans*. The workflow is illustrated in Figure 4.

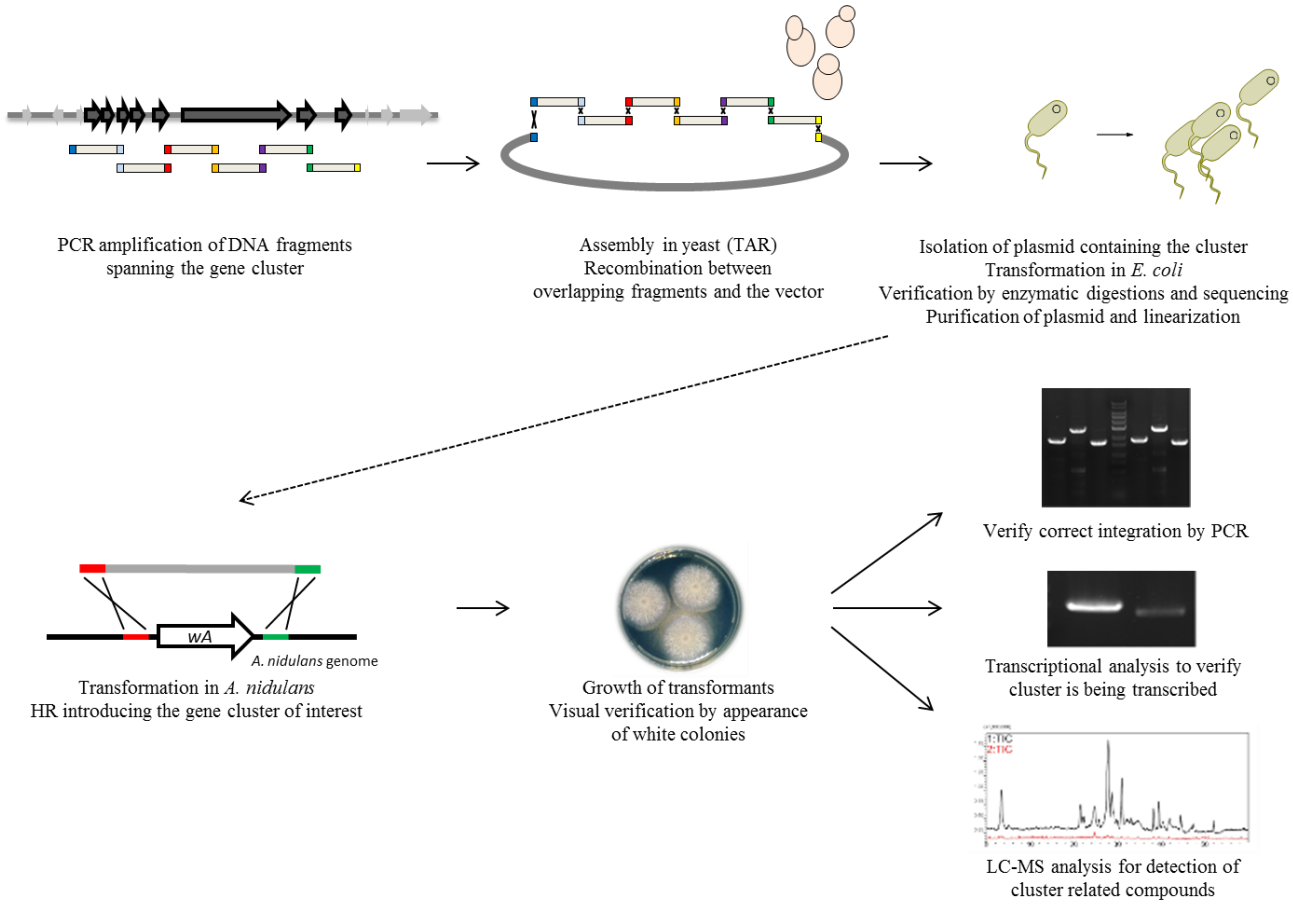

Figure 4 Workflow for cluster reconstitution by TAR.

DNA fragments of 5 kb, spanning the entire gene cluster of interest, were first amplified by PCR. The primers were designed to create overlapping regions of 150-200 bp between each PCR fragment (see Figure 5). The resulting sets of overlapping PCR fragments and a linearized vector, engineered to carry small homology regions corresponding to regions of the exterior primers, were introduced in *S. cerevisiae* by co-transformation. The fragments and vector recombine to yield a stable plasmid containing the targeted genomic region.

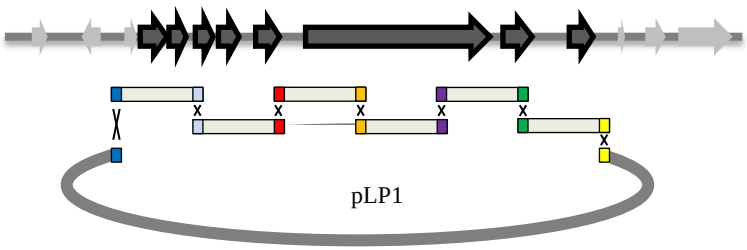

Figure 5 Custer reconstitution by PCR amplification and TAR in yeast. Primers are designed to create 150-200 bp overlapping regions between each PCR fragment, and with a 30-50 bp overlapping region to the linearized vector.

The CEN-based vector, was designed for transformation in three different organisms: Transformation in *S. cerevisiae*, replication in *E. coli* and transformation in *A. nidulans*. It therefore contains elements for all three organisms, see Table 2.

Table 2 Elements in the cluster capturing vector set up for transformation in *A. nidulans*, *E. coli* and *S. cerevisiae*.

A. nidulans		*E. coli*		*S. cerevisiae*	
pyrG	Selectable marker for *A. nidulans*	***ampR***	Antibiotic resistance gene.	***URA3***	Selectable marker for yeast
PgpdA	Promotor	**ori**	Origin of replication.	**CEN**	Yeast centromere sequence
TtrpC	Terminator			**ARS**	Autonomously replicating sequence
wAdown wAup	Targeting sequences for integration in *A. nidulans*				

The regulator gene *ccsR* was amplified separately and the plasmid was constructed with the strong constitutive promoter *PgpdA* followed by the TF encoding gene *ccsR* and then the remaining cluster. The resulting plasmid, pLP1, is depicted in Figure 6. The plasmid was verified by four enzymatic digestions, PCR of pieces spanning the cluster and into the plasmid as well as sequencing.

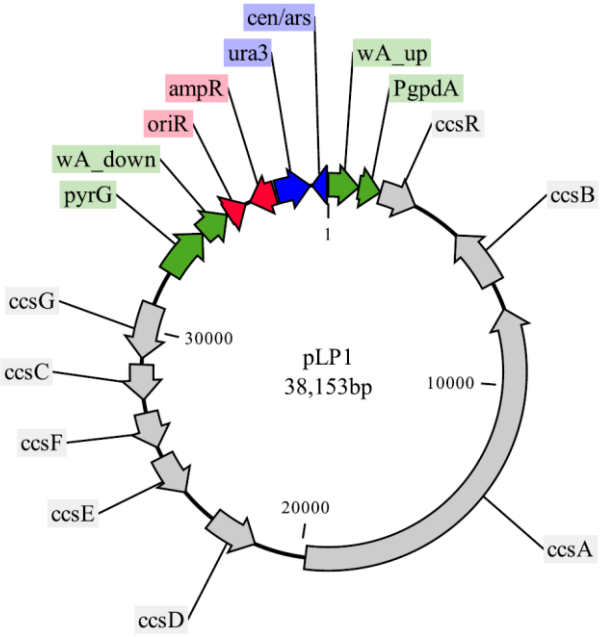

Figure 6 The plasmid, pLP1, designed for rapid assembly and transformation in yeast (CEN/ARS, URA3), transformation in *E. coli* (ORI, *ampR*) and for integrative transformation in *A. nidulans* (*pyrG*, *wA* PKS targeting sequences). It contains the *gpdA* promoter directly followed by the TF encoding gene *ccsR* and the remaining *ccs* cluster.

The plasmid was cleaved with SwaI creating a linearized plasmid for transformation in *A. nidulans*. Transformation in *A. nidulans* was achieved as earlier described [23][24][25], in the WA PKS gene *wA*, responsible for the green melanin production in *A. nidulans*, wherefore transformants will appear white. Four resulting transformants are depicted in Figure 7.

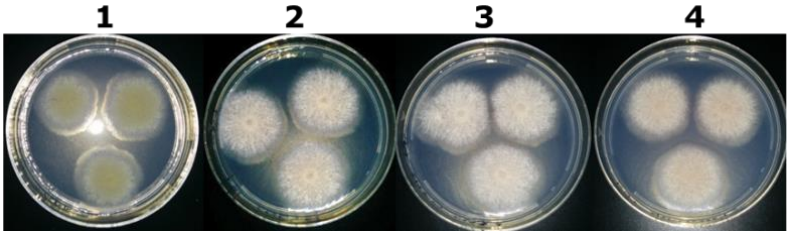

Figure 7 Appearance of four transformants where the *ccs* cluster has been integrated into the *A. nidulans* genome.

To determine if the *ccs* cluster was transcribed; RT-PCR analysis was performed. For each gene, a 600 bp segments was amplified, particularly around those regions having introns, to distinguish between the products from spliced cDNA and potential genomic DNA carryover during RNA extraction. In addition to the PKS-NRPS *ccsA*, all other genes believed to belong to the cluster were transcribed (*ccsB*-*ccsG*). The TF *ccsR* appeared to be transcribed in higher amounts, see Figure 8.

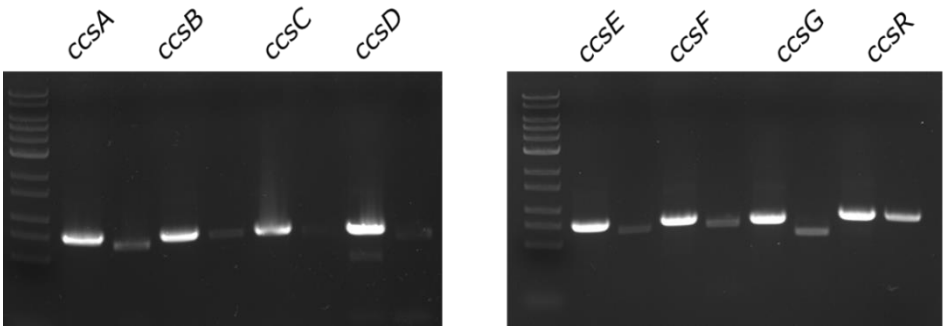

Figure 8 Transcriptional analysis of all genes in the *ccs* gene cluster in *A. nidulans*, showing that all cluster genes are transcribed. For each gene, the first band are from genomic DNA of *A. clavatus* for comparison.

The transformants were incubated on solid and liquid MM and extracted, and the metabolic profile examined by HPLC-MS. EICs of *m/z* corresponding to cytochalasin E and K are depicted in Figure 9, from a liquid extraction after three days.

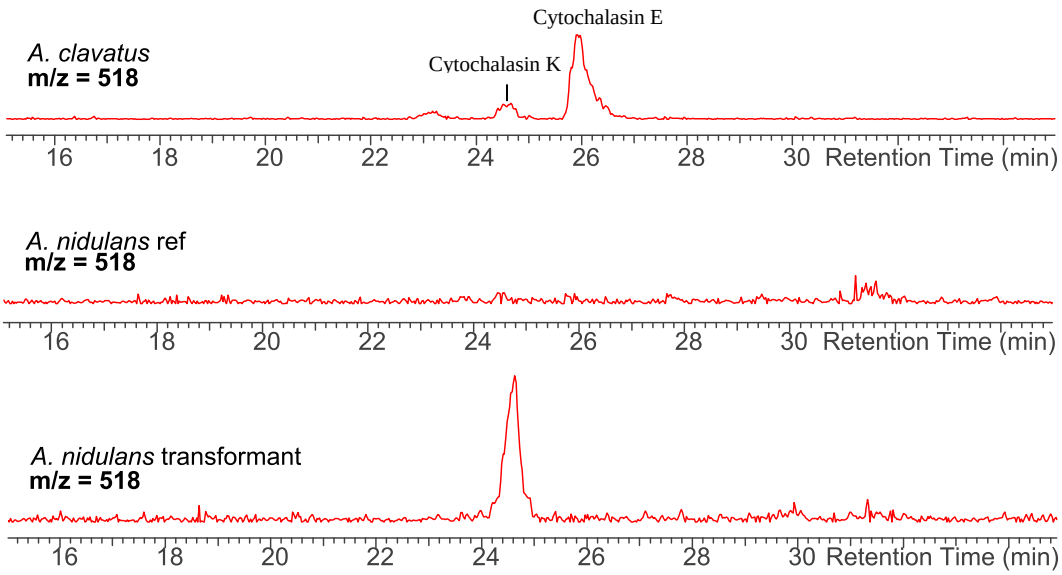

Figure 9 EIC of *m/z* = 518 (the most abundant adduct for both cytochalasin E and K, $[M+Na]^+$) in *A. clavatus*, the *A. nidulans* reference and the *A. nidulans* mutant containing the *ccs* cluster.

Cytochalasin E and K have the same molecular formula (see Figure 1) and hence the same *m/z* of 518 for the most abundant adduct $[M+Na]^+$. EICs of extracts from the host organism *A. clavatus*, show this was producing small amounts of cytochalasin K and vast amounts of cytochalasin E. In the *A. nidulans* transformants no cytochalasin E was observed, however, the end product of the pathway, cytochalasin K was detected. It is interestingly why cytochalasin E is favored in *A. clavatus*, while it is not produced even in trace amounts in *A. nidulans*. Cytochalasin E could be toxic to *A. nidulans* wherefore the biosynthesis is driven to the end product cytochalasin K. Nonetheless, the *ccs* gene cluster was successfully reconstituted and the end product cytochalasin K produced in *A. nidulans*.

3. Materials and methods

3.1 Strains, media and fungal growth.

The *A. clavatus* NRRL1 strain was used and the *A. nidulans* 1.49 (pyrG89, pyroA4, ΔnkuA::argB, veA) [25] was used for strain constructions in *A. nidulans*. *A. clavatus* was grown on MEPA (30 g/L malt extract, 3 g/L papaic digest of soybean meal and 15 g/L agar) at 25 ˚C, *A. nidulans* on glucose minimum medium (GMM) [26] at 37 ˚C. When necessary media were supplemented with 0.56 g uracil/L, 1.26 g uridine/L, and 0.5 µM pydroxine HCl.

E. coli strains XL-1 (Stratagene) was used for routine cloning. Luria-Bertani (LB) medium was used for cultivation of *E. coli* strains (25 g/L LB) and supplemented with 100 µg/ml ampicillin when needed.

S. cerevisiae BJ5464 was used for TAR cloning and yeast media was used (1 g bacto tech. grada cassa amino acid, 4 g dextrose, 4 g bacto agar,176 mL DI water, autoclaved, cooled and added 20 mL nitrogen base stock, 2 mL trp stock and 2 mL adenine stock).

Spheroplasts were prepared as described by Kouprina and Larionov [27].

3.2 Fungal transformation.

Transformation in *A. nidulans* was performed as earlier described [25].

3.3 Genetic manipulations.

Polymerase chain reactions were performed using Phusion high-fidelity DNA polymerase (New England Biolabs) for amplifications, and Quick-Load Taq 2X Master Mix (New England Biolabs) for screening.

Restriction enzymes (New England Biolabs) were used for digestions, and T4 ligase (Invitrogen) for ligation of DNA fragments. All primers used were synthesized by Integrated DNA Technologies and are listed in Table 3.

3.4 Transcriptional analysis.

Strains were inoculated into 10 mL LMM and cultivated at 37 ˚C for three days in the dark. Mycelia were harvested, dried and RNA was extracted using the Ambion RiboPure-Yeast extraction kit. RT-PCR was achieved using the Oligo-dT primer and Improm-II reverse transcription system (Promega). cDNA was then amplified with GoTaq Green Master Mix using specific primers for each gene (Table 3).

3.5 Small scale extraction.

Cultures were grown on either solid or liquid MM, at 37 ˚C for 2-7 days in the dark. The cultures were extracted with ethyl acetate/MeOH/acetic acid (89:10:1), by ultrasonification for 1h. The organic phase was transferred to a clean vial and evaporated to dryness. The dried extracts were dissolved in methanol and spun down prior to LC-MS analysis.

3.6 Chemical analysis.

Chemical analysis was performed on a Shimadzu 2010 EV liquid chromatography mass spectrometer with positive and negative electrospray ionization. Seperation was achieved with a Phenomenex Luna 5 µm, 2.0 mm x 100 mm C_{18} reverse-phase column, using a linear gradient from 5 % to 95 % with ACN/H_2O + 0.05 % formic acid solvent system for 15 minutes using a flow rate of 0.1 mL/min.

3.7 Yeast transformation.

TAR was achieved by transformation in *S. cerevisiae* BJ5464-NpgA by using a *S. c.* EasyComp Transformation Kit (Invitrogen). DNA was transferred to 50 µL cells on ice and 500 µL solIII was added. The sample was incubated at 30 °C for 1 hour, with vortexing every 15 min and the plated on selective media.

3.8 E. coli transformation.

E. coli strains XL-1 Blue (Stratagene) was used for transformation. DNA was transferred to 50 µL cells and the sample was incubated 30 minutes on ice followed by one minute heatchock at 42 °C and finally 5 minutes on ice. 1 mL LB was added to the sample and after incubation at 37 °C for 20 min the sample was plated on LB plate with 100 µg/mL ampicillin and incubated at 37 °C over night.

Table 3 Sequences of primers used in this study

Primer name	**Sequence (5' → 3')**
ccsR_F	**cttcagtatattcatcttcccatccaagaacctttaatc**atgcctttgccagaccatcg
ccsR_R	gatcagggataccgcgatgctctgattggcaactcagaccctgggagagattcaaattc
ccsP1_F	actcccgaatcgcttccatggaatttgaatctctcccagggtctgagttgccaatcagag
ccsP1_R	gccaggagtcatttgatcaaag
ccsP2_F	cgcaaggttcgagaatagcc
ccsP2_R	ggtccagcaggaattcttacgg
ccsP3_F	ccacgtaattgactctgactcg
ccsP3_R	gttcacacggctgctgaaggttg
ccsP4_F	gtagcgatcactaccatcttcc
ccsP4_R	gcaggaggatatggcgatattc
ccsP5_F	gcgtcgagtcgaagctgatgag
ccsP5_R	gccgcaagattgtggacttcac
ccsP6_F	cgtgccgaggatcgcataattc
ccsP6_R	**acacaacatatttcgtcagacacagaataactct**cgctagaccatccacgcaatgcactc
Transcriptional analysis	
IccsA_F	gtcgggccatttctgtgtac
IccsA_R	ctttgcattgggatcagctc
IccsB_F	caacgaccactgtggaagtg
IccsB_R	cccgtccagtgtactttctc
IccsD_F	cttgggtggagaagatccct
IccsD_R	atgttgcaggaggatatggc
IccsE_F	caacaacacggggcatatcac
IccsE_R	gcgttaccagggtacttgtatc
IccsF_F	gtgtaatgctgcatcctgcc
IccsF_R	cggctctctattgagttcgc
IccsC_F	ggtcgaatcccattcgacatg
IccsC_R	cagtactctcagaggatgcg
IccsG_F	ggttctgctacccatgaagt
IccsG_R	cccctaagcgaccaagatag
IccsR_F	cgaccactcctggtcatcaac
IccsR_R	gttcgcggatgtcctgttctc

REFERENCES

1. Flanagan, M. D.; Lin, S. Cytochalasins block actin filament elongation by binding to high affinity sites associated with F-actin. *J. Biol. Chem.* **1980**, *255*, 835–838.

2. Brown, S. S.; Spudich, J. A. Mechanism of action of cytochalasin: evidence that it binds to actin filament ends. *J. Cell Biol.* **1981**, *88*, 487–491.

3. Aldridge, D. C.; Armstron, J. J.; Speake, R. N.; Turner, W. B. Cytochalasins, a new class of biologically active mould metabolites. *Chem. Commun.* **1967**, 26–27.

4. Aldridge, D. C.; Armstrong, J. J.; Speake, R. N.; Turner, W. B. The structures of cytochalasins A and B. *J. Chem. Soc.* **1967**, 1667–1676.

5. Rampal, A.; Pinkofsky, H.; Jung, C. Structure of cytochalasins and cytochalasin B binding sites in human erythrocyte membranes. *Biochemistry* **1980**, 679–683.

6. Wagenaar, M. M.; Corwin, J.; Strobel, G.; Clardy, J. Three new cytochalasins produced by an endophytic fungus in the genus *Rhinocladiella*. *J. Nat. Prod.* **2000**, *63*, 1692–1695.

7. Udagawa, T.; Yuan, J.; Panigrahy, D.; Chang, Y. H.; Shah, J.; D'Amato, R. J. Cytochalasin E, an epoxide containing *Aspergillus*-derived fungal metabolite, inhibits angiogenesis and tumor growth. *J. Pharmacol. Exp. Ther.* **2000**, *294*, 421–427.

8. Binder, V. M.; Kiechel, J.-R.; Tamm, C. Zur Biogenese des Antibioticums Phomin. *Helv. Chim. Acta* **1970**, *53*, 1797–1812.

9. Probst, A.; Tamm, C. Biosynthetic Studies on Chaetoglobosin A and 19-O-Acetylchaetoglobosin A. *Helv. Chim. Acta* **1981**, *64*, 2065–2077.

10. Schümann, J.; Hertweck, C. Molecular basis of cytochalasan biosynthesis in fungi: gene cluster analysis and evidence for the involvement of a PKS-NRPS hybrid synthase by RNA silencing. *J. Am. Chem. Soc.* **2007**, *129*, 9564–9565.

11. Qiao, K.; Chooi, Y.-H.; Tang, Y. Identification and engineering of the cytochalasin gene cluster from *Aspergillus clavatus* NRRL 1. *Metab. Eng.* **2011**, *13*, 723–732.

12. Hu, Y.; Dietrich, D.; Xu, W.; Patel, A.; Thuss, J. a J.; Wang, J.; Yin, W.-B.; Qiao, K.; Houk, K. N.; Vederas, J. C.; Tang, Y. A carbonate-forming Baeyer-Villiger monooxygenase. *Nat. Chem. Biol.* **2014**, *10*, 552–554.

13. Kennedy, J.; Auclair, K.; Kendrew, S. G.; Park, C.; Vederas, J. C.; Hutchinson, C. R. Modulation of polyketide synthase activity by accessory proteins during lovastatin biosynthesis. *Science (80-.).* **1999**, *284*, 1368–1372.

14. Cox, R. J. Polyketides, proteins and genes in fungi: programmed nano-machines begin to reveal their secrets. *Org. Biomol. Chem.* **2007**, *5*, 2010–2026.

15. Larionov, V.; Kouprina, N.; Eldarov, M.; Perkins, E.; Porter, G.; Resnick, M. A. Transformation-associated recombination between diverged and homologous DNA repeats is induced by strand breaks. *Yeast* **1994**, *10*, 93–104.

16. Larionov, V.; Kouprina, N.; Graves, J.; Resnick, M. A. Highly selective isolation of human DNAs from rodent-human hybrid cells as circular yeast artificial chromosomes by transformation-associated recombination cloning. *Proc. Natl. Acad. Sci. U. S. A.* **1996**, *93*, 13925–13930.

17. Kim, J. H.; Feng, Z.; Bauer, J. D.; Kallifidas, D.; Calle, P. Y.; Brady, S. F. Cloning large natural product gene clusters from the environment: piecing environmental DNA gene clusters back together with TAR. *Biopolymers* **2010**, *93*, 833–844.

18. Larionov, V.; Kouprina, N. Specific cloning of human DNA as yeast artificial chromosomes by transformation-associated recombination. *Proc. Natl. Acad. Sci. U. S. A.* **1996**, *93*, 491–496.

19. Feng, Z.; Kim, J.; Brady, S. Fluostatins produced by the heterologous expression of a TAR reassembled environmental DNA derived type II PKS gene cluster. *J. Am. Chem. Soc.* **2010**, *132*, 11902–11903.

20. Candlla, M.; Graves, J.; Matesic, L.; Reeves, R.; Tainton, K.; Choo, K.; Resnick, M.; Larionov, V.; Kouprina, N. Rapid cloning of mouse DNA as yeast artificial chromosomes by transformation-associated recombination (TAR). *Mamm. Genome* **1998**, *9*, 157–159.

21. Kirchner, J. M.; Ivanova, V.; Samson, A.; Noskov, V. N.; Volff, J. N.; Resnick, M. a; Walter, R. B. Transformation-associated recombination (TAR) cloning of tumor-inducing Xmrk2 gene from *Xiphophorus maculatus*. *Mar. Biotechnol.* **2001**, *3*, 168–176.

22. Gaida, A.; Becker, M. M.; Schmid, C. D.; Bühlmann, T.; Louis, E. J.; Beck, H.-P. Cloning of the repertoire of individual *Plasmodium falciparum* var genes using transformation associated recombination (TAR). *PLoS One* **2011**, *6*, e17782.

23. Johnstone, I. L.; Hughes, S. G.; Clutterbuck, A. J. Cloning an *Aspergillus nidulans* developmental gene by transformation. *EMBO J.* **1985**, *4*, 1307–1311.

24. Nielsen, M. L.; Albertsen, L.; Lettier, G.; Nielsen, J. B.; Mortensen, U. H. Efficient PCR-based gene targeting with a recyclable marker for *Aspergillus nidulans*. *Fungal Genet. Biol.* **2006**, *43*, 54–64.

25. Yin, W.-B.; Chooi, Y. H.; Smith, A. R.; Cacho, R. A.; Hu, Y.; White, T. C.; Tang, Y. Discovery of cryptic polyketide metabolites from dermatophytes using heterologous expression in *Aspergillus nidulans*. *ACS Synth. Biol.* **2013**, *2*, 629–634.

26. Shimizu, K.; Keller, N. P. Genetic involvement of a cAMP-dependent protein kinase in a G protein signaling pathway regulating morphological and chemical transitions in *Aspergillus nidulans*. *Genetics* **2001**, *157*, 591–600.

27. Kouprina, N.; Larionov, V. Selective isolation of genomic loci from complex genomes by transformation-associated recombination cloning in the yeast *Saccharomyces cerevisiae*. *Nat. Protoc.* **2008**, *3*, 371–377.